

STANDARDS AND CODES  
OF PRACTICE IN  
MEDICAL RADIATION DOSIMETRY

VOLUME 2

**ALL BLANK PAGES HAVE BEEN  
RETAINED INTENTIONALLY  
IN THIS WEB VERSION.**

**BLANK**

PROCEEDINGS SERIES

# STANDARDS AND CODES OF PRACTICE IN MEDICAL RADIATION DOSIMETRY

PROCEEDINGS OF AN INTERNATIONAL SYMPOSIUM

HELD IN VIENNA, AUSTRIA,

25–28 NOVEMBER 2002,

ORGANIZED BY

THE INTERNATIONAL ATOMIC ENERGY AGENCY,

CO-SPONSORED BY THE EUROPEAN COMMISSION

(DIRECTORATE-GENERAL ENVIRONMENT),

THE EUROPEAN SOCIETY

FOR THERAPEUTIC RADIOLOGY AND ONCOLOGY,

THE INTERNATIONAL ORGANIZATION FOR MEDICAL PHYSICS

AND THE PAN AMERICAN HEALTH ORGANIZATION,

AND IN CO-OPERATION WITH

THE AMERICAN ASSOCIATION OF PHYSICISTS IN MEDICINE,

THE EUROPEAN FEDERATION OF ORGANISATIONS

FOR MEDICAL PHYSICS,

THE INTERNATIONAL COMMISSION ON RADIATION UNITS

AND MEASUREMENTS,

THE INTERNATIONAL SOCIETY FOR RADIATION ONCOLOGY

AND THE WORLD HEALTH ORGANIZATION

*In two volumes*

## VOLUME 2

INTERNATIONAL ATOMIC ENERGY AGENCY

VIENNA, 2003

Permission to reproduce or translate the information contained in this publication may be obtained by writing to the International Atomic Energy Agency, Wagramer Strasse 5, P.O. Box 100, A-1400 Vienna, Austria.

© IAEA, 2003

**IAEA Library Cataloguing in Publication Data**

International Symposium on Standards and Codes of Practice in Medical Radiation Dosimetry (2002 : Vienna, Austria)

Standards and codes of practice in medical radiation dosimetry : proceedings of an international symposium held in Vienna, Austria, 25–28 November 2002 / organized by the International Atomic Energy Agency ; co-sponsored by the European Commission, Directorate-General Environment...[et al.]. In 2 vols. — Vienna: The Agency, 2003.

2 v. ; 24 cm. — (Proceedings series, ISSN 0074–1884)

Contents : v. 2.

STI/PUB/1153

ISBN 92–0–111403–6

Includes bibliographical references.

1. Radiology, Medical — Congresses. 2. Radiation dosimetry — Standards — Congresses. I. International Atomic Energy Agency. II. Series: Proceedings series (International Atomic Energy Agency).

IAEAL

03–00338

Printed by the IAEA in Austria  
December 2003  
STI/PUB/1153

## FOREWORD

In technologically advanced societies, there are many applications and processes that employ ionizing radiation. In order to use radiation safely and effectively, it is necessary to be able to measure radiation properly. Dosimetry is the science of radiation measurement. Knowledge of dosimetry enables nuclear technology to be applied to meet the needs of society. Medical radiation dosimetry deals with those applications in which patients are irradiated for either diagnosis or therapy.

These Proceedings present a refereed selection of papers that were presented at the International Symposium on Standards and Codes of Practice in Medical Radiation Dosimetry, held in Vienna from 25 to 28 November 2002. Over 250 scientists from 62 countries attended the meeting, at which 140 presentations were delivered covering a broad range of topics in medical radiation dosimetry.

Since the last IAEA meeting on dosimetry (Measurement Assurance in Dosimetry, held in Vienna from 24 to 27 May 1993), three major activities have affected progress in medical radiation dosimetry. Firstly, in terms of measurement technology, much work has gone into perfecting calorimetric methods for the determination of absorbed dose to water, and so one entire session of the symposium was devoted to that topic. Secondly, since several primary standards dosimetry laboratories have developed the capability to provide instrument calibrations based on their newly refined standards of absorbed dose to water, the IAEA and other organizations developed new dosimetry codes of practice using these standards. In the opening session, one talk focused on the development of dosimetry codes of practice, in particular the international code of practice published by the IAEA in Technical Reports Series No. 398, Absorbed Dose Determination in External Beam Radiotherapy. The third major activity in dosimetry relates to the mutual recognition arrangement (MRA) of the Comité international des poids et mesures, which was signed by the laboratories, including the IAEA's, responsible for metrology in the field of ionizing radiation standards. One of the talks in the opening session dealt with the MRA explicitly, but several of the sessions on comparisons were motivated by the need to establish degrees of equivalence between the dosimetry standards of different laboratories. The new standards, the dosimetry protocols that use them and the MRA, which encourages comparisons, have together raised dosimetry to a new level.

Of course, the requirement for accuracy in dosimetry is driven primarily by the demands for cancer therapy — too low a dose leaves the patient to die from cancer and too high a dose may result in a dramatic increase in complication rates. An overt attempt was made during the symposium to highlight the

link between accuracy in dosimetry and cancer therapy. For example, a plenary session focused on the impending crisis in cancer management, and regular scientific sessions dealt with clinical radiotherapy dosimetry and with radiotherapy dosimetry auditing. In addition, scientific sessions were dedicated to dosimetry issues in brachytherapy, proton and hadron therapy and diagnostic radiology. One session was devoted to nuclear medicine, in an attempt to bridge the gap between the experts who measure radioactivity and those who deal with quality assurance in nuclear medicine.

The symposium programme comprised 14 scientific sessions, and at the end of each session there was a brief discussion arising from the material that had been presented. During these discussions, participants were encouraged to suggest recommendations that would provide guidance to everyone concerned with the field of dosimetry. Session 15 contains the list of the participants' recommendations as summarized by the Chair of the session, P.J. Allisy-Roberts of the Bureau international des poids et mesures. Many institutions and organizations have since incorporated elements of these recommendations into their own work plans. In addition, a meeting of symposium participants was held at the IAEA in July 2003 in order to draw up a plan of action in response to the recommendations. This action plan is available from the IAEA in a separate document entitled International Action Plan on Medical Radiation Dosimetry.

The IAEA would like to thank the Programme Committee and the co-sponsoring and collaborating organizations. Special thanks are due to the session Chairs and Co-chairs who, in advance of the symposium, acted as referees and editors of the material for their sessions in addition to preparing their own presentations. Their exceptional contribution increased the level of scientific interaction, thereby enhancing the success of the symposium. Owing to the important changes taking place in the field of dosimetry, participants would like to see the medical physics community hold the next meeting on medical radiation dosimetry in six years' time (2008).

**BLANK**

#### EDITORIAL NOTE

*The Proceedings have been edited by the editorial staff of the IAEA to the extent considered necessary for the reader's assistance. The views expressed remain, however, the responsibility of the named authors or participants. In addition, the views are not necessarily those of the governments of the nominating Member States or of the nominating organizations.*

*Although great care has been taken to maintain the accuracy of information contained in this publication, neither the IAEA nor its Member States assume any responsibility for consequences which may arise from its use.*

*The use of particular designations of countries or territories does not imply any judgement by the publisher, the IAEA, as to the legal status of such countries or territories, of their authorities and institutions or of the delimitation of their boundaries.*

*The mention of names of specific companies or products (whether or not indicated as registered) does not imply any intention to infringe proprietary rights, nor should it be construed as an endorsement or recommendation on the part of the IAEA.*

*The authors are responsible for having obtained the necessary permission for the IAEA to reproduce, translate or use material from sources already protected by copyrights.*

*Material prepared by authors who are in contractual relation with governments is copyrighted by the IAEA, as publisher, only to the extent permitted by the appropriate national regulations.*



## CONTENTS OF VOLUME 2

### NUCLEAR MEDICINE DOSIMETRY (Session 9)

Radiation dose assessment in nuclear medicine (IAEA-CN-96/63) . . . . .	3
<i>M.G. Stabin</i>	
Quality assurance programmes for radioactivity measurements in nuclear medicine (IAEA-CN-96/64) . . . . .	17
<i>B.E. Zimmerman</i>	
Monte Carlo techniques in diagnostic and therapeutic nuclear medicine (IAEA-CN-96/65) . . . . .	29
<i>H. Zaidi</i>	
Performance and quality control of radionuclide calibrators in nuclear medicine (IAEA-CN-96/66) . . . . .	45
<i>M.J. Woods, M. Baker</i>	

### Poster presentations

Relationship of bone uptake to radiation doses in bone pain treatment with $^{188}\text{Re}$ HEDP (IAEA-CN-96/67P) . . . . .	59
<i>J. Gaudio, E. Savio, A. Paolino</i>	
Comparisons of activity measurements in nuclear medicine with radionuclide calibrators in the Czech Republic (IAEA-CN-96/68P) . . . . .	67
<i>V. Olšovcová, P. Dryák</i>	

### BRACHYTHERAPY (Session 10)

Source specification and codes of practice for brachytherapy dosimetry (IAEA-CN-96/70) . . . . .	79
<i>C.G. Soares, H. Tölli</i>	
Development of a Dutch primary standard for beta emitting brachytherapy sources (IAEA-CN-96/71) . . . . .	93
<i>J. van der Marel, E. van Dijk</i>	
New developments on primary standards for brachytherapy at the National Institute of Standards and Technology and the Physikalisch-Technische Bundesanstalt (IAEA-CN-96/72) . . . . .	101
<i>H.-J. Selbach, C.G. Soares</i>	
The need for international standardization in clinical beta dosimetry for brachytherapy (IAEA-CN-96/73) . . . . .	111
<i>U. Quast, J. Böhm, T.W. Kaulich</i>	

Energy dependence of the air kerma response of a liquid ionization chamber at photon energies between 8 keV and 1250 keV (IAEA-CN-96/74) .....	121
<i>G. Hilgers, J. Bahar-Gogani, G. Wickman</i>	
Comparison of two different methods to determine the air kerma calibration factor, $N_k$ , for $^{192}\text{Ir}$ (IAEA-CN-96/75) .....	129
<i>E. van Dijk</i>	

## **RADIOTHERAPY DOSIMETRY AUDITS (Session 11)**

Worldwide quality assurance networks for radiotherapy dosimetry (IAEA-CN-96/76) .....	139
<i>J. Izewska, H. Svensson, G. Ibbott</i>	
ESTRO European assurance programme for radiation treatments (the EQUAL network) (IAEA-CN-96/77) .....	157
<i>I.H. Ferreira, A. Dutreix, A. Bridier, H. Svensson</i>	
Radiation therapy thermoluminescence dosimetry service in Germany: The experience of the first year (IAEA-CN-96/78) .....	167
<i>C. Pychlau</i>	
Audit of radiotherapy dosimetry in New Zealand: Practical considerations and results (IAEA-CN-96/79) .....	177
<i>V.G. Smyth, J.A. Laban</i>	
The United Kingdom's radiotherapy dosimetry audit network (IAEA-CN-96/81) .....	183
<i>D.I. Thwaites, S.K. Powley, A. Nisbet, M. Allahverdi</i>	
Thermoluminescence dosimetry as a tool for the remote verification of output for radiotherapy beams: 25 years of experience (IAEA-CN-96/82) .....	191
<i>J.F. Aguirre, R.C. Taylor, G. Ibbott, M. Stovall, W.F. Hanson</i>	

## **Poster presentations**

Role of the National Physical Laboratory in monitoring and improving dosimetry in radiotherapy in the United Kingdom (IAEA-CN-96/80P) .....	201
<i>R.A.S. Thomas, S. Duane, M.R. McEwen, K.E. Rosser</i>	
An anthropomorphic head and neck phantom for the evaluation of intensity modulated radiation therapy (IAEA-CN-96/85P) .....	209
<i>G. Ibbott, A. Nelson, D. Followill, P. Balter, W.F. Hanson</i>	

## **POSTERS ON BRACHYTHERAPY (Session 12a)**

- Design and implementation of a phantom for the quality control of high dose rate  $^{192}\text{Ir}$  sources used in brachytherapy (IAEA-CN-96/87P) ..... 221  
*R. Ochoa, I.H. Ferreira, C.E. de Almeida*
- New approach for standardizing absorbed dose from beta radioactive wires and seeds used for intravascular brachytherapy (IAEA-CN-96/88P) ..... 231  
*S. Pszona, B. Kocik, K. Wincel, B. Zareba, W. Bulski*
- Comparison of calibration techniques for  $^{192}\text{Ir}$  high dose rate brachytherapy sources (IAEA-CN-96/92P) ..... 239  
*C. Tannanonta, T. Layangkul, C. Orkongkiat*

## **POSTERS ON RADIOTHERAPY DOSIMETRY AUDITS (Session 12b)**

- IAEA supported national thermoluminescence dosimetry audit networks for radiotherapy dosimetry: Summary of the posters presented in Session 12b (IAEA-CN-96/137) ..... 249  
*J. Izewska, D.I. Thwaites*
- Thermoluminescence dosimetry quality assurance network for radiotherapy and radiology in the Czech Republic (IAEA-CN-96/97) ..... 269  
*D. Kroutilíková, J. Novotný, L. Novák*

## **PROTON AND HADRON DOSIMETRY (Session 13)**

- Codes of practice and protocols for the dosimetry in reference conditions of proton and ion beams (IAEA-CN-96/110) ..... 279  
*S.M. Vatnitsky, P. Andreo*
- Dosimetry with the scanned proton beam on the Paul Scherrer Institute gantry (IAEA-CN-96/111) ..... 295  
*A. Coray, E. Pedroni, T. Boehringer, S. Lin, A. Lomax, G. Goitein*
- Dosimetry of  $^{12}\text{C}$  ion beams at the German heavy ion therapy facility: Comparison of the currently used approach and TRS 398 (IAEA-CN-96/112) ..... 303  
*O. Jäkel, G.H. Hartmann, P. Heeg, C.P. Karger*

Proton dosimetry intercomparison using parallel-plate ionization chambers in a proton eye therapy beam (IAEA-CN-96/113) .....	311
<i>A. Kacperek, E. Egger, L. Barone Tonghi, G. Cuttone,</i>	
<i>L. Raffaele, A. Rovelli, M.G. Sabini, P. Tabarelli de Fatis,</i>	
<i>F. Luraschi, L. Marzoli</i>	

## Poster presentations

Proton beam dosimetry: Protocol and intercomparison in Japan (IAEA-CN-96/115P) .....	321
<i>A. Fukumura, T. Kanai, N. Kanematsu, K. Yusa, A. Maruhashi,</i>	
<i>A. Nohtomi, T. Nishio, M. Shimbo, T. Akagi, T. Yanou, S. Fukuda,</i>	
<i>T. Hasegawa, Y. Kusano, Y. Masuda</i>	
Parallel-plate and thimble ionization chamber calibrations in proton beams using the TRS 398 and ICRU 59 recommendations (IAEA-CN-96/116P) .....	327
<i>S.M. Vatnitsky, M.F. Moyers, A.S. Vatnitsky</i>	

## DEVELOPMENTS IN CLINICAL RADIOTHERAPY DOSIMETRY (Session 14)

Radiotherapy gel dosimetry (IAEA-CN-96/117) .....	339
<i>C. Baldock</i>	
Development of optical fibre luminescence techniques for real time in vivo dosimetry in radiotherapy (IAEA-CN-96/118) .....	353
<i>C.E. Andersen, M.C. Aznar, L. Bøtter-Jensen, S.Å.J. Bäck,</i>	
<i>S. Mattsson, J. Medin</i>	
An anthropomorphic head phantom with a BANG polymer gel insert for the dosimetric evaluation of intensity modulated radiation therapy treatment delivery (IAEA-CN-96/119) .....	361
<i>G. Ibbott, M. Beach, M. Maryanski</i>	
Clinical implementation and quality assurance for intensity modulated radiation therapy (IAEA-CN-96/120) .....	369
<i>C.-M. Ma, R. Price, S. McNeeley, L. Chen, J.S. Li, L. Wang,</i>	
<i>M. Ding, E. Fourkal, L. Qin</i>	
QUASIMODO: An ESTRO project for performing the quality assurance of treatment planning systems and intensity modulated radiation therapy (IAEA-CN-96/121) .....	381
<i>B.J. Mijnheer, C. de Wagter, S. Gillis, A. Olszewska</i>	

## Poster presentations

Factors affecting the extraction of absorbed dose information in 3-D polymer gel dosimeters by X ray computed tomography (IAEA-CN-96/122P) .....	389
<i>J.V. Trapp, G. Michael, Y. de Deene, C. Baldock</i>	
Acoustic evaluation of polymer gel dosimeters (IAEA-CN-96/123P) .....	397
<i>M.L. Mather, Y. de Deene, C. Baldock, A.K. Whittaker</i>	
Photon energy dependence of the electron paramagnetic resonance alanine dosimetry system: An experimental investigation (IAEA-CN-96/124P) .....	405
<i>E.S. Bergstrand, K.R. Shortt, C.K. Ross, E.O. Hole</i>	
Experience with in vivo diode dosimetry for verifying radiotherapy dose delivery: The practical implementation of cost effective approaches (IAEA-CN-96/131P) .....	415
<i>D.I. Thwaites, C. Blyth, L. Carruthers, P.A. Elliott, G. Kidane, C.J. Millwater, A.S. MacLeod, M. Paolucci, C. Stacey</i>	

## CONCLUSIONS AND RECOMMENDATIONS (Session 15)

Conclusions and recommendations .....	427
Chairs of Sessions .....	441
Co-chairs of Sessions .....	441
Rapporteurs of Sessions .....	442
Programme Committee .....	443
Secretariat of the Symposium .....	443
List of Participants .....	445
Author Index .....	495

**BLANK**

# NUCLEAR MEDICINE DOSIMETRY

(Session 9)

**Chair**

**B.E. ZIMMERMAN**

United States of America

**Co-Chair**

**M.G. STABIN**

United States of America

**Rapporteur**

**H. ZAIDI**

Switzerland

**BLANK**



## **RADIATION DOSE ASSESSMENT IN NUCLEAR MEDICINE**

**M.G. STABIN**

Department of Radiology and Radiological Sciences,  
Vanderbilt University,  
Nashville, Tennessee, United States of America  
E-mail: michael.g.stabin@vanderbilt.edu

### **Abstract**

Radionuclides are used in nuclear medicine in a variety of diagnostic and therapeutic procedures. Recently, interest has grown in therapeutic agents for a number of applications in nuclear medicine. Internal dose models and methods have been in use for many years, are well established and can give radiation doses to stylized models representing reference individuals. Kinetic analyses need to be carefully planned, and dose conversion factors should be chosen that are most similar to the subject in question and that can then be tailored to be more patient specific. Such calculations, however, are currently not relevant in patient management in internal emitter therapy, as they are not sufficiently accurate or detailed to guide clinical decision making. Great strides are being made at many centres regarding the use of patient image data to construct individualized voxel based models for more detailed and patient specific dose calculations. These recent advances make it likely that the relevance will soon change to be more similar to that of external beam treatment planning.

### **1. INTRODUCTION**

In any application involving the use of ionizing radiation in humans, risks and benefits must be properly evaluated and balanced. Radionuclides are used in nuclear medicine in a variety of diagnostic and therapeutic procedures. Recently, interest has grown in therapeutic agents for a number of applications in nuclear medicine, particularly in the treatment of haematologic and non-haematologic malignancies. This has heightened interest in the need for radiation dose calculations and challenged the scientific community to develop more patient specific and relevant dose models. Consideration of radiation dose in such studies is central to efforts to maximize the dose to the tumour while sparing normal tissues. In many applications a significant absorbed dose may be received by some radiosensitive organs, particularly the active marrow. This paper reviews the methods and models used in internal dosimetry in nuclear medicine and discusses some current trends and challenges in this field.

Internal dose estimates currently are not used in the management of individual patients in internal emitter therapy in the way that dose information is used in external beam radiation dose treatment planning. Internal dose calculations generally are well evaluated during clinical trials to establish the efficacy of and gain approval for new radiolabelled agents. In routine administrations, however, the same amount of activity is given to most patients, perhaps with slight adjustments for total body weight or external surface area, and a careful radiation dose plan to optimize the therapy is not developed for each patient. The basic reasons for this are that dosimetry analyses are far more difficult for internal emitters than for external radiation therapy (as patients must be imaged at multiple times and a fairly complex analysis performed) and because current models, which are based on stylized models representing average individuals, do not give dose estimates with the degree of accuracy needed for such careful analyses. Much attention is being given to improving models, for both general organs and red marrow; whether this ultimately leads to greater clinical relevance remains to be seen.

## 2. CURRENT NUCLEAR MEDICINE APPLICATIONS

Nuclear medicine continues to employ radionuclides such as  $^{99m}\text{Tc}$ ,  $^{67}\text{Ga}$ ,  $^{18}\text{F}$  (a positron emitter),  $^{111}\text{In}$ ,  $^{123}\text{I}$ ,  $^{131}\text{I}$  and  $^{201}\text{Tl}$  in diagnostic procedures. In developed countries about 25% of such procedures are used to scan bone, 15% to scan the cardiovascular system, 5% for the thyroid and 10% to scan the liver, spleen and lung. About 80% of diagnostic nuclear medicine scans are performed on patients of over 40 years of age [1]. Most therapeutic radiopharmaceuticals emit beta particles, which travel only a few millimetres in tissue. The most common procedure is the use of radioactive  $^{131}\text{I}$  for the treatment of hyperthyroidism and thyroid cancer. As in diagnosis, thyroid therapy is given predominantly to women (male:female ratio, 1:3). The activities of  $^{131}\text{I}$  given orally for hyperthyroidism are 200–1000 MBq, and those for thyroid cancer are 3500–6800 MBq [1]. Other therapeutic uses of unsealed radionuclides include the administration of monoclonal antibodies, antibody fragments or other targeted molecules to specific markers on the surface of tumour cells. In February 2002 a radiolabelled monoclonal antibody product ( $^{90}\text{Y}$  labelled Ibritumomab Tiuxetan, or Zevalin) was approved by the United States Food and Drug Administration for the therapy of non-Hodgkin's lymphoma in a limited patient population [2]. Many other products, labelled with a variety of beta as well as alpha emitters, are under active study. Investigation also continues into the use of bone seeking agents (such as  $^{89}\text{SrCl}$ ,  $^{153}\text{Sm}$  EDTMP,  $^{117m}\text{Sn}$  DTPA and  $^{188}\text{Re}$  HEDP) for the palliative treatment of osseous metastases, at a

typical intravenously administered activity of 150 MBq. Another bone seeking nuclide,  $^{166}\text{Ho}$  DOTMP [3], is in clinical trials for therapy against multiple myeloma. In this therapy up to 150 GBq of activity may be administered, in an attempt to ablate marrow, followed by marrow rescue after the reinfusion of marrow stem cells harvested from peripheral blood. Marrow doses in this procedure are obviously extremely high (up to 40 Gy), and doses to secondary organs such as the kidney are of concern for patient protection.

### 3. DATA ACQUISITION AND ANALYSIS

To design and execute a good kinetic study it is necessary to collect the correct data, enough data and express the data in the proper units. The basic data needed are the fraction (or per cent) of administered activity in important source organs and excreta samples. It is very important, in either animal or human studies, to take enough samples to characterize both the distribution and retention of the radiopharmaceutical over the course of the study. The following criteria are essential:

- (a) Catch the early peak uptake and rapid washout phase;
- (b) Cover at least three effective half-times of the radiopharmaceutical;
- (c) Collect at least two time points per clearance phase;
- (d) Account for 100% of the activity at all times;
- (e) Account for all the major paths of excretion (urine, faeces, exhalation, etc.).

Some knowledge of the expected kinetics of the pharmaceutical is needed for a good study design. For example, the spacing of the measurements and the time of the initial measurement will be greatly different if a  $^{99\text{m}}\text{Tc}$  labelled renal agent is studied, which is 95% cleared from the body in 180 min, or if an  $^{131}\text{I}$  labelled antibody is studied, which clears about 80% on the first day and the remaining 20% over the next two weeks. A key point that researchers can overlook is the characterization of excretion. Very often the excretory organs (the intestines and urinary bladder) are the organs that receive the highest absorbed doses, as 100% of the activity (minus decay) will eventually pass through one or both of these pathways at different rates. If excretion is not quantified, the modeller must make the assumption that the compound is retained in the body and removed only by radioactive decay. This may not be a problem for very short lived radionuclides, and in fact may be quite accurate. For moderately long lived nuclides, however, this can cause an overestimate of the dose to most body organs and an underestimate of the dose to the excretory organs, perhaps significantly.

Before beginning clinical trials with radiopharmaceuticals, biokinetic data are usually gathered in animal studies. Organ, blood and excreta measurements are made either after sacrificing the animal or by using quantitative imaging methods. Extrapolation to human values of uptake and clearance is far from certain, but these preliminary data provide a basis for going forward with clinical trials if the results are generally favourable. In clinical studies, quantitative imaging methods are used to obtain activity in various organs as a function of time. Planar or single photon emission computed tomography (SPECT) data may be acquired [4]. Obtaining quantitative estimates of the activity per organ is an arduous task, requiring careful attention to detail, including corrections for photon scatter, attenuation, septal penetration and other effects in the gamma camera [5]. When this phase is satisfactorily completed, data may be fitted to multicomponent exponential retention functions or in closed compartment models using the SAAM II software [6] or other tools. Time integrals of activity are calculated, and these may be used with dose conversion factors (DCFs) (as discussed below) to obtain radiation dose estimates.

#### 4. DOSE CALCULATION METHODOLOGIES

The principal quantity of interest in internal dosimetry is the absorbed dose, or the dose equivalent. Absorbed dose,  $D$ , is defined [7] as:

$$D = \frac{d\epsilon}{dm}$$

where  $d\epsilon$  is the mean energy imparted by ionizing radiation to matter of mass  $dm$ . The units of absorbed dose are typically erg/g or J/kg. The special units are rad (100 erg/g) or the gray (Gy) (1 J/kg = 100 rad =  $10^4$  erg/g). The dose equivalent,  $H$ , is the absorbed dose multiplied by a quality factor,  $Q$ , the latter accounting for the effectiveness of different types of radiation in causing biological effects:

$$H = DQ$$

Because the quality factor is in principle dimensionless, the pure units of this quantity are the same as absorbed dose (i.e. erg/g or J/kg). However, the special units have unique names, specifically the rem and sievert (Sv). Values for the quality factor have changed as new information about radiation effectiveness has become available. Current values, recommended by the International Commission on Radiological Protection (ICRP 30) [8], are given in Table I.

TABLE I. QUALITY FACTORS  
RECOMMENDED IN ICRP 30 [8]

Radiation type	Quality factor, $Q$
Alpha particles	20
Beta particles	1
Gamma rays	1
X rays	1

The quantity dose equivalent was originally derived for use in radiation protection programmes. The development of the effective dose equivalent by the ICRP in 1979, and of the effective dose in 1991 [9], however, allowed non-uniform internal doses to be expressed as a single value, representing an equivalent whole body dose.

A generic equation for the absorbed dose rate in an organ can be shown as:

$$D = \frac{k\tilde{A} \sum_i n_i E_i \phi_i}{m}$$

where

- $D$  is the absorbed dose (rad or Gy);
- $\tilde{A}$  is the cumulated activity ( $\mu\text{Ci}\cdot\text{h}$  or  $\text{MBq}\cdot\text{s}$ );
- $n$  is the number of radiations with energy  $E$  emitted per nuclear transition;
- $E$  is the energy per radiation (MeV);
- $\phi$  is the fraction of energy absorbed in the target;
- $m$  is the mass of the target region (g or kg);
- $k$  is the proportionality constant ( $\text{rad}\cdot\text{g}\cdot\mu\text{Ci}^{-1}\cdot\text{h}^{-1}\cdot\text{MeV}^{-1}$  or  $\text{Gy}\cdot\text{kg}\cdot\text{MBq}^{-1}\cdot\text{s}^{-1}\cdot\text{MeV}^{-1}$ ).

It is extremely important that the proportionality constant be properly calculated and applied. The results of a calculation will be useless unless the units within are consistent and correctly express the quantity desired. The application of quality factors to this equation to calculate the dose equivalent rate is a trivial matter; for most of this section only absorbed doses are considered.

#### 4.1. MIRD system for internal dose calculations

The equation for absorbed dose in the MIRD system [10] is deceptively simple:

$$D = \tilde{A}S$$

The cumulated activity is there; all other terms must be lumped in the factor  $S$ :

$$S = \frac{k \sum_i n_i E_i \phi_i}{m}$$

The factor  $k$  in the MIRD equation is 2.13, which gives doses in rad, from activity in microcuries, mass in grams and energy in MeV. The MIRD system was developed primarily for use in estimating radiation doses received by patients from administered radiopharmaceuticals; it is not intended to be applied to a system of dose limitation for workers.

#### 4.2. MIRDOSE software and RADAR system

The MIRDOSE computer program [11] was originally developed to eliminate the tedium of repetitive internal dose calculations (looking up DCFs from tables and adding contributions from every source to every target, even if of minor importance), to automate the calculation of organ doses in nuclear medicine. The evolution of the MIRDOSE software continues today. In order to provide more computer platform independence, M.G. Stabin recently rewrote the MIRDOSE code entirely in the Java language and incorporated a curve fitting algorithm for kinetic data [12]. The code was renamed OLINDA (Organ Level Internal Dose Assessment), partly to distinguish it from the activities of the MIRD Committee (which had expressed concern that the name MIRDOSE might imply that it was a product of that committee) and partly to integrate the name into a new unified system of internal and external dose assessment.

This unified system is deployed on a web site for rapid electronic access [13]. This site, called the Radiation Dose Assessment Resource (RADAR), provides decay data for over 800 radionuclides, absorbed fractions for all available stylized phantoms and some voxel phantoms, kinetic data, dose factors (for all phantoms and nuclides), risk information and other data via electronic transfer to users worldwide. The resource has several features that make it easier to understand and use than existing resources in these areas, and it is hoped that

this will greatly facilitate the work of professionals in the field who need access to such resources to do their work. As the system will be mostly accessible through web pages or ftp access, it should be of particular utility to professionals in developing countries, who may have difficulty obtaining all the necessary documents, data and guidance that they want. In the RADAR system the number of disintegrations will be called  $N$ , and the factor to convert disintegrations to dose will be called a DCF, thus permitting both systems to be used while learning only one equation, whose terms are perhaps more intuitive. For external dose the situation is similar — it is necessary to specify the number of disintegrations that have occurred in a particular source and then apply the appropriate DCFs to obtain doses to individual organs, effective doses, etc.:

$$D_T = \sum_S N_S \text{DCF}(T \leftarrow S)$$

A difficulty often encountered with the existing systems is that the published results usually appear only as printed text, at various intervals in time. To use the data, they must be entered by hand into computer programs, spreadsheets, etc. The RADAR system will be primarily an on-line system in which all data are available for access electronically, at any time. The system will be kept up to date at regular intervals. As new models, decay data, DCFs or methods become available, as soon as they can be incorporated into the RADAR system, they will be made available to users.

## 5. APPLYING DCFs TO PATIENTS

With suitable values for  $\tilde{A}$  and the DCF a series of dose estimates can be calculated for a patient. The MIRDOSE 3 software, discussed above, has made available  $S$  values for Reference Man, Reference Woman, paediatric phantoms and all the pregnant female phantoms. Typical results are shown in Table II.

These dose estimates are based on a standard kinetic model and absorbed fractions for the adult male phantom in the Cristy–Eckerman phantom series [14]. If patient specific biokinetic data were to be used for a nuclear medicine therapy agent with this same phantom, the result would be the same as in Table II (except that the effective dose quantities may not be used in therapy applications). These models, however, give the average dose to whole organs (not dose distributions within organs or tissues with possibly non-uniform activity distributions), and the reported doses are applicable only to a person whose size and weight are close to that of the reference individual after which

TABLE II. RADIATION DOSE ESTIMATES FOR THE REFERENCE ADULT FOR  $^{90}\text{Y}$  ZEVALIN

Organ	mGy/MBq	rad/mCi
Liver	$4.8 \times 10^0$	$1.8 \times 10^1$
Lungs	$2.0 \times 10^0$	$7.4 \times 10^0$
Lower large intestine wall	$4.8 \times 10^0$	$1.8 \times 10^1$
Upper large intestine wall	$3.6 \times 10^0$	$1.3 \times 10^1$
Red marrow	$1.3 \times 10^0$	$4.8 \times 10^0$
Spleen	$9.4 \times 10^0$	$3.5 \times 10^1$
Testes	$9.1 \times 10^0$	$3.4 \times 10^1$
Urinary bladder wall	$9.0 \times 10^{-1}$	$3.3 \times 10^0$
Other organs	$3.0 \times 10^{-1}$	$1.1 \times 10^0$

the model was derived. Thus the doses reported with such models really represent the dose to a phantom, not to a patient. If the biokinetic data to be applied were taken from the actual patient, then these data would be patient specific. In diagnostic applications in nuclear medicine, usually a standardized kinetic model is also applied.

### 5.1. Adaptation of model based dose estimates to individual patients

Dose estimates can be made more patient specific through mass based adjustments to the organ doses:

- (a) Absorbed fractions for electrons and alphas scale linearly with mass;
- (b) Absorbed fractions for photons scale with mass to a power of  $1/3$ .

Generally it is not possible to:

- (a) Account for patient specific differences in organ geometry;
- (b) Account for patient specific marrow characteristics;
- (c) Calculate dose distributions within organs.

To perform real patient specific dose calculations, a patient specific physical model is needed, to be used with patient specific biokinetic data. A one dose fits all approach to radiation therapy with these internal emitter treatments is not likely to be effective (owing to the narrow range between tumour ablation and bone marrow toxicity). Individual patients not only have significantly different uptake and retention half-times of activity of the radioactive



agent, but also have significantly different physical characteristics and radiosensitivities. Many cancer patients have failed other treatments, and may enter radiotherapy with compromised marrow, owing to their previous treatments. Thus their therapies should be optimized, taking into account individual parameters as much as possible.

If a radiation oncologist or medical physicist for an external beam therapy programme were to be approached and the suggestion made that all patients with a certain type of cancer should receive the exact same treatment schedule (beam type, energy, beam exposure time, geometry, etc.), the idea would certainly be rejected as not being in the best interests of the patient. Instead, a patient specific treatment plan would be implemented in which treatment times are varied to deliver the same radiation dose to all patients. Patient specific calculations of doses delivered to tumours and normal tissues have been routine in external beam radiotherapy and brachytherapy for decades. The routine use of a fixed GBq/kg, GBq/m<sup>2</sup> or simply GBq administration of radionuclides for therapy is equivalent to treating all patients in external beam radiotherapy with the same treatment schedule. Varying the treatment time to result in an equal absorbed dose for external beam radiotherapy is equivalent to accounting for the known variation in a patient's physical characteristics and radionuclide biokinetics to achieve similar tumour doses in internal emitter radiotherapy, while watching the doses received by healthy tissues.

## **5.2. Image based, patient specific dose calculations**

Great strides are being made at many centres in the use of patient image data to construct individualized voxel based models for more detailed and patient specific dose calculations. Many specially designed computer codes have been developed for patient specific dosimetry and treatment planning. A few groups have managed to fuse three dimensional (3-D) anatomical data, from computed tomography (CT) or magnetic resonance imaging images, with 3-D data on radionuclide distribution, from SPECT or positron emission tomography images, to provide a 3-D representation of the radionuclide distribution in the tissues of the patient. Efforts in this area include the 3D-ID code from the Memorial Sloan-Kettering Cancer Center, United States of America [15], the SIMIND code from the University of Lund, Sweden [16], the RMDP code from the Royal Marsden Hospital, United Kingdom [17], the VOXEL-DOSE code from Rouen, France [18], and the SCMS code from Vanderbilt University, United States of America [19]. Most of these codes are still research tools and have not yet entered the clinical area. The code with the most clinical experience to date is the 3D-ID code. This code produces 3-D dose distributions as well as dose-volume histograms (functions that show which fraction of

an organ received what dose) for normal organs and tumours. The RMDP and VOXELDOSE codes combine the MIRD voxel source kernels for soft tissue with beta point kernels to give dose distributions in unit density soft tissue regions of the body. The SCMS code uses MCNP Monte Carlo software to transport electrons and photons in heterogeneous voxel based phantoms, using fused CT and SPECT image data. Reference [19] shows an example of how different the geometries of the standardized phantom may be from those of real human subjects, in a figure (Fig. 1) showing the difference between the gastrointestinal tract and liver–kidney regions of the Cristy–Eckerman adult male phantom and that of the voxel based 75 kg individual image provided by the group at Yale [20].

### **5.3. Other patient specific modifications**

Knowledge continues to evolve about bone and marrow dose models and their appropriate application to individual patients in therapy. Much has been learned recently about patient specific adjustments to model based marrow dose estimates and about the use of biomarkers to indicate an individual patient's ability to tolerate radiation dose to the marrow [21]. Some data concerning dose–response relationships for tumours have also been established [22].

## **6. CONCLUSIONS**

Internal dose models and methods in use for many years are well established and can give radiation doses to stylized models representing reference individuals. Kinetic analyses need to be carefully planned, and DCFs should be chosen that are most similar to the subject in question and that can then be tailored somewhat to be more patient specific. Such calculations, however, are currently not relevant in patient management in internal emitter therapy, as they are not sufficiently accurate or detailed to guide clinical decision making. This is currently an area of active inquiry, and recent advances make it likely that the relevance will soon change to be more similar to that of external beam treatment planning.

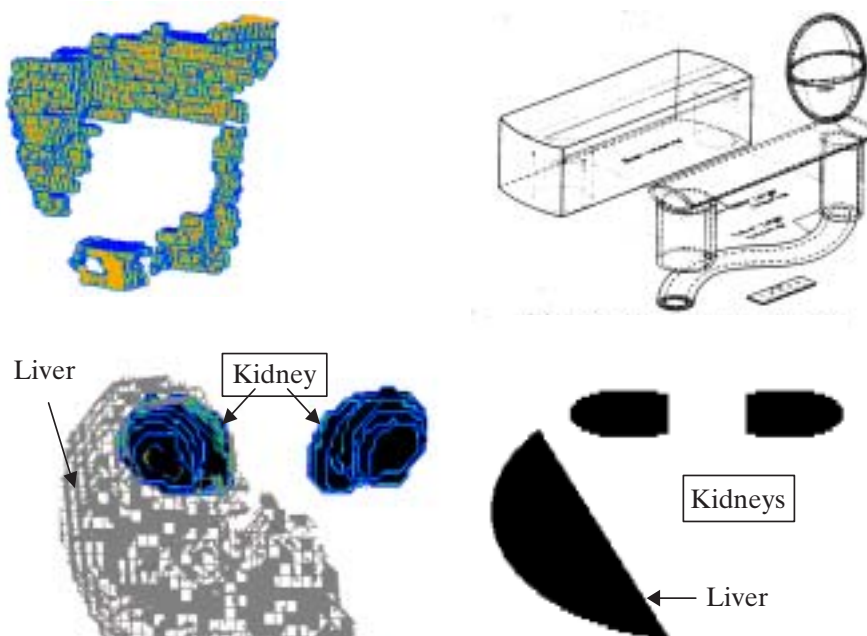


FIG. 1. Images showing the gastrointestinal tract (top) and kidney–liver region (bottom) from the Yale voxel phantom [20] (left) and the Cristy–Eckerman geometrical phantom [14] (right).

## REFERENCES

- [1] UNITED NATIONS, Sources and Effects of Ionizing Radiation (Report to the General Assembly), Volume I, Scientific Committee on the Effects of Atomic Radiation (UNSCEAR), UN, New York (2000).
- [2] WHITE, C.A., BERLFEIN, J.R., GRILLO-LOPEZ, A.J., Antibody-targeted immunotherapy for treatment of non-Hodgkin's lymphoma, *Curr. Pharm. Biotechnol.* **1** (2000) 303–312.
- [3] BREITZ, H., Dosimetry in a myeloablative setting, *Cancer Biother. Radiopharm.* **17** (2002) 119–128.
- [4] SIEGEL, J.A., et al., MIRD pamphlet no. 16: Techniques for quantitative radio-pharmaceutical biodistribution data acquisition and analysis for use in human radiation dose estimates, *J. Nucl. Med.* **40** (1999) 37S–61S.
- [5] KING, M., FARNCOMBE, T., An overview of attenuation and scatter correction of planar and SPECT data for dosimetry studies, *Cancer Biother. Radiopharm.* (in press).

- [6] FOSTER, D., BARRETT, P., "Developing and testing integrated multicompart-ment models to describe a single-input multiple-output study using the SAAM II software system", Sixth International Radiopharmaceutical Dosimetry Symposium (Proc. Symp. Gatlinburg, TN, 1999), Oak Ridge Associated Universities, TN (1999).
- [7] INTERNATIONAL COMMISSION OF RADIATION UNITS AND MEASUREMENTS, Radiation Quantities and Units, Rep. 33, ICRU, Bethesda, MD (1980).
- [8] INTERNATIONAL COMMISSION ON RADIOLOGICAL PROTECTION, Limits for Intakes of Radionuclides by Workers, Publication 30, Pergamon Press, Oxford and New York (1979).
- [9] INTERNATIONAL COMMISSION ON RADIOLOGICAL PROTECTION, 1990 Recommendations of the International Commission on Radiological Protection, Publication 60, Pergamon Press, Oxford and New York (1991).
- [10] LOEVINGER, R., BUDINGER, T., WATSON, E., MIRD Primer for Absorbed Dose Calculations, Society of Nuclear Medicine, Reston, VA (1988).
- [11] STABIN, M., MIRDOSE — The personal computer software for use in internal dose assessment in nuclear medicine, *J. Nucl. Med.* **37** (1996) 538–546.
- [12] STABIN, M.G., SPARKS, R.B., MIRDOSE4 does not exist, *J. Nucl. Med.* **40** (1999) 309P.
- [13] STABIN, M.G., et al., RADAR — The radiation dose assessment resource. An online source of dose information for nuclear medicine and occupational radiation safety, *J. Nucl. Med., Suppl.* **42** (2001) 243P.
- [14] CRISTY, M., ECKERMAN, K., Specific Absorbed Fractions of Energy at Various Ages from Internal Photon Sources, Rep. ORNL/TM-8381, V1–V7, Oak Ridge Natl Lab., TN (1987).
- [15] SGOUROS, G., et al., Three-dimensional dosimetry for radioimmunotherapy treatment planning, *J. Nucl. Med.* **34** (1993) 1595–1601.
- [16] JONSSON, L., LJUNDBERG, M., SJOGREEN, K., STRAND, S.E., The conjugate view method: Evaluation of activity and absorbed dose calculations from Monte Carlo simulated scintillation camera images using experimental data in an anthropomorphic phantom, *J. Nucl. Med., Suppl.* **41** (2000) 234P.
- [17] GUY, M.J., FLUX, G.G., PAPAVALSILEIOU, P., FLOWER, M.A., OTT, R.J., "RMDP-MC: A dedicated package for I-131 SPECT quantification, registration, patient-specific dosimetry and Monte-Carlo", Seventh International Radiopharmaceutical Dosimetry Symposium (Proc. Int. Symp. Nashville, TN, 2002), Oak Ridge Associated Universities, TN (2002).
- [18] GARDIN, I., et al., "VoxelDose: A computer program for 3D dose calculation in therapeutic nuclear medicine", Seventh International Radiopharmaceutical Dosimetry Symposium (Proc. Int. Symp. Nashville, TN, 2002), Oak Ridge Associated Universities, TN (2002).
- [19] YORIYAZ, H., STABIN, M.G., DOS SANTOS, A., Monte Carlo MCNP-4B-based absorbed dose distribution estimates for patient-specific dosimetry, *J. Nucl. Med.* **42** (2001) 662–669.

- [20] ZUBAL, I.G., et al., Computerized 3-dimensional segmented human anatomy, *Med. Phys.* **21** (1994) 299–302.
- [21] SIEGEL, J.A., et al., Red marrow radiation dose adjustment using plasma FLT3-L cytokine levels: Improved correlations between hematologic toxicity and bone marrow dose for radioimmunotherapy patients, *J. Nucl. Med.* **44** (2003) 67–76.
- [22] JONARD, P., et al., Tumor dosimetry based on PET 90Y-DOTA-Tyr-Octreotide (SMT487) and CT scan predicts tumor response to 90Y-SMT487 (Octreother), *J. Nucl. Med.* **41** (2000) 111P (abstract).

**BLANK**

# **QUALITY ASSURANCE PROGRAMMES FOR RADIOACTIVITY MEASUREMENTS IN NUCLEAR MEDICINE**

**B.E. ZIMMERMAN**

Ionizing Radiation Division,

Physics Laboratory, National Institute of Standards and Technology,

Gaithersburg, Maryland, United States of America

E-mail: bez@nist.gov

## **Abstract**

Accurate radioactivity measurements in the clinic are vital for ensuring that administered doses of radiopharmaceuticals are safe and effective. This accuracy is achieved both in the development phase of the drug and in its clinical application, when the instrumentation used is calibrated in a way that is traceable to national or international standards. For nearly 30 years the National Institute of Standards and Technology has maintained a dedicated programme aimed at developing and distributing reference sources and providing calibration services to the nuclear medicine community in North America. The result has been an overall improvement in measurement protocols by isotope producers and radiopharmaceutical manufacturers. The current emphasis of the programme is the development of secondary standards that can be used to enable a similar improvement in measurements in the clinic. The paper discusses the need for radioactivity standards in nuclear medicine and provides a review of this programme.

## **1. INTRODUCTION: THE NEED FOR STANDARDS AND TRACEABILITY**

The accuracy of radioactivity measurements in nuclear medicine is a primary determinant of the safety and efficacy of radionuclide based therapy. Dose estimates for radiopharmaceuticals are based on calculational models that use biodistribution information to predict the uptake of the drug, as well as radiation transport codes that predict the amount of absorbed radiation from the decaying radioactive component. Most of these Monte Carlo radiation transport codes express the calculated dose in terms of a dose per initial source particle (Gy/particle). Confirmation of the doses predicted from these transport codes can often be made by comparing the results of the calculations with experimental dosimetry and radioactivity measurements, and are expressed in units of Gy/s and Bq (decays/s), respectively.

The relationship between Monte Carlo calculations and experimental measurements is depicted in Fig. 1. The number of particles per decay having a particular energy is determined from the nuclear decay scheme and atomic data (in the case of X rays and Auger electrons); therefore, these values must be well determined in order to have the correct input energy spectrum for the theoretical calculations. In most cases the radioactivity component of this type of analysis is the one that is available with the best accuracy and precision, since the current state of technology for experimental dosimetry limits the uncertainty on such measurements to several times the uncertainty on the radioactivity determinations. Variability in the assumed biodistribution can also limit the accuracy of this analysis. However, accurate knowledge of the activity can reduce the overall uncertainty in the analysis.

In clinical practice the amount of the drug that is to be given to the patient is expressed in terms of the amount of radioactivity to be injected, and not the dose rate. It is therefore imperative to make an accurate assessment of the amount of radioactivity contained in the drug prior to its administration. This is most often done in the radiopharmacy using re-entrant ionization chambers, known as 'dose' or 'radionuclide' calibrators. While these instruments are, in principle, very simple to use, they require the instrument to be correctly calibrated. The electric current observed in the chamber as a result of the interaction of the chamber gas and the radiation emitted from the radioactive drug is related to the amount of activity present, and is different

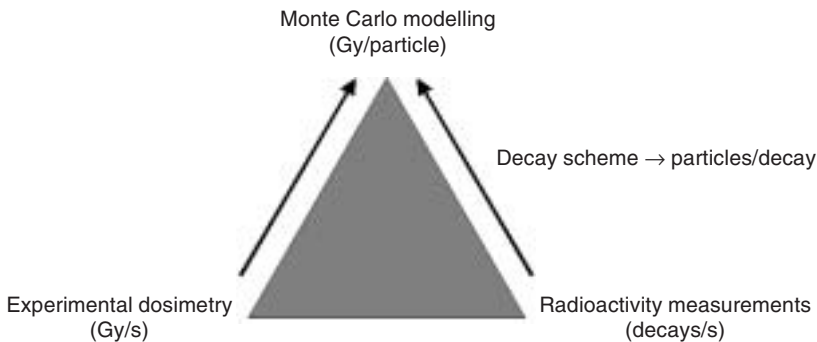


FIG. 1. Relationship between Monte Carlo modelling results (in units of Gy/particle), experimental dosimetry measurements (in Gy/s) and radioactivity measurements (in Bq or decays/s). The conversion between decays/s and particles/s is made through knowledge of the decay scheme. Only through the combination of accurate dosimetry and radioactivity measurements can modelling results be compared with experimental results.



for each radionuclide, being dependent upon the decay scheme. The conversion factor relating the observed current to an activity for the nuclide being measured is only accurate if a standard of that radionuclide is used in performing the calibration.

Finally, radioactivity standards also play an important role in the development of new radiopharmaceuticals. The consistency of dose estimates among a group of sites participating in clinical trials can only be ensured when the activity measurements are made in such a way as to be traceable to a single reference point. This is particularly important for multicentre trials, in which clinical sites in different locations (sometimes in different countries), using different types of instrument (from various manufacturers), make activity measurements that ultimately must be compared in order to draw conclusions about efficacy. The only way to ensure this is for each detection device used in the study to be calibrated using appropriate standards.

The Radioactivity Group of the National Institute of Standards and Technology (NIST) has an extremely active programme aimed at ensuring good radioactivity measurements at all levels of nuclear medicine practice in North America, and is the only national metrology institute to have a programme specifically aimed at the development of standards for medicine. This is done through an integrated programme that includes the continuous development of standards for new radionuclides under investigation for nuclear medicine applications, the development of secondary and transfer standards that allow clinical measurements to be made in such a way as to be directly traceable to those made at NIST, on-demand calibration services and a quality assurance programme that establishes NIST traceability for radiopharmaceutical manufacturers and isotope producers.

The relationship between NIST measurements and traceability from the various parts of the nuclear medicine community is depicted in Fig. 2. Typically, direct traceability is achieved only at the manufacturing and radiopharmacy levels since, in those instances, measurements are made directly against NIST calibrated sources. Secondary traceability for measurements can often be found in the radiopharmacy and clinic, but this requires that an unbroken chain of measurements exists back to NIST, which is often difficult to maintain. For example, if the radiopharmacy having direct traceability to NIST distributes a calibration source of a radionuclide in a syringe, and the clinic uses that same source to calibrate its instrumentation, then a direct link exists from the clinic back to NIST, and the calibration would be traceable for that radionuclide. If, however, the calibrated solution was shipped from the same radiopharmacy in a dose vial and the solution was taken up into a syringe at the clinic, the measurement of the amount of activity in the syringe is no longer traceable, since there is no direct comparison of the syringe back to its source.

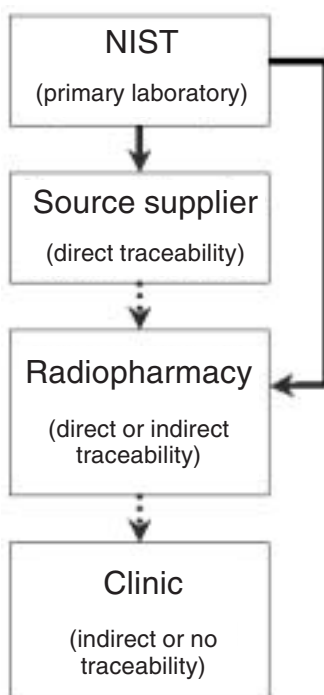


FIG. 2. Pathways for measurement traceability from different parts of the nuclear medicine community back to national standards (NIST). Solid arrows indicate pathways having direct traceability, while dotted arrows indicate possible pathways of secondary traceability.

## 2. MEASUREMENT QUALITY ASSURANCE FOR THE RADIOPHARMACEUTICAL INDUSTRY

An important aspect of the entire programme is the fact that all its functions are a response to issues raised during close interactions with researchers, manufacturers, radiopharmacies and clinical workers. Most of the research projects conducted as part of the overall programme were initiated at the request of the user community. Additionally, the Measurement Assurance Programme (MAP) was formed as a direct result of the need of radiopharmaceutical manufacturers and isotope suppliers to have a third party mediate in measurement disputes. The aim now is to establish good measurement practice so that conflicts do not arise.

The cornerstone of the overall nuclear medicine standards programme at NIST is the NIST/Nuclear Energy Institute MAP, which focuses on performance

based testing of the primary producers of radiopharmaceuticals and radioisotopes. The participants are most of the isotope suppliers, commercial radiopharmacies and radiopharmaceutical manufacturers in North America. Ten times per year (once per month for 10 months), solutions of a single radionuclide are calibrated for radioactivity content and distributed as blind samples to the participants, who perform activity measurements exactly as would normally be done in their facility and report the values back to NIST. The participants' results are compared to the NIST calibrated activity value and a Certificate of Traceability is issued to document the degree to which the measurements are traceable to NIST. Should any problems be evident in the measurement results, NIST and the participant work together to attempt to resolve the issues and will often attempt a second measurement trial.

The nuclides to be distributed are decided upon by the participants in the MAP, and this generally reflects the primary nuclides of interest to their respective institutions or companies. This, in turn, is indicative of the trends for radionuclide use in nuclear medicine in North America. The current distribution schedule, which is shown in Table I, has remained essentially unchanged since 1998. Only participants in the programme are entitled to receive the high level solutions as blind samples for the purposes of establishing traceability. The low level solutions are available for purchase by non-participating clinics, universities and companies, but they are distributed only as Standard Reference Materials (SRMs) with a certified activity value for use in calibrating instrumentation. The use of these SRMs does not establish traceability for the user for the purposes of regulatory compliance, but does provide a means for users to calibrate their instruments with NIST standard sources.

During the two months in which there is no radionuclide scheduled for distribution, participants have the option of submitting samples of any previously standardized radionuclide for calibration by NIST. This provides opportunities not only to receive calibrated solutions for the nuclides included in the normal yearly distribution, but also to receive more than a single SRM for a particular nuclide during the year.

Since its inception, the primary goal of the MAP has been to establish and maintain good measurement practice in nuclear medicine at the manufacturing level. By conducting yearly performance tests for a particular radionuclide and repeating this for a number of nuclides, manufacturers obtain continuous feedback on the state of their measurement capabilities. This is an important part of the documentation required to demonstrate compliance with various government regulations. Figure 3 shows a histogram of all the measurement results for  $^{131}\text{I}$  that have been submitted by participants over the more than 25 years that this nuclide has been distributed. The bulk of the results were found to be within 5% of the NIST calibrated value, which is well within the regulatory

TABLE I. CURRENT DISTRIBUTION SCHEDULE FOR CALIBRATED SOLUTIONS OF RADIONUCLIDES FROM THE NIST/NUCLEAR ENERGY INSTITUTE MAP

Month	Radionuclide	Nominal activity in 5 mL (high level)	Nominal activity in 5 mL (low level)
January	<sup>131</sup> I	750 MBq	25 MBq
February	<sup>99</sup> Mo	3 GBq	75 MBq
March	<sup>133</sup> Xe	7.5 GBq	750 MBq
April	<sup>67</sup> Ga	375 MBq	20 MBq
May	Open	—	—
June	<sup>201</sup> Tl	225 MBq	35 MBq
July	<sup>153</sup> Sm	375 MBq	20 MBq
August	<sup>111</sup> In	375 MBq	20 MBq
September	<sup>99m</sup> Tc	7.5 GBq	—
October	<sup>125</sup> I	750 MBq	6 MBq
November	Open	—	—
December	<sup>90</sup> Y	200 MBq	20 MBq

**Note:** Solutions with high level activities are only available to MAP participants, while the lower level solutions are available to non-participating organizations. During the months denoted ‘Open’, participants can submit samples of any previously standardized radionuclide for calibration.

limit of 10%. In fact, most of the results outside the 5% limits are from the early days of the MAP, before the measurement processes used by the participants were brought under control. Today, most of the submitted results are within 2–3% of the NIST value.

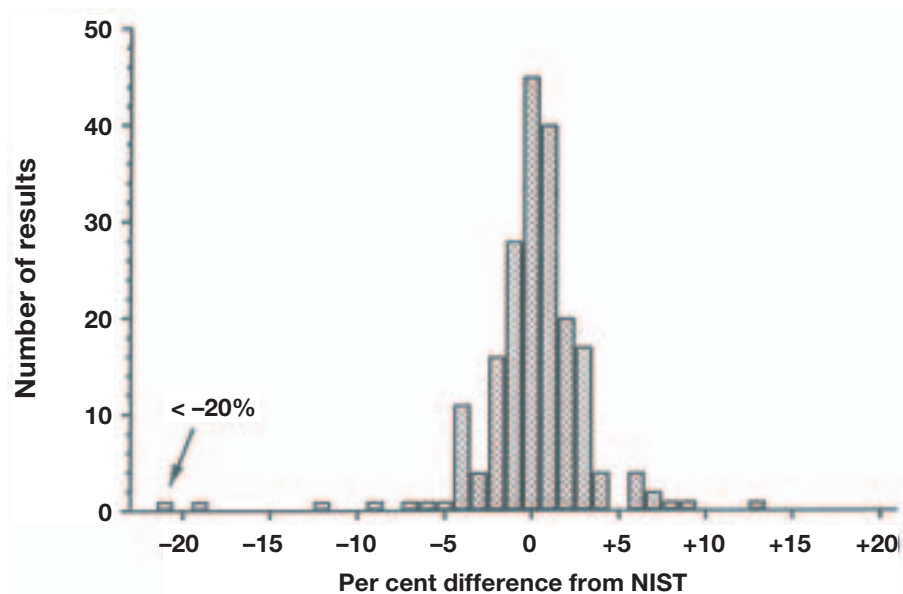


FIG. 3. Histogram of differences between participants' reported activity measurement results and NIST calibrated activity values for distributions of  $^{131}\text{I}$  from 1975 to 2001. Measurements were carried out as part of the NIST/Nuclear Energy Institute MAP for radiopharmaceuticals.

### 3. DEVELOPMENT OF RADIOACTIVITY STANDARDS FOR NUCLEAR MEDICINE

Another important part of the nuclear medicine quality assurance programme at NIST centres around providing standards for new radionuclides being considered for use in nuclear medicine. This includes the standardization of an ever growing list of radionuclides of interest for both therapy and diagnosis. Performing a primary standardization for a new radionuclide is a time and labour intensive undertaking, requiring a large number of measurements on many samples in order not only to determine accurately the amount of radioactivity in the sample being standardized but also to understand and characterize the uncertainties involved in the measurement process. A typical experimental scheme for a primary standardization is depicted in Fig. 4. Primary standardizations have recently been performed by NIST on such radionuclides as  $^{188}\text{W}$  (in equilibrium with  $^{188}\text{Re}$ ) [1],  $^{177}\text{Lu}$  [2],  $^{62}\text{Cu}$  [3] and

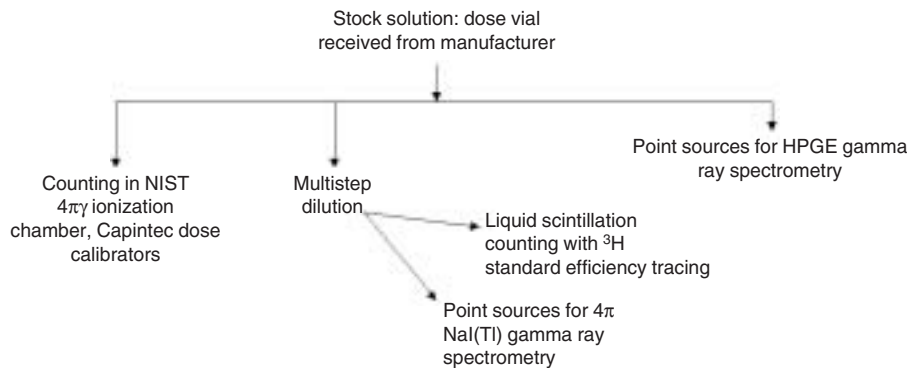


FIG. 4. Generalized source preparation scheme for a typical primary standardization of a radionuclide by LSC. Primary activity measurements are carried out by LSC and confirmatory activity measurements are made with  $4\pi\gamma$  ray spectrometry. Radionuclidic impurities are identified and quantified by high resolution gamma ray spectrometry. Primary measurements are transferred to secondary measurement systems (ionization chambers) to permit rapid measurements for future calibrations.

$^{177\text{m}}\text{Sn}$  [4]. Experiments are currently in progress to standardize the alpha emitter  $^{211}\text{At}$ .

The first step in the development of a new standard is the accurate measurement of the activity concentration, also known as the massic activity (in units of Bq/g), of a solution containing the radionuclide of interest. Because most radionuclides currently in use in nuclear medicine are beta emitters, the preferred method for making activity measurements is liquid scintillation counting (LSC). This method provides extremely high detection efficiencies (of the order of 95–99%) for nuclides with beta endpoint energies above a few hundred keV and requires relatively simple sample preparation.

Despite the advantage that LSC has over techniques for measuring beta emitters, it is always desirable to perform activity measurements with more than a single technique; techniques that measure different types of radiation should preferably be employed. For example, LSC might be the primary detection technique for measuring a beta emitting radionuclide such as  $^{166}\text{Ho}$ , but confirmatory activity measurements should also be carried out using gamma ray spectrometry, taking advantage of the fact that this radionuclide also emits a number of gamma rays in its decay. By obtaining the same measurement result with two or more different independent techniques measuring different types of radiation, there can be reasonable assurance that the result is correct.

Another consideration when performing a standardization is the presence of radionuclidic impurities. Because the radiations emitted by decaying impurities can interfere with the measurement of the nuclide of interest, it is

imperative that the solution being measured be as free from these interferences as possible. In some cases it may even be necessary to chemically remove some of the impurities prior to measurement. In the case of most solutions prepared for use in nuclear medicine, the impurities have already been removed in preparation for use as a drug product and are, therefore, less of a concern. Despite the best efforts to completely remove impurities, they are often present in small amounts and must be quantified so that the appropriate corrections can be made. Since most radionuclides emit some sort of photon radiation, they can be identified and quantified using high purity germanium detectors calibrated for energy and efficiency.

Once the solution has been calibrated for massic activity, gravimetrically related sources are prepared for measurement in the NIST  $4\pi\gamma$  ionization chamber. The result of these measurements will be a calibration factor for the ionization chamber that will allow subsequent measurements of solutions of that radionuclide to be made in that instrument. This is generally referred to as a secondary standard. Although LSC is a very accurate and relatively simple technique for measuring activity, counting times and the amount of time required for data reduction and analysis can be somewhat long. Measurements in the ionization chamber are quick and require minimal data analysis, resulting in much more rapid results and higher measurement throughput.

#### 4. DEVELOPMENT OF TRANSFER STANDARDS FOR CLINICAL MEASUREMENTS

In addition to the development of the primary standards mostly of interest to metrology laboratories, there is a strong effort in the programme to develop ways to make the primary measurements relevant in a clinical, manufacturing or research setting. This involves the derivation of calibration factors for the commercially available instrumentation, such as re-entrant ionization chambers (dose calibrators), currently used in many hospitals and clinics around the world. Because these devices respond only to photon radiation, the measurement of radionuclides whose decay schemes involve low energy gamma or X ray emissions (such as  $^{125}\text{I}$ ,  $^{166}\text{Ho}$ ,  $^{186}\text{Re}$  and  $^{177}\text{Lu}$ ) or which are pure beta emitters (which produce photons in the form of bremsstrahlung) can be very sensitive to any changes in the measurement geometry, which can: (a) vary the attenuation of the radiation of the source; (b) alter the spectrum of the emitted radiation, especially the bremsstrahlung; and/or (c) change the response of the measuring instrument to the source radiation. Such changes in the geometry that can cause this type of effect are differences in solution density, differences in container material and configuration, the filling volume of

solution in the container and the position of the container in the measuring instrument.

Since the activity measurements can be sensitive to these types of measurement variables, it is necessary to derive the calibration factor for the exact geometry in which the radionuclide will be measured in the clinic, or at the very least determine the correction factors needed to obtain the correct activity value using a single calibration factor. Normally standards are developed at NIST in a single, standard geometry, which is 5 mL of solution in a 5 mL thin walled flame-sealed glass ampoule. Several instrument manufacturers have also adopted the same geometry in determining calibration factors for different radionuclides using their instruments. However, this type of container does not have much practical use in a clinical or manufacturing setting. For this reason, the main focus of research for the programme during the past five years has involved the determination of calibration factors for nuclides such as  $^{90}\text{Y}$ ,  $^{125}\text{I}$  [5],  $^{186}\text{Re}$  [6],  $^{188}\text{Re}$  [7] and  $^{166}\text{Ho}$  in various geometries, including syringes and dose vials, for a variety of commercially available re-entrant ionization chambers.

## 5. CONCLUSION

The quality of radioactivity measurements made in the clinic and in the manufacturing sector plays a vital role in the quality of care received by the patient. The administration of accurate doses of established radiopharmaceuticals depends on having measurement instruments calibrated against standardized sources. Moreover, the determination of correction factors appropriate for measurement geometries other than those in which the original calibration factor was derived makes it possible to make measurements in those geometries in ways that can still be related to existing standards. NIST has an active programme aimed at improving measurement quality assurance in nuclear medicine at all levels: isotope producer, radiopharmaceutical manufacturer, researcher and clinical user. This is accomplished by the continuous development of standards for the radionuclides being considered for use in nuclear medicine applications, as well as the implementation of a quality assurance programme for the industrial sector. By maintaining strong interactions with the nuclear medicine community, the requirements for standards and calibrations can be anticipated and established when they are needed.



## REFERENCES

- [1] ZIMMERMAN, B.E., CESSNA, J.T., UNTERWEGER, M.P., The standardization of  $^{188}\text{W}/^{188}\text{Re}$  by  $4\pi\beta$  liquid scintillation spectrometry with the CIEMAT/NIST  $^3\text{H}$ -standard efficiency tracing method, *Appl. Radiat. Isot.* **56** (2002) 315–320.
- [2] ZIMMERMAN, B.E., UNTERWEGER, M.P., BRODACK, J.W., The standardization of  $^{177}\text{Lu}$  by  $4\pi\beta$  liquid scintillation spectrometry with  $^3\text{H}$ -standard efficiency tracing, *Appl. Radiat. Isot.* **54** (2001) 623–631.
- [3] ZIMMERMAN, B.E., CESSNA, J.T., The standardization of  $^{62}\text{Cu}$  and experimental determinations of dose calibrator settings for generator-produced  $^{62}\text{CuPTSM}$ , *Appl. Radiat. Isot.* **51** (1999) 515–526.
- [4] ZIMMERMAN, B.E., CESSNA, J.T., SCHIMA, F.J., The standardization of the potential bone palliation radiopharmaceutical  $^{117\text{m}}\text{Sn}(+4)\text{DTPA}$ , *Appl. Radiat. Isot.* **49** (1998) 317–328.
- [5] ZIMMERMAN, B.E., CESSNA, J.T., DORTON, J.A., Experimental investigation of dose calibrator response for  $^{125}\text{I}$  brachytherapy solutions contained in 5 ml plastic syringes and 2 ml conical glass v-vials as a function of filling mass, *Med. Phys.* **29** (2002) 1547–1455.
- [6] ZIMMERMAN, B.E., PIPES, D.W., Experimental determination of dose calibrator settings and study of associated volume dependence in v-vials for solution sources of  $^{186}\text{Re}$  perrhenate, *J. Nucl. Med. Technol.* **28** (2000) 264–270.
- [7] ZIMMERMAN, B.E., et al., A new experimental determination of the dose calibrator setting for  $^{188}\text{Re}$ , *J. Nucl. Med.* **40** (1999) 1508–1516.

**BLANK**

# MONTE CARLO TECHNIQUES IN DIAGNOSTIC AND THERAPEUTIC NUCLEAR MEDICINE

H. ZAIDI

Division of Nuclear Medicine, Geneva University Hospital,  
Geneva, Switzerland

E-mail: Habib.Zaidi@hcuge.ch

## Abstract

The use of the Monte Carlo method to simulate radiation transport has become the most accurate means of predicting absorbed dose distributions and other quantities of interest in radiation treatments of cancer patients using either external or radionuclide radiotherapy. This trend has continued for the estimation of absorbed dose in diagnostic procedures using radionuclides as well as for the assessment of image quality and the quantitative accuracy of radionuclide imaging. As a consequence of this generalized use, many questions are being raised, primarily about the need for and potential of Monte Carlo techniques, but also about how accurate they really are and what it would take to apply them clinically and to make them available widely to the nuclear medicine community at large. Many of these questions will be answered when Monte Carlo techniques are implemented and used for more routine calculations and for in-depth investigations. The conceptual role of the Monte Carlo method is briefly introduced in the paper, followed by a survey of its different applications in diagnostic and therapeutic nuclear medicine. Please note that, due to limited space, the references contained herein are for illustrative purposes and are not inclusive; no implication that those chosen are better than others not mentioned is intended.

## 1. CONCEPTUAL ROLE OF MONTE CARLO SIMULATIONS

The Monte Carlo method describes a very broad area of science, in which many processes, physical systems and phenomena are simulated by statistical methods employing random numbers. The general idea of Monte Carlo analysis is to create a model as similar as possible to the real physical system of interest and to create interactions within that system based on known probabilities of occurrence, with random sampling of the probability density functions (PDFs). As the number of individual events (called histories) is increased, the quality of the reported average behaviour of the system improves, meaning that the statistical uncertainty decreases. Almost any complex system can in principle be modelled; perhaps there is a desire to model the number of cars passing a particular intersection during certain times of the day, to optimize traffic

management, or to model the number of people that will make transactions in a bank, to evaluate the advantages of different queuing systems. If the distribution of events that occur in a system is known from experience, a PDF can be generated and sampled randomly to simulate the real system. A detailed description of the general principles of the Monte Carlo method is given in Refs [1, 2].

In the specific application of interest in this paper, the transport of ionizing radiation particles is simulated by the creation of particles or rays from a defined source region, generally with a random initial orientation in space, with tracking of the particles as they travel through the system, sampling the probability PDFs for their interactions to evaluate their trajectories and energy deposition at different points in the system. The interactions determine the penetration and motion of particles, but, more importantly, the energy deposited during each interaction gives the radiation absorbed dose, when divided by the appropriate values of mass. With sufficient numbers of interactions the mean absorbed dose at points of interest will be given with acceptable uncertainties. The central issues include how well the real system of interest can be simulated by a geometrical model, how many histories (i.e. how much computer time) are needed to obtain acceptable uncertainties (usually around 5%, no more than 10%) and how can measured data be used to validate theoretical calculations.

Monte Carlo techniques have become one of the most popular tools in different areas of medical physics, following the development and subsequent implementation of powerful computing systems for clinical use [3]. In particular, they have been extensively applied to simulate processes involving random behaviour and to quantify physical parameters that are difficult or even impossible to calculate analytically or to determine by experimental measurements. The applications of the Monte Carlo method in medical physics cover almost all topics, including radiation protection, diagnostic radiology, radiotherapy and nuclear medicine, with an increasing interest in exotic and new applications such as intravascular radiation therapy, boron neutron capture therapy and synovectomy. With the rapid development of computer technology, Monte Carlo based treatment planning for radiation therapy is becoming practicable.

This paper briefly reviews the conceptual role of the Monte Carlo method and summarizes its application in diagnostic and therapeutic nuclear medicine. Emphasis is given to applications in which photon and/or electron transport in matter is simulated. The historical developments and computational aspects of the Monte Carlo method, mainly related to random number generation, sampling and variance reduction, together with a description of widely used Monte

Carlo codes in diagnostic and therapeutic nuclear medicine, fall outside the scope of this paper and are discussed elsewhere [1–4].

## 2. DEVELOPMENT OF ANTHROPOMORPHIC MATHEMATICAL AND VOXEL BASED PHANTOMS

Computerized anthropomorphic phantoms can be defined either by mathematical (analytical) functions or digital (voxel based) volume arrays [4]. Analytic phantoms consist of regularly shaped continuous objects defined by combinations of simple mathematical geometries, whereas voxel based phantoms are mainly derived from segmented tomographic images of the human anatomy obtained by either X ray computed tomography (CT) or magnetic resonance imaging (MRI). Any complex activity and corresponding attenuation distributions can therefore be modelled. Analytical phantoms, however, have the advantage of being able to model anatomical variability and dynamic organs easily. The mathematical specifications for phantoms that are available assume a specific age, height and weight. People, however, exhibit a variety of shapes and sizes.

The first breakthrough in the use of Monte Carlo techniques was the development of the Fisher-Snyder heterogeneous, hermaphrodite, anthropomorphic model of the human body in the 1970s [5]. This phantom consisted of spheres, ellipsoids, cones, tori and subsections of such objects, combined to approximate the geometry of the body and its internal structures. The representation of internal organs with this mathematical phantom is very crude, since the simple equations can only capture the most general description of an organ's position and geometry. The original phantom developed was intended mainly to represent a healthy average adult male, which well characterized the working population of its time. The phantom did have both male and female organs, but most structures represented the organs of Reference Man, as defined by the International Commission on Radiological Protection (ICRP) from an extensive review of medical and other literature, restricted primarily to European and North American populations. Both due to the makeup of the nuclear medicine population and the diversifying worker population, the need for other phantoms arose.

In 1987 Cristy and Eckerman [6] of the Oak Ridge National Laboratory (ORNL) developed a series of phantoms representing children of different ages, one of which (the 15 year old) also served as a model for the adult female. Bouchet and Bolch [7] developed a series of five dosimetric head and brain models to allow more precise dosimetry in paediatric neuroimaging procedures. More recently, a new rectal model and a dynamic urinary bladder

model have also been proposed. To develop more patient specific dosimetry, new mathematical models for adults of different height have been developed using anthropometric data. Mathematical anthropomorphic phantoms are continuously being improved. Recent three and four dimensional computer phantoms seek a compromise between ease of use, flexibility and the accurate modelling of populations of patient anatomies, and attenuation and scatter properties as well as biodistributions of radiopharmaceuticals in patients. Current developments are aimed at computer phantoms that are flexible while providing the accurate modelling of patient populations. The use of dynamic anthropomorphic phantoms in Monte Carlo simulations is becoming possible, owing to the increasing availability of computing power. This includes the development of appropriate primitives that allow the accurate modelling of anatomical variations and patient motion, such as superquadrics and non-uniform rational B spline surfaces [8].

Modelling for imaging and dosimetry applications is best done with phantom models that match the gross parameters of an individual patient. Anthropomorphic phantoms with internally segmented structures make clinically realistic Monte Carlo simulations possible. Zubal et al. [9] developed a typical anthropomorphic voxel based adult phantom by the manual segmentation of CT transverse slices of a living human male performed by medical experts. A computerized three dimensional (3-D) volume array modelling all the major internal structures of the body was then created. Each voxel of the volume contains an index number designating it as belonging to a given organ or internal structure. These indexes can then be used to assign a value, corresponding to, for example, density or activity. The phantom data are available as a  $128 \times 128 \times 246$  matrix with a cubic resolution of 4 mm. The same group has also developed a high resolution brain phantom based on an MRI scan of a human volunteer, which can be used for detailed investigations in the head. The torso phantom was further improved by copying the arms and legs from the Visible Human (VH) and attaching them to the original torso phantom. However, the arms of the VH were positioned over the abdominal part, which limited the usefulness of the phantom for simulations of whole body scanning. This problem was tackled by mathematically straightening the arms out along the phantom's side [10]. More recently, a new voxel based whole body model, called VIP-Man, has been developed using high resolution transversal colour photographic images obtained from the National Library of Medicine's VH Project [11]. A group at the National Research Center for Environment and Health (GSF) in Germany has also been developing some voxel based phantoms. The GSF voxel phantom family tends to cover persons of individual anatomy and includes at the moment two paediatric and five adult phantoms of both sexes, different ages and stature, and several others are under construction [12].

### 3. MONTE CARLO TECHNIQUES IN NUCLEAR MEDICINE DOSIMETRY

#### 3.1. Calculation of absorbed fractions

There is broad consensus in accepting that the earliest Monte Carlo calculations in medical physics were made in the area of nuclear medicine, for which the technique was used for dosimetry modelling and computations. Formalism and data based on Monte Carlo calculations, developed by the Medical Internal Radiation Dose (MIRD) Committee of the Society of Nuclear Medicine, have been published as pamphlets in a series of supplements to the Journal of Nuclear Medicine, the first one in 1968 [13]. Some of these pamphlets made extensive use of Monte Carlo calculations to derive specific absorbed fractions (AFs) for photon sources uniformly distributed in organs of mathematical phantoms. This was extended later to electrons [14], beta particles and positron emitters [15].

Monte Carlo calculations for photons were performed using a computer code called ALGAM, which created photons at random positions within any source region (organ or tissue), gave these photons a random orientation in  $4\pi$  space and then followed them through various Compton and photoelectric interactions (coherent scattering was neglected because of its low contribution to the total cross-section, and pair production events were quite rare, as starting energies did not exceed 4 MeV) until the photon reached a certain critical low cut-off energy and was assumed to be locally absorbed, or until it escaped the surface of the body (at which point the probability of scatter from an air molecule and redirection towards the body was assumed to be negligibly low). With repeated sampling of the source, which at this time generally involved only tens of thousands of trials (histories), a statistical average behaviour of particles originating in this source could be obtained for other regions of the body of interest to radiation dose assessment (target regions). This behaviour was reported as the fraction of energy emitted in the source that was absorbed in a target (AF), with an associated uncertainty (reported as the coefficient of variation). These AFs were thus a considerable improvement over the values given in ICRP Publication 2, as the organ geometries were more realistic, and, more importantly, the organs could irradiate each other, whereas in the ICRP 2 model an organ could irradiate only itself. These AFs were used later by the ICRP in updated assessments for workers; of more interest for this paper is that they found a more immediate application in dose assessments for nuclear medicine patients, owing to the monumental efforts of the newly formed MIRD Committee. In a flurry of publications in its early years, this committee published decay data, methods for kinetic analyses, the AFs from the ALGAM

calculations, dose conversion factors for over 100 nuclides of interest to nuclear medicine, dose calculations for various radiopharmaceuticals, methods for small scale dose calculations with electrons, and other interesting practical scientific documents. AFs for these phantoms were developed using the ALGAMP code (the P signifying a parameterized version of the code, allowing the substitution of parameters giving the radii and positions of the various organs at different ages). These values were published in an ORNL document, but never officially adopted in the MIRD or other peer reviewed literature. Nonetheless, they were widely accepted and used for dose calculations for individuals of different ages.

Previously calculated AFs for unit density spheres in an infinite unit density medium for photon and electron emitters have been recently re-evaluated using both the EGS4 and MCNP-4B Monte Carlo codes. Moreover, Stabin and Yoriyaz [16] used the MCNP-4B code to calculate AFs for photons in the voxel based phantom of Zubal et al. [9], and the results were compared with reference values from traditional MIRD and ORNL phantoms, while Chao and Xu [17] used the EGS4 code to estimate specific AFs from internal electron emitters for the VIP-Man model with energies from 100 keV to 4 MeV.

The application of the Monte Carlo method to internal radiation dosimetry is further emphasized in two recent MIRD pamphlets. In MIRD Pamphlet No. 15 [18] the EGS4 Monte Carlo radiation transport code was used to revise substantially the dosimetric model of the adult head and brain originally published in MIRD Pamphlet No. 5 [5]. Pamphlet No. 17 [19] demonstrates the utility of the MIRD formalism for the calculation of the non-uniform distribution of radiation absorbed dose in different organs through the use of radionuclide specific *S* values defined at the voxel level. Figure 1 shows absorbed fractions for monoenergetic photons (the source and target are confounded) calculated using the EGS4 Monte Carlo system as a function of voxel size.

### 3.2. Derivation of dose point kernels

In most cases Monte Carlo calculations are used to simulate the random distribution of sources or targets, whereas the actual dosimetric calculation is performed using so called dose point kernels. Such kernels, usually spherical and calculated for monoenergetic sources, describe the pattern of energy deposited at various radial distances from photon and electron or beta point sources. Dose point kernels can be calculated using analytical or Monte Carlo methods. Hybrid approaches (analytical calculations using Monte Carlo data) have also been considered to decrease the computation time [20]. Three Monte Carlo systems have mainly been used for this purpose, namely ETRAN, the



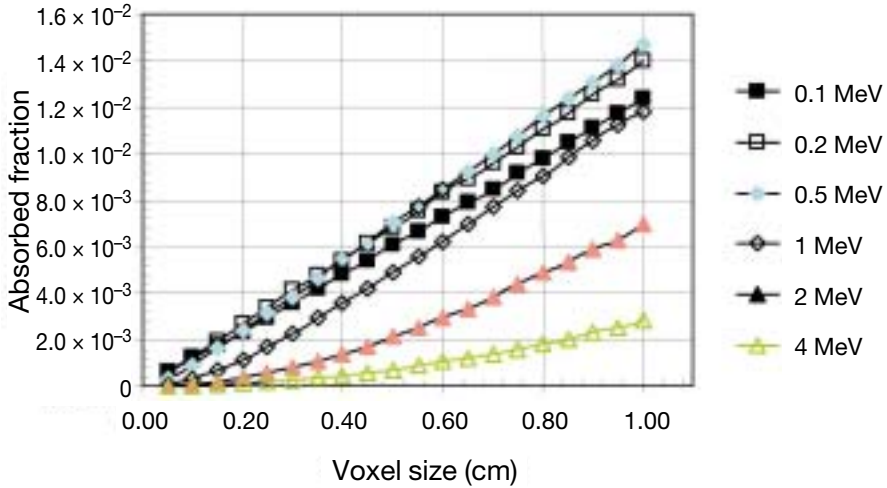


FIG. 1. AFs versus voxel size for monoenergetic photons (source = target) calculated using the EGS4 Monte Carlo system. Linear interpolation was used to estimate intermediate AFs between different voxel sizes (courtesy of L.G. Bouchet).

ACCEPT code of the ITS system and EGS4. Limitations and constraints of some of these codes have been reported in the literature; their impact on the calculated kernels is difficult to evaluate. ETRAN, for instance, had an incorrect sampling of the electron energy loss straggling, which has been corrected for in the ITS3 system (based on ETRAN). EGS4 did not include the accurate electron physics and transport algorithms, which have been incorporated in the recent EGSnrc system. Furhang et al. [21] generated photon point dose kernels and absorbed fractions in water for the full photon emission spectrum of the radionuclides of interest in nuclear medicine by simulating the transport of particles using Monte Carlo techniques. The kernels were then fitted to a mathematical expression.

A unified approach for photon and beta particle dosimetry has been proposed by Lechner [22] by fitting Berger's tables for photons and electrons to generate an empirical function that is valid for both photons and beta particles. Both point kernel and Monte Carlo techniques can therefore be effectively employed to calculate absorbed dose to tissue from radionuclides that emit photons or electrons. The latter are computationally much more intensive; however, point kernel methods are restricted to homogeneous tissue regions that can be mathematically described by analytical geometries, whereas Monte Carlo methods have the advantage of being able to accommodate heterogeneous tissue regions with complex geometric shapes.

### 3.3. Patient specific dosimetry and treatment planning

To perform real patient specific dose calculations, a patient specific physical model to be used with patient specific biokinetic data is required. Individual patients not only have significantly different uptake and retention half-lives of activity of the radioactive agent, but also have significantly different physical characteristics and radiosensitivities. If our goal is to optimize patient therapies, their individual parameters should be accounted for as much as possible during treatment planning. Currently, the preferred strategy with radiolabelled antibodies is to use personalized patient dosimetry, and this approach may become routinely employed clinically. The dose distribution pattern is often calculated by generalizing a point source dose distribution [23], but direct calculation by Monte Carlo techniques is also frequently reported, since it allows media of inhomogeneous density to be considered [24].

The development of a 3-D treatment planner based on nuclear imaging is an area of considerable research interest, and several dose calculation algorithms have been developed [2]. Figure 2 lists the essential steps required in developing a 3-D treatment planning program for radioimmunotherapy (RIT). Projection data acquired from an emission tomographic imaging system are processed to reconstruct transverse section images, which yields a count density map of source regions in the body. This count density is converted to an activity map using the sensitivity derived from a calibration phantom. In the final step this activity distribution is converted to a dose rate or dose map, either by convolving the activity distribution with dose point kernels or by direct Monte Carlo calculations. To elaborate a treatment plan for an individual patient, prospective dose estimates can be made by using the tracer activity of a radiolabelled antibody to obtain biodistribution information prior to the administration of a larger therapeutic activity. The clinical implementability of treatment planning algorithms will depend to a significant extent on the time required to generate absorbed dose estimates for a particular patient.

Many specially designed software packages have been developed for patient specific dosimetry and treatment planning. The MABDOSE and DOSE3D computer codes adapt the standard geometrical phantoms, allowing the placement of a single or multiple tumours in various locations to estimate dose contributions from these tumours to normal organs, but they do not at present use patient images. These codes work with stylized representations of average individuals, and give the average dose to whole organs. The RTDS code employs either the standard MIRDose phantom set or its own transport algorithms in a limited body space, based on voxel source kernels to produce average organ doses or dose distributions within specified organs or tissues of the body. More sophisticated approaches combine anatomical (CT or MRI) and

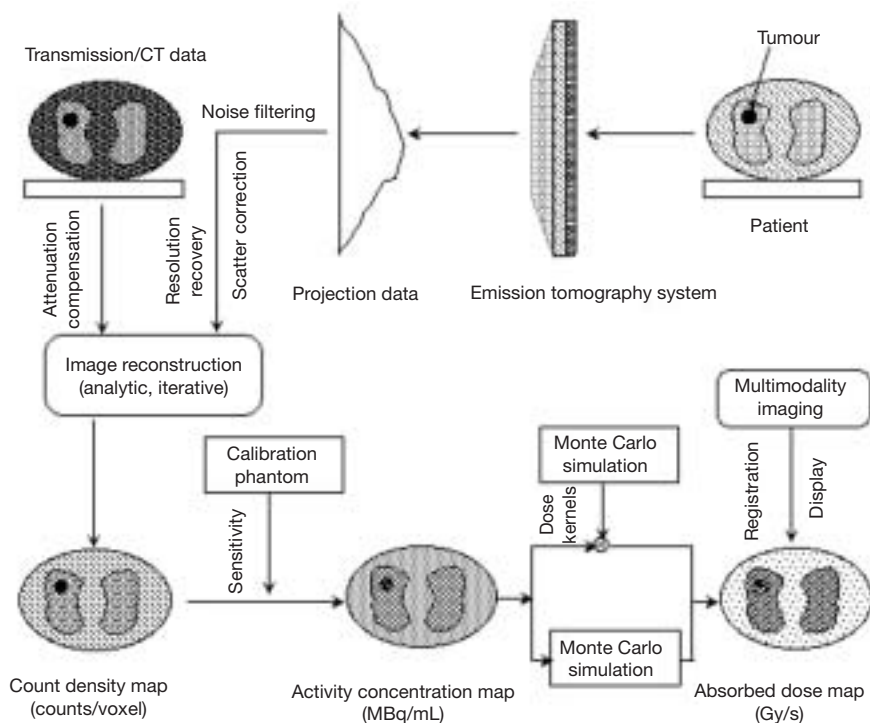


FIG. 2. Essential steps required in developing a 3-D internal dosimetry program for treatment planning with RIT based on quantitative nuclear medical imaging, for which Monte Carlo simulations play a crucial role.

functional radionuclide (single photon emission computed tomography (SPECT) and positron emission tomography (PET)) images to compute patient specific absorbed dose distributions and dose–volume histograms similar to the treatment planning programs used in external beam radiotherapy. Several software packages have been devised and validated by different research groups, including the 3D-ID code, SIMDOS and its more recent version based on the EGS4 system, the RMDP package, and the SCMS code. A detailed description of some of these tools is provided in Ref. [2]. It is worth emphasizing that, with some exceptions, very few have been used in clinical environments.

#### 4. MONTE CARLO TECHNIQUES IN NUCLEAR MEDICINE IMAGING

There has been an enormous increase and interest in the use of Monte Carlo techniques in all aspects of nuclear imaging, including planar imaging,

SPECT, PET and multimodality imaging devices [1, 4]. However, due to computer limitations, the method has not yet fully lived up to its potential. With the advent of high speed supercomputers the field has received increased attention, particularly with parallel algorithms, which have much higher execution rates. Figure 3 illustrates the principles and main components of Monte Carlo or statistical simulation as applied to a cylindrical PET imaging system [25]. Assuming that the behaviour of the imaging system can be described by PDFs, the Monte Carlo simulation can proceed by sampling from these PDFs, which necessitates a fast and effective way to generate uniformly distributed random numbers. Photon emissions are generated within the phantom and are transported by sampling from PDFs through the scattering medium (transmission image) and detection system until they are absorbed or escape the volume of interest without hitting the crystal matrices. The outcomes of these random samplings, or trials, must be accumulated or tallied in an appropriate manner to produce the desired result, but the essential characteristic of the Monte Carlo method is the use of random sampling techniques to arrive at a solution of the physical problem.

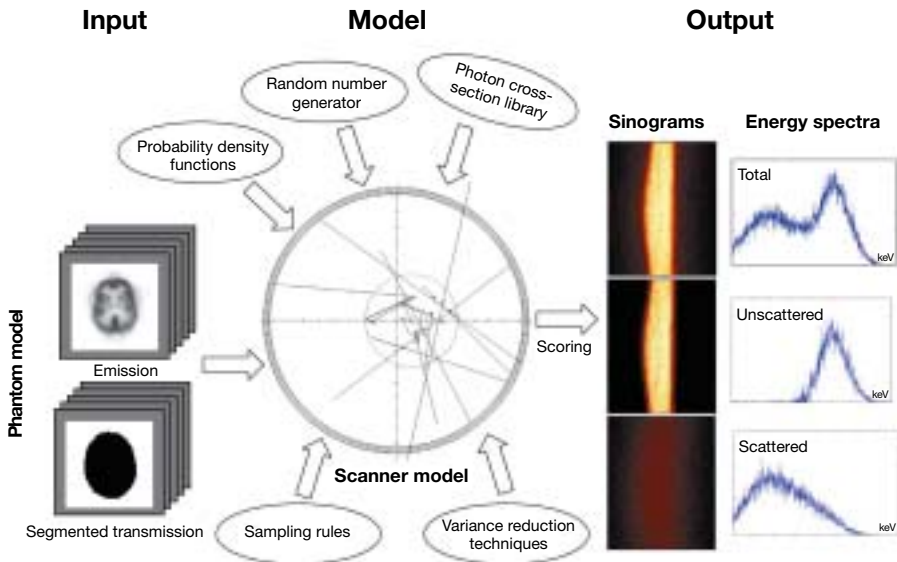


FIG. 3. Principles and main components of a Monte Carlo simulation environment for a cylindrical multiring PET imaging system.

#### 4.1. Applications in diagnostic nuclear medicine imaging

The Monte Carlo method is a widely used research tool for different areas of diagnostic nuclear imaging, such as detector modelling and systems design, image correction and reconstruction techniques, internal dosimetry and pharmacokinetic modelling. The method has proved to be very useful for solving complex problems that cannot be modelled by computer codes using deterministic methods, or when experimental measurements may be impracticable [4]. The design of SPECT and PET systems using the Monte Carlo method has received considerable attention, and a large number of applications were the result of such investigations. During the past two decades the simulation of scintillation camera imaging using both deterministic and Monte Carlo methods has been developed to assess qualitatively and quantitatively the image formation process and interpretation and to assist in the development of collimators. Several researchers have also used Monte Carlo simulation methods to study potential designs of dedicated small animal positron tomographs.

Another promising application of Monte Carlo calculations is the development and evaluation of image reconstruction algorithms and correction methods for photon attenuation and scattering in nuclear medicine imaging, since the user has the ability to separate the detected photons into their components: primary events, scatter events, contribution of downscatter events, etc. Monte Carlo modelling thus allows a detailed investigation of the spatial and energy distribution of Compton scatter, which would be difficult to perform using present experimental techniques, even with very good energy resolution detectors. A Monte Carlo study of the acceptance of scattered events in a depth encoding large aperture camera made of position encoding blocks modified to resolve the depth of interaction through a variation in the photopeak pulse height has been performed by Moison et al. [26]. The contribution of scatter from outside the field of view is a challenging issue, especially with the current large axial field of view 3-D PET scanners. Several researchers used Monte Carlo simulations to study scatter contribution from outside the field of view and the spatial characteristics of scatter for various phantoms. It was concluded that the spatial distribution of multiple scatter is quite different from the simple scatter component, which might preclude the rescaling of the latter to take into account the effect of the former for scatter correction purposes. Monte Carlo simulations have also been extensively used to evaluate and compare scatter correction schemes in both SPECT and PET [27]. The simulation of transmission scanning allowed the study of the effect of downscatter from the emission ( $^{99\text{m}}\text{Tc}$ ) photons into the transmission ( $^{153}\text{Gd}$ ) energy window in SPECT and the investigation of detected scattered photons in single photon transmission measurements using  $^{137}\text{Cs}$  single photon sources for PET [4].

Monte Carlo simulations have been shown to be very useful for the validation and comparative evaluation of image reconstruction techniques. Smith et al. [28] used Monte Carlo modelling to study photon detection kernels, which characterize the probabilities that photons emitted by radioisotopes in different parts of the source region will be detected at particular projection pixels of the projection images in the case of parallel hole collimators. The authors also proposed a reconstruction method using 3-D kernels, in which projection measurements in three adjacent planes are used simultaneously to estimate the source activity of the centre plane. The search for unified reconstruction algorithms led to the development of inverse Monte Carlo (IMC) reconstruction techniques. The principal merits of IMC are that, like direct Monte Carlo methods, the method can be applied to complex and multivariable problems, and variance reduction procedures can be applied. Floyd et al. [29] used IMC to perform tomographic reconstruction for SPECT with simultaneous compensation for attenuation, scatter and distance dependent collimator resolution. More recently, direct fully 3-D Monte Carlo based statistical reconstruction proved to be feasible within clinically acceptable computation times [30].

#### **4.2. Applications in therapeutic nuclear medicine imaging**

For internal radiation dose estimates, the biodistribution of a trace  $^{131}\text{I}$  labelled monoclonal antibody is generally used to predict the biodistribution of a high dose administration for therapy. Imaging therapeutic doses would further confirm the hypothesis that the biodistribution is similar; however, current generation scintillation cameras are unable to handle accurately the corresponding high counting rate. Monte Carlo calculations have been used in the development of a method for imaging therapeutic doses of  $^{131}\text{I}$  by using thick lead sheets placed on the front surface of a high energy parallel hole collimator [31]. Huili et al. [32] simulated point response functions for pinhole apertures with various aperture span angles, hole sizes and materials. The point responses have been parameterized using radially circular symmetric 2-D exponential functions, which can be incorporated into image reconstruction algorithms that compensate for the penetration effect. The effect of pinhole aperture design parameters on angle dependent sensitivity for high resolution pinhole imaging has been also investigated using Monte Carlo modelling.

The accuracy of  $^{131}\text{I}$  tumour quantification after RIT has been further investigated with an ultra-high energy collimator designed for imaging 511 keV photons. It has been shown that the difference in tumour size, relative to the size of a calibration sphere, has the biggest effect on accuracy, and recovery coefficients are needed to improve the quantification of small tumours.

Different strategies are being developed to improve image quality and quantitative accuracy in tumour SPECT imaging, including collimator detector response compensation and high energy scatter correction techniques. In a study by Dewaraja et al. [33], Monte Carlo simulations have been used to evaluate how object shape influences spill out and spill in, which are major sources of quantification errors associated with the poor spatial resolution of  $^{131}\text{I}$  SPECT, and to characterize energy and the spatial distributions of scatter and penetration.

## 5. FUTURE APPLICATIONS OF MONTE CARLO TECHNIQUES

On-line monitoring of the positron emitting activity created in patient tissues undergoing radiotherapy treatment has been a goal pursued by several investigators since the 1990s. Whereas the clinical application of on-line PET monitoring in photon radiotherapy has so far been limited by the reduced activity produced in a patient using today's clinical accelerators, its use in heavy particle radiotherapy has become a useful technique to visualize the  $\beta^+$  activity distributions that help to determine the effective range of heavy particles in the patient, as well as to evaluate blood flow in some organs. Several groups have reported the applicability of PET to in vivo dosimetry in radiotherapy treatments with photons, protons and light and heavy ions using different Monte Carlo codes to investigate this challenging field [34].

It is clear that a new generation of dose modelling tools needs to be developed for use with internal emitter therapy in nuclear medicine. It is unacceptable to use standardized, geometrical phantoms to perform dose calculations for individual patients if the physician is asking for meaningful information to be used in planning patient therapy. The evolution of the methodology followed for external beam radiotherapy treatment planning must be followed for internal emitter therapy. The technology now exists to develop patient specific 3-D dose distributions, based on a fusion of anatomical (CT or MRI) and functional (SPECT or PET) data, with individualized Monte Carlo calculations done in a reasonable amount of time using high powered computing workstations or distributed computing networks. The combination of realistic computer phantoms and accurate models of the imaging process allows the simulation of nuclear medicine data that are ever closer to actual patient data. Simulation techniques will find an increasingly important role in the future of nuclear medicine in light of the further development of realistic computer phantoms, the accurate modelling of projection data and computer hardware. However, caution must be taken to avoid errors in the simulation process, and verification via comparison with experimental and patient data is essential.



## REFERENCES

- [1] LJUNGBERG, M., STRAND, S.-E., KING, M.A. (Eds), Monte Carlo Calculations in Nuclear Medicine: Applications in Diagnostic Imaging, Institute of Physics Publishing, Bristol, UK (1998).
- [2] ZAIDI, H., SGOUROS, G. (Eds), Therapeutic Applications of Monte Carlo Calculations in Nuclear Medicine, Institute of Physics Publishing, Bristol, UK (2002).
- [3] ANDREO, A., Monte Carlo techniques in medical radiation physics, *Phys. Med. Biol.* **36** (1991) 861–920.
- [4] ZAIDI, H., Relevance of accurate Monte Carlo modeling in nuclear medical imaging, *Med. Phys.* **26** (1999) 574–608.
- [5] SNYDER, W., FORD, M.R., WARNER, G., Estimates of Specific Absorbed Fractions for Photon Sources Uniformly Distributed in Various Organs of a Heterogeneous Phantom, Pamphlet No. 5, revised, Society of Nuclear Medicine, New York (1978).
- [6] CRISTY, M., ECKERMAN, K.F., Specific Absorbed Fractions of Energy at Various Ages from Internal Photon Sources, Rep. ORNL/TM 8381, V1–V7, Oak Ridge Natl Lab., TN (1987).
- [7] BOUCHET, L.G., BOLCH, W.E., Five pediatric head and brain mathematical models for use in internal dosimetry, *J. Nucl. Med.* **40** (1999) 1327–1336.
- [8] SEGARS, W.P., LALUSH, D.S., TSUI, B.M.W., Modeling respiratory mechanics in the MCAT and spline-based MCAT phantoms, *IEEE Trans. Nucl. Sci.* **48** (2001) 89–97.
- [9] ZUBAL, I.G., et al., Computerized 3-dimensional segmented human anatomy, *Med. Phys.* **21** (1994) 299–302.
- [10] SJOGREEN, K., LJUNGBERG, M., WINGARDH, K., ERLANDSSON, K., STRAND, S.E., Registration of emission and transmission whole-body scintillation-camera images, *J. Nucl. Med.* **42** (2001) 1563–1570.
- [11] XU, X.G., CHAO, T.C., BOZKURT, A., VIP-Man: An image-based whole-body adult male model constructed from color photographs of the Visible Human Project for multi-particle Monte Carlo calculations, *Health Phys.* **78** (2000) 476–486.
- [12] PETOUSSI-HENSS, N., ZANKI, M., FILL, U., REGULLA, D., The GSF family of voxel phantoms, *Phys. Med. Biol.* **47** (2002) 89–106.
- [13] BERGER, M.J., MIRD Pamphlet 2: Energy deposition in water by photons from point isotropic sources, *J. Nucl. Med.* **9** (1968) 15–25.
- [14] STABIN, M.G., KONIJNENBERG, M.W., Re-evaluation of absorbed fractions for photons and electrons in spheres of various sizes, *J. Nucl. Med.* **41** (2000) 149–160.
- [15] BICE, A.N., LINKS, J.M., WONG, D.F., WAGNER, H.N., Absorbed fractions for dose calculations of neuroreceptor PET studies, *Eur. J. Nucl. Med.* **11** (1985) 127–131.



- [16] STABIN, M.G., YORIYAZ, H., Photon specific absorbed fractions calculated in the trunk of an adult male voxel-based phantom, *Health Phys.* **82** (2002) 21–44.
- [17] CHAO, T.C., XU, X.G., Specific absorbed fractions from the image-based VIP-Man body model and EGS4-VLSI Monte Carlo code: Internal electron emitters, *Phys. Med. Biol.* **46** (2001) 901–927.
- [18] BOUCHET, L.G., BOLCH, W.E., WEBER, D.A., ATKINS, H.L., POSTON, J.W., MIRD Pamphlet No. 15: Radionuclide S values in a revised dosimetric model of the adult head and brain. *Medical Internal Radiation Dose, J. Nucl. Med.* **40** (1999) 62S–101S.
- [19] BOLCH, W.E., et al., MIRD Pamphlet No. 17: The dosimetry of nonuniform activity distributions — Radionuclide S values at the voxel level, *J. Nucl. Med.* **40** (1999) 11S–36S.
- [20] BARDIES, M., MYERS, M.J., Computational methods in radionuclide dosimetry, *Phys. Med. Biol.* **41** (1996) 1941–1955.
- [21] FURHANG, E.E., SGOUROS, G., CHUI, C.S., Radionuclide photon dose kernels for internal emitter dosimetry, *Med. Phys.* **23** (1996) 759–764.
- [22] LEICHNER, P.K., A unified approach to photon and beta particle dosimetry, *J. Nucl. Med.* **35** (1994) 1721–1729.
- [23] SGOUROS, G., et al., Three-dimensional dosimetry for radioimmunotherapy treatment planning, *J. Nucl. Med.* **34** (1993) 1595–1601.
- [24] YORIYAZ, H., STABIN, M.G., DOS SANTOS, A., Monte Carlo MCNP-4B-based absorbed dose distribution estimates for patient-specific dosimetry, *J. Nucl. Med.* **42** (2001) 662–669.
- [25] ZAIDI, H., SCHEURER, A.H., MOREL, C., An object-oriented Monte Carlo simulator for 3D cylindrical positron tomographs, *Comput. Methods Programs Biomed.* **58** (1999) 133–145.
- [26] MOISAN, C., TUPPER, P., ROGERS, J.G., DE JONG, J.K., A Monte Carlo study of the acceptance to scattered events in a depth encoding PET camera, *IEEE Trans. Nucl. Sci.* **43** (1996) 1974–1980.
- [27] ZAIDI, H., Comparative evaluation of scatter correction techniques in 3D positron emission tomography, *Eur. J. Nucl. Med.* **27** (2000) 1813–1826.
- [28] SMITH, M.F., FLOYD, C.E., JASZCZAK, R.J., COLEMAN, R.E., Three-dimensional photon detection kernels and their application to SPECT reconstruction, *Phys. Med. Biol.* **37** (1992) 605–622.
- [29] FLOYD, C.E., JASZCZAK, R.J., GREER, K.L., COLEMAN, R.E., Inverse Monte Carlo as a unified reconstruction algorithm for ECT, *J. Nucl. Med.* **27** (1986) 1577–1585.
- [30] EEKMAN, F.J., DE JONG, H.W.A.M., VAN GELOVEN, S., Efficient fully 3-D iterative SPECT reconstruction with Monte Carlo-based scatter compensation, *IEEE Trans. Med. Imaging* **21** (2002) 867–877.
- [31] POLLARD, K.R., BICE, A.N., EARY, J.F., DURACK, L.D., LEWELLEN, T.K., A method for imaging therapeutic doses of iodine-131 with a clinical gamma camera, *J. Nucl. Med.* **33** (1992) 771–776.

- [32] HUILI, W., JASZCZAK, R.J., COLEMAN, R.E., Monte Carlo modeling of penetration effect for iodine-131 pinhole imaging, *IEEE Trans. Nucl. Sci.* **43** (1996) 3272–3277.
- [33] DEWARAJA, Y.K., LJUNGBERG, M., KORAL, K.F., Monte Carlo evaluation of object shape effects in iodine-131 SPET tumor activity quantification, *Eur. J. Nucl. Med.* **28** (2001) 900–906.
- [34] PARODI, K., ENGHARDT, W., Potential application of PET in quality assurance of proton therapy, *Phys. Med. Biol.* **45** (2000) N151–N156.

# **PERFORMANCE AND QUALITY CONTROL OF RADIONUCLIDE CALIBRATORS IN NUCLEAR MEDICINE**

M.J. WOODS

Ionising Radiation Metrology Consultants Ltd

E-mail: Michael.Woods@npl.co.uk

M. BAKER

National Physical Laboratory

Teddington, United Kingdom

## **Abstract**

Over recent years the divide between therapeutic and diagnostic applications of ionizing radiations has become increasingly blurred and the science between the two disciplines has become significantly closer. This merging has been accelerated by the increased use of radiolabelled pharmaceuticals for therapeutic purposes. This, in turn, has brought with it the requirement to use those same instruments that are commonly employed for the determination of the activity of diagnostic administrations. The principal difference is in the level of accuracy required. The paper presents and discusses the results of the various comparisons conducted by the National Physical Laboratory on those measuring instruments, particularly as they relate to the potential improvements in performance that can be achieved, and the necessary developments in the associated quality assurance protocols. It also addresses the developments in the calibration facilities available with these systems, especially as they relate to the measurement of, and achievable accuracies for, therapeutic radiation sources.

## **1. INTRODUCTION**

The use of ionizing radiations in nuclear medicine has traditionally been divided into two specific areas. Diagnostic use has generally been dominated by the injection or ingestion of unsealed sources of radionuclides. Therapeutic applications, however, have usually been accomplished by the use of ionizing radiation, primarily photons, both from machines and radionuclide sources, with the radiation source external to the patient. Over recent years this divide has started to disappear. The techniques of intracavitary and interstitial brachytherapy have introduced the radiation source into the body and even the tumour itself, using sealed sources of  $^{103}\text{Pd}$ ,  $^{125}\text{I}$ ,  $^{137}\text{Cs}$  and  $^{192}\text{Ir}$ . More recently, the practice of targeted radiotherapy, using unsealed sources of radionuclides, has gained

prominence: this involves radionuclides such as  $^{32}\text{P}$ ,  $^{67}\text{Cu}$ ,  $^{89}\text{Sr}$ ,  $^{90}\text{Y}$ ,  $^{131}\text{I}$ ,  $^{153}\text{Sm}$ ,  $^{166}\text{Ho}$ ,  $^{177}\text{Lu}$ ,  $^{186}\text{Re}$  and  $^{188}\text{Re}$  being administered to the target volume [1].

The successful application of both diagnostic and therapeutic administrations depends on many critical factors. One of these factors is an accurate knowledge of the activity or dose rate of the administered source. For diagnosis, it is generally accepted that the administered activity should be known to better than  $\pm 10\%$ : this, in turn, implies that the accuracy of the measuring device should be better than, approximately,  $\pm 5\%$ . The measuring instrument of choice is normally a radionuclide calibrator, which is a combination of a well type ionization chamber and an electrometer. The accuracy requirements for therapy applications are stricter, and the measurement device should be capable of providing accuracies of the order of  $\pm 2\text{--}3\%$ .

The radionuclide calibrator, traditionally a diagnostic tool, is a relatively simple to use device and can display exceptional long term stability coupled with minimal measurement geometry dependence. (It should be noted that any geometry effects will normally be radionuclide dependent.) Thus the radionuclide calibrator lends itself to being a particularly suitable instrument for the measurement of therapeutic radionuclides, provided it can deliver the required levels of accuracy and its operation is subject to a robust level of quality control. Knowledge of the calibrator construction and associated tolerances can provide a theoretical basis for determining accuracy limits; this should be validated experimentally.

A measure of the potential level of the performance of operational radionuclide calibrators can be determined by conducting comparison exercises by expert and impartial laboratories. Such exercises can have the added advantage of enabling the calibration of particular calibrators to be checked and even determined more accurately. A regular programme of such comparisons has been organized in the United Kingdom by the National Physical Laboratory (NPL) over the past 15 to 20 years, and follow-up workshops have been held for the participants to discuss the results and the potential avenues to performance improvements. The outputs from these comparisons, supplemented by regular dialogue and exchanges of information and experiences between the NPL and the user community, have identified a number of potential, but avoidable, sources of error.

In addition, the NPL, together with the relevant professional organization in the UK, the Institute of Physics and Engineering in Medicine, produced a quality assurance protocol in 1992, which was designed to establish and maintain the calibration of medical radionuclide calibrators and their quality control. This protocol is currently being revised to take into account both the increased emphasis on uncertainty estimation, the accumulation of comparison data and user experiences and the changes in equipment formats.

## 2. UK RADIONUCLIDE CALIBRATOR COMPARISONS

### 2.1. Comparison protocol

Since 1980 the NPL has conducted a series of comparisons [2–9] with UK hospitals. The number of participants varies but, typically, about 40 hospital departments take part and measurements are returned for up to 150 individual radionuclide calibrators.

The normal protocol adopted is that a series of identical sample containers are each filled with a weighed aliquot from a stock solution of the radionuclide being compared. Typically, 4 g of solution is dispensed to a 10 mL glass vial of the type commonly used by the principal radiopharmaceutical supplier in the UK. Radiometric check measurements are made on each sample to ensure homogeneity of the total batch, and then individual samples are despatched to the participants. At least two samples are assayed at the NPL using high pressure, re-entrant ionization chambers, the calibration factors of which are directly traceable to the UK primary standards of radioactivity.

The results from each participant are transmitted to the NPL and compared with the NPL determined activity values, and a report is compiled. The analytical breakdown differentiates between different calibrator types and sample containers (participants are normally requested to make additional measurements in syringe formats using the original solution in the vial despatched to them). These results are then discussed at a workshop of participants and NPL personnel, at which problems are highlighted and potential remedies discussed.

The accuracies of the primary standards, used by the NPL to calibrate its own ionization chambers, are confirmed by ongoing comparisons with other national metrology institutes (NMIs) via the international comparison system operated by the Bureau international des poids et mesures. A typical set of international comparison data is shown in Table I.

### 2.2. Comparison results

A variety of calibrators are in use in UK hospitals, but the principal systems are either the NPL secondary standard radionuclide calibrator [10] or one of the various Capintec models. Details of the comparison results for each calibrator and for each container are contained in the individual NPL reports, but it is instructive to examine some of the more significant findings. Typically, the results are plotted in a histogram form that expresses the difference between the reported and NPL values. Three such histograms are shown in Fig. 1 for measurements in the original 10 mL vials.

TABLE I. COMPARISON DATA BETWEEN NMIs FOR <sup>123</sup>I

NMI	Country/region	Uncertainty on NMI value ( <i>k</i> = 1) (%)	Difference between the NMI value and the mean of all values (%)
BCMNa	European Community	0.60	+0.14
NPL	UK	0.36	+0.44
SCK•CENb	Belgium	0.39	−0.98
LMRIc	France	0.54	−0.38
IERd	Switzerland	0.43	−0.40
PTBe	Germany	1.10	+1.17

a Bureau central de mesures nucléaires.  
b Studiecentrum voor Kernenergie—Centre d’étude de l’énergie nucléaire.  
c Laboratoire métrologie des rayonnements ionisants.  
d Institut d’électrochimie et de radiochimie.  
e Physikalisch-Technische Bundesanstalt.

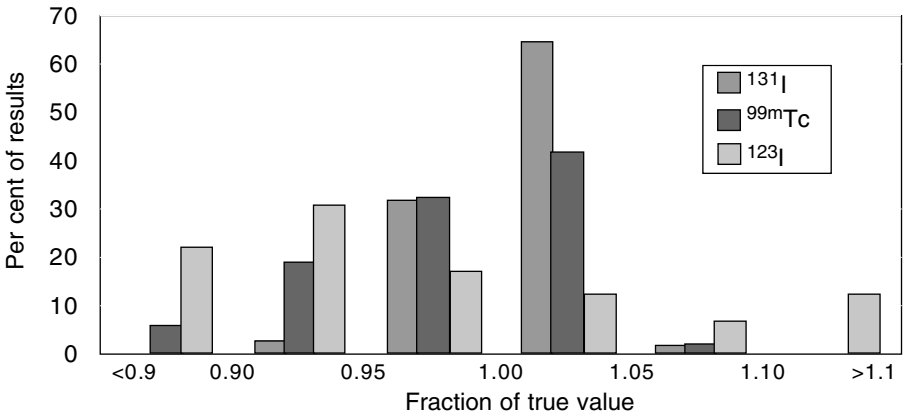


FIG. 1. Comparison results.

It is interesting to note that the three comparisons indicate varying levels of performance and, in particular, that there is a significant difference in the overall spread of the results between the three radionuclides. In the two extreme cases, all (100%) the results for <sup>131</sup>I lie within ±10% of the true (NPL) value, while for <sup>123</sup>I the corresponding figure is only 66%. Similar comparisons can be made for the overall spread of the results but, as in most exercises of this

type, there will always be a few outliers that make it difficult to determine the normal boundaries of the distributions with outliers excluded. In the two extreme cases considered in this paper, the actual spread of all the results without excluding outliers was 17% for  $^{131}\text{I}$ , while the corresponding figure for  $^{123}\text{I}$  was 112%. These results have been reproduced in comparison exercises in other countries. The results from comparisons in the Czech Republic [11], for example, show a remarkable similarity in spreads of results for both  $^{99\text{m}}\text{Tc}$  and  $^{131}\text{I}$ .

When the results of all the NPL comparisons are analysed, it becomes clear that the spreads of the results are a function of the effective energy of the radionuclide being compared. Since the ratio of responses at any two energies is dependent on the materials and thicknesses of the calibrator walls, the effective energy will depend on the individual radionuclide calibrator type. It is still possible, however, to make some crude ordering on this basis, and the breakdown of comparison results in Table II illustrates this effect.

TABLE II. ANALYSIS OF COMPARISON RESULTS WITH RADIO-NUCLIDE EFFECTIVE ENERGY

Radio-nuclide	Principal photon emissions (keV)	Photon emission probability (%)	Fraction of results within a given range of the NPL value (%)	
			$\pm 5\%$	$\pm 10\%$
$^{125}\text{I}$	~30	145	13	26
$^{123}\text{I}$	31	87	29	66
	159	83		
$^{57}\text{Co}$	122	86	52	76
	136	11		
$^{99\text{m}}\text{Tc}$	140	89	73	94
$^{201}\text{Tl}$	~80	28	73	94
	167	10		
$^{111}\text{In}$	26	83	84	92
	171	90		
	245	94		
$^{67}\text{Ga}$	~92	42	91	95
	185	21		
	300	17		
$^{131}\text{I}$	365	82	90	100

3. ACHIEVABLE PERFORMANCES

3.1. NPL secondary standard radionuclide calibrator (diagnostic sources)

The NPL calibrator [10] was specifically designed to provide secondary standard levels of performance for the measurement of those gamma emitting radionuclides used in diagnostic procedures. (It has been known variously as the 271/671, ISOCAL IV and NPL-CRC.) The most important feature is that the responses of all such chambers are closely controlled, to the extent that the calibration factors for each calibrator are identical to those of the master chamber held at the NPL, within specified limits. The controlling limits are as shown in Table III. Every calibrator chamber is tested at the NPL and compared with the master calibrator chamber, to ensure that these limits are met, before it can be released. This process has been continuing for almost 20 years, and the test results show a much better concurrence of responses than the limits allow. The actual spread of responses of all accepted chambers is also shown in Table III.

It can be seen that the agreement between the responses of any production chamber and those of the master chamber held at the NPL has been maintained within relatively small limits. Chambers that failed to meet these strict criteria by just a small margin have often been marketed by the manufacturer as an ISOCAL III, and these systems also appear in the comparison data. The ability to achieve these high levels of performance is also evidenced in practice by comparing the results of the NPL calibrator systems in the <sup>123</sup>I comparison with those of other systems (see Table IV).

TABLE III. REQUIRED AND ACTUAL PERFORMANCE REQUIREMENTS FOR THE NPL SECONDARY STANDARD RADIONUCLIDE CALIBRATORS

Radionuclide	Principal photon energy (keV)	Outer limits of difference in response compared with the NPL master chamber (all chambers since 1985) (%)	
		Required	Achieved
<sup>60</sup> Co	1250	±0.2	±0.2
<sup>57</sup> Co	125	±1.0	±0.7
<sup>125</sup> I	30	±6.0	±2.2



TABLE IV. COMPARISON BETWEEN PERFORMANCES OF THE NPL CALIBRATOR SYSTEMS AND OTHER SYSTEMS FOR  $^{123}\text{I}$  (EXCLUDING OBVIOUS OUTLIERS)

Calibrator system	Number of systems	Spread of results (%)
NPL (ISOCAL IV)	8	$\pm 2$
NPL (ISOCAL III)	6	$\pm 3$
Others	114	$\pm 30$

### 3.2. NPL secondary standard radionuclide calibrator (therapy sources)

Given the level of accuracy that can be achieved with the NPL calibrator, it lent itself to being employed also for the measurement of dose rates from therapy sources. Calibration factors have been developed for LDR (low dose rate) brachytherapy sources of  $^{192}\text{Ir}$  (wires and pins) and  $^{137}\text{Cs}$  (seeds and seed trains). Given the relatively high photon energies involved, it was possible to transfer measurements of the AKR (air kerma rate) to the calibrator with only a relatively small increase in uncertainty arising from the transfer process and variations between responses of individual NPL calibrators. This work has been published [12] and indicates that measurement uncertainties of 2–3% are readily achievable.

Further studies have demonstrated that the NPL calibrator can also be used for the accurate assay of the more difficult radionuclides — the activities of pure beta emitters such as  $^{32}\text{P}$ ,  $^{89}\text{Sr}$  and  $^{90}\text{Y}$  [13], and the dose rates of low photon energy emitters such as interstitial brachytherapy sources of  $^{125}\text{I}$  (seeds and trains) used for the treatment of prostatic cancer. For the  $^{125}\text{I}$  seeds the principal source of uncertainty arises from the potential anisotropy of dose distribution around the source [14], as shown in Fig. 2.

To measure the AKR using external measurement devices it is necessary to perform a series of angular measurements encompassing the whole  $360^\circ$  about the source axis and to aggregate these to give a mean value of AKR. The calibrator, however, is effectively a  $4\pi$  detector and the advantage is that the aggregation is incorporated into the single measurement. A series of investigations [14] has shown that the additional type B uncertainty (effectively synonymous with the previously used term, systematic uncertainty) that needs to be added to the uncertainty of the AKR measurement on any NPL calibrator, because of effects such as positional variations in the calibrator, is only of the order of about 2.5%. The overall uncertainty (at a coverage factor of  $k = 1$ ) that

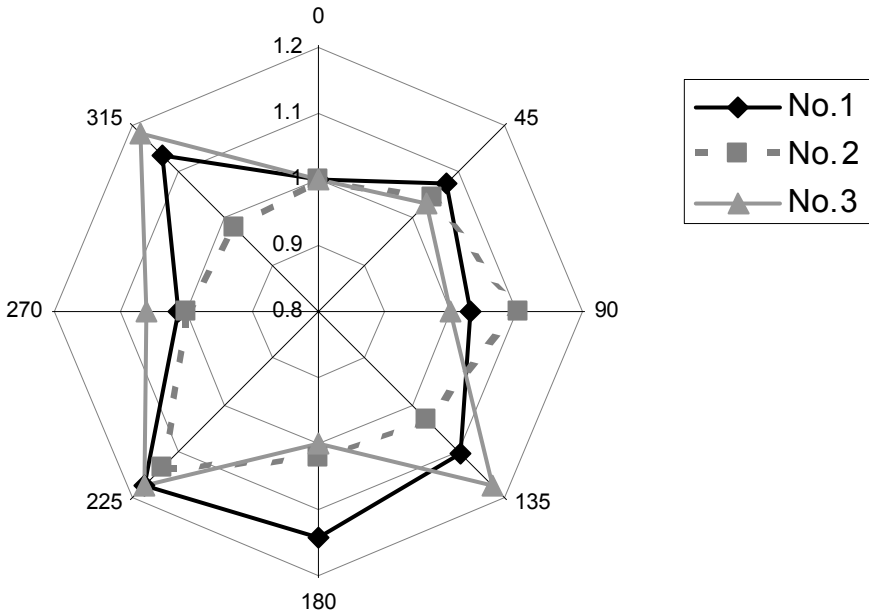


FIG. 2. Axial uniformity of  $^{125}\text{I}$  seeds. Angular responses relative to the response measured at the  $0^\circ$  measurement position [14].

can be achieved on the calibrator measured AKR value can therefore be of the order of 3%, only fractionally greater than that achieved by conventional dosimetric methods.

#### 4. QUALITY CONTROL

Following the publication of the first sets of comparison results in the UK, it became clear that there was scope for achieving better levels of measurement accuracy. To accomplish this, it was necessary to have a system of ongoing comparisons and workshops that would enable problems to be identified and possible remedies to be discussed. These workshops would also enable best practice to be disseminated more widely throughout the user community. It was also evident that these best practices should be documented. A joint collaboration between the user community and the NPL resulted in the production and publication in 1992 of a Protocol for Establishing and Maintaining the Calibration of Medical Radionuclide Calibrators and their Quality Control [15]. The principal recommendations were that users should maintain a regular series of quality assurance actions; these are summarized in Table V.

TABLE V. RECOMMENDED FREQUENCY OF RADIONUCLIDE CALIBRATOR QUALITY ASSURANCE ACTIONS

Source of uncertainty	Acceptance testing	Daily	Monthly	Annually
High voltage/display	✓	✓	✓	✓
Zero adjust	✓	✓	✓	✓
Background	✓	✓	✓	✓
Accuracy	✓			✓
Precision	✓		✓	✓
Relative responses	✓	✓	✓	✓
Subsidiary calibrations	✓			
Linearity	✓			✓
Electrical safety	✓			✓
Leakage radiation	✓			

This protocol is now being revised, again as a joint exercise between the NPL and the user community, to include the changes in both hardware and software that have been introduced in commercial systems. It will also incorporate the lessons learnt from the various comparisons and from metrological problems encountered since the protocol was first published.

Perhaps the most important item in Table V is that of accuracy. Irrespective of any claims made by the manufacturer of the calibrator system about accuracy and traceability, it is strongly recommended that users perform an independent check on the accuracy of the calibration factors for at least two radionuclides every year. For example, a user might check  $^{99m}\text{Tc}$  and  $^{67}\text{Ga}$  in the first year, then  $^{201}\text{Tl}$  and  $^{123}\text{I}$  the next, and so on, with priority being given to those radionuclides that are most commonly used. To that end, the NPL has been offering a service for many years now, whereby users can send samples of their radionuclides to the NPL for an assay that produces activity measurements that are directly traceable to national standards. The procedure is that the:

- (a) Users dispense solutions to their own containers;
- (b) Users measure samples in their own calibrator;
- (c) Users send a sample to the NPL;

- (d) NPL assays samples in the users' containers in the NPL ionization chamber;
- (e) NPL transfers samples to the NPL container;
- (f) NPL measures activities in the NPL ionization chamber;
- (g) NPL checks and corrects for transfer losses, adsorption and contaminants;
- (h) NPL issues certificates of measurement;
- (i) Users confirm the accuracy of the calibration factor or make appropriate corrections.

This system operates on a very rapid turnaround, and often provides users with provisional results on the same day.

Although the use of long lived check sources can provide some guarantee of the ongoing integrity of the ionization chamber and of the electronics of a calibrator system, it will not identify when the dimensions and composition of the sample container have changed. This is often the major source of error, and the NPL service described above will allow this problem to be identified.

The protocol described above is now the recommended procedure in all UK hospitals, and there is evidence to suggest that its introduction has played some part in improving the overall quality of measurements made in UK hospitals.

## 5. DISCUSSION

### 5.1. Diagnostic radionuclides

The two principal requirements of a calibrator system are to provide measurements of activity or dose rate that are:

- (a) Traceable to national standards of measurement. The generally available commercial calibrator systems were designed originally to accommodate the diagnostic user community. The validity of any claims of traceability is a matter that should be addressed to the individual manufacturers, and users are advised to seek such assurances and supporting documentation. It is recognized, however, that the container formats for which the manufacturer provides calibration factors are often different from those in routine use, and hence correction factors may be required, which are often not available. Within the UK the recommended quality assurance protocol and the NPL measurement service provide a reliable and independent mechanism for overcoming these problems and that ensures direct traceability to national standards.

- (b) Within the accuracy limits required by the user. The accuracy performance for diagnostic use should be such as to meet the  $\pm 10\%$  criterion. The evidence from comparison exercises, however, suggests that this criterion is not being met by some commercial calibrators for those radionuclides that emit a significant proportion of low energy photon radiation (X rays, bremsstrahlung, etc.). However, the NPL radionuclide calibrator does meet this criterion quite easily. This demonstrates that, if sufficient attention is paid to the manufacturing tolerances of the calibrator and other influences such as the selection of sample containers, this level of performance is fully attainable.

## 5.2. Therapeutic radionuclides

The traceability aspects are as important for therapeutic radionuclides as they are in the diagnostic area, and, in the UK, this requirement can be met using the same quality assurance protocol and calibration services that apply for diagnostic radionuclides.

The work conducted by the NPL with its radionuclide calibrator demonstrates that the stricter uncertainty requirements can be easily met for the higher energy, photon emitting radionuclides. For the lower energy photon emitters, such as  $^{125}\text{I}$ , and the pure beta emitters, such as  $^{32}\text{P}$ ,  $^{89}\text{Sr}$  and  $^{90}\text{Y}$ , the limiting factors may well be the anisotropy of the source and the uncertainty on the primary standardization technique, both of which are independent of the radionuclide calibrator. The investigations with the NPL calibrator indicate that, if sufficient care is given to the calibrator manufacture, the additional uncertainty arising from the operation of this instrument should not add significantly to the overall uncertainty of the activity or dose rate measurement.

The assertions above are based on the use of calibration factors that are produced for a master chamber and then transferred to other chambers of the same construction and using the same measurement geometry. The practice with the NPL calibrator is that all production models are compared with the NPL master chamber across a range of energies and radionuclides (including  $^{125}\text{I}$  and a long lived check source). The results of these comparisons can be applied to the measurements made with the production chamber and lead to a beneficial reduction in the overall uncertainty.

Additional benefits may be gained by using a radionuclide calibrator. The measurement is very straightforward and extremely rapid, and it also has the potential to minimize the radiation dose to the operator.

## 6. CONCLUSIONS

The radionuclide calibrator techniques employed in the measurement of diagnostic levels of radionuclides can be transferred to the measurement of therapeutic radionuclides. These methods offer an extremely stable measurement device that combines simplicity, traceability and levels of accuracy that are compatible with the requirements of the user community.

## REFERENCES

- [1] INTERNATIONAL ATOMIC ENERGY AGENCY, Summary Report of the Consultants' Meeting on Nuclear Data for Production of Therapeutic Radioisotopes (Mtg Vienna, 2002), Rep. INDC(NDS)-432, IAEA, Vienna (2002).
- [2] WOODS, M.J., Intercomparison of  $^{57}\text{Co}$  and  $^{125}\text{I}$  in U.K. Hospitals 1980/81, Rep. RS56, National Physical Laboratory, Teddington, UK (1981).
- [3] WOODS, M.J., Intercomparison of  $^{99\text{m}}\text{Tc}$  and  $^{131}\text{I}$  by Radionuclide Calibrators in UK Hospitals, 1986, Rep. RS(EXT)88, National Physical Laboratory, Teddington, UK (1987).
- [4] WOODS, M.J., KEIGHTLEY, J.D., CIOCANEL, M., Intercomparison of  $^{67}\text{Ga}$  Solution Sources in UK Hospitals, 1996, Rep. CIRA(EXT)012, National Physical Laboratory, Teddington, UK (1996).
- [5] WOODS, M.J., CIOCANEL, M., KEIGHTLEY, J.D., Intercomparison of  $^{123}\text{I}$  Solution Sources in UK Hospitals, 1996, Rep. CIRA(EXT)017, National Physical Laboratory, Teddington, UK (1997).
- [6] WOODS, M.J., CIOCANEL, M., KEIGHTLEY, J.D., Intercomparison of  $^{111}\text{In}$  Solution Sources in UK Hospitals, 1997, Rep. CIRM 001, National Physical Laboratory, Teddington, UK (1997).
- [7] CIOCANEL, M., KEIGHTLEY, J.D., SCOTT, C.J., WOODS, M.J., Intercomparisons of  $^{131}\text{I}$  Solution and Capsule Sources in UK Hospitals, 1999, Rep. CIRM 31, National Physical Laboratory, Teddington, UK (1999).
- [8] BAKER, M., WOODS, M.J., Intercomparison of  $^{123}\text{I}$  Solution Sources in UK Hospitals, 2000, Rep. CIRM 38, National Physical Laboratory, Teddington, UK (2000).
- [9] BAKER, M., WOODS, M.J., Intercomparison of  $^{201}\text{Tl}$  Solution Sources in UK Hospitals, 2001, Rep. CIRM 47, National Physical Laboratory, Teddington, UK (2001).
- [10] WOODS, M.J., CHRISTMAS, P., CALLOW, W.J., The NPL radionuclide calibrator – Type 271, *Int. J. Nucl. Med. Biol.* **10** (1983) 127–135.
- [11] OLŠOVCOVÁ, V., DRYÁK, P., “Comparisons of activity measurements in nuclear medicine with radionuclide calibrators in the Czech Republic”, these Proceedings, Vol. 2, pp. 67–75.

- [12] SEPHTON, J.P., et al., Calibration of the NPL secondary standard radionuclide calibrator for Ir-192 brachytherapy sources, *Phys. Med. Biol.* **38** (1993) 1157–1162.
- [13] WOODS, M.J., MUNSTER, A.S., SEPHTON, J.P., LUCAS, S.E.M., PATON WALSH, C., Calibration of the NPL secondary standard radionuclide calibrator for  $^{32}\text{P}$ ,  $^{89}\text{Sr}$  and  $^{90}\text{Y}$ , *Nucl. Instrum. Methods Phys. Res. A* **369** (1996) 698–702.
- [14] BAKER, M., BASS, G.A., WOODS, M.J., Calibration of the NPL secondary standard radionuclide calibrator for  $^{125}\text{I}$  seeds used for prostate brachytherapy, *Appl. Radiat. Isot.* **56** (2002) 321–325.
- [15] PARKIN, A., et al., “Protocol for establishing and maintaining the calibration of medical radionuclide calibrators and their quality control”, *Quality Standards in Nuclear Medicine* (Proc. Mtg London, 1992), Rep. 65, Institute for Physical Sciences in Medicine, York, UK (1992) 60.

**BLANK**



## RELATIONSHIP OF BONE UPTAKE TO RADIATION DOSES IN BONE PAIN TREATMENT WITH $^{188}\text{Re}$ HEDP

J. GAUDIANO

Centro de Medicina Nuclear, Hospital de Clínicas,  
Universidad de la República  
E-mail: gaudiano@hc.edu.uy

E. SAVIO, A. PAOLINO

Cátedra de Radioquímica,  
Universidad de la República

Montevideo, Uruguay

### Abstract

Dosimetric results for 29 therapeutic administrations of  $^{188}\text{Re}$  hydroxyethylidene diphosphonate (HEDP) to patients with painful bone metastases are presented along with a discussion of the administered activity and individual bone uptake. Bone marrow absorbed dose was calculated using the MIRDOSE Version 3.0 program. Residence times were calculated as  $(0.5 \times C/A \times 1.443 \times 16.9)$  h (where  $C$  is the bone uptake in mCi;  $A$  is the administered radioactivity in mCi; 16.9 h is the  $t_{1/2}$  of  $^{188}\text{Re}$ ) with equal apportionment to trabecular and cortical bone. Bone uptake was inferred from urine collection to 24 h, being estimated as  $A_0 - E_{\max}$  ( $A_0 = ^{188}\text{Re}$  HEDP administered radioactivity;  $E_{\max}$  = total accumulated urine excretion). The total volume of urine was collected over 24 h in five patients and over 6 h in the other patients for an estimate of the 24 h excretion. Urine collection was performed by catheterization in order to facilitate sample collection and minimize wall irradiation in the bladder. The total bone marrow dose was related to the administered activity: a correlation coefficient,  $r$ , of 0.27 was observed. When total bone marrow dose was correlated to bone uptake,  $r$  was 0.79.

### 1. INTRODUCTION

Cancer is the second most frequent cause of death in developed countries; progressive pain is one of the main symptoms in patients suffering from bone metastases. There has therefore been attention focused on a variety of treatments for pain management: chemotherapy, surgery, external beam radiotherapy, hormonal therapy and analgesic drugs (both opiates and non-opiates). In cases of non-respondent pain, usually due to diffuse and hormone resistant

metastases, treatment with  $\beta^-$  emitter radiopharmaceuticals has been proposed and has proved to be a complementary but useful aid [1, 2].

Rhenium-188 hydroxyethylidene diphosphonate (HEDP) is an agent that has several advantageous characteristics [1, 2]. Increased and multiple radioactivity administrations require a careful consideration of radiation dosimetry, although this radiopharmaceutical is estimated to deliver comparatively low absorbed doses to bone marrow [3]. Several other radionuclides have been proposed and have undergone multiple clinical trials, for example  $^{32}\text{P}$  and  $^{89}\text{Sr}$  [4, 5]. Several  $\beta^-$  emitting phosphonate radiopharmaceuticals were developed in the 1980s. In particular,  $^{186}\text{Re}(\text{Sn})$  HEDP and  $^{153}\text{Sm}$  ethylenediamine tetramethylenephosphonic acid (EDTMP) have shown favourable biodistributions and dosimetry, and have been used clinically [6, 7].

Similarly to  $^{186}\text{Re}$  and  $^{153}\text{Sm}$ ,  $^{188}\text{Re}$  emits both beta particles suitable for therapy ( $\beta_{\text{max}} = 2.1$  MeV) and a gamma ray (155 keV) that is adequate for diagnostic imaging to verify localization in the areas associated with the metastatic processes [8–10].

The objective of this study was to evaluate the influence of administered activity and bone uptake is 29 doses involving  $^{188}\text{Re}$  HEDP at two levels of activity (35 and 60 mCi) given to 21 patients. A correlation of these data to (a) the TBMD (total bone marrow dose) and (b) clinical results was made to optimize the amount of administered radioactivity and pre-administration dosimetry calculations.

## 2. METHODS

### 2.1. Equipment and software

Whole body images were acquired with a Sopha DSX, a 93 photo multiplier tube (PMT) camera with a medium energy high resolution collimator and a 20% window centred at 155 keV. A Capintec CRC-12 dose calibrator was used with a calibration factor of 496 ( $\times 10$ ) for the measurement of administered activity and radioactivity contained in urine samples. Blood samples for pharmacokinetic characterization were assessed in an NaI(Tl) Mini Assay Type G-20 gamma counter. The MIRDOSE 3.0 program was used for the dose calculations.

### 2.2. Radiopharmaceuticals

Rhenium-188 HEDP (radiochemical purity > 98%) was prepared from lyophilized and locally produced kits, with  $^{188}\text{Re}$  eluted from a  $^{188}\text{W}/^{188}\text{Re}$  generator. Radiochemical purity was determined by ascending chromatography

with acetone and NaCl 0.9% as mobile phases and Whatman 1M and 3M as stationary phases [11].

### 2.3. Patients

Twenty-nine doses were delivered to 21 patients suffering pain from bone metastases due to primary cancers in the prostate (No. = 11), breast (No. = 8), uterus (No. = 1) and thyroid (No. = 1). Inclusion criteria were: the presence of painful bone metastases, the failure of previous conventional analgesic therapies, bone scans showing multiple bone metastases and white blood cell and platelet counts higher than  $4000/\text{mm}^3$  and  $150\,000/\text{mm}^3$ , respectively, and serum creatinine concentrations of 1.5 mg/dL or less. Patients with renal failure, urinary incontinence, psychiatric disorders, spine compression or fracture on pathological bone were excluded.

### 2.4. Protocol

The dose administration protocol used was approved by the ethics committee of the Faculty of Medicine, Universidad de la República, Montevideo, Uruguay. Tracer doses were administered to assess bone uptake and derive a therapeutic dose tailored to each patient (on the basis of bone uptake and body weight), administered 24 h after the first injection.

Two groups of patients were distinguished: in the first group (12 patients, group I) the maximum administered activity for accumulated dose was set at 35 mCi (1295 MBq), which took into consideration radiation safety as well as the reasonable expectancy of the therapeutic benefit. In the second group (nine patients, group II) a scaled administered radioactivity protocol was used, with a proposed radioactivity of 60 mCi (2220 MBq) for a bone uptake of 40%.

Five patients from group I were hospitalized and remained for 24 h after the administration of a therapeutic dose for study and sample collection. The patients were not pre-hydrated. In these five patients blood samples were drawn from an antecubital vein opposite the injection site at preset approximate intervals (2, 4, 8, 12 and 30 min and 1, 2, 4, 6, 12 and 24 h post-injection) with heparinized syringes. Total urine was collected at various time intervals (0–1, 1–2, 2–4, 4–6, 6–12, 12–18 and 18–24 h) after the administration of the radioactivity. Urine was collected from the other patients (No. = 16) only up to 6 h after the administration of the dose (0–1, 1–2, 2–4, 4–6 h); 24 h excretion was estimated from these limited collections. Patients were catheterized to facilitate sample collection and minimize possible contamination and to reduce bladder wall irradiation due to urinary retention.

## 2.5. Dose calculations

The residence time in trabecular bone was considered equal to that in cortical bone, and calculated on the basis of experimental data as:

$$\text{residence time} = (0.5 \times C/A \times 1.443 \times 16.9) \text{ h}$$

where

$C$  is bone uptake (mCi);

16.9 is  $t_{1/2}$  of  $^{188}\text{Re}$ ;

$A$  is the administered radioactivity (mCi).

The absorbed dose to bone marrow was calculated using the MIRDOSE Version 3.0 program, entering residence time values calculated as described above. Typical residence times for the kidney, bladder wall and remainder of the body are reported based on our data and  $^{99\text{m}}\text{Tc}$  HEDP reported values [12].

## 2.6. Bone uptake

Bone uptake was calculated from the results of urine collection 6 h after the injection. In previous studies a 6 h urine collection was validated against a 24 h urine collection in order to calculate the bone uptake. The  $^{99\text{m}}\text{Tc}$  MDP bone uptake was also determined from bone scans of a group of patients, in order to validate the protocol.

## 3. RESULTS

The results for uptake, residence time and dose for all patients are shown in Table I, which considers only the trabecular and cortical bone contribution for the bone marrow absorbed dose calculation. Average radiation doses were estimated for the kidneys, bladder wall, bone surface, red marrow and total body (residence time for the remainder of the body) and are shown in Table II. These results overestimate the bladder wall absorbed dose because a voiding time of 4 h was used as the MIRDOSE 3.0 program input, while patients were under bladder catheterization during the procedure.

The following correlation coefficients,  $r$ , were calculated: AD/BMD ( $r = -0.248$ ), AD/TBMD ( $r = 0.332$ ), AD/DD ( $r = -0.018$ ), AD/PD ( $r = -0.243$ ), BU/TBMD ( $r = 0.740$ ), BU/DD ( $r = -0.205$ ), BU/PD ( $r = 0.127$ ) (Figs 1 and 2).

TABLE I. RHENIUM-188 HEDP ADMINISTRATION TO 21 PATIENTS (29 DOSES): CLINICAL AND ESTIMATED PARAMETERS

	Patient	AD (mCi)	Weight (kg)	AD/ kg	BU (%)	RT (h)	BMD (rad/mCi)	TBMD (rad)	DD (%)	PD (%)
1	L.H.	41.6	88.2	0.47	59	7.2	3.04	159.3	—	—
2	G.M	35.3	61	0.58	68.7	8.4	3.54	108.9	70	75
3	A.P	33.09	75	0.44	65.4	8	3.38	119.8	50	45
4	J.P.	34.8	80	0.44	43.5	5.3	2.24	89.1	—	—
5	E.S	30.7	62	0.5	63.6	7.8	3.29	89.5	33	33
6	F.C	30.7	67	0.46	43.7	5.3	2.24	65.8	63	59
7	S.V.	24.4	83	0.29	46.9	5.7	2.4	69.4	0	0
8	H.L	26.7	68	0.39	39.6	4.8	2.03	52.7	33	56
9	N.R	25.5	62	0.41	38.5	4.7	1.98	44.7	25	57
10	G.F	27.5	57	0.48	25.2	3.1	1.31	29.3	66	50
11	T.D.	19.4	65.5	0.3	25.3	3.1	1.31	23.8	100	100
12	B.B.	38.7	92	0.42	10.1	1.2	0.51	25.9	0	0
13	A.P.C.	60	60	1	41.2	5	2.11	108.5	—	—
14	M.M	38.3	62	0.62	36.6	4.5	1.9	64.5	—	50
15	J.F.	64.7	86	0.75	27.7	3.4	1.43	113.7	36	50
16	E.V.	42.5	93	0.46	39.8	4.9	2.07	116.9	0	0
17	C.B.	76.8	68	1.13	15.5	1.9	0.8	59.7	50	50
18	G.R.	63	60	1.05	53.4	6.5	2.74	148	70	75
19	E.U.	33.2	60	0.55	23	2.8	1.18	33.6	100	100
20	T.P.	41.7	59.5	0.7	58.5	7.1	3	106.33	50	50
21	Y.R.	30.4	88	0.34	67	8.5	3.59	137.15	0	80
22	N.D.	49.8	92	0.54	9.7	1.18	0.49	32.07	100	33
23	A.L.	63	79	0.79	42.7	5.2	2.19	155.7	0	50
24	A.L.	41.1	70	0.59	7.5	0.9	0.38	15.6	8	41
25	A.L.	44.3	70	0.63	7.5	0.9	0.38	16.8	83	70
26	M.M.	27	62	0.44	47.1	5.7	2.4	57.4	—	50
27	E.V.	72.9	92	0.79	12.6	1.5	0.63	60.4	50	0
28	E.U.	35.2	60	0.59	36.1	4.4	1.87	76.8	64	100
29	G.R.	54.9	60	0.92	64.7	7.9	3.33	156.7	—	33

AD: administered dose. BU: bone uptake. RT: residence time. BMD: bone marrow dose. TBMD: total bone marrow dose. DD: drug decrease. PD: pain decrease.

TABLE II. RADIATION DOSE ESTIMATES

Organ	Residence time (h)	Absorbed dose (rad/mCi)
Kidney	0.43	2.40
Bladder wall	3.6	14.3
Total body	3.2	0.31
Red marrow	4.6 <sup>a</sup>	2.01
Bone surfaces	4.6 <sup>a</sup>	2.79

<sup>a</sup> Residence time in cortical and trabecular bone (average value for 29 doses).

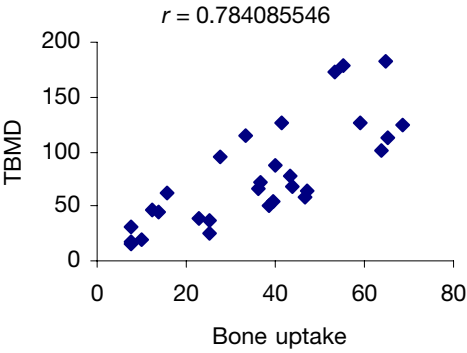


FIG. 1. Total bone marrow dose versus bone uptake.

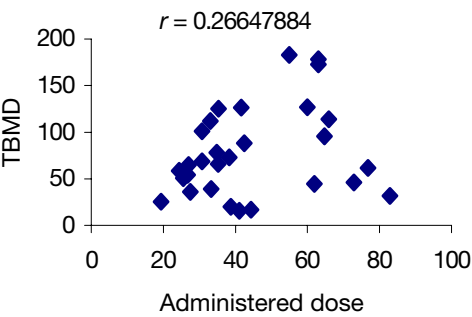


FIG. 2. Total bone marrow dose versus administered dose.

Bone uptake, bone marrow dose per unit activity (corrected to a total body weight of 70 kg) and total bone marrow dose are closely related. Depending on the number and extent of the lesions shown in the  $^{99m}\text{Tc}$  MDP bone scan, considerable variability in bone uptake was observed ( $44\% \pm 18$  in group I;  $31\% \pm 18$  in group II), resulting in a maximum total absorbed dose to bone marrow similar for both groups, despite receiving an average value of 31 or 55 mCi (1147 or 2035 MBq). However, while all the patients received 0.29–1.18 mCi/kg (10.7–43.7 MBq/kg), dose calculations show that a higher bone uptake correlated with higher absorbed doses to the bone marrow (as should be expected). Although the second group of patients received twice as much activity, absorbed doses were highly dependent on the rate of bone uptake. Overall, a 76% pain decrease and a 62% decrease in the need for pain relieving medication was observed in the patients receiving radiation treatment.

#### 4. CONCLUSIONS

As bone uptake is directly related to the total bone marrow dose, it can be used to determine the administered activity for each patient. Seventy-nine per cent of the patients reported an improved quality of life in terms of pain relief, reduction of analgesic intake and/or increase in daily activity. Studies will be carried out to determine bone uptake from scintigraphic images, in order to improve patient management. Most patients involved in this kind of treatment have considerable pain, which limits their daily functions; this therapy offers much promise for an improved quality of life for these patients.

#### REFERENCES

- [1] KNAPP, F.F., Jr., et al., Reactor produced radioisotopes from ORNL for bone pain palliation, *Appl. Radiat. Isot.* **49** (1998) 309–315.
- [2] MAXON, H.R., III, et al., Rhenium-188(Sn)HEDP for treatment of osseous metastases, *J. Nucl. Med.* **39** (1998) 659–663.
- [3] GAUDIANO, J., et al., “<sup>188</sup>Rhenium HEDP in the treatment of pain in bone metastases”, *Therapeutic Applications of Radiopharmaceuticals*, IAEA-TECDOC-1228, IAEA, Vienna (2001) 215–220.
- [4] SILBERSTEIN, E., ELGAZZAR, A., KAPILIVSKY, A., Phosphorus-32 radiopharmaceuticals for the treatment of painful osseous metastases, *Semin. Nucl. Med.* **XXII** 1 (1992) 17–27.
- [5] POTER, A.T., et al., Results of a randomized phase-III trial to evaluate the efficacy of strontium-89 adjuvant to local field external beam irradiation in the management of endocrine resistant metastatic prostate cancer, *Int. J. Radiat. Oncol. Biol. Phys.* **25** (1993) 805–813.
- [6] KETRING, A.R., <sup>153</sup>Sm-EDTMP and <sup>186</sup>Re-HEDP as bone therapeutic radiopharmaceuticals, *Nucl. Med. Biol.* **3** 14 (1987) 223–232.
- [7] MAXON, H.R., et al., Re-186 (Sn) HEDP for treatment of painful osseous metastases: Initial clinical experience in 20 patients with hormone-resistant prostate cancer, *Radiology* **176** (1990) 155–159.
- [8] CALLAHAN, A.P., RICE, D.E., KNAPP, F.F., Jr., Rhenium-188 for therapeutic applications from an alumina-based tungsten-188/rhenium-188 radionuclide generator, *Nucl. Compact.* **20** (1989) 3–6.
- [9] KAMIOKI, H., et al., <sup>188</sup>W/<sup>188</sup>Re generator for biomedical applications, *Radiochim. Acta* **65** (1994) 39–46.
- [10] PALMEDO, H., et al., Dose escalation study with rhenium-188 hydroxyethylidene diphosphonate in prostate cancer patients with osseous metastases, *Eur. J. Nucl. Med.* **27** (2000) 123–130.
- [11] VERDERA, E.S., et al., Rhenium-188-HEDP-kit formulation and quality control, *Radiochim. Acta* **79** (1997) 113–117.

- [12] SUBRAMANIAN, G., McAFEE, J.G., BLAIR, R.J., KALLFELZ, F.A., THOMAS, F.D., Technetium-99m-methylene diphosphonate — A superior agent for skeletal imaging: Comparison with other technetium complexes, *J. Nucl. Med.* **16** (1975) 744–755.



# COMPARISONS OF ACTIVITY MEASUREMENTS IN NUCLEAR MEDICINE WITH RADIONUCLIDE CALIBRATORS IN THE CZECH REPUBLIC

V. OLŠOVCOVÁ, P. DRYÁK

Czech Metrological Institute, Prague, Czech Republic

E-mail: volsovcova@cmi.cz

## Abstract

Radionuclide calibrators consisting of a well type ionization chamber and an electrometer are used in nuclear medicine for the determination of the activity of radioactive pharmaceuticals administered to patients. In order to maximize the safety of patients, it is important to ensure the long term accuracy of radionuclide calibrators. The paper presents data obtained in annual calibrator accuracy checks carried out in the Czech Republic by the Czech Metrological Institute during the past decade. Changes in radionuclide calibrator models, the range of radionuclides used and the development of measurement accuracies are also described. In addition, the results of a regional international comparison are given.

## 1. INTRODUCTION

Medical irradiation represents one of the main sources of exposure of the public to radiation. It is therefore important to measure the activity administered to a patient *in vivo* as accurately as possible, in order to reduce the received dose to that which is necessary — not only in radiotherapy, for which an error could have serious consequences, but also in diagnostics. Almost as important is the need to ensure that sufficient dose to be effective is administered, thereby reducing the need for repeat treatments.

Activity measurements in nuclear medicine using radionuclide calibrators or activimeters have been performed for several decades, although their reliability has varied. Many comparisons have been carried out, both national [1–3] and international (such as EUROMET project E634 (2001) and DUNAMET project D24 (1996)).

In this paper the results of measurements performed during the annual calibrator accuracy checks over the past decade in the Czech Republic are summarized. Since the Czech Metrological Act No. 137/2002 in its implementation into law by Edict No. 263 of the Ministry of Trade and Industry (2000) requires annual accuracy checks of “devices measuring activity of diagnostic and therapeutic pharmaceuticals applied to a patient *in vivo*”, each of the

48 nuclear medicine departments in the Czech Republic have been included and have participated in the checks. Seven of the nuclear medicine departments administer therapeutic as well as diagnostic doses.

## 2. METHODS

Only agreement of measured activity with the reference value is monitored in the annual calibrator accuracy checks. Long and short term stability tests are the responsibility of the user, according to the 1999 recommendation of the State Office for Nuclear Safety.

During the past decade the system of annual calibrator accuracy checks has undergone a gradual development. Originally, samples of one chosen radionuclide were prepared and their activities measured using the Czech Metrological Institute's (CMI)  $4\pi\gamma$  reference chamber [4]. Samples were then sent to the participants, who measured them for activity (the value of which was not disclosed to them) and then filled out a questionnaire. The answers were later evaluated by the CMI. Despite the fact that all the measurements were performed under common conditions (i.e. without pressure from the presence of an observer), this system was found to be unsatisfactory, mostly because of the long time intervals between the measurement and evaluation of its results. The main disadvantages arose from difficulties connected with the interpretation of the results (mainly the evaluation of questionnaires with incomplete data) and the impossibility of revealing retrospectively the true source of error in the event of a large difference between the conventionally true and the measured value of activity of the sample.

A different system of checks was therefore first introduced in 2000. Each participant can choose for the calibrator accuracy check a subset of or all the radionuclides offered. The offered set is being gradually enlarged; in 2001 it consisted of:  $^{99m}\text{Tc}$ ,  $^{131}\text{I}$ ,  $^{67}\text{Ga}$  and  $^{201}\text{Tl}$ . Solution samples (a 5 mL volume in a 10 mL standard serum bottle — the most commonly used in the Czech Republic) are prepared in advance for all the offered radionuclides, except for  $^{99m}\text{Tc}$ , and are measured with the CMI's  $4\pi\gamma$  reference chamber to obtain a conventionally true value of activity. For  $^{99m}\text{Tc}$  (for which the sample is provided by the participant), the true value is considered to be the activity value measured by the CMI's radionuclide calibrator, the calibration of which is periodically checked against the CMI's  $4\pi\gamma$  reference chamber. Since in most Czech hospitals activity is measured not only in serum bottles but also in syringes, the CMI recommends the performance of calibrator accuracy checks for both geometries.

The CMI's inspector responsible for the checks travels through the Czech Republic over the course of a week and, in co-operation with hospital staff, carries out the checks of accuracy of the calibrators. The main advantage of this approach is an immediate knowledge of the results and the possibility of tracking down unexpected errors and correcting them (e.g. changing the measuring routine or recommending a repair). Moreover, satisfaction with the service has grown, as it is more convenient for the customers than the previously used system.

### 3. RESULTS

#### 3.1. Devices

The distribution of the types of radionuclide calibrator used has changed significantly over the past decade (see Table I). After the detection of a design error in NNG 601 calibrators (manufactured by TESLA, Czech Republic) during the first large national comparison in 1991, they were replaced by other models. In 1992 a new domestic type of calibrator, the Bqmeter (manufactured by Consortium BQM, Czech Republic), was introduced. It is currently the second most commonly used calibrator in the Czech Republic, as its quality is comparable with Curiementors (manufactured by PTW), which are the most common.

A comparison of deviations from the conventionally true value of measured activity of the two most commonly used devices has revealed that, while Bqmeters tend to overestimate the measured activity, Curiementors almost

TABLE I. THE THREE MOST COMMONLY USED RADIONUCLIDE CALIBRATORS IN 1991, 1996 AND 2001

	Calibrator (manufacturer)	Share (%)
1991	Robotron (VEB Robotron)	27
	NNG 601 (TESLA)	26
	Curiementor (PTW)	20
1996	Curiementor (PTW)	46
	Robotron (VEB Robotron)	21
	Bqmeter (Consortium BQM)	21
2001	Curiementor (PTW)	56
	Bqmeter (Consortium BQM)	36
	Robotron (VEB Robotron)	6

always underestimate it. Figure 1 illustrates the case for  $^{99m}\text{Tc}$ . The mean values of deviations of measurements of activity in syringes are shifted from those in bottles by about 3–5%, so the results when compared with the limits of the European Pharmacopoeia [5] are somewhat poor (see Table II).

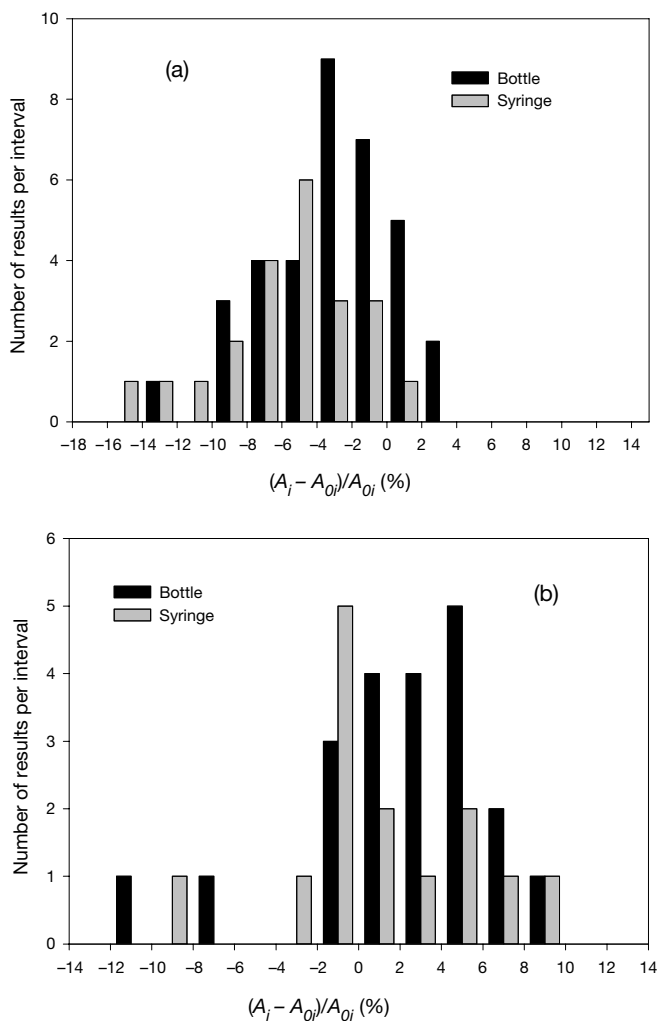


FIG. 1. Distribution of the results of the  $^{99m}\text{Tc}$  comparison. (a) Curielements. (b) Bq meters.  $A_i$ : activity measured by the participant;  $A_{0i}$ : activity measured by the CMI.

TABLE II. DISTRIBUTION OF THE RESULTS OF ACTIVITY MEASUREMENTS IN 2001  
(percentage of the results within a given range of the CMI value)

	Serum bottle				Syringe				European Pharmacopoeia
	$\pm 5\%$	$\pm 10\%$	$\pm 15\%$	Number of measurements	$\pm 5\%$	$\pm 10\%$	$\pm 15\%$	Number of measurements	
$^{67}\text{Ga}$	58	97	100	31	29	71	93	14	$\pm 10\%$
$^{99\text{m}}\text{Tc}$	71	95	100	65	45	90	98	40	$\pm 10\%$
$^{131}\text{I}$	77	100	100	35	60	100	100	15	$\pm 10\%$
$^{201}\text{Tl}$	24	68	100	25	0	40	90	10	$\pm 10\%$

### 3.2. Radionuclides

The range of radionuclides used in nuclear medicine has changed over the past decade. When we assign to the most frequently used radionuclide in a given nuclear medicine department a rank of usage equal to 1, and values 2, 3, etc., to the respectively less frequently used radionuclides, then from the weighted average of usage (WAU) we can follow a change of preference of the use of the various radionuclides (see Table III). Naturally, the most frequently used radionuclide remains  $^{99m}\text{Tc}$ , the frequency of use of which has further increased. While both the number of users and the WAU of  $^{131}\text{I}$  have been dropping slightly, the WAU of some other nuclides has been gradually rising, especially that of  $^{111}\text{In}$ .

### 3.3. Calibrator accuracy checks

Possibly owing to the regular comparisons of radionuclide calibrators, the majority of them meet the allowed limits for deviation from the conventionally true value of activity given in the European Pharmacopoeia [5]. If the limit value is exceeded the possible reason for the excess is investigated (e.g. whether a technician's error has occurred or whether repair or replacement of the device is needed).

The data in Tables II and III were obtained before a remedy had been applied. Table II shows that the limit values of  $\pm 10\%$  [5] of activity were exceeded significantly for  $^{201}\text{Tl}$ . The results are satisfactory, however, for  $^{67}\text{Ga}$  and  $^{99m}\text{Tc}$  and excellent for  $^{131}\text{I}$ . This is true for both the serum bottle and the syringe measurements.

TABLE III. NUMBER OF USERS AND THE WAU OF VARIOUS RADIONUCLIDES

	WAU			Number of users			
	1991	1999	2001	1991	1999	2001	2002
$^{51}\text{Cr}$	4.5	3.5	3.4	15	8	8	12
$^{67}\text{Ga}$	3.4	2.9	2.9	11	19	20	22
$^{99m}\text{Tc}$	1.1	1.1	1.0	45	46	48	41
$^{111}\text{In}$	5.5	3.3	2.6	4	10	10	17
$^{131}\text{I}$	2.0	2.0	2.3	41	38	30	21
$^{201}\text{Tl}$	3.3	2.6	2.7	15	21	21	19

**Note:** The WAU is not available for 2002.

Table IV shows the gradual improvement in the accuracy of activity measurements over the past decade for  $^{131}\text{I}$  and  $^{99\text{m}}\text{Tc}$ . On the whole, the results of the measurements are satisfactory.

### 3.4. Regional international comparison

The Slovak Institute of Metrology (Slovakia), Bundesamt für Eich- und Vermessungswesen (Austria) and CMI (Czech Republic) participated in a regional international comparison organized by the CMI in 2001. The participants measured, using radionuclide calibrators, the activities of  $^{18}\text{F}$ ,  $^{67}\text{Ga}$ ,  $^{99\text{m}}\text{Tc}$ ,  $^{123}\text{I}$ ,  $^{131}\text{I}$  and  $^{201}\text{Tl}$  in solutions,  $^{137}\text{Cs}$  in gels and  $^{133}\text{Xe}$  in gas ampoules. Determined activities were compared with the activity obtained using either the CMI's  $4\pi\gamma$  reference chamber or a calibrated HPGe spectrometer. Iodine-131 was in addition standardized by the  $4\pi\beta\text{--}\gamma$  coincidence absolute method and sent to the International Reference System at the Bureau international des poids et mesures, Sèvres, France, at which the CMI value was found to be within 0.67% of all entries since 1998.

A good agreement among the three institutes was found for  $^{137}\text{Cs}$ ,  $^{131}\text{I}$ ,  $^{99\text{m}}\text{Tc}$  and  $^{67}\text{Ga}$ , for which the differences did not exceed 3%. Measurements of  $^{133}\text{Xe}$  were illustrative only, since there were very large differences in geometry among the chambers. Values of the activity of  $^{123}\text{I}$  measured by the radionuclide calibrators were in good agreement with each other, but not with the value from the CMI's  $4\pi\gamma$  reference chamber. This highlighted an error in the calibration of the CMI's  $4\pi\gamma$  reference chamber. A similar problem was encountered for  $^{201}\text{Tl}$ . The results of this exercise are summarized in Table V.

TABLE IV. DISTRIBUTION OF RESULTS FROM COMPARISONS OF  $^{131}\text{I}$  AND  $^{99\text{m}}\text{Tc}$  ACTIVITY MEASUREMENTS  
(percentage of results within a given range of the CMI value)

	Year	$\pm 5\%$	$\pm 10\%$	$\pm 15\%$	Number of measurements
$^{131}\text{I}$	2001	77	100	100	35
	1996	76	93	98	44
	1991	62	80	91	41
$^{99\text{m}}\text{Tc}$	2001	71	95	100	65
	1996	73	93	98	55

**Note:**  $^{99\text{m}}\text{Tc}$  was not measured in 1991; the first complete data set was collected in 1996.

TABLE V. DEVIATIONS OF RESPONSES OF SECONDARY CHAMBERS FROM THE CMI'S  $4\pi\gamma$  REFERENCE CHAMBER(for  $^{201}\text{Tl}$  the deviation is given relative to the NPL-CRC chamber measurement)

	$(A_r - A)/A$ (%)			
	ISOCAL-IV	Vacutec	Bqmeter	NPL-CRC
$^{18}\text{F}$	+0.8	+4.7	-4.8	+1.2
	+0.8	+4.2	-4.9	+1.5
$^{67}\text{Ga}$	-0.3	-1.2	-8.7	+0.5
	-0.4	-1.1	-8.8	+0.3
$^{99\text{m}}\text{Tc}$	+0.9	+2.4	+1.3	+1.7
	+0.9	+2.4	+1.2	+1.7
$^{123}\text{I}$	-0.8	+1.0	+0.2	<sup>b</sup>
	-0.8	+1.0	+0.2	<sup>b</sup>
$^{131}\text{I}$	+0.6	+3.3	-2.9	+0.8
	+0.6	+3.4	-2.8	+0.7
$^{137}\text{Cs}$	-1.4	+1.2	-1.8	-1.5
	-1.4	+1.3	-1.0	-1.5
	-1.5	+1.1	-1.9	-1.5
	-1.5	+1.1	-1.5	-1.5
	-1.5	+1.2	-1.7	-1.3
$^{201}\text{Tl}$	+0.7	-4.5	-10.5	<sup>b</sup>
	+0.0	-5.3	-11.2	<sup>b</sup>
	+0.1	<sup>a</sup>	-10.8	<sup>b</sup>
$^{133}\text{Xe}$	<sup>a</sup>	+7.1	+0.2	<sup>a</sup>

**Note:** The ISOCAL-IV and the NPL-CRC have identical ionization chambers with calibrations traceable to the NPL.

<sup>a</sup> Not measured.

<sup>b</sup> The NPL-CRC value was taken as a reference.

#### 4. CONCLUSIONS

The data collected at the beginning of the 1990s, when regular checks were introduced, were compared with those obtained during the latter years. In general, it can be seen that, after the extensive replacement of radionuclide



calibrators and after the increase in the number of radionuclides used in the mid-1990s, the situation has stabilized.

Measurements with radionuclide calibrators performed in the Czech Republic during 2001 showed that the deviations of measured activities from the conventionally true values for the majority of devices lay within the limits given by the European Pharmacopoeia [5]. Although many of the devices still being used are relatively old, regular controls have prevented them from deviating from the required limits.

The international comparison of radionuclide calibrators has met its objective. It has revealed an agreement between participants and enabled an error in the calibration of the CMI's  $4\pi\gamma$  reference chamber for  $^{123}\text{I}$  and  $^{201}\text{Tl}$  to be discovered.

## REFERENCES

- [1] DEBERTIN, K., SCHRADER, H., Intercomparisons for quality assurance of activity measurements with radionuclide calibrators, Nucl. Instrum. Methods Phys. Res. A **312** (1992) 241–245.
- [2] BAKER, M., WOODS, M.J., Intercomparison of  $^{123}\text{I}$  Solution Sources in UK Hospitals, 2000, Rep. CIRM 38, National Physical Laboratory, Teddington, UK (2000).
- [3] BAKER, M., WOODS, M.J., Intercomparison of  $^{201}\text{Tl}$  Solution Sources in UK Hospitals, 2001, Rep. CIRM 47, National Physical Laboratory, Teddington, UK (2001).
- [4] DRYÁK, P., DVOŘÁK, L., Measurement of the energy response functions of the UVVVR and SIR  $4\pi\gamma$  ionisation chambers, Appl. Radiat. Isot. **37** (1986) 1071–1073.
- [5] EUROPEAN DIRECTORATE FOR THE QUALITY OF MEDICINES, European Pharmacopoeia, 4th edn, EDQM, Strasbourg (2001).

**BLANK**

# BRACHYTHERAPY

(Session 10)

**Chair**

**H. TÖLLI**  
IAEA

**Co-Chair**

**C.G. SOARES**  
United States of America

**Rapporteur**

**I.-L.C. LAMM**  
European Federation of Organisations for Medical Physics

**BLANK**

# **SOURCE SPECIFICATION AND CODES OF PRACTICE FOR BRACHYTHERAPY DOSIMETRY**

**C.G. SOARES**

National Institute of Standards and Technology,  
Gaithersburg, Maryland, United States of America  
E-mail: csoares@email.nist.gov

**H. TÖLLI**

Division of Human Health, International Atomic Energy Agency,  
Vienna

## **Abstract**

Issues concerned with source specification, methods to transfer calibrations between laboratories, radiation field parameterization for treatment planning and protocols for brachytherapy dosimetry are discussed in the paper. Comparisons are made between direct measurements of absorbed dose in tissue equivalent phantoms and indirect measurements using well type ionization chambers. The problems associated with the application of the most commonly recommended field parameterization method (American Association of Physicists in Medicine TG 43) to beta particle sources, the length of which are long compared with the range of their emitted radiation, are discussed and possible solutions are proposed. Finally, the commonalities and differences among various guidance documents on brachytherapy dosimetry measurements are explored.

## **1. SOURCE SPECIFICATION**

The goal of source specification is to produce a single quantity that represents the source output. The ideal quantity for specifying output for a brachytherapy source is the absorbed dose rate in water or tissue at a clinically relevant distance from the source. This distance varies with the application. For traditional interstitial brachytherapy treating tumours with dimensions of the order of centimetres, the relevant distance has been chosen [1] as 1 cm. For intravascular brachytherapy treating arteries with dimensions of the order of millimetres, the relevant distance has been chosen [2] as 2 mm. Measurements of absorbed dose rate at these short distances are very difficult to perform accurately because of the small source dimensions, very high dose rate gradients and the necessarily finite size of the available detectors. Therefore, for the

photon sources used in conventional brachytherapy ( $^{137}\text{Cs}$ ,  $^{192}\text{Ir}$ ,  $^{125}\text{I}$  and  $^{103}\text{Pd}$ ), recourse has been made to making source specification measurements in air at relatively large distances from the source, and specifying source output in terms of the air kerma rate at 1 m. Conversion factors are then used to obtain the absorbed dose rate at 1 cm. The advent of intravascular brachytherapy has led to the use of beta particle emitters ( $^{90}\text{Sr}/^{90}\text{Y}$  and  $^{32}\text{P}$ ), for which the use of any quantity at a large distance (e.g. 1 m) as a source specifier is inappropriate. Therefore, for these sources, direct measurements of the reference absorbed dose rate at 2 mm are necessary. The currently used primary standard for photon brachytherapy source specification is (in the United States of America) the wide angle free air chamber, which is a specially designed true free air chamber for realizing the quantity of the air kerma rate. For beta particle sources, extrapolation chambers equipped with very small (less than 1 mm diameter) collecting electrodes are used for primary standards of absorbed dose rate at 2 mm in the USA [3], the Netherlands [4] and Germany [5]. There is no primary standard for the dosimetry of high dose rate  $^{192}\text{Ir}$  sources; rather, indirect methods are used that are traceable to air kerma standards for X rays and gamma rays [6]. For low dose rate  $^{192}\text{Ir}$  a standard exists in the USA, based on the work of Loftus [7].

Other quantities have been employed in the past to specify the output of brachytherapy sources. Until relatively recently, mg Ra equivalency was used [1], which is related to the idea of apparent activity. Both of these specifiers are based on the effect of the sources on detectors at a distance, but have activity units, so are a mixture of radioactivity and dosimetry concepts. Recently, the measurement of contained activity of brachytherapy sources has matured [8] to the extent that it might be proposed that this quantity be used to specify these sources. The advantage of this is that the contained activity can be measured at a precision of the order of a few per cent, comparable with what is possible with the reference air kerma rate. The conversion from contained activity to the dose in water or tissue at the reference point can be determined by calculational techniques and confirmed by measurements, at least within the measurement uncertainty. The disadvantage is that the quantity contained activity conveys no information about the distribution of the radioactivity within the source matrix. Since uniform distribution is assumed in the theoretical modelling used to predict the reference dose rate per unit contained activity, real sources with less than perfect activity distributions can yield reference absorbed dose rates at some variance from that predicted from the contained activity.

Another alternative for a source specification for beta particle sources is the absorbed dose rate to water or tissue at a depth of 0.07 mm, measured in air at a distance of 30 cm from the source [9]. This is a direct analogy to the case

of photon emitting sources, for which the air kerma rate is the source specifier. The advantage of this quantity is that it is relatively easy to measure accurately with readily available equipment. Accuracies of 1–2% are achievable, in contrast to the 8–15% achievable with current methods [3–5]. The disadvantage is that the quantity measured is not the quantity desired, and a conversion factor is necessary to determine the absorbed dose rate in water at the reference distance. The uncertainty of the end result is the same by either method, since the conversion factor would carry the same large uncertainty that the direct measurement has. For this reason, the authors feel that the direct measurement of the absorbed dose rate at the reference distance is the preferred method for source specification by primary standards laboratories, both for beta particle sources and for photon sources.

## 2. TRANSFER OF CALIBRATIONS BETWEEN LABORATORIES

The primary standards are transferred to secondary laboratories and/or therapy centres using various transfer standard instruments. The most commonly used instrument for this purpose is the well type ionization chamber, which has the advantage of very high precision, simplicity of operation and a reasonable cost. Since the nature of the reading obtained from such a device is more akin to the contained activity, the disadvantage of the device is that it provides no information on the uniformity of the absorbed dose rate at the reference distance, either along the source length or around the source axis. It has been suggested that it is more appropriate, particularly for beta particle sources, to make a direct measurement of absorbed dose using another type of transfer instrument, such as a small volume plastic scintillator [10, 11]. Measurements of this type are quite difficult and fraught with pitfalls and uncertainties. Since the dose rate gradients at a reference distance of 2 mm are so high, around 100% per mm, positioning accuracies must be very high, since an error of even 0.1 mm can cause an error of 10% in the measurement. For this reason these measurements must be made carefully, with special equipment. If measurements of seed trains are made, several measurements around the source axis should be made, and repeated insertions and withdrawals of the source train should be performed, because of tumbling of the seeds in the delivery catheter. Special catheters with minimal inner diameters to position the sources more precisely in the measurement phantom must be used. Because well ionization chambers are less sensitive to variations of source positioning within the catheter, they are easier to use, although it is prudent to make measurements with several source orientations and insertions. To provide the information needed on source uniformity (at least), qualitative measurements

should be performed with an imaging detector, such as radiochromic film. The film need not be calibrated for uniformity measurements, since only relative measurements are needed. However, properly calibrated radiochromic film in an appropriate phantom is a third alternative for the measurement of the reference absorbed dose rate.

At the National Institute of Standards and Technology (NIST) all three methods are routinely used to measure the reference absorbed dose rate. Well chamber measurements are performed with Standard Imaging<sup>1</sup> chambers. For Guidant <sup>32</sup>P wire sources, the model high dose rate 1000+ chamber, equipped with the Guidant needle insert, is used, while for Novoste <sup>90</sup>Sr/<sup>90</sup>Y train sources the model IVB 1000 chamber equipped with the Novoste insert is used. Guidant sources are stepped along the chamber axis at 2 mm increments to determine the location of maximum response. This is repeated at four orthogonal source orientations, and the results are averaged. The chamber used for <sup>32</sup>P measurements is calibrated in terms of contained activity, with sources calibrated by the NIST Radioactivity Group [8]. Conversion factors between the measured contained activity and the reference absorbed dose rate were determined by a combination of extrapolation chamber measurements and Monte Carlo calculations, both for the 27 mm [12] and the 20 mm [13] source lengths. The chamber used for <sup>90</sup>Sr/<sup>90</sup>Y source train measurements was calibrated using reference sources that were calibrated using the primary standard extrapolation ionization chamber. Sources are injected into the chamber using the Novoste three lumen therapy catheter positioned against the stop of the insert, which has settings for each of the three lengths of sources used.

Radiochromic film is calibrated at NIST using an ophthalmic applicator, which was calibrated using the primary standard extrapolation chamber. A specially designed phantom, constructed using A150 tissue equivalent plastic, is used for Novoste sources. The sources are injected into the measurement position in special single lumen measurement catheters that have nominal inner diameters of 0.74 mm and outer diameters of 1.20 mm. For Guidant <sup>32</sup>P sources the source filming phantom supplied with the afterloader is used, which is made from polystyrene. GafChromic type HD-810 is used for the measurements; this film consists of a nominal 0.007 mm sensitive layer coated on to a 0.1 mm polyethylene terephthalate base. The films are read using a laser densitometer with a 0.1 mm diameter spot size, stepped in 0.16 mm increments in two dimensions across the film. The results are expressed as 1 mm (six pixel) averages along the

---

<sup>1</sup> In this paper certain commercially available products are referred to by name. This is done for informational purposes only and does not imply that these products are the best or only products available for the purpose, and does not imply endorsement by NIST or the IAEA.



source axis, with the central two thirds of the nominal source length averaged to yield the reference absorbed dose rate.

The third method employed for routine source measurements at NIST is the PTW OPTIDOSE scintillator system. This system uses a 1 mm diameter by 1 mm thick plastic scintillator as the detection element, and the sources are measured in special polymethylmethacrylate (PMMA) phantoms. The scintillator probe can be placed at one of several depths using PMMA plugs with end thicknesses to simulate the desired depth in water. The system was calibrated using brachytherapy sources calibrated at NIST. Precautions must be taken with this system, particularly with the phantom used for the  $^{32}\text{P}$  source measurements, because the diameter of the hole in the phantom into which the source is placed is too large, and errors as great as  $\pm 15\%$  can be made if multiple readings to obtain an average representation of the source in the centre of the hole are not made. For  $^{90}\text{Sr}/^{90}\text{Y}$  source measurements, the same single lumen catheter used for the film measurements is used in the special PTW/Novoste PMMA phantom.

In Tables I–III results using the three different methods are presented for a number of different sources. What is of interest in these comparisons is the standard deviations of the averages of the ratios. It is seen that those obtained

TABLE I. COMPARISON OF MEASUREMENTS OF  $^{32}\text{P}$  WIRE SOURCES

Source serial number	Length (mm)	Reference dose rate (Gy/min)			Ratio	
		WIC <sup>a</sup>	Radiochromic film	Scintillator	Film/WIC	Scintillator/WIC
010608003	27	17.16	—	18.16	—	1.058
010821015	20	3.95	—	4.34	—	1.099
011024011	20	34.5	34.0	36.1	0.986	1.046
011113013	20	23.1	21.4	22.7	0.926	0.983
020131006	27	7.37	7.18	7.66	0.975	1.039
020206018	20	24.7	22.5	24.5	0.912	0.992
020425003	20	18.32	16.43	18.78	0.897	1.025
020506001	20	34.7	34.0	35.1	0.980	1.011
020618002	27	10.67	10.32	10.79	0.967	1.011
020724015	20	32.1	28.6	34.5	0.892	1.074
020814003	20	19.89	17.49	19.57	0.879	0.984
				Average	0.935	1.029
				Standard deviation	0.042	0.038

<sup>a</sup> WIC: well ionization chamber.

TABLE II. COMPARISON OF MEASUREMENTS OF  $^{90}\text{Sr}/^{90}\text{Y}$  SEED TRAIN SOURCES

Source serial number	Length (mm)	Reference dose rate (mGy/s)			Ratio	
		WIC <sup>a</sup>	Radiochromic film	Scintillator	Film/WIC	Scintillator/WIC
151/98	30	93.1	89.6	92.6	0.962	0.995
743/99	40	103.5	101.2	100.5	0.978	0.971
769/99	40	101.9	103.7	—	1.018	—
N24	60	89.8	88.8	89.0	0.989	0.991
255/01	40	91.7	87.9	90.8	0.959	0.990
02/96	30	73.7	72.7	75.5	0.986	1.024
				Average	0.982	0.994
				Standard deviation	0.021	0.019

<sup>a</sup> WIC: well ionization chamber.

with  $^{90}\text{Sr}/^{90}\text{Y}$  sources are about a factor of two smaller than those obtained with  $^{32}\text{P}$  sources. This is a direct result of the tighter tolerances of the source placement in one system relative to the other. No conclusions concerning which system yields the most accurate results can be drawn from these data. All systems yield comparable results. It can be stated, however, that the well chamber is the easiest and most foolproof of the three, and is therefore recommended for routine use in the clinic, with the caveat that a qualitative assessment of the source uniformity must also be made for each source measured. Uniformities should be within  $\pm 10\%$  of the average over the central two thirds of the nominal source length [2] for the calibration of the well chamber to be relevant to the source being measured.

3. RADIATION FIELD PARAMETERIZATION

The determination of the reference absorbed dose rate for a source is just one part of the process of specifying the complete three dimensional representation of the absorbed dose distribution around the source needed for treatment planning. This specification can most conveniently be done by parameterizing the radiation field in a convenient co-ordinate system. For

TABLE III. COMPARISON OF MEASUREMENTS OF  $^{90}\text{Sr}/^{90}\text{Y}$  JACK-ETED TRAIN SOURCES

Source serial number	Length (mm)	Reference dose rate (mGy/s)			Ratio	
		WIC <sup>a</sup>	Radiochromic film	Scintillator	Film/ WIC	Scintillator/ WIC
ZA 100	30	66.4	67.9	67.4	1.023	1.015
ZA 123	60	98.7	98.5	100.4	0.998	1.017
ZA 138	40	98.8	99.1	98.2	1.003	0.994
ZA 427	30	97.2	96.3	97.7	0.991	1.005
ZA 428	30	97.0	95.9	98.5	0.989	1.015
ZA 348	40	96.8	97.6	98.9	1.008	1.022
ZA 105	40	97.6	99.6	96.8	1.020	0.991
ZA 352	40	93.0	93.4	90.8	1.004	0.976
ZA 262	60	97.6	98.6	98.6	1.010	1.010
ZA 522	30	101.5	97.0	104.7	0.956	1.031
ZA 525	30	101.6	99.7	106.9	0.982	1.052
ZA 511	40	119.4	119.5	117.4	1.001	0.983
ZA 614	40	119.8	122.4	121.9	1.022	1.017
ZA 301	60	103.4	105.6	107.2	1.021	1.036
ZA 302	60	99.6	101.0	105.8	1.015	1.063
ZA 307	60	102.2	102.6	102.6	1.003	1.004
				Average	1.003	1.015
				Standard deviation	0.018	0.023

<sup>a</sup> WIC: well ionization chamber.

brachytherapy sources, which are usually more line like at close distances than point like, a cylindrical co-ordinate system is convenient. If the dose profile is symmetric about the source axis (behaviour that is usually prudent to verify, particularly for intravascular applications), then the dose profile can be described in terms of the remaining two dimensions in a tabular form away from the source and along the source axis. In recent years such descriptions have given way to a description using a spherical co-ordinate system for which, again, symmetry about the source axis is assumed, and the remaining polar co-ordinates are used for field specification. However, in this approach [1] the large gradients due to the inverse square dependence of the field are accounted for in a separate parameter (the geometry function) and the remaining field

parameters (the radial dose function and the anisotropy function) are much more slowly varying with distance and hence easier to interpolate in tabular form. Use of this formalism, originally developed for interstitial brachytherapy applications, has been extended for use in intravascular applications [2].

The TG 43 formalism was the result of the American Association of Physicists in Medicine (AAPM) Task Group Number 43 recommendations on the dosimetry of interstitial brachytherapy sources [1]. The formalism was originally developed to apply only to photon emitting sources used for interstitial brachytherapy. These sources are not calibrated in terms of a reference absorbed dose rate, but rather in terms of an air kerma rate corrected to a distance of 1 m, defined as air kerma strength,  $S_k$ . To obtain the absorbed dose rate in water at the reference distance of 1 cm, a conversion factor,  $\Lambda$ , the dose rate constant, is used. The formalism uses a spherical co-ordinate system with symmetry assumed about the source axis ( $\phi$  direction). Thus positions are represented in the remaining two (polar) co-ordinates,  $r$  and  $\theta$ . Figure 1 shows a representation of this co-ordinate system. Using the formalism, the absorbed dose rate,  $\dot{D}(r, \theta)$ , is given by:

$$\dot{D}(r, \theta) = S_k \Lambda [G(r, \theta)/G(r_0, \theta_0)] g(r) F(r, \theta) \quad (1)$$

The definitions of the new parameters,  $G(r, \theta)$ ,  $g(r)$  and  $F(r, \theta)$ , are given in the following sections. The reference location  $(r_0, \theta_0)$  is  $r_0 = 1$  cm and  $\theta_0 = 90^\circ$ .

### 3.1. The geometry factor, $G(r, \theta)$

As stated above, the geometry function accounts for the inverse square dependence of the absorbed dose profile. It should be emphasized that it is only a convenient construct, meant to make the interpolations of the other parameters more accurate, so its definition can be somewhat arbitrary. The value of the geometry factor is calculated under the line source approximation as:

$$G(r, \theta) = \frac{\beta}{Lr \sin(\theta)} \quad (2)$$

where  $L$  is a length, usually taken as the active source length, and  $\beta$  is the angle subtended by the source length  $L$  at the point  $(r, \theta)$ . Referring to Fig. 1, it can be seen that  $\beta = \theta_2 - \theta_1$ . The geometry function is meant to represent the absorbed dose distribution in the absence of scattering and absorption for a line source of length  $L$ .

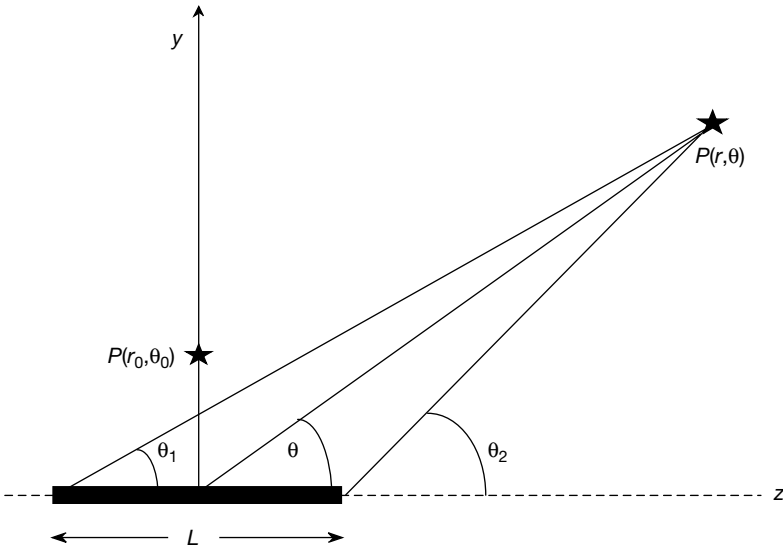


FIG. 1. AAPM TG 43 geometry.

### 3.2. The radial dose function, $g(r)$

The radial dose function represents the variation of the absorbed dose rate along the perpendicular bisector of the source, and includes the effects of absorption and scatter in water or tissue. It can be calculated from the radial dose profile,  $\dot{D}(r, \theta_0)$ , by:

$$g(r) = \left( \frac{\dot{D}(r, \theta_0)}{\dot{D}(r_0, \theta_0)} \right) \left( \frac{G(r_0, \theta_0)}{G(r, \theta_0)} \right) \quad (3)$$

The quantity in the first set of brackets is simply the radial dose profile, expressed in polar co-ordinates.

### 3.3. The anisotropy function, $F(r, \theta)$

The anisotropy function represents the variation of the absorbed dose rate around the source, in the  $\theta$  direction, and includes the effects of absorption and scatter in water or tissue. It can be calculated from the off-axis dose profile, appropriately converted to polar co-ordinates, by:

$$F(r, \theta) = \left( \frac{\dot{D}(r, \theta)}{\dot{D}(r, \theta_0)} \right) \left( \frac{G(r, \theta_0)}{G(r, \theta)} \right) \quad (4)$$

Again, the quantity in the first set of brackets is simply the off-axis dose function, normalized to unity at  $\theta_0$ .

### 3.4. Problems with the formalism for beta particle line sources

There are problems with the use of this formalism with beta particle sources, which are longer than the range of the emitted beta particles. Consider a point 2 mm out and 8 mm along a 27 mm long  $^{32}\text{P}$  wire source. If the source is uniform, then the dose rate at a distance of 2 mm from the source axis is known to be constant along the source axis to within about 5 mm from each end of the wire. Therefore,  $\dot{D}(r, \theta) = \dot{D}(r_0, \theta_0)$  for this point. However, the quantity  $\dot{D}(r, \theta_0)$  is nearly zero, since  $r = 8.246$  mm, which is near the end of the range of the beta particles of maximum energy emitted by  $^{32}\text{P}$ . Therefore, considering Eq. (4), the value for  $F(r, \theta)$  must be very large. Large values for  $F(r, \theta)$  bring us back to the situation of the large cell to cell differences in the away and along tables, a situation that the TG 43 formalism was designed to avoid. It has been suggested [14–16] that rather than use the spherical co-ordinate system of TG 43, a cylindrical co-ordinate system for long sources should be used. All these authors have suggested an alternative cylindrical formalism such that:

$$\dot{D}(\rho, z) = \dot{D}(\rho_0, z_0) [G(\rho, z)/G(\rho_0, z_0)] g(\rho) F(\rho, z) \quad (5)$$

where, as in Eq. (2),  $G(\rho, z)$  is calculated in the line source approximation, using the co-ordinate transformations  $\rho = r \sin(\theta)$  and  $z = r \cos(\theta)$ . In the central region where  $\dot{D}(\rho, z)$  is independent of  $z$ , Eq. (5) reduces to:

$$\dot{D}(\rho) = \dot{D}(\rho_0, z_0) [G(\rho, z_0)/G(\rho_0, z_0)] g(\rho) \quad (6)$$

This approach represents an improvement in the situation; however, the cell to cell variation is only marginally improved, especially near the source ends.

An alternative approach is to model long sources as a train of short segments. One of the motivations that drove one of the authors [17, 18] to calculate only a 3 mm wire segment for  $^{32}\text{P}$  was the desire to model dose distributions from non-uniform sources, as well as to study the effect of changes in source length. There was also the desire to maintain some degree of correspondence to the other two major systems that employ short (2.5 mm or 3 mm)

source segments. With a 3 mm wire segment there are no problems with breakdown in the TG 43 formalism. In addition, it is possible to make dose profile calculations for a curved source, as can also be done with seed based sources using the TG 43/TG 60 formalism. This is a very powerful argument for not changing the formalism, but rather to use data for a shorter wire segment to model the dose distribution for a longer source.

#### 4. STANDARDS, PROTOCOLS, RECOMMENDATIONS AND GUIDANCE DOCUMENTS

Modern protocols for brachytherapy dosimetry started with the work of the Interstitial Collaborative Working Group, published in 1990, which evolved into the AAPM TG 43 recommendations, published in 1995 [1]. Since then there have been a number of guidance documents and codes of practice published by AAPM working groups on brachytherapy, the latest being the work of TG 60 on intravascular brachytherapy [2]. These latter recommendations have been supplemented by the work of the Deutsche Gesellschaft für Medizinische Physik (DGMP) Working Group 18, which published Report 16 in 2001 [11]. The IAEA has published a series of technical documents on brachytherapy dosimetry, the latest being IAEA-TECDOC-1274 in 2002 [6]. Also, the International Commission of Radiation Units and Measurements (ICRU) is publishing recommendations on the dosimetry of beta particle and low energy photon sources used for medical applications [17], and the Endovascular Groupe Européen de Curiethérapie/European Society for Therapeutic Radiology and Oncology (EVA/ESTRO) has published recommendations for prescribing, recording and reporting in intravascular brachytherapy [19]. Finally, there is an initiative to create an International Organization for Standardization (ISO) standard on the dosimetry of beta particle brachytherapy sources [10]. There are commonalities and differences among these various guidance documents. Of interest in this paper are those that deal with dosimetry and source specification. Table IV shows a comparison of the various documents, indicating which sources are covered, which reference distances are recommended, and whether the documents contain data and recommended dose calculation formalisms and how calibrations are to be transferred and verified at the clinical level. From Table IV it can be inferred that there are two distinct genealogies of these documents, as indicated by the transfer methods recommended. The North American approach advocating that well chambers are sufficient for this purpose is taken in the AAPM, IAEA and ICRU documents. The European approach advocating that absorbed dose should be measured directly is taken in the DGMP and EVA/ESTRO docu-

TABLE IV. COMPARISON OF RECOMMENDATIONS DOCUMENTS FOR BRACHYTHERAPY

Document	Source	Reference distance	Data	Formalism	Transfer method
AAPM TG 43 [1]	$^{192}\text{Ir}$ , $^{125}\text{I}$ , $^{103}\text{Pd}$	1 cm	Yes	TG 43	—
AAPM TG 60 [2]	Intravascular sources	2 mm (seed and line), 0.5 mm shell	No	TG 43/TG 60	—
DGMP Report 16 [11]	Intravascular sources	2 mm (intracoronary), 5 mm (peripheral)	No	—	Measure reference absorbed dose
EVA/ESTRO [19]	Intravascular sources	—	No	Radial only, away and along, TG 43/TG 60	Measure reference absorbed dose
IAEA-TECDOC-1274 [6]	All brachytherapy sources	1 mm (ophthalmic), 2 mm (seed and line), 0.5 mm (shell)	No	TG 43/TG 60	Use well ionization chamber and film
ICRU Report No. 72 [17]	$^{125}\text{I}$ , $^{103}\text{Pd}$ , $^{90}\text{Sr}/^{90}\text{Y}$ (seed and planar), $^{106}\text{Ru}/\text{Rh}$ (concave), $^{32}\text{P}$ , others	1 mm (ophthalmic), 2 mm (seed and line), 0.5 mm (shell)	Yes	TG 43/TG 60	Use well ionization chamber and film
ISO ad hoc group [10]	Beta intravascular and ophthalmic only	1 mm (ophthalmic), 2 mm (intracoronary), 5 mm (peripheral)	?	Radial only, away and along, TG 43/TG 60	Measure reference absorbed dose and/or well ionization chamber/film



ments. It is the opinion of the authors that the two approaches should be thought of as being complementary, rather than favouring one over the other. It is hoped that this dual approach will be adopted in the forthcoming ISO recommendations.

## REFERENCES

- [1] NATH, R., et al., Dosimetry of interstitial brachytherapy sources: Recommendations of the AAPM Radiation Therapy Task Group No. 43, *Med. Phys.* **22** (1995) 209–234.
- [2] NATH, R., et al., Intravascular brachytherapy physics: Report of the AAPM Radiation Therapy Committee Task Group No. 60, *Med. Phys.* **26** (1999) 119–152.
- [3] SOARES, C.G., HALPERN, D., WANG, C.-K., Calibration and characterization of beta-particle sources for intravascular brachytherapy, *Med. Phys.* **25** (1998) 339–346.
- [4] VAN DER MAREL, J., VAN DIJK, E., “Development of a Dutch primary standard for beta emitting brachytherapy sources”, these Proceedings, Vol. 2, pp. 93–100.
- [5] SELBACH, H.-J., SOARES, C.G., “New developments on primary standards for brachytherapy at the National Institute of Standards and Technology and the Physikalisch-Technische Bundesanstalt”, *ibid.*, Vol. 2, pp. 101–110.
- [6] INTERNATIONAL ATOMIC ENERGY AGENCY, Calibration of Photon and Beta Ray Sources Used in Brachytherapy, IAEA-TECDOC-1274, IAEA, Vienna (2002).
- [7] LOFTUS, T.P., Standardization of iridium-192 gamma-ray sources in terms of exposure, *J. Res. Natl. Bur. Stand.* **85** (1980) 19–25.
- [8] COLLÉ, R., Chemical digestion and radionuclidic assay of TiNi-encapsulated  $^{32}\text{P}$  intravascular brachytherapy sources, *Appl. Radiat. Isot.* **50** (1999) 811–833.
- [9] SOARES, C.G., Consistency standards for source strength of beta-particle sources, *Vasc. Radiother. Monit.* **3** (2001) 59–63.
- [10] QUAIST, U., BÖHM, J., KAULICH, T.W., “The need for international standardization in clinical beta dosimetry for brachytherapy”, these Proceedings, Vol. 2, pp. 111–119.
- [11] QUAIST, U., KAULICH, T.W., FLÜHS, D., Guideline for medical physical aspects of intravascular brachytherapy. DGMP Report No. 16 (2001). Part I: Guideline, *Z. Med. Phys.* **12** (2002) 47–64; Part II: Samples and examples, *Z. Med. Phys.* **12** (2002) 133–148.
- [12] MOURTADA, F.A., SOARES, C.G., SELTZER, S.M., LOTT, S.H., Dosimetry characterization of a  $^{32}\text{P}$  catheter-based vascular brachytherapy source wire, *Med. Phys.* **27** (2000) 1770–1776.
- [13] MOURTADA, F.A., et al., Dosimetry characterization for  $^{32}\text{P}$  source wire used for intravascular brachytherapy with automated stepping, *Med. Phys.* (in press).

- [14] SCHAART, D.R., CLARJIS, M.C., BOS, A.J.J., On the applicability of the AAPM TG-60/TG-43 dose calculation formalism to intravascular line sources: Proposal for an adapted formalism, *Med. Phys.* **28** (2001) 638–653.
- [15] PATEL, N.S., CHIU-TSAO, S.T., TSAO, H., HARRISON, L.B., A new treatment planning formalism for catheter-based  $\beta$  sources used in intravascular brachytherapy, *Card. Rad. Med.* **2** (2001) 157–164.
- [16] WANG, R., LI, X.A., Monte Carlo characterization of a  $^{32}\text{P}$  source for intravascular brachytherapy, *Med. Phys.* **28** (2001) 1776–1785.
- [17] INTERNATIONAL COMMISSION ON RADIATION UNITS AND MEASUREMENTS, ICRU Report No. 72: Dosimetry of beta rays and low-energy photons for brachytherapy with sealed sources, J. ICRU (in press).
- [18] SOARES, C.G., “Dosimetric issues in vascular brachytherapy (TG-43/60)”, *Intravascular Brachytherapy/Fluoroscopically Guided Interventions* (BALTER, S., CHAN, R.C., SHOPE, T.B., Jr., Eds), Medical Physics Monograph No. 28, Medical Physics Publishing, Madison, WI (2002) 321–371.
- [19] PÖTTER, R., et al., Recommendations of the EVA GEC ESTRO working group: Prescribing, recording and reporting in endovascular brachytherapy. Quality assurance, equipment, personnel and education, *Radiother. Oncol.* **59** (2001) 339–360.

## DEVELOPMENT OF A DUTCH PRIMARY STANDARD FOR BETA EMITTING BRACHYTHERAPY SOURCES

J. VAN DER MAREL, E. VAN DIJK  
Nederlands Meetinstituut,  
Utrecht, Netherlands  
E-mail: hvdmarel@nmi.nl

### Abstract

The Nederlands Meetinstituut is developing a new primary standard for the dosimetry of beta radiation emitting brachytherapy sources in terms of absorbed dose to water. This standard is based on an extrapolation chamber with a small (1 mm diameter) collecting electrode. The electrode and guard are made of aluminium, which requires the determination of a correction that takes into account the different scattering behaviour of beta rays in aluminium with respect to the reference material, water. The extrapolation chamber has been tested successfully for the determination of the absorbed dose rate at the surface of a flat, cylindrical  $^{90}\text{Sr}/^{90}\text{Y}$  source. The dose distribution of the source has also been measured. The primary standard will play a key role in a quality assurance protocol for the clinical use of brachytherapy sources in Belgium and the Netherlands.

### 1. INTRODUCTION

The application of beta radiation emitting radioactive sources in medicine is rapidly expanding. An important new application is the use of beta radiation emitting radioactive sources in endovascular brachytherapy to avoid restenosis. The ophthalmic applicator (a flat or concave surface beta source) is a well known type of brachytherapy source for the treatment of tumours in the eye.

Dose and dose distributions are very important characteristics of brachytherapy sources. The absorbed dose in the treated tissue should be known accurately to ensure a good quality treatment and to develop new treatment methods and source configurations. However, owing to the short range of the beta rays, the dosimetry of these sources is quite difficult. Several detection systems, such as thermoluminescent dosimeters, radiochromic dye films, plastic scintillators, diodes, fixed volume ionization chambers and extrapolation chambers (see, for an overview, Refs [1, 2]), have been used in the dosimetry of brachytherapy sources. Most of the methods require calibration with other

radiation sources against other (primary) standards, giving rise to new problems and uncertainties. Only the extrapolation chamber can be used as a primary standard. Currently, only at the National Institute of Standards and Technology in the United States of America is such a primary standard in operation.

To serve the manufacturers and users of both endovascular and ophthalmic beta sources, a project was initiated in 2000 by the Nederlands Meetinstituut (NMI) for the development of a primary standard for the dosimetry of these sources. The primary standard consists of an extrapolation chamber with a small measuring electrode with a guard electrode, both made of aluminium, and a scanning mechanism to measure both dose and dose distributions. The standard will become a part of a quality assurance protocol for clinical practice, which is currently under development by a task group of the Nederlandse Commissie voor Stralingsdosimetrie (NCS).

## 2. THE DUTCH PRIMARY STANDARD

### 2.1. Extrapolation chamber

The measurement of absorbed dose in tissue with an extrapolation chamber is based on the Bragg–Gray principle. Owing to the limited range of beta rays, the best approach for the Bragg–Gray cavity is an infinitesimal volume. Obviously, ionization cannot be measured in such a volume, and therefore the ionization at zero volume is derived from the extrapolation of the measured values of the ionization current at a number of different (but small) air volumes. For an ionization chamber with a fixed electrode area and a variable electrode separation,  $d$ , the absorbed dose rate in water,  $\dot{D}_w$ , can be expressed as:

$$\dot{D}_w = s_{w/a} \left( \frac{\bar{W}_a k_1}{eA\rho_0} \right) \left( \frac{d(k_2 I)}{dd} \right)_{d \rightarrow 0} \quad (1)$$

where  $s_{w/a}$  is the ratio of the stopping powers between water and air,  $\bar{W}_a$  is the average energy required to produce an electron–ion pair in air,  $e$  is the electron charge,  $A$  is the surface of the collecting electrode,  $\rho_0$  is the density of air at standard pressure, temperature and humidity,  $I$  is the ionization current and  $k_1$  and  $k_2$  are groups of correction factors to compensate for the fact that a practical extrapolation chamber does not completely fulfil the Bragg–Gray conditions and that the measurement conditions can vary.

The set-up of the extrapolation chamber of the NMi is shown in Fig. 1. The central part of the extrapolation chamber is the electrode. It consists of a small central (collecting) electrode (diameter 1 mm) surrounded by a large guard electrode. Both the central and guard electrodes are made of aluminium; aluminium was chosen as it can be machined accurately and smoothly. Between the central and the guard electrode there is a small gap of 50  $\mu\text{m}$ . Measurements with different sizes of the central electrode in a parallel X ray beam showed that the effective area of the central electrode is equal to the area of the electrode plus the inner half of the gap.

The extrapolation chamber is mounted in the downward direction on a platform, which is supported by three legs. The central and guard electrode are mounted on a translation stage with a resolution of 0.1  $\mu\text{m}$ , equal to the accuracy of the calibration of the movement, which moves the electrode up and

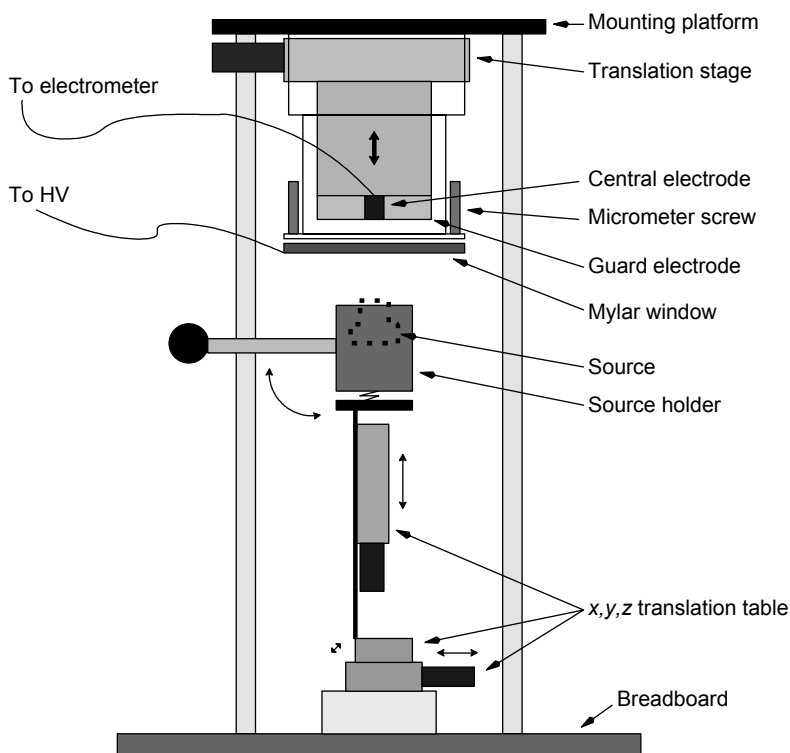


FIG. 1. Extrapolation chamber set-up at the NMi.

down. The entrance window of the extrapolation chamber (12  $\mu\text{m}$  thick single sided aluminized polyethylene terephthalate (Mylar)) is mounted statically on the platform over a hollow cylinder in which the electrode can move. The entrance window can be adjusted with three micrometer screws in order to be exactly parallel with the electrode. This adjustment can be done with an accuracy of 2 arcsec with the help of an autocollimator.

A source holder has been mounted on a motorized  $x,y,z$  translation table. This allows the accurate positioning of the source in the horizontal ( $x,y$ ) plane under the chamber and allows the making of a scan of the dose distribution of the source. For reproducible dose rate measurements it is required that the source (for surface dose rate measurements) or the phantom containing the source (for depth dose measurements) be just in contact with the entrance window. A special procedure in the data acquisition program, together with the  $z$  axis translation stage, enables the automatic positioning of the source in the direction of the entrance window of the extrapolation chamber.

The ionization current in the chamber is measured by means of a Keithley 6517A electrometer, which also supplies the voltage at the entrance window. Throughout the measurements a constant electric field of 100 V/mm is maintained. The whole set-up, including the monitoring of ambient conditions, is controlled by a data acquisition program, written in Delphi.

## 2.2. Correction factors

Owing to the fact that extrapolation chambers are never ideal, correction factors are needed to convert the measured data into an absolute dose rate. As can be seen in Eq. (1), the correction factors are divided into two groups:  $k_1$  contains correction factors that have a constant value (i.e. corrections for the entrance window, decay of the source and air density) and  $k_2$  contains correction factors that depend on the electrode separation,  $d$ . Owing to the application of aluminium central and guard electrodes,  $k_2$  contains (among others) a correction for the difference in backscatter properties between water and aluminium ( $k_{\text{backsc}}$ ). This dominant correction factor depends on the source geometry and on the energy spectrum of the beta radiation. For its determination it is combined with other source dependent corrections to form  $k_{\text{source}}$ , which also contains a correction for the radial inhomogeneity of the beta radiation field,  $k_{\text{rad}}$ , a correction for the divergence of the beta radiation field,  $k_{\text{div}}$ , and a correction for interface effects between the air volume and the electrode material,  $k_{\text{interf}}$ . The determination of  $k_{\text{source}}$  is strongly based on Monte Carlo calculations, for which the packages PENELOPE [3] and EGSnrc [4] have been employed, followed by experimental verification using radiochromic film. To this end, GafChromic HD-810 film is placed with the emulsion side on aluminium or a

water equivalent material and irradiated with a beta source. The ratio of the measured doses gives a value for  $k_{\text{source}}$ . It appears that  $k_{\text{source}}$  is significantly smaller than 1 and nearly constant in a range of distances close to the centre of the source, but increases rapidly at the edges of the source, reaching a maximum just outside the source area and dropping to 1 at large distances from the source. The precise shape of  $k_{\text{source}}$  mainly depends on the difference in scattering properties between water and aluminium, but is also dependent on the geometry of the source, on the energy spectrum of the beta radiation and on  $d$ . For other non-water-equivalent materials, like silicon, a similar behaviour is to be expected.

In general it is important to measure at small values of  $d$  (typically  $0.05 \text{ mm} < d < 0.2 \text{ mm}$ ) to minimize the corrections.

### 2.3. Measurement procedure

A determination of the dose rate as a function of the position on the source with the extrapolation chamber would require a complex correction,  $k_{\text{source}}$ . To avoid this we are developing a measurement procedure, which includes the use of radiochromic film. First, a source is scanned with the extrapolation chamber to create a map of the source. Next, at the centre of the source an extrapolation is performed, since at the centre  $k_{\text{source}}$  is almost constant. Subsequently, a radiochromic film is irradiated with the source, and a detailed dose rate map is created, with the dose rate from the extrapolation at the reference point taken as the normalization.

### 2.4. Measurements

Test measurements have been performed with the extrapolation chamber on a  $^{90}\text{Sr}/^{90}\text{Y}$  source from our Buchler secondary standard, which had an activity of 1.062 GBq on the date of the measurements. This source has a configuration comparable with that of ophthalmic applicators. It is a flat source with an active area diameter of 7.1 mm. The data acquisition program was used to position the source as close as possible to the entrance window. An example of an extrapolation measurement at the centre of the source is shown in Fig. 2. For this type of source  $k_{\text{source}} = 0.83 \pm 0.08$  ( $2\sigma$ ) at the centre of the source and within the range of measurements on which the extrapolation is based. The uncertainty in the correction factor is a conservative estimate, as this uncertainty is still under investigation. We obtained an absorbed dose rate in water of  $(0.27 \pm 0.03) \text{ Gy/s}$  ( $2\sigma$ ). The reproducibility of this value was better than 2% for subsequent remounting, repositioning and extrapolation.

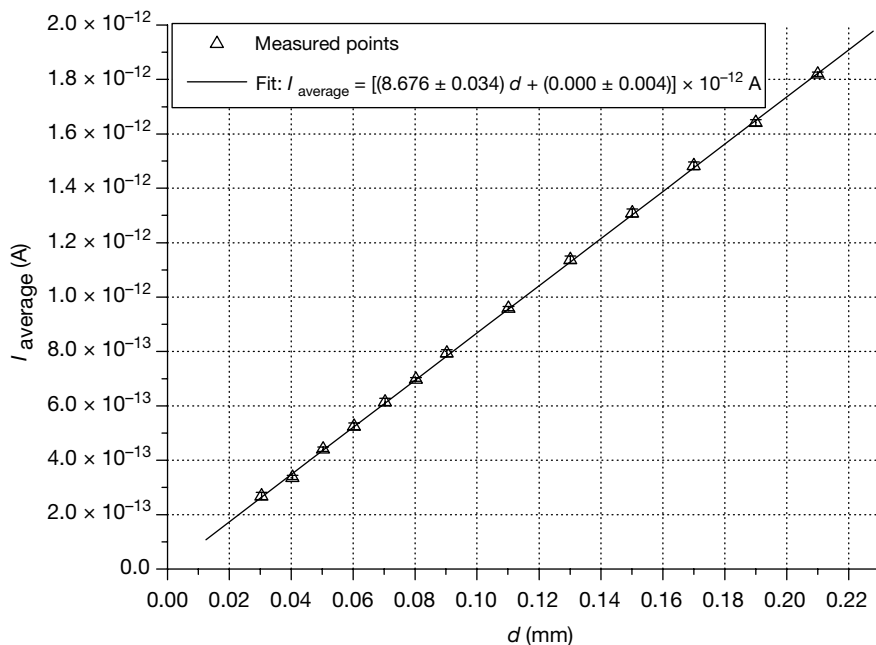


FIG. 2. Data points and fit of an extrapolation measurement at the centre of the Buchler source.

Using the above mentioned dose rate, and using the centre of the source as the reference point, we performed a measurement on the same source with radiochromic film. The resulting dose map is shown in Fig. 3. It can be seen that the activity is not completely homogeneously distributed over the surface of the source. This is in agreement with a scan with the extrapolation chamber over the surface of the source.

### 3. QUALITY ASSURANCE PROTOCOL

An investigation by a task group of the NCS in 2000 showed that little uniformity is present in the dosimetric quality control of beta emitting brachytherapy sources. A protocol for the quality assurance in the clinical practice is currently being developed by the NCS. According to this protocol both endovascular brachytherapy sources and ophthalmic applicators have to be checked regularly for strength and homogeneity; well type ionization chambers, plastic scintillators and radiochromic film will be used for this. The well type ionization chambers and the plastic scintillators will have calibration factors traceable to the extrapolation chamber at the NMI.



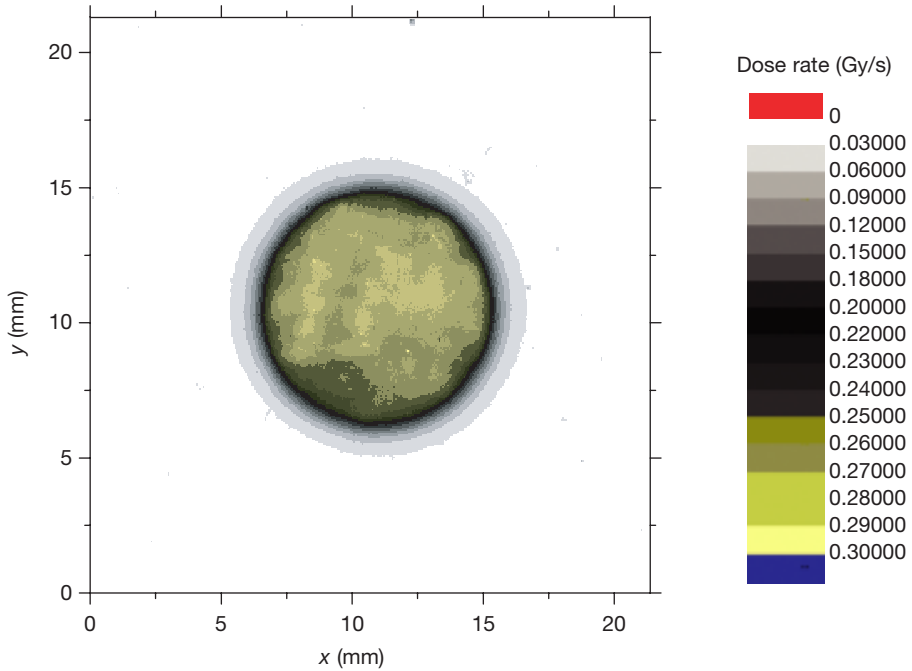


FIG. 3. Dose rate distribution of the Buchler  $^{90}\text{Sr}/^{90}\text{Y}$  source using the dose rate from extrapolation from Fig. 2 and radiochromic film.

#### 4. CONCLUSION

With the primary standard for the dosimetry of beta radiation emitting brachytherapy sources that is under development at the NMi it is possible to perform an accurate extrapolation for the determination of the dose rate in terms of absorbed dose in water. The measurement set-up is equipped with an automated positioning system for the source and an accurate translation stage for the movement of the electrode, which ensures a very good reproducibility in determining dose rates.

A number of corrections are required for the determination of the absolute dose rate, of which the combined correction factor ( $k_{\text{source}}$ ) for the source geometry and the backscattering properties of the electrode are the most difficult and dominant. The factor  $k_{\text{source}}$  has been obtained by means of Monte Carlo calculations and measurements. We are presently finalizing the determination of the corrections and the uncertainties of all the steps in the absorbed dose rate calculation. We believe that the uncertainty assigned to the dose rate in Section 2.4 can be further reduced. We are developing a procedure

to measure absolute dose rate distributions of sources with a combination of the extrapolation chamber and radiochromic film. The first results are encouraging.

## REFERENCES

- [1] SOARES, C.G., et al., Dosimetry of beta-ray ophthalmic applicators: Comparison of different measurement methods, *Med. Phys.* **28** (2001) 1373–1384.
- [2] SOARES, C.G., HALPERN, D.G., WANG, C.-K., Calibration and characterization of beta-particle sources for intravascular brachytherapy, *Med. Phys.* **25** (1998) 339–346.
- [3] SALVAT, F., FERNÁNDEZ-VAREA, J., ACOSTA, E., SEMP AU, J., PENELOPE — A Code System for Monte Carlo Simulation of Electron and Photon Transport (Proc. Workshop Issy-les-Moulineaux, France, 2001), OECD, Paris (2001).
- [4] KAWRAKOW, I., ROGERS, D.W.O., The EGSnrc Code system: Monte Carlo Simulation of Electron and Photon Transport, Rep. PIRS-701, National Research Council, Ottawa (2000).

# **NEW DEVELOPMENTS ON PRIMARY STANDARDS FOR BRACHYTHERAPY AT THE NATIONAL INSTITUTE OF STANDARDS AND TECHNOLOGY AND THE PHYSIKALISCH-TECHNISCHE BUNDESANSTALT**

H.-J. SELBACH

Physikalisch-Technische Bundesanstalt,  
Braunschweig, Germany  
E-mail: hans-joachim.selbach@ptb.de

C.G. SOARES

National Institute of Standards and Technology,  
Gaithersburg, Maryland, United States of America

## **Abstract**

As brachytherapy has become increasingly popular, mainly due to new techniques in cardiovascular and prostate cancer treatments, the traceability of clinical dose measurements to national standards has become more and more important. As a consequence, increasing activities in the field of the dosimetry of brachytherapy sources can be recognized in most of the national primary standards dosimetry laboratories (PSDLs). The status and new developments of primary standards for conventional brachytherapy sources ( $^{192}\text{Ir}$ ), low energy photon sources and beta particle seed and line sources at two PSDLs (the National Institute of Standards and Technology in the United States of America and the Physikalisch-Technische Bundesanstalt in Germany) are presented.

## **1. STANDARDS FOR THE CALIBRATION OF $^{192}\text{Ir}$ SOURCES**

The first calibration of a medical  $^{192}\text{Ir}$  source at the Physikalisch-Technische Bundesanstalt (PTB) in terms of a reference air kerma rate was performed about ten years ago. The calibration procedure, which is still maintained, consists of the calibration of a transfer ionization chamber against the PTB's primary standards for air kerma in the X ray range from 10 keV to 250 keV and in  $^{137}\text{Cs}$  and  $^{60}\text{Co}$  gamma radiation beams. By use of the known X ray spectra, the response of the transfer standard as a function of photon energy is calculated from the measured values. A subsequent integration over the  $^{192}\text{Ir}$  spectrum results in a calibration factor of the transfer standard for  $^{192}\text{Ir}$  radiation [1]. Additional shadow shield measurements are performed to determine the amount of backscatter and stray radiation.

At present, the National Institute of Standards and Technology (NIST) does not perform equivalent calibrations. Rather, the calibration established by Loftus [2] is maintained at NIST through the use of a re-entrant ionization chamber. Studies are under way at NIST to compare the method described in IAEA-TECDOC-1079 [3] with the method commonly used in the United States of America [4] for the calibration of  $^{192}\text{Ir}$  sources. Auxiliary measurements with the re-entrant ionization chamber and some additional measurements are also performed for  $^{192}\text{Ir}$  seeds at NIST. These include ‘fingerprinting’ measurements with radiochromic film, measurements in various types of well ionization chamber, high resolution gamma spectrometry and some measurements of the absorbed dose rate at various depths in a phantom with radiochromic film and scintillators.

## 2. STANDARDS FOR LOW ENERGY PHOTON SOURCES

### 2.1. Wide angle free air chamber

Starting in 1998 NIST began offering calibrations of  $^{125}\text{I}$  and  $^{103}\text{Pd}$  seeds in terms of air kerma strength using a wide angle free air chamber (WAFAC) developed by Loevinger [5]. The WAFAC has important advantages over conventional free air chambers as a primary standard for the radiation produced by these sources. It accepts a large solid angle of radiation incidence and its active volume is about 150 times larger than normal free air chambers. These advantages result in a much improved sensitivity and signal to background ratio, and allow the measurement of single sources with contained activities suitable for clinical use. The calibration of  $^{125}\text{I}$  and  $^{103}\text{Pd}$  seeds is affected by the presence of 4.5 keV Ti characteristic X rays from the seed encapsulation, which contribute to the reference air kerma but are of no therapeutic relevance. To cope with this, the source radiations are very lightly filtered to remove this component. The chamber has been compared with the existing, smaller volume standard free air chamber using NIST bremsstrahlung X ray beams with maximum energies of 40 keV and below. The relative measured air kerma rates in these beams with these chambers agree to better than  $\pm 0.5\%$ .

For measurements with the WAFAC the source is mounted on the tip of a rotating platform, which allows the averaging of any radiation field non-uniformities perpendicular to the source axis. An aluminium absorber with a mass thickness of  $23 \text{ mg/cm}^2$  is mounted about 10 cm from the source to remove the contaminant Ti K X rays from the source cladding. The front surface and reference plane of the WAFAC is 300 mm from the source and the entrance

aperture is 80 mm in diameter. Aluminized polyethylene terephthalate (PET) foils are used for both the polarizing electrode at voltage  $V$  and the 150 mm diameter collecting electrode at ground potential. The 250 mm diameter cylindrical middle electrode can be varied between 150 mm and 10 mm in length, and is kept at potential  $V/2$ , which results in a much more uniform potential distribution within the chamber volume and ensures the complete collection of the ionization charge within the chamber. Wall effects due to the front and back electrodes are removed by subtracting the current produced in the 10 mm long configuration from that produced in the 150 mm long configuration.

The air kerma strength,  $S$ , is given by:

$$S = \frac{(\overline{W}/e)I_{\text{net}}r^2}{\rho_0 V_{\text{eff}}} k \quad (1)$$

where

- $\overline{W}$  is the average energy needed to produce one coulomb of charge in dry air equal to  $33.97 \pm 0.05$  J/C;
- $I_{\text{net}}$  is the net current (corrected to reference conditions of temperature and pressure) between the 150 mm and 10 mm configurations, with leakage and background subtracted;
- $r$  is the distance from the source to the WAFAC aperture front surface;
- $\rho_0$  is the density of air at the reference temperature and pressure;
- $V_{\text{eff}}$  is the effective volume (aperture area times difference in middle electrode lengths);
- $k$  is the product of corrections to the measured current, as discussed below.

Besides the corrections for reference temperature and pressure, the current measurements are corrected for:

- (a) Radioactive decay using the half-life of the isotope being measured;
- (b) Recombination;
- (c) The attenuation of the primary radiations by the aluminium filter used to remove the Ti K X ray photons;
- (d) The attenuation of the primary photons in the air space between the source and the WAFAC front surface aperture;
- (e) The attenuation within the volume of the WAFAC;
- (f) The inverse square correction for the aperture diameter, to account for the differences in photon fluence rate over the diameter of the aperture;

- (g) Humidity;
- (h) The in-chamber photon scatter, to account for photons scattered out of the aperture defined beam, as well as for those scattered into the collection volume by the chamber itself;
- (i) The source holder stem scatter, to account for photons that are scattered into the WAFAC collection volume by the rotating platform on which the seed is placed during calibration;
- (j) The in-chamber electron loss, to account for secondary electrons that leave the collection volume before expending their entire energy in the form of ionization;
- (k) The aperture penetration, to account for incident primary photons penetrating the defining aperture;
- (l) The external photon scatter by the air between the source and the WAFAC aperture as well as by the filter, which causes a slight buildup.

For the WAFAC used with single seeds, the measurement uncertainty is largely driven by the reproducibility of the net ionization current,  $I_{\text{net}}$ . For sources of air kerma strength of less than  $25 \mu\text{Gy}\cdot\text{m}^2\cdot\text{h}^{-1}$  this can vary between 0.1% and 2.0% ( $k = 1$ ) from seed to seed. This reproducibility is affected by the magnitude of the measured currents and variations of the WAFAC leakage current during the measurement relative to these magnitudes.

In addition to measurements with the primary standard, various auxiliary measurements are made of submitted sources in order to understand better how transfer standard instruments will respond. These measurements also serve as a consistency check on the WAFAC calibration results. Source anisotropy is examined by observing the variations in the WAFAC signal as a function of seed orientation about its axis. Some types of seed can exhibit rather large relative anisotropies, exceeding  $\pm 10\%$  in some cases. All submitted sources are ‘fingerprinted’ using contact autoradiography with radiochromic film. These radiographs, when read by high resolution densitometry, reveal details of source structuring. The relationship between measured air kerma strength with the WAFAC and the response of various well type ionization chambers is established for each submitted seed [6]. This information is important for secondary laboratories and users who rely on these types of chamber to transfer NIST calibrations. Finally, photon spectra are obtained using high resolution spectrometric techniques. These measurements are important, since subtle variations in the emergent photon spectrum within a seed type explain the substantial variations observed in the responses of well ionization chambers.

## 2.2. Large volume extrapolation chamber

Although the PTB's activities are strongly orientated towards the concept of in the future providing calibrations only in terms of absorbed dose to water for all brachytherapy sources, including low and high energy photon sources (see Section 5), for the present a special extrapolation chamber with a large volume, suitable for measuring the reference air kerma rate of single  $^{103}\text{Pd}$  and  $^{125}\text{I}$  sources, has been constructed. The large volume extrapolation chamber (LVEC) is currently under investigation in regard to correction factors, which are mostly the same as those mentioned in Section 2.1. The LVEC is intended to go into operation in about one year.

Additional measurements, such as high resolution spectrometry, GafChromic film measurements and calibrations of well type ionization chambers, will also be performed to characterize the low energy photon source completely.

## 3. BETA PARTICLE SEED AND LINE SOURCES

### 3.1. NIST 1 mm extrapolation chamber

A special extrapolation chamber is used at NIST to determine the reference absorbed dose rate from a beta particle emitting seed or wire source. For these measurements the source is inserted into a hole in a tissue equivalent plastic block (A150), with the centre of the source at a distance of 2 mm from the block surface. At this depth the radiation field from a seed or wire source is such that a collecting electrode diameter of 1 mm can be used to measure the absorbed dose rate.

The absorbed dose rate is determined from current measurements at a series of air gaps; the slope of the current versus air gap function at the limit of zero air gap width is determined by curve fitting. The absorbed dose rate in water,  $\dot{D}_w$ , is then given by the Bragg–Gray relationship:

$$\dot{D}_w = \frac{(\overline{W}/e)s_{w,\text{air}}k}{\rho_0 a}(\Delta k' / \Delta \ell)_{\ell \rightarrow 0} \quad (2)$$

where

$s_{w,\text{air}}$  is the ratio of the mean mass collision stopping power of water to that of air;

- $a$  is the effective area of the collecting electrode;
- $k$  is the product of corrections to the ionization current, which do not depend on the chamber depth,  $\ell$ ;
- $k'$  is the product of corrections to the ionization current, which depend on chamber depth;
- $(\Delta I/\Delta \ell)_{\ell \rightarrow 0}$  is the rate of change of the ionization current with extrapolation chamber depth as the depth approaches zero.

The other symbols in this equation are as described for Eq. (1).

Corrections to the measured current, which depend on the chamber depth or may change during the measurement of a complete extrapolation curve, are corrections due to reference temperature and pressure, decay (for short half-life sources such as  $^{32}\text{P}$ ), recombination and the effects caused by the divergence of the radiation field. The only correction assumed to be independent of the chamber depth is that for the difference in backscatter between the material of the collecting electrode and the reference medium (water).

For the NIST extrapolation chamber with a 1 mm diameter collecting electrode, the major component of measurement uncertainty is the uncertainty in the effective area of the collecting electrode. While the physical area can be determined accurately using a travelling microscope, the fraction of the area of the insulating gap (which isolates the collecting electrode from the guard electrode), which should be included in the effective collecting electrode area, is not accurately known, owing to the relatively large width of the insulating gap (about 0.3 mm) in this electrode. Another large component of uncertainty is that in the stopping power ratio, which arises from the uncertainty in the beta particle spectrum at distances in water close to the source. This component could be reduced using careful Monte Carlo calculations to predict the beta particle spectrum, over which the stopping power ratio should be averaged.

There are limitations associated with the NIST extrapolation chamber because of the unacceptably large uncertainty ( $\pm 7.5\%$ ,  $k = 1$ ). These problems are associated with the construction of the 1 mm diameter collecting electrode (see above) and the uncertainty in the value of the limiting slope due to curvature in the current versus chamber depth function, caused mainly by the source radiation field divergence.

These problems are expected to be overcome by a new design of the collecting electrode of the extrapolation chamber, based on work already in progress at the PTB, which is described below. In addition, it is expected that a more complete analysis of the divergence effect will result in corrections that will largely remove the curvature in current versus chamber depth functions, yielding less ambiguous extrapolations of the terminal slope.



### 3.2. Multielectrode extrapolation chamber at the PTB

A new primary standard has been developed at the PTB that enables the realization of the unit of absorbed dose to water in the vicinity of beta brachytherapy sources [7]. In the course of its development, the recommendations of the American Association of Physicists in Medicine (AAPM) TG 60 [8] and the Deutsche Gesellschaft für Medizinische Physik (DGMP) Working Group 18 [9] were taken into account. The primary standard is based on a newly designed multielectrode extrapolation chamber (MEC), which meets in particular the requirements of a high spatial resolution and a small uncertainty. In contrast to a conventional extrapolation chamber, the central part of the MEC is a segmented collecting electrode, which was manufactured in the clean room centre of the PTB by means of electron beam lithography on a wafer. About 30 collecting electrodes (e.g. 1 mm × 1 mm in size) can be arranged in the centre of the wafer, with insulating gaps of only 2 µm. A precise displacement device consisting of three piezoelectric macrotranslators has been incorporated to move the wafer collecting electrode relative to the entrance window. The three piezoelectric macrotranslators, which are arranged at angles of 120° around the centre, ensure electrode positioning to within a standard uncertainty of 0.2 µm. The entire stroke mechanism has been built on a two axis positioning system, allowing the continuous scanning of the absorbed dose rate distribution. The spatial resolution can be improved using wafers with smaller collecting areas, and individual wafers can be designed for different measurement situations. An electromechanical adjustment system based on a capacitance bridge circuit has been developed for the adjustment of the wafer collecting electrode to be parallel to the entrance foil. This procedure allows the wafer to be adjusted parallel to the entrance foil within an angular deviation of less than 100 µrad.

The MEC allows a three dimensional dose distribution to be measured with high spatial resolution without having to rely on an additional relative dosimetry system, thus avoiding additional uncertainties. A measuring microscope insert is intended for the necessary lateral adjustment between the source axis and the collecting electrode. A defined lateral positioning of better than 50 µm should thus become possible. Extrapolation chamber measurements in the vicinity of a plane beta source have proved the suitability of the MEC as a primary standard. With sizes of collector electrodes as small as 1 mm × 1 mm and a dose rate of approximately 10 Gy/min, calibrations were performed with a relative combined standard uncertainty of 3.8%. The relative reproducibility of the MEC is 1.5% ( $k = 1$ ).

#### 4. BETA SECONDARY STANDARD

To enable clinics practising the irradiation of coronary vessels to ensure the traceability of their dose measurements, the PTB has developed a secondary standard for cardiovascular brachytherapy using beta radiation sources. This standard consists of a  $^{90}\text{Sr}/^{90}\text{Y}$  extended beam source about 15 mm in diameter with an activity of about 7.5 GBq, which is enclosed in a suitable protective casing. To provide different dose rates the source can be brought into five different beam positions (at distances of between 1.7 mm and 50 mm from a reference area) by means of a precise mechanical system almost free from play. This results in a 40 fold dose rate variation. Directly in the reference plane and behind several tissue equivalent layers, the thicknesses of which are 0.1–8 mm, the water absorbed dose rate is determined using an extrapolation chamber as a primary standard measuring device. In addition, the radial dose rate distribution is measured for each of the different layer thicknesses with the aid of a special ionization chamber of a high spatial resolution. With this secondary standard, which is produced under licence by a German manufacturer and calibrated at the PTB, the clinical user gets a beta radiation field in a water equivalent medium that is specified in three dimensions in terms of dose rate and shows properties similar to fields from clinical radiation sources. By the calibration of dosimeters in this radiation field, the user can ensure that the dose measurements are traceable to the national standards of the PTB.

The main uncertainties in the calibration of the secondary standard are due to the correction factors accounting for the radial dose distribution and the source radiation field divergence. The latter correction has been determined by Monte Carlo calculations using the MCNP4-C code, which has shown that the curvature in current versus chamber depth functions is nearly completely removed when this correction is applied.

The overall relative uncertainty ( $k = 2$ ) of the calibration of the secondary standard is 7.5%. In the future the specification of similar reference radiation fields for  $^{106}\text{Ru}/^{106}\text{Rh}$  is planned.

#### 5. PRIMARY STANDARD FOR ABSORBED DOSE TO WATER FOR PHOTON SOURCES

The German Radiology Standards Committee (NAR, Normenausschuss Radiologie) has made a decision in favour of the use of absorbed dose to water for all dose measurements in radiation therapy. Consequently, in the future all sources used in brachytherapy, including high and low energy photon sources, should be calibrated in units of absorbed dose to water in a water phantom

instead of in terms of the air kerma rate in free air, as performed now. To provide future calibrations of brachytherapy photon sources in the energy range from 20 keV to 1.2 MeV, the PTB is extending the energy range of its existing primary standard [10] for water absorbed dose for therapy X radiation to lower photon energies. The principle of the primary standard is based on extrapolation measurements in a graphite phantom, which allows the determination of the graphite kerma in a specified depth of the graphite phantom for low energy photons. A three component model, which separately considers the contributions of absorbed dose to air in the extrapolation volume from photo, Compton and Auger electrons, was developed for the determination of the graphite kerma [11]. By use of the graphite to water ratio of the mass energy absorption coefficients, the water kerma in graphite at this depth can be calculated, and a transfer standard can be calibrated in terms of water kerma at the same point in the phantom. By transferring this standard into a water phantom, the water kerma in water, which is identical to absorbed dose to water, can be measured. The different stray and scatter conditions between water and a graphite phantom are taken into account by corrections determined by Monte Carlo calculations.

Suitable transfer detectors for this calibration procedure are currently under investigation at the PTB. Possible types are ultrathin thermoluminescent dosimeters, GafChromic film, liquid ionization chambers and small scintillation detector systems; the properties of the latter are being improved for use in brachytherapy in a joint programme of the PTB and the universities of Essen and Dortmund.

## REFERENCES

- [1] BÜERMANN, L., KRAMER, H.-M., SCHRADER, H., SELBACH, H.-J., Activity determination of  $^{192}\text{Ir}$  solid sources by ionization chamber measurements using calculated corrections for self-absorption, Nucl. Instrum. Methods Phys. Res. A **339** (1994) 369–376.
- [2] LOFTUS, T.P., Standardization of iridium-192 gamma-ray sources in terms of exposure, J. Res. Natl. Bur. Stand. **85** (1980) 19–25.
- [3] INTERNATIONAL ATOMIC ENERGY AGENCY, Calibration of Brachytherapy Sources, IAEA-TECDOC-1079, IAEA, Vienna (1999).
- [4] GOETSCH, S.J., ATTIX, F.H., PEARSON, D.W., THOMADSEN, B.R., Calibration of  $^{192}\text{Ir}$  high-dose-rate afterloading systems, Med. Phys. **18** (1991) 462–467.
- [5] LOEVINGER, R., Wide angle free-air chamber for calibration of low-energy brachytherapy sources, Med. Phys. **20** (1993) 907 (abstract).

- [6] MITCH, M.G., et al., Well-ionization chamber response relative to NIST air-kerma strength standard for prostate brachytherapy seeds, *Med. Phys.* **27** (2000) 2293–2296.
- [7] BAMBYNEK, M., Development of a multi-electrode extrapolation chamber as a prototype of a primary standard for the realization of the unit of absorbed dose to water for beta brachytherapy sources, *Nucl. Instrum. Methods Phys. Res. A* **492** (2002) 264–275.
- [8] NATH, R., et al., Intravascular brachytherapy physics: Report of the AAPM Radiation Therapy Committee Task Group No. 60, *Med. Phys.* **26** (1999) 119–152.
- [9] QUAIST, U., KAULICH, T.W., FLÜHS, D., Guideline for medical physical aspects of intravascular brachytherapy. DGMP Report No. 16 (2001). Part I: Guideline, *Z. Med. Phys.* **12** (2002) 47–64; Part II: Samples and examples, *Z. Med. Phys.* **12** (2002) 133–148.
- [10] SCHNEIDER, U., “A new method for deriving the absorbed dose in phantom material from measured ion dose for x-rays generated at voltages up to 300 kV”, *Biomedical Dosimetry: Physical Aspects, Instrumentation, Calibration* (Proc. Symp. Paris, 1980), IAEA, Vienna (1981) 223–234.
- [11] KRAMER, H.M., GROSSWENDT, B., The role of de-excitation electrons in measurements with graphite extrapolation chambers, *Phys. Med. Biol.* **47** (2002) 801–822.

# **THE NEED FOR INTERNATIONAL STANDARDIZATION IN CLINICAL BETA DOSIMETRY FOR BRACHYTHERAPY**

U. QUAST\*

Clinical Radiation Physics, Essen University,  
Essen

J. BÖHM

Physikalisch-Technische Bundesanstalt,  
Braunschweig  
E-mail: Juergen.Boehm@ptb.de

T.W. KAULICH

Department of Medical Physics, Tübingen University,  
Tübingen

Germany

## **Abstract**

In addition to the curative brachytherapy of intraocular tumours, beta radiation has proved to be successful in intravascular brachytherapy and makes a significant contribution to reducing the risk of restenosis after the interventional revascularization of arterial stenosis. The rapidly increasing use of beta radiation requires international standardization for clinical beta radiation dosimetry. There seems to be a relatively wide agreement on the use of the measurand absorbed dose to water at the clinically relevant distance (e.g. 2 mm). IAEA-TECDOC-1274 recommends well type ionization chambers as working standards for calibration. Deutsche Gesellschaft für Medizinische Physik Report 16, however, recommends calibration by means of a (small) detector (e.g. a thin scintillator) positioned at the reference calibration distance. Although some degree of skill and knowledge is required to perform this method correctly, it is considered to be superior as it approximates a clean physical measurement of the radiation clinically used and at the point of clinical interest of the dose distribution. Based on these recommendations, the Dosimetry Task Group of the Deutsches Institut für Normung—Normenausschuss Radiologie has initiated an international ad hoc working group to prepare within one year an International Organization for Standardization new work item proposal on the standardization of clinical dosimetry, which will be used to prepare

---

\* Present address: Klinische Strahlenphysik, Universitätsklinikum Essen, Essen, Germany.

a code of practice for clinical beta radiation dosimetry. The topics are: beta sources and source data; calibration principles; primary, secondary and transfer standards; traceability; instrument requirements for in-phantom dosimetry, clinical dosimetry and dosimetric quality assurance; dose calculation and presentation of dose distributions; and dose specification and reporting. The results of its first meetings in March and September 2002 and further activities are reported.

## 1. INTRODUCTION

Beta radiation is of rapidly increasing interest for radiotherapy. In addition to the curative treatment of small and medium sized intraocular tumours by means of ophthalmic beta radiation applicators, intravascular brachytherapy has proved, in over 50 clinical trials with more than 5000 patients, to reduce significantly the risk of restenosis after interventional treatments of arterial stenosis in coronaries and peripheral vessels. Most of these treatments were performed using therapeutic beta radiation. Prior to initiating procedures applying beta radiation in radiotherapy, it will, however, be necessary to harmonize methods for the determination and specification of the absorbed dose to water or tissue and the spatial distributions they provide. In accordance with this global need for standardization in clinical beta radiation dosimetry, the Dosimetry Task Group of the Deutsches Institut für Normung—Normenausschuss Radiologie (DIN-NAR) has initiated an international ad hoc working group for an International Organization for Standardization (ISO) new work item proposal for the standardization of procedures in clinical dosimetry to ensure the reliable application of therapeutic means.

This paper explains the general background and the strategy of the committee to initiate this new work in the field of standardization. The shortcomings but also the merits of two guidelines recently published for brachytherapy are discussed, and the main new issues of the planned standard as well as the scope and the outline are touched upon. Moreover, the general question is raised as to whether the ISO and the International Electrotechnical Commission (IEC) should play a more active role in producing international standards in the field of medical physics, which would help to avoid the numerous national and international standards being drawn up, which often make conflicting recommendations.

## 2. IAEA-TECDOC-1274

IAEA-TECDOC-1274 [1] is a help in photon brachytherapy calibration. However, for beta sources the IAEA recommends well type ionization chambers as working standards calibrated in terms of absorbed dose to water, and as

a supplementary quantity the contained activity (see table I in Ref. [1]). No additional performances, for example the uniformity of the activity distribution of the source, have to be checked.

### 3. DEUTSCHE GESELLSCHAFT FÜR MEDIZINISCHE PHYSIK REPORT 16

Deutsche Gesellschaft für Medizinische Physik (DGMP) Report 16 [2] is a very detailed code of practice, especially for the calibration and clinical dosimetry of intravascular beta radiation sources. This report, which is more stringent than the American Association of Physicists in Medicine (AAPM) TG 60 report [3], recommends for all intravascular brachytherapy sources calibration in terms of absorbed dose to water at the clinically relevant distance of 2 mm for intracoronary applications and 5 mm for peripheral vessels. For all sources, the calibration in terms of absorbed dose to water should be checked:

- (a) At the calibration reference point at a depth of 2 mm for all intracoronary sources;
- (b) At the calibration reference point at a depth of 5 mm for all peripheral sources.

In addition to this reference absorbed dose, DGMP Report 16 also recommends measuring complete distributions of the absorbed dose to water during the first delivery while checking replaced sources by dose measurements only at selected points. The purity of the radionuclide should be checked indirectly by measuring at two depths within the range of the beta radiation. The contribution of the photon radiation to the measuring signal should be measured at a depth greater than the maximum range of the beta particles (within the region of background bremsstrahlung). The dose uniformity of the source should be checked at the radial distance of the calibration reference point (i.e. at 2 mm or 5 mm) at least at three points along the source and at one point opposite the calibration reference point.

### 4. ISO NEW WORK ITEM PROPOSAL: CLINICAL DOSIMETRY — BETA RADIATION SOURCES FOR BRACHYTHERAPY

#### 4.1. Background

The DIN-NAR celebrated its 75th anniversary in 2002. During the past few years it has shown a tendency to concentrate its efforts on international

standards, with particular reference to new radiological procedures. Existing national standards are re-examined after careful inspection, in co-operation with national educational and professional associations of medical physicists such as the DGMP and DEGRO (Deutsche Gesellschaft für Radioonkologie), with respect to their suitability for international application. Recommendations should be made to the ISO, as the DIN is a member of the ISO; problems associated with this are discussed in Section 4.4.

Against this general background and strongly stimulated by medical physicists and interested commercial enterprises, the Dosimetry Task Group within the DIN-NAR initiated an international ad hoc working group for the standardization project Clinical Dosimetry — Beta Radiation Sources for Brachytherapy. The aim of the group is to prepare an ISO new work item proposal on this subject.

#### **4.2. Concept of absorbed dose to water calibration**

The measurand absorbed dose to water, which is the clinically relevant dose quantity and is now being used in external beam dosimetry worldwide, should also be employed to calibrate brachytherapy sources. The Physikalisch-Technische Bundesanstalt (PTB) strongly supports this concept by developing new primary and secondary standards for realizing and disseminating the gray for the measurand absorbed dose to water. The primary standard is based on a newly designed multielectrode extrapolation chamber (MEC), which in particular meets the requirements for a high spatial resolution and a small measurement uncertainty [4]. In contrast to conventional extrapolation chambers, the central part of the MEC is a segmented collecting electrode, which was manufactured at the clean room centre of the PTB by electron beam lithography on a wafer. The MEC allows three dimensional dose distributions to be measured with a high spatial resolution and without having to fall back on an additional relative dosimetry system, thus avoiding additional uncertainties. A secondary beta radiation source, a planar  $^{90}\text{Sr}/^{90}\text{Y}$  applicator embedded in a suitable container, is available for calibrating dosimeters for brachytherapy in hospitals in terms of absorbed dose to water.

Different traceability concepts are recommended in Sections 2 and 3. When the well chamber is used as a working standard, the medical physicist in the clinical environment gets a calibration of high precision, owing to the relatively large output signal of the chamber. However, it must be trusted that the source is identically activated and that the manufacturer has not changed the design and construction of the source encapsulation on which the first calibration was based. Additional means, such as autoradiography, are not deemed necessary. However, in Ref. [2] calibration by means of a (small) detector (e.g.



a thin scintillator) positioned at the reference calibration distance is recommended. Although this calibration method requires some degree of skill and knowledge to perform it correctly, it is considered to be superior as it approximates a clean physical measurement of the radiation clinically used and at the point of interest of the dose distribution. This is of particular importance because of the low penetration of the beta radiation.

#### **4.3. Scope and outline of the standard**

The following scope was agreed during the first meeting of the working group in Essen on 18 and 19 April 2002:

“This standard specifies methods for the determination of absorbed dose distributions in water or tissue that are required prior to initiating procedures for the application of beta radiation in intravascular and ocular-tumour brachytherapy. The intent of this standard is to review methods and to give recommendations for beta source calibration, dosimetry measurements, dose calculation, dosimetric quality assurance as well as for beta radiation brachytherapy treatment planning and performance and gives guidance for estimating the uncertainty of the absorbed dose to water delivered. The standard is confined to “sealed” radioactive sources such as source trains of single seeds, line sources, shell and volume sources, plane and concave surface sources for which only the beta radiation emitted is of therapeutic relevance. The absorbed dose rate of these sources at the calibration reference point is of high dose rate in intravascular brachytherapy and of low dose rate in ocular-tumour brachytherapy, respectively.

“The standardization of procedures in clinical dosimetry described in this standard serves as a basis for the reliable application of beta radiation brachytherapy. The dosimetric methods apply to intravascular brachytherapy treatment for overcoming the problem of restenosis, which is the main late complication limiting the success of interventional treatment of vascular stenosis, and to curative treatment of ophthalmic disease.

“The document is geared towards organizations wishing to establish reference methods in dosimetry aiming at clinical demands for appropriate small uncertainty of the delivered dose. This standard does not exclude that there may be other methods leading to the same or smaller measurement uncertainties.”

Existing normative documents, as well as recommendations such as those of the AAPM, DGMP, European Society for Therapeutic Radiology and Oncology (ESTRO), IAEA, International Commission on Radiation Units and

Measurements (ICRU) and Nederlandse Commissie voor Stralingsdosimetrie, will be taken into account by the ad hoc working group. The planned standard will be structured as follows:

- (a) Scope, normative references and terminology.
- (b) Dosimetric quantities for the characterization of the radiation field.
- (c) Source data (characteristics of the radionuclides, source reference data and the source certificate).
- (d) Calibration and traceability.
- (e) General principles and requirements for absorbed dose measurements (e.g. scaling, the influence of detector geometry and the effective detector reference point of measurement).
- (f) In-phantom dosimetry (e.g. measurements in a water or water substituting phantom).
- (g) Theoretical modelling and the presentation of dose distributions.
- (h) Clinical dosimetry, clinical quality control and irradiation treatment planning.
- (i) Uncertainties.

#### **4.4. Role of the ISO and IEC for the production of standards for medical physics**

The need to develop and disseminate international standards with recommendations for dosimetry procedures for use in brachytherapy is widely accepted. What, however, is the present state of producing standards in medical physics (see Fig. 1 [5])? Medical physicists, manufacturers, authorities, representatives of national metrology institutes and others co-operate in organizations having strong relations with medical physics, such as the AAPM, DGMP, ESTRO, IAEA and ICRU, to satisfy their need for standardization by writing recommendations, guidelines, etc. The documents often allow for national features or reflect specific views of the individual organizations and, in general, frequently have only loose links to acknowledged standardization bodies such as the American National Standards Institute, DIN, IEC or ISO.

Both the ISO and IEC develop and maintain international standards through the activities of technical committees and their subsidiary bodies. The ISO and IEC directives define the basic procedures to be followed. A number of them are common to the ISO and IEC, and some are unique and published in separate supplements. There are strict definitions for the organizational structure and the responsibilities for the technical work. The development of international standards is subdivided into a number of stages, starting with a preliminary stage and ending with the publication stage. Members of the IEC

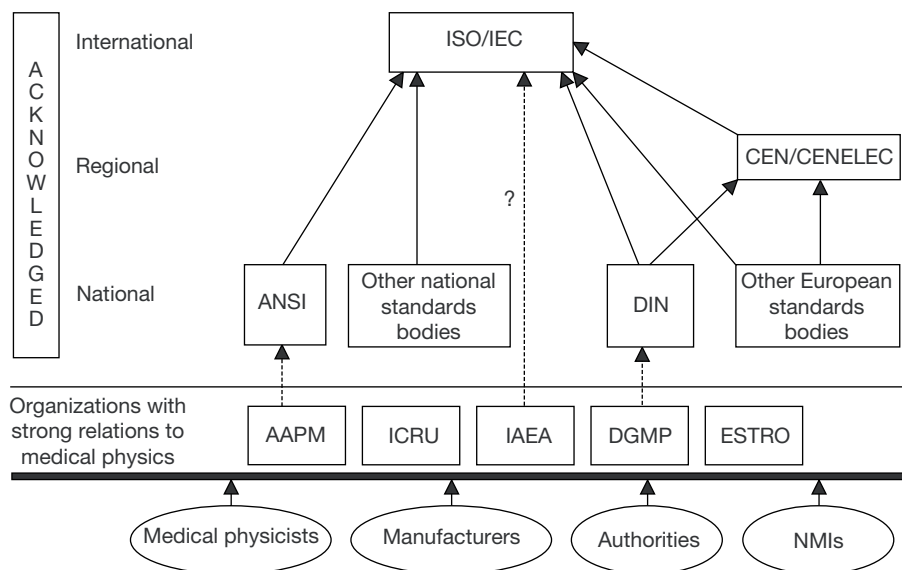


FIG. 1. Relationship between organizations setting up standards for medical physics.

or ISO are involved in the decision processes through votes and comments. Clear procedures for the maintenance of standards have been laid down. The maximum time elapsing before a systematic review of a standard is five years. A standard may be confirmed, amended, revised or withdrawn. The consistency of IEC and ISO standards is very important; this relates particularly to standardized terminology, quantities and units, bibliographic references, technical drawings and diagrams. A number of general documents published by the ISO and IEC should be followed; these deal with, for example, subjects such as the tolerancing of dimensions and the uncertainty of measurement, statistical methods, environmental conditions and associated tests, safety, conformity and quality. In addition, the content of a document published by the ISO or IEC is drawn up so as to facilitate direct application as a regional or national standard and adoption without modification.

All these long term quality management procedures and strategies are difficult to map out and maintain by national and international scientific, educational and professional organizations of medical physicists. The strong point of these organizations is the motivation of and co-operation and fast communication between their members. To transform their ideas and proposals into consolidated templates for standards is the role of the delegates of the members of the IEC and ISO.

The IEC has established Technical Committee No. 62 (TC 62), Electrical Equipment in Medical Practice, to prepare international standards for the manufacture, installation and application of electrical equipment as used in medical practice. Subcommittee SC 62C, Equipment for Radiotherapy, Nuclear Medicine and Radiation Dosimetry, prepares standards for the safety and performance of medical equipment using high energy radiation for the treatment of cancer, associated equipment such as simulators used in treatment planning, dosimeters for measuring the quantity of radiation delivered, and nuclear medicine equipment used for imaging the distribution of radioactive substances in the human body for diagnostic purposes. Working Group 3 of SC 62C deals with the performance of dosimeters.

The ISO does not yet have a technical committee equivalent to IEC TC 62 to match the concepts and methods of medical physics to the diagnosis and treatment of human disease. Recommendations for dosimetry procedures for use in brachytherapy could be established in such a committee. As an interim solution, however, the new work item proposal, Clinical Dosimetry — Beta Radiation Sources for Brachytherapy, could be addressed by TC 85, Nuclear Energy, which published the ISO/ASTM 51939:2002 standard, Practice for Blood Irradiation Dosimetry. This plan was supported during an advisory group meeting of TC 85/SC 2 on 29 May 2002 in Ringhals, Sweden. The completion of the new work item proposal for beta brachytherapy by the ad hoc working group is scheduled for spring 2003. Which technical committee of the ISO will address the matter will then be decided upon.

## 5. CONCLUSIONS

The bilingual DGMP Report 16 has found broad international acceptance as a guideline for the medical–physical aspects of intravascular brachytherapy and has partly been included in other recommendations (by ESTRO and the AAPM TG 60 update draft). Based on these and other normative documents, the DIN-NAR project, launched at the first meeting of the international working group on 18 and 19 March 2002, has already collected and prepared interesting material on the calibration and dosimetry of beta radiation brachytherapy sources in terms of absorbed dose to water. The detailed ISO new work item proposal will be completed in the spring of 2003.

## ACKNOWLEDGEMENTS

The authors gratefully acknowledge the contribution to the scope and outline of the ISO new work item proposal by the following delegates and consultants of the ad hoc working group: M. Andrassy, M. Bambynek, L. DeWerd, W. Dries, D. Flüh, C. Kirisits, J.L. Lobdell, F. Mourtada, R. Nath, E. Schüle, H.-J. Selbach, C. Soares, K. Thieme and H. Tölli.

## REFERENCES

- [1] INTERNATIONAL ATOMIC ENERGY AGENCY, Calibration of Photon and Beta Ray Sources Used in Brachytherapy, IAEA-TECDOC-1274, IAEA, Vienna (2002).
- [2] QUAIST, U., KAULICH, T.W., FLÜHS, D., Guideline for medical physical aspects of intravascular brachytherapy. DGMP Report No. 16 (2001). Part I: Guideline, Z. Med. Phys. **12** (2002) 47–64; Part II: Samples and examples, Z. Med. Phys. **12** (2002) 133–148.
- [3] NATH, R., et al., Intravascular brachytherapy physics: Report of the AAPM Radiation Therapy Committee Task Group No. 60, Med. Phys. **26** (1999) 119–152.
- [4] BAMBYNEK, M., Development of a multi-electrode extrapolation chamber as a prototype of a primary standard for the realization of the unit of the absorbed dose to water for beta brachytherapy sources, Nucl. Instrum. Methods A (in press).
- [5] REEVE, N., Visionen für die Zukunft, DIN-Mitt. **81** (2002) 170–174.

**BLANK**

# ENERGY DEPENDENCE OF THE AIR KERMA RESPONSE OF A LIQUID IONIZATION CHAMBER AT PHOTON ENERGIES BETWEEN 8 keV AND 1250 keV

G. HILGERS

Physikalisch-Technische Bundesanstalt,  
Braunschweig, Germany  
E-mail: gerhard.hilgers@ptb.de

J. BAHAR-GOGANI, G. WICKMAN

Radiation Physics Department, University of Umeå,  
Umeå, Sweden

## Abstract

The energy dependence of the response to air kerma of four different liquid ionization chambers (LICs) of various geometries and filled with various liquid mixtures has been investigated. Two LICs were filled with a mixture of 40% TMS (tetramethylsilane) and 60% isooctane. One of these LICs was a plane-parallel chamber 5 mm in diameter and with a 0.3 mm electrode spacing and the other was a thimble chamber with an inner diameter of 3.0 mm, an outer diameter of the inner electrode of 1.0 mm and a height of 3.0 mm. For both chambers the measured response to air kerma varies by a factor of about 2 to 3 in the photon energy range relevant for brachytherapy of 15 keV to 220 keV. Two LICs were filled with a mixture of 60% TMS and 40% isooctane. Both were plane-parallel chambers, one was 5 mm in diameter and with a 0.3 mm electrode spacing and the other was 2.5 mm in diameter and with a 0.35 mm electrode spacing. For both chambers the response to air kerma varies by a factor of about 1.5 in the same energy range. The energy dependence of the LICs cannot be explained only by the liquid to air ratio of the mass energy absorption coefficient. Monte Carlo calculations carried out with EGSnrc show a chamber response significantly different from the measured response. Measurements (assisted by Monte Carlo calculations) of the ion yield of the ionization liquid exhibit a pronounced energy dependence from about 1 keV/ion pair at about 10 keV to 250 eV/ion pair for  $^{137}\text{Cs}$  gamma radiation. Taking the ion yield of the ionization liquid into account, the deviation between the measured and the calculated response reduces to less than  $\pm 10\%$ .

## 1. INTRODUCTION

In its recent reports on cardiovascular brachytherapy the Deutsche Gesellschaft für Medizinische Physik recommends that the source strength of

brachytherapy sources be characterized in terms of absorbed dose to water at a distance of 2 mm from the central axis of the source [1]. As a consequence, the detection volume of the detector has to be sufficiently small for the necessary spatial resolution to be obtained. Additionally, the response of a detector suitable for characterizing such sources with respect to absorbed dose to water should depend only to a small extent on the radiation energy.

The liquid ionization chambers (LICs) described in Refs [2, 3] seem to be a promising means for this type of measurement. The two components of the ionization liquid (tetramethylsilane (TMS) and isooctane) can be mixed in a ratio that ensures that the mass energy absorption coefficient of the resulting mixture deviates from that of water by less than  $\pm 15\%$  down to photon energies of 10 keV. Owing to the high density of the ionization medium, the spacing between the two electrodes of the ionization chamber can be made as small as a few tenths of a millimetre, with the resulting ionization current remaining sufficiently large.

Previous investigations [4] of the properties of LICs have shown that the long term stability of LICs is in the range of less than 0.4%. Recombination effects can be accounted for by using appropriate correction formulas [3], and the temperature dependence of 0.5%/K of the response can be corrected for [3].

## 2. EXPERIMENTAL SET-UP AND MONTE CARLO CALCULATION

The LICs used in the investigation were two plane-parallel chambers, one 5 mm in diameter and with a 0.3 mm electrode spacing (a 'large plane-parallel chamber') and one 2.5 mm in diameter with a 0.35 mm electrode spacing (a 'small plane-parallel chamber'), and a thimble chamber with an inner diameter of the outer electrode of 3.0 mm, an outer diameter of the inner electrode of 1.0 mm and a height of 3.0 mm. The ionization medium for the two plane-parallel chambers was a mixture of 60% TMS and 40% isooctane, and for the thimble chamber and for the large plane-parallel chamber was a mixture of 40% TMS and 60% isooctane. All chambers were operated at a high voltage (300 V).

Owing to the relatively high leakage current of the LICs, sufficiently high dose rates were needed for the measurements. The irradiations were therefore carried out for all chambers with the International Organization for Standardization wide spectra series [5] and with additional series that represent an extension of this series down to tube voltages of 10 kV and that are part of the Physikalisch-Technische Bundesanstalt B series [6]. The large plane-parallel chamber filled with a mixture of 40% TMS and 60% isooctane was additionally irradiated with  $^{137}\text{Cs}$  and  $^{60}\text{Co}$  gamma radiation. The Monte Carlo



calculations to calculate the energy deposited in the ionization liquid were carried out using the EGSnrc user code DOSRZnrc, Version 2.

As a first step, the response of the LICs was investigated with respect to air kerma free in air, instead of absorbed dose to water, in a standardized water phantom.

### 3. RESULTS

Figure 1 shows the measured relative response with respect to air kerma for the various LICs and the various liquid fillings as a function of the mean photon energy,  $\bar{E}_{ph}$ , averaged over the spectral air kerma distribution. In the energy range below about 80 keV the relative air kerma response of the large plane-parallel chamber for the two mixtures shows differences of a factor of up to 2, whereas in the range of higher photon energies the differences are less than about 20%. The mixture containing 40% TMS and 60% isooctane shows an energy dependence by a factor of about 2 in the energy range from 15 keV

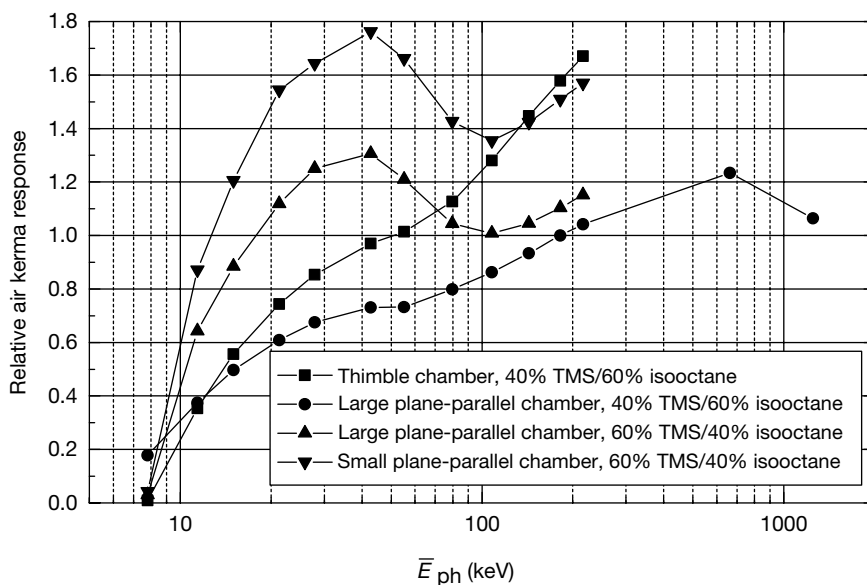


FIG. 1. Relative air kerma response of the large plane-parallel chamber for both liquid mixtures, of the small plane-parallel chamber filled with a mixture of 60% TMS and 40% isooctane and of the thimble chamber filled with a mixture of 40% TMS and 60% isooctane.

to 220 keV, while the mixture containing 60% TMS and 40% isooctane shows a variation by a factor of about 1.5 in this energy range.

The relative air kerma response for the large and the small plane-parallel chambers, both filled with a mixture containing 60% TMS and 40% isooctane, was normalized with respect to the chambers' active volumes and, as the response strongly depends on the chamber high voltage, to the strength of the electric field between the collecting electrodes. The two chambers show a similar relative energy dependence of the air kerma response, but the normalized air kerma response of the large chamber is about one third smaller than that of the small chamber.

The relative air kerma response for the thimble chamber and the large plane-parallel chamber, both filled with a mixture of 40% TMS and 60% isooctane, shows a similar energy dependence, with the air kerma response for the thimble chamber being about 50% larger at higher photon energies than the air kerma response for the large plane-parallel chamber.

The data show that the photon energy dependence of the LICs is mainly governed by the composition of the liquid mixture in the chamber collecting volume and that the geometry of the collecting volume is only of minor influence.

The energy dependence of the LICs cannot be explained only by the liquid to air ratio of the mass energy absorption coefficient: for the mixture of 40% TMS and 60% isooctane the mass energy absorption coefficient deviates from that of air by less than 10% over the photon energy range, but the measured chamber air kerma response varies by more than a factor of 3, whereas for the mixture of 60% TMS and 40% isooctane the mass energy absorption coefficient deviates from that of air by up to 70% over the energy range from 20 keV to 200 keV, but the measured chamber air kerma response varies only by a factor of less than 1.3.

Figure 2 shows the relative air kerma response measured and determined by Monte Carlo calculations for the large plane-parallel chamber filled with the two different liquid mixtures, 40% TMS and 60% isooctane (Fig. 2(a)) and 60% TMS and 40% isooctane (Fig. 2(b)). In both cases only poor agreement between the measurement and calculation is achieved.

Apart from the mass energy absorption coefficient, the response of an ionization chamber is also influenced by the amount of energy required for the production of an electron-ion pair in the detector material. The quantity considered is the energy,  $W_{fi}$ , required to create an electron-ion pair that escapes initial recombination [7].  $W_{fi}$  was determined for the two liquid mixtures. The LIC used for this purpose was the large plane-parallel chamber.

In an ionization chamber with a dielectric liquid, the ionization current never reaches saturation with respect to initial recombination within the experimentally accessible range of polarizing voltages [8]. The ions can escape

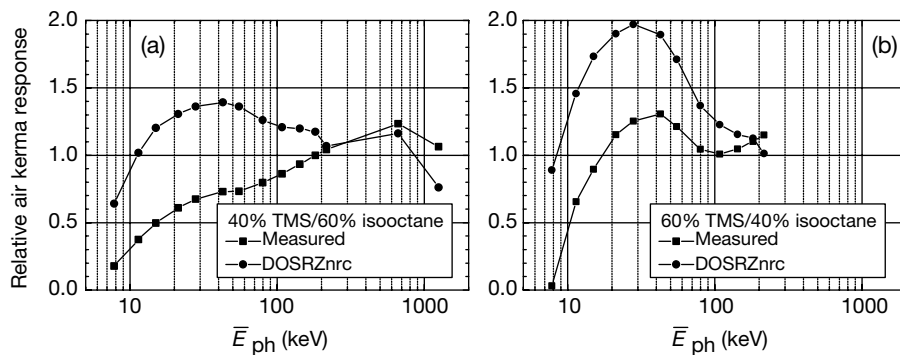


FIG. 2. Measured and calculated relative air kerma response for the large plane-parallel chamber filled with (a) 40% TMS and 60% isooctane and (b) 60% TMS and 40% isooctane.

initial recombination by diffusion or by a combination of diffusion and the influence of an external electric field.

Under constant fluence irradiation conditions and with negligible volume recombination, the ionization current increases linearly with the electric field strength. At low electric field strengths the ionization current deviates from the linear relationship, owing to volume recombination. The current at a chamber voltage of zero represents that fraction of the ionization current that escapes initial recombination by diffusion.

For both liquid mixtures the measurements for the determination of  $W_{fi}$  were carried out with the large plane-parallel chamber. The energy deposited in the liquid was calculated by DOSRZnrc. The determination of  $W_{fi}$  was carried out in the following way (see Fig. 3(a)). First, the chamber current dependence on the chamber high voltage was measured for the various photon spectra. The region in which the chamber current and the chamber high voltage show a linear relationship was linearly fitted and extrapolated to zero high voltage. The dose rate during all these measurements was chosen such that the volume recombination was negligible at higher chamber voltages. The energy  $W_{fi}$  was determined from this extrapolated chamber current at a chamber voltage of zero and from the Monte Carlo calculated deposited energy. The results are shown in Fig. 3(b). For both liquid mixtures and in the energy range between 10 keV and 220 keV,  $W_{fi}$  decreases by a factor of about 3 towards increasing energy.

The value of  $W_{fi}$  determined from the extrapolated chamber current at a chamber voltage of zero was then used to correct the relative air kerma response values obtained with DOSRZnrc. The comparison of the measured (under normal operating conditions with a chamber voltage of 300 V) and calculated corrected relative air kerma response is shown in Fig. 4. For the large

plane-parallel chamber, for both liquid mixtures, a good agreement was achieved (Figs 4(a) and (b)). Applying the values of  $W_{fi}$  that were obtained with the large plane-parallel chamber to the calculated air kerma response of the thimble chamber (Fig. 4(c)) and of the small plane-parallel chamber (Fig. 4(d))

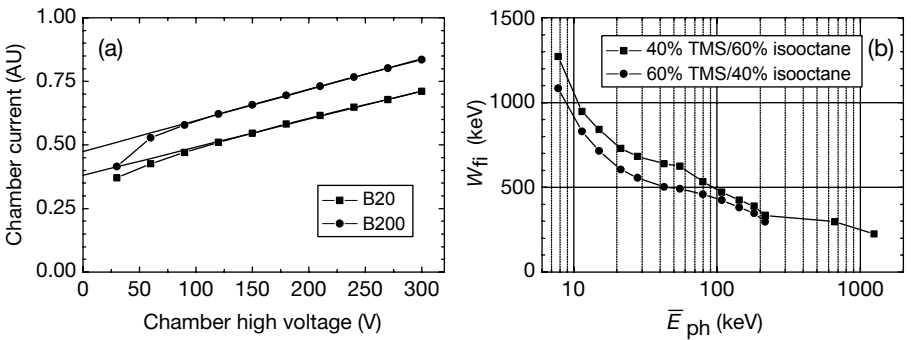


FIG. 3. (a) Chamber current versus chamber high voltage for two different photon spectra; (b)  $W_{fi}$  for the two different liquid mixtures.

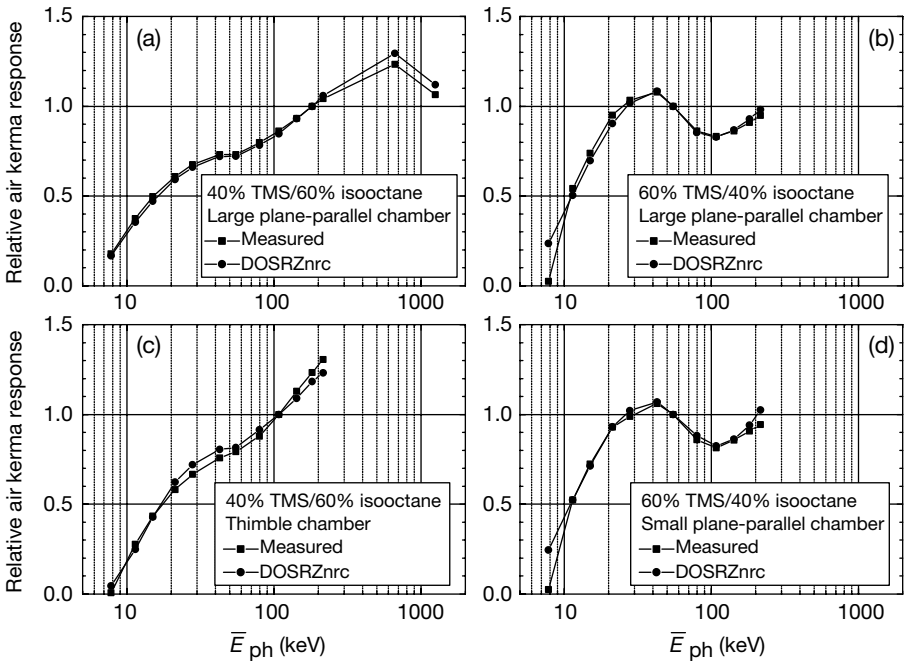


FIG. 4. Comparison of the measured and Monte Carlo calculated corrected responses relative to the air kerma response.

also leads to a good agreement. This indicates that the relative energy dependence of  $W_{fi}$  determined in the way described above is a property of the liquid mixture in the LIC and does not depend on the specific geometry of the collecting volume of the LIC.

#### 4. CONCLUSION

The energy dependence of the air kerma response of LICs filled with two different liquid mixtures was investigated. The energy dependence is mainly determined by the composition of the liquid, while the influence of the geometry of the collecting volume is only of minor importance. By taking into account the energy dependence of  $W_{fi}$ , a good agreement between the measured and Monte Carlo calculated air kerma responses is achieved.

By varying the mixing ratio it is possible to minimize the energy dependence of the air kerma response of a LIC. As the water to air ratio of the mass energy absorption coefficient varies with photon energy by only about 10%, a minimization of the response of a LIC with respect to absorbed dose to water should also be possible.

#### REFERENCES

- [1] QUAST, U., KAULICH, T.W., FLÜHS, D., Guideline for medical physical aspects of intravascular brachytherapy. DGMP Report No. 16 (2001). Part I: Guideline, *Z. Med. Phys.* **12** (2002) 47–64; Part II: Samples and examples, *Z. Med. Phys.* **12** (2002) 133–148.
- [2] BAHAR-GOGANI, J., WICKMAN, G., JOHANSSON, L., JOHANSSON, B.E., Assessment of the relative dose distribution around an  $^{192}\text{Ir}$  line source using a liquid ionization chamber, *Med. Phys.* **26** (1999) 1932–1942.
- [3] WICKMAN, G., JOHANSSON, B., BAHAR-GOGANI, J., HOLMSTRÖM, T., GRINDBORG, J.E., Liquid ionization chambers for absorbed dose measurements in water at low dose rates and intermediate photon energies, *Med. Phys.* **25** (1998) 900–907.
- [4] BAHAR-GOGANI, J., GRINDBORG, J.E., JOHANSSON, B.E., WICKMAN, G., Long-term stability of liquid ionization chambers with regard to their qualification as local reference dosimeters for low dose-rate absorbed dose measurements in water, *Phys. Med. Biol.* **46** (2001) 729–740.
- [5] INTERNATIONAL ORGANIZATION FOR STANDARDIZATION, X and Gamma Reference Radiations for Calibrating Dosimeters and Doserate Meters and for Determining their Response as a Function of Photon Energy — Part 1:

- Radiation Characteristics and Production Methods, ISO 4037-1, ISO, Geneva (1996).
- [6] PHYSIKALISCH-TECHNISCHE BUNDESANSTALT, PTB-Prüfregeln, Vol. 11, Strahlenschutzdosimeter für Photonenstrahlung mit Energien zwischen 5 keV und 3 MeV, PTB, Braunschweig (1977).
- [7] WICKMAN, G., NYSTRÖM, H., The use of liquids in liquid ionization chambers for high precision radiotherapy dosimetry, *Phys. Med. Biol.* **37** (1992) 1789–1812.
- [8] JOHANSSON, B., WICKMAN, G., General collection efficiency for liquid iso-octane and tetramethylsilane used as sensitive media in a parallel-plate ionization chamber, *Phys. Med. Biol.* **42** (1997) 133–145.

# COMPARISON OF TWO DIFFERENT METHODS TO DETERMINE THE AIR KERMA CALIBRATION FACTOR, $N_k$ , FOR $^{192}\text{Ir}$

E. VAN DIJK

Department of Temperature and Radiation,  
Nederlands Meetinstituut, Delft, Netherlands  
E-mail: evandijk@nmi.nl

## Abstract

Two different methods to determine the air kerma calibration factor for  $^{192}\text{Ir}$  high dose rate sources are described. One method is used by the Nederlands Meetinstituut (NMI), the national standards institute of the Netherlands, and is based on weighting the response curve of an ionization chamber over the  $^{192}\text{Ir}$  spectrum. Another method was developed by Goetsch et al. and is based on the determination of the absorption in the chamber wall for  $^{192}\text{Ir}$  and air kerma calibration factors for a 250 kV X ray quality and  $^{137}\text{Cs}$  gamma rays. The difference between both methods is discussed in the paper. A description of the NMI method is given.

## 1. INTRODUCTION

Iridium-192 is a radionuclide frequently used in high dose rate (HDR) and pulsed dose rate brachytherapy sources. Before a brachytherapy source can be used in clinical practice the source strength has to be determined, preferably in terms of a reference air kerma rate (in  $\mu\text{Gy/h}$ ) [1, 2]. The problem in deriving the air kerma calibration factor for  $^{192}\text{Ir}$  is that the most important part of the photon spectrum of an  $^{192}\text{Ir}$  brachytherapy source falls in an energy gap between the standards for X rays and the standards for gamma rays established at primary standards laboratories. It is therefore necessary to determine the air kerma calibration factor using an indirect method. This can be achieved by approximating the calibration factor for the spectrum of the radionuclide  $^{192}\text{Ir}$  using calibration factors obtained at the energies of the X ray and gamma ray standards on both sides of the energy gap.

When applying the method developed by Goetsch et al. [3] the calibration factor for  $^{192}\text{Ir}$  for an ionization chamber is approximated by interpolating between two known calibration factors. One calibration factor is determined at a mean photon energy below the energy gap (250 kV X rays). The other calibration factor is determined at a photon energy above that gap ( $^{137}\text{Cs}$  gamma rays). The measured wall absorption for the  $^{192}\text{Ir}$  spectrum and the measured

wall absorption for the spectra of 250 kV X rays and  $^{137}\text{Cs}$  gamma rays are used for a linear interpolation procedure between the two calibration factors.

However, the Nederlands Meetinstituut (NMI), the national standards laboratory of the Netherlands, derives the calibration factor for  $^{192}\text{Ir}$  by weighting the individual contributions of 22 significant photon peaks, between 9 keV and 884.5 keV, of the  $^{192}\text{Ir}$  spectrum [4] over the response curve of the ionization chamber determined at the photon energies for the primary standards for X rays and gamma rays. The response curve of the ionization chamber is a plot of the inverse values of the calibration factors versus the corresponding mean photon energies, determined with a set of International Organization for Standardization (ISO) quality X rays [5] and the radionuclides  $^{137}\text{Cs}$  and  $^{60}\text{Co}$  [4]. This method is recommended by the Nederlandse Commissie voor Stralingsdosimetrie (NCS) [1].

For the method used by the NMI, as well as for the method proposed by Goetsch et al., it is assumed that the response of the ionization chamber is linear in the energy gap between the standards for X rays and the standards for gamma rays established at primary laboratories. When inferring the calibration factor for  $^{192}\text{Ir}$  for the NE 2561 ionization chamber in accordance with these two methods, a significant difference in the calibration factors is found.

## 2. MATERIALS AND METHODS

The ionization chamber used in the NMI set-up was an NE 2561 ionization chamber, serial number 051. The Delrin buildup was placed on the ionization thimble not only during the calibration measurements with  $^{137}\text{Cs}$  and  $^{60}\text{Co}$  but also during the measurements with X rays. In order to apply the method used at the NMI and the method developed by Goetsch et al. it is necessary to determine the calibration factors of the ionization chamber by an extensive set of measurements. The inverse value of the calibration factors plotted against the corresponding mean photon energy (the response curve) and the most significant  $^{192}\text{Ir}$  spectrum lines are shown in Fig. 1.

### 2.1. Method recommended by Goetsch et al.

In the paper by Goetsch et al. [3] it is assumed that the air kerma calibration factor,  $N_k$ , depends on the photon energy distribution due to changes in the attenuation of the photons in the wall of the ionization chamber. This assumption enables the comparison of air kerma calibration factors for different photon spectra. It also gives the possibility of calculating air kerma calibration factors for other photon spectra if the wall attenuation for the different photon



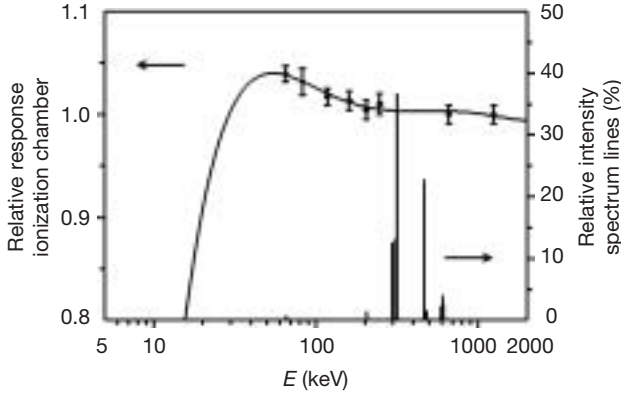


FIG. 1. Response curve of the NE 2561 ionization chamber, normalized to  $^{137}\text{Cs}$ , in relation to the air kerma weighted spectrum lines of an  $^{192}\text{Ir}$  HDR source.

spectra is known. The wall attenuation,  $A_w$ , is the ratio of the ionization current with the wall present to the ionization current with a wall thickness extrapolated to  $0 \text{ g/cm}^2$ . The ionization current at a thickness of  $0 \text{ g/cm}^2$  was determined by measuring the ionization current with different wall thicknesses and using a linear extrapolation of the measured values to a wall thickness of  $0 \text{ g/cm}^2$ . With the measured air kerma calibration factors, and with the wall attenuations for a 250 kV X ray quality, for  $^{137}\text{Cs}$  gamma rays and for the  $^{192}\text{Ir}$  spectrum obtained from the extrapolation of the wall thickness to  $0 \text{ g/cm}^2$ , the air kerma calibration factor for  $^{192}\text{Ir}$  can be approximated by:

$$A_{W^{192}\text{Ir}} N_{K^{192}\text{Ir}} = \frac{1}{2} (A_{W^{250\text{kV}}} N_{K^{250\text{kV}}} + A_{W^{137}\text{Cs}} N_{K^{137}\text{Cs}}) \quad (1)$$

Taking into account the measured values for  $A_w$  and the calibration factors for 250 kV X rays and  $^{137}\text{Cs}$  gamma rays, Eq. (1) can be rearranged to:

$$N_{K^{192}\text{Ir}} = \frac{(1+x)}{2} (N_{K^{250\text{kV}}} + N_{K^{137}\text{Cs}}) \quad (2)$$

where  $x = at$ , where  $t$  is the wall thickness in electrons per  $\text{cm}^2$  and  $a = 3.98 \times 10^{-26}$  [3].

One of the assumptions in the method developed by Goetsch et al. is that the relation between air kerma calibrations factors  $N_{K1}$  and  $N_{K2}$ , at photon energies with wall attenuations of  $A_{W1}$  and  $A_{W2}$ , respectively, can be described as:

$$N_{K1}A_{W1} = N_{K2}A_{W2} \quad (3)$$

## 2.2. Method used at the NMI

The method used at the NMI is based on a more complex relationship between the air kerma calibration factors. Borg et al. [6] have shown that application of Spencer–Attix cavity theory is allowed for  $^{192}\text{Ir}$  photon energies. The measured ionization current can be transformed into an air kerma rate:

$$\dot{K}_{\text{air}} = \frac{1}{V\rho} \frac{W}{e} \frac{1}{1-\bar{g}} \left( \frac{\bar{s}}{\rho} \right)_{\text{air}}^{\text{wall}} \left( \frac{\bar{\mu}_{\text{en}}}{\rho} \right)_{\text{wall}}^{\text{air}} k_{\text{att}} \quad (4)$$

where

$I$	is the ionization current;
$V$	is the volume of the ionization chamber;
$\rho$	is the mass density of dry air;
$W$	is the mean energy to produce a pair of ions in dry air by an electron with a charge $e$ ;
$\bar{g}$	is the fraction of energy lost by bremsstrahlung (assumed to be negligible);
$(\bar{\mu}_{\text{en}}/\rho)_{\text{wall}}^{\text{air}}$	is the restricted stopping power ratio of the effective wall material and air;
$(\bar{s}/\rho)_{\text{air}}^{\text{wall}}$	is the ratio of the mass energy absorption coefficients of the effective wall material and air;
$k_{\text{att}}$	is the $A_W^{-1}$ attenuation factor of the photons by the effective wall material of the ionization chamber ( $A_W$ is equivalent to the wall attenuation used by Goetsch et al.).

The air kerma calibration factor of an ionization chamber,  $N_K$ , is defined as:

$$N_K = \frac{\dot{K}}{I} \quad (5)$$

where

$\dot{K}$	is the kerma rate at a reference point in air in a photon beam when the ionization chamber is absent;
$I$	is the ionization current produced in the ionization chamber when placed at the same reference point in the photon beam.

When Eqs (4) and (5) are combined, the air kerma calibration factor can be expressed as:

$$N_K = \frac{\dot{K}}{I} = \frac{1}{V\rho} \frac{W}{e} \left( \frac{\bar{s}}{\rho} \right)_{\text{air}}^{\text{wall}} \left( \frac{\bar{\mu}_{\text{en}}}{\rho} \right)_{\text{wall}}^{\text{air}} k_{\text{att}} \quad (6)$$

In Eq. (6) only  $(1/V\rho)(W/e)$  is independent of the photon spectrum, when the assumption is made that  $W/e$  is energy independent.

Since the energy response of an ionization chamber also depends on the mean mass energy ratio  $(\bar{\mu}_{\text{en}}/\rho)_{\text{wall}}^{\text{air}}$  and the stopping power ratio  $(\bar{s}/\rho)_{\text{air}}^{\text{wall}}$  of the wall material and air, it is considered that, for a given energy  $E$ :

$$N_{KE} A_{WE} \left[ \left( \frac{\bar{s}}{\rho} \right)_{\text{air}}^{\text{wall}} \left( \frac{\bar{\mu}_{\text{en}}}{\rho} \right)_{\text{wall}}^{\text{air}} \right]_E^{-1} = \text{constant} \quad (7)$$

This means that the contributions to the air kerma calibration factor for the different photon energies of the  $^{192}\text{Ir}$  spectrum have to be weighted over the energy response of the ionization chamber. The method used at the NMi is to determine the calibration factors for the ionization chamber at ten different photon energies: eight X ray spectra (ISO narrow spectrum series [5]) with mean energies of 48, 65, 83, 100, 118, 160, 205 and 248 keV, and  $^{173}\text{Cs}$  and  $^{60}\text{Co}$ . The energy response curve is the inverse value of the calibration factors plotted as a function of the photon energy (see Fig. 1). Also shown in Fig. 1 is the relative kerma in air spectrum of  $^{192}\text{Ir}$  [4]. This kerma in air spectrum is emitted by an encapsulated HDR  $^{192}\text{Ir}$  source used in brachytherapy. A good approximation of the calibration factor for each of the  $^{192}\text{Ir}$  energy peaks can be made by determining the ratio of the energy dependent component in Eq. (6) for each peak of the  $^{192}\text{Ir}$  photon spectrum, with respect to the determined air kerma calibration factor. The calibration procedure used at the NMi for the  $^{192}\text{Ir}$  photon spectrum is to weight the calibration factors for the individual photon energy peaks with respect to the individual peak heights, as described in Section 3.

### 3. NMi CALIBRATION PROCEDURE FOR $^{192}\text{Ir}$

The calibration factor for  $^{192}\text{Ir}$  radiation was determined by weighting the response  $R = N_K^{-1}$ , in accordance with the kerma spectrum, using:

$$N_K^{192\text{Ir}} = \left( \sum_{i=1}^n \dot{K}_i \right) \left( \sum_{i=1}^n \dot{K}_i R_i \right)^{-1} \quad (8)$$

where

$N_K^{192\text{Ir}}$  is the air kerma calibration factor for  $^{192}\text{Ir}$  of the ionization chamber under consideration;

$i$  is the spectrum line index of the  $^{192}\text{Ir}$  spectrum with energy  $E_i$ ;

$n$  is the number of spectrum lines taken into account ( $n = 8$ );

$\dot{K}_i$  is the air kerma contribution of the  $i$ th spectrum line (in arbitrary units);

$R_i$  is the response for a mean energy of  $E_i$  of the ionization chamber under consideration.

### 3.1. Determination of the air kerma rate, $\dot{K}_i$

The air kerma spectrum contribution of the  $i$ th spectrum line 1 m from the  $^{192}\text{Ir}$  source was obtained by multiplying the relative intensity of each spectrum line with its photon energy, the mass energy absorption coefficient and the correction for photon attenuation in air:

$$\dot{K}_i = f_i E_i \left( \frac{\bar{\mu}_{\text{en}}}{\rho} \right)_i e^{-\mu_i r} \quad (9)$$

where

$f_i$  is the relative intensity of the  $i$ th spectrum line;

$(\bar{\mu}_{\text{en}}/\rho)_i$  is the mass energy absorption coefficient for photons of energy  $E_i$  in air;

$\mu_i$  is the attenuation coefficient for photons of energy  $E_i$  in air;

$r$  is the distance between the source and the detector (1 m).

### 3.2. Determination of the response, $R_i$

The response  $R_i$  is the inverse of  $N_{ki}$ .  $N_{ki}$  is determined by a linear interpolation between the air kerma calibration factors, measured by the NMI, for the set of ISO quality X rays and the radionuclides  $^{137}\text{Cs}$  and  $^{60}\text{Co}$  [4], in accordance with:

$$N_{ki} = N_{k1i} + (E_i - E_{k1i})(E_{k2i} - E_{k1i})^{-1}(N_{k2i} - N_{k1i}) \quad (10)$$

where

- $N_{k1i}$  is the air calibration factor, determined by the calibration laboratory, with the lower closest mean X ray energy  $E_{k1i}$  to  $E_i$ ;
- $N_{k2i}$  is the air calibration factor, determined by the calibration laboratory, with the higher closest mean X ray energy  $E_{k2i}$  to  $E_i$ .

#### 4. RESULTS

When using the method of Goetsch et al. the approximated air kerma calibration factor of the NE 2561 ionization chamber for  $^{192}\text{Ir}$  is 0.3% higher than the NMI air kerma calibration factor for  $^{137}\text{Cs}$ . There are no data available to determine the uncertainty in the former calibration factor.

The air kerma calibration factor of the NE 2561 ionization chamber for  $^{192}\text{Ir}$  found with the method used at the NMI is 0.6% lower than the NMI air kerma calibration factor for  $^{137}\text{Cs}$ , which gives a total difference of 0.9% in  $N_K^{192\text{Ir}}$  compared with Goetsch et al. The total uncertainty in the air kerma calibration factor, derived by the NMI, is 0.85% (with a coverage factor of 2). The estimated uncertainty that should therefore be taken into account when the calibration factor is determined using the method recommended by Goetsch et al. should be raised by at least 1% over the combined uncertainty derived from the 250 kV and the  $^{137}\text{Cs}$  calibration factors.

#### 5. DISCUSSION AND CONCLUSIONS

The calibration factor for the NE 2561 ionization chamber found with Goetsch et al.'s method gives a value that is about 0.9% higher than the calibration factor determined by the procedure of weighting over the air kerma spectrum of a  $^{192}\text{Ir}$  brachytherapy source. The NMI method described in this paper is recommended by the NCS [2]. Further measurements at the NMI have shown that the calibration factor determined by weighting over the  $^{192}\text{Ir}$  spectrum is almost equal to a two point calibration (i.e. the air kerma calibration factor can be approximated as the average between the calibration factors for a 250 kV X ray quality and  $^{137}\text{Cs}$ ). The difference between this two point method and the method based on weighting the response curve of an ionization chamber over the  $^{192}\text{Ir}$  spectrum [4] is about 0.1% for the NE 2561 chamber. The method of weighting over the  $^{192}\text{Ir}$  spectrum is time consuming, which results in relatively high costs. The NMI therefore uses the two point method in routine calibrations.

In conclusion, two practical methods have been compared for determining the  $^{192}\text{Ir}$  air kerma calibration factor. Goetsch et al.'s method relies on an

extrapolation of chamber wall correction factors, while the NMi method is based on Spencer–Attix theory and weighting over the air kerma spectrum, and accounts for the energy dependence of air kerma calibration factors. The two methods yield a significant difference. The NMi method is recommended for all ionization chambers. If, however, it is chosen to use Goetsch et al.'s method, then it is advised that an additional uncertainty of at least 1% be assigned to the  $^{192}\text{Ir}$  air kerma calibration factor.

### ACKNOWLEDGEMENTS

The author wishes to thank J. Venselaar and I.K.K. Kolkman-Deurloo for their valuable comments on this work.

### REFERENCES

- [1] NEDERLANDSE COMMISSIE VOOR STRALINGSDOSIMETRIE, Recommendations for the Calibration of Iridium-192 High Dose Rate Sources, Rep. 7, NCS, Delft (1994).
- [2] NEDERLANDSE COMMISSIE VOOR STRALINGSDOSIMETRIE, Quality Control in Brachytherapy, Current Practice and Minimum Requirement, Rep. 13, NCS, Delft (2000).
- [3] GOETSCH, S.J., ATTIX, F.H., PEARSON, D.W., THOMADSON, B.R., Calibration of  $^{192}\text{Ir}$  high-dose-rate afterloading systems, *Med. Phys.* **18** (1991) 462–467.
- [4] GRIMBERGEN, T.W.M., VAN DIJK, E., Comparison of methods for derivation of  $^{192}\text{Ir}$  calibration factors for NE2561 & 2571 ionization chambers, Activity Rep. No. 7, Nucletron-Oldelft (1995).
- [5] INTERNATIONAL ORGANIZATION FOR STANDARDIZATION, X and Gamma Reference Radiations for Calibrating Dosimeters and Dose Ratemeters and for Determining their Response as a Function of Photon Energy, ISO 4037-1, ISO, Geneva (1993).
- [6] BORG, J., KWARAKOW, I., ROGERS, D.W.O., SEUNTJENS, J.P., Monte Carlo study of correction factors for Spencer–Attix cavity theory at photon energies at or above 100 keV, *Med. Phys.* **27** (2000) 1804–1813.

# **RADIOTHERAPY DOSIMETRY AUDITS**

(Session 11)

**Chair**

**H. SVENSSON**

European Society for Therapeutic Radiology and Oncology

**Co-Chair**

**J. IZEWSKA**

IAEA

**Rapporteur**

**R. HUNTLEY**

Australia

**BLANK**



## **WORLDWIDE QUALITY ASSURANCE NETWORKS FOR RADIOTHERAPY DOSIMETRY**

**J. IZEWSKA**

Division of Human Health, International Atomic Energy Agency,  
Vienna

E-mail: j.izewska@iaea.org

**H. SVENSSON**

European Society for Therapeutic Radiology and Oncology,  
Villejuif

**G. IBBOTT**

University of Texas M.D. Anderson Cancer Center,  
Houston, Texas, United States of America

### **Abstract**

Several national and international organizations have developed various types and levels of external audit systems for radiotherapy dosimetry, either based on on-site review visits or using mailed dosimetry systems. Three major TLD (thermoluminescence dosimetry) networks make available postal dose audits to a large number of radiotherapy centres on a regular basis. These are the IAEA/WHO (World Health Organization) TLD postal dose audit service, which operates worldwide; the European Society for Therapeutic Radiology and Oncology (ESTRO) network, known as EQUAL, which operates in the European Union; and the Radiological Physics Center (RPC) network in North America. Other external audit programmes are either associated with national and international clinical trial groups or perform national dosimetry comparisons that check radiotherapy dosimetry at various levels. The paper discusses the present status of the worldwide quality assurance networks in radiotherapy dosimetry and reviews the activities of the three main TLD networks: the IAEA/WHO, EQUAL and RPC networks.

### **1. INTRODUCTION**

The physical and technical aspects of quality assurance (QA) programmes in radiotherapy include the regular control of equipment, the dosimetry of radiotherapy beams, treatment planning procedures and treatment

delivery. A fundamental step in any dosimetry QA programme is an audit performed by an independent external body, a national or international organization, or a peer review by qualified medical radiation physicists.

Both on-site audit systems and mailed dosimetry programmes exist in parallel. On-site audit systems typically provide a thorough review of hospital QA programmes, and include checks of local dosimetry systems, tests of dosimetric, electrical, mechanical and safety parameters of radiotherapy equipment, tests of treatment planning systems (TPSs) and reviews of clinical dosimetry records. Some on-site systems have been designed to verify specific treatment techniques for use in national or international clinical trial groups.

The basic tool for on-site dosimetry audits is an ionization chamber. The measurements are conducted principally in water phantoms, although some audit systems use solid phantoms of various complexity, depending on the audit programme. The use of a portable calorimeter for on-site audits has recently been reported [1].

Most on-site review programmes operate at the national level for a limited number of hospitals, whereas mailed systems provide cost effective audits on a larger scale, involving radiotherapy facilities in hundreds of hospitals.

Thermoluminescent dosimeters in the form of powder is the type of transfer dosimeter preferred by the major postal audit systems [2–7], although some systems are based on thermoluminescent chips [8] or rods. A few one-off comparisons, such as the dosimetry exercise in the Nordic radiotherapy centres, France and Italy, involved Fricke dosimeters [9–11]. Some audit systems combine thermoluminescence dosimetry (TLD) and film techniques to increase the level of information audited from single point doses to two dimensional dose distributions [12–15]. With recent advances in technology, alanine and gel techniques may become a complementary tool or an attractive alternative to the traditional dose audit methodology.

## 2. TYPES AND LEVELS OF DOSE AUDIT SYSTEMS

There have been extensive debates on the range of dosimetry procedures that should undergo external audits so that they serve the purpose of enhancing confidence that the clinical dosimetry is accurate and that the hospital QA procedures are adequate. For practical reasons, typical postal dose audit systems have a limited scope and are capable of providing the verification of a few selected dose points or beam parameters only. The complexity of audit programmes depends on the local conditions, and it increases with the technical level of the participating hospitals and the experience of the auditing organization.

A four level flexible audit system may be adapted to allow the experience gained from preceding audit levels to be incorporated into subsequent audit steps:

- (a) Level 1. Postal dose audits for photon beams in reference conditions. It is necessary for any postal audit system to implement this step before launching a subsequent audit level.
- (b) Level 2. Postal dose audits for photon and electron beams in reference and non-reference conditions on the beam axis. This includes checks of beam quality (depth dose) and dose variation with field size and shape, and wedge transmission for photon beams, and checks of electron beam output, as well as of dose variation with field size and treatment distance.
- (c) Level 3. Audits for photon beams in reference and non-reference conditions off-axis and for dose at depth on the beam axis for electron beams. This includes checks of beam profiles, with and without wedges, for symmetric and asymmetric fields for photon beams, and a check of the electron beam energy in a standard field size and of the dose in a clinically relevant small field.
- (d) Level 4. Audits for photon and electron beams in anthropomorphic phantoms. This step is used to verify the dose distribution in more realistic treatment situations, such as for the breast, prostate or lung [16–18], or special treatment techniques, such as intensity modulated radiation therapy of the head and neck [13].

Most auditing systems focus on megavoltage photon and electron beams, although a few organizations extend their audit programmes to orthovoltage X rays and brachytherapy [19–21] using various set-ups and phantoms.

### 3. NATIONAL AND INTERNATIONAL QA NETWORKS FOR RADIOTHERAPY DOSIMETRY

Many national and international organizations have developed various types and levels of external audit (Fig. 1). There are three major TLD networks offering postal dose audits to over 2400 hospitals: the IAEA/WHO (World Health Organization) TLD postal dose audit programme, which operates worldwide; the ESTRO (European Society for Therapeutic Radiology and Oncology) system, EQUAL, set up for the European Union countries, and the Radiological Physics Center (RPC) network in North America. The EQUAL network has been linked to another European network (the European Commission (EC) network), which acted as a testing system for audit method-

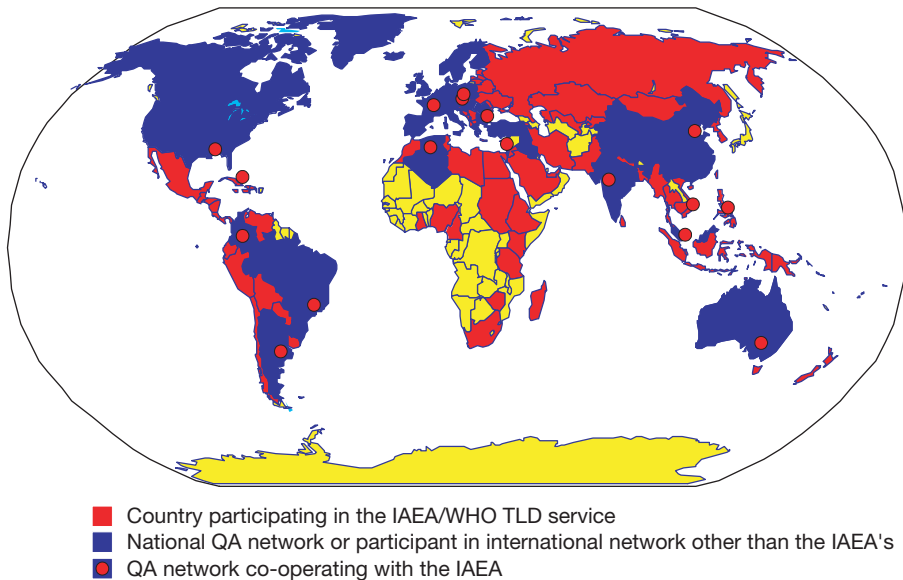


FIG. 1. Worldwide TLD audit networks for radiotherapy dosimetry.

ology [22]. Another QA project, for the transfer of know-how to a few countries in central and eastern Europe [23], was funded by the Flemish Government. In these projects, in addition to the extensive check of beam output in reference conditions, the feasibility of the methodology for electron dosimetry has been tested and a multipurpose solid phantom has been designed to check beam profiles in various geometrical conditions with mailed films [15, 24].

Other currently operating external audit programmes have been associated either with national or international clinical trial groups, similar to the RPC, for example the EORTC (European Organisation for Research in Treatment of Cancer) in Europe [17, 20], the RTOG (Radiotherapy Oncology Group) in the United States of America [25], the MRC (Medical Research Council) in the United Kingdom [16], or have been single dosimetry comparison exercises, carried out to test various levels of radiotherapy dosimetry, for example in Australia, Belgium, the Netherlands, Sweden and Switzerland [9, 19, 26, 27]. Some individual countries have set up regular audits of radiotherapy centres, including for QA programmes, equipment and dosimetry, for example Finland and the UK [18, 28].

The IAEA is currently encouraging, supporting and assisting Member States, and has traditionally done so, in the development of national audits, and offers technical backup at the same time as providing a link to the international

dosimetry chain. Several countries in various world regions have established TLD programmes to audit radiotherapy beams in hospitals with the assistance of the IAEA [29, 30]. The IAEA supports 18 national networks that encompass approximately 1400 hospitals with 870  $^{60}\text{Co}$  units and 1040 linacs. Owing to the different stages of the implementation of the national systems in these countries, at present only about 45% of local hospitals are involved in a regular audit programme.

#### 4. IAEA/WHO TLD POSTAL DOSE AUDIT SERVICE

The IAEA/WHO TLD postal programme for external audits of the calibration of high energy photon beams used in radiotherapy has been in operation since 1967 [6, 7, 31]. The programme aims at improving the accuracy and consistency of clinical dosimetry in radiotherapy hospitals worldwide. In its early years TLD audits were offered to hospitals both in developing and developed countries, but at present they are provided mainly to developing countries. TLD audits for radiotherapy dosimetry are also offered to the secondary standards dosimetry laboratories (SSDLs) [32, 33] that disseminate dosimetry standards to end user institutes by calibrating their local reference dosimeters for use in radiotherapy.

##### 4.1. IAEA TLD system

The dosimeters used in the IAEA/WHO TLD programme consist of polyethylene capsules filled with approximately 155 mg of annealed lithium fluoride ( $\text{LiF}$ ) powder, type TLD-100 (Harshaw). A PCL3 TLD automatic reader is used for the measurements. A calibration of the IAEA TLD system is performed in a  $^{60}\text{Co}$  beam, and several correction factors and coefficients are applied to account for the non-linearity in the dose response, the variation in sensitivity due to changes in beam quality and in the TLD holder attenuation, which is also a function of beam quality [34], and the fading of the thermoluminescent signal with time.

A thorough set of quality control procedures is maintained for the TLD system. The dose response and fading of the thermoluminescent dosimeter are verified at the commissioning of every new lot of powder, and the dosimeter calibration is verified at every reading session. The QA of the IAEA system includes reference irradiations provided by the Bureau international des poids et mesures, some primary standards dosimetry laboratories, major TLD audit networks and a few reference radiotherapy centres.

The IAEA exchanges dosimeters or carries out cross-measurements with EQUAL, the RPC and the EC network to ensure that there is a close correspondence in outcome. In this way the systems are interlinked to ensure that all international radiotherapy networks are working to the same levels and standards. The results of the reference irradiations from 1997 to 2001 provided by the major TLD networks and a few reference hospitals are presented in Fig. 2.

#### 4.2. Results of the thermoluminescent dosimeter irradiations

The dosimeters are sent to hospitals along with instructions and data sheets prepared for  $^{60}\text{Co}$  and high energy X ray beams. Users are requested to irradiate them in a water phantom, in the same way that a patient would be irradiated using a simple one beam configuration, with either the source to skin distance (SSD) or the isocentric (source to axis distance) set-up, depending on the normal practice of the hospital. The dose to water at the position of the dosimeters should be calculated in the same way as for patient treatments (i.e. using routine clinical data).

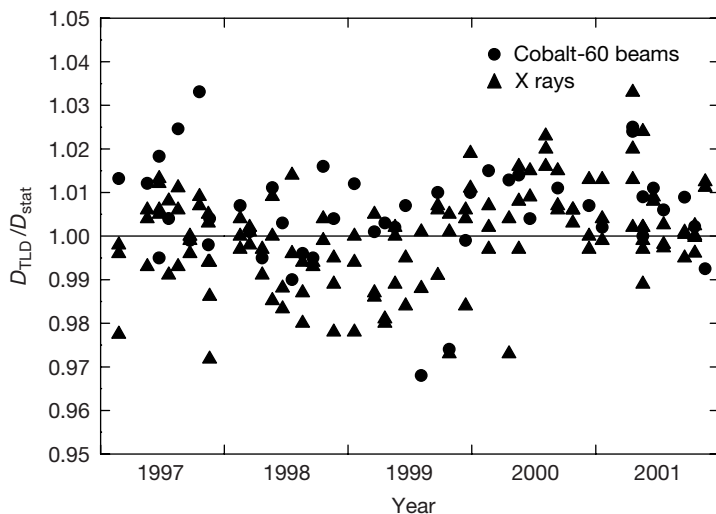


FIG. 2. Results of the reference irradiations from 1997 to 2001 provided by reference hospitals and major TLD networks. The symbols correspond to the ratios of the IAEA's determined dose ( $D_{TLD}$ ) relative to the dose stated by the reference centre ( $D_{stat}$ ). Each data point corresponds to the average of three dosimeters. A total of 180 reference irradiations were provided during this period. The mean of the distribution is 1.002 and the standard deviation is 1.1%.

The acceptance limit of 5% defines the maximum discrepancy between the stated and measured doses, which does not require further investigation. The 5% limit corresponds to the classical International Commission on Radiation Units and Measurements recommendation [35]. All results outside the acceptance limit are followed up and assistance is provided to reconcile discrepancies.

Over a period of about 33 years the IAEA/WHO TLD programme has verified the calibration of more than 4500 photon beams in approximately 1200 radiotherapy hospitals. From 1997 to 2001 the number of beams checked was 1520, which corresponds to approximately one third of the total. These checks were made in 626 hospitals in 90 countries in Africa, the eastern Mediterranean, Europe, Latin America and the Caribbean, Southeast Asia and the western Pacific. The distribution of the number of beams checked per region is shown in Fig. 3. Participation from the various regions corresponds to the requests received at the different regional offices of the WHO; for example, 35% of the beams checked were in hospitals in Latin America and the Caribbean, whereas only 6% were in Africa. Since 1996 the IAEA/WHO TLD audits have been initiated in some countries of eastern and southeastern Europe, raising the percentage of beams checked in Europe to 31%. A single thermoluminescent dosimeter batch was provided in 1998, on special request, to hospitals in Australia [36].

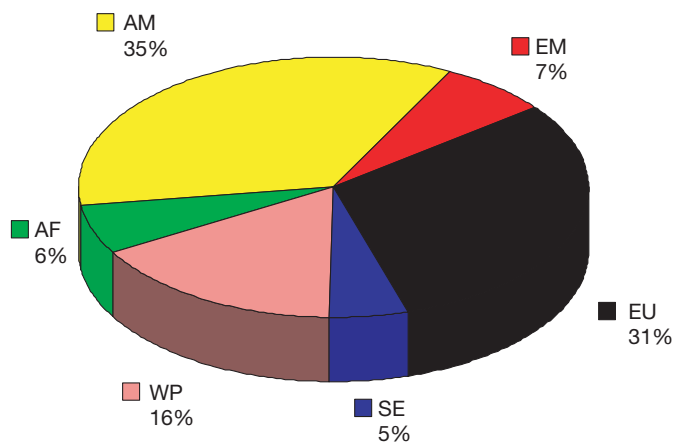


FIG. 3. Distribution of the number of beams checked in different regions from 1997 to 2001. The results pertain to 1520 photon beams in 626 hospitals in 90 countries in six world regions: Africa (AF), Latin America (AM), the eastern Mediterranean (EM), Europe (EU), Southeast Asia (SE) and the western Pacific (WP).

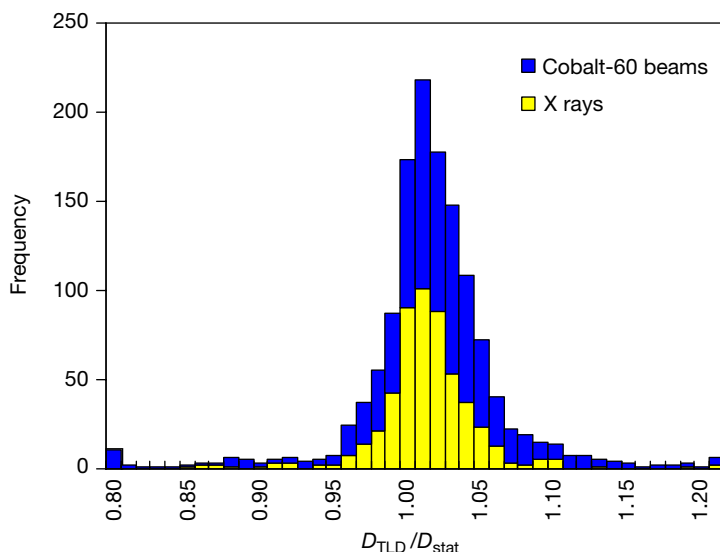


FIG. 4. Distribution of the results of the IAEA/WHO TLD postal dose audits of radiotherapy hospitals for the delivery of absorbed dose to water under reference conditions from 1997 to 2001. The histograms correspond to ratios of the IAEA's determined dose ( $D_{TLD}$ ) relative to the dose stated by the hospital ( $D_{stat}$ ). Each data point corresponds to the average of two dosimeters.

The distribution of the results for 1997 to 2001 is shown in Fig. 4; they include 936  $^{60}\text{Co}$  beams and 584 high energy X ray beams. The results correspond to the ratios of the IAEA TLD measured dose to that stated by the user,  $D_{TLD}/D_{stat}$ . Each value represents the average of two dosimeters. The mean of the distribution is 1.010, its standard deviation is 8.2% and the outliers range between a minimum of 0.06 and a maximum of 2.12. In 82% of cases the results were within the acceptance limit of 5%, whereas 2.6% (25 beams) had discrepancies larger than 20%, pointing at major problems in the delivery of dose to the dosimeters. All results outside the 5% acceptance limit were followed up with a second check. The majority of participants improved their results in the second irradiation but, unfortunately, 87 deviations outside 5% (5.7% of the beams checked) could not be resolved in 1997 to 2001. This was due either to a persistent error or to a failure in responding to the efforts by the IAEA to help resolve the problem. On-site visits were organized to several hospitals in which dosimetry practices were revised, and recommendations were made to the local staff.

Experience from the TLD service demonstrates the significance for a hospital of participating in an external audit programme. Only 75% of those hospitals that received thermoluminescent dosimeters for the first time had results



with a deviation between the measured and stated dose within the acceptance limit of 5%, while approximately 88% of the users that benefited from a previous TLD audit were successful in subsequent tests.

It is important to note that the distribution of the results for 50 high energy X ray beams audited in Australia in 1998 had a mean ratio of 1.002 and a standard deviation of 1.1%, with no results outside the acceptance limit of 5% [36].

## 5. ESTRO EUROPEAN ASSURANCE PROGRAMME FOR RADIATION TREATMENTS (THE EQUAL NETWORK)

The ESTRO Quality Assurance Network for radiotherapy (EQUAL) was set up in 1998 for the countries of the European Union [3]. This TLD postal dose service includes photon and electron beam checks in reference and non-reference conditions. By September 2002 the service had provided audits for more than 450 radiotherapy centres by checking about 2200 beams (see Fig. 5). Dosimetric problems in the beam calibration, errors in beam data used as input to the TPS and uncertainties in the algorithms used in the TPS can be detected through the EQUAL audit.

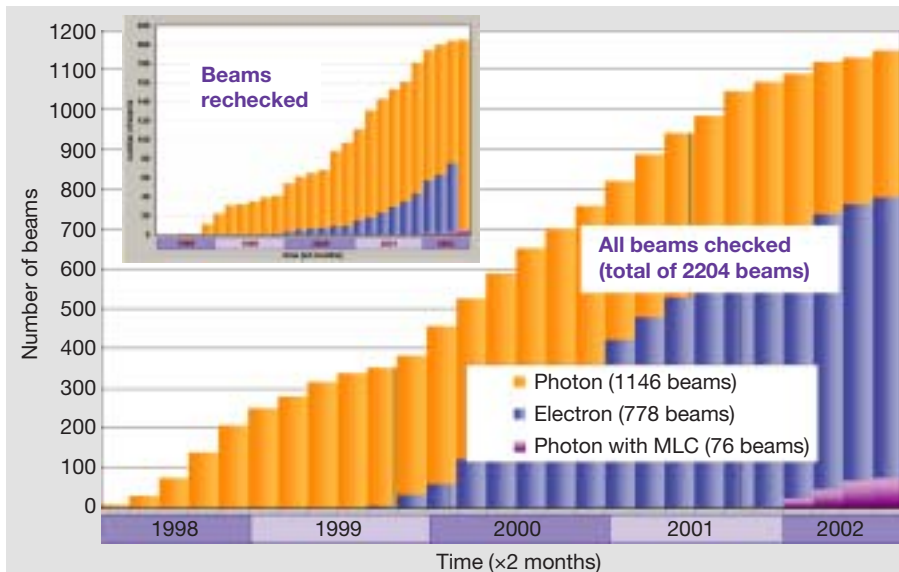


FIG. 5. Cumulative number of beam checks in the EQUAL programme.

The participating centres are instructed to irradiate the thermoluminescent dosimeter (LiF) capsules to a dose of 2 Gy, based on calculations using the TPS applied routinely for clinical use. Four dosimetric parameters were checked for photon beams: the beam output in reference conditions; the percentage depth doses; the beam output variation for open and wedged fields; and the wedge transmission factor. Measurements with electrons beams were carried out for three different field sizes and two SSDs.

About 13% of all beams had to be rechecked (Fig. 5), owing to deviations larger than 5%. In some of these cases the deviations could be traced to set-up errors or other mistakes, for example the wrong SSD being used, the wedge forgotten or the wrong depth being used. It was proven that 6% of the deviations were due to real dosimetry problems. Site visits were then offered, and have been carried out in 13 centres.

Most of the large deviations in dose were for non-reference conditions. The deviations have progressively decreased for the reference geometry. Thus for photon beams in the checks between 1998 and 1999, 3.1% of the centres were outside 5%, while only 1.2% were outside 5% between 1998 and 2002. The real improvement is even larger, as the latter value also includes the early period. The effort in Europe, including the introduction of new dosimetry protocols, training courses by ESTRO, etc., seems to have paid off.

The EQUAL programme is extended in parallel with changes in radiotherapy techniques. Checks were recently included for photon fields shaped by multileaf collimators (MLCs). In the MLC dose audit, five fields were checked with shapes and dimensions defined by the MLC. Since the launch of the programme in early 2002, the MLC dose checks have been performed for 76 beams, showing the great interest of radiotherapy centres in this new service. A programme for brachytherapy audits is now being prepared. Detailed results from ESTRO are reported in a separate paper in these Proceedings [4].

## 6. RPC

The RPC has been funded continuously since 1968 [2, 5] to monitor radiation therapy dose delivery at institutes participating in clinical trials sponsored by the US National Cancer Institute (NCI). The RPC also serves as a national resource in radiation dosimetry and physics for co-operative clinical trial groups and for all radiotherapy facilities that deliver radiation treatments to patients entered into co-operative group protocols. To accomplish this, the RPC has implemented a QA programme that monitors the basic machine output or brachytherapy source strength, the dosimetry data utilized by the institute, the calculational algorithms used during treatment planning and the institute's QA

procedures. The methods of monitoring include: (a) on-site dosimetry reviews by an RPC physicist; and (b) various remote audit tools. During the on-site evaluation, the institute's physicist and radiation oncologist are interviewed, physical measurements are made on the radiotherapy machines, dosimetry and QA data are reviewed, and patient dose calculations are evaluated. When deficiencies are detected, the RPC issues recommendations to the institute. A list of recently issued recommendations and their frequencies is shown in Table I.

The remote audit tools include: (a) mailed thermoluminescent dosimeters evaluated on a periodic basis to verify output calibrations and simple questionnaires to document changes in personnel, equipment or dosimetry practices; (b) the comparison of dosimetry data with RPC 'standard' data to verify the comparability of the dosimetry data; (c) the evaluation of reference and/or actual patient calculations to verify the validity of the treatment planning algorithms; (d) the review of the institute's written QA procedures and records; and (e) mailable anthropomorphic phantoms to verify tumour dose delivery for special treatment techniques. Any discrepancy identified by the RPC is followed up to help the institute find the origin of the discrepancy and to identify and implement methods to resolve it. Thus the RPC's QA review programme affects not only the quality of the treatment of patients in clinical

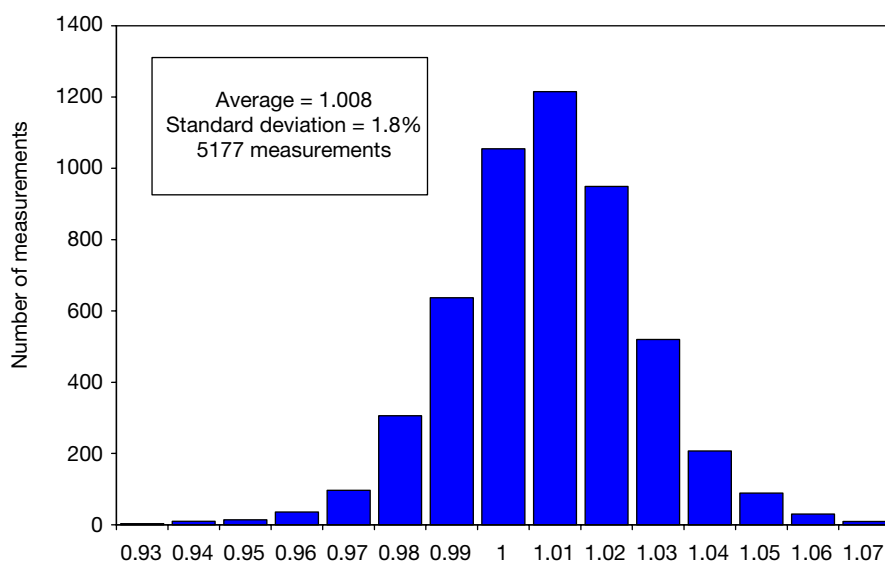


FIG. 6. Ratio of the institute's stated dose to the RPC's dose measured with mailed TLD. The figure covers photon beam data collected during 2000, following the introduction of the American Association of Physicists in Medicine TG 51 calibration protocol [37].

TABLE I. RECOMMENDATIONS MADE TO INSTITUTES FOLLOWING ON-SITE VISITS TO 56 INSTITUTES IN 2000

*(The frequency with which each recommendation was made is shown in parentheses.)*

Area of recommendation	Number of institutes receiving the recommendation
Inadequate QA programme	46 (82%)
Wedge transmission factors	28 (50%)
Electron calibration	14 (25%)
Off-axis factors	14 (25%)
Photon depth dose	12 (21%)
Electron depth dose	11 (20%)
Electron cone ratios	8 (14%)
Brachytherapy source calibration	7 (13%)
Asymmetric jaw calculations	7 (13%)
Photon calibration	6 (11%)
Using multiple sets of data	6 (11%)
Beam asymmetry	5 (9%)
Mechanical problems (lasers, optical distance indicator, collimator dial)	4 (7%)
Photon field size dependence	3 (5%)

trials but also the quality of the treatment of all patients treated at an institute. Figure 6 shows the agreement between the RPC's measurement of photon beam dose by mailed TLD and the institute's stated dose.

The RPC routinely monitors all conventional therapies, including external beam megavoltage photon and electron therapy as well as low and high dose rate brachytherapy. Monitoring procedures are modified to accommodate new techniques and special procedures used in co-operative group trials. Therefore, asymmetric jaws, multileaf collimators, dynamic wedges and non-coplanar beam procedures are monitored, as well as some special procedures, including

total body photon irradiation, intraoperative electron beam therapy, stereotactic radiosurgery and conformal radiotherapy.

More details on the RPC's activities are presented in a separate paper [2] in these Proceedings.

## 7. SUMMARY AND CONCLUSIONS

Owing to recent developments in external audit systems at the international and national level, better access to an audit programme is now available for many hospitals, although the number of hospitals that have not participated in an external audit is still significant. According to the IAEA's database, there are approximately 5700 radiotherapy centres in the world, of which not more than about 60% have participated in an audit programme within the past five years; that is, about 630 hospitals participated in the IAEA/WHO programme, 450 participated in the EQUAL network, 1300 are included in the RPC's checks and not more than 600 hospitals participate in regular audits at the national level. It is estimated that other QA networks probably involve fewer than 500 hospitals.

On-site systems provide an opportunity to review in depth the local clinical dosimetry, whereas mailed systems spot check either one or a few parameters of a radiotherapy beam and can verify hospital dosimetry practices to a lesser extent. Mailed systems mostly help to detect and correct fundamental problems in basic dosimetry, which can be followed up and corrected.

It is vital for a hospital to participate regularly in dosimetry audits. The experience of the various networks indicates that those hospitals that receive thermoluminescent dosimeters for the first time have a lower probability to achieve results within the acceptance limit than hospitals that have benefited from a previous audit. Some, or even many, facilities not involved in external quality audits may deliver inferior radiotherapy treatments, owing to inadequate dosimetry practices.

The clinical relevance of deviations detected in audit programmes was confirmed in many cases, but, fortunately, not all poor dosimetric results reflect deficiencies in the calibration of clinical beams or machine faults. Some dosimetry errors would have no direct impact on the actual doses delivered to a patient, as they are caused by common mistakes in the TLD irradiation exercise or are related to misunderstandings of the audit instructions.

In general, audits in developing countries, as noted by the IAEA, show a significantly lower percentage of results within the acceptance limits than those in developed countries, even though the hospitals participate in the audits reg-

ularly. Technical and scientific inadequacies exist that may handicap the level of clinical dosimetry in these countries. Some problems are caused by obsolete dosimetry equipment or poor treatment machine conditions. Other problems are due to the insufficient training of staff working in radiotherapy.

For all the QA networks that have carried out audits in conditions other than reference conditions, the results and experience show that the good performance of a radiotherapy centre delivering dose under reference conditions does not imply that there are no problems under non-reference dose conditions. Significant numbers of deviations under non-reference conditions, as used clinically on patients, have been observed in all audit systems. Therefore, it has been recognized that an external independent audit should be carried out under non-reference conditions as well as under reference conditions.

### ACKNOWLEDGEMENTS

This work refers to the system of external audit levels analysed at the IAEA Consultants Meeting in Vienna, 18–22 June 2001. The authors wish to thank A. Dutreix, D.S. Followill, D. Huyskens and D.I. Thwaites for their contribution to that meeting.

### REFERENCES

- [1] McEWEN, M.R., DUANE, S., “Portable graphite calorimeter for measuring absorbed dose in the radiotherapy clinic”, these Proceedings, Vol. 1, pp. 115–121.
- [2] AGUIRRE, J.F., TAILOR, R.C., IBBOTT, G.S., STOVALL, M., HANSON, W.F., “Thermoluminescence dosimetry as a tool for the remote verification of output for radiotherapy beams: 25 years of experience”, *ibid.*, Vol. 2, pp. 191–199.
- [3] FERREIRA, I.H., et al., “Radiotherapy dosimetry audit: A European programme to improve quality and safety in radiation treatments”, Radiological Protection of Patients in Diagnostic and Interventional Radiology, Nuclear Medicine and Radiotherapy (Proc. Int. Conf. Malaga, 2001), IAEA, Vienna (2001) 309–330.
- [4] FERREIRA, I.H., DUTREIX, A., BRIDIER, A., CHAVALUDRA, J., SVENSSON, H., “ESTRO European assurance programme for radiation treatments (the EQUAL network)”, these Proceedings, Vol. 2, pp. 157–165.

- [5] HANSON, W.F., SHALEK, R.J., KENNEDY, P., Dosimetry quality assurance in the United States from the experience of the Radiological Physics Center, SSDL Newsletter No. 30 (1991) 18–34.
- [6] IZEWSKA, J., ANDREO, P., The IAEA/WHO TLD postal programme for radiotherapy hospitals, *Radiother. Oncol.* **54** (2000) 65–72.
- [7] SVENSSON, H., HANSON, G.P., ZSDANSKY, K., The IAEA/WHO TL dosimetry programme for radiotherapy centres 1969–1987, *Acta Oncol.* **29** (1990) 461–467.
- [8] PYCHLAU, C., “Radiation therapy thermoluminescence dosimetry service in Germany: The experience of the first year”, these Proceedings, Vol. 2, pp. 167–175.
- [9] JOHANSSON, K.-A., SVENSSON, H., Dosimetric intercomparison at the Nordic radiation therapy centres. Part II. Comparison between different detectors and methods, in the Thesis by K.-A. Johansson, Univ. Gothenburg (1982).
- [10] WAMBERSIE, A., DUTREIX, A., PRIGNOT, M., Résultats d’une comparaison intercentres de l’étalonnage des dosimeters pour le  $^{60}\text{Co}$  au moyen de  $\text{FeSO}_4$ , *J. Radiol. Electrol.* **54** (1973) 835–839.
- [11] MILANO, F., Mailed Fricke dosimetry of radiotherapy electron and photon beams, *Nukleonika* **41** (1996) 83–92.
- [12] BRIDIER, A., NYSTRÖM, H., FERREIRA, I., GOMOLA, I., HUYSKENS, D., A comparative description of three multipurpose phantoms (MPP) for external audits of photon beams in radiotherapy: The water MPP, the Umeå MPP and the EC MPP, *Radiother. Oncol.* **55** (2000) 285–293.
- [13] IBBOTT, G., NELSON, A., FOLLOWILL, D., BALTER, P., HANSON, W.F., “An anthropomorphic head and neck phantom for the evaluation of intensity modulated radiation therapy”, these Proceedings, Vol. 2, pp. 209–217.
- [14] KROUTILÍKOVÁ, D., NOVOTNÝ, J., NOVÁK, L., “Thermoluminescence dosimetry quality assurance network for radiotherapy and radiology in the Czech Republic”, *ibid.*, Vol. 2, pp. 269–276.
- [15] NOVOTNY, J., GOMOLA, I., IZEWSKA, J., HUYSKENS, D., DUTREIX, A., External audit of photon beams by mailed film dosimetry, *Phys. Med. Biol.* **42** (1997) 1277–1288.
- [16] AIRD, E.G., WILLIAMS, C., MOTT, G.T., Quality Assurance in the CHART clinical trial, *Radiother. Oncol.* **36** (1995) 235–245.
- [17] DAVIS, J.B., MILTCHEV, V., Tangential breast irradiation: A multi-centric intercomparison of dose using a mailed phantom and thermoluminescent dosimetry, *Radiother. Oncol.* **52** (1999) 65–68.
- [18] THWAITES, D.I., WILLIAMS, J.R., AIRD, E.G., KLEVENHAGEN, S.C., WILLIAMS, P.C., A dosimetric intercomparison of megavoltage photon beams in UK radiotherapy centres, *Phys. Med. Biol.* **37** (1992) 445–461.
- [19] ELFRINK, R.E., et al., Quality control of brachytherapy equipment in the Netherlands and Belgium: Current practice and minimum requirements, *Radiother. Oncol.* **62** (2002) 95–102.
- [20] HANSSON, U., JOHANSSON, K.A., HORIOT, J.C., BERNIER, J., Mailed TL dosimetry programme for machine output check and clinical application in the EORTC radiotherapy group, *Radiother. Oncol.* **29** (1993) 85–90.

- [21] THWAITES, D.I., POWLEY, S.K., NISBET, A., ALLAHVERDI, M., "The United Kingdom's radiotherapy dosimetry audit network", these Proceedings, Vol. 2, pp. 183–190.
- [22] DUTREIX, A., DERREMAUX, S., CHAUAUDRA, J., VAN DER SCHUEREN, E., Quality control of radiotherapy centres in Europe: Beam calibration, *Radiother. Oncol.* **32** (1994) 256–264.
- [23] IZEWSKA, J., et al., Quality assurance network in Central Europe: External audit on output calibration for photon beams, *Acta Oncol.* **34** (1995) 829–838.
- [24] GOMOLA, I., et al., External audits of electron beams using mailed TLD dosimetry: Preliminary results, *Radiother. Oncol.* **58** (2001) 163–168.
- [25] PALIWAL, B.R., et al., A solid water pelvic and prostate phantom for imaging, volume rendering, treatment planning, and dosimetry for an RTOG multi-institutional, 3-D dose escalation study, *Int. J. Radiat. Oncol. Biol. Phys.* **42** (1998) 205–211.
- [26] KRON, T., HAMILTON, C., ROFF, M., DENHAM, J., Dosimetric intercomparison for two Australasian clinical trials using an anthropomorphic phantom, *Int. J. Radiat. Oncol. Biol. Phys.* **52** (2002) 566–579.
- [27] SCHIEFER, H., SEELENTAG, W., STUCKI, G., "Ein nationaler Dosimetrie-vergleich durch Postversand von TLDs", paper presented at the Ann. Conf. of the Swiss Society of Radiobiology and Medical Physics, Sion, 2001.
- [28] JÄRVINEN, H., SIPILÄ, P., PARKKINEN, R., KOSUNEN, A., JOKELAINEN, I., "Quality systems for radiotherapy: Impact by a central authority for improved accuracy, safety and accident prevention", paper presented at the IAEA Symp. on Radiological Protection of Patients in Diagnostic and Interventional Radiology, Nuclear Medicine and Radiotherapy, Malaga, 2001.
- [29] IZEWSKA, J., et al., Guidelines for the preparation of a quality manual for external audit groups on dosimetry in radiotherapy, *SSDL Newsletter* No. 46 (2002) 2–13.
- [30] IZEWSKA, J., THWAITES, D.I., "IAEA supported national thermoluminescence dosimetry audit networks for radiotherapy dosimetry: Summary of the posters presented in session 12b", these Proceedings, Vol. 2, pp. 249–267.
- [31] NETTE, P., SVENSSON, H., Radiation dosimetry in health care: Expanding the reach of global networks, *Int. At. Energy Agency Bull.* **4** (1994) 33–36.
- [32] INTERNATIONAL ATOMIC ENERGY AGENCY, *SSDL Network Charter: The IAEA/WHO Network of Secondary Standard Dosimetry Laboratories*, IAEA, Vienna (1999).
- [33] SVENSSON, H., ZSDANSKY, K., NETTE, P., "Dissemination, transfer and inter-comparison in radiotherapy dosimetry: The IAEA concept", *Measurement Assurance in Dosimetry (Proc. Int. Symp. Vienna, 1993)*, IAEA, Vienna (1994) 165–176.
- [34] IZEWSKA, J., NOVOTNY, J., DUTREIX, A., VAN DAM, J., VAN DER SCHUEREN, E., The influence of the IAEA standard holder on dose evaluated from TLD samples, *Phys. Med. Biol.* **41** (1996) 465–473.
- [35] INTERNATIONAL COMMISSION ON RADIATION UNITS AND MEASUREMENTS, *Determination of Absorbed Dose in a Patient Irradiated by*



Beams of X or Gamma rays in Radiotherapy Procedures, Rep. 24, ICRU, Bethesda, MD (1976).

- [36] HUNTLEY, R., IZEWSKA, J., The 1998 Australian external beam radiotherapy survey and IAEA/WHO TLD postal dose quality audit, *Australas. Phys. Eng. Sci. Med.* **23** (2000) 21–29.
- [37] AMERICAN ASSOCIATION OF PHYSICISTS IN MEDICINE, AAPM's TG-51 protocol for clinical reference dosimetry of high-energy photon and electron beams, *Med. Phys.* **26** (1999) 1847–1870.

**BLANK**

## **ESTRO EUROPEAN ASSURANCE PROGRAMME FOR RADIATION TREATMENTS (THE EQUAL NETWORK)**

I.H. FERREIRA, A. DUTREIX

ESTRO EQUAL Measuring Laboratory, Service de physique,  
Institut Gustave-Roussy,  
Villejuif, France  
E-mail: equal@igr.fr

A. BRIDIER

Service de physique, Institut Gustave-Roussy,  
Villejuif, France

H. SVENSSON

Radiation Physics Department, University of Umeå,  
Umeå, Sweden

### **Abstract**

The European Society for Therapeutic Radiology and Oncology (ESTRO) Quality Assurance Network for Radiotherapy (EQUAL) was set up in 1998. The EQUAL programme checks, using thermoluminescent dosimeters, four dosimetric parameters for photon beams: the reference beam output, the percentage depth dose, the beam output variation for open and wedged fields, and the wedge transmission factor. For electron beams, outputs are checked for four different field sizes in electron thermoluminescence dosimetry audits. The EQUAL programme has recently been extended to include dose checks in photon fields shaped with multileaf collimators (MLCs). In the MLC audit the EQUAL programme checks doses in five fields with shapes and dimensions defined by the MLC. The ESTRO quality assurance programme shows that dosimetry accuracy is fairly good in the reference condition, but that improvements are often needed in non-reference conditions (i.e. in irradiation geometries closely simulating those used in patient treatments).

## **1. INTRODUCTION**

Since 1998 the European Society for Therapeutic Radiology and Oncology (ESTRO) has run a thermoluminescence dosimetry (TLD) quality assurance programme known as EQUAL, which uses thermoluminescent dosimeters. The programme currently covers 23 European and two Mediterranean Basin countries.

Under the terms of the EQUAL programme the accuracy in dose is checked on the beam axis in both reference and non-reference conditions. The measuring laboratory is part of the Physics Department of the Institut Gustave-Roussy (IGR) in Villejuif, France. The traceability of the ionization chamber calibration to the Bureau international des poids et mesures is assured through a periodical reference chamber calibration at the French primary laboratory and by annual intercomparisons with the IAEA/World Health Organization network and other TLD networks, and with one of the French secondary standards dosimetry laboratories [1–3].

The EQUAL audit can detect dosimetric problems in beam calibration, errors in the beam data used as input to the treatment planning system (TPS) and uncertainties in the algorithms used in the TPS.

The service provided by EQUAL is supported by the European Union's (EU) Europe against Cancer action plan, is free of charge and is available to all EU countries. A memorandum of understanding has been signed with the IAEA, and, in agreement with the IAEA, the service can be offered to the countries neighbouring the EU that have no national programme.

## **2. MATERIALS AND METHODS**

### **2.1. EQUAL TLD system**

The EQUAL measuring laboratory uses for photon and electron beam dosimetry a method developed by the Medical Physics Department of the IGR. The dosimeters are made of lithium fluoride (LiF); LiF powder type DTL937 (Philitech) is encapsulated into IAEA black polyethylene cylindrical containers. The dosimeters are read on a PCL3 automatic reader (Fimel PTW). All dosimeter irradiations (photon and electron checks) in the participating centres are performed in a water phantom using IAEA holders.

The absorbed doses to water in photon and electron beams, measured by ionization chambers, are determined following the procedure described in the IAEA code of practice in Technical Reports Series No. 398 [4].

The EQUAL reference dosimetry is linked by periodic intercomparisons [1, 2] to the IAEA Dosimetry Laboratory and to the Radiological Physics Center's dosimetry laboratory in Houston, Texas.

### **2.2. Dosimetric parameters checked in the EQUAL programme**

Four dosimetric parameters are checked for photon beams: the beam output in reference conditions (RBO), percentage depth doses (PDDs), beam

output variations (BOVs) for open and wedged fields, and the wedge transmission factor (WTF). For electrons, the beam outputs for three different field sizes are checked for each energy (10 cm  $\times$  10 cm, 15 cm  $\times$  20 cm and 7 cm  $\times$  7 cm) [1, 2].

The EQUAL programme has been recently extended to include dose checks on the axis of photon fields shaped with multileaf collimators (MLCs). This extension to MLC fields and the combination of offset fields with wedges takes into account the increasing use of these tools in conformal photon beam therapy. The purpose of the MLC TLD audits is to check dosimetric data for fields tailored by an MLC as used for patient treatments. The dose at the reference depth is checked for six fields in this protocol: the reference field (10 cm  $\times$  10 cm) and five other fields with shapes and dimensions defined by the MLC (Fig. 1).

### 3. RESULTS

Figure 2 shows the percentage of European radiotherapy centres checked by the EQUAL laboratory or by a national quality assurance (QA) network for photon and electron beams in each country. All centres in four countries have been checked through the respective national centre, but a large proportion of

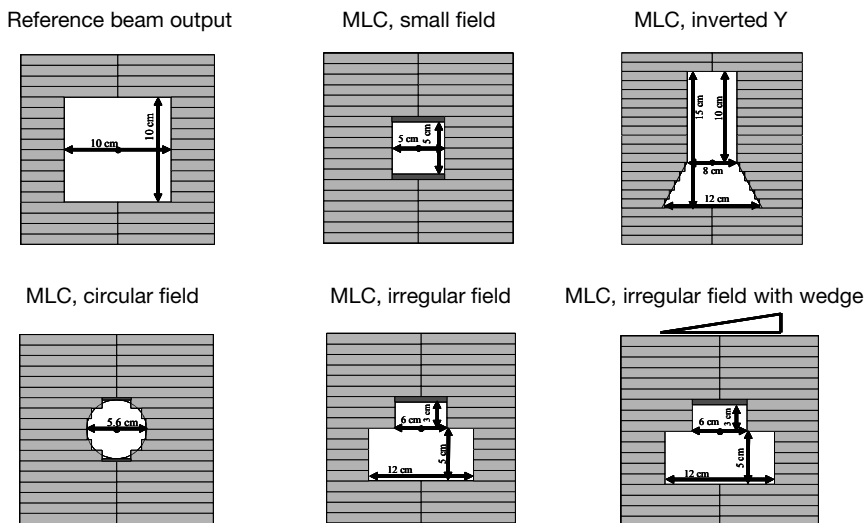


FIG. 1. Fields shaped by an MLC checked by the EQUAL programme.

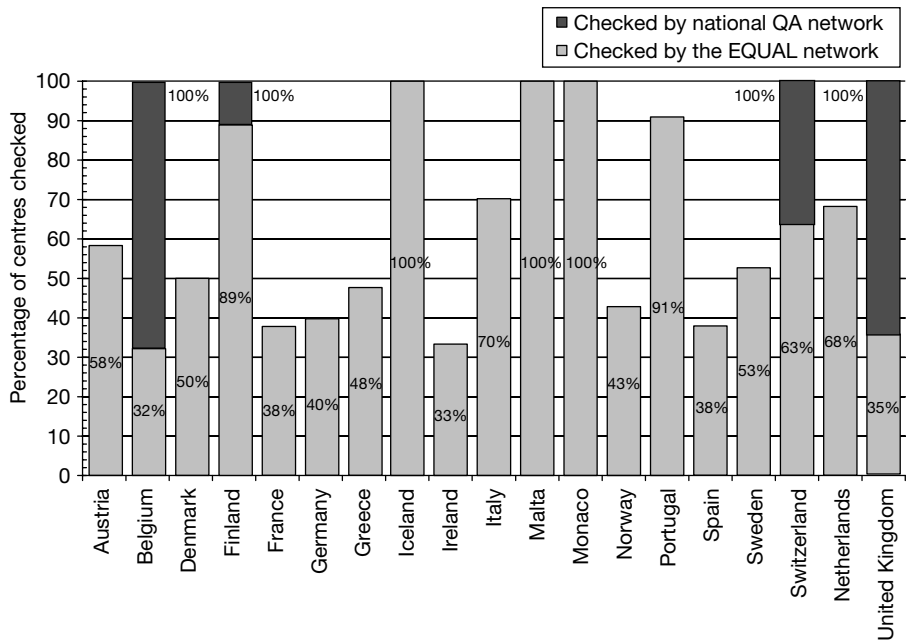


FIG. 2. Percentage of centres per country checked by the EQUAL programme (in grey) and by national QA networks (in black) expressed in per cent of the total number of radiotherapy centres in each country (as of July 2002).

centres have nevertheless applied to join the EQUAL programme. More than 50% of centres in the EU have applied to join the EQUAL programme or a national QA network, which shows the great interest of radiotherapy centres in participating in external audits in order to improve the accuracy of patient treatments.

In order to evaluate the agreement between the measured dose,  $D_m$ , and the dose stated by the participating centre,  $D_s$ , deviations,  $\delta$  ( $|\delta| = |(D_s - D_m)| \times 100/D_m$ ), are calculated for photon and electron beams. Tables I and II give the number of beams with deviations,  $\delta$ , at each level considered in the EQUAL protocol ( $|\delta| \leq 3\%$ ,  $3\% < |\delta| \leq 5\%$ ,  $5\% < |\delta| \leq 10\%$  and  $|\delta| > 10\%$ ) for the parameters checked.

The results concern only the deviations confirmed in the second check, those for which the number of monitor units was modified between the first and second check, and those for which some parameters have been corrected by the physicist after the first check.

Out of the 160 photon beams rechecked, 54 beams had deviations  $|\delta| > 5\%$ , due to possible set-up errors or to a recalibration of the monitor, and

TABLE I. NUMBER OF PHOTON BEAMS AND PERCENTAGES AT EACH DEVIATION LEVEL FOR RBO, BOV, PDD AND WTF

Parameter	Deviation levels on $ \delta $				Number of beams
	$ \delta  \leq 3\%$	$3\% <  \delta  \leq 5\%$	$5\% <  \delta  \leq 10\%$	$ \delta  > 10\%$	
RBO	1037 (91%)	94 (8%)	12 (1%)	2 (0.2%)	1145
PDD	1078 (97%)	25 (2%)	9 (1%)	2 (0.2%)	1114
BOV					
Open beams	999 (89%)	93 (8%)	28 (3%)	1 (0.1%)	1121
Wedged beams	907 (87%)	99 (10%)	15 (1.5%)	3 (0.3%)	1024
WTF	922 (88%)	89 (8.5%)	27 (3%)	7 (0.7%)	1045

106 beams presented identified proven dosimetric problems. The main dosimetric problems observed for the photon beams were: errors in the TPS data (PDD, WTF and output variations with field sizes); errors in the reference dose; errors in the dose calculations (use of the wrong PDD, wedge, etc.); errors in electrometer readings; errors in the WTF; errors in the timer for the cobalt machine; errors in field size; and errors in the beam calibration (i.e. the use of a plastic phantom instead of a water phantom without correcting for the equivalent depth).

The results (Table I) show that 91% of the beam outputs checked in reference conditions (RBO) were at the optimal level ( $|\delta| \leq 3\%$ ), 8% had deviations between 3% and 5%, and only 1.2% had deviations outside the tolerance level ( $|\delta| > 5\%$ ). Regarding the PDDs, 93% of the beams were at the optimal level, 5% had deviations between 3% and 5%, and 2% of the checked beams had deviations outside the tolerance level.

For the BOV, 89% (open beams) and 87% (wedged beams) were at the optimal level, and 3.1% (open beams) and 1.8% (wedged beams) had  $\delta$  outside the tolerance level; 88% of the WTFs were at the optimal level, and 3.7% had deviations outside the tolerance level. The BOV (open beams) and the WTF presented the highest number of deviations (8% and 8.5%, respectively) outside the optimal level but within the tolerance level ( $|\delta|$  between 3% and 5%).

The results of the EQUAL programme show significant improvements in dosimetry in European centres. Table III shows the improvements in the results of EQUAL checks between 1999 and 2002. For the BOV, 1.2% of the checked beams in 2002 were found with deviation  $|\delta| > 5\%$ , compared with 3.1% in 1999. The improvement of the QA results is also remarkable for the BOV and the WTF.

TABLE II. NUMBER OF DEVIATIONS,  $\delta$ , FOR 769 ELECTRON BEAM OUTPUTS CHECKED BY THE EQUAL PROGRAMME

*(Deviations observed in the first check and not in the second are not included.)*

Field size	Dosimeter used	Deviation levels on $ \delta $				Total number of checks
		$ \delta  \leq 3\%$	$3\% <  \delta  \leq 5\%$	$5\% <  \delta  \leq 10\%$	$ \delta  > 10\%$	
10 cm $\times$ 10 cm	1 and 2	637 (83%)	95 (12%)	33 (4%)	4 (0.5%)	769
15 cm $\times$ 20 cm	3	547 (79%)	110 (16%)	30 (4%)	6 (0.9%)	693
7 cm $\times$ 7 cm	4	562 (81%)	94 (14%)	29 (4%)	8 (1.2%)	693
10 cm $\times$ 10 cm (SSD <sup>a</sup> $\geq$ 105 cm)	5	281 (80%)	37 (10.5%)	29 (8%)	5 (1.4%)	352
Total	All dosimeters	2027 (81%)	336 (13%)	121 (5%)	23 (1%)	2507

<sup>a</sup> SSD: source to surface distance.



TABLE III. EVOLUTION OF THE EQUAL RESULTS FOR CHECKED PHOTON BEAM PARAMETERS (1998–2002)

Parameter	Deviation $ \delta  > 5\%$ (%)	
	1998–1999 <sup>a</sup>	1998–2002 <sup>b</sup>
RBO	3.1	1.2
BOV	4.7	1.8
WTF	10.4	3.3

<sup>a</sup> From 1998 to 1999, 387 beams were checked.

<sup>b</sup> From 1998 to 2002, 1145 beams were checked.







The values of the deviations,  $\delta$ , are shown for the electron beam checks in Table II. For electron beams, 83% of the RBOs (10 cm  $\times$  10 cm) were at the optimal level (i.e. deviations  $|\delta|$  below 3%). Compared with photon dose checks for the RBO, there were more deviations between 3% and 5%.

Fifteen beams with deviations larger than 5% on one or more parameter were remeasured; dosimetric problems were identified for 20 of these parameters. The principal problems on the electrons beams were:

- (a) Beam calibration errors due to a leakage in the plane-parallel ionization chamber, problems with the ionization chamber correction factors used and problems due to the calibration of a Markus chamber;
- (b) Technical problems with the accelerator during the irradiation of a thermoluminescent dosimeter;
- (c) Incorrect depth dose curve data used in the TPS.

Table IV shows the results of the MLC dose checks for 44 radiotherapy centres, including 73 beams tailored by an MLC. Five of these centres were rechecked, and one presented a proven dosimetric problem for an MLC field combined with wedges, corresponding to field No. 6 in Table IV. In addition, the MLC results show that 94% of the beam outputs checked in reference conditions (RBO) were at the optimal level ( $|\delta| \leq 3\%$ ), and 6% had deviations between 3% and 5%. Similar results are found for the small square fields (5 cm  $\times$  5 cm). However, for complex fields tailored by an MLC (the circular and inverted Y fields), a large percentage of beams (10–14%) had deviations between 3% and 5%. For the 73 checked MLC beams, no deviation larger than 10% was found.

TABLE IV. NUMBER OF DEVIATIONS,  $\delta$ , OBSERVED IN 73 MLC PHOTON BEAMS AT 44 RADIOTHERAPY CENTRES

Field No.	MLC fields checked	MLC field shape	Field size (maximum length and width)	$ \delta  \leq 3\%$	$3\% <  \delta  \leq 5\%$	$5\% <  \delta  \leq 10\%$
1	Reference beam output		10 cm $\times$ 10 cm	68 (94%)	5 (6%)	—
2	MLC, small field		5 cm $\times$ 5 cm, with MLC	67 (93%)	5 (7%)	—
3	MLC, circular field		5.6 cm diameter, with MLC	65 (90%)	7 (10%)	—
4	MLC, inverted Y		15 cm $\times$ 12 cm, with MLC	62 (86%)	10 (14%)	—
5	MLC, irregular field		12 cm $\times$ 8 cm, with MLC	69 (96%)	3 (4%)	—
6	MLC, irregular field with wedge		12 cm $\times$ 8 cm, with MLC and wedge	57 (81%)	11 (16%)	2 (3%)

#### 4. CONCLUSIONS

A real improvement in radiotherapy dosimetry has been found since the start of the EQUAL programme in 1998 for European radiotherapy centres, and the reduction of uncertainties in dosimetry gives the possibility of optimizing doses in radiotherapy. This would lead to an increased percentage of local controls of tumours, with a constant or reduced number of complications.

The EQUAL project was, for a large number of European centres, the first opportunity to take part in an external audit both for photon (both standard fields and MLC fields) and electron beams, for non-reference conditions and, in many cases, for reference conditions.

The EQUAL network and national QA networks in Europe have checked more than 50% of the radiotherapy centres in Europe.

The results from measurements in the reference geometry are very good both for photon and electron beams (the mean ratio of measured and stated doses is 0.998 and 1.003, respectively, and the standard deviation is 1.9% and 2.1%, respectively).

All beams with dosimetry problems are followed up, and in some cases on-site visits have been undertaken. The EQUAL dosimetry audit in radiotherapy offers the European radiation oncologist an important tool for improving the quality of treatments.

#### REFERENCES

- [1] FERREIRA, I.H., DUTREIX, A., BRIDIER, A., CHAVAUDRA, J., SVENSSON, H., The ESTRO-QUALity assurance network (EQUAL), *Radiother. Oncol.* **55** (2000) 273–284.
- [2] FERREIRA, I.H., et al., The ESTRO-EQUAL quality assurance network for photon and electron radiotherapy beams in Germany, *Strahlenther. Onkol.* **177** (2001) 383–393.
- [3] FERREIRA, I.H., et al., “Radiotherapy dosimetry audit: A European programme to improve quality and safety in radiation treatments”, *Radiological Protection of Patients in Diagnostic and Interventional Radiology, Nuclear Medicine and Radiotherapy* (Proc. Int. Conf. Malaga, 2001), IAEA, Vienna (2001) 309–330.
- [4] INTERNATIONAL ATOMIC ENERGY AGENCY, Absorbed Dose Determination in External Beam Radiotherapy, Technical Reports Series No. 398, IAEA, Vienna (2000).

**BLANK**

## **RADIATION THERAPY THERMOLUMINESCENCE DOSIMETRY SERVICE IN GERMANY: THE EXPERIENCE OF THE FIRST YEAR**

C. PYCHLAU  
PTW-Freiburg,  
Freiburg, Germany  
E-mail: pychlau@ptw.de

### **Abstract**

An external audit service for radiotherapy dosimeters using thermoluminescence dosimetry has been established in Germany. Technical and administrative structures have been put in place to comply with the strict scientific and legislative requirements. The results of the first comparison measurements confirm the practical value of the service.

### **1. INTRODUCTION**

The external audits of therapy dosimeters by mailed thermoluminescence dosimetry mandatory today in Germany are the result of a long technical, legal and administrative development process. The origins and history of this process are presented first, followed by technical details and the results of the first year.

### **2. ORIGIN AND REQUIREMENTS**

Until 1 January 1999 the measuring quality of therapy dosimeters in Germany was ensured by a legally enforced calibration. Each dosimeter (both the electrometer and the chamber), in addition to the manufacturer's calibration, had to be calibrated by a State agency and recalibrated at regular intervals. This calibration checked the correct functioning of a dosimeter over the energy range up to the  $^{60}\text{Co}$  beam quantity. The use of dosimeters at energies higher than this range was based on the cobalt calibration value and on dosimetry protocols, and was not subject to further control. Comparisons on a voluntary basis first using ferrous sulphate and later also thermoluminescence dosimetry (TLD) gave additional safety.

As early as 1989 a committee was established to extend the scope of legislative calibrations to higher energies. This was to be done using compulsory comparison measurements with solid state dosimeters.

During the long working period of this committee the European Medical Device Directive was issued, and in 1993 the direction of the work changed to implementing such comparison measurements as calibration controls in accordance with the German medical device user directive. This finally resulted in 2001 in guidelines for therapy dosimeter surveillance, which define the current legislative requirements for the control of therapy dosimeters in Germany [1].

The guidelines require a measuring agency capable of reproducibility better than 0.3% in comparison with the national primary standards dosimetry laboratory and an uncertainty of the comparison measurement procedure for the customer of less than 1%. All uncertainties are stated as equivalent to one standard deviation ( $k = 1$ ). Comparison results are classified in three categories: for high energy photon radiation a comparison resulting in a deviation below 3% is classified A, and means that the user's dosimetry is fully compliant with the guidelines. Category B encompasses deviations of 3–4% and calls for a check of the dosimetry used. Category C is for deviations above 4% and results in checking the dosimetry and a prohibition against the use of the dosimeter concerned until the cause of the deviation is found and rectified. The category B limit for electrons is set at 5%.

Doubt over the final requirements and especially the precision demanded by these guidelines caused a delay until a measuring agency could become operational.

### 3. ESTABLISHING A MEASURING AGENCY

Following the decision to establish a postal dosimetry service it soon became obvious that this could only be done by using TLD. The use of TLD in radiation therapy is common, especially for evaluation of the dose in body phantoms or during whole body irradiation. Following the implementation of increasingly precise procedures to compensate for various influence factors, the TLD method has over the past few years been developed to a high level of precision [2]. Various measuring agencies in Europe are performing extensive comparison measurements on the basis of this method [3–10].

The literature on TLD measurements in radiation therapy describes various systems, two of which were investigated. One of these systems is especially suitable and is already in use at two organizations that carry out comparable tasks (the European Society for Therapeutic Radiology and Oncology (ESTRO) and the IAEA [4, 7]). This same system was finally chosen for the PTW-Freiburg measuring agency and, following some not unexpected initial difficulties, has been found to be very stable and reproducible.

The choice of the thermoluminescent dosimeters to be used was mainly influenced by knowledge and experience gained in earlier investigations in Germany. After a prolonged qualification process of repeated irradiations and annealing, several groups of TLD-100 dosimeters were characterized by reproducible calibration factors.

The implementation of the measuring procedure was an intensive learning process. Without trained specialists and recent TLD experience the demanded reproducibility and uncertainty of the procedure pushed the capabilities of the laboratory to its limits. Experiments to establish parameters such as the optimal reading temperature and the temperature distribution in the annealing oven took several months. An important point occasionally overlooked by TLD users is the necessary, almost clinical, cleanness required during the processing of the thermoluminescent dosimeters. The slightest contamination by dust or, for example, hair must be avoided.

The calibration of the TLD system was facilitated by a test irradiation of thermoluminescent dosimeters carried out by the German national laboratory, the Physikalisch-Technische Bundesanstalt (PTB), early in 2001. A blind comparison in July 2001 resulted in a comfortably small deviation (well below 0.3%) between the PTB and PTW values. Following this, the measuring agency was officially assigned its task by the State authority.

Parallel to the absolute calibration, the energy dependence of the measuring system between 6 MV and 18 MV photons and 4 MeV and 20 MeV electrons was determined. This was done by comparison measurements between TLD and ionization chamber dosimetry according to the Deutsches Institut für Normung (DIN) standard DIN 6800-2 [11]. In contrast to the procedure used in comparable projects in other countries [9], these values were not determined by a national laboratory but in co-operation with hospitals. First measurements on one type of accelerator (Philips) were validated by independent measurements performed in other hospitals with Siemens and Varian accelerators. The calibration factors now used by the measuring agency for TLD measurements at high energies are not directly determined from the TLD comparison measurement with the PTB, but are nevertheless traceable to the PTB through ionization chamber dosimetry. This method has the advantage of being identical to the dosimetry used by customers following the DIN code of practice.

Before starting operations, an organizational structure for customer communications and the routine execution of the comparisons had to be implemented. The measuring agency, as an organizational unit of PTW-Freiburg, is subject to the certified quality assurance system of PTW. The medical device test guidelines in conjunction with the necessity of a complete quality assurance system stress the importance of clear agreements between the measuring agency and its customers. Accordingly, in addition to producing a number of

internal quality assurance documents, PTW implemented a standard operating procedure that listed the obligations of the measuring agency and its customers. The procedure practised is the following:

- (a) The user informs PTW of its need for a comparison measurement;
- (b) The measuring agency sends a copy of the standard operating procedure, including order forms;
- (c) The user orders the comparison measurement, and the date of the measurement is agreed during a telephone conversation;
- (d) On the agreed date the measuring agency sends the thermoluminescent dosimeters, phantoms and, if necessary, adapters;
- (e) The user irradiates the thermoluminescent dosimeters and sends them back, together with the irradiation protocol;
- (f) The measuring agency evaluates the thermoluminescent dosimeters and compares the results with the user's data;
- (g) The measuring agency informs the user, the PTB and, by the end of every year, the State authority of the results (the PTB is informed of the data only, not of the name of the user).

Usually the order procedure takes between two days and a week, and the measurement procedure from the sending of the thermoluminescent dosimeters to giving the results to the customer takes between one and two weeks, depending on the response time of the user.

#### 4. MATERIALS AND METHODS

The measuring agency uses a Fimel PCL3 automatic reader, the original PTW TLD oven and dosimeter probes with round TLD-100 chips. These probes are comparable with those used by Feist in Munich [2]. Six TLD chips are arranged in a circle within a waterproof housing of about the size and form of a Roos chamber. These probes can essentially be mounted in any water phantom. The necessary dimensions are communicated to the user, if required. So far the probes have been used either in the recommended calibration phantom type 4322 (a 30 cm × 30 cm × 30 cm water phantom for horizontal irradiation with waterproof adaptors for many different chambers) or in a large beam analyser phantom (only for waterproof chambers, since usually no waterproof adaptors are available).

Each of the TLD-100 chips used has its own calibration factor, which is always determined from reference irradiations before and after its use at a hospital. Every mailed batch consists of 13 probes with six TLD chips each. These



are opened only by the measuring agency for evaluation. During the evaluation, in accordance with European practice [6], the smallest and largest values are omitted, and the comparison value is determined from the mean value of the remaining four chips. The standard deviation of these values during daily practice is below 1%. Mean standard deviations of 0.4% for single TLD chips and of 0.2% for complete probes were determined during experiments on reproducibility. Eight of these probes can be used by the customer for the actual comparison, and one additional preirradiated probe accompanies the mailed batch as a record of unintentional irradiation, if any. The remaining four probes are used for internal control and are irradiated at the same time as the customer's thermoluminescent dosimeters with a defined dose to identify fading and possible changes of the response of the entire batch. All 13 probes, with 78 TLD chips, are always evaluated together in one process, and thus have a common irradiation and thermal history. The nominal dose for irradiation is always 1 Gy. Deviations from this nominal dose are accounted for using a supralinearity correction based on a second degree polynomial, which is determined individually for each TLD batch using points at 0.5, 1 and 2 Gy. Typical deviations at the ends of this range for uncorrected values are of the order of 5%. The external control probe also enables a correction for fading following temperature differences during transport. This must be done carefully, since it can be disadvantageous to base a correction on one single probe. All other corrections used are determined from the results of several probes.

In accordance with the requirements of the guidelines, the customer irradiates the TLDs using the lowest and the highest available photon and electron energies. Since the legal basis and the main purpose of the audits is quality assurance of the customer's dosimetry equipment, during the comparison each chamber and each electrometer has to be checked by comparing it at one measuring point at least. The dose must be determined using DIN 6800-2 [11].

## 5. RESULTS

After the comparison measurements for the energy dependence determination had shown the practicability of the system when mailed, it was not surprising that the first customer audit run, very much in accordance with the experience of the ESTRO service, also mainly gave first class results. Difficulties only developed from the planning of transporting the material back and forth, especially in the event that the user could not irradiate on the date planned, owing to problems with the accelerator. Some difficulties also developed in connection with the technical and administrative documentation, which had to be amended several times during the first weeks of operation.

Although the results were generally good, three types of measuring problem were observed:

- (a) Set-up difficulties. Users having no experience with the calibration phantom had some trouble with the correct set-up. Changes and amendments to the phantom user manual solved these problems. Furthermore, some trivial set-up and handling problems occurred (e.g. the incorrect choice of measuring depth).
- (b) Electron dosimetry. In some cases there were deviations of more than 3% for electrons. These problems were partially caused by the behaviour of older Markus chambers, and led in one case to an exchange of the chamber. Other problems with deviations in some cases far beyond 3% arose following the use of inconsistent dosimetry procedures. These were, for example, the combination of elements of the Markus protocol with parts of the DIN protocols or the use of the DIN protocol with the calibration factors for the Markus protocol. Some of these problems could be solved by giving advice over the telephone, by a cross-calibration of the Markus chamber by the user with a comparison with a compact chamber at high electron energies or by a recalculation of the results based on this calibration factor.
- (c) Modification of the DIN protocol following earlier comparisons. In at least one case deviations of more than 3% were caused by a user modifying calibration factors following an earlier comparison using ferrous sulphate. Similar effects within category A were observed for several users. It must be stressed that comparison measurements are not calibrations, and any change of calibration factor following a comparison measurement may lead to very erroneous results.

During the first nine months of operation 33 comparison series were completed; of these, five were repeat comparisons following problems with the initial measurements. The 28 users audited produced the results given in Table I.

Repeat comparisons were necessary mainly as a result of positioning errors in the phantom and missing air density corrections.

The initial results show that the results for photons are better than for electrons and that low energy measurements are liable to lead to questionable results more often than high energy measurements (see Table II).

Table II shows that more than 90% of the photon beam measurements at energies above 12 MV were within category A; in contrast, nearly 10% of the electron measurements below 12 MeV were in category C.

An interesting point is that, in accordance with the ESTRO results [3], a limited selection of chambers has so far been presented. Also, the results of this

TABLE I. RESULTS AFTER THE FIRST NINE MONTHS

Result	Number
Only category A without further discussion	12
Only category A after discussion and amendment	2
Only category A after a repeat comparison	3
Category A including 'unimportant B or C'	8
Category A with some B or C disqualifying single chambers	2
Category A with some category B still under discussion	1

**Note:** 'Unimportant B or C' means that the measuring agency will consider a comparison as successful when all chambers concerned show at least one result in category A (meaning that the dosimetry equipment is measuring correctly) and when category A results are shown for the lowest and highest electron and photon energies. If in such a case additional category B results appear, for example for medium electron energies or during the experimental use of a compact chamber for low electron energies, the user is informed of this result, but it is not considered relevant.

TABLE II. NUMBER OF BEAMS CHECKED ACCORDING TO ENERGY RANGE AND CATEGORY  
(situation on 31 July 2002)

	Category		
	A	B	C
Photons <12 MV	79	8	3
Photons ≥12 MV	51	1	2
Electrons <12 MeV	57	14	7
Electrons ≥12 MeV	60	12	4

national study, although occasionally outside category A, mainly show smaller deviations than those reported for international audits [9].

All deviations, regardless of their size, are first discussed with the physicist concerned. In contrast to ESTRO practice [5], all data are given to the user immediately. Many deviations can be identified and corrected during the telephone conversation that takes place when the results are communicated to the user. Repeat comparison measurements have been found necessary only in the event of actual technical problems with a chamber (e.g. a damaged chamber or an expired calibration factor) or irreproducible errors in the measuring procedure (e.g. a missing air density correction).

## 6. CONCLUSION

The first experiences of the measuring service indicate that the high standard of radiation therapy dosimetry in Germany can be improved upon by this additional general control system. In some cases substantial improvements have been made possible. Medical physicists are now advised not only to compare the results of their different calibrated ionization chambers but also to check their complete dosimetry by comparing the results of two basically different processes: calibration at  $^{60}\text{Co}$  followed by the dosimetry procedure according to the DIN protocol and a TLD comparison, both of which are traceable to national standards.

It has been observed that while the, rather rare, deviations of over 3% immediately lead to corrective actions (e.g. changes in internal protocols or recalibrations) being taken by the user, smaller deviations of between 1% and 2% will also usually trigger an internal procedure optimization process (i.e. changes in the application of the code of practice), which can lead to additional improvements.

It can be concluded that the installation of a measuring service for comparison measurements of medical devices, which was initially considered to be problematic, has been found to be practicable. Its successful implementation has led to an improvement for the medical physics community in Germany.

## REFERENCES

- [1] MIEKE, S., SCHADE, T. (Eds), Leitfaden zu messtechnischen Kontrollen von Medizinprodukten mit Messfunktion (LMKM) (Ausgabe 2.1), Teil 2, Physikalisch-Technische Bundesanstalt, Braunschweig (2001).
- [2] FEIST, H., Entwicklung der Thermolumineszenzdosimetrie mit LiF zu einer Präzisionsmethode für absolute Energiedosis-Bestimmungen in der Strahlentherapie mit Photonen- und Elektronenstrahlungen hoher Energie, Habilitation, Univ. Munich (1992).
- [3] FERREIRA, I., et al., The ESTRO-EQUAL quality assurance network for photon and electron radiotherapy beams in Germany, *Strahlenther. Onkol.* **177** (2001) 383–393.
- [4] FERREIRA, I.H., et al., “Radiotherapy dosimetry audit: A European programme to improve quality and safety in radiation treatments”, *Radiological Protection of Patients in Diagnostic and Interventional Radiology, Nuclear Medicine and Radiotherapy* (Proc. Int. Conf. Malaga, 2001), IAEA, Vienna (2001) 309–330.
- [5] FERREIRA, I.H., DUTREIX, A., BRIDIER, A., CHAVAUDRA, J., SVENSSON, H., The ESTRO-QUALity assurance network (EQUAL), *Radiother. Oncol.* **55** (2000) 273–284.

- [6] GOMOLA, I., et al., External audits of electron beams using mailed TLD dosimetry: Preliminary results, *Radiother. Oncol.* **58** (2001) 163–168.
- [7] IZEWSKA, J., ANDREO, P., The IAEA/WHO TLD postal programme for radiotherapy hospitals, *Radiother. Oncol.* **34** (2000) 65–72.
- [8] IZEWSKA, J. (Ed.), Guidelines for the preparation of a quality manual for external audit groups on dosimetry in radiotherapy, *SSDL Newsletter No. 46* (2002) 6–16.
- [9] SCHIEFER, H., SEELENTAG, W., STUCKI, G., “Ein nationaler Dosimetrievergleich durch Postversand von TLDs”, paper presented at the Annual Conference of the Swiss Society of Radiobiology and Medical Physics, Sion, 2001.
- [10] VATNITSKY, S., IZEWSKA, J., Reasons for deviations outside the acceptance limits in the IAEA/WHO TLD audits for radiotherapy hospitals, *SSDL Newsletter No. 46* (2002) 24–26.
- [11] DEUTSCHES INSTITUT FÜR NORMUNG, Dosismessverfahren nach der Sondenmethode für Photonen- und Elektronenstrahlung — Teil 2: Ionisationsdosimetrie, DIN 6800-2, DIN, Berlin (1997).

**BLANK**

# **AUDIT OF RADIOTHERAPY DOSIMETRY IN NEW ZEALAND: PRACTICAL CONSIDERATIONS AND RESULTS**

V.G. SMYTH, J.A. LABAN  
National Radiation Laboratory,  
Christchurch, New Zealand  
E-mail: Vere\_Smyth@nrl.moh.govt.nz

## **Abstract**

In order to verify regulatory compliance, every two years staff of the National Radiation Laboratory (NRL) of New Zealand visit each of the radiotherapy departments in New Zealand to carry out an independent audit of the dosimetry of their external radiation beams. The audit is carried out under Technical Reports Series No. 277 reference conditions using dosimetry equipment belonging to the NRL to maximize the independence of the measurements. Audits have been carried out regularly since 1991 and the results show that discrepancies of up to 2% for linac beams are within normal output variability. However, much greater discrepancies are observed in kilovoltage X ray beams. This is due to the use of different dosimetry protocols rather than error. Experience to date suggests that the dosimetry audit is of continuing benefit to radiotherapy departments, but should be supplemented with dosimetry of planned treatments in an anthropomorphic phantom.

## **1. INTRODUCTION**

The New Zealand Radiation Protection Regulations 1982 state that the dose delivered to a radiotherapy patient must be within  $\pm 5\%$  of the prescribed dose. Following the overdose of 153 patients because of an error in dosimetry at the Royal Devon and Exeter Hospital, United Kingdom, in 1988 it was decided to audit compliance with this dose limit routinely. Since 1991 every high energy beam in New Zealand used for teletherapy has been independently measured every two years by staff of the National Radiation Laboratory (NRL) of New Zealand. Since 1997 all kilovoltage X ray beams have also been measured. The audits cover 16 linacs and ten kilovoltage X ray machines distributed among the six radiotherapy centres in New Zealand.

## 2. DOSIMETRY EQUIPMENT

The following equipment is used in the dosimetry audits:

- (a) A Keithley 35617EBS dosimeter;
- (b) An NE 2571 0.6 cm<sup>3</sup> graphite chamber;
- (c) A PTW Roos plane-parallel electron chamber;
- (d) A PTW M23342 0.02 cm<sup>3</sup> soft X ray chamber;
- (e) A 30 cm × 30 cm × 20 cm water phantom, exposed from the top;
- (f) Mercury in a glass thermometer;
- (g) An aneroid barometer;
- (h) Strontium-90 check sources.

Before each round of audits is completed, the ionization chambers are calibrated against the primary standards of New Zealand for air kerma, and the thermometer and barometer are calibrated against local reference standards.

## 3. MEASUREMENT METHODS

The measurements follow the IAEA dosimetry protocols of Technical Reports Series No. 277 (TRS 277) [1] and TRS 381 [2]. A <sup>90</sup>Sr check of the ionization chambers is made at each site to verify that the dosimetry system has reached a stable state before any measurements are taken. Agreement within 0.5% of the long term mean response is accepted. The source to surface distance on a linac is set using the optical distance indicator after verifying it against a mechanical front pointer. Beam quality parameters are accepted as provided by the hospital physicist. The depth of measurement of electrons is taken to be the same as that used by the hospital. All electron beams are measured using the PTW Roos plane-parallel chamber, which is calibrated against the NE 2571 cylindrical chamber in a high energy electron beam in accordance with TRS 381. Recombination corrections are measured on each linac beam and polarity corrections are also measured for the electron beam measurements.

For medium energy kilovoltage X rays, in a locally agreed departure from TRS 277, beams with a half-value layer (HVL) greater than 4 mm Al are measured at a depth of 2 cm in water. When each beam is measured the dose at 2 cm is related to the maximum dose by taking relative dose measurements with the Roos chamber at depths of between 2 cm and 0.1 cm. This is done to give a consistent point of comparison, since not all hospitals measure such beams at a depth of 2 cm. (Beams with an HVL of less than 4 mm Al are measured in air.)



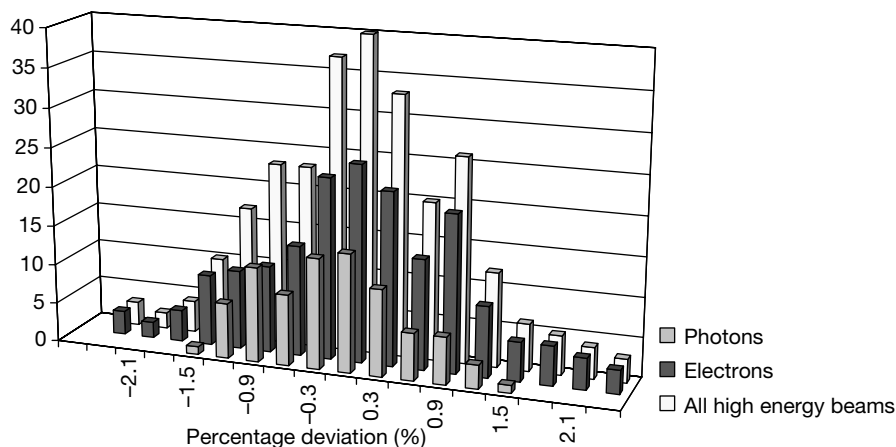


FIG. 1. High energy photons and electrons: audit results, 1991–1999.

Once the measurements are complete the hospital is asked to supply reference data, corresponding to current clinical use, for each beam. Thus not only dosimetry practice is tested but also verified is machine stability since the last dose measurements were taken.

#### 4. RESULTS

The results for high energy beams (Fig. 1) are reassuring, both to the regulators and to the physicists, who appreciate the independent check. The only disagreements significantly greater than 2% have been caused by the use of a cylindrical chamber on a 4 MeV electron beam by a hospital, and confusion between the source to surface distance and isocentric set-ups. (When the measurements were repeated using the same set-up as the hospital, the difference was resolved.)

The kilovoltage results (Fig. 2) are more widely scattered. Differences greater than 10% were observed. These were not resolved by uncovering any errors, but rather they were due to inconsistencies in dosimetry protocols — particularly between measurements in air and in water.

#### 5. DISCUSSION

The exercise has raised some interesting questions and issues. Some of these are:

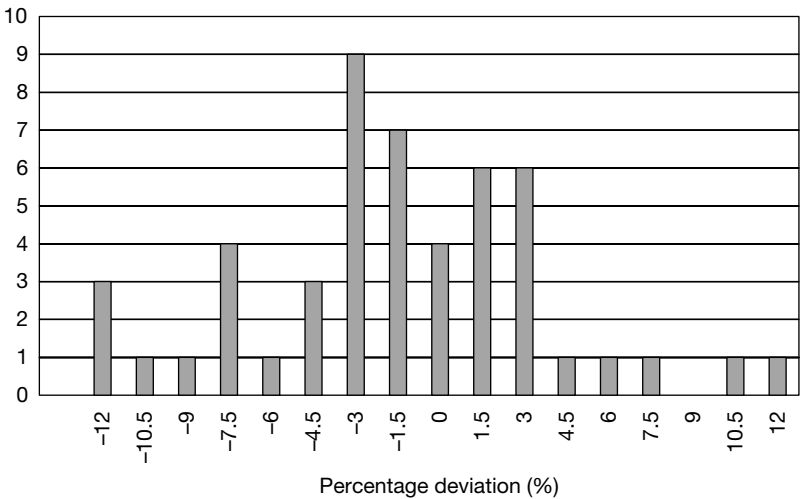


FIG. 2. Kilovoltage X rays: audit results, 1993 and 1999.

- (a) What should the NRL measurement be compared with, a measurement carried out by the hospital physicist at the same time to look for errors in method, or the most recent measurement to look for errors and to check the quality control of the machine, or the dose that the treatment planning system calculates for an exposure of the water phantom under reference conditions to check the clinical dosimetry? It was chosen to take the last option, since it checks the greatest number of links in the dosimetry chain.
- (b) What are the uncertainties and what level of agreement should be expected? The expanded combined standard uncertainty of the NRL measurements (with a coverage factor of 2) is estimated to be 1% for linacs and 2–3% for kilovoltage X ray machines. This excludes the uncertainty of the primary standards, since the same standards are used throughout New Zealand. Machine stability and local policy on output adjustment place lower limits on the expected level of agreement.
- (c) How much is not tested that may be significant? The hospital values for beam quality specification are accepted, and the geometrical set-up is assumed to be accurate. Factors used in common by both the hospital and the NRL, such as the primary standards and the dosimetry protocols, are not tested. However, the NRL is confident that significant errors in reference dosimetry will be detected.

- (d) Is the right audit being done? Is there any benefit from doing this every two years? Should the focus just be on new machines? Is there another check that would be more effective? There are many steps in the dosimetry process before the dose is delivered to the patient. It is also planned to test the delivery of the planned dose to an anthropomorphic phantom rather than just under reference conditions. This will be particularly important with the introduction of intensity modulated radiation therapy. However, such a dosimetry system will not have the resolution to detect discrepancies at the level of a few per cent, so it is intended to alternate between audits of reference dosimetry and clinical dosimetry.
- (e) There was a definite problem uncovered in kilovoltage X ray dosimetry. This has largely been resolved by getting hospitals to adopt a uniform dosimetry protocol. The reason that this had not previously happened was because of perceived deficiencies in the kilovoltage section of TRS 277. However, it gained wider acceptance after a few minor local changes to the reference conditions.

## 6. CONCLUSION

The NRL programme of dosimetry audits at all of the radiotherapy departments in New Zealand has proved to be valuable both for verifying regulatory compliance and for providing assurance to the departments that gross errors in reference dosimetry have not been made. In the time since the start of the programme (1991) there have been no major errors detected. After the experience gained in the first ten years it was decided to continue the programme and to include the audit of the clinical dosimetry of planned treatments, as well as that of reference dosimetry.

## REFERENCES

- [1] INTERNATIONAL ATOMIC ENERGY AGENCY, Absorbed Dose Determination in Photon and Electron Beams, 2nd edn, Technical Reports Series No. 277, IAEA, Vienna (1997).
- [2] INTERNATIONAL ATOMIC ENERGY AGENCY, The Use of Plane Parallel Ionization Chambers in High Energy Electron and Photon Beams, Technical Reports Series No. 381, IAEA, Vienna (1997).

**BLANK**

## THE UNITED KINGDOM'S RADIOTHERAPY DOSIMETRY AUDIT NETWORK

D.I. THWAITES\*, S.K. POWLEY\*\*, A. NISBET\*\*\*,  
M. ALLAHVERDI\*

\* Western General Hospital, University of Edinburgh, Edinburgh  
E-mail: dit@holyrood.ed.ac.uk

\*\* Lincoln County Hospital, Lincoln

\*\*\* Raigmore Hospital, Inverness

United Kingdom

### Abstract

The first comprehensive national dosimetry intercomparison in the United Kingdom involving all UK radiotherapy centres was carried out in the late 1980s. Out of this a regular radiotherapy dosimetry audit network evolved in the early 1990s. The network is co-ordinated by the Institute of Physics and Engineering in Medicine and comprises eight co-operative regional groups. Audits are based on site visits using ionization chambers and epoxy resin water substitute phantoms. The basic audit methodology and phantom design follows that of the original national intercomparison exercise. However, most of the groups have evolved more complex methods, to extend the audit scope to include other parameters, other parts of the radiotherapy process and other treatment modalities. A number of the groups have developed phantoms to simulate various clinical treatment situations, enabling the sharing of phantoms and expertise between groups, but retaining a common base. Besides megavoltage external beam photon dosimetry, a number of the groups have also included the audit of kilovoltage X ray beams, electron beams and brachytherapy dosimetry. The National Physical Laboratory is involved in the network and carries out basic beam calibration audits to link the groups. The network is described and the methods and results are illustrated using the Scottish+ group as an example.

### 1. INTRODUCTION

Radiotherapy dosimetry intercomparisons have been carried out in limited studies in the United Kingdom since at least the 1960s. However, the first national dosimetry intercomparison involving all centres was conducted in the

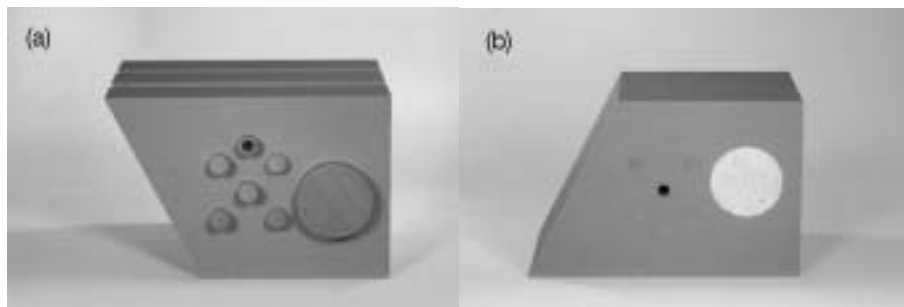


*FIG. 1. The trapezoidal phantom. (a) All inserts are water substitute plastic; the chamber is inserted into the top hole for the beam calibration audit. (b) Five points are measured within a defined target volume, irradiated by a three-field technique. The large insert can be water substitute or lung substitute plastic.*

late 1980s [1], organized under the auspices of the Institute of Physics and Engineering in Medicine (IPEM). This was based on visits to each centre, using Farmer ionization chamber dosimetry. The intercomparison audited megavoltage photon beam calibrations and other single field parameters and measured doses in a three-field treatment in a trapezoidal phantom constructed from epoxy resin water-equivalent material (Fig. 1), and compared these with locally planned doses. This included off-axis points, points at different depths and a range of field sizes, wedges, oblique incidences and inhomogeneities.

The study found mean measured beam calibration doses close to stated values (ratio, measured/stated, 1.003), with a standard deviation (SD) of the distribution of 1.5%. Ninety-seven per cent of doses were observed to be within the pre-set 3% tolerance. The study did find one very significant beam miscalibration [2]. For the planned multifield irradiations, mean dose ratios (measured/stated) were 1.01 (SD 3%, 90% of results within 5%). A number of discrepancies were identified, leading to improved practice. A follow-up study was carried out in the mid-1990s [3] to audit electron beams, but it also repeated the megavoltage photon calibration audit. An improvement was noted for photons in that the SD was reduced (mean ratio 1.003, SD 1.0%), and 100% of the measurements were now observed to be within the pre-set tolerance of 3%. The mean ratio of measured/stated dose for electron beams was 0.994 (SD 1.8%, 94% within 3%, 99% within 5%). This intercomparison also identified causes of discrepancies and led to improved practice. The national exercises gave an impetus for the development of a regular audit network.

## 2. UK AUDIT NETWORK STRUCTURE AND ORGANIZATION

Growing out of the first of the national dosimetry intercomparison exercises, and initially using a very similar approach, a national interdepartmental audit network began to develop in 1991 and 1992 [4–8]. A network approach of co-operative regional groups of radiotherapy and medical physics departments evolved, which allowed different groups to be set up and develop at their own pace and also enabled the scope of the system to be broadened quickly, when the situation and resources allowed. The network has eight regional groups, each with up to ten radiotherapy centres, serving average populations of 7 to 8 million. The groups organize audits of their own centres and have developed rather differently in their approach, although with a common basic core to the audits. Most groups began with a copy of the original IPEM trapezoidal phantom and repeated the national intercomparison checks, using a very similar methodology. However, the audits in some areas included tests of more of the basic geometric and dosimetric performance characteristics of treatment units and simulators [7, 8]. A number of groups have piloted methodologies and phantoms for new audits that can then be shared, or experience transferred, to other groups [8–10]. The network collaborates with the UK primary standards dosimetry laboratory (the National Physical Laboratory (NPL)) to co-ordinate first level dosimetry audits in at least one centre per group at two-yearly intervals. This audits the dissemination of chamber calibration factors from the NPL to the centres and links the network groups at the level of basic dosimetry.

The network is co-ordinated by an IPEM steering committee of one representative from each group and one from the NPL. It reviews experience and results once a year and oversees standards and progress. It makes recommendations on minimum frequencies and the content of the audits; the current aim is that each centre should participate in an audit at least once every two years. It also allows developments or the sharing of different approaches to be co-ordinated. This central review ensures uniformity for intergroup comparisons of audit performance.

All UK radiotherapy centres (approximately 65) are included in one of the regional groups. Participation is now a requirement of the National Cancer Services Standards [11], which are seen as accreditation criteria. Some of the groups operate by having one or two central auditors visiting each centre in the group, while some operate under a peer review system, in which each centre audits, and is audited by, one other in the group in each audit round. Such a system is cost effective but requires a good level of mutual trust and co-operation between departments. It also may seem that there might not be total independence in the audits, but this again relies on trust in the professionalism of the staff involved. The data are considered confidential between the auditor and

the centre. The audited centre is asked to investigate any observed discrepancies and to explain the causes. In the event that this is not possible, the audit group could provide assistance, but this has never been found to be necessary. Anonymized data are analysed at the group level (see, for example, Refs [7, 8, 12]) and at the national level for dissemination to the radiotherapy community. The overall data over ten years are currently being analysed by the steering committee for publication. As one example of the overall results, for megavoltage photon beam calibration audits the mean ratio (audit/centre) is 1.002, with an SD of 1%. Only one result (of 300) was outside the 3% tolerance, at 3.3%.

The normal minimum recommended audit covers megavoltage photons and includes ionization chamber and beam calibrations, the beam quality, beam modifiers and other single field parameters, geometric parameters and simple multifield planned irradiations, using the trapezoidal phantom. Various groups have extended the scope of the audits to kilovoltage X rays, electrons and brachytherapy dosimetry. A number are using more sophisticated phantoms to audit more complex, more realistic treatment situations. Some use phantoms developed for clinical trial audits (e.g. CHART head and neck and lung, START breast, RTO1 prostate; see, for example, Ref. [9]). Others have developed specific phantoms for the audit group [8, 10]. Some audits follow the process through from a simulator or CT scanner to volume delineation to planning and then to delivery. Some groups are currently developing audits for conformal, stereotactic and other sophisticated treatments, including intensity modulated radiotherapy (IMRT). In addition to practical measurement audits, there is always a degree of procedural audit, considering dosimetry, quality control, treatment planning, etc., in the visited centre in terms of procedures, documentation and records.

### 3. AN EXAMPLE OF ONE NETWORK GROUP: THE SCOTTISH+ GROUP

#### 3.1. Group structure

The Scottish+ group [8, 13] includes the six centres in Scotland, the two most northerly centres in England and the one centre in Northern Ireland. It has also worked in co-operation with physicists in Ireland to establish an audit system there [14] and retains links with that group. It began operation in 1992, following on from the UK national intercomparison exercise [1], which was co-ordinated from Edinburgh. It obtained initial money from the Scottish Health Department to purchase an independent set of measuring equipment, to cover the system set-up and initial travel costs and to develop phantoms. The original



aim was to carry out annual audits. In practice the frequency has, on average, been every two years. Most of the audit visits have been carried out by one auditor (D. Thwaites).

The group is linked to other national audit systems via the NPL inter-comparisons and to international systems via Edinburgh's participation as a reference or development centre, including for the IAEA, the EQUAL network (the audit system operated by the European Society of Therapeutic Radiology and Oncology (ESTRO), with a measuring centre in Villejuif, France) and the EC network (a developmental audit network funded by the European Commission (EC), with its measuring centre in Leuven, Belgium).

### **3.2. Basic dosimetry audits**

Over the ten year period of operation the audits have included the basic tests using the trapezoidal phantom, testing beam calibrations, a range of single field parameters, equipment geometric performance and simple multifield planning and delivery. The group has also audited the basic dosimetry of kilovoltage X rays, electrons and brachytherapy source specification, as well as megavoltage X rays. Tolerances were set at the beginning to be compatible with UK recommendations on radiotherapy equipment and process quality control, with the tolerances for beam calibrations set at 3% and for multifield dose delivery at 5%. Examples of overall results (1992–2002) for calibration and single field parameters include:

- (a) Megavoltage photon beam calibration: the mean ratio audited/locally stated was 1.001 (SD 1.1%) for the approximately 120 beams audited.
- (b) Other single field dosimetric parameters: 0.998 (SD 1.5%).
- (c) A range of geometric parameters: 1.00 (SD 1 mm).
- (d) Electron beam calibration: 0.997 (SD 1.8%).
- (e) Kilovoltage beam calibration: 1.001 (SD 1.6%).

Since 1996 no single field dosimetric parameter or machine geometric parameter has been observed outside the tolerances for megavoltage photon and electron beams, and the SD for these distributions has reduced to 1% or less. On this basis the beam calibration tolerance was reduced to 2%.

### **3.3. Semi-anatomic phantom for audits of treatment sites**

Over the same period a semi-anatomic epoxy resin based phantom was developed [8, 15], which to date has been used in three audit rounds covering irradiations representative of treatments for breast, lung–thorax and three

head and neck sites, respectively. This phantom has, for normalization, two 2 cm diameter holes to take the same Farmer chamber inserts as the geometric (trapezoidal) phantom, but the rest of the holes are machined to take smaller inserts and a 0.125 cm<sup>3</sup> PTW chamber. It has a fixed 'lung' and some bone equivalent areas, but also takes the same interchangeable water or lung substitute 8 cm diameter cylinders as the geometric phantom (Fig. 2). Audit visits have included an audit of the whole planning and delivery process for one of these 'sites', and at the same time an audit of another aspect of radiotherapy dosimetry, for example kilovoltage X rays and electrons. This has given an effective use of time; the visits usually take 4–5 h, but many parameters and modalities are tested within the cycle of a few visits.

The 'treatment site' audits incorporate many imaging, dosimetry, planning and machine parameters into one audit. If a discrepancy is then observed it is not immediately clear which parameter or part of the process may be responsible. However, as this is based on the very good experience of the basic audit performance, which was previously carried out at all the centres, and as the centres are then asked to investigate any discrepancies and report on them, this approach is justified. In the event that a cause could not be identified, a repeat visit would be organized, using the simpler audit phantom and protocol. This, however, has not been found to be necessary. The overall results to date in the 'target volumes' are:

- (a) The 'breast' plan: mean (audit/locally stated), 0.978 (SD 2.3%), 96% of measurements within a tolerance of 5%.
- (b) The 'thorax' plan: 0.991 (SD 1.1%), 100% within tolerance.
- (c) The 'head and neck' plan (parallel opposed): 0.993 (SD 1.6%), 97% within tolerance.

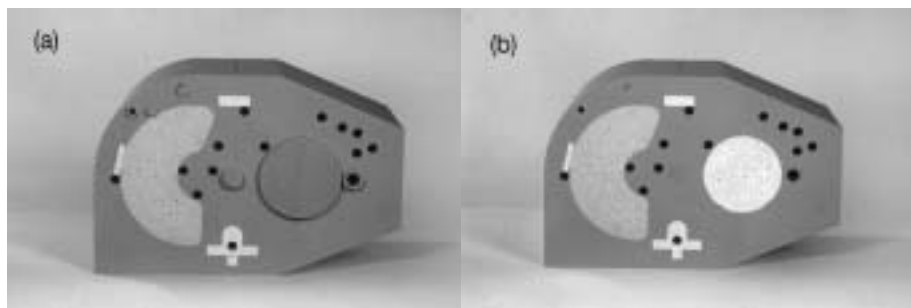


FIG. 2. The semi-anatomic phantom: (a) with the water substitute cylinder in place; (b) with the lung substitute cylinder in place. For a measurement, all the holes are filled with solid inserts, except for the one containing the ionization chamber. Some are left open in the figure simply to make them more visible.

- (d) The 'head and neck' (90° wedge pair): 0.993 (SD 2.2%), 97% within tolerance.
- (e) The 'head and neck' (oblique wedge pair): 0.995 (SD 1.8%), 100% within tolerance.

### 3.4. Developments

The audit group is developing audits of brachytherapy treatment planning, cross-centre in vivo dosimetry and multileaf collimator dosimetry, and is beginning to consider requirements and methods for stereotactic, conformal and IMRT audits.

The results of the audits in the group have improved with time. As stated above, since 1996 all single field parameters have been observed within the pre-set tolerances for megavoltage X rays and electrons. The simple routine audits have therefore now been discontinued, as they are not a cost effective use of the limited time available for auditing. Instead, more complex audits are being pursued, which inherently incorporate the more basic levels. However, at each audit visit beam calibrations are audited, as this is needed to normalize the results of the more complex audits. The more basic audit visits are available on request to departments as independent checks after the installation of a new treatment unit or after a major change, for example of a planning system or of software.

## 4. CONCLUSIONS

The network has provided a flexible and cost effective audit system for the UK. The co-operative approach has proved effective and efficient. The groups have developed at different speeds, but the experience of groups that have developed more advanced approaches can be shared and utilized by others. The parallel development of different approaches has produced a robust audit system, which has developed rapidly to include a range of modalities and complex radiotherapy situations. The audit results have generally been good. However, they have identified problems and have shown improvements with time, proving the value of audit participation. Auditing of radiotherapy dosimetry and of the radiotherapy process should be undertaken regularly, with the scope of the audit under continual development, to include more complex levels when it is observed that the basic levels have been met.

## REFERENCES

- [1] THWAITES, D.I., WILLIAMS, J.R., AIRD, E.G., KLEVENHAGEN, S.C., WILLIAMS, P.C., A dosimetric intercomparison of megavoltage photon beams in UK radiotherapy centres, *Phys. Med. Biol.* **37** (1992) 445–461.
- [2] THWAITES, B., BURLIN, T.E., JOSLIN, C.A.F., The Report of the Committee of Enquiry into the Overdoses Administered in the Department of Radiotherapy, Royal Devon and Exeter Hospital (Wonford), Exeter District Health Authority, Exeter, UK (1988).
- [3] NISBET, A., THWAITES, D.I., A dosimetric intercomparison of electron beams in UK radiotherapy centres, *Phys. Med. Biol.* **42** (1997) 2393–2409.
- [4] MILLS, J.A., AUKETT, R.J., BONNETT, D.E., MARTIN-SMITH, P., A pilot inter-departmental audit: Description, results and recommendations, *SCOPE* **1** (1992) 12.
- [5] THWAITES, D.I., The role of quality audit in clinical dosimetry, *SCOPE* **1** (1992) 14.
- [6] THWAITES, D.I., “Quality audit network in the UK”, *Physics in Clinical Radiotherapy* (Proc. Mtg Prague, 1993), European Society of Therapeutic Radiology and Oncology, Brussels (1993) 116.
- [7] BONNETT, D.E., MILLS, J.A., AUKETT, J.A., MARTIN-SMITH, P., The development of an inter-departmental audit as part of a physics quality assurance programme for external beam therapy, *Br. J. Radiol.* **67** (1994) 275–282.
- [8] THWAITES, D.I., “External audit in radiotherapy dosimetry”, *Radiation Incidents*, British Institute of Radiology, London (1996) 21–28.
- [9] AIRD, E.G., WILLIAMS, C., MOTT, G.T., Quality assurance in the CHART clinical trial, *Radiother. Oncol.* **36** (1995) 235–245.
- [10] PERRIN, B., JORDAN, T.J., HOUNSELL, A.R., The design and evaluation of a phantom for the audit of the treatment chain for prostate radiotherapy, *Radiother. Oncol.* **60** (2001) 37–43.
- [11] DEPARTMENT OF HEALTH, *Manual of Cancer Services Standards*, Department of Health, London (2000).
- [12] BLAKE, S.W., CASEBOW, M.P., A pragmatic approach to dosimetric audit in radiotherapy, *Br. J. Radiol.* **75** (2002) 754–762.
- [13] MCKENZIE, A.L., KEHOE, T.M., THWAITES, D.I., “Quality assurance in radiotherapy physics”, *Radiotherapy Physics in Practice* (WILLIAMS, J.R., THWAITES, D.I., Eds), 2nd edn, Oxford University Press, Oxford (2000).
- [14] NISBET, A., THWAITES, D.I., SHERIDAN, M.E., A dosimetric intercomparison of kilovoltage x-rays, megavoltage photons and electrons in the Republic of Ireland, *Radiother. Oncol.* **48** (1998) 95–101.
- [15] THWAITES, D.I., ALLAHVERDI, M., The development of interdepartmental audit methods, *Radiother. Oncol.* **37** (1995) S40.

# **THERMOLUMINESCENCE DOSIMETRY AS A TOOL FOR THE REMOTE VERIFICATION OF OUTPUT FOR RADIOTHERAPY BEAMS: 25 YEARS OF EXPERIENCE**

J.F. AGUIRRE, R.C. TAILOR, G. IBBOTT, M. STOVALL,  
W.F. HANSON

Department of Radiation Physics,  
University of Texas M.D. Anderson Cancer Center,  
Houston, Texas, United States of America  
E-mail: faguirre@mdanderson.org

## **Abstract**

The University of Texas M.D. Anderson Cancer Center has extensive experience with thermoluminescence dosimetry (TLD) as a quality assurance tool for output and the energy monitoring of radiation therapy beams. Over the past 25 years TLD results of the monitored institutions, commissioning data for TLD readers, the characterization data of lithium fluoride TLD-100 powder and the records of a quality assurance programme for the system have accumulated. Nearly 1600 TLD sessions over the past seven years on a cobalt unit reveal an accuracy in dose determination of 0.9% (one standard deviation), which represents a measure of the best achievable accuracy for TLD measured therapy doses. Based on this experience, the windows of acceptability may be tightened from 5% in dose to 3% and from 5 mm in electron depth to 3 mm.

## **1. INTRODUCTION**

The University of Texas M.D. Anderson Cancer Center (UTMDACC) has two separate groups that operate mailed thermoluminescence dosimetry (TLD) services: the Radiological Physics Center (RPC) and the Radiation Dosimetry Services (RDS). Both groups monitor the output of the therapeutic photon beams ( $^{60}\text{Co}$  to 25 MV) and electron beams (6–25 MeV) used in radiation therapy.

The RPC, under a grant from the United States National Cancer Institute (NCI), monitors the quality of radiation dosimetry performed at institutions participating in NCI funded co-operative clinical trials. This ensures that the institutions participating in the trials have adequate quality assurance procedures and that no major systematic dosimetry discrepancies exist. The methodology has been described in detail in Ref. [1]. This programme includes the

periodic monitoring of beam output for photon and electron beams, and of electron beam energy. Agreement between the RPC TLD measurement and the output as stated by the institution is expected to be better than 5%. If the disagreement exceeds 5%, the discrepancy is resolved through telephone calls, correspondence, a repeat TLD irradiation or an on-site visit, in which ionization chamber measurements are performed.

The RDS has a similar programme that shares the same TLD and techniques as the RPC. It offers its services for a fee to customers, who can request verifications of photon or electron beams at any frequency. Discrepancies and acceptability criteria are very similar to those of the RPC, but there is no clear option for an on-site review to resolve intractable discrepancies.

The RPC system started photon beam verifications in 1977, and verifications for electrons in 1982. The RDS initiated its for a fee service in 1987. A total of about 3600 treatment units at radiation therapy facilities have been involved in the two programmes. Approximately 6000 X ray beams and 7500 electron beams are monitored per year. In the past three years on average 3% of photons and 7% of electrons have been outside the 5% criterion and have resulted in a repeat irradiation. Most of these cases are resolved by communication.

## 2. MATERIALS AND METHODS

The methodology of the remote audit TLD programme within the UTM-DACC has been explained in detail in Ref. [2]. A summary of the procedures is presented below.

### 2.1. Thermoluminescent material

Both centres use lithium fluoride powder (Harshaw, TLD-100) provided in disposable polyethylene capsules. Each capsule holds approximately 25 mg of powder. A large number of the capsules are filled with the same single batch of TLD powder, thereby ensuring uniform characteristics. Each batch is subjected to a commissioning process prior to its use.

### 2.2. Phantom design

For photon beams, TLD capsules are placed in an acrylic miniphantom that provides for electronic equilibrium. The miniphantom is supported in air by a nearly massless stand during irradiation. A larger acrylic, full scatter phantom is provided for electrons. Both types of phantom have three TLD capsules

placed at the depth of maximum dose,  $d_{\max}$ . For electrons, a second set of three capsules is placed at a depth of 30–80% dose in order to monitor energy by measuring the percentage depth dose.

### 2.3. Instrumentation

The UTMDACC uses single sample TLD readers. All thermoluminescent dosimeters are weighted and the thermoluminescent signal is normalized to the weight. Each instrument is commissioned prior to regular use by optimizing signal to noise ratios with respect to photomultiplier tube voltage settings. This verifies its ability to reproduce the TLD signal per weight within an acceptable standard deviation (SD) (1.2% at  $1\sigma$ ) and confirms that the operating parameters are appropriate and produce glow curves of an acceptable appearance. Each sample is read in a 2 min cycle that aims at a careful replication of the reading cycle. Currently, the reading cycle includes preheating for 5 s at 110°C, after which the signal is acquired for 46 s, with a temperature ramp of 5°C per second up to 320°C. Nitrogen gas flows throughout the entire session, beginning 30 min before a reading session starts, to eliminate non-radiation induced signals. Each sample is weighted while the system cools from the previous reading and is placed on the planchet after it has cooled to below 50°C. Thermoluminescent readings are provided with a reading precision of 0.01  $\mu\text{C}$  and a weighting precision of 0.01 mg. The reading is typically 15–50  $\mu\text{C}$  for an approximately 25 mg sample.

### 2.4. TLD characterization

Prior to the use of a new batch, a representative sample is tested in order to establish its reproducibility, dose response, fading characteristics and energy dependence. The last term combines corrections for two effects: the TLD powder dependence on beam energy and the effects of attenuation and scatter by the miniphantom, which also vary with energy. These tests are also performed on the batch in current use as a redundant check.

### 2.5. Dose calibration of the TLD system

Standard dosimeters are irradiated in a  $^{60}\text{Co}$  beam to a known dose of about 300 cGy. The  $^{60}\text{Co}$  unit is precalibrated with an ionization chamber dosimetric system traceable to the National Institute of Standards and Technology. The current protocol used for calibration is the American Association of Physicists in Medicine TG 51 protocol [3]. Standard samples are read in each session, three at the start and three at the end of the session. The dose per unit

signal per milligram corrected for linearity and fading is determined, which is identified as the system sensitivity.

## 2.6. Dose determination from the customer's dosimeters

The customer's dosimeters are read between the two sets of standards. A session normally involves around 12 sets of the customer's dosimeters, one third of them for electrons, which have six capsules. The signal per unit mass is obtained, corrected for fading, linearity and energy dependence, and the dose to the thermoluminescent dosimeter is calculated. The dose is then adjusted to match the institution's dose specification conditions by including backscatter, inverse square effects, percentage depth dose adjustments, etc.

Interspersed throughout the session, four additional dosimeters, identified as controls, are read. These controls are preirradiated on a second cobalt unit, the beam of which is precalibrated with an ionization chamber. Controls provide a check of the system's reliability to measure the dose from control dosimeters that are irradiated under a very tightly reproducible set-up. Thus the control dosimeters are expected to provide the best results. The controls also serve to identify and measure drift in the reader's response during a session.

## 3. QUALITY ASSURANCE OF THE SYSTEM

The expected quality of the results is maintained through a comprehensive quality assurance programme that includes the following aspects:

- (a) The acceptance and commissioning of the instrumentation.
- (b) The acceptance and commissioning of the thermoluminescent powder.
- (c) Tests per session. During the course of each reading session the dosimeter reader and the TLD results are tested for the following parameters:
  - (i) Background and test signals.
  - (ii) The SD of the signal from standard dosimeters ( $\sigma = 1.2\%$ ).
  - (iii) The SD of the signal from control dosimeters ( $\sigma = 1.2\%$ ).
  - (iv) The agreement between the measured and predicted dose to controls ( $\sigma = 1\%$ ).
  - (v) The outliers in each set of three dosimeters (3% criterion).
  - (vi) The weighing scale's reproducibility ( $\pm 0.05$  mg).
  - (vii) The institutional TLD results against their historical averages.
- (d) Monthly checks. Several parameters that may indicate anomalous variations are reviewed every month.



- (i) The system sensitivity.
- (ii) The SD of standards and controls per technician and per reading unit.
- (iii) The measured to predicted dose to the control irradiations.
- (e) Intercomparison. The RPC and RDS perform a quarterly intercomparison of  $^{60}\text{Co}$  beams, 6 MV and 18 MV photon beams, and 6 MeV and 12 MeV electron beams. Yearly intercomparisons with the IAEA are performed. Comparisons have also been performed with the quality assurance programme (EQUAL) of the European Society for Therapeutic Radiology and Oncology.
- (f) Record keeping. Records of results of reading sessions, quality assurance, malfunctions, maintenance and repairs are kept.

## 4. RESULTS

The TLD material (Harshaw, TLD-100) has not changed over the 25 years of TLD work. Other equipment and procedures, such as readers, weighing scales, the duration of routines and heating cycles, have changed over time. Most of the conclusions drawn in this paper are based on the data accumulated since 1991. There are, however, some conclusions that could very well apply to longer periods of time.

### 4.1. Batch characteristics

The signal per unit mass per unit dose (sensitivity) for a particular batch is dependent on the dosimeter reader, and it varies over time as the planchet gets used. Two different batches of TLD powder, read simultaneously on the same reader, generally yield different sensitivities. Batch to batch sensitivity changes of up to 15% have been observed. However, other characteristics, such as dose linearity, fading and energy correction, have been found to remain the same (within the limits of the accuracy of the measurement) from batch to batch.

### 4.2. Precision of dose determination

Statistics of 1646 TLD measurements over seven years on a cobalt unit at the UTMDACC are presented in Fig. 1. The  $x$  axis represents the dose ratio measured by TLD versus that measured by an ionization chamber. The distribution approximates to a Gaussian shape and shows a 0.9% SD that correlates well with the predicted precision [4] discussed in Section 4.5.

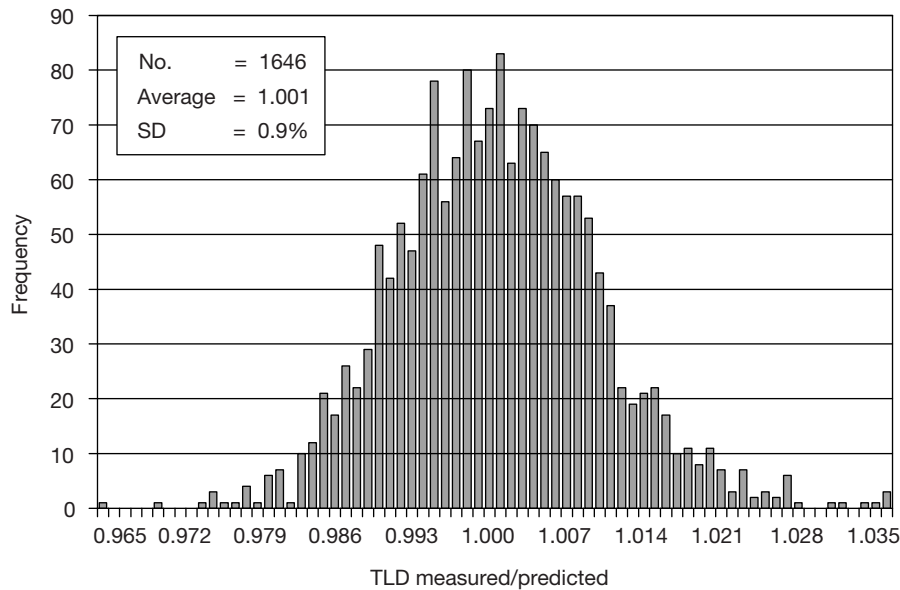


FIG. 1. Agreement between the TLD measured dose and the predicted dose from decay after ionization chamber calibration. Each value is the average of ten dosimeter samples per session.

Since these data correspond to dosimeters irradiated routinely under tightly reproducible geometry at the UTMDACC, the 0.9% precision represents the best possible result of our system.

4.3. Institutional results

Figure 2 shows the frequency distribution of TLD measurements of approximately 27 000 photon beams and 23 500 electron beams at participating institutions. These data are the results of measurements over a seven year period (1993–2000). Over this period most institutions used the TG 21 protocol [5]. SDs of the distributions are 1.9% for photons and 2.2% for electrons, which are higher than previously shown for the case of a cobalt unit. This higher SD is a result of the compounding of additional uncertainties, among which the calibration measurements and the use of a nominal dose rate instead of a measured value, drifts in the units between calibration, and irradiation and set-up uncertainties are significant contributors.

Figure 3 shows how the dose agreement has improved over the past 25 years. The ordinate is the percentage of institutions that have an acceptable agreement with the TLD measurements. From this figure can be seen an

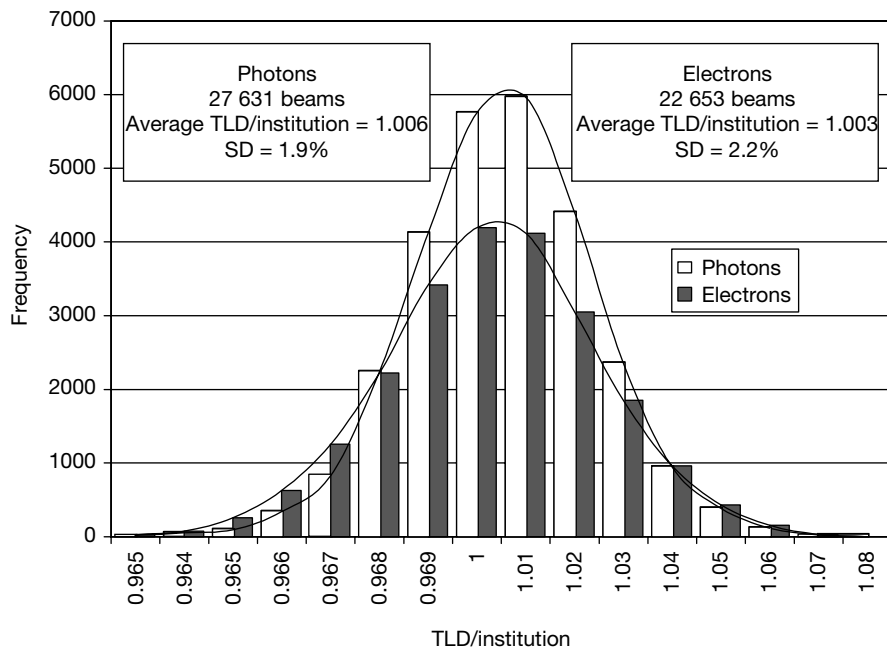


FIG. 2. Institutional results, excluding outliers ( $TLD/institution > 7\%$ ).

obvious steady improvement in the dose agreement. It is believed that this is in part due to the RPC's programme, which has ensured that the monitored institutions are continuously alert.

Figure 4 shows a distribution of SD for photon beams that have been verified five times or more. The location of the peak shows the most probable SD to be 1.5%. Based on this concept, the RPC may change its current window of acceptability from  $\pm 5\%$  to  $\pm 3\%$  ( $2\sigma$ ). Based on similar arguments, the RPC is considering changing its current window of  $\pm 5$  mm in electron depth dose measurements to  $\pm 3$  mm.

#### 4.4. Uncertainty in dose determination

The detailed analysis of uncertainty in dose determined from mailable TLD is given in Ref. [4]. Dose,  $D$ , is determined from TLD signal/mass,  $T$ , using:

$$D = TS k_f k_l k_E$$

where  $k_f$ ,  $k_l$  and  $k_E$  are fading, linearity and energy (nominal beam energy) correction factors, respectively.  $S$  represents system sensitivity in terms of

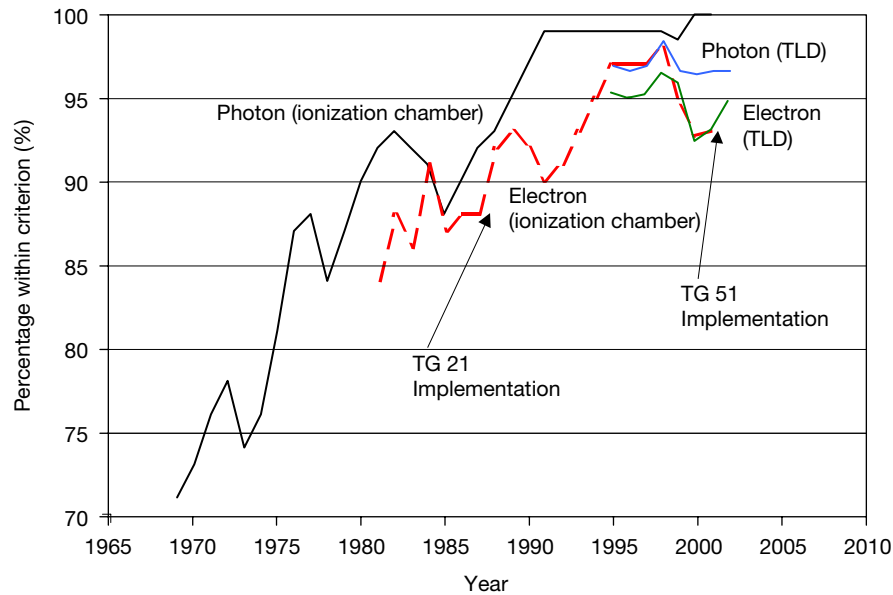


FIG. 3. Calibration verifications with an ionization chamber and with TLD. Percentage within criteria ( $\pm 5\%$  for TLD,  $\pm 3\%$  for the ionization chamber).

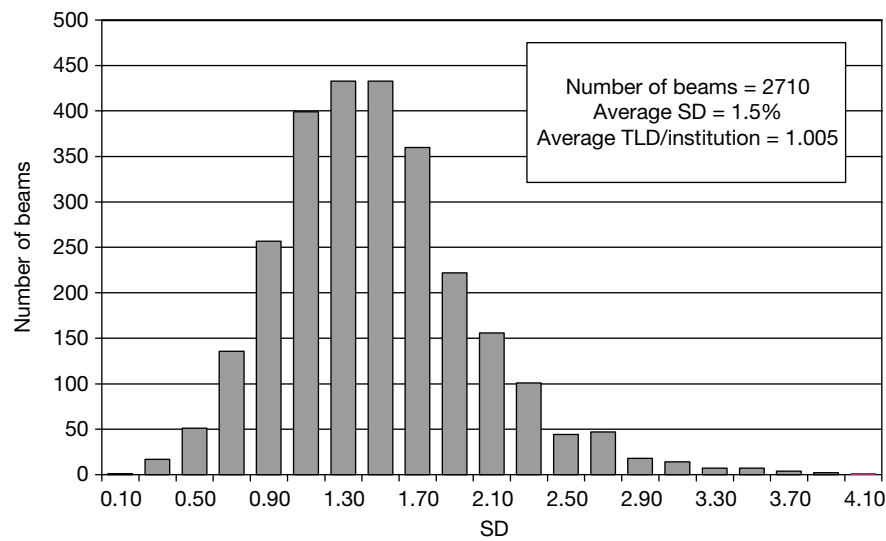


FIG. 4. SD of five or more repeat results of TLD on institutional photon beams.

dose/signal, and is determined by using the above equation applied to a cobalt unit, for which  $k_E = 1$  by definition and dose,  $D$ , is known through an ionization chamber measurement.

The standard error in dose is determined by compounding the standard errors in each of the factors in the above equation. For a cobalt unit this leads to a standard error of 0.9%, based on an average reading of six thermoluminescent dosimeter samples. This matches well with the measured SD in Fig. 1. For linac generated beams the estimated standard error is 1.5, based on an average of three TLD samples.

### ACKNOWLEDGEMENT

This work was supported by Public Health Service Grant CA 10953, awarded by the National Cancer Institute, US Department of Health and Human Services.

### REFERENCES

- [1] HANSON, W.F., SHALEK, R.J., KENNEDY, P., Dosimetry quality assurance in the U.S. from the experience of the Radiological Physics Center, SSDL Newsletter No. 30 (1991) 18–34.
- [2] KIRBY, T.H., HANSON, W.F., GASTORF, R.J., CHU, C.H., SHALEK, R.J., Mailable TLD system for photon and electron therapy beams, *Int. J. Radiat. Oncol. Biol. Phys.* **12** (1986) 261–265.
- [3] AMERICAN ASSOCIATION OF PHYSICISTS IN MEDICINE, AAPM's TG-51 protocol for clinical reference dosimetry of high-energy photon and electron beams, *Med. Phys.* **26** (1999) 1847–1870.
- [4] KIRBY, T.H., HANSON, W.F., JOHNSTON, D.A., Uncertainty analysis of absorbed dose calculations from thermoluminescence dosimeters, *Med. Phys.* **19** (1992) 1427–1433.
- [5] AMERICAN ASSOCIATION OF PHYSICISTS IN MEDICINE, TASK GROUP 21, A protocol for the determination of absorbed dose from high-energy photon and electron beams, *Med. Phys.* **10** (1983) 741–771.

**BLANK**

## **ROLE OF THE NATIONAL PHYSICAL LABORATORY IN MONITORING AND IMPROVING DOSIMETRY IN RADIOTHERAPY IN THE UNITED KINGDOM**

R.A.S. THOMAS, S. DUANE, M.R. McEWEN\*, K.E. ROSSER  
National Physical Laboratory,  
Teddington, United Kingdom  
E-mail: russell.thomas@npl.co.uk

### **Abstract**

The National Physical Laboratory, in collaboration with the Institute of Physics and Engineering in Medicine, operates an audit programme to ensure national consistency in radiotherapy dosimetry in the United Kingdom. The present programme covers the dosimetry of megavoltage photons, electrons (3–19 MeV) and low and medium energy (10–300 kV) photons. The aim of each audit is to verify the local measurement of absorbed dose at the radiotherapy centre. The audit measurements, principally beam quality and linac output, are made following the same UK codes of practice (CoPs) used by the clinic, but using different equipment. The audit is not an absolute measurement of the absorbed dose, but amounts to a check that the equipment used by the centre is operating as expected and that the CoP is being implemented correctly. The protocols used in the UK are the Institute of Physical Sciences in Medicine 1990 protocol for high energy photons, the Institution of Physics and Engineering in Medicine and Biology (IPEMB) 1996 protocol for electrons and the IPEMB 1996 protocol for low energy photons. Measurements are made using NE 2561, NE 2571, NACP-02 and PTW Roos ionization chambers.

### **1. INTRODUCTION**

Radiotherapy centres in the United Kingdom are organized by the Institute of Physics and Engineering in Medicine (IPEM) into eight geographical regions for the purpose of interdepartmental audits. Within each region hospitals audit dosimetry, treatment planning, record keeping, etc. A national audit was reported by Thwaites et al. [1], who carried out a dosimetric comparison of megavoltage photon beams in all UK centres, obtaining a mean value for the ratio audit/local dose of 1.003, with a standard deviation of 1.5%. In three cases the results differed from unity by 3% or more. In 1997 Nisbet et al. [2] carried out a similar exercise for photon and electron beams, finding standard deviations of 1% for photons and 1.8% for electrons. For photon beams,

---

\* Present address: National Research Council, Ottawa, Canada.

the worst case agreement was 2.6%. Since 1994 the intraregional audits organized by the IPEM have been supplemented by dosimetry audits carried out by the National Physical Laboratory (NPL), whose staff visit one department from each region in turn. The aim of these extra audits is twofold: to pick up any interregional differences that would be missed by the IPEM and to check the dissemination of the UK standard of absorbed dose to the end of the calibration chain, by measuring absorbed dose under reference conditions by following the appropriate UK code of practice (CoP). The scope of these audits was extended in 2000 to include electron beams, and low energy kilovoltage X ray audits are presently being piloted.

## 2. MEGAVOLTAGE PHOTON AUDITS

The UK CoP [3] for megavoltage photon dosimetry is based on the NPL absorbed dose to water calibration service [4], traceable to the primary standard graphite calorimeter. The calibrated secondary standard chamber is used in the clinic to calibrate field instruments (most commonly a Farmer type NE 2571 chamber). The procedure for an NPL audit is as follows, using NPL owned instruments, traceably calibrated to national standards:

- (a) The host department selects the beam quality, often 6 MV or 8 MV.
- (b) NPL staff make measurements in water, on the axis of a horizontal beam, in an NPL phantom, at depths of 5 (or 7), 10 and 20 g/cm<sup>2</sup> from the front face. The source to chamber distance is set at 100 cm, with a field size of 10 cm × 10 cm at the chamber.
- (c) The calibration of the NPL secondary standard chamber in the clinical beam is based on the measured beam quality index, TPR<sub>20,10</sub>.
- (d) The machine output is obtained, including the recombination correction.
- (e) The local field instrument is calibrated by substitution against the NPL chamber in the NPL phantom. Recombination is also measured for the field instrument.
- (f) The results are compared with local values, possibly measured on the same day.

Over the past six years around 25 audits based on the UK CoP [3] have been carried out; the results are summarized in Table I.

As can be seen from Table I, the ratio of the local to audit measurement is unity within the standard uncertainty (estimated to be ±0.4%). Experimental procedures within the centres appear to have improved in recent years, with a marked reduction in the scatter of the results. Solid state alanine dosimeters



have been used to investigate the effectiveness of  $\text{TPR}_{20,10}$  as a beam quality parameter in the transfer of calibrations from the standards laboratory to the clinic. The initial conclusion from the measurements, shown in Fig. 1, is that the absolute error in the transfer of dose in photon beams is unlikely to be more than 1% (see Fig. 1, in which the error bars indicate only the internal consistency of dose measurements at a given site). The audits cover linacs from a wide range of manufacturers, with no statistically significant variation from one manufacturer to another.

TABLE I. SUMMARY OF RESULTS OF MEGAVOLTAGE PHOTON AUDITS

Quantity	Mean ratio (NPL/host)	Standard deviation (%)
TPR	0.998	0.6
Machine output	1.003	0.8
Field instrument calibration	1.000	0.7

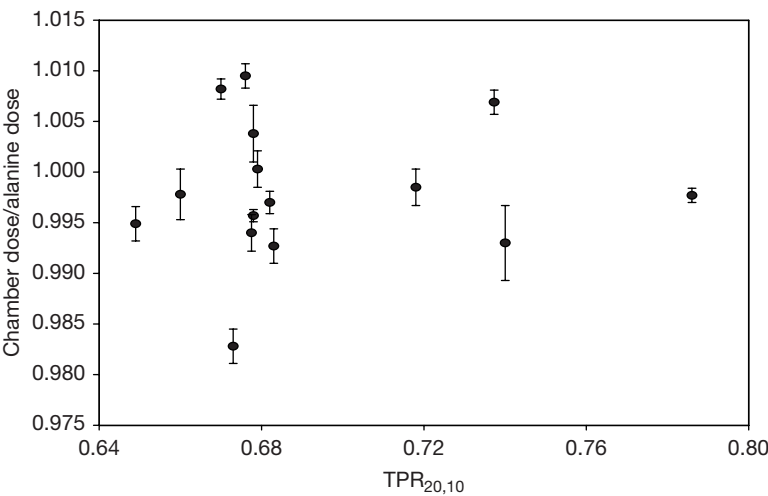


FIG. 1. Comparison of ionometric and alanine doses in megavoltage photon beams.

### 3. ELECTRON AUDITS

The NPL has launched an absorbed dose calibration service based on a calorimetric primary standard [5], for which a new CoP is in preparation by the IPEM. However, this new CoP has not yet been adopted and, for the moment at least, dosimetry for electron beam radiotherapy is traceable to  $^{60}\text{Co}$  air kerma standards [6]. Audits of electron beam dosimetry therefore follow the air kerma based CoP [6], as follows:

- (a) Prior to the audit, the host supplies depth ionization data for the electron beams selected. These data are analysed by the NPL to obtain reference depths, perturbation factors and stopping power ratios. (There is not time to measure depth ionization data afresh.)
- (b) NPL staff derive the  $N_{D,\text{air}}$  factor for an NPL Farmer chamber using an NPL NE 2611 chamber in the user's 6 MV photon beam.
- (c) NPL staff derive  $N_{D,\text{air}}$  factors for a number of parallel-plate chambers, using NPL equipment in a high energy electron beam ( $>15$  MeV).
- (d) NPL staff measure recombination and polarity corrections and machine output for the chosen electron beam(s) using NPL equipment.
- (e) The host measures the recombination and machine output using local equipment.

The Institution of Physics and Engineering in Medicine and Biology (IPEMB) 1996 CoP [7] recommends that all measurements in electron beams be carried out in a water phantom, but allows the use of solid phantoms. For these audits a WTe phantom was used (manufactured by St Bartholomew's Hospital, London). Investigation of the water equivalence of this epoxy based material at the NPL supports the conclusions of others (e.g. Ref. [8]) that 1 cm of WTe is equivalent to 1 cm of water, with a fluence ratio correction of unity, within the measurement uncertainty. To date four electron audit visits have been completed using eight electron beams in total. These have included linacs from three manufacturers: Philips (Elekta), Varian and Siemens. Output was measured using both NACP and PTW Roos chambers; the results are listed in Table II.

In any air kerma based CoP an error in the determination of  $N_{D,\text{air}}$  for the NE 2571 chamber will affect all dose measurements in an electron beam. Although  $N_{D,\text{air}}$  is best measured in a  $^{60}\text{Co}$  beam, such facilities are no longer widely available, and so the CoP allows the use of a low energy linac photon beam (usually 6 MV). X ray measurements in the clinic have been compared with measurements at the NPL using a  $^{60}\text{Co}$  beam, and indicate that there may be a difference of up to 0.5% in the value of  $N_{D,\text{air}}$  derived by these two routes.

TABLE II. COMPARISON OF OUTPUT FACTORS FOR NACP AND ROOS CHAMBERS

Centre	$E_{\text{nom}}$ (MeV)	Machine output (NPL/host)	
		NACP	PTW Roos
1	9	1.010	0.992
1	12	1.004	0.996
2	6	1.004	1.003
2	10	1.001	0.995
3	6	1.003	1.002
3	9	1.006	1.005
4	6	1.012	1.018
4	12	1.010	—
Mean		1.006	1.002
Standard deviation		0.4%	0.8%

The IPEMB 1996 CoP gives a figure of around  $\pm 2\%$  for the overall uncertainty of a measurement of dose, but the standard uncertainty in the ratios given in Table II was estimated to be only  $\pm 0.5\%$ , as a result of correlations in the uncertainties (in physical data and in the air kerma primary standard) of the host and NPL measurements.

The mean level of agreement is around 0.6%, which indicates that there are no significant errors in the application of the IPEMB 1996 CoP. There is, in general, good agreement (i.e. better than 0.5%) when comparing the NACP and Roos results in Table II, although these initial results show a greater variability in the measurements made with Roos chambers. Differences between the results for the chamber types arise only in the chamber readings, either in the high energy comparison with the Farmer chamber or in the output measurement. This may be due to beam non-uniformity (the Roos chamber having a larger diameter collector), differences in chamber perturbation, chamber positioning or some other effect. Further audits should clarify whether there is a significant difference between the Roos and NACP chambers.

It is interesting to note that, from the NACP data, the NPL measured dose is always higher than the host value: since the NPL measurements are made in WTe and the host measurements are made in water, it may be that the fluence correction for the WTe material is not unity after all. Further measurements have been made at the NPL using an ionization chamber to compare the

fluence in water and WTe. This work is described in detail in Ref. [9] and summarized in Fig. 2. As can be seen, the measured fluence in WTe is perhaps 0.3% higher than that in water at the same depth. This means that a correction of  $-0.3\%$  should be applied to the NPL dose values in Table II, which would result in a mean value for the ratio NPL/host for the NACP data of 1.0032, which is consistent with unity within the estimated uncertainty. Further work is required to determine whether the sample to sample variation is around the 0.4% level, or whether instead one should consider revising the fluence correction given in the IPEMB 1996 CoP.

#### 4. FUTURE WORK

A working party of the IPEM is currently developing a new, simpler CoP for electron beam dosimetry, based on the NPL absorbed dose calibration service. This will lead to a significant reduction in uncertainty. Once this CoP has been published and implemented, further electron audits will be carried out to evaluate its implementation and for comparison with the earlier CoP. Low and medium energy kilovoltage photon audits will start next year. Trial audits of kilovoltage photon dosimetry show reproducibility at the  $\pm 2\%$  level, but have highlighted problems at very low photon energies and the need for more accurate chamber data. Discrepancies have been shown to occur at the overlap

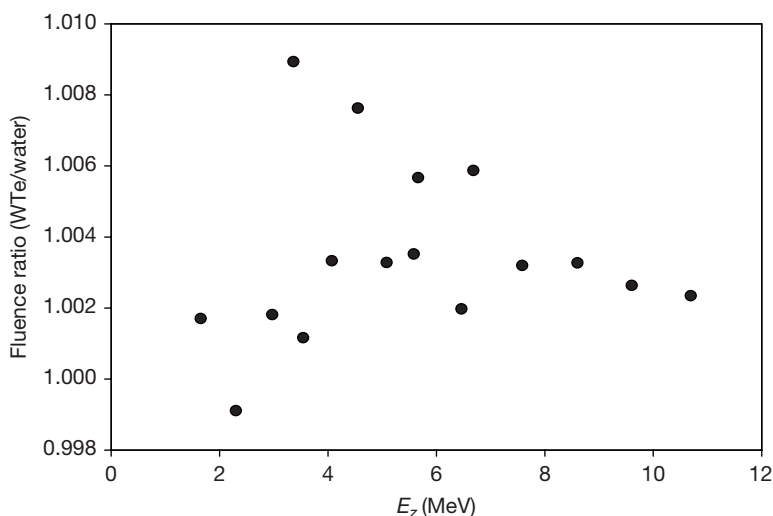


FIG. 2. Fluence correction for the WTe phantom used for NPL audits.

between the different energy ranges of the CoP. An addendum to the 1996 photon CoP, which will address these issues, is currently in preparation by the IPEM. It is also hoped to pilot further audit measurements of dosimetry for brachytherapy, mammography and diagnostic X rays. A portable calorimeter has also been developed at the NPL [10], which can be operated in clinical beams, allowing the measurement of absolute dose and the independent investigation of beam quality issues. The standard uncertainty in measuring absorbed dose to water using this device is  $\pm 0.9\%$ , which is comparable with that of the NPL primary standards.

### ACKNOWLEDGEMENTS

This work was funded as part of the UK National Measurement System, Ionizing Radiation Metrology Programme, by the NMS Policy Unit of the UK Department of Trade and Industry. Thanks are due to the IPEM for instigating and developing this system of audits, and for inviting the NPL to take part, and to the many UK radiotherapy centres that participated so willingly in these measurements. The audits described in this paper were developed in close collaboration with colleagues in the IPEM, which pioneered the system of regional radiotherapy dosimetry audit in the UK.

### REFERENCES

- [1] THWAITES, D.I., WILLIAMS, J.R., AIRD, E.G., KLEVENHAGEN, S.C., WILLIAMS, P.C., A dosimetric intercomparison of megavoltage photon beams in UK radiotherapy centres, *Phys. Med. Biol.* **37** (1992) 445–461.
- [2] NISBET, A., THWAITES, D.I., A dosimetric intercomparison of electron beams in UK radiotherapy centres, *Phys. Med. Biol.* **42** (1997) 2393–2409.
- [3] INSTITUTE OF PHYSICAL SCIENCES IN MEDICINE, Code of Practice for high-energy photon therapy dosimetry based on the NPL absorbed dose calibration service, *Phys. Med. Biol.* **35** (1990) 1355–1360.
- [4] BURNS, J.E., DALE, J.W.G., DuSAUTOY, A.R., OWEN, B., PRITCHARD, D.H., “New calibration service for high-energy x-radiation at NPL”, *Dosimetry in Radiotherapy* (Proc. Int. Symp. Vienna, 1987), Vol. 2, IAEA, Vienna (1988) 125–132.
- [5] McEWEN, M.R., DuSAUTOY, A.R., WILLIAMS, A.J., The calibration of therapy level electron beam ionization chambers in terms of absorbed dose to graphite, *Phys. Med. Biol.* **43** (1998) 2503–2519.

- [6] INSTITUTION OF PHYSICS AND ENGINEERING IN MEDICINE AND BIOLOGY, The IPEMB code of practice for electron dosimetry for radiotherapy beams of initial energy from 2 to 50 MeV based on an air kerma calibration, *Phys. Med. Biol.* **41** (1996) 2557–2603.
- [7] INSTITUTION OF PHYSICS AND ENGINEERING IN MEDICINE AND BIOLOGY, The IPEMB code of practice for the determination of absorbed dose for x-rays below 300 kV generating potential (0.035 mm Al–4mm Cu HVL; 10–300 kV generating potential), *Phys. Med. Biol.* **41** (1996) 2605–2625.
- [8] NISBET, A., THWAITES, D.I., Polarity and ion recombination correction factors for ionization chambers employed in electron beam dosimetry, *Phys. Med. Biol.* **43** (1998) 435–443.
- [9] McEWEN, M.R., DuSAUTOY, A.R., OATEY, M., Measurement of Water Equivalence of a WTe Phantom for Electron Beam Dosimetry (in preparation).
- [10] McEWEN, M.R., DUANE, S., A portable calorimeter for measuring absorbed dose in the radiotherapy clinic, *Phys. Med. Biol.* **45** (2000) 3675–3691.

## **AN ANTHROPOMORPHIC HEAD AND NECK PHANTOM FOR THE EVALUATION OF INTENSITY MODULATED RADIATION THERAPY**

G. IBBOTT, A. NELSON, D. FOLLOWILL, P. BALTER, W.F. HANSON  
University of Texas M.D. Anderson Cancer Center,  
Houston, Texas, United States of America  
E-mail: gibbott@mdanderson.org

### **Abstract**

Intensity modulated radiation therapy (IMRT) has gained acceptance as an improved treatment technique for several disease sites. As the use of IMRT increases, national cancer study groups are beginning to initiate clinical trials that involve its use. Because IMRT offers the possibility of high dose gradients, it is possible to deliver high doses to target volumes while maintaining low doses to nearby critical normal structures. The use of high gradients means that the localization of the dose distribution is critical. Consequently, it is important that the institutions participating in clinical trials administer IMRT consistently and accurately. The Radiological Physics Center (RPC) has been funded by the United States National Cancer Institute to assure study groups that participants in clinical trials have adequate quality assurance procedures and that their patient dosimetry is accurate. The RPC also reviews and accredits institutions to participate in some high technology clinical trials. To evaluate the delivery of IMRT and to accredit institutions for IMRT head and neck trials, the RPC has developed a mailable anthropomorphic head and neck phantom. The phantom contains dosimeters and structures to represent anatomy and target volumes, and has been used to evaluate the imaging, planning and delivery of IMRT at ten institutions. An evaluation of the results indicates significant variations and surprising trends in the delivery of IMRT.

### **1. INTRODUCTION**

#### **1.1. Intensity modulated radiation therapy and quality assurance requirements**

Intensity modulated radiation therapy (IMRT) has gained acceptance as an improved treatment technique for a number of disease sites [1–4]. Several manufacturers of radiation therapy equipment provide devices to enable the delivery of IMRT, including multileaf collimators and inverse planning (optimization) treatment planning systems. Because IMRT offers the possibility of

larger dose gradients than conventional radiation therapy, it is possible to deliver higher doses to target volumes while maintaining low doses to nearby critical normal structures. At the same time, the high dose gradients achievable with IMRT mean that the localization of the dose distribution is critical. Small errors in the positioning of the patient can mean that a target volume is missed, or that a sensitive normal structure is irradiated to a higher dose than intended, and perhaps higher than can be tolerated.

Consequently, comprehensive quality assurance (QA) procedures are necessary [5]. A QA programme for IMRT must address characteristics that stress procedures and the abilities of the equipment. For example, the nature and advantages of IMRT demand that patient positioning be considerably more precise and reproducible than for conventional treatments. Devices to facilitate reproducible positioning and patient immobilization are available for imaging, simulation and treatment equipment, and QA procedures should be implemented to ensure proper functioning and correct usage. Other alignment devices, such as lasers, video systems and ultrasound imaging systems, must be evaluated on a regular basis to ensure their correct functioning.

## **1.2. Radiological Physics Center**

The Radiological Physics Center (RPC) is funded by the United States National Cancer Institute to assure the co-operative study groups that conduct multi-institutional clinical trials that institutions participating in the trials have adequate QA procedures and that no major systematic dosimetry discrepancies exist. Remote monitoring procedures include the use of mailed thermoluminescent dosimeters (TLDs) to verify machine output, the comparison of an institution's dosimetry data with RPC standard data to identify potential discrepancies, the evaluation of reference or actual patient calculations to verify the treatment planning algorithms and manual calculations, the review of the institution's written QA procedures and records to verify adherence to recommendations published by the American Association of Physicists in Medicine (AAPM) [6], and the use of mailed anthropomorphic phantoms to verify tumour dose delivery for special treatment techniques.

In some cases, the RPC participates in the accreditation of institutions wishing to participate in specific clinical trials. These institutions are required to submit the details of their treatment planning capabilities, representative treatment plans for benchmark cases or actual patient treatments, and, in some cases, actual measured data. Recently, several study groups have begun to require, or encourage, the use of IMRT for the treatment of patients submitted to some clinical trials. The RPC was asked to develop a head and neck phantom to evaluate the quality of the IMRT treatment process from imaging, through planning,



to treatment delivery. The results of the phantom irradiation were to be used in accrediting institutions wishing to participate in an IMRT protocol.

## 2. MATERIALS AND METHODS

### 2.1. Phantom design

The phantom was to have an anthropomorphic outer plastic shell, be lightweight to reduce shipping costs, use water as a substitute for tissue where possible, and contain imageable targets that included radiation dosimeters. The outer plastic shell of the head was purchased commercially (The Phantom Laboratory) and modified to hold an imaging and dosimetry insert in a water-tight environment. The remainder of the phantom was filled with water. All modifications were performed without metal parts that would interfere with imaging or the treatment of the phantom. The exterior plastic shell was of a sufficiently realistic anthropomorphic shape that the phantom would fit in most treatment immobilization devices used for IMRT treatments.

The target–dosimeter insert was constructed as a block of water equivalent plastics. Planning target volumes (PTVs) were designed to mimic head and neck disease involving primary and secondary targets, with an organ at risk (OAR) adjoining the primary target. The water equivalent plastics used for the targets and OAR were of a slightly different density than the surrounding water and plastics, to enable imaging, but had an insignificant effect on treatment delivery. The target–dosimeter insert was designed to hold TLDs in the two PTVs and the OAR. Radiochromic films (RCFs) were placed in the axial plane through the targets and critical structure and in the sagittal plane through the primary PTV. Since the dosimeters would be irradiated during imaging as well as treatment delivery, TLDs were located on the exterior of the phantom to monitor the dose given during imaging.

### 2.2. Phantom dosimeters

TLD-100 powder, placed in custom made reusable capsules, was used as an absolute dosimeter. The capsules were small cylinders with outer dimensions of 5 mm height  $\times$  5 mm diameter, with a 1 mm wall thickness. Each capsule held approximately 40 mg of powder, which yielded two readings. The capsules were constructed of high impact polystyrene, contained very little air and approximated a small sphere.

Powder used in the mailout system was evaluated for dose response, energy dependence, dose uniformity and fading. The accuracy of the thermoluminescence

dosimetry system is  $\pm 4\%$  at the 90% confidence interval [7]. The system is precise to within  $\pm 3\%$  and capable of detecting dose errors of the order of  $\pm 5\%$ . Readout procedures described earlier were followed [8], except that a filter was used to dampen the thermoluminescent signal, and high dose thermoluminescence dosimetry standards were used.

RCFs (GafChromic MD-55-2 film) were used to measure dose distributions and field localization. RCFs have a high spatial resolution, a low spectral sensitivity, an insignificant angular dependence and are approximately tissue equivalent [9]. RCFs are therefore well suited to measure IMRT produced high dose gradient radiation fields. AAPM recommendations for the handling and evaluation of RCFs for use in dosimetry were followed [9]. Films were scanned with a 633 nm laser densitometer (Personal Densitometer), with a scanning resolution of 0.1 mm. RCFs were investigated for dose response, fading, energy independence and uniformity [10, 11].

### **2.3. Data comparison**

Each institution irradiating the IMRT head and neck phantom was instructed to provide dose calculations and dose distribution information for comparison with the TLD and RCF measurements. The institution was asked to outline the TLD powder on computed tomography images and report the minimum, mean and maximum dose to the TLD capsule. The institution was also asked to provide dose distributions in the planes corresponding to the location of the films. A comparison of the treatment plan and measured dose profiles in the two planes of measurement was performed.

## **3. RESULTS**

### **3.1. Phantom design**

Figure 1 shows the hollow phantom head with the imaging–dosimetry insert in place. The crown of the head is removable so that the insert can be dropped into its watertight housing. The base is equipped with adjustable screws for alignment prior to imaging and treatment. The head can be placed on the type of headrest commonly used by most institutions.

Figure 2 shows the 7.5 cm  $\times$  10.5 cm  $\times$  13 cm polystyrene imaging–dosimetry insert. The primary and secondary PTVs were made of Solid Water and were 5 cm in length. The primary PTV was 4 cm in diameter and held two TLDs. One TLD was superior to the axial film, and the other was inferior to it. The secondary PTV was 2 cm in diameter and held one TLD located in its

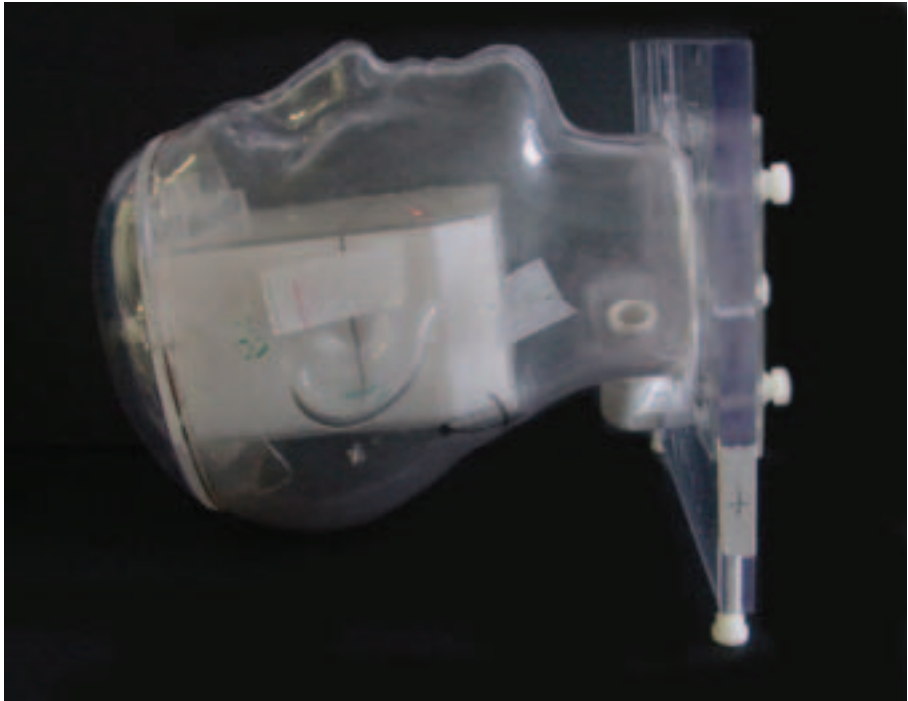


FIG. 1. The head and neck phantom showing the imaging–dosimetry insert in place.

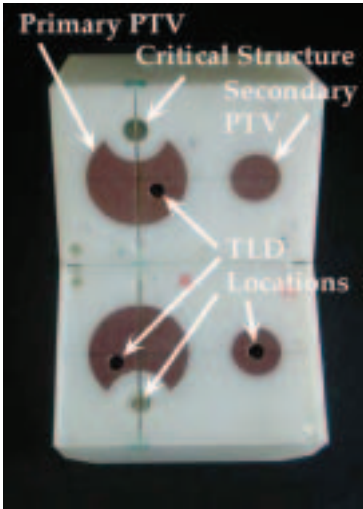


FIG. 2. The imaging–dosimetry insert showing the two PTVs and the OAR.

centre directly inferior to the axial film. The centres of the two PTVs were separated by 5.2 cm. The OAR was made of acrylic, was 1 cm in diameter and extended the length of the insert. It held one TLD located in the centre of its cross-section directly inferior to the axial film. The edge of the OAR was 0.8 cm away from the edge of the primary PTV in the posterior direction. The location of the RCF can also be seen in Fig. 2. A single sheet was placed in the axial plane. Sagittal films were placed above and below the axial film in the slits bisecting the primary PTV.

### 3.2. Phantom dosimetry reproducibility

The reproducibility of the TLD results was established by delivering a benchmark treatment plan three times in one evening. The phantom set-up was not disturbed between the irradiations. The TLD results are shown in Table I. The standard deviation (SD) was less than 1.6% at each point.

The reproducibility of the film scanning system was established by scanning the films from one irradiation three times. Profiles in the two planes were determined for each scan and normalized to unity at the centre of the primary PTV. The profiles from the three scans were compared in a high gradient region at a level of 75%. The maximum uncertainty in film reproducibility for the three scans was  $\pm 0.35$  mm.

### 3.3. Phantom irradiation

Ten institutions irradiated the phantom as part of this commissioning. The TLD dose results from these irradiations are shown in Table II. The results are presented as the ratio of the RPC TLD reading to the mean dose to the TLD as predicted by the institution.

TABLE I. REPRODUCIBILITY OF TLD RESULTS AS DETERMINED FROM THREE IDENTICAL EXPERIMENTS

TLD	Average dose (cGy) $\pm$ SD
Primary PTV (superior)	714 $\pm$ 8.1
Primary PTV (inferior)	804 $\pm$ 10.8
Secondary PTV	663 $\pm$ 6.7
OAR	178 $\pm$ 2.3

TABLE II. RATIO OF THE RPC TLD DOSE MEASUREMENT TO THE DOSE STATED BY THE INSTITUTION

Institution	Primary PTV (superior)	Primary PTV (inferior)	Secondary PTV	OAR
1	0.97	1.04	1.10	0.99
2	0.93	0.96	0.93	0.82
3	1.04	—	1.01	1.16
4	0.96	1.00	0.98	—
5	1.09	1.07	1.11	1.35
6	1.01	1.03	0.99	1.10
7	1.02	1.03	1.00	0.95
8	0.98	0.98	0.97	0.88
9	1.04	1.04	1.06	1.09
10	1.04	1.05	1.04	1.18
Average	1.01	1.02	1.02	1.07
SD	4.8%	3.5%	5.7%	15.6%

Two TLD results are missing, because one TLD capsule from institution 3 was lost, and institution 4 was not able to give a mean dose to the OAR TLD capsule. The agreement was good between the TLD doses and the institution doses in both PTVs, with a maximum SD of 5.7%. The dose agreement in the OAR was not as good, with an average TLD/institution ratio of 1.07 and an SD of 15.6%. In all cases the RPC TLD dose fell between the minimum and maximum doses reported by the institution.

#### 4. DISCUSSION

Institution 5 was not included in the data analysis to develop acceptance criteria because it reported point doses, not average doses. The acceptance criteria were set at  $\pm 7\%$  for the primary and secondary PTVs. This value was 1.64 times the SD, excluding institution 5. The criterion for the OAR was set at  $\pm 18\%$ , which is the range of TLD values, excluding institution 5. A larger error for the OAR was deemed appropriate considering the high gradients in this area combined with the relatively large size of the TLD.

Film profiles from the axial film were taken through the centre of the primary PTV in the anterior–posterior and right–left directions. Profiles in the superior–inferior direction were taken from the sagittal film. The profiles were normalized to the TLD results from the primary PTV. A preliminary analysis indicated that distance to agreement values of 5 mm or more were not infrequent. Calculated doses were generally lower than measurements in regions of a steep gradient. Some planning systems may underestimate the contributions of head scatter and transmission through rounded leaf ends, contributing to the differences seen in low dose regions [12].

### ACKNOWLEDGEMENTS

This work was supported by Public Health Service Grant CA 81647, awarded by the National Cancer Institute, US Department of Health and Human Services.

### REFERENCES

- [1] STERNICK, E.S., CAROL, M.P., GRANT, W.H., “Intensity-modulated radiotherapy”, *Treatment Planning in Radiation Therapy* (KHAN, F.M., POTISH, R.A., Eds), Williams & Wilkins, Baltimore, MD (1998) 187–213.
- [2] GRANT, W., CAIN, R.B., Intensity-modulated conformal therapy for intracranial lesions, *Med. Dosim.* **23** (1998) 237–241.
- [3] HONG, G.L., et al., Intensity-modulated tangential beam irradiation of the intact breast, *Int. J. Radiat. Oncol. Biol. Phys.* **44** (1999) 1155–1164.
- [4] HUNT, M.A., et al., Treatment planning and delivery of intensity-modulated radiation therapy for primary nasopharynx cancer, *Int. J. Radiat. Oncol. Biol. Phys.* **49** (2001) 623–632.
- [5] BOYER, A.L., et al., “Quality assurance for treatment planning dose delivery by 3DRTP and IMRT”, *General Practice of Radiation Oncology Physics in the 21st Century* (SHIU, A.S., MELLEBERG, D.E., Eds), Medical Physics Publishing, Madison, WI (2000) 187–230.
- [6] KUTCHER, G.J., et al., Comprehensive QA for radiation oncology, report of Task Group No. 40, Radiation Therapy Committee, *Med. Phys.* **21** (1994) 580–618.
- [7] KIRBY, T.H., HANSON, W.F., GASTORFF, R.J., JOHNSTON, D.A., Uncertainty analysis of absorbed dose calculations for thermoluminescence dosimeters, *Med. Phys.* **19** (1992) 1427–1433.
- [8] KIRBY, T.H., HANSON, W.F., GASTORFF, R.J., CHU, C.H., SHALEK, R.J., Mailable TLD system for photon and electron therapy beams, *Int. J. Radiat. Oncol. Biol. Phys.* **12** (1986) 261–265.

- [9] NIROOMAND-RAD, A., et al., Radiochromic film dosimetry: Recommendations of AAPM Radiation Therapy Committee Task Group 55, *Med. Phys.* **25** (1998) 2093–2115.
- [10] BALTER, P., STOVALL, M., HANSON, W.F., An anthropomorphic head phantom for remote monitoring of stereotactic radiosurgery at multiple institutions, *Med. Phys.* **26** (1999) 1164 (abstract).
- [11] RADFORD, D.A., FOLLOWILL, D.S., HANSON, W.F., A standard method of quality assurance for intensity modulated radiation therapy of the prostate, *Med. Phys.* **28** (2001) 1211 (abstract).
- [12] CADMAN, P., BASSALOW, R., SIDHU, N.P.S., IBBOTT, G., NELSON, A., Dosimetric considerations for validation of a sequential IMRT process with a commercial treatment planning system, *Phys. Med. Biol.* **47** (2002) 3001–3010.

**BLANK**



## POSTERS ON BRACHYTHERAPY

(Session 12a)

**Chair**

**I.-L.C. LAMM**

European Federation of Organisations for Medical Physics

**Co-Chair**

**H. TÖLLI**

IAEA

**Rapporteur**

**I.-L.C. LAMM**

European Federation of Organisations for Medical Physics

**BLANK**

# DESIGN AND IMPLEMENTATION OF A PHANTOM FOR THE QUALITY CONTROL OF HIGH DOSE RATE $^{192}\text{Ir}$ SOURCES USED IN BRACHYTHERAPY

R. OCHOA\*, I.H. FERREIRA\*\*, C.E. DE ALMEIDA\*

\* Laboratório de Ciências Radiológicas,  
Universidade do Estado de Rio de Janeiro,  
Rio de Janeiro, Brazil  
E-mail: ric8ap@hotmail.com

\*\* ESTRO EQUAL Laboratory, Institut Gustave-Roussy,  
Villejuif, France

## Abstract

A new phantom has been developed that uses thermoluminescent dosimeters for the quality control of high dose rate  $^{192}\text{Ir}$  sources used in brachytherapy. This phantom can be used to verify the air kerma at 10 cm in air and the absorbed dose 2 cm deep in water calculated by the treatment planning system. The formalism used for the verification of the air kerma and the absorbed dose, as well as the methods used for the determination of the correction factors that are needed, are described.

## 1. INTRODUCTION

Brachytherapy is an essential part of the treatment of several types of cancer, especially of the cervix, lung and prostate. The use of high dose rate  $^{192}\text{Ir}$  sources requires appropriate calibration in order to ensure the desired level of accuracy of the dose delivered to the tumour.

Primary standards for high dose rate  $^{192}\text{Ir}$  sources have yet to be developed. Metrological traceability in many countries, including Brazil, is established by indirect methods using an energy weighted average of air kerma calibration factors for 250 kV X rays (half-value layer of 2.5 mm Cu, effective energy of 131 keV) and  $^{60}\text{Co}$  or  $^{137}\text{Cs}$  gamma ray beams, as described elsewhere [1–4].

A set of calibration procedures for low and high dose rate brachytherapy sources has recently been published by the IAEA [5, 6]. These documents emphasize the recommendations made previously by the IAEA and the American Association of Physicists in Medicine [7, 8], which are that all radiation therapy centres should have a quality assurance programme to

guarantee the consistency of operational procedures, including for source calibration and the absorbed dose calculated by the treatment planning system. As a part of such a quality assurance programme it is highly desirable that an independent evaluation be included, which can either be done by site visits or through well established postal dosimetry programmes. A postal dosimetry programme is a very useful, reliable and economical option, especially when a large number of geographically dispersed institutions are involved. Site visits are planned to clarify inconsistent data or unresolved discrepancies [9].

There are essentially no postal systems in operation for brachytherapy targeted at high dose rate  $^{192}\text{Ir}$  sources. The main goals of this work were to design a phantom that uses thermoluminescent dosimeters (TLDs) to verify the air kerma and the absorbed dose calculations made with the treatment planning system. In order to develop a reliable system, it was necessary to evaluate the physical parameters involved in the calculation formalism, such as the energy dependence of the TLD, the contribution of the scattering from the phantom to the measured air kerma and the doses involved. It was also necessary to develop and evaluate irradiation protocols and to investigate the feasibility of transporting the phantom. This phantom was devised as part of a national quality assurance programme that involves the majority of the radiation therapy centres in Brazil.

## 2. METHOD

### 2.1. Phantom design and construction

The phantom was designed to measure two important dosimetric parameters needed to ensure the desired level of accuracy in the dose delivered to the patient: (a) the source calibration in terms of air kerma calibration 10 cm from the source in air [10]; and (b) the absorbed dose 2 cm deep in water. The latter point coincides with the point A used in gynaecological brachytherapy [11–14]. The phantom was designed for TLD lithium fluoride DTL937 (Philitech) powder encapsulated in cylindrical polyethylene capsules [15, 16].

An important change was made in the shape of the dosimeter holder, making it curved, with circumferences with radii of 10 cm and 2 cm (Fig. 1), in order to avoid unacceptable dose gradient values across the capsule.

### 2.2. Evaluation of the TLDs for air kerma and absorbed dose

A new formalism for the evaluation of the TLD response was used, which was primarily based on TLD calibration in a  $^{60}\text{Co}$  beam, corrected for the

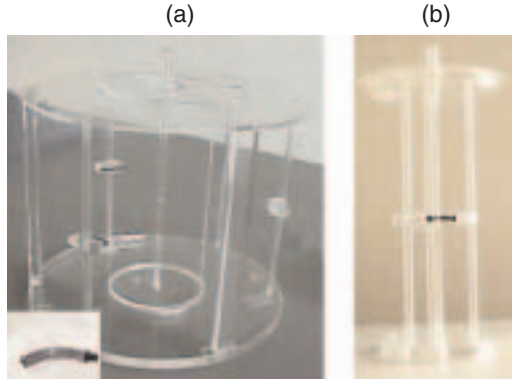


FIG. 1. Design of the phantom composed of two parts: (a) for the in-air measurements 10 cm from the source and (b) for in-water measurements 2 cm from the source. A closer view of the curved dosimeter holder is shown in (a).

energy dependence of the TLD to the  $^{192}\text{Ir}$  spectra, the phantom attenuation and scattering, and the inhomogeneous irradiation of the capsule.

The formalisms used were:

$$(a) \quad \text{Air kerma at 10 cm: } K_{\text{air}}^{192\text{Ir}} = L N_{K,\text{air}}^{60\text{Co}} F_{E,\text{air}}^{192\text{Ir}} F_H F_P$$

$$(b) \quad \text{Water dose at 2 cm: } D_{\text{water}}^{192\text{Ir}} = L N_{K,\text{air}}^{60\text{Co}} F_M F_{E,\text{water}}^{192\text{Ir}} F_H F_P$$

where

$L$	is the thermoluminescence reading corrected for background, dose linearity and fading;
$N_{K,\text{air}}^{60\text{Co}}$	is the calibration coefficient for a $^{60}\text{Co}$ beam in terms of air kerma;
$F_M$	is the absorbed dose ratio (air to water) for the same geometry (see Section 2.3.4);
$F_{E,\text{air}}^{192\text{Ir}}, F_{E,\text{water}}^{192\text{Ir}}$	are the energy dependence correction factors for lithium fluoride DTL937 powder in air and water, relative to $^{60}\text{Co}$ , as described in Section 2.3.3;
$F_H, F_P$	are the dose homogeneity and phantom perturbation factors, as described in Sections 2.3.5 and 2.3.6.

The calibration coefficient for  $^{60}\text{Co}$  and X rays was experimentally obtained in reference beams of the Ionizing Radiation Metrology National

Laboratory in Rio de Janeiro. The correction factors were calculated with Monte Carlo simulations using the PENELOPE code [17] and experimentally validated taking into account the geometric irradiation conditions, the spectral variations in the media and the phantom structure. The measured absorbed dose at 2 cm in water was directly compared with the value calculated by the treatment planning system, and the measured air kerma values at 10 cm were compared with data in clinical use.

### **2.3. Correction factors evaluated by Monte Carlo simulations**

The PENELOPE Monte Carlo code described elsewhere [17] was used to simulate the  $^{192}\text{Ir}$  sources with capsule spectra from the bare sources emission spectrum taken from Duchemin and Coursol [18], and to estimate the magnitude of the different parameters involved.

#### *2.3.1. Source and dosimeter geometry*

The sources used in the microSelectron and VariSource systems were simulated, taking into account the differences in their physical dimensions and encapsulation materials [19].

The dosimeter (Fig. 2) was simulated as if it were a complete ring of lithium fluoride DTL937, and was surrounded by polyethylene rings, which represented the capsule. This approach was taken in order to reduce the uncertainties in the Monte Carlo calculation and the excessively large calculation time; this simplification does not influence significantly the parameters that were evaluated, since they are relative values, the result of comparisons of two or more similar processes. A cylindrical co-ordinate system was chosen, centring the active source volume on the axis of symmetry (the  $z$  axis) and the dosimeter axis parallel to the  $x$ - $y$  plane.

#### *2.3.2. Evaluation of the spectrum changes*

The gamma ray spectrum from the  $^{192}\text{Ir}$  source was evaluated for three different geometric conditions of interest in air and water. Initially, the source encapsulation composition was considered for the calculations in air and water for distances varying between 1 cm and 10 cm. The TLD and capsule were then added to the calculation carried out at a point inside the capsule, at 10 cm in air and at 2 cm in water. Finally, the phantom structure (the acrylic source support and the dosimeter holders) was added and the spectrum inside the TLD capsule was evaluated.

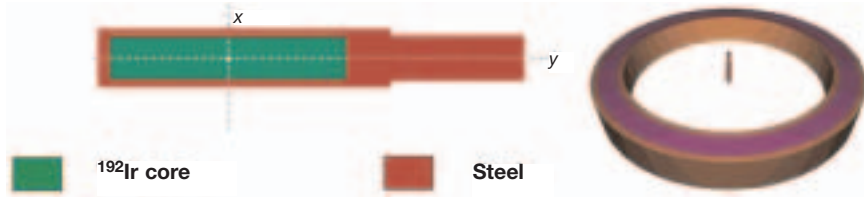


FIG. 2. Source and dosimeter geometries used for the simulations with the PENELOPE code.

### 2.3.3. Energy dependence correction factors, $F_{E,\text{air}}^{192\text{Ir}}$ , $F_{E,\text{water}}^{192\text{Ir}}$

The energy dependence of the DTL937 TLD powder was initially evaluated experimentally using reference beams of X rays with effective energies varying from 35 keV to 125 keV, and with gamma rays from  $^{137}\text{Cs}$  and  $^{60}\text{Co}$ . Since there was no beam available in the energy interval between 125 keV and 662 keV, and considering that most of the  $^{192}\text{Ir}$  spectrum is in this energy region, a Monte Carlo calculation of the TLD material response was carried out. For the sake of simplicity, the simulation considered the dosimeter irradiated by monoenergetic beams with energies varying between 11 keV and 1250 keV, with the responses normalized to the readings obtained for  $^{60}\text{Co}$  (which have an average energy of 1250 keV). In these simulations the distance between the source and the dosimeter was 10 cm in air and 2 cm in water. For each case, the calculation was made using the spectrum previously obtained for the sources used by the microSelectron and VariSource systems.

### 2.3.4. Absorbed dose ratio (air to water) correction factor, $F_M$

The difference between the calculated absorbed dose values in air and water,  $F_M$ , was calculated by simulating the dosimeter in the phantom placed at 2 cm in air and then in water. The ratio of the absorbed dose was obtained for both situations.

### 2.3.5. Dose homogeneity factor, $F_H$

The dose homogeneity correction factor,  $F_H$ , accounts for the inhomogeneous dosimeter irradiation and is evaluated by considering the dose gradient across the depth of the capsules due to its attenuation. For the work described in this paper, the dosimeter geometry was divided into layers to assess the absorbed energy in each one.

### 2.3.6. Phantom perturbation factor, $F_p$

The phantom perturbation factor,  $F_p$ , is the ratio of the dose to the TLD with the phantom in place to that without the phantom, keeping all other parameters constant. The numerical values were calculated with Monte Carlo simulations.

## 3. RESULTS

### 3.1. Correction factors evaluated by Monte Carlo simulations

Figure 3 presents the results of the gamma ray spectrum calculated by Monte Carlo simulations inside the TLD powder inserted in the phantom for the sources used by the microSelectron and VariSource systems. The results presented are normalized to the total fluence at 10 cm in air and 2 cm in water. The correction factors calculated by Monte Carlo methods and used for the air kerma and absorbed dose calculations are presented in Table I. The energy dependence correction factors were obtained by a fourth order polynomial fit of the data adjusted to each different energy region and weighted by their respective spectra in air and water. Since it is difficult to discriminate experimentally the thermoluminescence readings coming from the different parts of the dosimeter, the homogeneity dose correction factor was obtained from the average dose absorbed in each simulated layer.

The total combined uncertainty of 2.8% with  $k = 2.03$  (confidence interval of 95.7%) was obtained following the procedure adopted by the

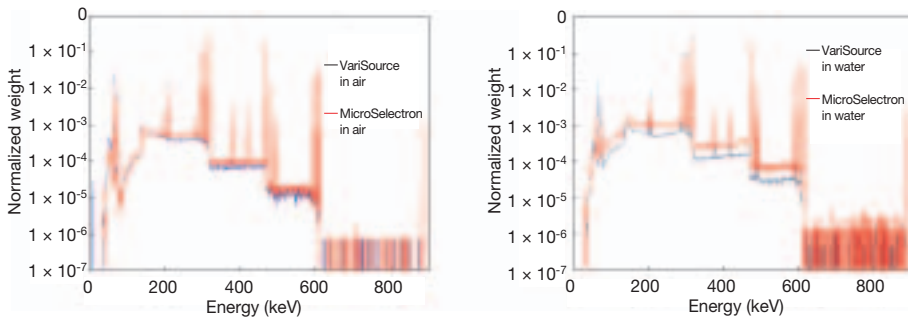


FIG. 3. Comparison between the calculated spectra for microSelectron and VariSource sources in air (a) and in water (b) for the full geometry, which includes the phantom and TLD capsule.



TABLE I. CORRECTION FACTORS USED IN THE FORMALISM PROPOSED FOR THE AIR KERMA AND ABSORBED DOSE CALCULATIONS

Correction factor	Numerical value	
	In air	In water
Air kerma calibration (mGy/ $\mu$ C)	82.6 ( $N_{K,air}^{60Co}$ )	—
Energy dependence (microSelectron source)	1.0068 ( $F_{E,air}^{192Ir}$ )	0.9673 ( $F_{E,water}^{192Ir}$ )
Energy dependence (VariSource)	1.0103 ( $F_{E,air}^{192Ir}$ )	0.9725 ( $F_{E,water}^{192Ir}$ )
Dose homogeneity	1.001 ( $F_H$ )	0.994 ( $F_H$ )
Phantom perturbation	0.995 ( $F_P$ )	1.05 ( $F_P$ )
Absorbed dose ratio (water/air)	—	0.9735 ( $F_M$ )
Overall correction factor	1.003	0.983
	1.006	0.988
Final corrected value (microSelectron source)	82.8 ( $F_{air}$ )	81.2 ( $F_{water}$ )
Final corrected value (VariSource)	83.1 ( $F_{air}$ )	81.6 ( $F_{water}$ )

European Society for Therapeutic Radiology and Oncology (ESTRO) EQUAL programme [20].

#### 4. CONCLUSIONS

A new dedicated phantom was constructed for the quality control of high dose rate  $^{192}Ir$  brachytherapy sources using TLD powder contained in cylindrical capsules. This phantom is very simple to use, requiring only one source stop, and it allows the simultaneous irradiation of three TLD capsules, which yield 15 readings per irradiation under the same geometry. This procedure is bound to have a lower uncertainty than the technique of moving the source to three different positions and irradiating one capsule each time, as used in the ESTRO programme, since the source positioning uncertainty and the transit dose effect are minimized.

The lithium fluoride DTL937 powder used shows an energy dependence with the different  $^{192}Ir$  sources and spectra changes with the irradiation geometries, distances, depths and media. For this reason it is necessary to calculate a correction factor for each experimental geometry used. The homogeneity,  $F_H$ , and phantom,  $F_P$ , correction factors for the microSelectron source and energy

factors in air and water for the microSelectron and VariSource sources have been evaluated. The small differences found between the spectra generated by the microSelectron and VariSource sources allow the use of the same dose homogeneity,  $F_H$ , and phantom,  $F_P$ , correction factors for both sources, although the difference in the energy dependence factor,  $F_E$ , is more significant, owing to the TLD being sensitive to spectral variations.

An irradiation protocol was devised and tested and is sent by mail with the phantom to the participating institutions of the dosimetry quality assurance programme in Brazil (Programa de Qualidade em Dosimetria). This phantom has been shown to be useful for verifying the source calibration in air and the consistency of the treatment planning system for calculating the absorbed dose to be delivered to the patient.

### ACKNOWLEDGEMENTS

The authors wish to thank the support provided by the IAEA, F. Gutt, the co-ordinator of the Regional Masters Degree programme in Venezuela, and ESTRO.

### REFERENCES

- [1] DE ALMEIDA, C.E., et al., Intercomparison of calibration procedures for  $^{192}\text{Ir}$  HDR sources in Brazil, *Phys. Med. Biol.* **44** (1999) N31–N38.
- [2] EZZEL, G., “Evaluation of calibration techniques for the microSelectron”, *Brachytherapy 2* (Proc. Conf. The Hague, 1988) (MOULD, R.F., Ed.), Nucletron International, Leersum, Netherlands (1989) 61–69.
- [3] GOETSCH, S.J., ATTIX, F.H., PEARSON, D.W., THOMADSEN, B.R., Calibration of  $^{192}\text{Ir}$  high-dose-rate afterloading systems, *Med. Phys.* **18** (1991) 462–427.
- [4] MARÉCHAL, M.H., DE ALMEIDA, C.E., SIBATA, C.H., “Calibration of  $^{192}\text{Ir}$  high dose rate brachytherapy sources”, *Radiation Dose in Radiotherapy from Prescription to Delivery*, IAEA-TECDOC-896, IAEA, Vienna (1996) 203–206.
- [5] INTERNATIONAL ATOMIC ENERGY AGENCY, Calibration of Brachytherapy Sources, IAEA-TECDOC-1079, IAEA, Vienna (1999).
- [6] INTERNATIONAL ATOMIC ENERGY AGENCY, Calibration of Photon and Beta Ray Sources Used in Brachytherapy, IAEA-TECDOC-1274, IAEA, Vienna (2002).
- [7] INTERNATIONAL ATOMIC ENERGY AGENCY, Aspectos Físicos de la Garantía de Calidad en Radioterapia: Protocolo de Control de Calidad, IAEA-TECDOC-1151, IAEA, Vienna (2000).

- [8] AMERICAN ASSOCIATION OF PHYSICISTS IN MEDICINE, Code of practice for brachytherapy physics: Report of AAPM Radiation Therapy Committee Task Group No. 56, *Med. Phys.* **24** (1997) 1557–1598.
- [9] INSTITUTO NACIONAL DE CÂNCER, MINISTÉRIO DA SAÚDE DO BRASIL, Programa de Qualidade em Radioterapia. Recomendações para Calibração de Fontes de  $^{192}\text{Ir}$  de Alta Taxa de Dose Usadas em Braquiterapia, Ministério de Saúde do Brasil (2000).
- [10] DEWERD, L.A., THOMADSEN, B.R., “Source strength and calibration of HDR/PDR sources”, *Brachytherapy Physics*, Medical Physics Publishing, Madison, WI (1995).
- [11] AMERICAN ASSOCIATION OF PHYSICISTS IN MEDICINE, Specification of Brachytherapy Source Strength: Report of AAPM Task Group 32, AAPM Rep. 21, Institute of Physics, New York (1987).
- [12] INTERNATIONAL COMMISSION ON RADIATION UNITS AND MEASUREMENTS, Dose Volume Specification for Reporting Intracavitary Therapy in Gynecology, Rep. 38, ICRU, Bethesda, MD (1985).
- [13] HANSON, W.F., “Brachytherapy source strength: Quantities, units and standards”, *Brachytherapy Physics*, Medical Physics Publishing, Madison, WI (1995).
- [14] EIFEL, P.J., “Clinical intracavitary systems for treatment of gynecologic malignancies”, *Brachytherapy Physics*, Medical Physics Publishing, Madison, WI (1995).
- [15] FERREIRA, I.H., DUTREIX, A., BRIDIER, A., CHAVAUDRA, J., SVENSSON, H., The ESTRO-QUALity assurance network (EQUAL), *Radiother. Oncol.* **55** (2000) 273–284.
- [16] IZEWSKA, J., ANDREO, P., The IAEA/WHO postal programme for radiotherapy hospitals, *Radiother. Oncol.* **54** (2000) 65–72.
- [17] BARO, J., SEMP AU, J., FERNANDEZ-VAREA, J.M., SALVAT, F., PENELOPE: An algorithm for Monte Carlo simulation of the penetration and energy loss of electrons and positrons in matter, *Nucl. Instrum. Methods B* **100** (1995) 31–46.
- [18] DUCHEMIN, B., COUR SOL, N., Reevaluation de l' $^{192}\text{Ir}$ , Technical Note LPRI/93/018, DAMRI, Commissariat à l'énergie atomique, Saclay (1993).
- [19] BORG, J., ROGERS, D., Spectra and air-kerma strength for encapsulated  $^{192}\text{Ir}$  sources, *Med. Phys.* **26** (1999) 2441–2444.
- [20] MARRE, D., et al., Energy correction factors of LiF powder TLDs irradiated in high energy electron beams and applied to mailed dosimetry for quality assurance networks, *Phys. Med. Biol.* **45** (2000) 3657–3674.

**BLANK**

# **NEW APPROACH FOR STANDARDIZING ABSORBED DOSE FROM BETA RADIOACTIVE WIRES AND SEEDS USED FOR INTRAVASCULAR BRACHYTHERAPY**

S. PSZONA, B. KOCIK, K. WINCEL, B. ZAREBA

Soltan Institute for Nuclear Studies,

Swierk-Otwock

E-mail: pszona@ipj.gov.pl

W. BULSKI

Oncology Institute, Warsaw

Poland

## **Abstract**

A new method for standardizing beta particle emitting radioactive sources (in the form of wires or seeds) used in the intravascular brachytherapy of coronary disease has been devised and investigated. The method is based on the use of a new type of ionization chamber, called the ring ionization chamber (RIC). The RIC has a design that encompasses both a phantom and an ionization chamber. It has a cylindrical shape, and a catheter housing the source (a wire or seeds) passes through the chamber along its axis. Owing to its similarity to a cylindrical ionization chamber, the dosimetric protocol given in Technical Reports Series No. 277 can be applied for determining the absorbed dose to air chamber (and to water) calibration factors,  $N_D$ , as well as the absorbed dose to water calibration factor,  $N_{D,w}$ . Owing to this similarity, the overall uncertainty in the standardization of absorbed dose for beta radioactive sources used in intravascular brachytherapy could be substantially reduced compared with that presently achieved. The RIC can be used in a new code of practice for dose standardization and quality assurance in intravascular brachytherapy.

## **1. INTRODUCTION**

Intravascular radiotherapy (IVR) is accepted as an effective treatment that reduces the incidence of stenosis following balloon angioplasty. As evidenced from many randomized clinical trials, the rates of reduction of restenosis are from 30% to 60%. It is expected that the efficacy of IVR could be increased by improving the precision of dose delivery to the target tissues.

The majority of IVR catheter based radioactive source systems are equipped with beta emitters:  $^{90}\text{Sr}/^{90}\text{Y}$  and  $^{32}\text{P}$  in the form of thin wires or seeds. Dosimetry at short distances from these radioactive sources is a difficult task, which needs new developments both in dose standardization and quality assurance methods. The requirements for the dosimetric characterization of the radioactive sources used for IVR are summarized in Ref. [1]. One of the basic requirements is that the source strength of a catheter based system with beta emitters should be expressed in terms of dose rate in water at a reference distance of 2 mm. Several approaches and specially shaped detectors, such as scintillators, thermoluminescent dosimeters and GafChromic films, have been applied for these purposes. A new type of ionization chamber, called the ring ionization chamber (RIC), designed especially for catheter based radioactive sources, has been devised and is described in this paper. Based on this new detector a new method for standardizing absorbed dose measurement from beta particle sources used in intravascular brachytherapy is proposed. A full description of this method as well as of its practical application to the dosimetry and quality assurance of  $^{32}\text{P}$  radiotherapy sources is presented.

## 2. MATERIALS AND METHODS

### 2.1. RIC

The RIC has a design that encompasses both a phantom and an ionization chamber. It has a cylindrical shape, and a catheter housing the source (a wire or seeds) passes through the chamber along its axis. The cross-section of a RIC is shown in Fig. 1. A model of a RIC, with an air vented sensitive volume in the form of a 10 mm long wall cylinder, with a distance of 0.4 mm between the electrodes, has been tested. The inner diameter of sensitive volume is 3.8 mm and the hole in the inner electrode for a catheter based radioactive source is 1 mm in diameter. The external chamber dimensions are 35 mm in length and 19 mm in diameter. The model tested was made of polymethylmethacrylate (PMMA), with the conducting parts made by graphite coating. In the next design a water equivalent material will be used. The inner electrode of the RIC is adjusted in such a way as to obtain the equivalent depth in water close to 2 mm, which is the recommended reference point.

The RIC has the following characteristics:

- (a) The phantom and ionization chamber is one body made of PMMA;
- (b) It is designed specifically for wire and seed train sources;

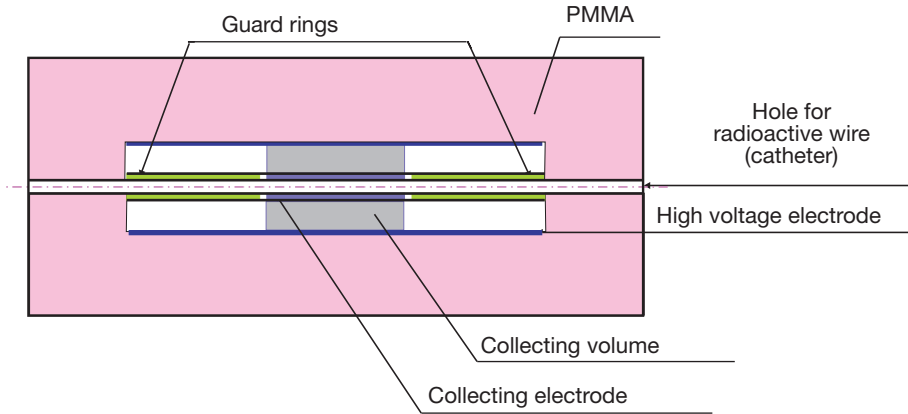


FIG. 1. Cross-section (not to scale) of a RIC.

- (c) The collecting electrode is in the form of a thin conducting layer 10 mm wide;
- (d) Along the axis of the RIC there is a hole for a source catheter;
- (e) The distance between the electrodes is 0.4 mm;
- (f) The collection volume is 0.0527 cm<sup>3</sup>;
- (g) Guard rings, 5 mm wide, are placed symmetrically to the collecting electrode;
- (h) It has an air vented volume.

## 2.2. Calibration

Owing to the similarity of a RIC to a cylindrical ionization chamber, the dosimetric protocol given in Technical Reports Series No. 277 (TRS 277) [2] has been applied for determining the absorbed dose to air chamber calibration factor,  $N_D$ . The  $N_D$  factor for the RIC model described in Section 2.1 has been derived from calibration in a <sup>60</sup>Co beam at a secondary standards dosimetry laboratory (traceable to a national standard). The absorbed dose to water calibration factor,  $N_{D,w}$ , values for <sup>60</sup>Co and <sup>90</sup>Y (which are assumed also to be valid for <sup>32</sup>P) were derived from  $N_D$  and are shown in Table I, together with the relevant interaction coefficients. As seen in Table I, the values of  $N_{D,w}$  for <sup>60</sup>Co and <sup>90</sup>Y sources differ by only 1%. This means that the absorbed dose to water calibration factors for beta radioactive sources actually used for intravascular

TABLE I. VALUES OF APPLIED INTERACTION COEFFICIENTS (SYMBOLS AS IN TRS 277)

	$s_{\text{PMMA,air}}$	$s_{\text{water,air}}$	$N_{D,w}$ (cGy/nC)
$^{60}\text{Co}$ beam	1.102	1.133	54.35
$^{90}\text{Y}$ ( $^{32}\text{P}$ ) source	1.098	1.129	54.16

brachytherapy can be obtained with a very high accuracy, close to those for cylindrical chambers for  $^{60}\text{Co}$ . An absorbed dose to PMMA calibration factor,  $N_{D,\text{PMMA}}$ , can also be derived with a high precision from  $N_D$ .

2.3. Effective surface of measurements

The sensitive air gap of the RIC model presently being investigated is not an infinitesimal one, therefore it perturbs the depth dose distribution. Additionally, because of the large dose rate gradient across this gap, the effective depth of measurements in PMMA has to be estimated. The Monte Carlo code MCNP4C was used to investigate these effects, particularly for an air gap of

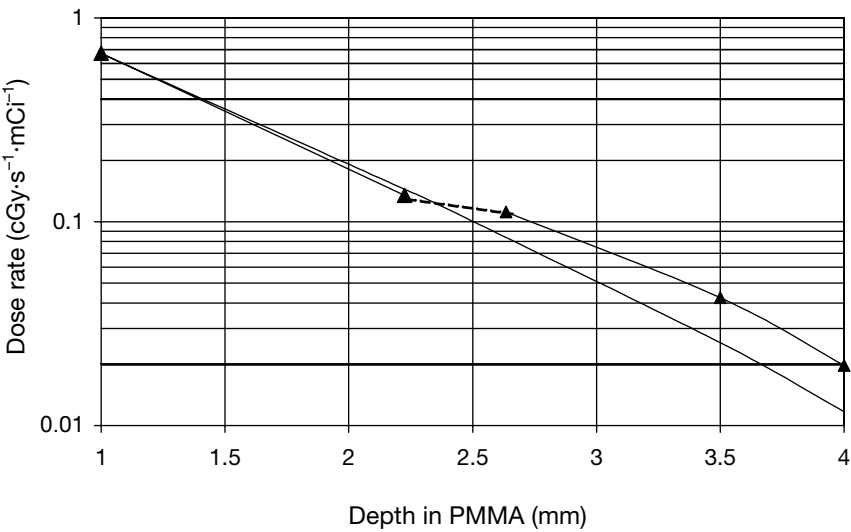


FIG. 2. Calculated radial dose rate distribution in PMMA. Filled triangles: 0.4 mm air gap; dashed line: exponential fit marking radial dose rate across the air gap; full line: without an air gap.



TABLE II. SUMMARY OF THE DOSE RATE COMPARISON AT 2 mm IN WATER

DSF	$r_{\text{ef}}$ (mm)	Experiment (cGy/s)	Certificate (cGy/s)	Experiment/ certificate
1.192	2.009	47.8	45.52	1.05

0.4 mm at around 2 mm deep in PMMA. A model of a  $^{32}\text{P}$  source wire, as described for the Guidant system, was applied in these calculations [3]. The results in the forms of dose rate per unit activity as a function of depth in PMMA are shown in Fig. 2. Two curves can be seen, namely with and without the 0.4 mm air gap. The effective depth (cylindrical surface),  $r_{\text{ef}}$ , of dose measurements has been derived based on this figure and is shown in Table II. The effective depth of measurements is shifted 0.109 mm from the edge towards the cavity; the effective depth in PMMA is therefore equal to 2.009 mm.

#### 2.4. Depth scaling factor

The depth scaling factor (for depth dose) of PMMA to water, DSF, was calculated [3] using the Monte Carlo code MNCP4C. The results are shown in Fig. 3 in the form of the dependence of depth in water,  $r_w$ , as a function of depth in PMMA,  $r_{\text{PMMA}}$ , for equal values of absorbed dose in these two media. The calculated value of the DSF was 1.1192, valid for a depth in PMMA of up to

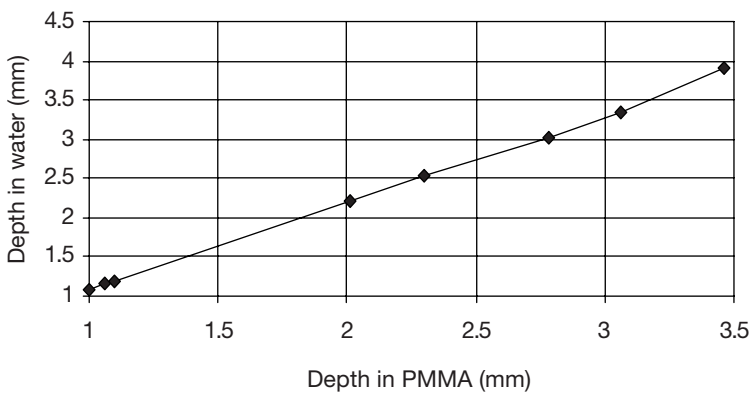


FIG. 3. Depths in water and PMMA for the same values of absorbed dose for a  $^{32}\text{P}$  brachytherapy source.

3.5 mm. The following relation holds as the best fit in the range of  $r_{\text{PMMA}}$  up to 3.5 mm:

$$r_w = 1.1192 r_{\text{PMMA}} \quad (1)$$

## 2.5. Absorbed dose to water at the reference point

The standardization procedure for the dosimetric characterization of a radioactive source requires that the absorbed dose rate to water at a depth of 2 mm,  $d_w(2 \text{ mm})$ , has to be reported. The following chain of steps was undertaken to determine this quantity based on measurements with the RIC. The ionization current,  $I$  (in nA), was measured (pressure, temperature, saturation and polarization corrected) and the following relations were used:

$$d_{\text{PMMA}}(r_{\text{ef}}) = IN_{D,\text{PMMA}} \quad (2)$$

$$d_w(1.1192r_{\text{ef}}) = d_{\text{PMMA}}(r_{\text{ef}}) \quad (3)$$

$$d_w(2 \text{ mm}) = d_w(1.1192r_{\text{ef}}) k \quad (4)$$

where  $k$  is the dose correction factor taken from Monte Carlo calculation ((dose rate at 2 mm in water)/(dose rate at  $1.1192r_{\text{ef}}$  in water)).

## 3. RESULTS AND DISCUSSION

### 3.1. Comparison with a certified $^{32}\text{P}$ radioactive wire

The absorbed dose rate at a depth of 2 mm in water from a  $^{32}\text{P}$  source (Guidant certified (Certificate for Sealed Radioactive Source, model number GDT-P32-1, serial number 0202/5005 (2002)), traceable to the United States National Institute of Standards and Technology standard) [3], was estimated based on the measurements by methods presented in this paper and compared with the certified value. The result is 5% higher than that based on the Guidant certificate. The Guidant certificate estimates the uncertainty of the absorbed dose rate to be  $\pm 16\%$ . The uncertainty of measuring the absorbed dose with a properly designed RIC (water equivalent material) could be close to that obtained for parallel-plate chambers (i.e.  $\pm 4\%$ ). The uncertainty of dose measurements at the reference point in water with the present model of the RIC is 8–12%. The largest contribution to the uncertainty is due to some remaining air space between the source and the cylindrical hole housing the

catheter. This may partly explain the higher value of the dose obtained from the measurements.

#### 4. CONCLUDING REMARKS

The proposed method opens a new way for improving the existing codes of practice for the standardization of absorbed dose and quality procedures for radioactive sources used in intravascular brachytherapy.

One of the advantages of the new method over the current standardization methods is the very good geometrical reproducibility of the source relative to the detector, which in turn gives the excellent reproducibility of the dose readings.

The described method is equally applicable to the standardization of absorbed dose from  $^{192}\text{Ir}$  sources used for brachytherapy.

#### REFERENCES

- [1] AMERICAN ASSOCIATION OF PHYSICISTS IN MEDICINE, Intravascular brachytherapy physics: Report of the AAPM Radiation Committee Task Group No. 60, Med. Phys. **26** (1999) 119–152.
- [2] INTERNATIONAL ATOMIC ENERGY AGENCY, Absorbed Dose Determination in Photon and Electron Beams, Technical Reports Series No. 277, IAEA, Vienna (1987).
- [3] WINCEL, K., ZAREBA, B., Monte Carlo calculation of absorbed dose for P-32 brachytherapy wire source, Pol. J. Med. Phys. Eng. (in press).

**BLANK**

## COMPARISON OF CALIBRATION TECHNIQUES FOR $^{192}\text{Ir}$ HIGH DOSE RATE BRACHYTHERAPY SOURCES

C. TANNANONTA, T. LAYANGKUL, C. ORKONGKIAT

Department of Radiology, Ramathibodi Hospital,

Bangkok, Thailand

E-mail: ractn@mahidol.ac.th

### Abstract

Iridium-192 high dose rate sources need to be calibrated to verify the value certified by the manufacturer before their clinical use. Three calibration techniques, in air, in a cylindrical phantom and in a well type chamber, were performed to calibrate eight sources of  $^{192}\text{Ir}$  between March 1999 and January 2002. It was found that the kerma rates obtained from all calibration systems were less than the manufacturer's by a maximum of 2.35%. The mean discrepancies were  $-1.67\% \pm 0.56$  in the range of  $-0.96\%$  to  $-2.35\%$  in air,  $-1.12\% \pm 0.53$  in the range of  $-0.40\%$  to  $-2.19\%$  in a phantom and  $-1.25\% \pm 0.37$  in the range of  $-0.73\%$  to  $1.36\%$  for a well type chamber. The results of all calibration systems agreed to within 1.5%. It is not only more reproducible and simpler to set up, but also less time consuming to use well type chambers for source calibration compared with the other two techniques. For an institute in which only a Farmer chamber is available, the measurements in a phantom are easier and quicker to set up than using in-air measurement techniques.

### 1. INTRODUCTION

High dose rate (HDR) brachytherapy using an  $^{192}\text{Ir}$  source with an activity of about 10 Ci ( $3.7 \times 10^{11}$  Bq) is a common treatment modality. Independent verification of the source strength provided by the manufacturer is needed before starting clinical use [1–3]. The reference air kerma rate (the kerma rate, in air, at a reference distance of 1 m, corrected for air attenuation and scattering, expressed in mGy/h at 1 m or  $\mu\text{Gy/h}$  at 1 m) is the recommended quantity for the specification of gamma ray brachytherapy sources [4].

The protocols for the calibration of sources with well type ionization chambers, and in air and in a phantom using ionization chambers, are well established [2, 3]. For in-air measurements with Farmer type chambers, a source to chamber distance (SCD) of between 10 cm and 40 cm is recommended by the IAEA [3]. To minimize scatter from the holder, a calibration jig of low density plastic is used [2, 3, 5, 6]. Source calibration in a solid phantom (cylindrical or plate) has been

reported by many authors [5, 7, 8], and is preferred because of its improved reproducibility.

The main purpose of the experiments reported in this paper was to compare the calibration of HDR  $^{192}\text{Ir}$  brachytherapy sources using the three systems available at the Department of Radiology, Ramathibodi Hospital, Bangkok, in air, in a cylindrical phantom and using a well type chamber, and to compare the results obtained with those given on the source certificate provided by the manufacturer. A difference from the manufacturer's certificate value within  $\pm 5\%$  is required by the Ramathibodi Hospital.

## 2. MATERIALS AND METHODS

A  $0.6\text{ cm}^3$  PTW 30001 Farmer chamber was used for the calibration of HDR  $^{192}\text{Ir}$  brachytherapy sources in air and in a cylindrical phantom. The well type chamber used in this study was a Nucletron Source Dosimetry System 077.094. A PTW Unidos 10002 electrometer was used for all measurements.

### 2.1. Interpolative calibration of a cavity chamber

The Farmer chamber system is calibrated in terms of exposure,  $N_x$ , at the secondary standards dosimetry laboratory of Thailand for 250 kVp X rays (half-value layer of 3.01 mm Cu, 137 keV (effective)) and  $^{60}\text{Co}$  energy (1250 keV), with the buildup cap used for both energies.

The exposure calibration factor for  $^{192}\text{Ir}$  (average energy of 380 keV [9, 10]) of  $5.460 \times 10^9$  R/C was determined by interpolation between these two energies. A  $^{137}\text{Cs}$  gamma beam, as used by other investigators [11, 12], is not available in Thailand. The air kerma calibration factor,  $N_K$ , was calculated by [13]:

$$N_K = N_x(W/e)(1/(1 - g)) \quad (1)$$

where

$W/e$  is the mean energy expended in air per ion pair formed and per electron charge (= 33.97 J/C for dry air) [13].

$g$  is the fraction of the energy of secondary charge particles that is lost to bremsstrahlung. The value of 0.001 was used in this study [14].

The  $N_K$  value of  $4.790 \times 10^7$  Gy/C for  $^{192}\text{Ir}$ , calculated from Eq. (1), was used for source measurements in air and in the phantom.

## 2.2. Calibration of $^{192}\text{Ir}$ sources

Between March 1999 and January 2002 eight sources of  $^{192}\text{Ir}$  for the micro-Selectron HDR unit were calibrated using the three systems as described above. The outer source dimensions are 0.9 mm in diameter and 4.5 mm in length, and the active source dimensions are 0.6 mm in diameter and 3.5 mm in length.

Each measurement was made with the source position at the maximum sensitivity for each technique. To investigate the influence of wall scattering on calibration for each technique, the measurements were made at various distances of the chamber centre to the wall, with the distance above the floor fixed at 1000 mm.

An externally triggered electrometer was used for all systems, and the charge was collected during an interval after the source had stopped moving [13], to exclude transit effects. The interval time of 600 s with +400 V was used for the in-air and in-phantom measurements, and 180 s with +300 V for the well type chamber. Owing to the long measurement time, the leakage current for each calibration was also checked, and it was found to be very much less than 0.1% of the ionization reading. At least five readings in nC and nA were performed in each calibration for the Farmer type and well type chambers, respectively. The average value was then corrected for recombination losses [15] and for the ambient temperature and pressure [13].

### 2.2.1. Calibration in air

The Nucletron source calibration jig was used to hold the ionization chamber and source during the calibration in air. It has two metal tubes (430 mm long) with thin polymethylmethacrylate (PMMA) rods 50 mm long in the middle for holding the source at a distance of 100 mm from the centre of the chamber. The measurements were made using the Farmer chamber with a buildup cap.

The reference air kerma rate,  $K_R$ , at 1 m was determined by using [3]:

$$K_R = N_K (M_u/t) k_{\text{air}} k_{\text{scatt}} k_n (d/d_{\text{ref}})^2 \quad (2)$$

where

$M_u$  is the measured charge collected during time  $t$  and corrected for ambient temperature and pressure, and recombination.

$k_{\text{air}}$  is the correction for attenuation in air of the primary photons (the value of 1.001 for the 100 mm source to chamber distance from table XI of Ref. [3] was used in this study).

- $k_{\text{scatt}}$  is the correction for scattered radiation from the wall, floor, measurement set-up, air, etc. (since other authors [6, 11] report the values of 0.9987 and 0.997, which are very close to 1.0, and the investigational method is very complex, the value of 1.0 was used in this study).
- $k_n$  is the non-uniformity correction (the value of 1.0111 was calculated using eq. (14) in Ref. [3]).
- $d$  is the measurement distance (the value of 100 mm was used in this study).
- $d_{\text{ref}}$  is the reference distance of 1 m.

### 2.2.2. Calibration in a phantom

A PTW 9193 PMMA cylindrical phantom with a diameter of 200 mm and a height of 120 mm was used. The phantom was placed on a Cullmann tripod at a distance of about 1100 mm above the floor. The distance between the source and the reference point of the detector was 8 cm. The reference air kerma rate,  $K_R$ , at a distance of 1 m was determined using [16]:

$$K_R = N_K(M_u/t)k_{a \rightarrow p}k_{zp}(d/d_{\text{ref}})^2 \quad (3)$$

where  $(M_u/t)$  and  $(d/d_{\text{ref}})^2$  are the same as in Eq. (2) and

- $k_{a \rightarrow p}$  is the perturbation factor for the transition from air to acrylic glass for a cylindrical compact chamber with PMMA walls and inner graphite, for which the approximation value of 1.0 was used in this study [16].
- $k_{zp}$  is the geometry factor accounting for the presence of the absorbing and scattering cylindrical phantom instead of air; the value of 1.187 reported by Krieger [14] was used in this study.

### 2.2.3. Calibration by a well type chamber

The reference air kerma rate,  $K_R$ , for the well type chamber was determined by [3]:

$$K_R = N_K(M_u/t) \quad (4)$$

where

- $N_K$  is the reference air kerma rate calibration factor for the well type chamber; the value of  $9.251 \times 10^7 \text{ cGy} \cdot \text{m}^2 \cdot \text{h}^{-1} \cdot \text{A}^{-1}$ , from the manufacturer's calibration certificate, was used. (At the time of the study, a well type chamber for a comparison measurement of the  $^{192}\text{Ir}$  source was not available in Thailand.)
- $(M_u/t)$  is the same as in Eqs (2) and (3).



### 3. RESULTS

The influence of the lateral wall scattering on the measurements for each calibration system is shown in Fig. 1. A minimum distance of the chamber centre to the lateral wall of 500 mm for in-air calibrations, 700 mm for the cylindrical phantom and 300 mm for the well type chamber measurements, was needed to keep the scattering contribution below 0.1% of the reading for the 1000 mm distance.

Table I shows the comparison of the air kerma rate for all calibration systems with the manufacture's values for eight  $^{192}\text{Ir}$  sources. The value of each calibration technique was less, with the maximum difference of 2.35% for an in-air calibration. (The  $^{192}\text{Ir}$  half-life of 74.02 days, as specified by the planning system, was used for decay calculations.) The mean discrepancies were  $-1.67\% \pm 0.56$  in the range of  $-0.96\%$  to  $-2.35\%$  in air,  $-1.12\% \pm 0.53$  in the range of  $-0.40\%$  to  $-2.19\%$  in the phantom and  $-1.25\% \pm 0.37$  in the range of  $-0.73\%$  to  $-1.36\%$  for the well type chamber. The results of all calibration systems were in agreement to within 1.5%.

### 4. DISCUSSION AND CONCLUSIONS

All the calibration techniques used in the study show very comparable results, with a maximum discrepancy of 1.5%, and are in agreement with the values reported by the manufacturer, with a maximum difference of  $-2.35\%$ . For the measurements in the phantom, the reading was not corrected for the attenuation of the stainless steel applicator used in the calibration. Baltas et al.

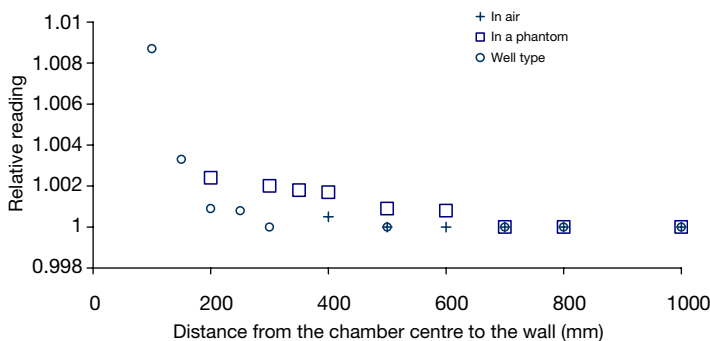


FIG. 1. Influence of wall scattering on the measurements for the three systems used in the study.

TABLE I. PERCENTAGE DIFFERENCE OF THE AIR KERMA RATE OF EIGHT  $^{192}\text{Ir}$  SOURCES MEASURED BY THE THREE TECHNIQUES COMPARED WITH THE MANUFACTURER'S VALUES

Calibration technique	Source number								Mean	SD <sup>b</sup>
	1	2	3	4	5	6	7	8		
In air	-1.98	-1.80	-2.35 <sup>a</sup>	-0.96	-2.31	-1.54	-1.50	-0.88	-1.67	0.56
In a phantom	-2.19 <sup>a</sup>	-1.40	-1.08	-1.12	-1.43	-1.12	-0.84	-0.79	-1.12	0.53
Well type chamber	-0.73	-1.06	-1.51	-1.27	-1.36	-1.51	-1.78 <sup>a</sup>	-0.79	-1.25	0.37

<sup>a</sup> Maximum percentage difference of each system.

<sup>b</sup> SD: standard deviation.

[8] report a 1.7% correction for the wall thickness of 0.56 mm for the stainless steel applicator. If the correction for the attenuation of the calibration applicator is used for the measurements made in this study, the results should be closer to the manufacturer's values. Venselaar et al. [6] reported the higher maximum difference of -6.8% from the certificate for in-air measurements, which may be due to the no correction for non-uniformity (non-collimated geometry) recommended by the IAEA [3].

From the study of the influence of wall scattering on the measurements (Fig. 1), the well type chamber is less affected by scattering from the wall than the other two systems.

The data from this work illustrate that all the systems are appropriate for the routine calibration of HDR brachytherapy sources, but the authors prefer to use the well type chamber because of its higher reproducibility, simpler set-up and reduced measurement times. For institutes in which only a Farmer chamber is available, measurement in a phantom is easier and quicker to set up and also more reproducible than in the in-air geometry.

## REFERENCES

- [1] KUTCHER, G.J., et al., Comprehensive QA for radiation oncology: Report of AAPM Radiation Therapy Committee Task Group 40, Med. Phys. **21** (1994) 581-618.
- [2] AMERICAN ASSOCIATION OF PHYSICISTS IN MEDICINE, Remote Afterloading Technology: A Report of AAPM Task Group No. 41, Rep. 41, AAPM, New York (1993).
- [3] INTERNATIONAL ATOMIC ENERGY AGENCY, Calibration of Brachytherapy Sources, IAEA-TECDOC-1079, IAEA, Vienna (1999).

- [4] INTERNATIONAL COMMISSION ON RADIATION UNITS AND MEASUREMENTS, Dose and Volume Specification for Reporting Interstitial Therapy, Rep. 58, ICRU, Bethesda, MD (1997).
- [5] EZZEL, G., "Evaluation of calibration techniques for the microSelectron", Brachytherapy 2 (Proc. Conf. The Hague, 1988) (MOULD, R.F., Ed.), Nucletron International, Leersum, Netherlands (1989) 61–69.
- [6] VENSELAAR, J.L.M., BROUWER, W.F.M., VAN STRAATEN, B.H.M., AALBERS, A.H.L., Intercomparison of calibration procedures for Ir-192 HDR sources in the Netherlands and Belgium, Radiother. Oncol. **30** (1994) 155–161.
- [7] BALTAS, D., "Quality assurance in brachytherapy with special reference to the microSelectron-HDR", Activity: Int. Selectron Brachyther. J., Special Rep. No. 2 (1993) 2–11.
- [8] BALTAS, D., et al., Comparison of calibration procedures for  $^{192}\text{Ir}$  high-dose rate brachytherapy, Int. J. Radiat. Oncol. Biol. Phys. **43** (1999) 653–661.
- [9] KHAN, F.H., "Brachytherapy", The Physics of Radiation Therapy, 2nd edn, Williams & Wilkins, London (1994) 418–473.
- [10] HENDEE, W.R., IBBOTT, G.F., "Sources for implant therapy", Radiation Therapy Physics, 2nd edn, Mosby, New York (1996) 365–384.
- [11] NAIR, M.T.K., CHENG, M.C., HDR calibration methods and discrepancies, Int. J. Radiat. Oncol. Biol. Phys. **38** (1997) 207–211.
- [12] GOETSCH, S.J., ATTIX, F.H., PEARSON, D.W., THOMADSEN, B.R., Calibration of  $^{192}\text{Ir}$  high-dose-rate afterloading systems, Med. Phys. **18** (1991) 462–467.
- [13] INTERNATIONAL ATOMIC ENERGY AGENCY, Absorbed Dose Determination in Photon and Electron Beams, Technical Reports Series No. 277, IAEA, Vienna (1987).
- [14] KRIEGER, H., Messung der Kenndosisleistung punkt-und linien-förmiger HDR-192-Iridium Afterloadingstrahler mit einem PMMA-Zylinderphantom, Z. Med. Phys. **1** (1991) 38–41.
- [15] ATTIX, F.H., Determination of  $A_{\text{ion}}$  and  $P_{\text{ion}}$  in the new AAPM radiotherapy dosimetry protocol, Med. Phys. **11** (1984) 714–716.
- [16] PTW, "For measurements of the nominal air kerma rate of 192-iridium-HDR afterloading sources with a PMMA cylindrical phantom", Afterloading Calibration Phantom Type 9193 Instruction Manual, D402.131.0/1, PTW, Freiburg.

**BLANK**

## POSTERS ON RADIOTHERAPY DOSIMETRY AUDITS

(Session 12b)

**Chair**

**D.I. THWAITES**

European Society for Therapeutic Radiology and Oncology and  
International Society for Radiation Oncology

**Co-Chair**

**J. IZEWSKA**

IAEA

**Rapporteur**

**R. HUNTLEY**

Australia

**BLANK**

# **IAEA SUPPORTED NATIONAL THERMOLUMINESCENCE DOSIMETRY AUDIT NETWORKS FOR RADIOTHERAPY DOSIMETRY: SUMMARY OF THE POSTERS PRESENTED IN SESSION 12b**

J. IZEWSKA

Division of Human Health, International Atomic Energy Agency,  
Vienna

E-mail: j.izewska@iaea.org

D.I. THWAITES

Western General Hospital, University of Edinburgh,  
Edinburgh, United Kingdom

## **Abstract**

The IAEA has supported its Member States over many years by providing thermoluminescence dosimetry (TLD) based quality assurance audits for radiotherapy dosimetry. Over recent years it has extended this role by encouraging, supporting and assisting the development of national audit programmes, building on the IAEA's experience of operating a TLD system. Whenever possible, the IAEA establishes links between the national programmes and the IAEA Dosimetry Laboratory. The IAEA disseminates its standardized TLD methodology and provides technical backup to national TLD networks, ensuring at the same time traceability to primary dosimetry standards. Several countries have established TLD programmes to audit radiotherapy beams in hospitals with assistance from the IAEA, and the paper presents an overview of the activities in Algeria, Argentina, Australia, Brazil, China, Colombia, Cuba, India, the Republic of Korea, the Philippines and Poland.

## **1. INTRODUCTION**

The most basic level of a radiotherapy dosimetry audit is a beam output check. The most cost effective method of carrying out an external dosimetry audit for large numbers of centres and for large geographical areas is with the use of mailed thermoluminescent dosimeters. In 1969 the IAEA, together with the World Health Organization (WHO), implemented a thermoluminescence dosimetry (TLD) postal dose assurance service to verify the calibration of radiotherapy beams in developing countries [1, 2]. Over the subsequent 33 years the IAEA/WHO TLD audit service has verified the calibration of

more than 4500 radiotherapy beams in approximately 1200 hospitals worldwide. At present the IAEA Dosimetry Laboratory processes thermoluminescent dosimeters for about 400 hospital beam audits per year, and with its limited capacity can only partially satisfy the current demand. To make TLD audits available to the largest possible number of hospitals in developing countries, the IAEA has encouraged and supported the development and operation of national activities for quality assurance in radiotherapy.

An IAEA co-ordinated research project (CRP), Development of a Quality Assurance Programme for Radiation Therapy Dosimetry in Developing Countries, was initiated in 1995 with the aim of transferring know-how on TLD postal dose audits for radiotherapy hospitals to the national level. Twelve countries participated in this exercise<sup>1</sup>. The IAEA's TLD methodology was provided to national centres at which existing resources enabled the set-up of external audit groups (EAGs), nationally recognized teams of experts in charge of operating external quality audits for radiotherapy dosimetry. The CRP offered a standardized methodology, the same for all participating countries, and provided a technical backup to the national EAG activities. It developed the Guidelines for the Preparation of a Quality Manual for External Audit Groups on Dosimetry in Radiotherapy [3]. In addition, the TLD standard operating procedures of the IAEA Dosimetry Laboratory were distributed as an example of the TLD audit methodology. The countries set up their TLD systems with technical support from the IAEA, which acted as an external quality control of the performance of their national TLD systems. First, pilot TLD runs were conducted at the national level with a selected number of hospitals and, later, the regular audit programme was implemented. After the completion of the CRP in 2001 the methodology was made available to other countries willing to establish national TLD audits. This paper provides an overview of the TLD audit activities carried out within this programme in Algeria, Australia, Argentina, Brazil, China, Colombia, Cuba, India, the Republic of Korea, the Philippines and Poland, as given in the individual country presentations. The authors of each presentation are listed in the summary subheading. Aspects common to each of the national programmes are briefly described in the next section.

---

<sup>1</sup> The IAEA CRP E2.40.07, Development of a Quality Assurance Programme for Radiation Therapy Dosimetry in Developing Countries, involved the following countries: Algeria, Argentina, China, Colombia, Cuba, the Czech Republic, India, Israel, Malaysia, the Philippines, Poland and Vietnam.



## 2. COMMON TLD METHODOLOGY OF THE NATIONAL AUDIT SYSTEMS

The EAGs typically use the IAEA standard thermoluminescent dosimeters, which consist of polyethylene capsules filled with approximately 160 mg of annealed lithium fluoride (LiF) powder. A calibration of the TLD system (i.e. the thermoluminescent dosimeter response per unit absorbed dose to water) is performed using  $^{60}\text{Co}$  gamma rays. Several correction factors and coefficients are applied to account for the non-linearity in dose response, the variation in sensitivity due to changes in beam quality and the thermoluminescent dosimeter holder attenuation [4], and the fading of the thermoluminescent signal with time. A set of quality control procedures is maintained, which include verification of the thermoluminescent dosimeter calibration at every reading session and verification of the dose response and fading at the commissioning of every new lot of powder. External quality control of the system calibration is provided by the IAEA Dosimetry Laboratory.

The TLD sets are sent to hospitals with the standard IAEA holders and instructions and data sheets for  $^{60}\text{Co}$  beams and high energy X rays. Hospitals are requested to irradiate the thermoluminescent dosimeters in a water phantom in reference conditions. The dose delivered to the thermoluminescent dosimeters should be calculated using routine clinical data, in the same way as for patient treatments.

Upon arrival at the TLD laboratory, the thermoluminescent signal is measured and the doses are calculated for each TLD set. The results are reported to participants as the participant's stated dose, the EAG TLD determined dose and the relative deviation and/or the ratio (measured/stated) of these doses. The acceptance limit of 5% defines the maximum discrepancy between stated and measured doses, which does not require further investigation. All results outside the acceptance limit of 5% are followed up with a repeat thermoluminescent dosimeter irradiation, and the reasons for the discrepancies are investigated. An on-site visit is recommended if the deviations persist. Immediate action by the EAG is required if a deviation falls outside 10%. Some EAGs have introduced more detailed deviation categories, for example an optimum level of 3–3.5%, which corresponds to the expanded standard uncertainty of their TLD systems with the coverage factor  $k = 2$ .

## 3. ESTABLISHMENT OF A QUALITY AUDIT PROGRAMME FOR RADIATION THERAPY DOSIMETRY IN ALGERIA (M. ARIB, M. OUSSAID, M.S. BALI, S. KHOUDRI)

A quality audit programme for external beam radiotherapy dosimetry was set up by the secondary standards dosimetry laboratory (SSDL) of Algeria.

The EAG comprises a radiation physicist from the SSDL, medical physicists and a radiation oncologist working in radiotherapy.

The TLD capsules, using TLD-100, were calibrated in terms of absorbed dose to water by comparison with an ionization chamber whose calibration factor is traceable to the Bureau international des poids et mesures. The calibration curve was validated by reference irradiations performed by the IAEA, the radiotherapy centres of Leuven (Belgium) and Villejuif (France) and the primary standards dosimetry laboratory of Canada. The programme initially covered  $^{60}\text{Co}$  beams, but was later extended to include high energy X ray beams.

A comparison with the reference centres listed above and with two other national EAGs involved in similar programmes was made for absorbed doses between 1.4 Gy and 2.8 Gy. The maximum deviation observed was 2%.

All five Algerian radiotherapy hospitals take part in the audits, which are performed once a year. At present there are nine  $^{60}\text{Co}$  beams and four accelerator beams operational. The service is being extended to biannual checks in reference and non-reference conditions. The results of the beam calibration checks performed by the EAG from 1997 to 1999 are presented in Fig. 1. All but two results are within the acceptance limit of 5%. On-site visits by the EAG to the hospitals with poor results were organized to assist them in investigating the deviation and in recalibrating the beam.

For the beam audits in non-reference conditions the range of deviations was slightly higher (up to 7%), especially when using wedge filters.

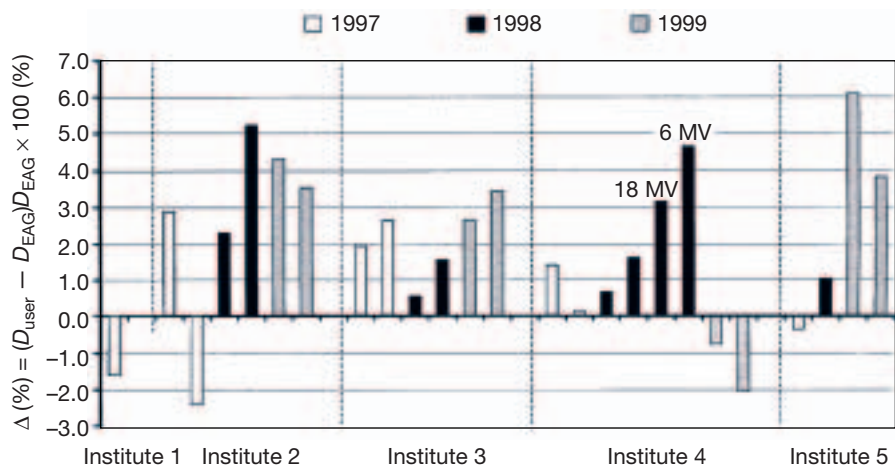


FIG. 1. National TLD audits of high energy photon beams in Algeria.

4. DOSIMETRIC QUALITY CONTROL IN RADIOTHERAPY USING TLD METHODOLOGY IN ARGENTINA (M. SARAVI, C. KESSLER, P.E. ALVAREZ, D.B. FELD)

An EAG was set up in Argentina in 1996 with the aim of upgrading the TLD programme run by the SSDL since 1978. The EAG is composed of the SSDL, which has responsibility for dose determination, traceability to international standards and TLD measurements, and two medical physicists from the Comisión Nacional de Energía Atómica, who work at the Buenos Aires Marie Curie Oncology Hospital. A total of 90 radiotherapy centres are registered in the EAG database, with 69  $^{60}\text{Co}$  units and 42 linacs operating in the country. Eighteen of the linacs produce X ray and electron beams. The TLD audit of dose in reference conditions is intended to be used on each  $^{60}\text{Co}$  and megavoltage X ray beam at least once per year. The EAG physicists make a visit to the centre if significant deviations are observed and persist after further action and checks.

The results for  $^{60}\text{Co}$  units show that 97% of results are within the acceptance limit of 5%. From 1998 to 2001, year by year, the percentages of the successful checks were 97, 89, 98 and 95%, and the standard deviation of the distribution of the results decreased from 5% to 3%. The results for 44 high energy X ray beams show that the percentages of results within the 5% limit were 98–100%, and the standard deviation 2–3%. Since 1999 no deviations greater than 10% have occurred in any beam,  $^{60}\text{Co}$  or high energy X rays.

Two pilot studies for dose audits in non-reference conditions were performed for 17  $^{60}\text{Co}$  units and 25 linacs. Depth dose ratios were analysed from irradiation at different depths in water (5 cm and 10 cm). Measurements on the axis for varying field size and with a wedge filter were performed. In reference conditions 93% of beams showed a deviation within 5%; for other field sizes the percentages of beams with the deviation within 5% were: 81% for 5 cm  $\times$  5 cm; 88% for 20 cm  $\times$  20 cm; 93% for 5 cm  $\times$  7 cm; and 91% for 10 cm  $\times$  10 cm with a wedge.

Typical reasons for deviations outside acceptance limits are: percentage depth dose errors, source to axis distance and/or source to surface distance set-up errors and misunderstandings of applied correction factors. Isolated cases revealed a lack of re-calibration of a dosimeter and a malfunctioning of the timer in a  $^{60}\text{Co}$  machine.

The procedure for on-site visits to hospitals was also implemented. The procedure includes mechanical and radiation beam checks, verification of the calibration factor of a dosimeter, determination of the dose rate in reference conditions, verification of percentage depth dose and output factor charts used at the hospital and a review of the documentation related to the irradiation

unit. Since 2000 five follow-up visits have been made. Reasons for dose discrepancies occurring in the analysis of the data sheets were verified at these visits.

5. A TLD THERAPY DOSIMETRY QUALITY ASSURANCE PROGRAMME FOR AUSTRALIA<sup>2</sup> (M. COX, R. HUNTLEY, D. WEBB)

The Australian Radiation Protection and Nuclear Safety Agency (ARPANSA) is in the process of developing a TLD quality assurance service for Australian radiotherapy centres that will be calibrated against the national primary standard of absorbed dose to water.

A pilot study during May and June 2002 involved six Australian centres. In addition to beam output checks, thermoluminescent dosimeters were exposed to measure PDD(10), TPR<sub>20,10</sub> or  $D_{20}/D_{10}$  for each beam used.

Calibration capsules were exposed at ARPANSA to precisely 2 Gy at <sup>60</sup>Co each day within the specified date window. Calibration capsules appropriate to the date of each hospital irradiation were read out on the same day as the hospital capsules, thus automatically correcting for fading effects. A fading study allowed corrections to be made in the event that no calibration capsule was available for the date of any particular hospital irradiation.

A bulk quantity of powder was exposed to approximately 2 Gy at <sup>60</sup>Co a few weeks before the irradiation window. This powder was used as a control during the readout of the hospital capsules, to eliminate the effects of drift in the TLD reader and variations in operator technique.

Background capsules travelled with the hospital capsules but were unexposed. Readouts from the background capsules were subtracted from the exposed hospital capsule readouts.

Energy corrections were applied, using a relationship supplied by the IAEA. ARPANSA intends to determine its own energy correction factors in future work.

A linearity curve was developed for the batch of powder used. As the doses delivered were all close to the requested dose of 2 Gy, the non-linearity corrections were insignificant and were not applied.

Good results were obtained for the dose at 5 cm (Fig. 2). The mean ratio of measured to stated dose ( $D_m/D_s$ ) for the 12 beams at six radiotherapy centres was 1.004, with a standard deviation of 0.015.

---

<sup>2</sup> The authors are grateful to the IAEA for the previous audits on radiotherapy centres in Australia and for guidance in developing Australia's own programme.

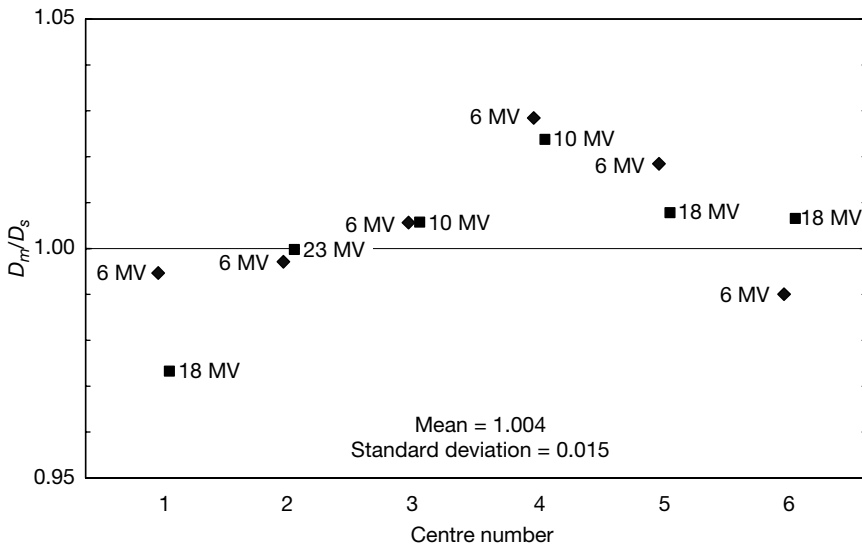


FIG. 2. Ratio of measured to stated dose.

The pilot study has allowed problems with the TLD method to be identified before the regular TLD quality assurance programme begins. There are approximately 100 linacs in Australia at 40 locations, administered by 30 radiotherapy centres. All centres will be expected to participate when the service is offered regularly, starting late in 2002 or early in 2003. Initially the Australian TLD quality assurance service will be offered for two photon beams per centre. Future work at ARPANSA will include the development of procedures so that audits of up to three photon beams and up to two electron beams will be offered annually to each centre.

#### 6. QUALITY CONTROL PROGRAMME FOR RADIOTHERAPY IN BRAZIL<sup>3</sup> (A.M. CAMPOS DE ARAUJO, C.C.B. VIEGAS, A.M. VIAMONTE, M.E. MORAES)

Brazil currently has 170 radiotherapy services (144 with megavoltage machines). The quality audit programme conducted by the National Cancer Institute (NCI) has been in operation for three years and covers 33 public radiotherapy centres distributed over 19 Brazilian states. The main activities

<sup>3</sup> Work supported by the IAEA under Technical Co-operation Project BRA/6/016. The work describes one of the TLD networks operating in Brazil.

are: on-site quality control evaluations, postal TLD audits in reference and off-axis conditions, and training.

On-site quality control reviews of dosimetric, electrical, mechanical and safety tests have been performed for 69 machines (36  $^{60}\text{Co}$  units and 33 linacs). As expected, more problems were found for obsolete  $^{60}\text{Co}$  machines than for linacs. The most frequent problems (percentage of occurrences  $\geq 25\%$ ) for the  $^{60}\text{Co}$  machines were related to the field and wedge factors, field symmetry and flatness, collimator axis rotation, laser alignment and field size indicators. For linacs they were mainly related to field flatness and laser alignment. The problems revealed were corrected wherever possible at the site visit. Those that needed action by maintenance engineers were to be corrected as soon as feasible, and the results communicated to the audit team.

Postal TLD audits for photon beams in reference conditions were conducted in four irradiation runs. The percentages of results within the specified deviation ranges are shown in Table I. All beams with deviations in the investigation and the emergency ranges have been rechecked. The audit team has found a highly significant decrease in the deviations between the first and the second audit.

The postal TLD audit in off-axis conditions started later, with the development and testing of a special thermoluminescent dosimeter holder. This has now been sent to all participants, to be irradiated with photon beams in a standard water phantom. It checks the beam output in reference conditions, depth

TABLE I. RESULTS OF FOUR AUDITS IN REFERENCE CONDITIONS: RELATIVE DEVIATIONS

Evaluation	Number of institutions	Number of beams ( $^{60}\text{Co}/\text{linac}$ )	Optimum (%)	Tolerance (%)	Investigation (%)	Emergency (%)
1	32	70 (37/33)	77.1	7.1	10.0	5.7
2	29	60 (34/26)	83.3	15.0	1.7	0
3	33	68 (34/34)	79.4	19.1	1.5	0
4	33	67 (35/32)	74.6	25.4	0	0

The relative deviation ranges for ratios of measured and stated doses ( $D_m/D_s$ ):

- (a) Optimum:  $0.97 \leq D_m/D_s \leq 1.03$ ;
- (b) Tolerance:  $0.95 \leq D_m/D_s < 0.97$  or  $1.03 < D_m/D_s \leq 1.05$ ;
- (c) Investigation:  $0.90 \leq D_m/D_s < 0.95$  or  $1.05 < D_m/D_s \leq 1.10$ ;
- (d) Emergency:  $D_m/D_s < 0.90$  or  $D_m/D_s > 1.10$ .

dose data, beam output variations with field size, wedge transmission factor, field flatness and symmetry, and dose calculation for an oblique beam incidence. In the future the audits will be expanded to cover checks of dose on-axis at different depths for electron beams.

## 7. QUALITY ASSURANCE IN RADIOTHERAPY DOSIMETRY IN CHINA (KAIBAO LI, SUMING LUO, JINSHENG CHENG, ZHIJIAN HE, JINGGANG AN, YIMIN HU, NINGYUAN FENG)

Since 1983 the Laboratory of Industrial Hygiene (LIH), Ministry of Health, has been involved in the IAEA/WHO TLD postal dose quality audit activities for hospitals in China. The SSDL of the LIH has participated in a yearly IAEA SSDL postal TLD dose comparison since 1989, with the results within the 3.5% acceptance limit.

In 1995 the SSDL started co-operation with the Beijing Cancer Hospital, Chinese Academy of Medical Science, to join the IAEA CRP. An EAG was established in 1996 with the responsibility of operating a TLD based quality audit for radiotherapy dosimetry. Since then, TLD audits have been carried out in seven provinces of China. The results are given in Table II.

The results for 132  $^{60}\text{Co}$  units and 86 high energy X ray beams checked from 1996 to 2000 indicated that 78% of hospitals were within the acceptance limit of 5%. Assistance was provided to 21 hospitals with poor results, including five on-site visits. All deviations were corrected.

In addition to the work above, national programmes for brachytherapy and stereotactic radiosurgery dosimetry were initiated in 2001. At the end of 2000 there were 41 gamma knives and 92 X knives in use in Chinese hospitals. So far 31 of these machines have been checked for dose rates and field dose

TABLE II. RESULTS OF NATIONAL TLD AUDITS (1996–2000)

Total number of beams checked	218
4–15 MV X rays	86
$^{60}\text{Co}$ gamma rays	132
Deviations within 5%	77.5%
Number of repeated TLD checks	35
Number of on-site visits to hospitals	5
Number of persisting deviations	0

profiles using dosimetric film and miniature ionization chambers ( $0.015 \text{ cm}^3$ ). The preliminary results indicate that problems exist with some of these machines.

8. NATIONAL TLD NETWORK FOR BEAM CALIBRATION  
QUALITY CONTROL IN COLOMBIA (M.E. CASTELLANOS,  
U.O. CHICA, H. OLAYA)

A national network for radiotherapy beam calibration quality control was established in Colombia in 1999. The network is supported by the SSDL and the TLD Laboratory (TLDL) of the Nuclear Safety and Radiation Protection Unit of INGEOMINAS. An EAG of five experienced medical physicists was created to assist in solving discrepancies found during the postal quality audits performed by the network. The aim is the establishment of a radiotherapy quality assurance programme (RQAP) for the 32 radiotherapy centres, with 56 photon beams, in the country.

The verification of the beam output in reference conditions for  $^{60}\text{Co}$  and high energy X ray beams is made by a postal TLD audit system, following IAEA procedures. The accuracy of the dose calibration by the SSDL is checked by comparisons with the IAEA.

To check the performance of the TLD procedures a few dosimeters were irradiated at the SSDL at doses near 2 Gy in reference conditions in a  $^{60}\text{Co}$  beam and then read at the TLDL following the established procedures. To check the postal procedure a similar test was performed in co-operation with the IAEA Dosimetry Laboratory. The agreement between the absorbed dose to water determined by the TLDL,  $D_m$ , and the absorbed dose stated,  $D_s$ , by the national SSDL and the IAEA was better than 2%.

The first trial run was performed with six radiotherapy centres in which experienced medical physicists work. The results are reported in Fig. 3, in which the dose stated by the centre is compared with the values measured by the TLDL. A total of 13 beams have been checked, including four  $^{60}\text{Co}$  beams and nine X ray beams from 4 MV to 18 MV. In general, the results were acceptable: the ratios of  $D_m/D_s$  for nine of the 13 beams were within 3% and only one 6 MV beam was outside 5%.

Additionally, as a result of this project the EAG assisted the IAEA to solve discrepancies that occurred in Colombian hospitals during the last IAEA/WHO TLD audit run. The EAG performed visits to these centres, investigated discrepancies and found causes of deviations such as a malfunction of the electrometers, a confusion of clinical reference conditions and calibration reference conditions, and a beam calibration misunderstanding.



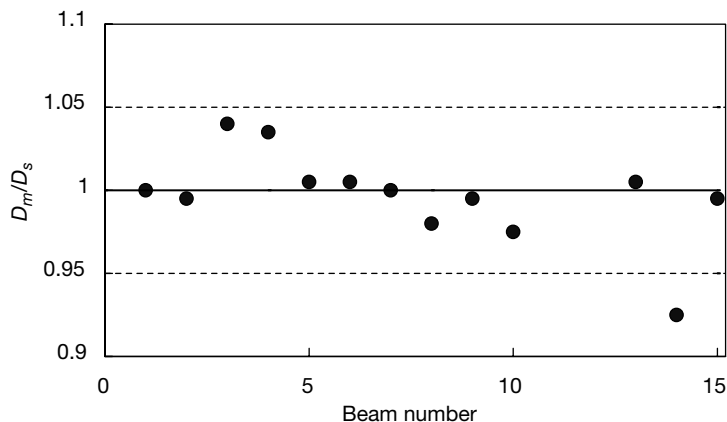


FIG. 3. First trial run in Colombia with six radiotherapy centres and 13 photon beams.

Now that the national network for radiotherapy beam calibration quality control is established, the procedures for external audits of high energy photon beams have been checked and the EAG manual has been completed.

9. CUBAN EXPERIENCE IN A DOSIMETRY QUALITY AUDIT PROGRAMME FOR RADIOTHERAPY (J.L. ALONSO-SAMPER, L. DOMINGUEZ, F.G. YIP, R.A. LAGUARDIA, J.L. MORALES, E. LARRINAGA)

In 1997 the Centro de Control Estatal de Equipos Médicos, in co-operation with the Instituto Nacional de Oncología y Radiobiología, started a national programme of quality assurance in radiotherapy. With the support of the IAEA a total of ten complete dosimetry sets has been acquired and a large number of medical physicists has been trained<sup>4</sup>. In addition, nine cobalt units have been installed, all of which are running at present.

For more than 20 years Cuba has taken part in the IAEA/WHO TLD postal dose audit programmes, the results of which have been inside the 5% acceptance limit. Cuba also joined the IAEA CRP to extend at a national level the experience of the TLD based audits, using the capability of its SSDL to measure thermoluminescent dosimeters. At the same time, the work of the already existing EAG was consolidated.

<sup>4</sup>This programme was possible thanks to co-operation between the Cuban Ministry of Health and the IAEA in projects ARCAL XXX and CUB/6/011.

The national programme for quality assurance in radiotherapy works on the basis of external on-site visits. The main objective is to avoid accidents and to improve the quality of radiotherapy treatments. Every year each radiotherapy service is visited by a qualified team of physicists, with the objective to check the physical aspects of the quality of radiotherapy treatments. The visit includes a review of documents and records, safety, mechanical and dosimetric aspects, treatment planning and tests in the fixed depth phantom to simulate and verify several techniques.

Although the TLD postal audit results were acceptable, the quality assurance audit visits have detected problems that may have affected the dose delivery to patients by more than 5%; for example, not all clinical plans are redundantly checked by an independent person; not all controls (daily, monthly and annual) are performed in accordance with the protocols approved by the National Quality Assurance Committee; in some cases the controls are not well recorded; clinical protocols are not strictly followed; there are problems with patient data acquisition; problems in the set-up of patients; mechanical malfunctions.

As a result of the visits, during the past three years of auditing these problems have been reduced in magnitude. Recently a radiation oncologist has joined the quality assurance programme as a part of the audit team.

10. ESTABLISHMENT OF A NATIONAL QUALITY AUDIT NETWORK FOR DOSIMETRIC QUALITY CONTROL IN RADIOOTHERAPY USING TLD METHODOLOGY IN INDIA (G. RAMANATHAN, V.D. KADAM, S.P. VINATHA, A.T. SOMAN, P.S. JADHAVGAONKAR, M. VIJAYAM, V.V. SHAHA, M.C. ABANI)

The programme of quality audits of dosimetry in radiation therapy centres in India has been carried out since 1976 by the Bhabha Atomic Research Centre (BARC), which is a member of the IAEA/WHO network of SSDLs. At present, approximately 220  $^{60}\text{Co}$  machines and about 35 linacs are covered by the programme, which has been extended to the neighbouring countries of Myanmar, Nepal and Sri Lanka.

The SSDL of BARC conducts two to three national TLD runs every year; approximately 50 radiotherapy centres are audited in each run. The IAEA TLD methodology has been adopted and the uncertainties in the evaluation have been reduced to less than 2% by optimization of the TLD procedure. Follow-up actions are taken for those hospitals that have deviations in the audit outside the acceptance limit of 5% by sending detailed worksheets to analyse the discrepancies and by a repeat TLD audit. If needed, visits to the hospitals are performed in order to improve the local dosimetry practices.

The SSDL participates in a reciprocal comparison with the IAEA every year and has also had comparisons with EAGs in Argentina, the Republic of Korea and Malaysia. The results have shown good agreement.

Figure 4 shows the evolution over time of the results of the national TLD programme in terms of the percentage of hospitals that had deviations within the 5% acceptance limit in the period from 1976 to 2000. The data have been averaged over five-year periods to smooth the yearly fluctuations. The results include the quality audits carried out for  $^{60}\text{Co}$  photon beams as well as high energy X ray photons from linacs.

As can be seen from Fig. 4, currently approximately 80% of hospitals have acceptable dosimetry procedures. In order to improve the performance of the remaining 20%, they have been advised to make dosimetry measurements in water following IAEA Technical Reports Series No. 277 (TRS 277) [5] (if the chamber is calibrated in terms of air kerma,  $N_K$ ) or TRS 398 [6] (if the chamber is calibrated in terms of absorbed dose to water,  $N_{D,w}$ ). Workshops have been organized on the recent IAEA protocols [6, 7].

The reasons for deviations beyond acceptable limits in the quality audit results have been identified as:

- (a) Calculational mistakes in converting measured output, mostly in air to absorbed dose in water;
- (b) Improper dosimetric measurements;
- (c) Auxiliary instruments, such as barometers, not functioning properly;

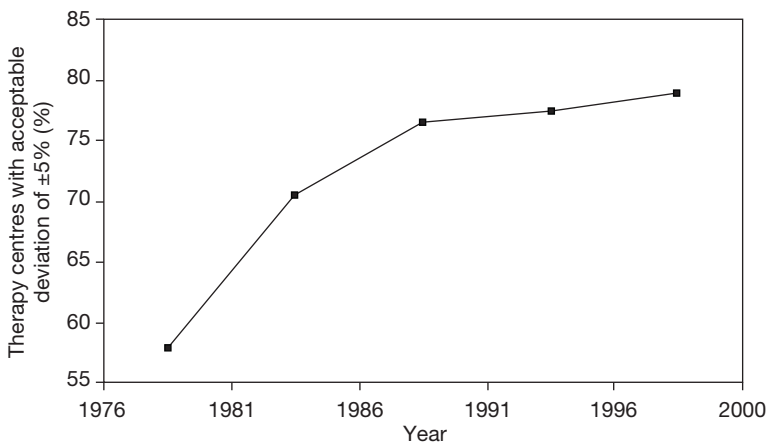


FIG. 4. Results of the comparison in terms of the percentage of therapy centres that had deviations within 5% over the period from 1976 to 2000.

- (d) Defective machine parameters.

At present, the quality audit is carried out for dosimetry under reference conditions. It is proposed to extend the audit to cover dosimetry under non-reference conditions by developing a suitable TLD methodology.

11. QUALITY ASSURANCE PROGRAMME FOR  
RADIOTHERAPY CENTRES IN THE REPUBLIC OF KOREA<sup>5</sup>  
(G.Y. KIM, H.K. LEE, K.J. PARK, H.J. OH)

In 1999 the SSDL of the Korea Food and Drug Administration (KFDA) started a national quality assurance programme for ensuring accuracy in radiotherapy dosimetry. On-site visits have been performed to verify dosimetry practices in 43 radiotherapy hospitals that have four <sup>60</sup>Co units and 47 high energy photon beams from accelerators. The measurements were carried out in a water phantom in accordance with TRS 277 [5]. The distribution of deviations is given in Table III. The results showed deviations varying between -7.1% and +8.4%. The KFDA followed up the large deviations observed in the programme.

In the past two years the KFDA successfully set up the national TLD postal dose audit programme. The method was based on the original IAEA technique using a PCL3 Fimel TLD readout system. There have been three TLD irradiation runs, in which 22 radiotherapy centres participated. The results showed deviations varying between -3.7% and +4.2%. All 52 radiotherapy centres in the Republic of Korea have applied to participate in the 2002 TLD programme.

The discrepancies outside the 5% limit were followed up by the KFDA. The lack of traceability of ionization chamber calibrations to the SSDL was a major reason for discrepancies in dosimetry. Also, the correction for air density (temperature and pressure) is a factor that sometimes introduces errors. Most hospitals do not calibrate their own barometers and sometimes rely on the air pressure that is quoted by local meteorological offices. In one case the barometer and thermometer of the clinic deviated from the KFDA's instruments by about 23 mm Hg and 2°C, respectively, even if the temperature was measured in air. In one case a variation in output of about 4% due to the gantry head angle (horizontal vs. vertical) was discovered.

---

<sup>5</sup>Training in TLD methodology at the IAEA Dosimetry Laboratory was provided within IAEA Technical Co-operation Project ROK/9/042.

TABLE III. RESULTS OF THE QUALITY ASSURANCE PROGRAMME IN THE REPUBLIC OF KOREA

	Linacs				$^{60}\text{Co}$			
	Number of beams	Deviation (%)			Number of beams	Deviation (%)		
		$\leq 3\%$	3–5%	5–10%		$\leq 3\%$	3–5%	5–10%
1999 <sup>a</sup>	47	36	3	8	4	2	—	2
2001	—	—	—	—	5	4	1	—
2002	18	16	2	—	—	—	—	—

<sup>a</sup> Audits were performed by on-site dosimetry review visits.

## 12. QUALITY AUDIT OF PHILIPPINE RADIOTHERAPY CENTRES (N. LINGATONG, M.D. SALADORES, E. CASERIA)

A quality audit programme for Philippine radiotherapy centres has been developed under the IAEA CRP. The programme includes annual on-site visits and a TLD based dose assurance programme using mailed dosimeters.

The EAG organized for the project implementation has obtained formal recognition from the national authorities. Its members are medical physicists and radiation oncologists from hospitals, and they have extensive training and experience in radiotherapy. The members of the measuring group are from the Philippine SSDs.

A total of 19 radiotherapy centres was visited from 2000 to 2001. These included all operational facilities, those with newly installed teletherapy equipment and those undergoing source replacement before the machines were used for clinical application. All centres have at least one medical physicist. A total of 19  $^{60}\text{Co}$  machines and eight linacs were evaluated for performance.

The TLD procedures were developed with the technical assistance and supervision of the IAEA Dosimetry Laboratory. Comparisons of the response of the TLD systems of the SSDL and the IAEA were undertaken from 2000 to 2001, with good results (within 1%).

A test TLD audit run for  $^{60}\text{Co}$  and megavoltage X ray beams was conducted in 2001. Sixteen sets of dosimeters were issued to participants; the results are shown in Fig. 5. All deviations were within 5%. However, a careful study of the data sheets shows that 14 dosimeter sets had been irradiated using the newly measured beam output and not the clinical data used in the treatment of patients. The difference of the doses was, however, less than 2%.

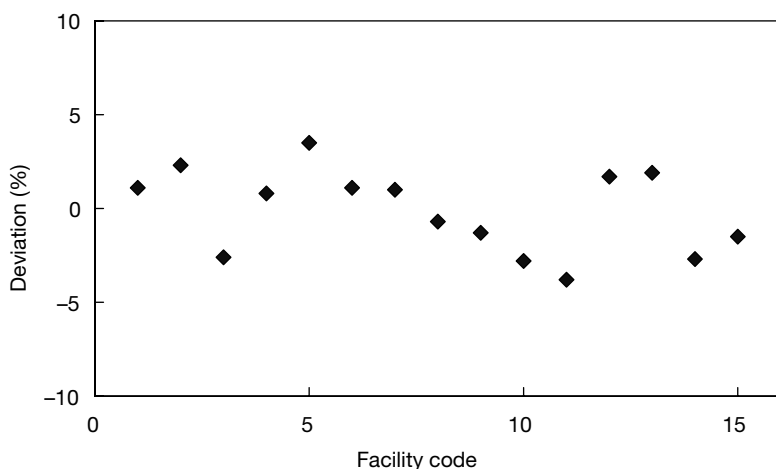


FIG. 5. Results of the TLD dose quality audit test run in the Philippines.

The radiotherapy quality audit programme was developed by the Department of Health under the Health Sector Reform Agenda and continues after the expiration of the IAEA research contract.

### 13. EXTERNAL QUALITY AUDITS IN RADIOTHERAPY IN POLAND (W. BULSKI, J. ROSTKOWSKA, M. KANIA, B. GWIAZDOWSKA)

The SSDL in Poland co-ordinates all activities carried out in radiotherapy quality assurance programmes nationwide. The EAG was set up as a part of the SSDL. The EAG is in charge of the management of the quality assurance programme and organization of the TLD measurements. The SSDL takes the responsibility for the metrological aspects of the programme.

There are in Poland 21 radiotherapy centres with 64 megavoltage units: 21  $^{60}\text{Co}$  units and 43 linacs. The first audit, supported by the IAEA, was carried out from 1991 to 1993. It yielded interesting results on the magnitude and sources of uncertainties of dose measurements. Between 1993 and 1995 a nationwide TLD check for photon beams in the framework of the Pan-European Radiation Oncology Programme for Assurance of Treatment Quality (EROPAQ) was performed. Audits supported by the IAEA under the CRP covering  $^{60}\text{Co}$  and accelerator photon beam output measurements in standard conditions were performed from 1999 to 2000. Audits in non-standard conditions started in 2001.

TABLE IV. CHRONOLOGY OF TLD AUDITS IN POLAND

	Number of audits in reference conditions		
	$^{60}\text{Co}$	Linac photons	Linac electrons
1991–1993	11	11	12
1994–1995 <sup>a</sup>	32	24	—
1999–2000	12	17	—
2001	16	—	32

<sup>a</sup> Performed within the framework of the EROPAQ project.

Since starting the programme in 1991 a total of four TLD runs for  $^{60}\text{Co}$  units, three for high energy X rays and two TLD runs for electron beams have been organized (Table IV). All dose checks were performed in reference conditions, and the participants measured the beam output prior to TLD irradiation. In 2001 an audit for  $^{60}\text{Co}$  beams was repeated, but this time the participants were requested to calculate the time of TLD irradiation using their clinical data rather than ionization chamber measurements. Among the total number (167) of checks performed from the inception of the programme, eight deviations beyond 5% have been detected, and they appeared mostly during the early audits (Fig. 6). All results in 2001 for  $^{60}\text{Co}$  units were within 3%. No deviations outside 5% occurred for electron beams.

#### 14. CONCLUSIONS

Several countries have established their own TLD based national audit systems with the support and technical assistance of the IAEA. A uniform methodology was implemented in Algeria, Australia, Argentina, Brazil, China, Colombia, Cuba, the Republic of Korea, the Philippines and Poland, and a few other countries. All the evidence points to the audit systems being an effective means of detecting problems, which when rectified improve the quality of radiotherapy treatment delivery and outcome.

A few quality assurance networks conduct TLD audits in parallel with on-site reviews of the local dosimetry practices in hospitals; the others organize on-site visits in order to follow up poor results of TLD audits. All networks have implemented, at least in the stage of a pilot TLD run, dose checks in reference conditions for photon beams. Most network systems perform regular audits for all hospitals in their countries. In addition to the basic programme, more developed networks incorporate dose audits in non-reference conditions on-axis for photon beams and audits in reference conditions for electron beams.

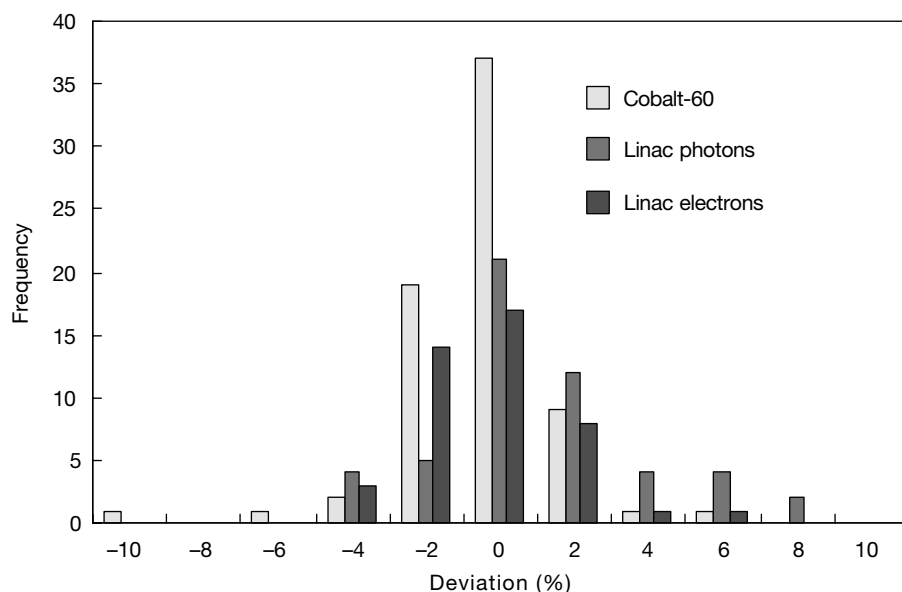


FIG. 6. Results of the national TLD audits in Poland performed from 1991 to 2001. A total of 167 beam checks were performed, including 71 checks for  $^{60}\text{Co}$ , 52 checks for high energy X rays and 44 checks of electron beams. The mean ( $m$ ) and standard deviation ( $SD$ ) of the distribution were:  $m = -0.4\%$ ,  $SD = 2.0\%$  for  $^{60}\text{Co}$ ;  $m = 1.0\%$ ,  $SD = 2.9\%$  for high energy X rays; and  $m = -0.2\%$ ,  $SD = 2.1\%$  for electron beams.

There are over 1400 radiotherapy hospitals with about 1040  $^{60}\text{Co}$  units and 870 linacs in the 11 countries presenting their work in this paper. Owing to the different stages of implementation of the national systems, at present about 43% of local hospitals are involved in the regular audit programme. Once the TLD networks are fully operational, the EAGs will be able to expand the number of beam checks in their countries and consider extension to other non-reference conditions and other modalities.

Thanks to these developments at the national level, access for a local hospital to a regular audit programme is now easier and assistance in resolving problems in dosimetry is now closer at hand and therefore more rapid. Also, the IAEA/WHO can now shift the focus of their TLD postal dose service to hospitals that have not yet participated in external dose audit programmes or to those countries in which there is no critical mass to establish a national quality assurance system, either owing to the small number of radiotherapy hospitals or owing to limitations in the national expertise or resources.



## ACKNOWLEDGEMENTS

The authors wish to thank the members of the EAGs who participated in setting up and operating quality assurance programmes for radiotherapy dosimetry and numerous colleagues who co-operated with the audits in their countries. A. Dutreix deserves special thanks for her personal involvement in and contribution to IAEA CRP E2.40.07, Development of a Quality Assurance Programme for Radiation Therapy Dosimetry in Developing Countries.

## REFERENCES

- [1] SVENSSON, H., HANSON, G.P., ZSDANSKY, K., The IAEA/WHO TL dosimetry programme for radiotherapy centres 1969–1987, *Acta Oncol.* **29** (1990) 461–467.
- [2] IZEWSKA, J., ANDREO, P., The IAEA/WHO TLD postal programme for radiotherapy hospitals, *Radiother. Oncol.* **54** (2000) 65–72.
- [3] IZEWSKA, J., et al., Guidelines for the preparation of a quality manual for external audit groups on dosimetry in radiotherapy, *SSDL Newsletter* No. 46 (2002) 2–13.
- [4] IZEWSKA, J., NOVOTNY, J., DUTREIX, A., VAN DAM, J., VAN DER SCHUEREN, E., The influence of the IAEA standard holder on dose evaluated from TLD samples, *Phys. Med. Biol.* **41** (1996) 465–473.
- [5] INTERNATIONAL ATOMIC ENERGY AGENCY, Absorbed Dose Determination in Photon and Electron Beams, Technical Reports Series No. 277, IAEA, Vienna (1987).
- [6] INTERNATIONAL ATOMIC ENERGY AGENCY, Absorbed Dose Determination in External Beam Radiotherapy, Technical Reports Series No. 398, IAEA, Vienna (2000).
- [7] INTERNATIONAL ATOMIC ENERGY AGENCY, The Use of Plane Parallel Ionization Chambers in High Energy Electron and Photon Beams, Technical Reports Series No. 381, IAEA, Vienna (1997).

**BLANK**

# **THERMOLUMINESCENCE DOSIMETRY QUALITY ASSURANCE NETWORK FOR RADIOTHERAPY AND RADIOLOGY IN THE CZECH REPUBLIC**

D. KROUTILÍKOVÁ\*,\*\*, J. NOVOTNÝ\*\*\*, L. NOVÁK\*

\* National Radiation Protection Institute  
E-mail: dkroutil@suro.cz

\*\* First Faculty of Medicine, Charles University

\*\*\* Hospital Na Homolce

Prague, Czech Republic

## **Abstract**

The Czech thermoluminescence dosimetry (TLD) quality assurance network provides independent audits for external beam radiotherapy and dental X ray radiology, primarily for the purposes of State supervision. Two modes of audit are used in radiotherapy. The basic mode includes beam calibration checks for all clinically used photon and electron beams, while the advanced mode covers TLD measurements for photon beams both on and off the central beam axis for a few simple treatment set-ups using a multipurpose phantom. The audit aims to check for dental radiology not only some basic dosimetric characteristics of the X ray apparatus but also the film developing process used by the dentists. The audits are performed by means of mailed dosimetry.

## **1. INTRODUCTION**

The Czech thermoluminescence dosimetry (TLD) quality assurance (QA) network was established in 1997 [1], as a part of the external auditing group (EAG) that originated in 1995, in order to perform an independent quality audit in external beam radiotherapy for two purposes:

- (a) To unify the dose within radiotherapy departments;
- (b) To strengthen and support the State supervision operated by the State Office for Nuclear Safety (SONS).

The network's measuring centre was established at the National Radiation Protection Institute (NRPI) in Prague. On the basis of positive

experience in radiotherapy with this network, new methods have been developed to expand it to radiology in order to simplify the application of State supervision. The TLD QA network for dental radiology began operation in 2001 [2].

## 2. TLD AUDIT IN RADIOTHERAPY

### 2.1. TLD system

Waterproof polyethylene capsules, identical to those used by the IAEA, are used for the thermoluminescent dosimeter's powder [3]. Each capsule contains about 160 mg of LiF:Mg,Ti powder that provides nine to ten identical portions to be read after the powder is dispensed into metallic containers that are small enough to be placed on the reader's planchette. The thermoluminescent dosimeter reader used is the manual Harshaw model 4000. Glow curves are recorded in every case in order to eliminate possible errors due to temperature shift in the reader. The thermoluminescence responses of the identical samples previously irradiated to 2 Gy exhibit a Gaussian distribution with a standard deviation for a single thermoluminescence reading of  $\nu = 1.9\%$ . The relative standard deviation for the mean related to a single thermoluminescent capsule does not exceed 0.7%. The absorbed dose was calculated using a generally accepted equation including correction for dose linearity, holder influence, fading and energy dependence [1]. The combined standard uncertainty is 1.5% for  $^{60}\text{Co}$  beams, 1.9% for X ray beams and 2.3% for electron beams.

### 2.2. Basic TLD audit

The basic TLD audit, which has been carried out since 1997, mostly covers beam calibration checks for all clinically used photon and electron beams. Photon and electron IAEA holders [3–5] were distributed to all Czech radiotherapy centres. When the audit is required, the audited radiotherapy centre is provided with a set of dosimeter capsules, an instruction sheet describing the method of irradiating the dosimeters, a data sheet to enter specifications regarding the radiotherapy treatment machine, other dosimetry equipment and details about the irradiation of the dosimeters. For photon beams the capsule is fixed by the holder positioned at a depth of 5 cm or 10 cm in an appropriate water phantom for a field size of 10 cm  $\times$  10 cm with a source to surface distance (SSD) or source to axis distance (SAD) set-up, as normally used by the centre. A dose of 2 Gy is required to be delivered. If necessary, a beam quality

check can be performed for X ray beams, for which the capsules are positioned at depths of 10 cm and 20 cm, with a field size of 10 cm  $\times$  10 cm and an SSD = 100 cm set-up, and a dose of 2 Gy is required for the upper capsule. For electron beams the capsule is positioned in a special holder to be irradiated at a depth of  $d_{\text{max}}$  to a dose of 2 Gy in a field size of 10 cm  $\times$  10 cm and at the normal SSD. The radiotherapy centres are requested to irradiate the dosimeters during a predetermined period. At the same time the TLD system is calibrated, which helps to keep fading under control.

According to the Czech regulations, every radiotherapy beam must be checked in this way at least once every two years.

### 2.3. Advanced TLD audit

The advanced TLD audit consists of measurements under both reference and non-reference conditions using a solid multipurpose phantom for photon beams, developed in Leuven for the European Commission network project, (the 'Leuven phantom') [6] that enables checks of a substantial part of the treatment planning process, including the dose delivery to the target volume. Some procedures that patients usually undergo during the radiotherapy process can be modelled in this way, including the sequence from computed tomography (CT) data acquisition to treatment planning and then finally the phantom irradiation in accordance with the calculated plan.

The audit procedure consists of a sequence of several steps that simulate the process of treatment preparation and realization. The phantom is first assembled in accordance with the requested set-up. Thereafter, a CT scan image through the central transversal plane of the phantom is taken using the markers on the phantom surface. The CT slice is transferred by normal means to the treatment planning computer, and a few irradiation set-ups are simulated. The planned dose for the point containing dosimeters on the central beam axis is 2 Gy. The phantom with dosimeters or a film in is then irradiated in accordance with the calculated plan. Consequently, it is possible to compare the planned dose for the thermoluminescent dosimeter points with the doses measured by dosimeters. Films are also irradiated in a reference set-up, using an applied dose within a range of 0.3 Gy to 0.4 Gy. Evaluation of the film is used to check the parameters of the dose profiles of the beam.

Irradiation of the phantom containing dosimeters is usually performed for seven simple irradiation set-ups currently used in clinical radiotherapy, basically with normal SSD (or SAD), open fields and a vertical incidence set-up, at depths of 5 cm or 10 cm, depending on the beam quality. The set-ups are summarized in Table I.

TABLE I. IRRADIATION SET-UPS TESTED IN THE ADVANCED TLD AUDIT

Set-up	Description	TLD measurements	
		On central beam axis	Off central beam axis
1	Reference conditions (10 cm × 10 cm)	Yes	No
2	Asymmetrical field (5 cm, 2 cm) × 10 cm, either with an asymmetrical collimator or with a block	Yes	No
3	Rectangular field (9 cm × 15 cm)	Yes	No
4	Wedge fields (9 W × 15 cm <sup>2</sup> , wedges from 15° to 60°)	Yes	Yes
5	Oblique incidence (15 cm × 15 cm, depth of 8.3 cm on central beam axis)	Yes	Yes
6	Open large field (15 cm × 15 cm, depth of 10 cm)	Yes	Yes
7	Inhomogeneities (15 cm × 15 cm, depth of 10 cm)	Yes	Yes

## 2.4. Reporting of deviations

The measured doses are compared with the doses stated (calculated) by the radiotherapy centre. For all dose measurements the deviation between measured and stated dose is reported:

$$\Delta_D = (D_{\text{TLD}}/D_s - 1) \times 100\%$$

An acceptance level of  $\pm 3\%$  has been set for this deviation. Deviations from  $\pm 3\%$  to  $\pm 6\%$  are considered minor, deviations exceeding  $\pm 6\%$  are regarded as major and deviations exceeding  $\pm 10\%$  are emergency values.

The full detailed results are mailed to the chief physicist of the audited radiotherapy centre if the deviation is within the acceptance level. In the event of a minor deviation the chief physicist is informed that it was detected and that the audit will be repeated shortly. If a major deviation is found the radiotherapy centre is informed and must investigate the situation to find a possible cause for the discrepancy and have the TLD audit repeated at its own expense.

Deviations exceeding  $\pm 10\%$  are reported immediately to SONS, which can execute proper sanctions on the radiotherapy centre. A detailed in situ audit by the EAG is usually ordered and the activities of the radiotherapy centre may be suspended temporarily.

Except for major and emergency deviations, the results of all performed TLD audits are mailed to SONS monthly.

These described actions for detected deviations are currently consistently applied only for the basic version of the audit; for the advanced audit no sanctions are currently applied to the radiotherapy centre. The current practice is such that if some deviations exceeding the acceptance level are found, they are reported to the chief physicist, who is asked to investigate the situation and check the treatment planning system, including the dosimetric data.

## 2.5. Results and discussion

There are 34 centres in the Czech Republic that provide external beam radiotherapy. From 1997 to 2001 each of the centres underwent the basic TLD audit for all its clinically used beams at least three times. Those showing some dosimetric discrepancies were audited more frequently. A total of 362 photon and electron beam checks were performed. For the total number of beams the mean value,  $m$ , for the  $\Delta_D$  (%) distribution was  $-0.04$  and the relative standard deviation was  $2.83\%$ . The emergency level was exceeded for four machines: one  $^{137}\text{Cs}$  unit, two  $^{60}\text{Co}$  units and one betatron (19 MV X ray beam). The deviations exceeding the emergency level were carefully investigated. In situ measurements were performed shortly after the TLD audit, which proved that the discrepancies were connected with mistakes caused by local physicists or incorrect performance of the outdated machines. The latter was especially obvious for the betatron, as keeping it stable was evidently difficult. The emergency levels were exceeded mostly from 1997 to 1999; the situation has improved as some outdated machines have been decommissioned. Currently about 90% of the results comply with the acceptance level. The remaining 10% mainly show deviations of up to  $\pm 6\%$ . Deviations higher than  $\pm 6\%$  are very rare.

Eight different types of treatment planning system (TPS) are used in the Czech Republic. The advanced audit was piloted for ten radiotherapy centres from 1999 to 2000. Within the pilot study, 11 TPSs (including seven different types) were tested for the use of cobalt and X ray beams. According to the multipurpose performance checks, most of the TPSs were found to comply with the tolerance level for simple treatment set-ups for central beam axis measurements. Some showed discrepancies for off-axis measurements above the acceptance level, especially for set-ups with inhomogeneities, oblique incidence and wedges. Only two of the tested TPSs showed deviations within the

acceptance level of  $\pm 3\%$ , another two showed a few minor deviations of up to  $\pm 6\%$  and the rest showed a few major deviations exceeding  $\pm 6\%$ . It was proved that the results were not dependent only on the quality of a particular TPS but rather on the quality of a particular radiotherapy centre. In any case, the purpose of the study was not to test TPS algorithms. The best results were achieved for large radiotherapy centres that were equipped adequately to perform modern quality radiotherapy. Such centres predominantly used systems such as CadPlan (Varian Medical Systems, Dosetec) or Focus (Computerized Medical Systems) with an on-line connection to the CT, simulator and verification system. These centres also had very good dosimetric equipment and the experience to acquire quality dosimetric data. Unfortunately, in the Czech Republic only ten of the 34 existing centres could be considered adequately equipped in this way.

### 3. TLD AND FILM AUDIT IN DENTAL RADIOLOGY

In dental radiology the audit is aimed at checking not only some basic dosimetric characteristics of the X ray apparatus but also the conditions of film processing by the dentists. It is well known that dentists often do not follow recommended chemical procedures for film processing, but deliver higher exposures to patients in order to speed up the film developing process.

#### 3.1. Method

For audit purposes the dentist receives a dosimetric set with instructions. The dosimetric part of the method includes irradiation of a large radiographic film simultaneously with an attached thermoluminescent dosimeter in order to check output in terms of air kerma ( $K_a$ ), irradiation field size and exposure reproducibility. The dentist is instructed to apply the usual setting for an upper molar exposure. The film processing is checked by means of two dental films and a standardized phantom. The dentist is required to develop an enclosed dental film irradiated under reference conditions in the measuring centre laboratory (the NRPI). In addition the dentist is asked to provide his or her own dental film and irradiate it with the phantom. This film is developed later in the measuring centre using a standard optimized process. The measurement of the sensitometric characteristics of both the dental films, and their mutual comparison, provide information on the quality of the film processing. It also indicates a relationship between the applied  $K_a$  value and the quality of the developing process. The  $K_a$  value should not exceed 5 mGy and the structures imaged on the developed dental films should be adequately visible and distinguishable. Evaluation of a particular case also depends on the type of film used by the



dentist, because most high sensitivity films can provide good quality radiographs for  $K_a$  values less than 5 mGy if a correct film processing procedure is observed. If this  $K_a$  value is exceeded, the dentist is informed and asked to improve the film processing. The diameters of the two radiation areas shown on the large radiographic film should be less than 6 cm.

### 3.2. Results and discussion

There are about 4000 X ray dental apparatuses in use in the Czech Republic, and therefore an audit system with a large operating capacity is required. The requirement is to check about 2000 apparatuses each year; the test run of this large number of apparatuses started in 2002. The main initial purpose is to familiarize the dentists with the method before the audit starts to be used as an instrument of State supervision, which should be in 2003. During the first six months of 2002 a total of 927 dosimetric sets were sent to dentists, although, unfortunately, 20% of the dentists refused to carry out the required procedures. Consequently, a total of 742 audits were performed.

Even though the measured  $K_a$  values were less than 5 mGy in most cases, only 10% of the results complied fully with the acceptance levels for all the checked parameters. Frequently,  $K_a$  was less than 5 mGy, but it was evident that the dentist did not observe the optimal conditions for film processing. The  $K_a$  value of 5 mGy was exceeded in 17% of cases; the radiation area diameter was exceeded in 24% of cases and unsatisfactory irradiation reproducibility was observed for 15% of the X ray apparatuses. These problems were evident especially for five models of X ray machine, unfortunately those that account for about 50% of those used in the Czech Republic. Film processing, however, causes the main problems. The sensitometric parameters measured within the film processing test conformed with the acceptance intervals only in 20% of cases. The results confirm the original assumption that incorrect methods of film processing lead to higher doses than necessary being applied to patients. Also, there are still many outdated types of X ray apparatus in use that do not meet the present criteria for radiation protection.

## 4. CONCLUSIONS

The importance of the national TLD quality assurance network has been proved. It has contributed to the improvement of clinical radiation dosimetry in the radiotherapy centres and to the improvement of the radiation protection of patients in dental X ray investigations. In addition, it significantly helps the

regulatory authority to monitor radiotherapy and radiology institutions effectively and regularly.

### ACKNOWLEDGEMENTS

Part of the work was sponsored by the Ministry of Health of the Czech Republic under project NC/5948-3 and also by IAEA contract No. 9468 under CRP E2.40.07.

### REFERENCES

- [1] KROUTILÍKOVÁ, D., ŽÁČKOVÁ, H., TLD audit in radiotherapy in the Czech Republic, *Radiat. Prot. Dosim.* **85** (1999) 393–396.
- [2] KROUTILÍKOVÁ, D., NOVÁK, L., “A method of postal audit in dental radiodiagnosics”, *Radiation Protection in Central Europe: Radiation Protection and Health (Proc. Congr. Dubrovnik, 2001)*, Croatian Radiation Protection Association, Zagreb (2001) (CD-ROM).
- [3] IZEWSKA, J., ANDREO, P., The IAEA/WHO TLD postal programme for radiotherapy hospitals, *Radiother. Oncol.* **54** (2000) 65–72.
- [4] IZEWSKA, J., NOVOTNY, J., VAN DAM, J., DUTREIX, A., VAN DER SCHUEREN, E., The influence of the IAEA standard holder on dose evaluated from TLD samples, *Phys. Med. Biol.* **41** (1996) 465–473.
- [5] DUTREIX, A., et al., “Performance testing of dosimetry equipment. Postal dose intercomparison of electron beams”, *Radiation Dose in Radiotherapy from Prescription to Delivery*, IAEA-TECDOC-734, IAEA, Vienna (1994) 305–309.
- [6] BRIDIER, A., NYSTRÖM, H., FERREIRA, I., GOMOLA, I., HUYSKENS, D., A comparative description of three multipurpose phantoms (MPP) for external audits of photon beams in radiotherapy: The water MPP, the Umeå MPP and the EC MPP, *Radiother. Oncol.* **55** (2000) 285–293.

# PROTON AND HADRON DOSIMETRY

(Session 13)

**Chair**

**P. ANDREO**

Sweden

**Co-Chair**

**S.M. VATNITSKY**

IAEA

**Rapporteur**

**A. KACPEREK**

United Kingdom

**BLANK**

# **CODES OF PRACTICE AND PROTOCOLS FOR THE DOSIMETRY IN REFERENCE CONDITIONS OF PROTON AND ION BEAMS**

S.M. VATNITSKY

Division of Human Health, International Atomic Energy Agency,  
Vienna

E-mail: s.vatnitsky@iaea.org

P. ANDREO

Medical Radiation Physics,  
Stockholm University–Karolinska Institute,  
Stockholm, Sweden

## **Abstract**

The advantages of radiotherapy protons and heavier charged particle beams, their technological feasibility and the clinical results obtained so far have led to the establishment of about 20 medical treatment facilities worldwide and plans to open another 20 proton and light ion therapy centres in the next five years. In order to meet the expanding capabilities of treatment techniques and to provide an extensive exchange of clinical experience, considerable effort has been devoted during the past 15 years to the development of the dosimetry and calibration of such beams. The paper reviews these developments and summarizes the present status of codes of practice and protocols for the dosimetry in reference conditions of proton and ion beams.

## **1. INTRODUCTION**

There has in recent years been an increased interest in the medical community throughout the world in establishing dedicated hospital based facilities employing proton and light ion beams for radiotherapy. A recent review [1] reports the establishment of about 20 treatment facilities worldwide and plans for opening another 20 proton and light ion therapy centres in the next five years. The advantages offered by the physical dose distributions of proton and light ion beams of a strongly increasing energy deposition at the end of the particle's range and a sharp lateral dose fall-off allow the tailoring of the dose distribution to the target volume. The planning of this high precision conformal therapy requires accurate dosimetry and beam calibration in order to ensure

the exact delivery of the prescribed dose<sup>1</sup>. However, the extensive exchange of clinical experience and medical treatment protocols needs to be based on consistent and harmonized dosimetry procedures.

Absorbed dose determinations in reference conditions in conventional radiotherapy are usually performed with air filled ionization chambers having calibrations traceable to standards laboratories. However, the lack of national and international dosimetry standards for proton and light ion beams, and the lack of the understanding of the details of the relevant physics, made calorimeters and Faraday cups (FCs) become the reference dosimetry instruments of choice for the calibration of these beams. This trend can also be understood from the perspective that the dosimetry of medical proton and light ion beams was carried out by physicists from nuclear physics research centres, who were more familiar with such instruments. Through the years considerable effort has been devoted to the development of a theoretical background and practical guidelines for the ionization chamber dosimetry of these beams. Currently, air filled thimble ionization chambers with <sup>60</sup>Co calibration factors are recognized as the most practical and reliable reference instrument for proton and light ion dosimetry. This paper reviews the efforts to standardize the dosimetry of therapeutic proton and light ion beams and summarizes the current status of codes of practice and protocols for their dosimetry in reference conditions.

## 2. EARLY DEVELOPMENTS IN THE DOSIMETRY OF PROTON AND LIGHT ION BEAMS

The following sections overview the recent dosimetry recommendations for absorbed dose determination in proton and light ion beams, with the emphasis on ionization chamber dosimetry. Conceptually, all the recommendations are based on the use of an air filled ionization chamber that behaves like a Bragg–Gray cavity. The formalisms that relate the absorbed dose to the medium to ionization in the air differ, but basically use the same approximation: to consider that the contribution to the ionization in the chamber air by particles other than protons and light ions can be neglected. The main features of the codes of practice and protocols discussed in this paper are summarized in Table I.

---

<sup>1</sup> When relevant, as in the case of ion beams, enhanced biological effects are taken into account during the clinical treatment planning procedure.

TABLE I. MAIN FEATURES OF THE CODES OF PRACTICE AND PROTOCOLS FOR DOSIMETRY IN REFERENCE CONDITIONS OF PROTON AND ION BEAMS

	AAPM TG 20 [2]	ECHED [5]	ECHED supplement [6]	ICRU 59 [12]	TRS 398 [13]
Particle type	Protons, ions	Protons	Protons	Protons	Protons, ions
Reference phantom material	‘Tissue’	‘Tissue’	Water	Water	Water
Reference dosimeter	Calorimeter/FC	Calorimeter/FC	Ionization chamber: thimble	Ionization chamber: thimble	Ionization chamber: thimble or parallel-plate
Calibration quality	Proton/ion beam	Proton beam	$^{60}\text{Co}$	$^{60}\text{Co}$	$^{60}\text{Co}$
Ionization chamber calibration factor	$N_X$	$N_K (N_X)$	$N_K (N_X)$	$N_X, N_K, N_{D,w}$	$N_{D,w}$
Ionization chamber wall material	A150	A150	No restriction	No restriction	No restriction
Beam quality specifier	None	60 MeV and 200 MeV	Effective energy	Effective energy	Residual range
Stopping powers	Ref. [4]	Ref. [4]	Ref. [7]	Ref. [7]	Ref. [14]
$W_{\text{air}}$	$34.3 \pm 4\%$ , $33.7 \pm 4\%$ ions	$35.2 \pm 4\%$	$35.2 \pm 4\%$	$34.8 \pm 2\%$	$34.2 \pm 0.4\%$ , $34.5 \pm 1.5\%$ ions
Use of chamber specific factors	No	No	Yes	Yes	Yes
$u_c(D_w), 1\sigma$	4.4%; 2.1% (based on calorimetry)	4.4%; 2.1% (based on calorimetry)	4.4%	2.8%	<i>Protons:</i> 2.0%: thimble 2.3%: parallel-plate <i>Ions:</i> 3.0%: thimble 3.4%: parallel-plate

## 2.1. American Association of Physicists in Medicine (AAPM) TG 20

The pioneer dosimetry protocol for heavy charged particle radiotherapy beams, TG 20 [2], was published by the AAPM in 1986. It was based on the use of FCs and calorimeters as reference instruments and gave little attention to ionization chamber dosimetry. Following the current trends in nuclear particle radiotherapy, TG 20 recommended specifying the dose to tissue. If a calorimeter or an FC were not available, an A150 walled ionization chamber with a  $^{60}\text{Co}$  calibration factor,  $N_X$ , traceable to a standards laboratory, was recommended. The lack of a harmonized set of data for the different particles made it necessary for this protocol to include data for stopping powers and for the mean energy required to produce an ion pair in air,  $w_{\text{air}}$ ,<sup>2</sup> that were not necessarily consistent and that came from different references in the literature. No beam quality specifier was introduced to select dosimetric quantities, and stopping power data [4] were provided for two chamber locations (the plateau and peak) only. As shown in Table I, the stated overall standard uncertainty of calorimetry based dosimetry,  $u_c(D_w)$ , was 2.1%, but the uncertainty of the ionization chamber dosimetry was larger by a factor of two, mainly due to the uncertainty of  $w_{\text{air}}$ .

## 2.2. European Clinical Heavy Particle Dosimetry Group (ECHED) code of practice and its supplement

The increased interest in radiotherapy with proton beams led to the publication of the ECHED code of practice [5], dedicated exclusively to protons, in which ionization dosimetry received more attention than in TG 20. However, it was not until the publication of the supplement to the ECHED recommendations [6] that ionization chambers having a  $^{60}\text{Co}$  calibration factor were recommended as a reference detector for proton dosimetry and data were supplied for chambers with different wall materials. The emphasis on ionization chamber based proton dosimetry was complemented with a recommendation for using water as the dosimetry phantom material, and the necessary data on tissue and water to air stopping power ratios and  $W_{\text{air}}$  were provided. Some of the most interesting aspects of the ECHED supplement were the use of the proton stopping power data in the then just released Report 49 of the International Commission on Radiation Units and Measurements (ICRU) [7] and the introduction of the effective energy of protons as the beam quality specifier.

---

<sup>2</sup> Note that the symbol  $w_{\text{air}}$  stands for the differential value, whereas the symbol  $W_{\text{air}}$  denotes the integral value. The difference between  $w_{\text{air}}$  and  $W_{\text{air}}$  is small, owing to the small variation of this quantity in the energy region of clinical proton beams [3], and the two symbols have been used in different codes of practice and protocols.



Another important aspect was the adoption of a new value of  $W_{\text{air}}$ ,  $35.2 \pm 4\%$  J/C, recommended in ICRU 31 [8]. As can be seen in Table I, all the new features recommended by ECHED did not change substantially the overall standard uncertainty of ionization chamber dosimetry, as  $u_c(D_w)$  was still estimated to be larger than 4%, because of the large uncertainty of  $W_{\text{air}}$ .

### 2.3. Dosimetry comparisons of proton dosimetry

In order to achieve homogeneity in dosimetry at institutions implementing proton radiotherapy and to facilitate the exchange of clinical experience, the two protocols, TG 20 and ECHED, recommended periodic dosimetry comparisons among the various centres. Several ionization chamber comparisons were performed in proton beams in the early 1990s [9, 10]. The measurements used low energy proton beams and were mainly focused on evaluating the consistency of ionization chamber dosimetry at the participating institutions. The goals of these studies were to compare the results of absorbed dose determination following TG 20 and ECHED and to verify the consistency of the results when one particular protocol was used with different types of ionization chamber. The results published in Ref. [11] showed agreement within 1% in the results for eight ionization chambers from five proton facilities when the ECHED recommendations were used.

The dose difference between facilities using TG 20 and ECHED was 2.2%, due to the different  $W_{\text{air}}$  values recommended in the two protocols. It is interesting to note that the results of ionization chamber and FC dosimetry differed by more than 5%. Similar discrepancies between the two methods were reported in Ref. [15] for measurements in a 173 MeV proton beam.

An international proton dosimetry comparison between 13 institutions was held in 1995 at the Loma Linda University Medical Center (LLUMC) [16]. The measurements were performed in an unmodulated beam of 250 MeV and in range modulated beams of 100 MeV and 155 MeV. The results showed differences within  $\pm 3\%$  when ionization chambers with  $^{60}\text{Co}$  calibration factors and institution specific conversion factors and protocols were used. However, one measurement based on a chamber having a proton calibration factor determined from FC measurements differed from the mean value of the other methods by 8%.<sup>3</sup>

---

<sup>3</sup> It is widely accepted today that FCs cannot be used directly for absorbed dose measurements, as the method does not provide information on energy deposition [2]. The collected charge must be converted into an absorbed dose to a medium, a process that requires the accurate determination of the spectrum of all particles reaching the FC. Even when careful measurements were made [17], errors in FC dosimetry caused by the lack of information on secondary particles introduced errors in the calibration of proton beams [18]. This limitation of FC dosimetry, which was highlighted by the results of the comparison, reduced substantially the use of FCs in proton and ion beam dosimetry, even after substantial improvements in the accuracy of FC measurements were proposed [19].

Presumably the differences in stated dose delivered to patients shown in Fig. 1 have existed systematically among the participating institutions, and were mainly due to the use of different dosimetry protocols. On the other hand, the LLUMC comparison demonstrated that the use of  $^{60}\text{Co}$  calibrated ionization chambers, identical dosimetry protocols and conversion factors, and specifying dose to the same material, would decrease the maximum difference between institutions to 1.5%. This reduction was consistent with the results of multi-institutional dosimetry comparisons in high energy photon and electron beams [20].

Since calorimetry is the most direct way to determine absorbed dose to water, and because this material became the reference for dose specification, several studies compared the results of dose measurements using ionization chambers and water calorimetry. Schulz et al. [21] used a calorimeter operated at a water temperature of  $4^\circ\text{C}$  in a 160 MeV range modulated proton beam and reported a calorimetry to ionometry (TG 20 based) dose ratio of  $0.99 \pm 0.01$ . Reference [22] used the Schulz calorimeter in a 155 MeV proton range modulated beam and measured a calorimetry to ionometry (ECHED based)

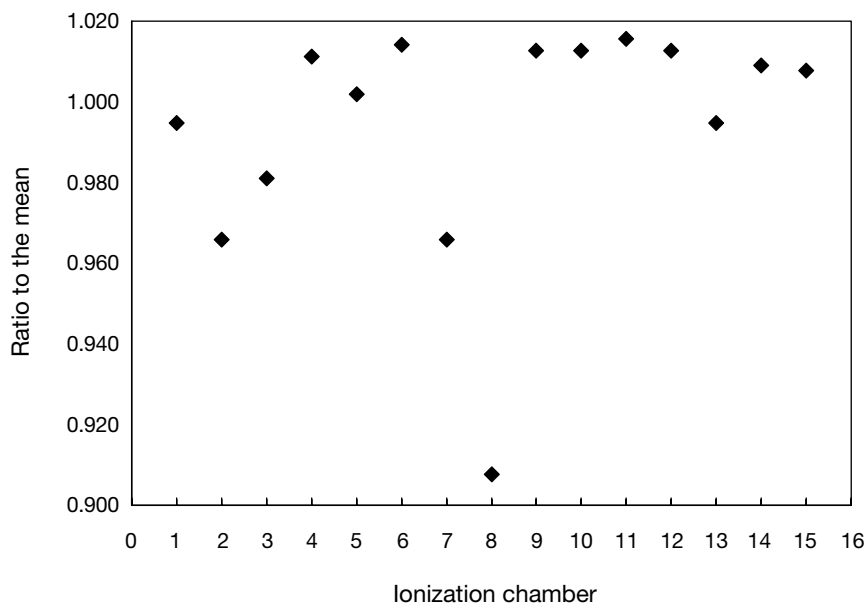


FIG. 1. Comparison of absorbed dose determinations in the Loma Linda 155 MeV proton beam in 1995 [16].

dose ratio of  $0.978 \pm 0.005$ . Similar results were obtained in Ref. [23] in an 85 MeV range modulated proton beam, finding calorimetry 2.6% lower than ionization chamber dose determination (ECHED based). This group used a water calorimeter described in Ref. [24], also operated at 4°C. A re-evaluation of the results from Ref. [21] using the ECHED code of practice yields a ratio of  $0.98 \pm 0.01$ . The close agreement of the results from these groups indicated that the recommended  $W_{\text{air}}$  value of  $35.2 \pm 4\%$  J/C for protons was too high, and that the use of the lower value of  $34.2 \pm 4\%$  J/C recommended in TG 20 yields a better agreement between ionometry and calorimetry. These calorimetry studies confirmed the conclusions of the ionization chamber dosimetry comparisons of adopting a uniform set of data and a common dosimetry protocol in order to achieve consistency in the dose delivered to patients in all proton centres.

### 3. MODERN TRENDS IN THE DOSIMETRY OF HEAVY CHARGED PARTICLES

#### 3.1. Procedures based on standards of absorbed dose to water

The idea of using solid state detectors calibrated in terms of absorbed dose to water for dose measurements in clinical proton beams was originally proposed in Refs [25, 26]. For ionization chamber based dosimetry, the authors of Ref. [27] extended the air kerma based formalism of the IAEA code of practice in Technical Reports Series No. 277 (TRS 277) [28] to proton beams, and developed the formalism based on absorbed dose to water standards for these type of beam, which was later adopted in TRS 398 [13]. The absorbed dose to water under reference conditions in a clinical proton beam of quality  $Q$ ,  $D_{w,Q}$ , is given by:

$$D_{w,Q} = M_Q N_{D,w,Q_0} k_{Q,Q_0}$$

$$k_{Q,Q_0} = \frac{(s_{w,\text{air}})_Q (w_{\text{air}})_Q P_Q}{(s_{w,\text{air}})_{Q_0} (w_{\text{air}})_{Q_0} P_{Q_0}} \quad (1)$$

where  $M_Q$  is the chamber electrometer reading in the proton beam corrected for influence quantities (temperature, pressure, etc.) and the subscript  $Q_0$  indicates the reference beam quality for the calibration of the ionization chamber. The lack of standards in the field of proton dosimetry meant that  $N_{D,w,Q_0}$ , the absorbed dose to water chamber calibration factor, had to be referenced to  $^{60}\text{Co}$  gamma rays.  $k_{Q,Q_0}$  is the beam quality correction factor that converts

$N_{D,w,Q_o}$  into the chamber calibration factor for a proton beam. In the definition of  $k_{Q,Q_o}$ ,  $s_{w,air}$  is the water to air stopping power ratio for protons ( $Q$ ) and a  $^{60}\text{Co}$  beam ( $Q_o$ ), respectively, and  $p_Q$  and  $p_{Q_o}$  are the ionization chamber perturbation factors at the qualities  $Q$  and  $Q_o$ . Initial experimental determinations of the factor  $k_Q$  for clinical proton beams ( $k_{Q,Q_o}$  for the case in which  $Q_o$  is  $^{60}\text{Co}$ ) were reported in Ref. [29].

### 3.2. ICRU 59

The publication of ICRU 59 [12] represented the first attempt to harmonize clinical proton dosimetry worldwide and included both  $^{60}\text{Co}$  air kerma and absorbed dose to water based procedures. The practical problems associated with the use of FCs and calorimeters were fully recognized in ICRU 59, and the role of these methods in proton dosimetry was minimized, favouring the use of ionization chamber dosimetry.

Follow the notation in ICRU 59, in which an ionization chamber calibrated in terms of air kerma,  $N_K$ ,<sup>4</sup> is used, the absorbed dose to water in a proton beam,  $D_{w,p}$ , is given by:

$$D_{w,p} = M_p^{\text{corr}} N_{D,g} C_p \quad (2)$$

where  $M_p^{\text{corr}}$  is the meter reading corrected for pressure and temperature, ion recombination and all other quantities that can modify the chamber response relative to the calibration condition, and:

$$N_{D,g} = \frac{N_K (1-g) A_{\text{wall}} A_{\text{ion}}}{s_{\text{wall},g} (\mu_{\text{en}}/\rho)_{\text{air,wall}} K_{\text{hum}}} \quad (3)$$

$$C_p = (s_{w,\text{air}})_p \frac{(w_{\text{air}})_p}{(W_{\text{air}})_c}$$

where  $g$  is the fraction of secondary electron energy lost to bremsstrahlung,  $s_{\text{wall},g}$  is the mean ratio of restricted mass stopping powers from the chamber

---

<sup>4</sup> Equations for using an exposure calibration factor were also given in ICRU 59.

wall material to the gas for the secondary electrons,  $(\mu_{\text{en}}/\rho)_{\text{air,wall}}$  is the mass energy absorption coefficient ratio from the air to the wall for  $^{60}\text{Co}$  photons,  $A_{\text{wall}}$  is the correction factor for the absorption and scatter in the wall and buildup cap,  $A_{\text{ion}}$  corrects for ion recombination during  $^{60}\text{Co}$  calibration,  $K_{\text{hum}}$  corrects for the difference in response of a chamber filled with ambient air versus dry air,  $(w_{\text{air}})_p$  and  $(W_{\text{air}})_c$  are the mean energies required to form an ion pair in the chamber gas for protons and  $^{60}\text{Co}$  photons, respectively, and  $(s_{w,\text{air}})_p$  is the mean water to air stopping power ratio for protons. As in the ECHED recommendations, an effective energy was used to select proton stopping power data, adapted from the ICRU 49 report.

For the absorbed dose to water formalism (i.e. the case in which an ionization chamber has a calibration factor in  $^{60}\text{Co}$ ,  $N_{D,w,c}$ ), ICRU 59 provided a simplified formalism, in which the absorbed dose to water was given by:

$$D_{w,p} = M_p^{\text{corr}} N_{D,w,c} k_p$$

$$k_p = \frac{(s_{w,\text{air}})_p (w_{\text{air}})_p}{(s_{w,\text{air}})_c (W_{\text{air}})_c} \quad (4)$$

ICRU 59 introduced some important changes in proton dosimetry, but some controversy resulted (see Ref. [30] for a detailed discussion):

- (a) A new value of  $34.8 \pm 0.7$  J/C for  $(w_{\text{air}})_p$ , for humid air, was adopted, which was higher than the value derived from comparisons of calorimetry and ionometry [22, 23]. Reference [31] indicates that the new value was in reality “an ideal best guess near the global average of existing data”, which represented a compromise between the value from ICRU 31 [8] and the value deduced from calorimetry and ionometry comparison results.
- (b) Equation (4) for the beam quality factor was a simplification compared with the expression previously proposed in Refs [25, 27] (compare Eqs (1) and (4)), as it omitted chamber specific perturbation factors ( $k_p$  thus became independent of the type of ionization chamber used). Whereas for proton beams this is a reasonable approximation, it ignores the chamber perturbation factor for  $^{60}\text{Co}$  in the denominator of  $k_p$ , which for some chamber types is significantly different from 1.
- (c) By adding explicitly a humidity correction in Eq. (3) and using a  $(w_{\text{air}})_p$  value for humid air, the resulting formalism became inconsistent, as other factors (the chamber calibration, stopping powers, etc.) did not correspond to the same situation.

The impact of these aspects is discussed below. Upon the adoption of ICRU 59 in multiple proton centres, international dosimetry using ionization chambers calibrated in terms of  $N_K$  and  $N_{D,w}$  in  $^{60}\text{Co}$  showed a considerable improvement in homogeneity, as expected. A comparison among various institutions, described in Ref. [32], resulted in agreements within  $\pm 0.9\%$  for all participants in the calibration of a common beam using their own instrumentation. Results for  $N_K$  calibrated chambers are given in Fig. 2. This homogeneity encouraged the use of ICRU 59 worldwide for the calibration of clinical proton beams. Compared with previous recommendations, the overall uncertainty of ionization chamber dosimetry based on ICRU 59,  $u_c(D_w)$ , was reduced to 2.8%, because of the uncertainty stated for  $w_{\text{air}}$ .

ICRU 59 limited its recommendations to the use of thimble chambers only, but subsequent studies [33, 34] extended these recommendations to parallel-plate ionization chambers, as they were often used in the calibration of ocular therapy and radiosurgery proton beams. For example, Ref. [33] used the data from ICRU 59, and different cross-calibration procedures were tested for a Markus plane-parallel chamber, including that against a thimble chamber in

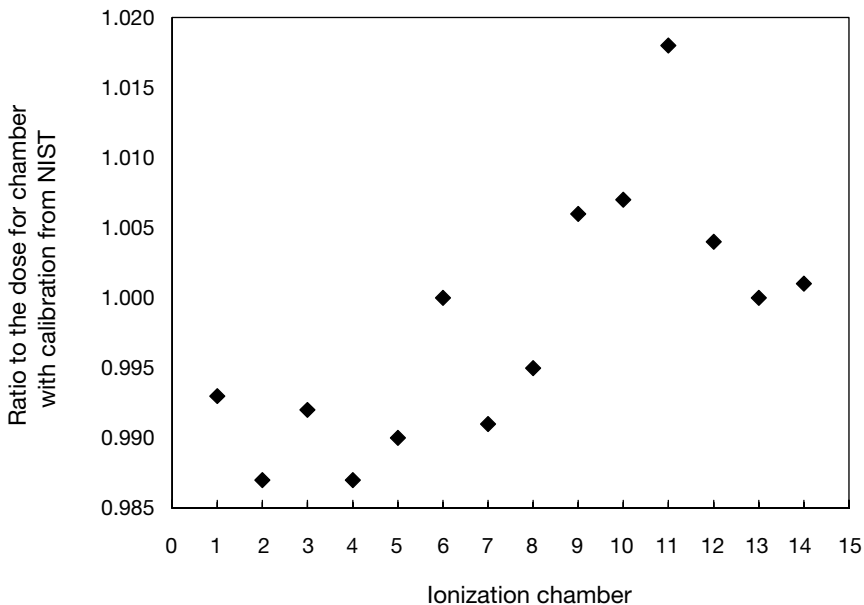


FIG. 2. Results of the proton dosimetry comparison [27] using ICRU 59 with ionization chambers having an  $N_K$  calibration.

a proton beam. The agreement of this procedure versus the direct use of a thimble chamber in a 100 MeV beam was within 0.4%. The authors of Ref. [34] compared results obtained with a Markus chamber, based on ICRU 59, with an FC in a 160 MeV proton radiosurgery beam, finding both techniques in agreement within 4%. As the ionization chamber dosimetry with plane-parallel chambers exhibited superior reproducibility than other techniques and allowed calibrations even in regions of a large depth dose gradient or in a narrow spread out Bragg peak, these studies provided support for the use of plane-parallel chambers as a standard method in clinical practice, with the appropriate modifications of ICRU 59.

### 3.3. Dosimetry of light ion beams

Although the number of light ion beam radiotherapy facilities is still small, and neither ECHED nor ICRU 59 made recommendations for absorbed dose determination in ion beams, several dosimetry studies and dose comparisons, mostly performed with carbon beams [35–37], provided progress comparable with that of proton beams.

The group at the Gesellschaft für Schwerionenforschung (GSI) applied the absorbed dose to water formalism to the ionization chamber dosimetry of carbon beams [35]. Based on the analysis of published data of  $W_{\text{air}}$  for different particles they proposed the value of 34.8 J/C, recommended by ICRU 59 for protons, for carbon beams as well as for all lighter fragments, down to protons. As the water to air stopping power ratio does not depend considerably on the particle type in the energy range above 1 MeV, Ref. [35] used the value of 1.13, close to that of the ICRU for protons and alpha particles [7]. Studies of the displacement of the effective point of measurement of a cylindrical chamber have been made in Ref. [36], which find a value of 72% of the inner radius.

The group at the Heavy Ion Medical Accelerator in Japan applied the air kerma based formalism of ICRU 59 to carbon beams and performed an ion chamber dosimetry comparison [37] in a 290 MeV/nucleon carbon beam with the GSI group, which used an absorbed dose to water formalism. The result of this comparison yielded agreement within 1%, even if different basic data were used. On the other hand, both groups estimated an uncertainty,  $u_c(D_w)$ , of 5% in the dose determination and agreed to establish a standard protocol for carbon beam dosimetry.

A comparison of different dosimetry methods in proton and light ion beams is made in Ref. [38]. It is worth noticing that the results with a Markus chamber (using the absorbed dose to water formalism of ICRU 59) were higher than those of a fluence method (single particle counting) by several per cent, thus being similar to the results reported by other authors [35, 37].

### 3.4. TRS 398

TRS 398 [13], which is based on standards of absorbed dose to water for external radiotherapy beams, includes recommendations for the calibration of proton and heavy ion radiotherapy beams. In conformity with previous IAEA codes of practice, TRS 398 adopted the most recent developments in the field of ionization chamber dosimetry for these beams; this includes a thorough revision of the physical quantities involved in their dosimetry.

For protons, TRS 398 differs substantially from ICRU 59. A detailed comparison of the two recommendations has been made in Ref. [30], which provides a discussion of the source of the differences. Important from a numerical point of view, these are the  $W_{\text{air}}$  value for protons, stopping power ratios and chamber perturbation factors:

- (a) The ratio of  $W_{\text{air}}$  values, protons to  $^{60}\text{Co}$ , differs by 2.3%, mostly due to the procedure to determine a mean value for protons from the experimental data available; about 0.6% of the difference is due to the conceptually different use of  $W_{\text{air}}$  values for humid air (ICRU 59) versus dry air (TRS 398).
- (b) The use in TRS 398 of the more accurate fluence averaged stopping power ratios, which include nuclear interactions and secondary electron production [14], results in a minor difference of 0.5%.
- (c) Both protocols recommend that chamber perturbation factors in proton beams be taken to unity, but TRS 398 includes perturbation factors for  $^{60}\text{Co}$  in the denominator of  $k_Q$ .

When these components are taken into account, differences in  $k_Q$  values, and therefore in  $D_w$ , vary between  $-2.6\%$  and  $+1.5\%$ , depending on the chamber type and proton beam quality. An experimental comparison of  $D_w$  determined in 100 MeV and 155 MeV clinical proton beams using ICRU 59 and TRS 398 is made in Ref. [39]. For various ionization chamber types the determinations of  $D_w$  based on TRS 398 agreed within 1.5%. The differences between TRS 398 and ICRU 59, using the same set of chambers, were up to 3.1%, in conformity with the remarks on  $W_{\text{air}}$  values and the chamber perturbation factors for  $^{60}\text{Co}$  mentioned above.

Compared with previous recommendations, the estimated overall uncertainty of ionization chamber dosimetry in TRS 398,  $u_c(D_w)$ , has been reduced to 2.0% for thimble chambers and to 2.3% for parallel-plate chambers, because of the stated lower uncertainty of  $W_{\text{air}}$ .

For the dosimetry of heavier ion beams the recommendations of TRS 398 are still based on approximate values for most of the physical parameters, since



very few experimental and theoretical data are available on the spectral distribution of ion beams and their fragmentation produced by nuclear interactions. A constant value of 1.13 was adopted for  $s_{w,air}$ , consistent with that proposed in Ref. [35]. Recent Monte Carlo calculations [40] for 391 MeV/u  $^{12}\text{C}$  ions at depths of 10 cm and 26 cm (for the plateau and Bragg peak front end) yield values of 1.135 and 1.151, which are in good agreement with the  $s_{w,air}$  value recommended in TRS 398.  $W_{air}$  for ion beams was determined using the same procedure as for proton beams, and until more information is available the value of 34.50 J/C with a standard uncertainty of 1.5% is recommended for ion beams. The TRS 398 estimated relative standard uncertainty,  $u_c(D_w)$ , is 3.0% for thimble chambers and 3.4% for parallel-plate chambers.

#### 4. RECENT AND FUTURE IMPROVEMENTS IN DOSIMETRY IN REFERENCE CONDITIONS

Recent improvements in proton dosimetry have been focused on chamber specific factors and perturbation effects. A systematic study of 17 thimble ionization chambers [41] has derived perturbation factors (relative to an NE 2571 chamber), concluding that they are the same within 1% and within the experimental uncertainty; this agrees with Monte Carlo calculated values [42]. The assumption made in TRS 398 that perturbation factors for plane-parallel chambers are unity has recently been confirmed by measurements in a 75 MeV proton beam [43]. Currently it is not possible to resolve the departure of perturbation factors from unity, owing to the experimental uncertainties of the data [41]. A systematic study using Monte Carlo calculations may possibly improve the accuracy of the calibration of proton and light ion beams. The lack of primary standards of absorbed dose to water for proton and light ion beams makes the availability of an experimental  $k_{Q,Q_0}$  a rather distant possibility, and in the foreseeable future possibly only calculated values of the beam quality factors will be used.

The adoption of TRS 398 by proton and light ion therapy facilities will allow them to achieve consistency in the dose delivered to patients and to establish ionization chamber dosimetry in reference conditions at a level consistent with that of high energy photon and electron beams. Key steps in this process will be testing the procedures recommended in TRS 398 for clinical proton and light ion beams with different ionization chambers, and comparing the results obtained with the existing protocols.

## REFERENCES

- [1] SISTERSON, J., "Ion beam therapy: Overview of the world experience", Application of Accelerators in Research and Industry (Proc. Int. Conf. Denton, TX, 2000) (DUGGAN, J.L., MORGAN, I.L., Eds), American Institute of Physics, College Park, MD (2001) 865–868.
- [2] AMERICAN ASSOCIATION OF PHYSICISTS IN MEDICINE TASK GROUP 20, Protocol for Heavy Charged-particle Therapy Beam Dosimetry, Rep. 16, AAPM, New York (1986).
- [3] GROSSWENDT, B., BAEK, W.Y., W values and radial dose distributions for protons in TE-gas and air at energies up to 500 MeV, *Phys. Med. Biol.* **43** (1998) 325–337.
- [4] JANNI, J.F., Proton range-energy tables, 1 keV–10 GeV, part 1, *At. Data Nucl. Data Tables* **27** (1982) 147–339.
- [5] VYNCKIER, S., BONNETT, D.E., JONES, D.T.L., Code of practice for clinical proton dosimetry, *Radiother. Oncol.* **20** (1991) 53–63.
- [6] VYNCKIER, S., BONNETT, D.E., JONES, D.T.L., Supplement to the code of practice for clinical proton dosimetry, *Radiother. Oncol.* **32** (1994) 174–179.
- [7] INTERNATIONAL COMMISSION ON RADIATION UNITS AND MEASUREMENTS, Stopping Powers and Ranges for Proton and Alpha Particles, Rep. 49, ICRU, Bethesda, MD (1993).
- [8] INTERNATIONAL COMMISSION ON RADIATION UNITS AND MEASUREMENTS, Average Energy Required to Produce an Ion Pair, Rep. 31, ICRU, Bethesda, MD (1979).
- [9] KACPEREK, A., VYNCKIER, S., BRIDIER, A., HERAULT, J., BONNETT, D.E., "A small scale European proton dosimetry intercomparison", Proton Radiotherapy Workshop at PSI (Proc. Workshop Villigen, Switzerland, 1991), Paul Scherrer Institute, Villigen (1991) 76–79.
- [10] JONES, D.T.L., et al., "Proton dosimetry intercomparison at NAC", NAC/AR/92-01, Annual Report, National Accelerator Center, Cape Town (1992) 61–63.
- [11] JONES, D.T.L., et al., "National accelerator centre: Proton dosimetry intercomparisons", Application of Heavy Ion Accelerator in Radiation Therapy of Cancer (Proc. Int. Sem. Chiba, 1994), National Institute of Radiological Science, Chiba (1994) 222–230.
- [12] INTERNATIONAL COMMISSION ON RADIATION UNITS AND MEASUREMENTS, Clinical Proton Dosimetry. Part I: Beam Production, Beam Delivery and Measurement of Absorbed Dose, Rep. 59, ICRU, Bethesda, MD (1998).
- [13] INTERNATIONAL ATOMIC ENERGY AGENCY, Absorbed Dose Determination in External Beam Radiotherapy, Technical Reports Series No. 398, IAEA, Vienna (2000).
- [14] MEDIN, J., ANDREO, P., Monte Carlo calculated stopping-power ratios, water/air, for clinical proton dosimetry (50–250 MeV), *Phys. Med. Biol.* **42** (1997) 89–105.

- [15] GALL, K.P., ROSENTHAL, S.P., SMITH, A., "Proton dosimetry protocol comparisons", Application of Heavy Ion Accelerator in Radiation Therapy of Cancer (Proc. Int. Sem. Chiba, 1994), National Institute of Radiological Science, Chiba (1994) 231–233.
- [16] VATNITSKY, S., et al., Proton dosimetry intercomparison, *Radiother. Oncol.* **41** (1996) 169–177.
- [17] VERHEY, L.J., et al., The determination of absorbed dose in a proton beam for purposes of charged particle radiation therapy, *Radiat. Res.* **79** (1979) 34–54.
- [18] NEWHAUSER, W.D., et al., A report on the change in the proton absorbed dose measurement protocol for the clinical trials conducted at the Harvard Cyclotron Laboratory, *Med. Phys.* **25** (1998) A144–A145.
- [19] GRUSELL, E., ISACSSON, U., MONTELIUS, A., MEDIN, J., Faraday cup dosimetry in a proton therapy beam without collimation, *Phys. Med. Biol.* **40** (1995) 1831–1840.
- [20] JOHANSSON, K.A., Studies of Different Methods of Absorbed Dose Determination and a Dosimetric Intercomparison at the Nordic Radiotherapy Centres, Thesis, Gothenburg Univ. (1982).
- [21] SCHULZ, R.J., VERHEY, L.J., SAIFUL HUQ, M., VENKATARAMANAN, N., Water calorimeter dosimetry for 160 MeV protons, *Phys. Med. Biol.* **37** (1992) 947–953.
- [22] VATNITSKY, S.M., SIEBERS, J.V., "Comparison of water calorimeter with reference ionization chamber dosimetry in high-energy photon and proton beams", paper presented at the NPL Calorimetry Workshop, Teddington, UK, 1994.
- [23] PALMANS, H., et al., Water calorimetry and ionization chamber dosimetry in the 85 MeV clinical proton beam, *Med. Phys.* **23** (1996) 643–650.
- [24] SEUNTJENS, J., VAN DER PLAETSEN, J.A., VAN LAERE, K., THIERENS, H., "Study of correction factors and the relative heat defect of a water calorimetric determination of absorbed dose to water in high energy proton beams", Measurement Assurance in Dosimetry (Proc. Int. Symp. Vienna, 1993), IAEA, Vienna (1994) 45–59.
- [25] VATNITSKY, S.M., KHRUNOV, V.I., FOMINYCH, V.I., SCHUELE, E., Diamond detector dosimetry for medical applications, *Radiat. Prot. Dosim.* **47** (1993) 515–518.
- [26] VATNITSKY, S.M., MILLER, D.W., SIEBERS, J.V., MOYERS, M.F., Application of solid state detectors for dosimetry of therapeutic proton beams, *Med. Phys.* **22** (1995) 469–473.
- [27] MEDIN, J., et al., Ionization chamber dosimetry of proton beams using cylindrical and plane parallel chambers.  $N_w$  versus  $N_K$  chamber calibrations, *Phys. Med. Biol.* **40** (1995) 1161–1176.
- [28] INTERNATIONAL ATOMIC ENERGY AGENCY, Absorbed Dose Determination in Photon and Electron Beams, Technical Reports Series No. 277, IAEA, Vienna (1987).
- [29] VATNITSKY, S.M., SIEBERS, J.V., MILLER, D.W.,  $k_O$  factors for ionization chamber dosimetry in clinical proton beams, *Med. Phys.* **23** (1996) 25–31.

- [30] MEDIN, J., ANDREO, P., VYNCKIER, S., Comparison of dosimetry recommendations for clinical proton beams, *Phys. Med. Biol.* **45** (2000) 3195–3211.
- [31] VERHEY, L.J., Response to comparison of dosimetry recommendations for clinical proton beams, *Phys. Med. Biol.* **45** (2000) L51–L52.
- [32] VATNITSKY, S., et al., Proton dosimetry intercomparison based on the ICRU Report 59 protocol, *Radiother. Oncol.* **51** (1999) 273–279.
- [33] VATNITSKY, S.M., The Practical Use of Plane Parallel Chambers in Calibration of Therapeutic Proton Beams Based on the ICRU 59 Report Dosimetry Protocol, Rep. LLUMCTN02-99, Loma Linda University Medical Center, Loma Linda, CA (1999).
- [34] NEWHAUSER, W.D., MYERS, K.D., ROSENTHAL, S., SMITH, A., Proton beam dosimetry for radiosurgery: Implementation of the ICRU Report 59 at the Harvard Cyclotron Laboratory, *Phys. Med. Biol.* **47** (2002) 1369–1389.
- [35] HARTMANN, G., JAEKEL, O., HEEG, P., KARGER, C.P., KRIESSBACH, A., Determination of absorbed dose in a carbon beam using thimble ionization chambers, *Phys. Med. Biol.* **44** (1999) 1193–1206.
- [36] JAEKEL, O., HARTMANN, G.H., HEEG, P., SCHARDT, D., Effective point of measurement of cylindrical ionization chambers for heavy charged particles, *Phys. Med. Biol.* **45** (2000) 599–607.
- [37] FUKUMURA, A., et al., Carbon beam dosimetry intercomparison at HIMAK, *Phys. Med. Biol.* **43** (1998) 3459–3463.
- [38] BESSERER, J., et al., Dosimetry of low-energy protons and light ions, *Phys. Med. Biol.* **46** (2001) 473–485.
- [39] VATNITSKY, S.M., MOYERS, M.F., VATNITSKY, A.S., “Parallel-plate and thimble ionization chamber calibrations in proton beams using the TRS 398 and ICRU 59 recommendations”, these Proceedings, Vol. 2, pp. 327–336.
- [40] GUDOWSKA, I., ANDREO, P., SOBOLEVSKY, N., “Secondary particle production in tissue-like and shielding materials for light and heavy ions calculated with the Monte-Carlo code SHIELD-HIT”, paper presented at the 2nd Int. Workshop on Space Radiation Research, Nara, Japan, 2002.
- [41] PALMANS, H., VEGHAEGEN, F., DENIS, J.-M., VYNCKIER, S., THIERENS, H., Experimental  $p_{\text{wall}}$  and  $p_{\text{cell}}$  correction factors for ionization chambers in low-energy clinical proton beams, *Phys. Med. Biol.* **46** (2001) 1187–1204.
- [42] VERHAEGEN, F., PALMANS, H., A systematic Monte Carlo study of secondary electron fluence perturbation in clinical proton beams, *Med. Phys.* **28** (2001) 2088–2095.
- [43] PALMANS, H., VEGHAEGEN, F., DENIS, J.-M., VYNCKIER, S., Dosimetry using plane-parallel ionization chambers in a 75 MeV clinical proton beam, *Phys. Med. Biol.* **47** (2002) 2895–2905.

## **DOSIMETRY WITH THE SCANNED PROTON BEAM ON THE PAUL SCHERRER INSTITUTE GANTRY**

A. CORAY, E. PEDRONI, T. BOEHRINGER,  
S. LIN, A. LOMAX, G. GOITEIN  
Department of Radiation Medicine, Paul Scherrer Institute,  
Villigen, Switzerland  
E-mail: Doelf.Coray@psi.ch

### **Abstract**

The spot scanning technique is used at the Paul Scherrer Institute to treat tumours with proton pencil beams with energies of up to 270 MeV. The calibration of the main dose monitor is described in the paper. The doses measured with different ionization chambers are consistent when using the IAEA code of practice in Technical Reports Series No. 398. The dosimetric procedures for quality control are presented and results to illustrate the reliability of the dose delivery are shown.

### **1. INTRODUCTION**

Owing to the physical properties of protons, which result in a high dose peak in a well defined range and no dose behind this Bragg peak, proton beams are an excellent tool for radiation therapy. The irradiation facility at the Paul Scherrer Institute (PSI) is designed for the treatment of deep seated tumours with a proton beam with an energy of up to 270 MeV [1]. The spot scanning technique, which uses a proton pencil beam to deposit dose into the patient in three dimensions, is performed on a compact isocentric gantry. An optimal three dimensional conformation of the dose distribution to the target volume can be realized.

The beam is deflected by a fast magnet in one direction; the range of the protons in the second direction is modified with a set of 40 range shifter plates, which can be put into the beam one by one. The movement in the third direction is performed with a linear motion of the patient table. The dose is delivered as a superposition of discrete dose spots, with the beam being shut off for the movement to the next spot position. A fast magnetic beam kicker with a rise time of 50  $\mu$ s is used to stop the beam between the spots. The steering system is based on two independent processors to steer the treatment and check the dose and position of each spot, based on two separate data tables provided by the therapy planning system. The gantry can be rotated over 360°, and for head irradiations the patient table can be rotated over  $\pm 120^\circ$ . This enables a large choice of field incidence directions on the patient.

The most pronounced advantages of the PSI scanning method are that: (a) the system can deliver complex shaped dose distributions without the use of patient specific hardware; (b) the scanning can be used with inverse planning algorithms; (c) the scanning is Cartesian; and (d) the discrete scanning method is safe.

The dose delivery is controlled by a grid type ionization chamber, with two parallel-plate ionization chambers used as redundant monitors. The monitors are placed at the exit of the 90° bending magnet, before the range shifter.

## 2. CALIBRATION OF THE PRIMARY MONITOR

### 2.1. Primary monitor

Until 2000 a parallel-plate ionization chamber monitor with a 0.5 cm gap between Mylar foils was used as the main monitor. However, this monitor, which had a window size of 2.5 cm × 20 cm, was sensitive to the range shifter noise and produced microphonic effects. To overcome this problem a grid chamber type monitor has been developed and tested. In the grid chamber the beam passes parallel to the ion collection plates. A grid placed in front of the anode shields the anode from induction produced by positive ions. A guard ring electrode is placed around the anode in order to get a uniform electric field over the whole range of the swept beam. The monitor is operated under a continuous nitrogen flow. The resulting charge collection time is faster than 100 μs. Since the beam period of 2001 the monitoring has been based on the use of the grid monitor.

The PSI therapy planning system calculates the dose distribution from a superposition of individual pencil beams, taking into account the density information from the corresponding computed tomography (CT) slices. An empirical model of the pencil beam is used, which takes into account the attenuation of the primary protons, the effects of multiple coulomb scattering and losses due to nuclear interactions. The therapy planning can predict absolute doses on the basis of this model and on parameterization data in data tables. The primary monitor has therefore been calibrated in terms of protons per monitor units (MUs).

### 2.2. Calibration procedure

During the calibration the volume of 10 cm × 10 cm × 10 cm is filled with scanned beams to deliver a dose of 1 Gy. A reference ionization chamber is placed in a water phantom and the dose is measured in the centre of the field at a residual range of 5 g/cm<sup>2</sup>. As the dose model is able to predict the number of protons per gray required for any dose field, the monitor calibration

derived in the calibration procedure is valid as a global factor for one energy.

The reference dosimeters used are thimble ionization chambers with a  $^{60}\text{Co}$  calibration factor in terms of absorbed dose to water provided by the Swiss Federal Office of Metrology and Accreditation (METAS), a secondary standards dosimetry laboratory. Two reference systems with a calibration from the federal dosimetry laboratory are available:

- (a) An Exradin T2 chamber,  $0.5\text{ cm}^3$  with an A150 wall and a PTW Unidos electrometer;
- (b) A Farmer NE 2571 chamber,  $0.6\text{ cm}^3$  with a graphite wall and a Farmer NE 2570/A electrometer.

The absolute dose to water was calculated using the recommendations in ICRU Report 59 [2]. The ratio between the nominal dose value predicted by the therapy planning and the measured dose was then input as a correction factor in the dose calculation procedure of the therapy planning. To get a second and independent fluency calibration of the primary monitor, a Faraday cup was built in house. The cup, which has a diameter of 12 cm, was made of copper and has a guard ring and a magnetic field to minimize secondary electron effects. The charge produced by a proton pencil beam within the Faraday cup was measured and a second monitor calibration was calculated.

### 2.3. Results

Table I shows the results of the two calibration procedures of the beam monitor (in protons per MU) at different energies of the incident protons. The one sigma standard deviation (SD) of the Faraday cup and ionization chamber data is 0.5%. The ionization measurement was carried out with the Exradin T2 reference chamber. The measurements show a good agreement, with a variation of the order of 1% between the two methods. This is mainly due to the fact that a small uncollimated pencil beam is used; in addition, there is no requirement to know the beam area in the Faraday cup.

The ICRU recommendations were used at the PSI for dose determination up to 2001. The doses measured with the two reference systems, however, differ by more than 2% unless a chamber perturbation correction for the NE 2571  $^{60}\text{Co}$  calibration is applied; this modification is recommended in Ref. [3].

The IAEA code of practice in Technical Reports Series No. 398 (TRS 398) [4] takes into account this chamber specific correction in the quality factor  $k_Q$  and introduces  $W_{\text{air}}$ , based on a detailed analysis of the available data. It was therefore decided to use the IAEA recommendations in 2002.

TABLE I. MEASURED MONITOR CALIBRATION DATA FOR FOUR PROTON ENERGIES

Proton energy (MeV)	Faraday cup (protons/MU)	Ionization chamber (protons/MU)	Ratio Faraday cup/ ionization chamber
138	6555	6473	1.012
160	7333	7333	1.00
177	7921	7984	0.992
214	8983	9136	0.983

Table II shows dose measurements carried out in 2002 using the two PSI reference chambers. The data taken at the residual range ( $R_{\text{res}}$ ) and calculated using TRS 398 are very consistent: the dose values are within 0.3%. The same measurements calculated in accordance with the ICRU recommendations illustrate the difficulties that this protocol has with different ionization chambers: the dose shift due to the protocol change is approximately 1%.

All the monitor calibration data have been measured using a water phantom, as is recommended. However, as some of the quality assurance measurements were carried out in a Perspex phantom, it was of interest to find out the effect of these phantom materials on dose measurements. The effect on the dose measured in the centre of a 10 cm  $\times$  10 cm  $\times$  10 cm field when as much as 24 cm of water (214 MeV) was replaced by the corresponding amount of Perspex was less than 0.5%. A large calibration dose field is used, so as not to be sensitive to the size of the halo produced by nuclear reaction products in the centre of the field. Care must be taken when using only small fields or pencil beams, as has been shown in Ref. [5].

### 3. PROCEDURES FOR QUALITY CONTROL IN SCANNED BEAM DOSIMETRY

A precise and safe application of the spot scanning fields requires an extensive and regular check of the whole irradiation system. The dosimetric procedures introduced to check that the dose delivery is accurate in both dose and location are described below.

#### 3.1. Yearly procedures

The yearly procedures include a check of the beam characteristics of each beamline tune, a calibration of the whole dosimetry system and a check of the



TABLE II. ABSORBED DOSE TO WATER, MEASURED USING TWO DOSIMETERS

Energy (MeV)	$R_{\text{res}}$ (g/cm <sup>2</sup> )	ICRU Report 59		TRS 398	
		Exradin T2 (Gy)	NE 2571 (Gy)	Exradin T2 (Gy)	NE2571 (Gy)
138	5	1.016	0.992	1.004 (SD 0.2%)	1.003 (SD 0.1%)
	3	—	—	0.996 (SD 0.3%)	0.993 (SD 0.1%)
177	5	1.008	0.982	0.992 (SD 0.4%)	0.993 (SD 0.1%)
	7	—	—	0.993 (SD 0.3%)	0.993 (SD 0.1%)

performance of the scanning system in terms of dose linearity and dose rate dependence. Doses are measured with a thimble ionization chamber placed in the centre of a geometrical field. The relative deviation as planned versus the measured dose is less than 0.5% in the dose range of 0.2 Gy to 10 Gy. Changing the dose rate by a factor of three results in a deviation from the nominal dose of less than 1%.

### 3.2. Half-yearly procedures

The calibration of the main dose monitor is checked every half-year using the reference ionization chamber. In addition, also at a half-yearly interval, the phase space of the beam tunes is measured, using a fluorescent screen placed at various distances from the nozzle and a charged coupled device (CCD) camera to look at the screen.

### 3.3. Weekly procedures

Once a week one patient irradiation field is applied to a stack of Perspex plates with X ray films in between. This allows a qualitative three dimensional check of the outline and range of the dose distribution.

### 3.4. Daily procedures

The daily quality control of the system takes about 30 min. This includes the machine set-up, safety and system tests and a dosimetry quality assurance procedure with the following steps:

- (a) The measurement of the dose rate and monitor ratios of the pencil beam.
- (b) A check of the performance of the beam position monitors. The beam position is measured with two orthogonal strip ionization chambers placed behind the dose monitor chambers.
- (c) The measurement of a depth dose curve of a pencil beam using a parallel-plate, 8 cm diameter chamber. The depth is modified using the range shifter plates. The measured range is within 0.5% (SD) of the nominal range.
- (d) The measurement of the dose when a geometrical proton field is applied using the scanning system. The dose is measured with Exradin T2 chambers, one in the centre of the field and one at the distal fall-off.

Figure 1 shows the daily measured doses in the centre of a homogeneous volume of 6 cm × 6 cm × 6 cm during the last beam period. The energy and the gantry angle (−90°, 0°, 90°) are regularly swapped. The data taken from the last beam period are very reproducible and stable and exhibit an SD of less than 1%.

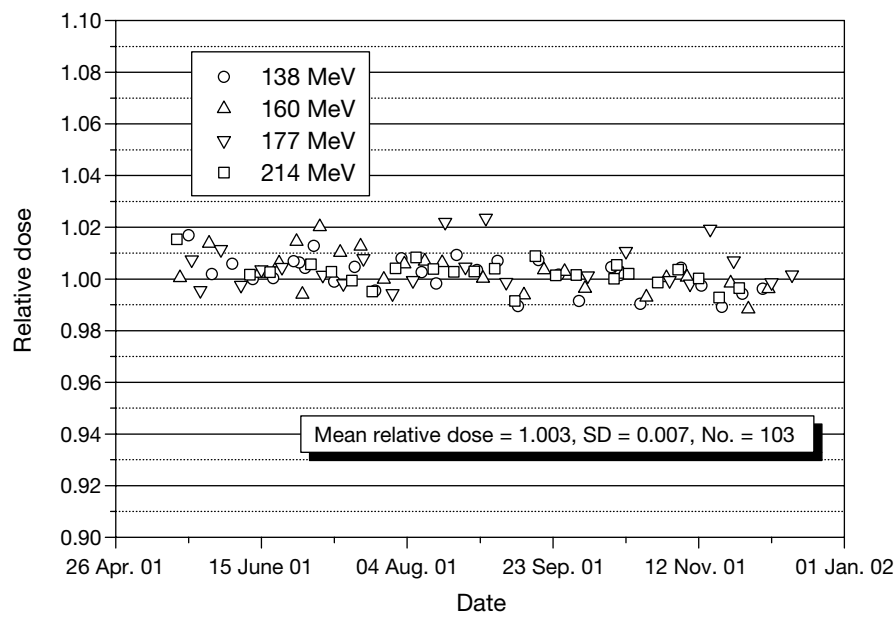


FIG. 1. Dose measured daily in the centre of a 6 cm × 6 cm × 6 cm box.

### 3.5. Procedures before first delivery

Before the first delivery of a new field to the patient, the dose distribution is checked, using a water phantom with an array of ionization chambers. The thickness of the water column can be set to the required depth of measurement. The array is made of a cross of  $2 \times 13$  cylindrical ionization chambers ( $0.08 \text{ cm}^3$ ). The water phantom is irradiated, using the same steering data as for the patient treatment. The measured dose profiles are then compared with the dose distribution recalculated by the therapy planning system when using a homogeneous medium instead of the patient CT data.

Figure 2 shows two orthogonal dose profiles taken during a routine patient verification. The solid line represents the calculated profile, the crosses show the measured doses. The routine dosimetry with ionization chambers agrees well with the expected dose from the therapy plan. The overall dose error for one year is 0.7% (SD 2%). Some minor systematic effects, due to nuclear reactions in the range shifter plates, have been observed for small fields.

The PSI CCD based dosimetry system, which uses a scintillating screen, has been used to study complex dose distributions and details of the pencil beam scanning. This experience has shown that this two dimensional device has an excellent position resolution and that a precise and fast overview of the

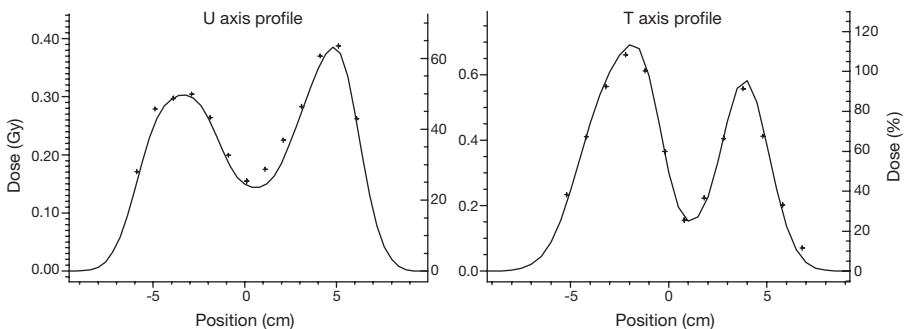


FIG. 2. Verification of patient treatment. The calculated orthogonal dose profiles and the data points measured using the cross-array are plotted.

three dimensional dose distribution is possible. A small correction for the quenching effect of the scintillator is applied. It is planned to use this instrument in the future at the PSI for routine dosimetry, together with a built-in ionization chamber to provide an absolute calibration of the dose profiles.

#### 4. CONCLUSIONS

TRS 398 has been used for dosimetry on the scanned proton beam at the PSI. The formalism was used for two ionization chambers made of completely different materials and has given identical results. The implementation of regularly repeated dosimetry intercomparisons within the proton user community would increase the consistency in absorbed dose delivered and be of a benefit for all patients. The method of the dosimetric verification of patient plans used at the PSI is time consuming and gives only a limited view of a dose distribution. The authors are still looking for a simple and reliable way to acquire the whole three dimensional information in one go.

#### REFERENCES

- [1] PEDRONI, E., et al., The 200-MeV proton therapy project at the Paul Scherrer Institute: Conceptual design and practical realization, *Med. Phys.* **22** (1995) 37–53.
- [2] INTERNATIONAL COMMISSION ON RADIATION UNITS AND MEASUREMENTS, Clinical Proton Dosimetry, Part I: Beam Production, Beam Delivery and Measurement of Absorbed Dose, Rep. 59, ICRU, Bethesda, MD (1999).
- [3] MEDIN, J., ANDREO, P., VINCKIER, S., Comparison of dosimetry recommendations for clinical proton beams, *Phys. Med. Biol.* **45** (2000) 3195–3211.
- [4] INTERNATIONAL ATOMIC ENERGY AGENCY, Absorbed Dose Determination in External Beam Radiotherapy, Technical Reports Series No. 389, IAEA, Vienna (2001).
- [5] SCHNEIDER, U., et al., “The water equivalence of solid materials used for dosimetry with small proton beams”, Annual Meeting of the Deutsche Gesellschaft für Medizinische Physik, Gmunden, Austria, 2002 (abstract).

# **DOSIMETRY OF $^{12}\text{C}$ ION BEAMS AT THE GERMAN HEAVY ION THERAPY FACILITY: COMPARISON OF THE CURRENTLY USED APPROACH AND TRS 398**

O. JÄKEL, G.H. HARTMANN, P. HEEG, C.P. KARGER

Department of Medical Physics, Deutsches Krebsforschungszentrum,  
Heidelberg, Germany

E-mail: o.jaekel@dkfz.de

## **Abstract**

A radiotherapy unit using a scanned  $^{12}\text{C}$  beam and an active energy variation of the synchrotron has been in operation at the German heavy ion research centre (GSI) since 1997. A code of practice for carbon ions was developed at the Deutsches Krebsforschungszentrum (DKFZ) for the clinical dosimetry of thimble ionization chambers calibrated in terms of dose to water, and a  $k_Q$  factor for  $^{12}\text{C}$  was derived, which was very similar to the new IAEA code of practice in Technical Reports Series No. 398 (TRS 398). The differences in measured doses using both codes of practice are below 0.8% for Farmer type chambers. A conceptual difference arises from the reference conditions for dosimeters. A reference depth of 7 mm in a plastic material in a monoenergetic beam is used at the GSI. This eliminates a number of uncertainties arising in measurements within the dynamically generated spread out Bragg peak of carbon ions. Measurements also indicate that the saturation correction discussed in TRS 398 for ions is not always well suited. In the near future TRS 398 will be implemented at the German ion therapy facility, although with small adaptations.

## **1. INTRODUCTION**

A radiotherapy unit using a  $^{12}\text{C}$  beam started treating patients at the German heavy ion research centre, the GSI (Gesellschaft für Schwerionenforschung), in December 1997. A magnetic beam scanning system is used for beam shaping, together with an active variation of the synchrotron energy [1], which enables a three dimensional modulation of the dose in the target to be achieved. For the purpose of clinical dosimetry a code of practice (CoP) for carbon ions was developed at the Deutsches Krebsforschungszentrum (German cancer research centre, DKFZ). This CoP was developed for thimble ionization chambers calibrated in terms of dose to water and incorporates most of the suggestions made in the IAEA code of practice in Technical Reports Series No. 398 (TRS 398), which covers heavy ion beams. There are, however, a number of differences, which are outlined in this paper.

## 2. DOSIMETRIC APPROACH USED CURRENTLY AT THE GSI RADIOTHERAPY FACILITY

The CoP developed at the DKFZ for carbon ions [2] is based on the use of thimble type ionization chambers calibrated in terms of dose to water in a field of  $^{60}\text{Co}$  gamma rays ( $N_{D,w,\text{Co60}}$ ). The calibration can be traced to the Physikalisch-Technische Bundesanstalt (PTB).

The absorbed dose to water at the effective point of measurement,  $P_{\text{eff}}$ , of the chamber in an ion beam is determined by:

$$D_w(P_{\text{eff}}) = M_{\text{corr}} N_{D,w,\text{Co60}} k_Q$$

where  $M_{\text{corr}}$  is the dosimeter reading  $M$ , corrected for changes in air density,  $p_\rho$ , incomplete saturation,  $p_{\text{sat}}$ , and polarity effects of the chamber,  $p_{\text{pol}}$ :

$$M_{\text{corr}} = M p_\rho p_{\text{sat}} p_{\text{pol}}$$

The calibration factor,  $N_{D,w,\text{Co60}}$ , is given by the manufacturer.  $k_Q$  is a chamber specific factor that corrects for the different beam quality of  $^{12}\text{C}$  ions and the calibration quality ( $^{60}\text{Co}$ ). This formulation followed a suggestion by Medin et al. [3] and is in accordance with TRS 398.

### 2.1. Correction factors

#### 2.1.1. Correction for air density

The correction for air density is derived using a radioactive check source ( $^{90}\text{Sr}$ ). From the ratio of the measured charge given in the certificate of the chamber,  $M_K$ , and the measurement at the actual date,  $M_m$ , and a decay factor for the radioactive decay of the check source in the time,  $t$ , elapsed between the certification and measurement, the correction is:

$$p_\rho = (M_K / M_m) \exp[-\ln 2(t / T_{1/2})]$$

The resulting correction is then identical to the one given in TRS 398 using direct measurements of temperature and pressure.

#### 2.1.2. Saturation and polarization correction

Although a pulsed and scanning beam is used at the GSI, it was assumed that the correction method for continuous radiation applied, owing to: (a) the

slow accelerator extraction mode, which has pulses of about 1 s duration; and (b) the scanning keeping the beam stable at each spot for several milliseconds, which is far more than the average transit times of the ions in the chamber.

Measurements of the saturation effects were performed at voltages of between 50 V and 400 V. Figure 1 shows the results for the Farmer chamber at 100 MeV/u (MeV per nucleon) energy, using a flux of  $10^8 \text{ s}^{-1}$ . The chambers were placed at a depth of 7 mm, where the linear energy transfer (LET) was 300 MeV/cm. The data are well described by a quadratic fit, which leads to the conclusion that the conditions for continuous radiation are met. The determined saturation corrections for the Farmer, Wellhöfer IC 03 and Exradin T1 chambers were all very small ( $\leq 0.2\%$ ). Using the formula for pulsed radiation, as suggested in TRS 398,  $p_{\text{sat}}$  is around 1.01 for the Farmer chamber.

To investigate the effect of initial recombination, a Roos chamber was irradiated using different angles between the chamber and the beam (250 MeV/u, LET = 150 MeV/cm). The resulting saturation correction at this moderate LET is consistent with unity within the uncertainties of the measurement. The measured polarity corrections for thimble chambers are also consistent with unity.

### 2.1.3. Effective point of measurement

The effective point of measurement for thimble type chambers was determined [4] by a comparison of measured depth dose curves for a Farmer chamber and a plane-parallel chamber (Markus chamber), for which it was

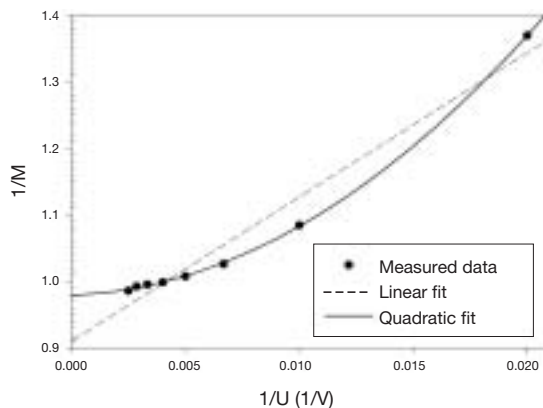


FIG. 1. Data for the saturation effect (Farmer chamber M30001-1023).

assumed that the point of measurement of the plane-parallel chamber was known. The resulting depth dose for the thimble chamber was calculated using an averaging of depth dose values over the curved inner surface of the chamber. The resulting  $P_{\text{eff}}$  was 0.72 of the inner radius of the chamber, with an uncertainty of 10%. TRS 398 suggests a value of 0.75 of the inner radius.

## 2.2. $k_Q$ values

As in TRS 398, the  $k_Q$  factor was calculated theoretically in accordance with:

$$k_Q = \frac{(w_{\text{air}}/e)^{\text{C12}}}{(w_{\text{air}}/e)^{\text{Co60}}} \frac{\bar{s}_{w,\text{air}}^{\text{C12}}}{(\bar{L}/\rho)_{w,\text{air}}^{\text{Co60}}} \frac{p^{\text{C12}}}{p^{\text{Co60}}}$$

which is a product of the ratios of the  $w$  values, the stopping power ratios water to air and the chamber specific perturbation factors for  $^{12}\text{C}$  and  $^{60}\text{Co}$ , respectively. The calculation of the stopping power ratio has to take into account not only the fluence of primary carbon ions but also the fragments that arise from nuclear interactions (mainly target fragmentation with  $Z = 1-5$ ), and also their energy distribution. It was found in Ref. [2] that for energies above 10 MeV/u an average constant value of 1.13 can be used. This leads to an uncertainty in dose determination of below 2%.

The  $w$  value in Ref. [2] was adopted from an International Commission on Radiation Units and Measurements recommendation for protons of 34.8 eV [5]. A compilation of the available data for protons, alpha particles and ions leads to an uncertainty in dose of 4%, if this value is also adopted for  $^{12}\text{C}$  ions [2].

The perturbation factor,  $p$ , for the different beam qualities includes all departures from ideal Bragg–Gray detectors (i.e. the correction for cavity effects, the displacement factor, and the effects from the chamber wall and central electrode). The value of  $p^{\text{Co60}}$  in Ref. [2] was adopted from Refs [6, 7] and accounts for the cavity and wall correction factors for  $^{60}\text{Co}$  radiation. The corrections for the central electrode and the displacement were taken to be unity. The combined correction of cavity effects and the effects of the chamber wall and central electrode for a Farmer chamber in a  $^{12}\text{C}$  ion beam were set to unity, since no data exist that indicate a significant deviation from unity. Since this assumption is made for protons [3], it is justified also for heavy ions, for which the range of secondary electrons is even shorter. A displacement correction is not necessary for ions, as the depth of reference is replaced by the effective point of measurement.



TABLE I. COMPARISON OF THE DIFFERENT NUMERICAL VALUES USED IN THE CALCULATION OF  $k_Q$  FACTORS FOR THE FARMER CHAMBER M30001 IN REF. [2] AND TRS 398

Parameter	$(w/e)^{C12}$ (J/C)	$(w/e)^{Co60}$ (J/C)	$\bar{s}_{W,L}^{C12}$	$(\bar{L}/\rho)_{W,L}^{Co60}$	$P^{C12}$	$p^{Co60}$ (M30001)	$k_Q$ (M30001)
Ref. [2]	34.8 [5]	33.77 [5]	1.13 [8]	1.133 [6]	1.0	0.994 [7]	1.034
TRS 398	34.5	33.97	1.13	1.133	1.0	0.982	1.031

### 2.3. Calibration procedure and reference conditions

The depth dose distribution can be actively modulated at the GSI by the use of an energy variation of the synchrotron, and a spread out Bragg peak (SOBP) is produced from a superposition of many energies with different weights. The weights are optimized individually for each field in order to achieve a homogeneous biological effect in the target volume. The SOBP therefore looks different at every scan point in every field. The plateau region of the depth dose was consequently chosen as the reference depth for dosimetry. The beam monitors are then calibrated in terms of particle number at different energies. As a reference, the measurement is performed with a Farmer type ionization chamber (a PTW M30001) in a water equivalent phantom material (PTW RW3) at a depth of 7 mm. The phantom is positioned in the isocentre and irradiated with a 5 cm × 5 cm scanned field.

## 3. DOSE MEASUREMENTS

Differences in dose measurements arise mainly with the different CoPs from the values of  $k_Q$  and the saturation correction,  $p_{sat}$ . Doses measured in an SOBP will depend crucially on the validity of the calibration performed in the plateau. Measurements were performed with different Farmer chambers in the plateau region using a 250 MeV/u carbon ion field of 5 cm × 5 cm size, with the chambers positioned at a depth of 7 mm. The Exradin T1 was used in addition for the SOBP measurement, for which the measuring depth was 12 cm in the centre of a 5 cm SOBP. To test the influence of the phantom medium, the measurement in the SOBP was repeated in water with the waterproof Farmer chamber using a depth scaled with the range. The results obtained with the two CoPs are shown in Table II.

TABLE II. COMPARISON OF DOSES OBTAINED WITH DIFFERENT CHAMBERS IN THE PLATEAU REGION (250 MeV/u) AND IN A 5 cm SOBP OBTAINED WITH THE TWO CoPs

	Energy = 250 MeV/u, plateau			Centre of the SOBP, 12 cm depth				
	PTW 30001	PTW 30002	PTW 30006	PTW 30001	PTW 30002	PTW 30006	Exradin T1	30006 in water
TRS 398	1.005	1.0	0.991	1.002	0.989	0.985	0.991	1.000
Ref. [2]	1.000	1.012	0.999	0.998	0.985	0.980	1.02	0.995
TRS 398/ Ref. [2]	1.005	0.988	0.992	1.004	1.004	1.005	0.972	1.005

**Note:** The data were taken in RW3 water equivalent material (for the plateau), PMMA (polymethylmethacrylate) (for the SOBP) and water (data in the last column). The values in the plateau are normalized to the PTW 30002 for TRS 398.

## 4. DISCUSSION

### 4.1. Comparison between the procedures

Since the CoP presented in Ref. [2] was developed from a suggestion by Medin et al. [3] and Vatnitsky et al. [6], it is nearly identical to TRS 398. Differences arise mainly from the numerical values for the calculation of  $k_Q$  and from the saturation correction,  $p_{\text{sat}}$ . Other differences are more conceptual, such as the chosen reference conditions.

The relative deviation of the numerical value of  $k_Q$  for the Farmer chamber (M30001) in Ref. [2] and in TRS 398 is only 0.3%. This small difference, however, results from a cancellation of differences in the  $w$  value and the perturbation factor,  $p^{\text{Co60}}$ . The value of  $p^{\text{Co60}} = 0.982$  in TRS 398 is dominated by the value of the displacement correction of 0.988, while the combined wall and central electrode perturbation factor is 0.994 (the cavity perturbation factor is unity). The value of  $p^{\text{Co60}} = 0.994$  in Ref. [2] does not include a displacement correction.

The differences in measured doses are below 1% for the Farmer chamber, for which the slightly smaller value of  $k_Q$  in TRS 398 is partially compensated by a larger value for  $p_{\text{sat}}$ . The difference for the Exradin T1 is nearly 3%, which is due to the different values for  $p^{\text{Co60}}$  (0.992 in Ref. [7] versus 1.005 in TRS 398).

The dose in the SOBP was calculated to be 1 Gy, using the calibration in the plateau region. The measured doses are thus a measure of the quality of this calibration. The measured doses for the Farmer chamber agree within 1.5% with this value. The dose measured in water is 1.5% higher than in the PMMA phantom and deviates only 0.5% from the calculated dose. This difference of 1.5% in dose measured in water and PMMA may be due to fluence variations, which were not considered.

## 4.2. Conclusion and outlook

The suggested reference conditions for heavy ion beams in TRS 398 are to measure in water in the centre of an SOBP. This is suitable for a facility with passive range modulation, but not for an active modulation system, for which the shape of the SOBP differs at each scan spot of each patient. Furthermore, additional uncertainties are introduced if the SOBP is a superposition of a finite number of fixed energy beams with different intensities. Owing to the discrete energies and variations in the intensities, such an SOBP is never absolutely continuous and reproducible. Furthermore, the dosimetric uncertainties in the SOBP, with its mixture of energies and low and high LET components, are larger than in the entrance region. Also, the fluence corrections for a plastic material should decrease with smaller depths of measurement, as observed for protons [9]. The authors therefore think that measurements in a plastic material in the entrance region of the depth dose are suitable as a reference for an active beam delivery system.

Another difference between TRS 398 and the approach the authors have taken is in the handling of saturation corrections. In contrast with TRS 398, the authors do not think that the conditions for a pulsed scanned beam are fulfilled for the GSI scanned beam. The measurements match better with the conditions for a continuous beam. Furthermore, initial recombination does not necessarily play a role, even for a plane-parallel chamber, as was demonstrated by measurements with only moderate LET values.

The authors will certainly apply the recommendations of TRS 398 for carbon ions in the near future for dosimetry at the German carbon ion facility; the reference conditions chosen in Ref. [2], however, will be kept. Further systematic studies will be performed on the recombination effects.

To improve the knowledge of  $w$  values for ions, measurements are currently being performed by the GSI. First measurements resulted in a preliminary value of 34.2 J/C, with an uncertainty of 3% [10] for carbon ions at an energy of 7.6 MeV/u. Ionization chamber dosimetry will also be checked against a water calorimeter run by the PTB.

## ACKNOWLEDGEMENTS

The work was funded in part by the strategy fund of the Helmholtz-Gemeinschaft Deutscher Forschungszentren, under grant number 01SF9906/1.

## REFERENCES

- [1] HABERER, T., BECHER, W., SCHARDT, D., KRAFT, G., Magnetic scanning system for heavy ion therapy, Nucl. Instrum. Methods A **330** (1993) 296–305.
- [2] HARTMANN, G.H., JÄKEL, O., HEEG, P., KARGER, C.P., KRIEBBACH, A., Determination of water absorbed dose in a carbon ion beam using thimble ionization chambers, Phys. Med. Biol. **44** (1999) 1193–1206.
- [3] MEDIN, J., et al., Ionization chamber dosimetry of proton beams using cylindrical and plane parallel chambers.  $N_w$  versus  $N_k$  ion chamber calibrations, Phys. Med. Biol. **40** (1995) 1161–1176.
- [4] JÄKEL, O., HARTMANN, G.H., HEEG, P., SCHARDT, D., Effective point of measurement of cylindrical ionization chambers for heavy charged particles, Phys. Med. Biol. **45** (2000) 599–607.
- [5] INTERNATIONAL COMMISSION ON RADIATION UNITS AND MEASUREMENTS, Clinical Proton Dosimetry. Part I: Beam Production, Beam Delivery and Measurement of Absorbed Dose, Rep. 59, ICRU, Bethesda, MD (1998).
- [6] VATNITSKY, S.M., SIEBERS, J.V., MILLER, D.W.,  $k_Q$  factors for ionization chamber dosimetry in clinical proton beams, Med. Phys. **23** (1996) 1–7.
- [7] AMERICAN ASSOCIATION OF PHYSICISTS IN MEDICINE TASK GROUP 21, A protocol for the determination of absorbed dose from high-energy photon and electron beams, Med. Phys. **10** (1983) 741–771.
- [8] INTERNATIONAL COMMISSION ON RADIATION UNITS AND MEASUREMENTS, Stopping Powers for Protons and Alpha Particles, Rep. 49, ICRU, Bethesda, MD (1993).
- [9] PALMANS, H., et al., Fluence correction factors in plastic phantoms for clinical proton beams, Phys. Med. Biol. **47** (2002) 3055–3071.
- [10] RODRIGUEZ-COSSIO, J., et al., W-value Measurements for Carbon Ions, GSI Scientific Rep. 2000, GSI, Darmstadt, Germany (2001).

# PROTON DOSIMETRY INTERCOMPARISON USING PARALLEL-PLATE IONIZATION CHAMBERS IN A PROTON EYE THERAPY BEAM

A. KACPEREK\*, E. EGGER\*\*, L. BARONE TONGHI\*\*\*,  
G. CUTTONE\*\*\*, L. RAFFAELE\*\*\*, A. ROVELLI\*\*\*,  
M.G. SABINI\*\*\*, P. TABARELLI DE FATIS<sup>+</sup>,  
F. LURASCHI<sup>+</sup>, L. MARZOLI<sup>+</sup>

\* Clatterbridge Centre for Oncology, Wirral, United Kingdom  
E-mail: andrzej.kacperek@ccotrust.nhs.uk

\*\* Paul Scherrer Institute, Villigen, Switzerland

\*\*\* INFN-Laboratori Nazionali del Sud, Catania, Italy

<sup>+</sup>TERA-Fondazione per Adroterapia Oncologica, Novara, Italy

## Abstract

A four centre proton dosimetry intercomparison was performed at the Paul Scherrer Institute on the OPTIS 63 MeV clinical beam in order to compare results for four Markus ionization chambers and six cylindrical chambers. The local reference ionization chambers had calibration factors obtained either directly from a standards laboratory or by a cross-calibration against a secondary standard chamber, traceable to an accredited standards laboratory. The absorbed dose to air chamber factors for the Markus chambers,  $N_{D,air,Q_0}^{pp}$ , were obtained by comparison with reference chambers in high energy electron or  $^{60}\text{Co}$  beams. The proton dosimetry comparison was performed in two proton beam conditions: at full incident energy (corresponding to the entrance dose of the pure Bragg peak) and at a depth of 15 mm in a fully modulated beam. The International Commission on Radiation Units and Measurements Report 59 recommendations were extended to parallel-plate chambers to derive the absorbed dose to water. The results showed a standard deviation of less than 1% for both beam conditions for all chambers, and a maximum difference of approximately 3%. The Markus chamber group, however, showed a difference in the mean dose of approximately 1.1% from the thimble chamber group, for both beam conditions.

## 1. INTRODUCTION

One of the most successful treatments with proton beams is their use on tumours of the eye, especially choroidal melanomas [1]. Clinical proton beams

used for this treatment are characterized by their short range (less than 35 mm), steep dose gradients (1–2 mm distal, 1.5–3 mm lateral at 90–10% dose) [2], relatively narrow fields (diameter smaller than 30 mm) and high dose rates (10–40 Gy/min). Proton dosimetry protocols [3–5] suggest that small volume cylindrical ionization chambers, including the Far West Technology (FWT) IC-18 and the Exradin T1 chambers, may be used for the calibration of eye therapy beams. The caps of these chambers are, however, made of A150, a hygroscopic material, and the relatively large volume limits their use in smaller fields and at modulation depths (the constant dose region created by the spread out Bragg peak).

The treatment of small posterior tumours and superficial iris lesions, which requires very restricted modulations, has posed a particular measurement problem (Fig. 1). The design of parallel-plate Markus chambers makes such chambers eminently suitable for proton beams, since their thin windows permit measurement at surfaces and near steep depth dose gradients. Parallel-plate chambers are also unlikely to be subject to perturbation effects. Proton dosimetry protocols [3–6], however, do not offer methods for the calibration of parallel-plate chambers in proton beams (this study was performed prior to the publication of Ref. [7]). The objective of this work was to compare the absorbed dose to water values for cylindrical and parallel-plate chambers. To perform such a comparison the International Commission on Radiation Units and Measurements (ICRU) Report 59 recommendations were extended for parallel-plate chambers using the formalism proposed by Medin et al. [8]. Each

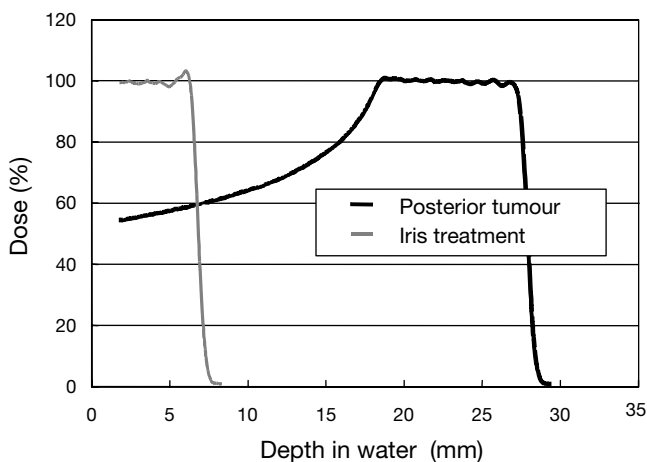


FIG. 1. Typical proton depth doses for eye therapy (at the CCO).

participating centre used different measurement techniques to obtain absorbed dose to air calibration factors,  $N_{D,air,Q_0}^{pp}$ , for the Markus chambers.

## 2. MATERIALS AND METHODS

### 2.1. Reference calibration of chambers used in the study

The Markus chambers are of the PTW M23343 (or NE 2534D) type. The 0.055 cm<sup>3</sup> nominal sensitive volume is enclosed by a graphite coated CH<sub>2</sub> window (which has a diameter of 6 mm and a thickness of 0.0023 g/cm<sup>2</sup>). The collecting electrode has a diameter of 5.4 mm. Details of the cylindrical chambers used in this study are given in Refs [4, 9]. The Clatterbridge Centre for Oncology (CCO) and the Terapia con Radiazioni Adroniche (TERA) used Keithley 617 and 6517 electrometers, respectively, while the Paul Scherrer Institute (PSI) and the Istituto Nazionale di Fisica Nucleare Laboratori Nazionali del Sud (INFN-LNS) used PTW Unidos 10001 instruments. The Markus chambers were biased at +300 V (the CCO used +270 V).

Each centre had at least one cylindrical chamber calibrated in terms of air kerma and traceable to an accredited standards laboratory, as summarized in Table I. The PSI and INFN-LNS cylindrical chambers were calibrated by the PTW in a <sup>60</sup>Co beam. The CCO and TERA calibrated their cylindrical

TABLE I. METHODS OF CROSS-CALIBRATION FOR MARKUS CHAMBERS

	PSI	CCO	INFN-LNS	TERA
Reference cylindrical chamber	PTW 30001	NE 2561	PTW 30001	NE 2561
Traceability	PTW-Freiburg	National Physical Laboratory	PTW-Freiburg	LMRI <sup>d</sup>
Method <sup>a</sup>	<sup>60</sup> Co, in air	<sup>60</sup> Co, in a phantom <sup>b</sup>	Electrons, 20 MeV, in a phantom <sup>c</sup>	Electrons, 20 MeV, in a phantom <sup>c</sup>

<sup>a</sup> Method for calibrating a Markus chamber in a reference beam [9].

<sup>b</sup> In polymethylmethacrylate (PMMA) at a depth of 5 cm.

<sup>c</sup> In water or PMMA at the reference depth.

<sup>d</sup> Laboratorio di Metrologia delle Radiazioni Ionizzanti.

chamber against a secondary standard in a  $^{60}\text{Co}$  beam. The  $N_k$  values for cylindrical chambers were converted to absorbed dose to air factors,  $N_{D,\text{air}}$ , using chamber dependent parameters described in Technical Reports Series No. 277 [4]. The Markus chambers were cross-calibrated against cylindrical chambers in  $^{60}\text{Co}$  and high energy electron beams, as shown in Table I.

The absorbed dose to water in the clinical proton beam,  $D_{w,Q}$ , is related to the absorbed dose to air chamber air factor,  $N_{D,\text{air},Qo}^{\text{PP}}$ , determined at a reference quality beam,  $Q_o$ , as follows [8, 9]:

$$D_{w,Q} = M_Q N_{D,\text{air},Qo}^{\text{PP}} \left[ (W_{\text{air}})_Q / (W_{\text{air}})_{Qo} \right] (s_{w,\text{air}})_Q p_Q \tag{1}$$

where

- $(s_{w,\text{air}})_Q$  is the water to air proton stopping power ratio in the user’s beam;
- $M_Q$  is the electrometer charge reading per monitor unit (MU), with influence corrections;
- $p_Q$  is the the product of the proton perturbation factor.

$p_Q$  values were set to unity in this study, as suggested in Ref. [8]. The values of the physical parameters in Table II were obtained from Ref. [3].

2.2. Proton beams

2.2.1. Paul Scherrer Institute OPTIS proton therapy beam

The clinical beam was provided directly by a 72 MeV proton injector cyclotron, which is analysed effectively by two large bending magnets [1]. An upstream copper scattering foil limits the beam current, which is further scattered by a lead foil as it enters the treatment room, in order to provide beam

TABLE II. VALUES OF PHYSICAL PARAMETERS USED IN PROTON DOSE CALCULATIONS

$W_{\text{Co,air}}$	$W_{\text{proton,air}}$	$s_{w,\text{air},40\text{MeV}}$
33.77 J/C	34.8 J/C	1.134



homogeneity. Thus a nominal 63 MeV full energy proton beam and a 61.5 MeV fully modulated beam were available for the two irradiation conditions (Fig. 1).

### 2.3. Irradiation procedures

The chambers were irradiated at the isocentre, at a distance of 50 mm from a copper ovoid collimator (26 mm  $\times$  32 mm) that defined the beam area. Approximately 10 Gy was delivered in 5 s. All chambers were placed in the treatment room several hours before the irradiation. The beam area was scanned with a diode, laterally and vertically, to ensure dose homogeneity prior to each irradiation condition. Four proton measurements per chamber were made.

#### 2.3.1. Ionization chamber positioning

In order to confirm the spatial position of the chambers, Polaroid X ray films were exposed, using the patient positioning X ray sets, which enabled a positional reproducibility better than 1 mm. The Markus and FWT chambers were fitted into custom made PMMA holders for easier handling. The Markus waterproof caps (0.87 mm PMMA) were retained for the full energy irradiations, to approximate the cap thickness of the thimble chambers; no further corrections were made. The chambers were positioned in the fully modulated beam by the use of preabsorbers of 14.2 mm and 15 mm of PMMA for the thimble chambers and Markus chambers, respectively. No cap was placed on the Markus chambers when using the fully modulated beam.

### 2.4. Other chamber factors

The polarity correction factor [10],  $p_{\text{pol}}$ , was measured as 1.012 and 0.995 for the TERA and CCO Markus chambers, respectively, but was considered to be 1.000 by the PSI and INFN-LNS. The factors  $p_{\text{pol}}$  for the cylindrical chambers were found to be less than 0.2%. The proton saturation correction,  $p_s$ , was measured to be less than 0.2%, and thus was considered negligible for all the chambers.

## 3. RESULTS AND DISCUSSION

The proton dose determination results are shown in Table III. The differences between the maximum and minimum dose readings,  $\Delta_{\text{max}}$ , for the ten chambers were 3.2% and 2.7% for the unmodulated and modulated beams, respectively. The standard deviation was less than 1% for both irradiation

conditions. These values are of the same order as a previous large scale inter-comparison [11]. Each participating centre estimated the reproducibility of proton beam measurements better than 0.2%. The results are further summarized in Fig. 2 and Table IV. The standard deviations for each group of chambers and each irradiation condition were 1.06% or less, with maximum differences between 2.7% and 0.8%. The main observations are that: (a) the

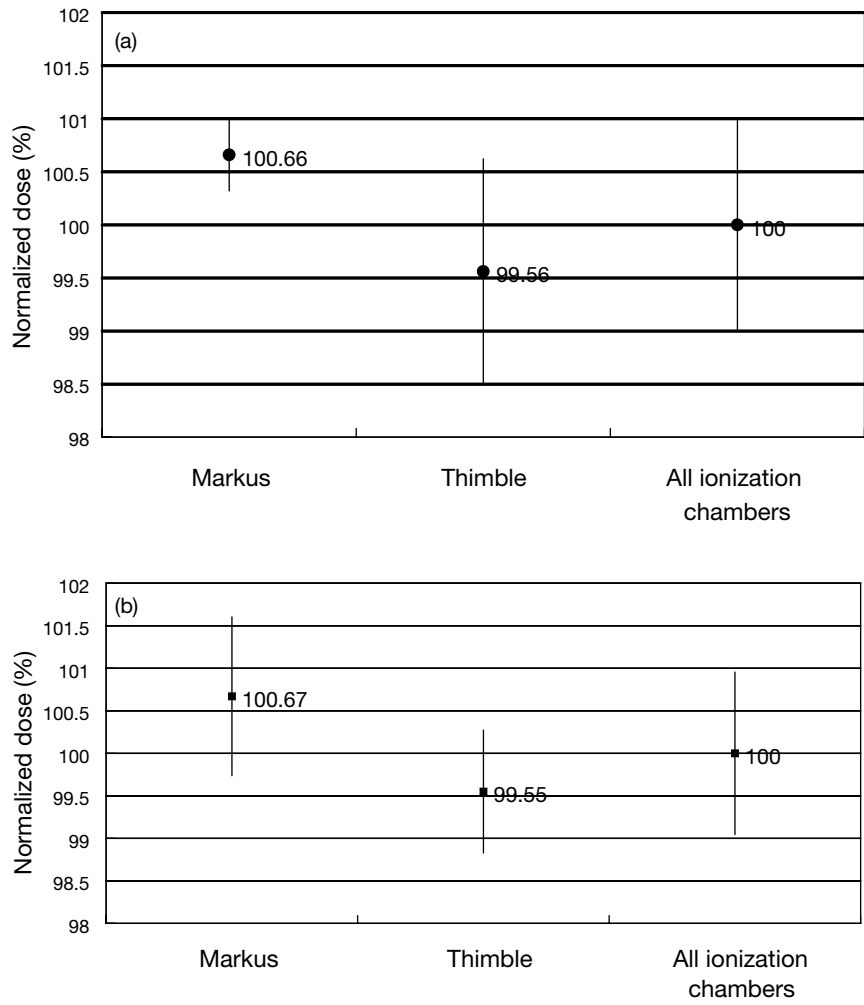


FIG. 2. Summary of comparison between groups of chambers for (a) modulated and (b) unmodulated proton beams. The bar length represents the standard deviation of an ionization chamber group and the centre of the bar indicates the mean per cent dose value.

TABLE III. INTERCOMPARISON DOSE RESULTS FOR MODULATED AND UNMODULATED PROTON BEAMS

Chamber type and number	Centre (country)	Unmodulated beam (cGy/1000 MU)	Modulated beam (cGy/1000 MU)
Markus No. 1036	PSI (Switzerland)	1015	1007.2
Markus No. 1916	CCO (United Kingdom)	1027.7	1003.4
Markus No. 2485	INFN-LNS (Italy)	1030	999.2
Markus No. 2824	TERA (Italy)	1038	1005
Exradin T1 No. 218	INFN-LNS (Italy)	1018	983
Exradin T1 No. 999	TERA (Italy)	1009	985
PTW 30001 No. 1371	PSI (Switzerland)	1015	1001.1
PTW 30001 No. 1384	INFN-LNS (Italy)	1026	991.4
FWT (IC-18) No. 683	CCO (United Kingdom)	1005.7	985
FWT (IC-18) No. 725	CCO (United Kingdom)	1022.4	1016.4

TABLE IV. SUMMARY OF INTERCOMPARISON DIFFERENCES BY BEAM CONDITION AND CHAMBER TYPE

		Proton irradiation condition	
		Unmodulated beam	Modulated beam
Standard deviation (%)	Markus	0.93	0.34
	Cylindrical	0.72	1.06
Maximum difference (%) ( $\Delta_{\max}$ )	Markus	2.25	0.80
	Cylindrical	1.99	2.69
Difference of means (%) (Markus–cylindrical)		1.12	1.10

standard deviation between the measurements appears to be less than  $\Delta_{\max}$ ; and (b) for both proton beam conditions the mean dose results are approximately 1% higher for the Markus chamber group than for the cylindrical chambers.

It is known that small volume chambers are more susceptible to slight beam inhomogeneities, such as tungsten cross-wires in the beam, than larger volume cylindrical chambers. Small differences in the positioning on the beam axis between Markus and cylindrical chambers were considered negligible [12]. It is suggested that: (a) the metal cross-wires, which are a feature of eye therapy

beams, should be withdrawn for such studies, or the small chambers should be systematically aligned off centre; and (b) if time permits, the mean reading of several positions of the chamber within the beam area should be taken (or at least the dose uncertainty due to the positioning of the Markus chambers should be ascertained).

The relatively small deviation of the Markus chambers results does not suggest differences in chamber specific values, differences that have been noted between other, similar chambers [9]. Also, the  $^{60}\text{Co}$  beam cross-calibration technique is subject to larger uncertainties than the high energy electron method [9], mainly due to the positioning of the cylindrical reference chamber. It would be of interest to revisit the intercomparison with all Markus chambers calibrated earlier in high energy electron beams to minimize variations due to perturbation factors and positional uncertainties.

#### 4. CONCLUSIONS

In spite of different measurement techniques for the estimation of  $N_{D_{\text{air},Q_0}}^{\text{pp}}$ , and the use of chamber calibrations traceable to different standards laboratories, the proton dose results show reasonable agreement within a 1% standard deviation, and within a  $\pm 1.5\%$  maximum difference. These results support the use of Markus chambers as instruments for the calibration of proton eye therapy beams. However, a single intercomparison provides only a spot check for gross differences, not a final check. Definitive checks of small inconsistencies, for example in chamber positioning and polarity effects, would require further intercomparisons.

#### REFERENCES

- [1] EGGER, E., ZAGROFOS, L., PERRET, C., GAILLOUD, C., "Proton beam irradiations of choroidal melanomas at the PSI: Techniques and results", Medical Radiology — Radiotherapy of Intraocular and Orbital Tumors (ALBERTI, W.E., SAGERMAN, R.H., Eds), Springer-Verlag, Berlin and Heidelberg (1993) 57–72.
- [2] KACPEREK, A., "Ophthalmological proton facilities", Ion Beams in Tumour Therapy (LINZ, U., Ed.), Chapman & Hall, London (1995) 360–370.
- [3] INTERNATIONAL COMMISSION ON RADIATION UNITS AND MEASUREMENTS, Clinical Proton Dosimetry. Part I: Beam Production, Beam Delivery and Measurement of Absorbed Dose, Rep. 59, ICRU, Bethesda, MD (1998).

- [4] INTERNATIONAL ATOMIC ENERGY AGENCY, Absorbed Dose Determination in Photon and Electron Beams, Technical Reports Series No. 277, IAEA, Vienna (1987).
- [5] VYNCKIER, S., BONNETT, D.E., JONES, D.T., Code of practice for clinical proton dosimetry, *Radiother. Oncol.* **20** (1991) 53–63.
- [6] VYNCKIER, S., BONNETT, D.E., JONES, D.T., Supplement to the code of practice for clinical proton dosimetry, *Radiother. Oncol.* **32** (1994) 174–179.
- [7] INTERNATIONAL ATOMIC ENERGY AGENCY, Absorbed Dose Determination in External Beam Radiotherapy, Technical Reports Series No. 398, IAEA, Vienna (2000).
- [8] MEDIN, J., et al., Ionization chamber dosimetry of proton beams using cylindrical and plane parallel plate chambers.  $N_w$  versus  $N_k$  ion chamber calibrations, *Phys. Med. Biol.* **40** (1995) 1161–1176.
- [9] INTERNATIONAL ATOMIC ENERGY AGENCY, The Use of Plane Parallel Ionization Chambers in High Energy Electron and Photon Beams, Technical Reports Series No. 381, IAEA, Vienna (1997).
- [10] INTERNATIONAL ATOMIC ENERGY AGENCY, Calibration of Dosimeters Used in Radiotherapy, Technical Reports Series No. 374, IAEA, Vienna (1994).
- [11] VATNITSKY, S., et al., Proton dosimetry intercomparison, *Radiother. Oncol.* **41** (1996) 169–177.
- [12] PALMANS, H., VERHAEGEN, F., On the effective point of measurement of cylindrical ionization chambers for proton beams and other heavy charged particle beams, *Phys. Med. Biol.* **45** (2000) L20–L22.

**BLANK**

## PROTON BEAM DOSIMETRY: PROTOCOL AND INTERCOMPARISON IN JAPAN

A. FUKUMURA\*, T. KANAI\*, N. KANEMATSU\*,  
K. YUSA\*, A. MARUHASHI\*\*.§, A. NOHTOMI\*\*, T. NISHIO\*\*\*,  
M. SHIMBO\*\*\*, T. AKAGI<sup>+</sup>, T. YANO<sup>+</sup>, S. FUKUDA<sup>++</sup>,  
T. HASEGAWA<sup>+++</sup>, Y. KUSANO<sup>+++</sup>, Y. MASUDA<sup>+++</sup>

\* Department of Medical Physics, Research Center for  
Charged Particle Therapy,  
National Institute of Radiological Sciences,  
Chiba  
E-mail: fukumura@nirs.go.jp

\*\* Proton Medical Research Center, University of Tsukuba,  
Tsukuba

\*\*\* National Cancer Center East, Kashiwa

<sup>+</sup> Hyogo Ion Beam Medical Center, Shingu

<sup>++</sup> Wakasa Wan Energy Research Center, Tsuruga

<sup>+++</sup> Accelerator Engineering Corporation, Chiba  
Japan

### Abstract

A new protocol for dosimetry in external beam radiotherapy was published by the Japan Society of Medical Physics in September 2002. The protocol deals with proton and heavy ion beams and with electron and photon beams, using the absorbed dose to water formalism with calculated  $N_{D,w}$  factors. An intercomparison programme was carried out with the new protocol to establish interinstitutional uniformity in proton beam dosimetry. The absorbed doses were measured with different cylindrical ionization chambers in a water phantom at a position of 30 mm residual range for a proton beam that had a range of 155 mm and a spread out Bragg peak 60 mm wide. As a result, the intercomparison showed that the use of the new protocol would improve the  $\pm 1.0\%$  (one standard deviation) and 2.7% (maximum discrepancy) differences in absorbed doses stated by the participating institutions to  $\pm 0.3\%$  and 0.9%, respectively. The new protocol will be adopted by all the participants.

---

§ Present address: Research Reactor Institute, Kyoto University, Kumatori, Japan.

## 1. INTRODUCTION

The Japan Society of Medical Physics (JSMP) is publishing a new code of practice for dosimetry [1]. The principal reasons for the revision are to adopt the absorbed dose to water based formalism, to update physical data, to harmonize with international protocols, to mention narrow beam dosimetry and to deal with proton and carbon beams.

The number of proton and carbon beam therapy facilities in Japan has recently increased [2]. Consistency in absorbed dose is essential to compare clinical results between the facilities. International organizations such as the International Commission on Radiation Units and Measurements (ICRU) recommend a periodic dosimetry intercomparison in order to verify the interinstitutional uniformity of proton beam dosimetry [3, 4]. Although the National Institute of Radiological Sciences (NIRS) group had attended international dosimetry intercomparisons for proton and carbon beams [5, 6], domestic intercomparisons involving new facilities had not been carried out in Japan. The first nationwide proton dosimetry intercomparison, using the new dosimetry protocol, was held in 2002 at the Proton Medical Research Center (PMRC) of the University of Tsukuba, with the participation of personnel from the NIRS, PMRC, National Cancer Center East (NCC), Hyogo Ion Beam Medical Center (HIBMC) and Wakasa Wan Energy Research Center (WERC). The aims of the intercomparison were to evaluate the differences in absorbed dose determined at different proton therapy facilities in Japan and to establish consistency in absorbed dose to water for protons.

## 2. MATERIALS AND METHODS

### 2.1. The new Japanese dosimetry protocol

The new Japanese dosimetry protocol mostly follows Technical Reports Series No. 398 (TRS 398) [7], which is based on  $N_{D,w,Q_0}$  (i.e. the calibration factor in terms of absorbed dose to water for a dosimeter at a reference beam quality,  $Q_0$ ). According to the protocols, absorbed dose is given by:

$$D_{w,Q} = M_Q N_{D,w,Q_0} k_{Q,Q_0} \quad (1)$$

where

$D_{w,Q}$  is the absorbed dose to water at the reference depth in a water phantom irradiated by a beam of quality  $Q$ ;



- $M_Q$  is the reading of a dosimeter at quality  $Q$ , corrected for influence quantities other than beam quality;
- $k_{Q,Q_0}$  is the factor to correct for the difference between the response of an ionization chamber in the reference beam quality,  $Q_0$ , used for calibrating the chamber and in the actual user beam quality,  $Q$ .

However,  $N_{D,w,Q_0}$  has not been supplied by the Japanese primary standards dosimetry laboratory. The new Japanese protocol alternatively gives the calculated values of  $N_{D,w,Q_0}/N_{X,Q_0}$ , which depend upon the ionization chamber. The value of  $N_{X,Q_0}$  is the calibration factor in terms of exposure for a dosimeter at a reference beam quality  $Q_0$ , which is supplied by the Japanese standards dosimetry laboratories.

To calculate  $k_{Q,Q_0}$  for a proton beam, the new Japanese protocol recommends using the values of  $W_{\text{air}}$ , the mean energy expended in air per ion pair formed by a proton beam, and  $s_{w,\text{air}}$ , the proton mass stopping power ratio of water to air, which are given in TRS 398 [7].

## 2.2. Proton beam dosimetry

The proton beam used for the intercomparison had a range of 155 mm and a spread out Bragg peak (SOBP) with a width in water of 60 mm. The field size of the proton beam was 15 cm  $\times$  15 cm. Each cylindrical ionization chamber was inserted into a water phantom, with a 1 mm thick polymethylmethacrylate (PMMA) sleeve for waterproofing. The centre of the chamber was set at the middle of the SOBP and of the field. Each chamber was irradiated with a preset proton beam, for which a given signal was recorded by the upstream beam monitor. Participants separately determined the absorbed dose to water per monitor unit (Gy/MU) from the ionization chamber measurements, using the new protocol and their respective dosimetry procedures.

Table I compares the dosimetry procedures used for the proton beam by each institute. NIRS had used the dosimetry procedure based on Ref. [3], while the other institutions followed ICRU Report 59 [4]. The model protocols were independently modified for their respective dosimetry procedures with various correction factors, since the dosimetric data for ionization chambers were significantly limited in the protocols. It should be noted that non-uniformity in the proton dosimetry procedure had existed between the participants before the intercomparison. Exposure measurements in a  $^{60}\text{Co}$  gamma ray field with all ionization chambers were also carried out, for comparison.

TABLE I. COMPARISON OF DOSIMETRY PROCEDURES BETWEEN THE PARTICIPANTS

Institution	Protocol	$W_{\text{air}}$ (J/C)	$s_{w,\text{air}}$
NIRS	Ref. [3]	35.2	1.123
PMRC	ICRU 59	34.8	1.132
NCC	ICRU 59	35.18	1.133
HIBMC	ICRU 59	34.8	1.133
WERC	ICRU 59	34.8	1.134

3. RESULTS AND DISCUSSION

Table II summarizes the results of the intercomparison. The ‘old’ column shows the absorbed dose to water per monitor unit (Gy/MU), which was determined with the procedure routinely used at each institution. The ‘new’ column shows the values determined by the new Japanese protocol. In the ‘old’ column a maximum discrepancy of 2.7% exists and a standard deviation of 1.0% is shown. In this case, participants calculated the absorbed dose with different dosimetric parameters (i.e. a  $w$  value for the proton beam, proton stopping power ratio, etc.) in accordance with the respective dosimetry procedures. The lack of unity in dosimetry procedures between the participants resulted in the observed significant discrepancies.

A maximum discrepancy of 1.0% exists and a standard deviation of 0.3% is shown in the ‘new’ column. The standard deviation is equal to that of exposure measurements in a  $^{60}\text{Co}$  gamma ray field. This means that the obtained consistency of proton beam dosimetry is nearly identical to the consistency obtained for  $^{60}\text{Co}$  gamma rays. As a result, it is shown that the use of the new protocol decreases the differences in absorbed doses stated by the participants.

4. CONCLUSION

To establish interinstitutional uniformity in proton beam dosimetry, an intercomparison programme was carried out using the new Japanese dosimetry protocol, which followed TRS 398, especially in selecting the dosimetric parameter for the proton beam. The dose measurements using different cylindrical ionization chambers were carried out in a water phantom at a position of 30 mm residual range for a proton beam that had a range of 155 mm and an SOBP 60

TABLE II. RESULTS OF PROTON DOSIMETRY INTERCOMPARISON

Institution	Ionization chamber	Co-60 exposure (C/kg)	Proton/absorbed dose to water		Ratio of new/old
			Old (Gy/MU)	New (Gy/MU)	
NIRS	PTW 30001 (ICT2)	0.00902	0.1121	0.1125	1.004
	PTW 30001 (ICS0)	0.00899	0.1119	0.1124	1.004
PMRC	C-110 (0.6 mL) No. 823	0.00898	0.1132	0.1125	0.994
NCC	C-110 (0.6 mL) No. 754	0.00895	0.1140	0.1121	0.983
	C-110 (0.6 mL) No. 967	0.00901	0.1149	0.1129	0.983
HIBMC	PTW 30001	0.00895	0.1144	0.1129	0.987
	PTW 31003	0.00902	0.1145	0.1133	0.989
WERC	PTW 30001	0.00894	0.1131	0.1123	0.993
Mean		0.00898	0.1135	0.1126	0.992
Standard deviation/mean (%)		0.3	1.0	0.3	0.9

mm wide. As a result, the use of the new protocol decreased the  $\pm 1.0\%$  (one standard deviation) and  $2.7\%$  (maximum discrepancy) differences in absorbed doses stated by the participating facilities, the improved figures being  $\pm 0.3\%$  and  $0.9\%$ , respectively. The results show that the lack of consistency in dosimetry procedures between the institutions resulted in significant discrepancies and that it is necessary to have a common dosimetry protocol. The new Japanese protocol will be adopted by all the participants.

## REFERENCES

- [1] JAPAN SOCIETY OF MEDICAL PHYSICS, Standard Dosimetry of Absorbed Dose in External Beam Radiotherapy, Tsuushou Sangyou Kenkyuusha, Tokyo (2002) (in Japanese).
- [2] PARTICLE THERAPY COOPERATIVE GROUP, Particle Newsletter No. 29 (2002).
- [3] VYNCKIER, S., BONNETT, D.E., JONES, D.T.L., Supplement to the code of practice for clinical proton dosimetry, Radiother. Oncol. **32** (1994) 174–179.

- [4] INTERNATIONAL COMMISSION ON RADIATION UNITS AND MEASUREMENTS, Clinical Proton Dosimetry. Part I: Beam Production, Beam Delivery and Measurement of Absorbed Dose, Rep. 59, ICRU, Bethesda, MD (1998).
- [5] VATNITSKY, S., et al., Proton dosimetry intercomparison based on the ICRU Report 59 protocol, *Radiother. Oncol.* **51** (1999) 273–279.
- [6] FUKUMURA, A., et al., Carbon beam dosimetry intercomparison at HIMAC, *Phys. Med. Biol.* **43** (1998) 3459–3463.
- [7] INTERNATIONAL ATOMIC ENERGY AGENCY, Absorbed Dose Determination in External Beam Radiotherapy, Technical Reports Series No. 398, IAEA, Vienna (2000).

# PARALLEL-PLATE AND THIMBLE IONIZATION CHAMBER CALIBRATIONS IN PROTON BEAMS USING THE TRS 398 AND ICRU 59 RECOMMENDATIONS

S.M. VATNITSKY

Division of Human Health, International Atomic Energy Agency,  
Vienna

E-mail: s.vatnitsky@iaea.org

M.F. MOYERS, A.S. VATNITSKY

Loma Linda University Medical Center,

Loma Linda, California,

United States of America

## Abstract

The IAEA has recently introduced a new code of practice, in Technical Reports Series No. 398 (TRS 398), to improve and standardize the radiation dosimetry of external photon, electron, proton and ion beams. The paper compares the results of proton beam calibrations based on the recommendations of TRS 398 and the International Commission on Radiation Units and Measurements Report 59 (ICRU 59). Measurements were performed in clinical range modulated proton beams with energies of 155 MeV and 100 MeV at the Loma Linda University Medical Center Proton Therapy Facility using thimble and parallel-plate ionization chambers. The absorbed dose to water calibrations based on the recommendations of TRS 398 agree for various thimble and parallel-plate chambers within 1.1% for the 155 MeV beam and within 1.5% for the 100 MeV beam. The results showed that the proton doses obtained with the different ionization chambers using the TRS 398 recommendations differed by as much as 3.1% compared with dose determinations based on the ICRU 59 recommendations. These differences were mainly due to differences in the recommended stopping powers, the  $W_{\text{air}}$  value for proton beams and the perturbation factors in a  $^{60}\text{Co}$  beam. The results obtained with parallel-plate chambers cross-calibrated in a proton beam showed close agreement with proton beam calibrations made with a thimble chamber using the recommendations of TRS 398.

## 1. INTRODUCTION

The adoption of a common dosimetry code of practice by proton therapy facilities is an important step in achieving consistency in determining the absorbed dose delivered to patients and in providing for the exchange of clinical results. The International Commission on Radiation Units and Measurements

Report 59 (ICRU 59) [1] was the first publication aimed at harmonizing clinical proton dosimetry with air filled thimble ionization chambers and promoting uniformity of the standards. The IAEA has introduced a new code of practice, in Technical Reports Series No. 398 (TRS 398) [2], which is based on the use of ionization chambers calibrated in terms of absorbed dose to water and includes recommendations for absorbed dose determination in proton beams with both thimble and parallel-plate chambers. Implementation of TRS 398 and its subsequent adoption by the proton beam user community requires testing the recommendation and a comparison of the results obtained with existing protocols. A detailed theoretical comparison of the recommendations of TRS 398 and ICRU 59 is presented in Ref. [3]. This paper reports the experimental results of proton beam calibrations in terms of absorbed dose to water following the recommendations of both TRS 398 and ICRU 59. The measurements were made using several thimble and parallel-plate ionization chambers in 155 MeV and 100 MeV range modulated proton beams. The lack of information in ICRU 59 for dose determination with parallel-plate chambers and missing data in TRS 398 for some types of parallel-plate chambers in use at proton facilities makes a direct comparison of results for parallel-plate chambers obtained with both the TRS 398 and ICRU 59 recommendations impossible. To overcome these difficulties, the cross-calibration formalism recommended for the dosimetry of high energy electron beams [4] was applied to parallel-plate chambers by using chamber specific factors determined from a cross-calibration procedure in a non-modulated 250 MeV proton beam. The results of absorbed dose determinations in 155 MeV and 100 MeV range modulated beams with cross-calibrated parallel-plate chambers were compared with the results for thimble chambers.

## 2. MATERIALS AND METHODS

The determination of absorbed dose in a proton beam using an ionization chamber and the recommendations of TRS 398 and ICRU 59 depends upon a calibration of the chamber in reference conditions. The equations related to both sets of recommendations are given below in a general form; the reader is referred to the original publications for details [1, 2]. ICRU 59 allows calibrations in a  $^{60}\text{Co}$  beam based upon exposure, air kerma or absorbed dose to water. Following the original notation of ICRU 59, the absorbed dose to water for protons,  $D_{w,p}$ , when using an ionization chamber with exposure,  $N_X$ , or air kerma,  $N_K$ , calibration factors for a  $^{60}\text{Co}$  beam, can be written as:

$$D_{w,p} = M_p^{\text{corr}} N_{D,g} C_p \quad (1)$$

$$C_p = (s_{w,air})_p \frac{(w_{air})_p}{(W_{air})_c} \quad (2)$$

where

- $M_p^{\text{corr}}$  is the meter reading corrected for influence quantities;
- $N_{D,g}$  is the absorbed dose to gas calibration factor;
- $C_p$  is the overall proton correction factor;
- $(W_{air})_c$  is the mean energy required to form an ion pair in the chamber air for  $^{60}\text{Co}$  gamma rays;
- $(w_{air})_p$  is the mean energy required to form an ion pair in the chamber air for protons;
- $(s_{w,air})_p$  is the mean water to air stopping power ratio for protons.

The absorbed dose to water for protons when using an ionization chamber with an absorbed dose to water calibration factor for a  $^{60}\text{Co}$  beam,  $N_{D,w,c}$ , can be written as:

$$D_{w,p} = M_p^{\text{corr}} N_{D,w,c} k_p \quad (3)$$

where  $k_p$  is the beam quality correction factor, defined as:

$$k_p = \frac{(s_{w,air})_p (w_{air})_p}{(s_{w,air})_c (W_{air})_c} \quad (4)$$

where  $(s_{w,air})_c$  is the ratio of restricted mass stopping powers of water to air for electrons produced by  $^{60}\text{Co}$  gamma rays.

The TRS 398 formalism gives the absorbed dose to water under reference conditions in a clinical proton beam,  $D_{w,Q}$ , using a slightly different notation, as the equation for the beam quality correction factor,  $k_{Q,Qo}$ , includes perturbation factors:

$$D_{w,Q} = M_Q N_{D,w,Qo} k_{Q,Qo} \quad (5)$$

$$k_{Q,Qo} = \frac{(s_{w,air})_Q (W_{air})_Q P_Q}{(s_{w,air})_{Qo} (W_{air})_{Qo} P_{Qo}} \quad (6)$$

where subscript  $Q$  relates to the user's beam quality (i.e. a proton beam) and subscript  $Qo$  relates to the calibration beam quality (i.e. a  $^{60}\text{Co}$  beam).

$p_Q$  and  $p_{Qo}$  are chamber perturbation factors for the proton and  $^{60}\text{Co}$  beams, respectively.

A list of chambers used in this study is shown in Table I. A detailed comparison of the results of absorbed dose determination using the procedures recommended in TRS 398 and ICRU 59 requires that both the  $N_{D,w}$  and  $N_K$  calibration factors, traceable to the same standards laboratory, be available for the chambers employed in the measurements. As seen in Table I, the specific chambers had official  $N_{D,w}$  and  $N_K$  calibrations from two calibration institutions (the Accredited Dosimetry Calibration Laboratory at the University of Wisconsin (ADCL UW) and the Dosimetry Laboratory at the IAEA). For two

TABLE I. IONIZATION CHAMBER DESCRIPTIONS AND CALIBRATION FACTORS

Chamber model: serial number (type)	Wall material	$N_K$ (Gy/C)	$N_{D,w}$ (Gy/C)	$N_{D,g}$ (Gy/C)	$N_{D,g,Qcross}^{pp}$ (Gy/C)	$N_{D,w,Qcross}^{pp}$ (Gy/C)
Exradin T1 No. 222 (thimble)	A150	$6.930 \times 10^8$ (ADCL UW)	$7.649 \times 10^8$ (ADCL UW)	$6.627 \times 10^8$	—	—
PTW 30001 No. 008 (thimble)	PMMA <sup>a</sup>	$4.759 \times 10^7$ (ADCL UW)	$5.259 \times 10^7$ <sup>b</sup>	$4.597 \times 10^7$	—	—
Capintec PR-06 No. 5965 (thimble)	C552	$4.392 \times 10^7$ (ADCL UW)	$4.875 \times 10^7$ <sup>b</sup>	$4.348 \times 10^7$	—	—
NE 2571 No. 1423 (thimble)	Graphite	$4.158 \times 10^7$ <sup>b</sup>	$4.565 \times 10^7$ <sup>b</sup>	$4.080 \times 10^7$	—	—
NE 2571 No. 208 (thimble)	Graphite	$4.152 \times 10^7$ (IAEA)	$4.559 \times 10^7$ (IAEA)	$4.074 \times 10^7$	—	—
PTW Markus No. 1771 (plane-parallel)	Graphited polyethyl	—	$5.516 \times 10^8$ (ADCL UW)	—	$4.736 \times 10^8$ <sup>c</sup>	$5.505 \times 10^8$ <sup>c</sup>
Memorial WPC No. 80 (plane-parallel)	Polystyrene	—	—	—	$9.209 \times 10^8$ <sup>c</sup>	$1.070 \times 10^9$ <sup>c</sup>
Exradin P11 No. 111 (plane-parallel)	Polystyrene	—	—	—	$5.520 \times 10^7$ <sup>c</sup>	$6.416 \times 10^7$ <sup>c</sup>

<sup>a</sup> PMMA: polymethylmethacrylate.  
<sup>b</sup> Cross-calibrated to NE 2571 No. 208 in a  $^{60}\text{Co}$  beam.  
<sup>c</sup> Cross-calibrated to Exradin T1 No. 222 in a non-modulated 250 MeV proton beam.



thimble chambers without an official calibration (Capintec PR-06 No. 5945 and NE 2571 No. 1423), the cobalt  $N_K$  and  $N_{D,w}$  calibration factors were determined by cross-calibrating these chambers to the NE 2571 No. 208 thimble chamber free in air and in water. The  $N_{D,w}$  calibration factor for the PTW W30001 No. 008 chamber was also obtained from the cross-calibration to the NE 2571 No. 208 chamber in a  $^{60}\text{Co}$  beam. With this arrangement the impact of the known discrepancy in  $N_{D,w}/N_K$  between the United States (ADCL UW) and Bureau international des poids et mesures traceable (IAEA) laboratories on the comparison results was minimized [5].

TRS 398 states that the uncertainty of a proton dose determination with a parallel-plate chamber is higher than that for a thimble chamber. The uncertainty of a proton dose determination with a parallel-plate chamber may be reduced, however, by using the procedure recommended for dose determination in high energy electron beams [4]. This procedure was tested by cross-calibrating a parallel-plate chamber against a thimble chamber in a proton beam of quality  $Q_{\text{cross}}$ . The use of this procedure also allowed the extension of the ICRU 59 formalism to parallel-plate chambers and to chambers not listed in the TRS 398 data tables. The absorbed dose to gas calibration factor,  $N_{D,g,Q_{\text{cross}}}^{\text{pp}}$  (ICRU 59) and the calibration factor in terms of absorbed dose to water,  $N_{D,w,Q_{\text{cross}}}^{\text{pp}}$  (TRS 398) for the chambers under calibration, at the cross-calibration quality  $Q_{\text{cross}}$ , can be derived as:

$$N_{D,g,Q_{\text{cross}}}^{\text{pp}} = \frac{M_{Q_{\text{cross}}}^{\text{ref}}}{M_{Q_{\text{cross}}}^{\text{pp}}} [N_{D,g}]^{\text{ref}} \quad (7)$$

$$N_{D,w,Q_{\text{cross}}}^{\text{pp}} = \frac{M_{Q_{\text{cross}}}^{\text{ref}}}{M_{Q_{\text{cross}}}^{\text{pp}}} [N_{D,w,Q_o}]^{\text{ref}} k_{Q_{\text{cross}},Q_o}^{\text{ref}} \quad (8)$$

where

$M_{Q_{\text{cross}}}^{\text{ref}}$ and $M_{Q_{\text{cross}}}^{\text{pp}}$	are the dosimeter readings for the reference thimble chamber and the parallel-plate chamber under calibration, respectively, corrected for the influence quantities;
$[N_{D,g}]^{\text{ref}}$	is the factor in terms of absorbed dose to gas in a $^{60}\text{Co}$ beam;
$[N_{D,w,Q_o}]^{\text{ref}}$	is the calibration factor in terms of absorbed dose to water for the reference chamber at quality $Q_o$ ;
$k_{Q_{\text{cross}},Q_o}^{\text{ref}}$	is the beam quality correction factor for the reference chamber.

The cross-calibrated chamber with calibration factor  $N_{D,w,Q_{\text{cross}}}^{\text{pp}}$  or  $N_{D,g,Q_{\text{cross}}}^{\text{pp}}$  may be used subsequently for the determination of absorbed dose in the user's beam of quality  $Q$  using the basic equation of TRS 398 (Eq. (5)) or equation (1) of ICRU 59. The beam quality correction factor from quality  $Q_{\text{cross}}$  to quality  $Q$  (TRS 398) is defined as:

$$k_{Q,Q_{\text{cross}}}^{\text{pp}} = \frac{(s_{w,\text{air}})_Q P_Q}{(s_{w,\text{air}})_{Q_{\text{cross}}} P_{Q_{\text{cross}}}} \tag{9}$$

Both proton perturbation factors in Eq. (9) were set to unity [2]; the factor  $k_{Q,Q_{\text{cross}}}^{\text{pp}}$  is the ratio of proton stopping powers. In general, the factor  $k_{Q,Q_{\text{cross}}}^{\text{pp}}$  for the parallel-plate chambers listed in TRS 398 can be calculated as a ratio of factors  $k_{Q,Q_o}^{\text{pp}}$  and  $k_{Q_{\text{cross}},Q_o}^{\text{pp}}$ , where  $Q_o$  is a  $^{60}\text{Co}$  beam. The cross-calibration procedure utilized the horizontal beam line (HBL) of the Loma Linda University Medical Center Proton Therapy Facility, which provided a non-modulated proton beam with an accelerator energy of 250 MeV (Table II).

The TRS 398 and ICRU 59 comparison measurements utilized two clinical proton beams. The first beam was the HBL proton beam, which had an accelerator energy of 155 MeV. The second beam used an ocular beam line that provided a range modulated proton beam with an accelerator energy of 100 MeV. Prior to the cross-calibrations and proton dose measurements, the chambers and water phantom were stored in the irradiation room for 24 h to equilibrate with the room temperature. Chambers were positioned in the water phantom so that the centre of the sensitive volume of each chamber was at a water equivalent depth of 10.00 cm for the 250 MeV proton beam, at a depth of 10.27 cm

TABLE II. PROTON BEAM PARAMETERS

Accelerator energy (MeV)	100	155	250
Aperture size (cm)	5.0 <sup>a</sup>	14 × 14	14 × 14
90% to 90% modulation width (cm)	2.36	5.8	—
Range ( $R$ ) in water to distal 10% dose (cm)	2.82	13.79	31.8
Depth ( $D$ ) of measurements in water (cm)	1.42 (COM <sup>b</sup> )	10.27 (COM)	10.00 (plateau)
Residual range ( $R - D$ ) (cm)	1.40	3.52	21.8

<sup>a</sup> To provide a uniform dose across the chamber, the end of the snout was removed, which increased the field size.

<sup>b</sup> COM: centre of modulation.

(COM) for the 155 MeV beam and at a depth of 1.42 cm (COM) for the 100 MeV beam. The effective point of measurement for the cylindrical chamber was considered to be at the geometric centre of the chamber, whereas the effective point of measurement for the parallel-plate chamber was considered to be at the inner surface of the air cavity.

### 3. RESULTS AND DISCUSSION

Absorbed dose to water values for the two proton beams for each chamber were calculated using Eqs (1)–(4) for ICRU 59 or Eqs (5) and (6) for TRS 398. The results of these calculations are shown in Tables III and IV for the 155 MeV beam and in Table V for the 100 MeV beam. It can be seen that the absorbed dose to water calibrations based only upon the recommendations of TRS 398 agree within 1.1% for both thimble and parallel-plate chambers in the 155 MeV beam and within 1.5% for the 100 MeV beam. A comparison between absorbed dose determinations using TRS 398 and ICRU 59 (for the absorbed dose to

TABLE III. ABSORBED DOSE TO WATER VALUES (Gy/10<sup>6</sup> MU) FOR MEASUREMENTS IN A 155 MeV PROTON BEAM

Chamber	TRS 398	TRS 398/ NE 2571 No. 208	ICRU 59 ( $N_k$ )	ICRU 59 ( $N_{D,w,c}$ )	TRS 398/ ICRU 59 ( $N_k$ )	TRS 398/ ICRU 59 ( $N_{D,w,c}$ )	TRS 398/ ICRU 59 ( $N_{D,w,c}$ ) [3]
NE 2571 No. 208	1.393	1.000	1.398	1.381	0.996	1.009	1.011
NE 2571 No. 1423	1.397	1.003	1.402	1.385	0.996	1.009	1.011
PTW W30001 No. 008	1.390	0.998	1.383	1.390	1.005	1.000	—
Capintec PR-06 No. 5965	1.382	0.992	1.390	1.375	0.994	1.005	—
Exradin T1 No. 222	1.387	0.996	1.390	1.419	0.998	0.978	0.978
PTW Markus No. 1771	1.382	0.992	—	—	—	—	—

water based formalism) for the various thimble chambers in the 155 MeV beam showed a maximum difference of 3.1%, while a comparison between TRS 398 and ICRU 59 (for the air kerma based formalism) for the same set of chambers showed a 1.1% maximum difference. As discussed in Ref. [3], the origin of these differences stems from the debate concerning the components of the two recommendations: the  $(W_{air})_p$  value, the proton stopping powers, humidity effects and the chamber perturbation factors. Following the analysis of Ref. [3], it can be seen that some of the recommended factors in the air kerma based formalism counteract, thus providing a better agreement of the results obtained with the air kerma based formalism of ICRU 59 and TRS 398 than with TRS 398 and the absorbed dose to water based formalism of ICRU 59. The differences between the results obtained with TRS 398 and ICRU 59 (for the absorbed dose to water based formalism) calculated in Ref. [3] for NE 2571 and Exradin T1 chambers (last column of Table III) are consistent with the measured ratios.

The calibration factors for parallel-plate chambers derived from cross-calibration measurements in a proton beam with the Exradin T1 No. 222 chamber using Eqs (7) and (8) are listed in Table I, and the comparison results for the 155 MeV and 100 MeV beams are listed in Tables IV and V.

It can be seen that the calibration of both proton beams with the cross-calibrated parallel-plate chambers results in a difference in reported dose less than 1.2%, when compared with the results for a thimble chamber with TRS 398 used for dose calculations. The use of the ICRU 59 formalism through the proton cross-calibration procedure demonstrates similar comparison results.

TABLE IV. ABSORBED DOSE TO WATER VALUES (Gy/10<sup>6</sup> MU) FOR MEASUREMENTS IN A 155 MeV PROTON BEAM: CROSS-CALIBRATED PARALLEL-PLATE CHAMBERS

Chamber	TRS 398	TRS 398 ( $N_{D,w,Q_{cross}}^{pp}$ )	ICRU 59 ( $N_{D,g}^{pp}$ )	TRS 398 ( $N_{D,w,Q_{cross}}^{pp}$ )/ NE 2571 No. 208	ICRU 59 ( $N_{D,g}^{pp}$ )/ NE 2771 No. 208
NE 2571 No. 208	1.393	—	—	—	—
Exradin P11 No. 111	—	1.392	1.403	1.000	1.007
Memorial WPC No. 80	—	1.376	1.379	0.988	0.990
PTW Markus No. 1771	1.382	1.376	1.380	0.988	0.991

TABLE V. ABSORBED DOSE TO WATER VALUES (Gy/10<sup>6</sup> MU) FOR MEASUREMENTS IN A 100 MeV PROTON BEAM: CROSS-CALIBRATED PARALLEL-PLATE CHAMBERS

Chamber	TRS 398	TRS 398/ NE 2571 No. 1423	TRS 398 ( $N_{D,w,Q_{cross}}^{pp}$ )	ICRU 59 ( $N_{D,g}^{pp}$ )	TRS 398 ( $N_{D,w,Q_{cross}}^{pp}$ )/ NE 2571 No. 1423	ICRU 59 ( $N_{D,g}^{pp}$ )/ NE 2571 No. 1423
NE 2571 No. 1423	15.778	1.000	—	—	—	—
PTW W30001 No. 008	15.858	1.005	—	—	—	—
Capintec PR-06 No. 5965	15.704	0.995	—	—	—	—
Exradin T1 No. 222	15.850	1.005	—	—	—	—
Exradin P11 No. 111	—	—	15.870	15.941	1.006	1.010
Memorial WPC No. 80	—	—	15.850	15.920	1.004	1.009
PTW Markus No. 1771	15.933	1.010	15.858	15.929	1.005	1.010

#### 4. CONCLUSIONS

The absorbed dose to water calibrations based on the recommendations of TRS 398 agree for various thimble and parallel-plate chambers within 1.1% for a 155 MeV beam and within 1.5% for a 100 MeV beam. A comparison of absorbed dose to water calibrations for a 155 MeV beam using the recommendations of TRS 398 and ICRU 59 (for the air kerma formalism) results in an agreement for thimble chambers of within 1.1%; however, the difference in the results for calibrations based on the recommendations of TRS 398 and ICRU 59 (for the absorbed dose to water formalism) increases, by up to 3.1%. A cross-calibration procedure for parallel-plate chambers yielded agreements at the same level as for thimble chambers, thereby enabling parallel-plate chambers to be a reliable alternative as standard reference detectors.

## REFERENCES

- [1] INTERNATIONAL COMMISSION ON RADIATION UNITS AND MEASUREMENTS, Clinical Proton Dosimetry. Part I: Beam Production, Beam Delivery and Measurement of Absorbed Dose, Rep. 59, Bethesda, MD (1998).
- [2] INTERNATIONAL ATOMIC ENERGY AGENCY, Absorbed Dose Determination in External Beam Radiotherapy, Technical Reports Series No. 398, IAEA, Vienna (2000).
- [3] MEDIN, J., ANDREO, P., VYNCKIER, S., Comparison of dosimetry recommendations for clinical proton beams, *Phys. Med. Biol.* **45** (2000) 3195–3211.
- [4] INTERNATIONAL ATOMIC ENERGY AGENCY, The Use of Plane Parallel Ionization Chambers in High Energy Electron and Photon Beams, Technical Reports Series No. 381, IAEA, Vienna (1997).
- [5] ANDREO, P., et al., Protocols for the dosimetry of high-energy photon and electron beams: A comparison of the IAEA TRS-398 and previous international Codes of Practice, *Phys. Med. Biol.* **47** (2002) 3033–3053.

# DEVELOPMENTS IN CLINICAL RADIOTHERAPY DOSIMETRY

(Session 14)

**Chair**

**B. MIJNHEER**

European Society for Therapeutic Radiology and Oncology

**Co-Chairs**

**C. BALDOCK**

Australia

**C.-M. MA**

United States of America

**Rapporteur**

**A. KACPEREK**

United Kingdom

**BLANK**



## **RADIOTHERAPY GEL DOSIMETRY**

**C. BALDOCK**

Centre for Medical, Health and Environmental Physics,  
Queensland University of Technology,  
Brisbane, Australia  
E-mail: c.baldock@qut.edu.au

### **Abstract**

The use of radiation sensitive gels for dosimetry measurements was first suggested in the 1950s. It was subsequently shown that radiation induced changes in the nuclear magnetic resonance relaxation properties of gels infused with conventional Fricke dosimetry solutions could be measured. Owing to diffusion related limitations in the use of Fricke gels, alternative polymer gel dosimeters were suggested. Both magnetic resonance imaging and optical laser techniques have been used to evaluate gel dosimeters and to produce three dimensional dose distributions. More recently, the use of X ray computer tomography, ultrasound and vibrational spectroscopy have also been demonstrated as valuable techniques in the evaluation of polymer dosimetry gels. Gel dosimetry has been shown to have great potential in the evaluation of complex dose distributions, such as in external beam radiotherapy, including intensity modulated radiation therapy and brachytherapy.

### **1. INTRODUCTION**

Over many years individuals have endeavoured to measure absorbed radiation dose distributions using gels. As long ago as the 1950s the radiation induced colour change in dyes was used to investigate radiation doses in gels [1]. Depth doses of X rays and electrons in agar gels were investigated using spectrophotometry [2]. Gel dosimetry today, however, is founded mainly on the work of Gore et al., who in 1984 demonstrated that changes due to ionizing radiation in Fricke dosimetry solutions could be measured using nuclear magnetic resonance (NMR) and magnetic resonance imaging (MRI) methods [3]. This paper gives an introductory overview of the basic principles of gel dosimetry. For further details on this dosimetry technique, including specific clinical applications, see Refs [4, 5] and the references therein.

### **2. ADVANTAGES OF GEL DOSIMETRY**

There are certain advantages of gel dosimetry over conventional dosimetry techniques. Measurements using conventional dosimeters, such as

thermoluminescent dosimeters, ionization chambers and film, are potentially time consuming if a full three dimensional (3-D) dose distribution is required, as only a limited number of points or planes can be measured at any one time. Steep dose gradients require that dosimeters be as small as possible, otherwise the true dose gradient may not be determined. Gel dosimeters have the potential to integrate the radiation dose from different directions, which enables the evaluation of volumes, resulting in the potential for true 3-D dosimetry.

### 3. GEL DOSIMETER TYPES

Gel dosimeters can generally be divided into two different types: Fricke gels based on the well established Fricke dosimetry and polymer gels. It should be noted, however, that dosimeters based on other gel systems have also been developed, including superheated bubble dosimetry [6].

#### 3.1. Fricke gel dosimeters

In 1984 it was proposed that NMR relaxation measurements of particular irradiated materials could be used to determine the absorbed dose of ionizing radiation [3] in a Fricke or ferrous sulphate dosimeter [7]. In the Fricke dosimeter, ionizing radiation causes ferrous ( $\text{Fe}^{2+}$ ) ions to be converted to ferric ions ( $\text{Fe}^{3+}$ ) through the radiolysis of the aqueous system. In the presence of the paramagnetic  $\text{Fe}^{3+}$  the NMR longitudinal or spin-lattice relaxation rate,  $R_1$  ( $= 1/T_1$ ), and the transverse or spin-spin relaxation rate,  $R_2$  ( $= 1/T_2$ ), of the irradiated dosimeter are significantly increased and found to be proportional to the concentration of the  $\text{Fe}^{3+}$  produced, and hence to the absorbed radiation dose [3]. Ferrous sulphate solutions were subsequently incorporated into aqueous gel matrices of gelatin [3], sephadex [8], agarose [9] and polyvinyl alcohol (PVA) [10] in order to stabilize spatially the absorbed dose distribution. When used in conjunction with MRI, the gel dosimetry system was found to exhibit potentially unique features for radiation dosimetry, including the ability to measure 3-D absorbed radiation dose distributions. A major limitation of ferrous sulphate dosimetry systems is the continual post-irradiation diffusion of ions in the dosimeter, resulting in a blurred dose distribution. The range of diffusion coefficients measured and reported in the literature by different authors has been summarized in Ref. [11]. Owing to the diffusion limitations encountered in Fricke gel type dosimeters, alternative gel dosimetry systems were proposed based on polymer systems or gel networks [12]. The remainder of this paper concentrates on polymer gel dosimeters.

### 3.2. Polymer gel dosimeters

The use of polymer systems as radiation dosimeters was suggested as early as 1954 [13]. An alternative gel dosimetry system to Fricke gel dosimeters was proposed based on the polymerization of acrylamide (AA) and N,N'-methylene-bis-acrylamide (BIS) monomers dispersed in an aqueous agarose gel matrix [12]. This dosimetry system was given the acronym BANANA (BIS, AA, nitrous oxide and agarose). As was the case for Fricke gel dosimeters [3], when used in conjunction with MRI the dosimetry system was found to exhibit unique features for radiation dosimetry, including the ability to determine 3-D absorbed dose distributions [14]. AA and agarose were subsequently replaced in the BANANA formulation with acrylic acid (ACA) and gelatin, respectively, and with sodium hydroxide added [15]. ACA was subsequently replaced with AA and sodium hydroxide removed with this new formulation, being given the acronym BANG (BIS, AA, nitrogen and gelatin) [16]. The BANG polymer dosimetry gel system was subsequently commercialized [17], and BANG became a registered trademark of MGS Research, Inc. These BANG type polyacrylamide gel dosimeters are now generally referred to in the literature as PAG dosimeters [18]. Over the last few years a number of different polymer gel formulations have been proposed in the literature by different authors. A summary of these formulations is given in Ref. [19]. Fong et al. suggested in 2001 a new formulation for polymer gel dosimeters, which consists of methacrylic acid, ascorbic acid, hydroquinone and copper sulphate gelatin, and has the name MAGIC (methacrylic and ascorbic acid in gelatine initiated by copper) gel [20]. The advantage of the MAGIC normoxic gel formulation is that the polymer is not as sensitive to the presence of atmospheric oxygen. Further research has suggested that these normoxic gels have great potential as polymer gel dosimeters [21, 22].

## 4. MANUFACTURE OF POLYMER GEL DOSIMETERS

Polymer gel dosimeters are usually manufactured using conventional chemistry apparatus (Fig. 1(a)) from aqueous solutions of monomers, such as AA and BIS, and a gelling agent, such as gelatin. Care is always essential when handling such chemicals. Normal laboratory safety procedures ensure that polymer gel dosimeters are manufactured safely [23]. Radiation induced free radical polymerization takes place in polymer gel dosimeters. A significant manufacturing problem of PAG dosimeters is the inhibition of the free radical polymerization by atmospheric oxygen [24], which must be excluded during and after the manufacturing process. This is usually achieved by manufacturing

the dosimeters in an inert nitrogen atmosphere in a reaction flask [16, 18, 25]. A glovebox containment facility is often used as part of the manufacturing process [25–27]. There has been anecdotal evidence reported of polymerization due to exposure to light, which may be a consideration during manufacture, storage, transport and evaluation [26]. In the case of normoxic gels [20–22], manufacture can take place on the bench top without the need to use a glovebox containment facility. The aqueous polymer gel mixture is usually poured into a suitable airtight phantom before being left to gel and/or solidify (Fig. 1(b)). Phantoms are usually manufactured from glass, Perspex or plastics with low oxygen transport properties, such as Barex (Arbo Plastics Ltd). The advantage of a material such as Barex is that it may be heat moulded to the desired shape of an anthropomorphic phantom [28].

After the polymer gel phantom has been prepared it is irradiated, usually with a linac or brachytherapy source (Fig. 1(c)). After a period of time, post-irradiation and after the radiation induced chemical reactions have taken place, the gel phantom is evaluated using, for example, MRI (Fig. 1(d)). The acquired data are subsequently processed to calculate, in the case of nuclear magnetic resonance, a relaxation map (Fig. 1(e)). A spatial distribution of the absorbed dose distribution (Fig. 1(f)) is calculated by applying a calibration curve to the relaxation map. This may be compared quantitatively with a radiotherapy treatment plan. A calibration curve is often not used for relative dosimetry, and linearity of the dose response in the range of doses under consideration is assumed. It has been observed, however, that the relationship between  $R_2$  and dose is quasi-linear [27, 30–32].

## 5. EVALUATION OF GELS

### 5.1. Magnetic resonance methods

To date, MRI has been used for the majority of investigations reported in the polymer gel literature. This measurement technique is used to determine radiation induced changes in relaxation times in polymer gels and to relate them to absorbed dose by means of a calibration curve. To date the majority of studies have been undertaken to investigate  $R_2$  or  $T_2$ . It is known that the determination of relaxation times using clinical MRI systems is inherently difficult [33]. In clinical imaging an uncertainty of up to 10% is considered acceptable in the determination of  $T_2$  [34]. In polymer gel dosimetry a number of the technical difficulties in measuring relaxation times *in vivo*, such as patient movement and blood flow, do not exist, and so it is possible to reduce uncertainties to a much lower level [35]. In the context of gel dosimetry, clinical MRI

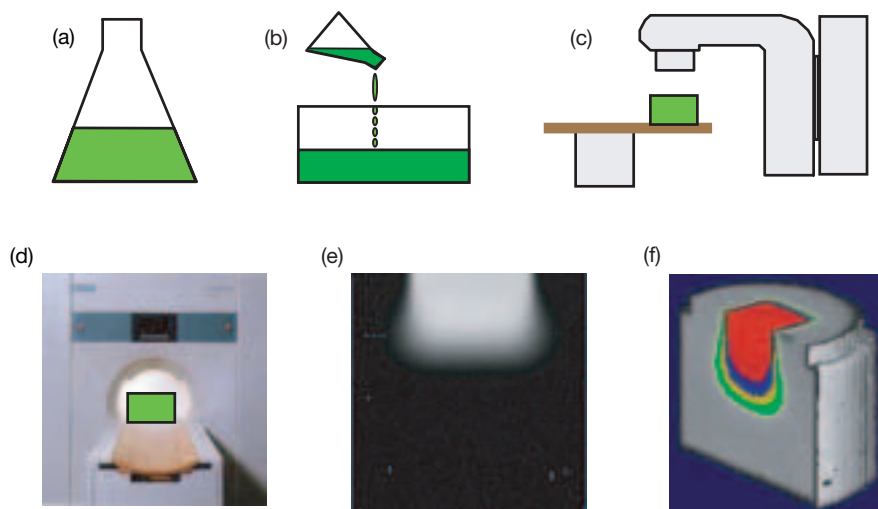


FIG. 1. Principles of gel dosimetry (modified from Ref. [29] and used with permission). (a) Manufacture of polymer gel dosimeter; (b) polymer gel dosimeter poured into a phantom; (c) irradiation of a polymer gel dosimeter on a linac; (d) evaluation of a polymer gel dosimeter; (e) map of the dose distribution; (f) 3-D reconstruction of the dose distribution.

scanners may contribute imaging artefacts to calculated dose maps. A suitable pulse sequence is chosen or developed so as to avoid imaging artefacts while optimizing the signal to noise ratio for a particular scanning time and image resolution. Variations in scanner type may result in the optimal pulse sequence, depending on field and gradient strengths and gradient rise and fall times. Imaging artefacts may be generally grouped in gel dosimetry into two categories: those that cause geometrical distortions and those that cause dose or  $T_2$  inaccuracies. Field inhomogeneities, gradient non-linearities and eddy currents cause machine related geometrical distortions, while susceptibility and chemical shift variations cause object related geometrical distortions. Eddy currents, slice profile variations,  $B_1$  field inhomogeneities and stimulated echoes cause machine related dose or  $T_2$  inaccuracies, while temperature drift and inhomogeneous temperature distributions may cause object related dose or  $T_2$  inaccuracies. In polymer gel dosimetry different methodologies have been extensively explored by De Deene et al. [36–39] to evaluate the various uncertainties associated with the use of MRI pulse sequences.

## **5.2. Optical tomography methods**

As solid polymer forms in the irradiated polymer gel dosimeter, the optical turbidity of the dosimeter changes. This phenomenon has been used to determine absorbed dose by measuring optical density changes [40, 41]. Optical techniques have been considered as an alternative to MRI for the evaluation of polymer gel dosimeters, as they may have the potential to be simpler and easier to implement [42]. Phantoms are typically rotated and scanned with a moving laser beam. Under these circumstances cylindrical phantoms are most suitable and are rotated in an optically matched fluid so as to minimize any effects originating from refraction and reflection. Optical techniques do, however, pose a technical challenge, especially when considering complex 3-D dose distributions in anthropomorphically shaped phantoms.

## **5.3. X ray computed tomography methods**

The use of X ray computed tomography (CT) has been shown to have potential as a method of evaluation for 3-D dose distributions in polymer gel dosimeters [43–45]. This technique relies on the radiation induced change in CT number due to a change in density of the irradiated polymer. A significant advantage of this method is the ready access to CT scanners by radiotherapy departments compared with MRI equipment. To date, results have indicated that the technique is somewhat inferior to MRI and optical gel dosimetry techniques, owing to the limited dynamic range of CT numbers.

## **5.4. Vibrational spectroscopy methods**

FT (Fourier transform) Raman spectroscopy has been shown to be a useful analytical tool for determining radiation induced changes in polymer gel dosimeters [27, 46–51]. Raman microscopy has further been demonstrated to have potential in the determination of dose distributions to resolutions approaching 1  $\mu\text{m}$  [49].

## **5.5. Ultrasound**

A new technique for the evaluation of absorbed dose distributions in these dosimeters using ultrasound was recently introduced [52, 53]. Ultrasound attenuation and speed were shown to vary with absorbed dose. The full potential of ultrasound evaluation techniques, however, is yet to be realized, as this method of investigation has not been optimized.

## 6. PROPERTIES OF POLYMER GEL DOSIMETERS

### 6.1. Dose response and sensitivity

The dose response in gel dosimetry has traditionally been represented in terms of an  $R_1$  or  $R_2$  relaxation rate versus absorbed dose graph. The  $R_1$  or  $R_2$  dose sensitivity, calculated from the initial gradient of the quasi-linear part of an  $R_1$  or  $R_2$  versus absorbed dose graph, is often quoted as the parameter defining the performance of the gel dosimeter. There has been a general assumption by numerous groups working in the polymer gel dosimetry field of the existence of a linear relationship between  $R_2$  and absorbed dose. However, as previously stated, it has been observed that the relationship is only quasi-linear [27, 30–32]. A number of studies have shown that altering both the percentage and chemical composition of the constituent chemicals of polymer gel dosimeters will alter the response to radiation. The  $R_2$  dose sensitivity has been shown to increase with the percentage of comonomers [54–56], up to a maximum above which the monomer will not dissolve. A number of studies have utilized alternative monomers [19–21] (Fig. 2).

### 6.2. Radiological water equivalence

Owing to the large proportion of water, polymer gel dosimeters are virtually radiologically water equivalent [57].

### 6.3. Linear energy transfer and dose rate

No significant linear energy transfer (LET) effects have been observed for BANG-1 polymer gel dosimeters [26]; however, an effect has been observed for BANG-3 [26, 58]. The extent to which there may be an LET effect in polymer gel dosimeters has not been quantified. No significant dose rate effects have been observed in polymer gel dosimeters in the dose rate range of 0.2 Gy/min to 4 Gy/min using MRI [59]. LET effects were observed for clinically relevant protons using vibrational spectroscopy [50].

### 6.4. Temperature

Temperature changes during and after the irradiation of polymer gel dosimeters have been noted [60]. The dose response of polymer gel dosimeters has been shown to be dependent on the temperature at which the dosimeters are evaluated using MRI [31, 55, 61].

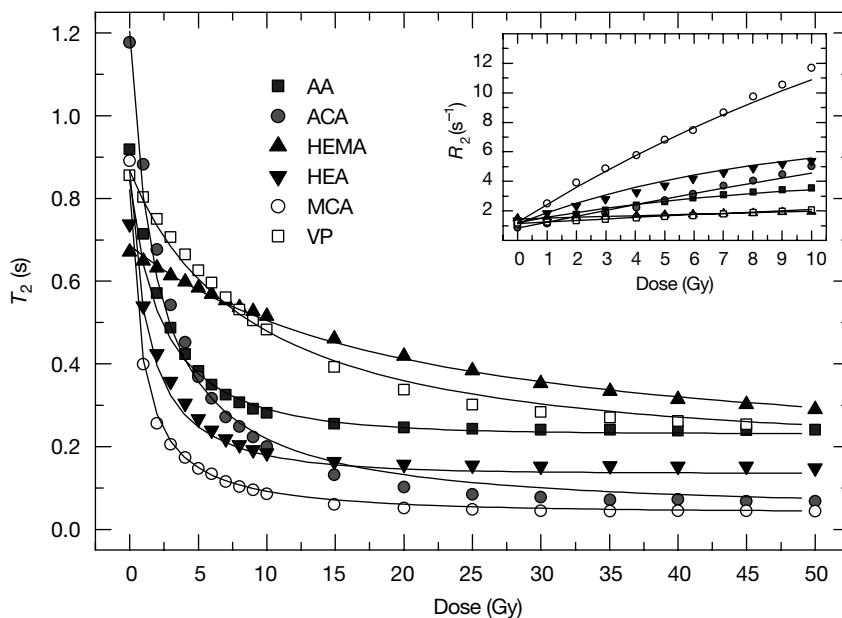


FIG. 2.  $T_2$  changes as a function of the absorbed dose for different polymer gel dosimeter formulations. In each formulation the percentage weight fraction of the different comonomers was 3%, with the remaining constituents being 3% BIS, 5% gelatin (300 bloom) and 89% water. The solid curves are obtained from the model of fast exchange of magnetization [19]. The inset shows the quasi-linear increase of  $R_2$  ( $1/T_2$ ) at low doses. AA: acrylamide; ACA: acrylic acid; MCA: methacrylic acid; VP: 1-vinyl-2-pyrrolidinone; HEMA: 2-hydroxyethyl methacrylate; HEA: 2-hydroxyethyl acrylate.

## 6.5. Magnetic field strength

The dose response of polymer gel dosimeters has been shown to have some dependence on the field strength of the MRI system with which the dosimeters are evaluated [14, 27, 62].

## 6.6. Ageing and temporal stability

The post-irradiation events taking place in polymer gel dosimeters have been investigated by a number of authors. Initially it was thought that observed continual changes in  $T_2$  post-irradiation were due to a continuous polymerization reaction [16, 63]. However, it has been shown that the properties of gelatin



in the polymer gel dosimeter also evolve with time [31]. More recent studies have explained the post-irradiation events taking place in polymer gel dosimeters as due to continual polymerization, ongoing gelation and strengthening of the gel matrix [47].

## 7. CONCLUSIONS

It has been demonstrated in the literature that gel dosimetry is a highly promising technique and it is currently being further investigated and developed by numerous research groups. As all groups work with slightly different gel compositions and evaluation techniques there is not yet a standard for polymer gel dosimetry, and developments are ongoing to produce better polymer gel dosimetry systems. Polymer gel dosimetry should benefit from the continuing improvements in instrumentation and software. Some features of polymer gel dosimetry are unique for the dosimetry of ionizing radiation. No other dosimeter can determine 3-D dose distributions in soft tissue equivalent phantoms that are 3-D shaped. It is likely that gel dosimetry will eventually establish a permanent role in clinical radiotherapy dosimetry. The most important applications in the near future may be the verification of 3-D treatment planning systems, intensity modulated radiation therapy and high dose rate brachytherapy, including cardiovascular brachytherapy.

## REFERENCES

- [1] DAY, M.J., STEIN, G., Chemical effects of ionizing radiation in some gels, *Nature* (London) **166** (1950) 146–147.
- [2] ANDREWS, H.L., MURPHY, R.E., LEBRUN, E.J., Gel dosimeter for depth dose measurements, *Rev. Sci. Instrum.* **28** (1957) 329–332.
- [3] GORE, J.C., KANG, Y.S., SCHULZ, R.J., Measurement of radiation dose distributions by nuclear magnetic resonance (NMR) imaging, *Phys. Med. Biol.* **29** (1984) 1189–1197.
- [4] SCHREINER, L.J., AUDET, C. (Eds), *DosGel'99*, 1st International Workshop on Radiation Therapy Gel Dosimetry (Proc. Int. Workshop Lexington, KY, 1999), Canadian Organization of Medical Physicists, Edmonton, Alberta (1999).
- [5] BALDOCK, C., DE DEENE, Y. (Eds), *DOSGEL 2001*, 2nd International Conference on Radiotherapy Gel Dosimetry (Proc. Int. Conf. Brisbane, 2001), Queensland University of Technology, Brisbane (2001).
- [6] HARPER, M.J., BAKER, B.W., NELSON, M.E., Investigation of alternate droplet material bubble dosimeters, *Health Phys.* **68** (1995) 670–673.

- [7] FRICKE, H., MORSE, S., The chemical action of roentgen rays on dilute ferrous sulfate solutions as a measure of radiation dose, *Am. J. Roentgenol. Radium Ther. Nucl. Med.* **18** (1927) 430–432.
- [8] HIRAOKA, T., et al., Digital imaging of dose distributions by magnetic resonance, *Nippon Igaku Hoshasen Gakkai Zasshi* **46** (1986) 503–505.
- [9] APPLEBY, A., CHRISTMAN, E.A., LEGHROUZ, A., Imaging of spatial radiation dose distribution in agarose gels using magnetic resonance, *Med. Phys.* **14** (1987) 382–384.
- [10] CHU, K.C., JORDAN, K.J., BATTISTA, J.J., VAN DYK, J., RUTT, B.K., Polyvinyl alcohol–Fricke hydrogel and cryogel: Two new gel dosimetry systems with low  $\text{Fe}^{3+}$  diffusion, *Phys. Med. Biol.* **45** (2000) 955–969.
- [11] BALDOCK, C., HARRIS, P.J., PIERCY, A.R., HEALY, B., Experimental determination of the diffusion coefficient in two-dimensions in ferrous sulphate gels using the finite element method, *Australas. Phys. Eng. Sci. Med.* **24** (2001) 19–30.
- [12] MARYANSKI, M.J., GORE, J.C., SCHULZ, R.J., 3-D radiation dosimetry by MRI: Solvent proton relaxation enhancement by radiation-controlled polymerisation and cross-linking in gels, *Proc. Soc. Magn. Reson. Med.* (1992) 1325.
- [13] ALEXANDER, P., CHARLESBY, A., ROSS, M., The degradation of solid polymethylmethacrylate by ionizing radiations, *Proc. R. Soc. A* **223** (1954) 392.
- [14] MARYANSKI, M.J., GORE, J.C., KENNAN, R.P., SCHULZ, R.J., NMR relaxation enhancement in gels polymerized and cross-linked by ionizing radiation: A new approach to 3D dosimetry by MRI, *Magn. Reson. Imag.* **11** (1993) 253–258.
- [15] MARYANSKI, M.J., IBBOTT, G.S., SCHULZ, R.J., XIE, J., GORE, J.C., Magnetic resonance imaging of radiation dose distributions in tissue-equivalent polymer-gel dosimeters, *Proc. Soc. Magn. Reson. Med.* (1994) 204.
- [16] MARYANSKI, M.J., et al., Magnetic resonance imaging of radiation dose distributions using a polymer-gel dosimeter, *Phys. Med. Biol.* **39** (1994) 1437–1455.
- [17] MARYANSKI, M.J., GORE, J.C., SCHULZ, R., Three-dimensional detection, dosimetry and imaging of an energy field by formation of a polymer in a gel, *US Patent 5,321,357* (1994).
- [18] BALDOCK, C., et al., Experimental procedure for the manufacture and calibration of polyacrylamide gel (PAG) for magnetic resonance imaging (MRI) radiation dosimetry, *Phys. Med. Biol.* **43** (1998) 695–702.
- [19] LEPAGE, M., JAYASEKERA, M., BÄCK, S.Å.J., BALDOCK, C., Dose resolution optimization of polymer gel dosimeters using different monomers, *Phys. Med. Biol.* **46** (2001) 2665–2680.
- [20] FONG, P., KEIL, D.C., DOES, M.D., GORE, J.C., Polymer gels for magnetic resonance imaging of radiation dose distributions at normal room atmosphere, *Phys. Med. Biol.* **46** (2001) 3105–3113.
- [21] DE DEENE, Y., VENNING, A., HURLEY, C., HEALY, B.J., BALDOCK, C., Dose–response stability and integrity of the dose distribution of various polymer gel dosimeters, *Phys. Med. Biol.* **47** (2002) 2459–2470.
- [22] DE DEENE, Y., et al., A basic study of some normoxic polymer gel dosimeters, *Phys. Med. Biol.* **47** (2002) 3441–3463.

- [23] BALDOCK, C., WATSON, S., "Risk assessment for the manufacture of radiation dosimetry polymer gels", DosGel'99, 1st International Workshop on Radiation Therapy Gel Dosimetry (Proc. Int. Workshop Lexington, KY, 1999) (SCHREINER, L.J., AUDET, C., Eds), Canadian Organization of Medical Physicists, Edmonton, Alberta (1999) 154–156.
- [24] FLORY, P.J., Principles of Polymer Chemistry, Cornell University Press, Ithaca, NY (1953).
- [25] DE DEENE, Y., et al., Three-dimensional dosimetry using polymer gel and magnetic resonance imaging applied to the verification of conformal radiation therapy in head-and-neck cancer, *Radiother. Oncol.* **48** (1998) 283–291.
- [26] MARYANSKI, M.J., "Radiation-sensitive polymer gels: Properties and manufacturing", DosGel'99, 1st International Workshop on Radiation Therapy Gel Dosimetry (Proc. Int. Workshop Lexington, KY, 1999) (SCHREINER, L.J., AUDET, C., Eds), Canadian Organization of Medical Physicists, Edmonton, Alberta (1999) 63–73.
- [27] LEPAGE, M., WHITTAKER, A.K., RINTOUL, L., BALDOCK, C.,  $^{13}\text{C}$ ,  $^1\text{H}$  NMR and FT-Raman study of the radiation-induced modifications in radiation dosimetry polymer gels, *J. Appl. Polym. Sci.* **79** (2001) 1572–1581.
- [28] BALDOCK, C., et al., A dosimetry phantom for external beam radiation therapy of the breast using radiation-sensitive polymer gels and MRI, *Med. Phys.* **23** (1996) 1490.
- [29] BÄCK, S.Å.J., Implementation of MRI in Radiation Therapy, PhD Thesis, Lund Univ., Malmö (1998).
- [30] OLDHAM, M., MCGJURY, M., BAUSTERT, I.B., WEBB, S., LEACH, M.O., Improving calibration accuracy in gel dosimetry, *Phys. Med. Biol.* **43** (1998) 2709–2720.
- [31] DE DEENE, Y., HANSELAER, P., DE WAGTER, C., ACHTEN, E., DE NEVE, W., An investigation of the chemical stability of a monomer/polymer gel dosimeter, *Phys. Med. Biol.* **45** (2000) 859–878.
- [32] MURPHY, P.S., COSGROVE, V.P., SCHWARZ, A.J., WEBB, S., LEACH, M.O., Proton spectroscopic imaging of polyacrylamide gel dosimeters for absolute radiation dosimetry, *Phys. Med. Biol.* **45** (2000) 835–845.
- [33] FOSTER, M., HAASE, A., "Relaxation measurements in imaging studies", *Encyclopaedia of Nuclear Magnetic Resonance* (GRANT, D., HARRIS, R., Eds), Wiley, Chichester (1996).
- [34] LERSKI, R., DEWILDE, J., BOYCE, D., RIDGWAY, J., Quality Control in Magnetic Resonance Imaging, Rep. 80, Institute of Physics and Engineering in Medicine, York, UK (1998).
- [35] BALDOCK, C., et al., Dose resolution in radiotherapy polymer gel dosimetry: Effect of echo spacing in MRI pulse sequence, *Phys. Med. Biol.* **46** (2001) 449–460.
- [36] DE DEENE, Y., DE WAGTER, C., DE NEVE, W., ACHTEN, E., Artefacts in multi-echo  $T_2$  imaging for high-precision gel dosimetry: I. Analysis and compensation of eddy currents, *Phys. Med. Biol.* **45** (2000) 1807–1823.

- [37] DE DEENE, Y., DE WAGTER, C., DE NEVE, W., ACHTEN, E., Artefacts in multi-echo  $T_2$  imaging for high-precision gel dosimetry: II. Analysis of  $B_1$ -field inhomogeneity, *Phys. Med. Biol.* **45** (2000) 1825–1839.
- [38] DE DEENE, Y., DE WAGTER, C., Artefacts in multi-echo  $T_2$  imaging for high-precision gel dosimetry: III. Effects of temperature drift during scanning, *Phys. Med. Biol.* **46** (2001) 2697–2711.
- [39] DE DEENE, Y., BALDOCK, C., Optimization of multiple spin-echo sequences for 3D polymer gel dosimetry, *Phys. Med. Biol.* **47** (2002) 3117–3141.
- [40] GORE, J.C., RANADE, M., MARYANSKI, M.J., SCHULZ, R.J., Radiation dose distributions in three dimensions from tomographic optical density scanning of polymer gels: I. Development of an optical scanner, *Phys. Med. Biol.* **41** (1996) 2695–2704.
- [41] MARYANSKI, M.J., ZASTAVKER, Y.Z., GORE, J.C., Radiation dose distributions in three dimensions from tomographic optical density scanning of polymer gels: II. Optical properties of the BANG polymer gel, *Phys. Med. Biol.* **41** (1996) 2705–2717.
- [42] OLDHAM, M., SIEWERDSEN, J.H., SHETTY, A., JAFFRAY, D.A., High resolution gel-dosimetry by optical-CT and MR scanning, *Med. Phys.* **23** (2001) 699–705.
- [43] HILTS, M., AUDET, C., DUZENLI, C., JIRASEK, A., Polymer gel dosimetry using x-ray computer tomography: A feasibility study, *Phys. Med. Biol.* **45** (2000) 2559–2571.
- [44] TRAPP, J., BÄCK, S.Å.J., LEPAGE, M., MICHAEL, G., BALDOCK, C., An experimental study of the dose response of polymer gel dosimeters imaged with x-ray computed tomography, *Phys. Med. Biol.* **46** (2001) 2939–2951.
- [45] TRAPP, J.V., MICHAEL, G., DE DEENE, Y., BALDOCK, C., Attenuation of diagnostic energy photons by polymer gel dosimeters, *Phys. Med. Biol.* (in press).
- [46] BALDOCK, C., RINTOUL, L., KEEVIL, S.F., POPE, J.M., GEORGE, G.A., Fourier transform Raman spectroscopy of polyacrylamide gels (PAGs) for radiation dosimetry, *Phys. Med. Biol.* **43** (1998) 3617–3627.
- [47] LEPAGE, M., WHITTAKER, A.K., RINTOUL, L., BÄCK, S.Å.J., BALDOCK, C., Modelling of post-irradiation events in polymer gel dosimeters, *Phys. Med. Biol.* **46** (2001) 2827–2839.
- [48] LEPAGE, M., WHITTAKER, A.K., RINTOUL, L., BÄCK, S.Å.J., BALDOCK, C., The relationship between radiation-induced chemical processes and transverse relaxation times in polymer gel dosimeters, *Phys. Med. Biol.* **46** (2001) 1061–1074.
- [49] JIRASEK, A.I., DUZENLI, C., AUDET, C., ELDRIDGE, J., Characterization of monomer/crosslinker consumption and polymer formation observed in FT-Raman spectra of irradiated polyacrylamide gels, *Phys. Med. Biol.* **46** (2001) 151–165.
- [50] JIRASEK, A.I., DUZENLI, C., Relative effectiveness of polyacrylamide gel dosimeters applied to proton beams: Fourier transform Raman observations and track structure calculations, *Med. Phys.* **29** (2002) 569–577.

- [51] RINTOUL, L., LEPAGE, M., BALDOCK, C., Radiation dose distribution in polymer gels by Raman spectroscopy, *Appl. Spectrosc.* (in press).
- [52] MATHER, M., WHITTAKER, A.K., BALDOCK, C., Ultrasound evaluation of polymer gel dosimeters, *Phys. Med. Biol.* **47** (2002) 1449–1458.
- [53] MATHER, M., DE DEENE, Y., WHITTAKER, A.K., SIMON, G., RUTGERS, R., BALDOCK, C., Investigation of ultrasonic properties of PAG and magic polymer gel dosimeters, *Phys. Med. Biol.* (in press).
- [54] BALDOCK, C., BURFORD, R.P., BILLINGHAM, N., COHEN, D., KEEVIL, S.F., Polymer gel composition in magnetic resonance dosimetry, *Proc. Soc. Magn. Reson. Med.* (1996) 1594.
- [55] MARYANSKI, M.J., AUDET, C., GORE, J.C., Effects of crosslinking and temperature on the dose response of a BANG polymer gel dosimeter, *Phys. Med. Biol.* **42** (1997) 303–311.
- [56] FARAJOLLAHI, A.R., BONNETT, D.E., RATCLIFFE, A.J., AUKETT, R.J., MILLS, J.A., An investigation into the use of polymer gel dosimetry in low dose rate brachytherapy, *Br. J. Radiol.* **72** (1999) 1085–1092.
- [57] KEALL, P.J., BALDOCK, C., A theoretical study of the radiological properties and water equivalence of Fricke and polymer gels used for radiation dosimetry, *Australas. Phys. Eng. Sci. Med.* **22** (1999) 85–91.
- [58] RAMM, U., et al., Three-dimensional BANG<sup>TM</sup> gel dosimetry in conformal carbon ion radiotherapy, *Phys. Med. Biol.* **45** (2000) N95–N102.
- [59] MARYANSKI, M.J., IBBOTT, G.S., EASTMAN, P., SCHULZ, R.J., GORE, J.C., Radiation therapy dosimetry using magnetic resonance imaging of polymer gels, *Med. Phys.* **23** (1996) 699–705.
- [60] SALOMONS, G.J., PARK, Y.S., McAULEY, K.B., SCHREINER, L.J., Temperature increases associated with polymerization of irradiated PAG dosimeters, *Phys. Med. Biol.* **47** (2002) 1435–1448.
- [61] MARYANSKI, M.J., AUDET, C., GORE, G.C., Dose response of BANG polymer gel dosimeter: Temperature dependence, *Med. Phys.* **22** (1995) 951.
- [62] HARALDSSON, P., BÄCK, S.Å.J., MAGNUSSON, P., OLSSON, L.E., Dose response characteristics and basic dose distribution data for a polymerization-based dosimeter gel evaluated using MR, *Br. J. Radiol.* **73** (2000) 58–65.
- [63] McJURY, M., OLDHAM, M., LEACH, M.O., WEBB, S., Dynamics of polymerization in polyacrylamide gel (PAG) dosimeters: (I) ageing and long-term stability, *Phys. Med. Biol.* **44** (1999) 1863–1873.

**BLANK**

## **DEVELOPMENT OF OPTICAL FIBRE LUMINESCENCE TECHNIQUES FOR REAL TIME IN VIVO DOSIMETRY IN RADIOTHERAPY**

C.E. ANDERSEN, M.C. AZNAR, L. BØTTER-JENSEN  
Radiation Research Department, Risø National Laboratory,  
Roskilde, Denmark  
E-mail: claus.andersen@risoe.dk

S.Å.J. BÄCK, S. MATTSSON, J. MEDIN  
Department of Radiation Physics, Malmö University Hospital,  
Malmö, Sweden

### **Abstract**

As a consequence of increased precision in radiotherapy and international safety recommendations, there is a growing demand for methods for accurate in vivo measurements of absorbed doses to patients. A flexible optical fibre dosimeter system with the capability of measuring the dose rate and total absorbed dose in real time (i.e. during the treatment), either on the surface of the body or in cavities near the organs and tissues of interest, has therefore been developed. The system is based on radioluminescence and optically stimulated luminescence (OSL) from a 1 mm × 1 mm × 2 mm solid state dosimeter of carbon doped aluminium oxide ( $\text{Al}_2\text{O}_3\text{:C}$ ). A focused laser beam is used as the stimulation source for the OSL, and all signals between the dosimeter probe and the rest of the system are transmitted through a thin (1 mm core diameter), 15 m long fibre optical cable. The main advantages of the system described in the paper compared with the currently available clinical radiation detectors are the small sensor, the high sensitivity and the real time measurement capability. The features of the new system and results from measurements carried out both in air and in phantoms using different experimental and clinical radiation beams are described. The system was found to be highly linear in the dose range tested (0–3 Gy), to have an almost identical response to 6 MV and 18 MV photons and 20 MeV electrons (the closeness of agreement is better than 1%) and to have a short term stability better than 0.2% (one standard deviation).

### **1. INTRODUCTION**

The need for an improved accuracy of absorbed dose measurements in radiotherapy is increasing, owing to new and more precise diagnostic methods (e.g. computed tomography, positron emission tomography and magnetic

resonance imaging), better treatment planning methods and treatment approaches (e.g. intensity modulated radiation therapy) and international safety recommendations for avoiding accidental exposures of patients undergoing radiation therapy [1]. Currently, in vivo patient monitoring is performed using mainly silicon diode detectors, thermoluminescent dosimeters (TLDs) and MOSFETs [2, 3]. However, these systems have various shortcomings, such as a limited reproducibility and no provision for real time information (TLDs) [4] or poor tissue equivalence (silicon diode detectors and MOSFETs).

To help meet the requirements outlined above, the authors have developed a real time optical fibre dosimeter based on radioluminescence (RL) and optically stimulated luminescence (OSL) from small solid state chips of carbon doped aluminium oxide ( $\text{Al}_2\text{O}_3\text{:C}$ ) [5]. Optical fibre dosimeters have previously been described by other groups [6–9].

The phenomenon of OSL is physically related to thermoluminescence. The latter phenomenon uses heating of the sample (usually up to  $500^\circ\text{C}$ ) to stimulate the luminescence, whereas OSL is based on stimulation with a light source (e.g. a laser). During exposure to radiation (e.g. electrons or X rays), a small fraction of the radiation energy is stored in the  $\text{Al}_2\text{O}_3\text{:C}$  crystal in the form of electrons that are trapped at lattice defects. During optical stimulation, these trapped electrons are released and luminescence is emitted in the subsequent electron–hole recombination process. This OSL signal is thus related to the dose of absorbed radiation. RL does not involve traps, and the luminescence occurs promptly during irradiation. A simple protocol for the use of RL and OSL in radiotherapy is illustrated in the right hand part of Fig. 1: the RL signal generated in the dosimeter provides continuous information about the dose rate during treatment, whereas the total absorbed dose can be read out after (or during) the treatment using OSL. A relatively accurate dose estimate can be obtained within a few seconds by reading the peak value of the OSL decay curve. The OSL signal is completely cleared after some minutes of stimulation, and the dosimeter is ready for a new measurement.

The main advantages of the new optical fibre dosimeter over currently available radiation detectors used in clinical applications are: (a) the small sensor; (b) its high sensitivity over a wide range of dose rates and absorbed doses; and (c) its unique capability of measuring both the dose rate and integrated absorbed dose in real time. Ultra-thin fibre dosimeters can be placed either on the surface of the body or in cavities near the organs and tissues of interest.

This paper describes the features of the new optical fibre dosimeter based on measurements made in phantoms and in air using laboratory X ray, beta and gamma sources, and various clinical photon and electron therapy beams.



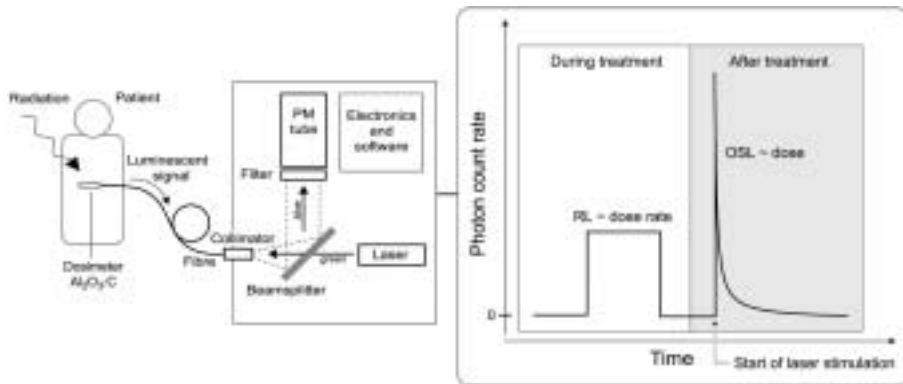


FIG. 1. Outline of the dosimeter system.

## 2. INSTRUMENTATION AND METHODS

A schematic diagram of a prototype optical fibre dosimetry system is shown in Fig. 1. To produce the OSL a green (532 nm, 20 mW) laser beam is focused through a dichroic colour beamsplitter positioned at a 45° angle relative to the incident beam, and via the light fibre into the Al<sub>2</sub>O<sub>3</sub>:C dosimeter. The stimulated OSL signal, which mainly consists of blue light, is carried back from the dosimeter in the same fibre and reflected through a 90° angle by the beamsplitter into a photomultiplier tube. A filter in front of the tube rejects the scattered green light from the laser. The dosimeter probe consists of a small (1 mm × 1 mm × 2 mm) single crystal of Al<sub>2</sub>O<sub>3</sub>:C coupled to the end of a 10 m or 15 m long, 1 mm core diameter fibre made of plastic. The dosimeter system is controlled from a standard desktop computer.

The dosimeter was tested using the following sources of radiation: (a) a linac (Varian Clinac 2100C; 6 MV and 18 MV photons and 20 MeV electrons); (b) a gamma calibration facility (<sup>60</sup>Co and <sup>137</sup>Cs sources); (c) a laboratory <sup>90</sup>Sr/<sup>90</sup>Y source; and (d) an X ray generator (Varian VF-50J; 50 kV, 1 mA) [10]. In-phantom measurements were performed at the linac using Solid Water (Gammex RMI) at the depth dose maximum (100 cm source to surface distance; 10 cm × 10 cm field for photons and 15 cm × 15 cm for electrons). Other measurements were made in air.

## 3. RESULTS

All experiments were carried out in accordance with the protocol outlined in the right hand part of Fig. 1. As an example, Fig. 2 shows the RL

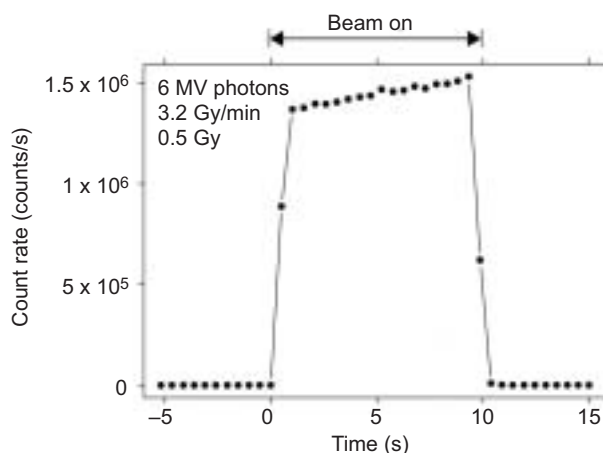


FIG. 2. RL response during irradiation with 6 MV photons.

response during an irradiation with 6 MV photons. The irradiation lasted about 10 s, and there is a data point for every 0.5 s. When the beam is switched on, the count rate changes abruptly from about 20 to  $1.4 \times 10^6$  counts per second. It is observed that the RL signal is not constant during the irradiation; it increases by 1.2% per second. This is a result of the RL characteristics of  $\text{Al}_2\text{O}_3\text{:C}$ .

### 3.1. Linearity

Figures 3(a) and (b) show that there is a clear linear relation between the RL response and dose rate in the experimental range of 0 Gy/min to 3.2 Gy/min; the correlation coefficients are larger than 0.9994 for both data sets. Figures 3(c) and (d) show that the OSL dose response is linear in the range of 0 Gy to 3 Gy; the correlation coefficient is 0.9995 for the log scale and 0.9999 for the linear scale. On the basis of the literature [11], the authors expect linearity to extend beyond 20 Gy.

### 3.2. Reproducibility

The reproducibility of the system was tested with a small laboratory X ray generator that was programmed to give a fixed dose (500 s irradiation at 50 kV and 0.3 mA) every 32 min. The system ran for 38 h, while the OSL signals from the  $\text{Al}_2\text{O}_3\text{:C}$  dosimeter between irradiations were monitored. The

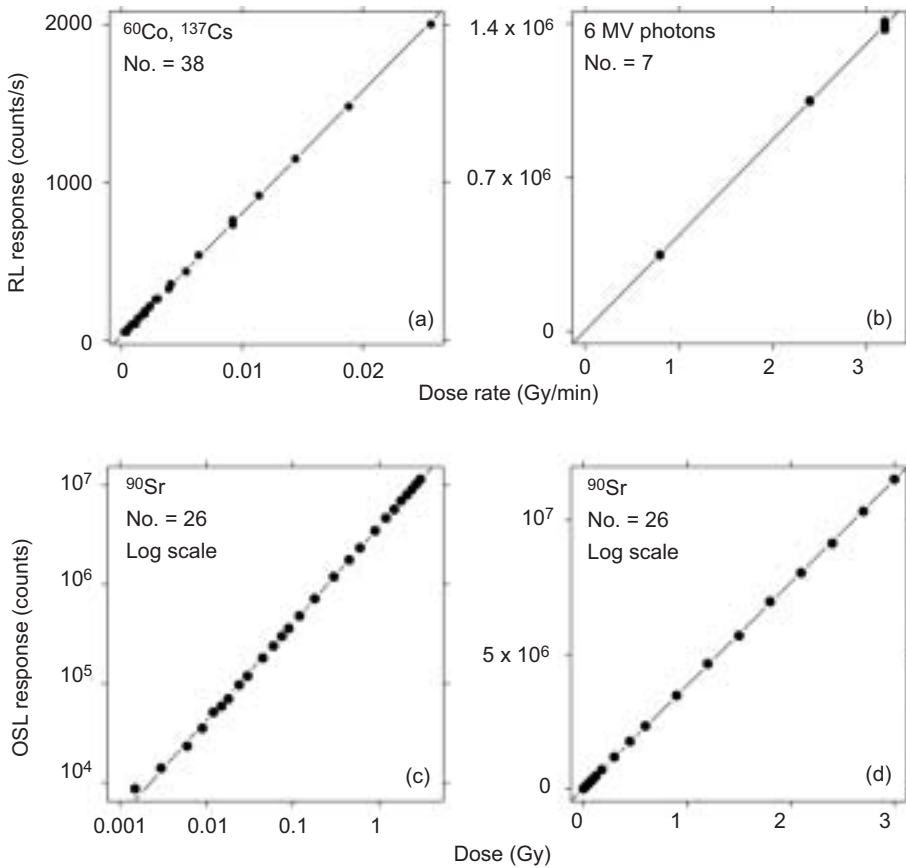


FIG. 3. Linearity plots. (a) and (b): RL response versus dose rate for low and high dose rates. The two sets of experiments were carried out with different experimental configurations, and the RL response per dose rate unit is therefore different in the two plots. (c) and (d): OSL response versus dose for 26  $^{90}\text{Sr}/^{90}\text{Y}$  irradiations shown both on (c) logarithmic and (d) linear scales.

distribution of results is shown in Fig. 4(a). The standard deviation is 0.2%, and the majority of results are very closely centred around the mean. The main deviations occur for the initial irradiations in the sequence (probably because of temperature effects). It must be emphasized that the observed variability includes contributions from the dosimeter system, as well as from the X ray unit. These results show that the system has an excellent short term reproducibility and that the dosimeter can be regenerated as part of the measurement procedure.

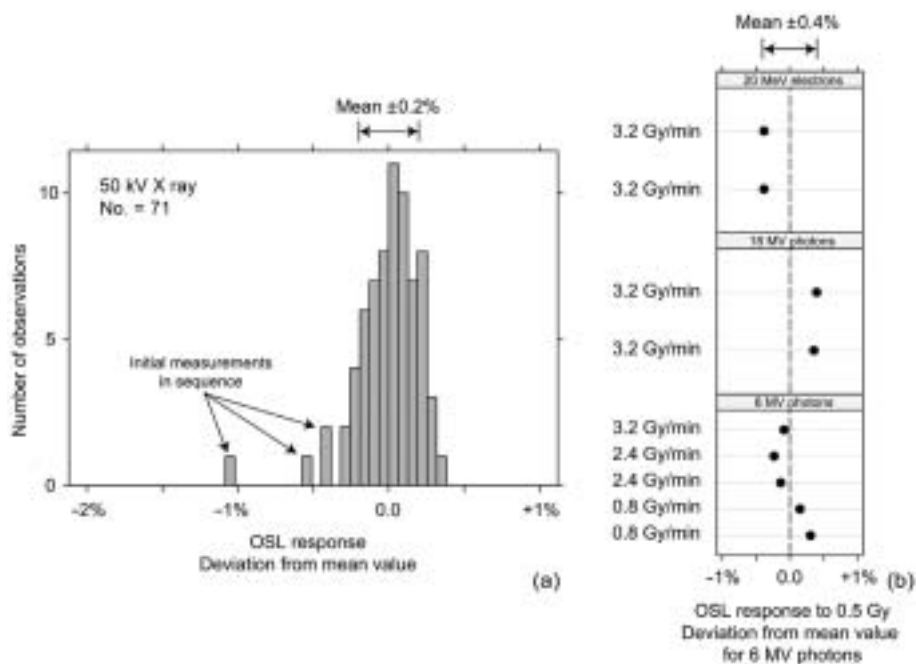


FIG. 4. OSL response to (a) 71 identical soft X ray doses and (b) 0.5 Gy delivered using various linac beams and dose rates.

### 3.3. Energy and dose rate dependence

Figure 4(b) shows the OSL response of the dosimeter to 0.5 Gy delivered using different energies (6 MV and 18 MV photons and 20 MeV electrons) and dose rates (0.8, 2.4 and 3.2 Gy/min). The results have been normalized to the mean value of the response to 6 MV photons. The standard deviation of the results is about 0.4%, which suggests that the OSL response is essentially independent of energy and dose rate for the conditions tested.

### 3.4. Other characteristics

The response of the bare fibre (i.e. without an  $\text{Al}_2\text{O}_3\text{:C}$  dosimeter attached) shows that the so called stem effect (e.g. caused by Cerenkov radiation) is less than 1.5% of the RL response for the linac radiation qualities mentioned above. Basic in-air experiments with 6 MV photons indicate that the angular dependence is better than 5% (expressed as the difference in signal for gantry angles from  $0^\circ$  to  $270^\circ$ , with the detector at the isocentre).

## 4. CONCLUSIONS

A prototype of an optical fibre luminescence dosimeter system has been developed and tested. The system was found to be highly linear in the dose range tested (0–3 Gy), to have an almost identical response to 6 MV and 18 MV photons and 20 MeV electrons (the closeness of agreement is better than 1%) and to have a short term stability better than 0.2% (expressed as one standard deviation of repeated measurements). These characteristics, combined with the small size of the dosimeter probe and the ability to provide real time measurements of dose rate and integrated absorbed dose during or immediately after irradiation, demonstrate a large potential for *in vivo* dosimetry in radiotherapy. The high sensitivity of this technique also makes it highly suitable for applications in diagnostics and nuclear medicine.

## ACKNOWLEDGEMENTS

This work was supported by the Malmö University Hospital Cancer Foundation and Landauer, Inc.

## REFERENCES

- [1] INTERNATIONAL COMMISSION ON RADIOLOGICAL PROTECTION, Prevention of Accidental Exposures to Patients Undergoing Radiation Therapy, Publication 86, Pergamon Press, Oxford and New York (2000).
- [2] ESSERS, M., MIJNHEER, B.J., *In vivo* dosimetry during external photon beam radiotherapy, *Int. J. Radiat. Oncol. Biol. Phys.* **43** (1999) 245–259.
- [3] RAMANI, R., RUSSELL, S., O'BRIEN, P., Clinical dosimetry using MOSFETs, *Int. J. Radiat. Oncol. Biol. Phys.* **37** (1997) 959–964.
- [4] LONCOL, T., GREFFE, J.L., VYNCKIER, S., SCALLIET, P., Entrance and exit dose measurements with semiconductors and thermoluminescent dosimeters: A comparison of methods and *in vivo* results, *Radiother. Oncol.* **41** (1996) 179–187.
- [5] AKSELROD, M.S., KORTOV, V.S., KRAVETSKY, D.J., GOTLIB, V.I., Highly sensitive thermoluminescent anion-defective  $\alpha\text{-Al}_2\text{O}_3\text{:C}$  single crystal detectors, *Radiat. Prot. Dosim.* **32** (1990) 15–20.
- [6] BEDDAR, A.S., MACKIE, T.R., ATTIX, F.H., Water-equivalent plastic scintillator detectors for high-energy beam dosimetry: II. Properties and measurements, *Phys. Med. Biol.* **37** (1992) 1901–1913.
- [7] HUSTON, A.L., et al., Remote fiber dosimetry, *Nucl. Instrum. Methods Phys. Res. B* **184** (2001) 55–77.

- [8] RANCHOUX, G., MAGNE, S., BOUVET, J.P., FERDINAND, P., Fibre remote optoelectronic gamma dosimetry based on optically stimulated luminescence of  $\text{Al}_2\text{O}_3\text{:C}$ , *Radiat. Prot. Dosim.* **100** (2002) 255–260.
- [9] POLF, J.C., McKEEVER, S.W.S., AKSELROD, M.S., HOLMSTROM, S., A real-time, fiber optic dosimetry system using  $\text{Al}_2\text{O}_3\text{:C}$  fibers, *Radiat. Prot. Dosim.* **100** (2002) 301–304.
- [10] ANDERSEN, C.E., BØTTER-JENSEN, L., MURRAY, A.S., A mini X-ray generator as an alternative to a  $^{90}\text{Sr}/^{90}\text{Y}$  beta source in luminescence dating, *Rad. Meas.* (in press).
- [11] McKEEVER, S.W.S., AKSELROD, M.S., MARKEY, B.G., Pulsed optically stimulated luminescence dosimetry using  $\alpha\text{-Al}_2\text{O}_3\text{:C}$ , *Radiat. Prot. Dosim.* **65** (1996) 267–272.

# **AN ANTHROPOMORPHIC HEAD PHANTOM WITH A BANG POLYMER GEL INSERT FOR THE DOSIMETRIC EVALUATION OF INTENSITY MODULATED RADIATION THERAPY TREATMENT DELIVERY**

G. IBBOTT, M. BEACH

University of Texas M.D. Anderson Cancer Center,  
Houston, Texas

E-mail: gibbott@mdanderson.org

M. MARYANSKI

MGS Research, Inc.,  
Guilford, Connecticut

United States of America

## **Abstract**

Radiation therapy has seen remarkable advances in the ability to plan complex three dimensional treatments to tumour target volumes. Intensity modulated radiation therapy (IMRT) is one such method used to conform dose distributions to irregularly shaped tumour volumes while minimizing the dose to nearby critical structures. IMRT offers the possibility of high dose gradients, and it is therefore possible to deliver high doses to target volumes while maintaining low doses to nearby critical normal structures to a much greater extent than is the case with conventional radiation therapy. Comprehensive quality assurance procedures are critical if IMRT is to be delivered consistently. The Radiological Physics Center has developed a mailable anthropomorphic head phantom to assist in the evaluation of IMRT head and neck treatment delivery. To improve the ability of the phantom to provide three dimensional dose information, modifications have been made to accommodate a polymer gel dosimeter. A gel dosimeter insert, made of Barex plastic, has been designed and constructed. The insert can be replaced with a similar insert containing structures of water equivalent plastics, as well as conventional dosimeters. A preliminary evaluation of the gel dosimeter phantom insert has been conducted.

## 1. INTRODUCTION

### 1.1. Intensity modulated radiation therapy and requirements for quality assurance

Radiation therapy has seen remarkable advances in the ability to plan complex three dimensional treatments to tumour target volumes. Intensity modulated radiation therapy (IMRT) is one such method used in cancer treatments to conform doses to irregularly shaped tumour volumes while minimizing the dose to nearby critical structures [1–4]. IMRT offers the possibility of high dose gradients, and it is therefore possible to deliver high doses to target volumes while maintaining low doses to nearby critical normal structures to a much greater extent than is the case with conventional radiation therapy. At the same time, the high gradients achievable with IMRT mean that the localization of the dose distribution is critical. Small errors in the positioning of the patient can mean that a target volume is missed, or that a sensitive normal structure is irradiated to a higher dose than intended, and perhaps higher than can be tolerated. Consequently, comprehensive quality assurance procedures are critical if IMRT is to be delivered consistently [5].

### 1.2. Radiological Physics Center

The Radiological Physics Center (RPC) is funded by the United States National Cancer Institute to assure the co-operative study groups that conduct multi-institutional clinical trials that institutions participating in the trials have adequate quality assurance procedures and that no major systematic dosimetry discrepancies exist. Remote monitoring procedures include the use of mailed thermoluminescent dosimeters (TLDs) to verify machine output, the comparison of an institution's dosimetry data with RPC standard data to identify potential discrepancies, the evaluation of reference or actual patient calculations to verify the treatment planning algorithms and manual calculations, the review of the institution's written quality assurance procedures and records to verify adherence to published standards, and the use of mailed anthropomorphic phantoms to verify tumour dose delivery for special treatment techniques.

In some cases the RPC participates in the accrediting of institutions wishing to participate in specific clinical trials. These institutions are required to submit the details of their treatment planning capabilities, representative treatment plans for benchmark cases or actual patient treatments and, in some cases, actual measured data. Recently, several study groups have begun to require, or encourage, the use of IMRT for the treatment of patients submitted to some clinical trials.



The RPC has developed a mailable anthropomorphic head phantom to assist in the evaluation of IMRT head and neck treatment delivery. The phantom currently has a dosimetry insert that uses film and TLDs to evaluate the dose distributions. While these conventional dosimeters have well known characteristics, they can only provide a one dimensional (TLD) and two dimensional (film) evaluation of treatment delivery. However, it is desirable to use a volumetric dosimeter in the evaluation of the complex distributions offered by IMRT.

### **1.3. Polymer gel dosimeter**

The BANG polymer gel dosimeter (MGS Research, Inc.) was chosen for this project. BANG polymer gel dosimetry has been shown to be a promising alternative to film and TLDs, since it allows for the three dimensional evaluation of treatment planning. Previous investigations have demonstrated that complex dose distributions can be measured and displayed accurately with the BANG gel [6–11]. This project was undertaken to design and construct a BANG gel insert for the RPC head and neck IMRT phantom, to provide for volumetric dosimetry evaluations.

## **2. METHODS AND MATERIALS**

### **2.1. Phantom design and construction**

A cylindrical insert container made of Barex plastic was designed and constructed to accommodate the polymer gel dosimeter. Barex was chosen because it has low permeability to oxygen and can be thermomoulded in accordance with design parameters. The insert was designed to fit within the RPC head and neck phantom in order to encompass a simulated treatment region (Fig. 1). A second imaging insert was constructed that contained TLD and film dosimeters, which mimicked the original imaging–dosimetry insert designed for this phantom; this was done to facilitate a direct comparison between conventional dosimeters and the gel. The imaging insert was designed with a primary target volume, a secondary target volume and an organ at risk that were of similar material and geometry to that of the original block style insert (Fig. 2). Owing to the change in the insert's dimensions, the phantom itself was redesigned to accommodate the insert. The cylinders had a radius of 5 cm and a depth of 8.5 cm.

An optical computed tomography (OCT) scanner was used to determine the optical density (OD) throughout the gel and to relate the OD to the dose. A straightforward relationship between OD and dose has been demonstrated



*FIG. 1. The RPC's redesigned IMRT head and neck phantom with imaging insert installed. The Barex BANG gel insert is shown in the foreground.*

previously [12]. The cylindrical design of the gel insert was chosen to facilitate OCT densitometry.

Both the gel and imaging–conventional dosimeter inserts were fitted with a registration pin. The pin served several purposes: (a) it ensured that the inserts were registered within the phantom in a reproducible orientation; (b) it served as an alignment marker for the X ray CT image taken of the phantom with the imaging insert (which was used for treatment planning); and (c) it served as an alignment marker for the OCT measurement and dosimetry image reconstruction of the gel insert. The registration pin also provided a reference for the alignment of isodose distributions (based upon X ray CT images of the imaging insert) with the measured distributions from the gel dosimeter.

### 3. RESULTS

#### 3.1. Simple treatment evaluation

An initial test was conducted to confirm the correct functioning of the components of the phantom and the dosimetry procedure. A uniform dose was



*FIG. 2. The BANG gel and imaging–dosimetry inserts. Note the planning target volumes, organ at risk and film–TLD provisions in the disassembled imaging insert.*

delivered to the gel insert while the insert was submerged in a water tank. This allowed measured gel dose points to be compared with ionization chamber measurements, as well as with calculated doses.

The calibration of the treatment machine, a Varian Clinac 2100C/D, was first verified through dose output measurements made using the American Association of Physicists in Medicine TG 51 [13] formalism. Test tubes filled with the same batch of BANG gel were irradiated with doses of 2, 6 and 10 Gy and were used to determine an OD versus dose response curve. One of the gel insert canisters was also irradiated to 6 Gy. This gel provided a correction factor that accounted for volumetric dependencies affecting the OD readings. The water tank containing the gel insert was irradiated with equally weighted parallel opposed 6 MV beams with a dose of 7 Gy at the isocentre. Ionization chamber measurements were taken along the three principal axes of the water tank, with the origin acting as the common isocentre for the ionization chamber measurements, treatment planning calculations and gel measurements.

The relative dose comparisons proved to be promising, considering that this was the first analysis using the recently commissioned OCT scanner. Representative plots along the  $x$  (transverse) axis and the  $z$  (longitudinal) axis demonstrated general agreement with ionization chamber measurements and with the treatment planning calculations (Figs 3 and 4). As can be seen, the gel measurement process was perturbed by the reflections of the laser along the

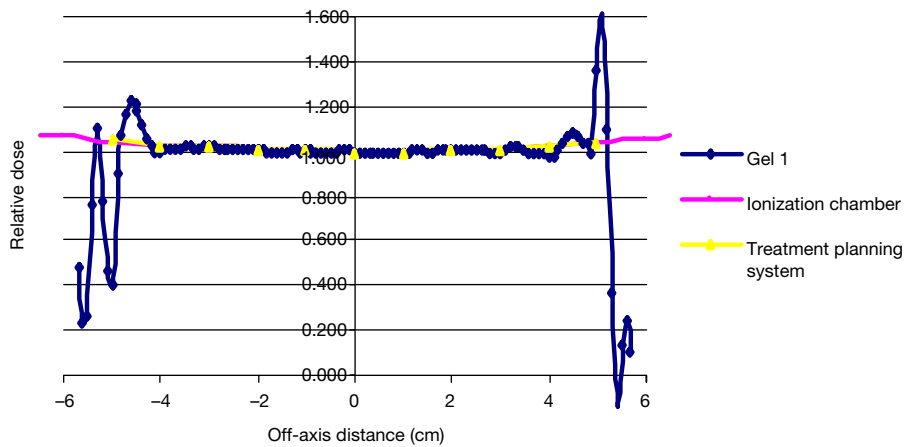


FIG. 3. Relative dose measured from the gel dosimeter compared with ionization chamber readings along the x axis.

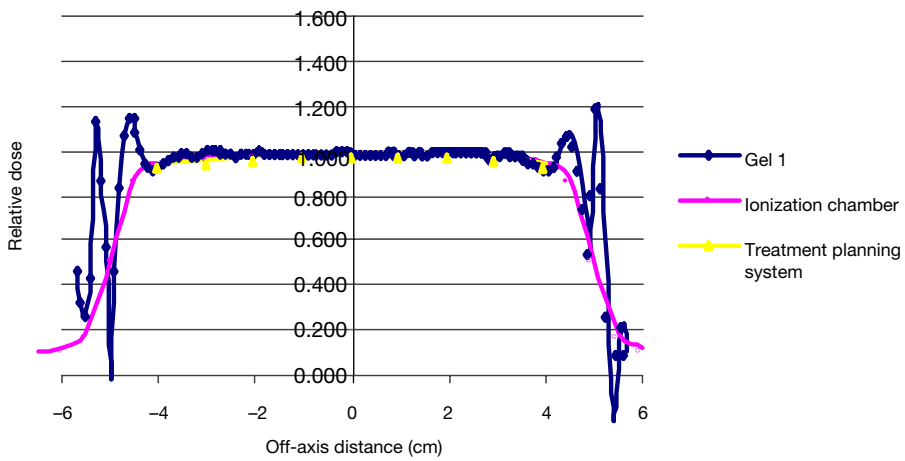


FIG. 4. Relative dose measured from the gel dosimeter compared with ionization chamber readings along the z axis.

sides of the canister walls. As a result, only the central 70% of the canister provided reliable data.

#### 4. CONCLUSIONS

The phantom with gel dosimetry insert is proposed as an evaluation tool for IMRT and for accrediting institutions participating in national clinical trials. Dose distributions measured with the gel dosimeter in the simulated target volumes and critical structure region should agree with the calculated distributions to within  $\pm 5\%$ . Spatial localization is expected to be within 5 mm.

#### ACKNOWLEDGEMENTS

This investigation was supported by Public Health Service grants CA 10953 and CA 81647 awarded by the National Cancer Institute, US Department of Health and Human Services.

#### REFERENCES

- [1] STERNICK, E.S., CAROL, M.P., GRANT, W.H., "Intensity-modulated radiotherapy", *Treatment Planning in Radiation Therapy* (KHAN, F.M., POTISH, R.A., Eds), Williams & Wilkins, Baltimore, MD (1998) 187–213.
- [2] GRANT, W., CAIN, R.B., Intensity-modulated conformal therapy for intracranial lesions, *Med. Dosim.* **23** (1998) 237–241.
- [3] HONG, G.L., et al., Intensity-modulated tangential beam irradiation of the intact breast, *Int. J. Radiat. Oncol. Biol. Phys.* **44** (1999) 1155–1164.
- [4] HUNT, M.A., et al., Treatment planning and delivery of intensity-modulated radiation therapy for primary nasopharynx cancer, *Int. J. Radiat. Oncol. Biol. Phys.* **49** (2001) 623–632.
- [5] BOYER, A.L., et al., "Quality assurance for treatment planning dose delivery by 3DRTP and IMRT", *General Practice of Radiation Oncology Physics in the 21st Century* (SHIU, A.S., MELLEMBERG, D.E., Eds), Medical Physics Publishing, Madison, WI (2000) 187–232.
- [6] MARYANSKI, M.J., et al., Magnetic resonance imaging of radiation dose distributions using a polymer-gel dosimeter, *Phys. Med. Biol.* **39** (1994) 1437–1455.
- [7] MARYANSKI, M.J., et al., Radiation therapy dosimetry using MRI of polymer gels, *Med. Phys.* **23** (1996) 699–705.
- [8] IBBOTT, G.S., et al., Three-dimensional visualization and measurement of conformal dose distributions using magnetic resonance imaging of BANG polymer gel dosimeters, *Int. J. Radiat. Oncol. Biol. Phys.* **38** (1997) 1097–1103.

- [9] KEALL, P., BALDOCK, C., A theoretical study of the radiological properties and water equivalence of Fricke and polymer gels used for radiation dosimetry, *Australas. Phys. Eng. Sci. Med.* **22** (1999) 85–91.
- [10] OLDHAM, M., et al., An investigation into the dosimetry of a nine-field tomotherapy irradiation using BANG-gel dosimetry, *Phys. Med. Biol.* **43** (1998) 1113–1132.
- [11] DE DEENE, Y., VENNING, A., HURLEY, C., HEALY, B.J., BALDOCK, C., Dose–response stability and integrity of the dose distribution of various polymer gel dosimeters, *Phys. Med. Biol.* **47** (2002) 2459–2470.
- [12] MARYANSKI, M.J., et al., Radiation dose distributions in three dimensions from tomographic optical density scanning of polymer gels: II. Optical properties of the BANG polymer gel, *Phys. Med. Biol.* **41** (1996) 2705–2718.
- [13] AMERICAN ASSOCIATION OF PHYSICISTS IN MEDICINE, AAPM’s TG-51 protocol for clinical reference dosimetry of high-energy photon and electron beams, *Med. Phys.* **26** (1999) 1847–1870.

## **CLINICAL IMPLEMENTATION AND QUALITY ASSURANCE FOR INTENSITY MODULATED RADIATION THERAPY**

C.-M. MA, R. PRICE, S. McNEELEY, L. CHEN, J.S. LI,  
L. WANG, M. DING, E. FOURKAL, L. QIN  
Department of Radiation Oncology, Fox Chase Cancer Center,  
Philadelphia, Pennsylvania, United States of America  
E-mail: c\_ma@fccc.edu

### **Abstract**

The paper describes the clinical implementation and quality assurance of intensity modulated radiation therapy (IMRT), based on experience at the Fox Chase Cancer Center, and reviews the procedures for the clinical implementation of the IMRT technique and the requirements for patient immobilization, target delineation, treatment optimization, beam delivery and system administration. The dosimetric requirements and measurement procedures for beam commissioning and dosimetry verification for IMRT are discussed and the details of model based dose calculation for IMRT treatment planning and the potential problems with such dose calculation algorithms are examined. The paper also discusses the effect of beam delivery systems on the actual dose distributions received by the patient and the methods to incorporate such effects in the treatment optimization process. Finally, the use of the Monte Carlo method for dose calculation and treatment verification for IMRT is investigated.

### **1. INTRODUCTION**

The use of computer controlled multileaf collimators (MLCs) to deliver intensity modulated beams has provided the possibility of achieving a conformal dose distribution to the tumour target while sparing nearby critical normal structures. However, the treatment complexity with intensity modulated radiation therapy (IMRT) has also greatly increased compared with three dimensional conformal radiation therapy (3-D CRT). The sequences of leaf movement and their associated effects on the dose delivered to the patient may vary significantly, depending on the accelerator and MLC design. Careful considerations must be given to the variation of the accelerator head scatter component in the MLC collimated beam [1–3], the amount of photon leakage through the leaves [4, 5], the scatter from the leaf ends, the tongue and groove effect [4, 6] and the effect of backscattered photons from the moving jaws and MLC leaves on the monitor chamber signal [7]. Furthermore, the inverse

planning algorithms for plan optimization have all used approximations to speed up the dose computation, which may introduce uncertainty in the calculated dose distributions, especially in the presence of heterogeneities. Patient positioning and organ motion will also increase the uncertainty in the dose delivered to the patient. All the above implies a potential problem with the prediction of the dose distribution in a patient for an IMRT treatment. Proper quality assurance (QA) procedures are needed to ensure the accuracy of treatment planning and beam delivery using IMRT techniques.

The requirements for the clinical implementation of IMRT are discussed in this paper; the treatment planning and beam delivery process, based on experience with IMRT at the Fox Chase Cancer Center (FCCC), is also described.

## 2. IMPLEMENTATION REQUIREMENTS

### 2.1. Requirements in equipment, space and shielding

Special equipment is needed to provide IMRT functionality. This includes software for treatment optimization and leaf sequencing and hardware for intensity modulated beam delivery. Existing record and verify systems may need to be upgraded to accommodate IMRT treatments. Computer networks may need to be enlarged or improved in order to permit the file transfers needed. Additional dosimetry equipment may be needed for the commissioning and ongoing QA of IMRT. It is important to have an efficient film scanning system to accomplish these tasks. Additional phantoms may also be needed. Extra space may be needed for additional equipment, such as computers to host the treatment planning software and add-on collimators or dosimetry devices. IMRT treatments require more beam-on time than conventional treatments, so room shielding should be re-evaluated. Additional materials may be needed for the secondary barriers, although not the primary barriers, owing to the increased beam-on time [8].

### 2.2. Time and personnel

Extra time and resources are needed for the initial implementation and routine clinical operation of IMRT. The implementation team, including radiation oncologists, physicists, dosimetrists, therapists, service engineers, nurses and administrators, must work together to set up and test every step in the IMRT process. Proper QA procedures must be implemented and special training should be arranged for the personnel involved in the IMRT process. These tasks will likely require an initial investment of several person-months of



work on the part of the physics staff and other members of the implementation team.

### **2.3. Treatment scheduling and billing**

IMRT treatments take at least 50% longer than conventional treatments, owing to changes in patient immobilization, target localization, beam delivery and dosimetry verification. The staff responsible for scheduling need to be advised of new scheduling requirements, and should be consulted early in the implementation process so that the consequences of these changes can be anticipated and adjustments made. Care must be given to compliance issues. Administrators and other staff need to develop tools for cost analysis (billing) and documentation.

### **2.4. Personnel training**

Personnel training and education is an essential part of the clinical implementation of IMRT. Experience gained by staff in three dimensional treatment planning and delivery is helpful but not sufficient for IMRT, since there are significant differences between the two that necessitate additional specialized training. In order to use this technology safely and effectively, each member of the IMRT team should understand the whole process. IMRT differs significantly enough from traditional radiation therapy that it can be considered a special procedure, necessitating didactic training for key members before they implement this new modality in their clinics. The training curriculum for each IMRT team member must include all the critical steps in the IMRT process. For example, oncologists and planners should be trained to adjust the treatment optimization parameters to steer the results in the desired direction, in order to avoid treating a patient with a suboptimal IMRT treatment plan. Radiation oncology physicists must have a good understanding of the mathematical principles of dose optimization, computer controlled delivery systems and the dosimetry issues related to small and complex shaped radiation fields. They also need to have a better understanding of the treatment set-up, planning and delivery uncertainties and of their impact on patients treated with IMRT. Therapists need to be trained to use any new immobilization or localization systems implemented in the new procedures. Performing mock procedures with phantoms needs to be part of the process of testing the new procedures. Therapists need to be provided with the means of knowing that the treatment they are about to deliver is correct, verifying for themselves that the record and verify system is running properly, knowing how to respond to unplanned events, how to interrupt and restart a treatment and how to recover from a

partial treatment that requires the console to be reprogrammed. Service engineers must have a good knowledge of all aspects of the IMRT beam delivery process and of the equipment required. With the co-operation of the radiation physicist, preventive maintenance programmes should be implemented to meet the special needs of IMRT.

## **2.5. Patient education**

Patient education is another important aspect of IMRT. Patients should be informed of the goal of the treatment and of the potential side effects and be given realistic estimates of the time required for each treatment as well as a description of the immobilization method used and of the beam delivery process they will experience.

## **3. QA CONSIDERATIONS**

The IMRT technique is a major departure from the way radiotherapy is currently delivered. The improved treatment efficacy with IMRT is associated with increased treatment complexity and therefore requires a well established QA programme to ensure its safe, effective and efficient operation. The following is a brief description of the QA considerations for IMRT, based on experience at the FCCC.

### **3.1. Patient immobilization**

Adequate patient immobilization will facilitate imaging and target localization to ensure accurate dose delivery. New immobilization devices and techniques may be necessary to use the technology safely, such as supplementing thermoplastic masks with a bite block fixation for head and neck treatments and using body localizers and vacuum fixation devices for abdominal treatments (Fig. 1). Techniques to reduce the effect of organ motion due to breathing, such as respiratory gating, may be desired for thoracic and abdominal lesions. Experience at the FCCC has shown the effectiveness of immobilizing and marking the patient as closely as possible to the anticipated treatment isocentre and then performing target localization prior to a treatment, if necessary, for example using the BAT (B mode, Acquisition, and Targeting, NOMOS Corp.) ultrasound system for prostate IMRT (see below).



*FIG. 1. A body localizer with vacuum fixation for patient immobilization and repositioning for stereotactic body surgery and IMRT.*

### **3.2. Image acquisition and structure segmentation**

Image guidance is playing an increasingly important role in structure segmentation, target (treatment volume) determination, inter- and intra-fraction target localization and/or target redefinition. IMRT will require more precise information about the target and normal tissue structures for treatment planning. The use of contrast agents for computed tomography (CT) and the registration of images from other modalities, such as magnetic resonance imaging (MRI) or positron emission tomography (PET), that provide additional anatomical as well as functional information is therefore often needed and may represent a change in typical practice. Figure 2 shows images from CT, MRI and PET. MRI can provide better soft tissue contrast compared with CT and is less affected by high Z material. The hip replacement in Fig. 2(b) caused significant artefact in the CT image. The FCCC PET-CT scanner can provide PET and CT image data at the same time, eliminating the uncertainty due to image fusion. Functional imaging has been used for IMRT treatment planning to improve target delineation for hypofractionated radiotherapy treatments. Methods to add additional reference structures (Fig. 3) to assist the optimization process in order to improve target dose conformity have also been investigated [9].

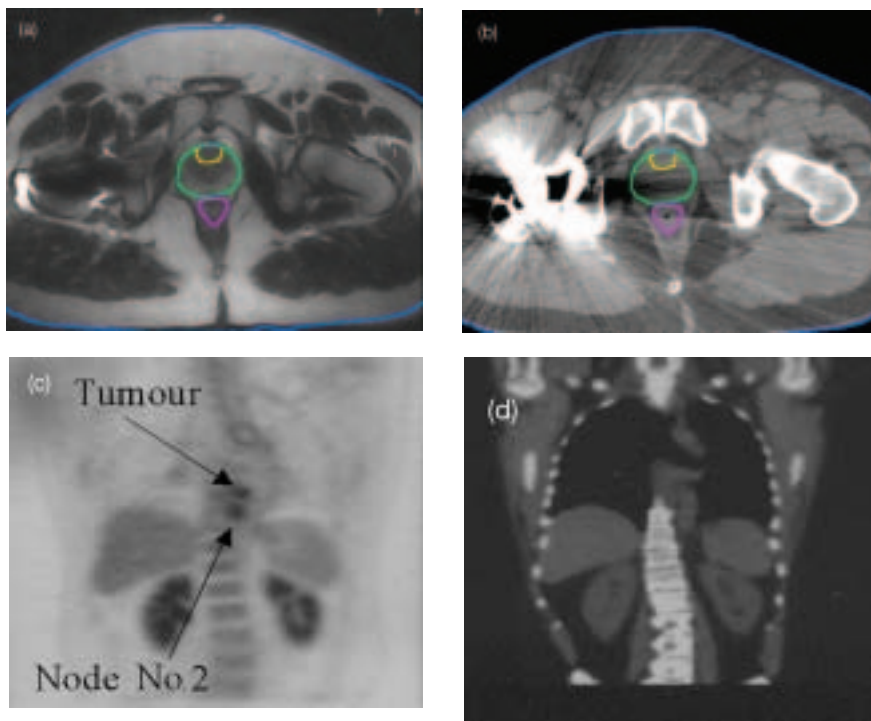


*FIG. 2. Images obtained using different modalities at the FCCC: (a) MRI, prostate; (b) CT, prostate; (c) PET, oesophagus; (d) CT, oesophagus. MRI can provide better soft tissue contrast and is less affected by high Z materials. PET images can provide functional information for target delineation.*

### **3.3. Treatment planning**

Different treatment planning optimization systems have been investigated at the FCCC, including the NOMOS Corvus system, the CMS FOCUS system, the Radionics system and a Monte Carlo based inverse planning system. Clinical protocols are established with quantitative dose criteria for different treatment sites, which ensures proper planning parameters and dose–volume limits for controlling the planning process and/or direction and for achieving an acceptable plan quickly. The FCCC has developed guidelines and forms for physicians to communicate complex planning goals to the planners and for the planners to keep track of the parameters that have been tried and to report the final plan results. The planning parameters and dose criteria are modified based on experience gained.

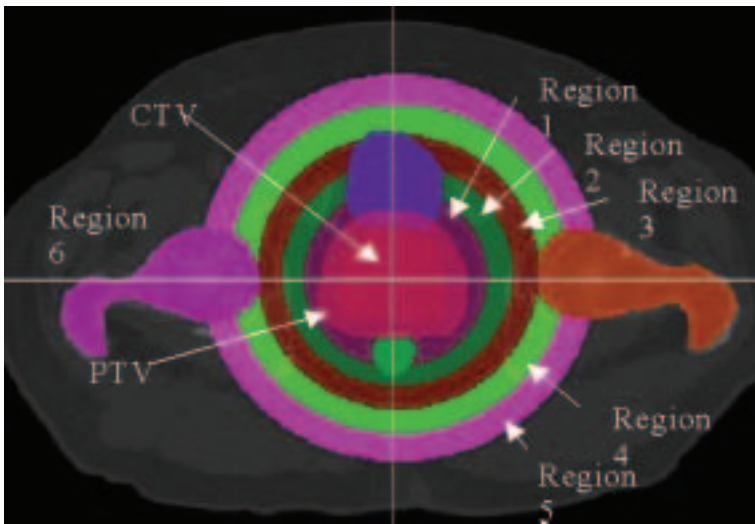


FIG. 3. Circular reference structures with different dose criteria are added around the prostate to assist treatment optimization to improve dose conformity.

### 3.4. Plan validation

The goal of patient specific dosimetry validation is to verify that the correct dose distribution will be delivered to the patient [4, 10, 11]. This QA procedure ensures that the plan has been properly computed and that the leaf sequence files and treatment parameters charted and/or stored in the record and verify system are correct and will be executable. The items checked before the first treatment include:

- (a) Monitor units (the absolute dose at a point): using an ionization chamber in a phantom.
- (b) MLC leaf sequences or fluence maps: using film or digital imaging devices.
- (c) The relative dose distribution: using film or a dosimeter array (e.g. thermoluminescent dosimeters and ionization chambers).
- (d) Collision avoidance: performing a dry run before treatment.

Figure 4 compares doses predicted by the Corvus treatment planning system with those measured using an ionization chamber for over 300 IMRT patients. The FCCC results showed that the differences were within 1% for 41.9% of the cases and within 2% for 78.3% of the cases. Differences of more

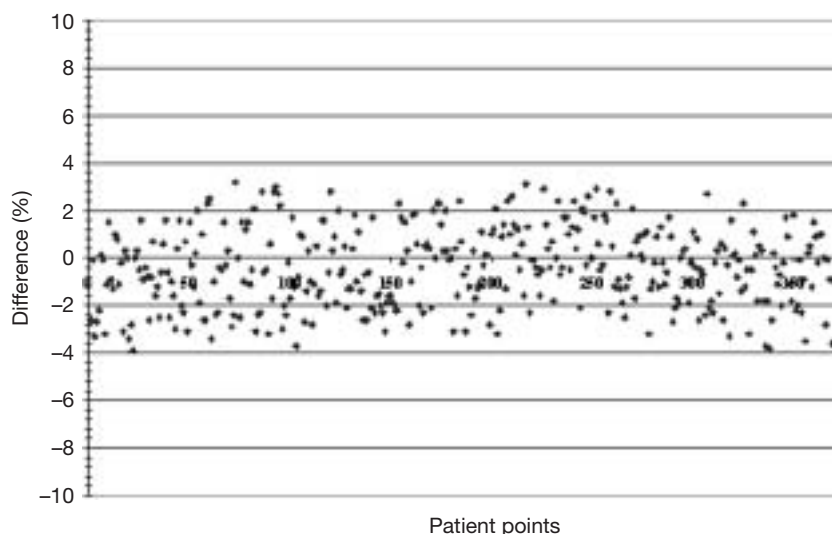


FIG. 4. Comparison of doses predicted by the Corvus treatment planning system and measured by an ionization chamber in a phantom.

than 3% were investigated individually to ensure the accuracy of the dose distribution. So far direct measurements have been performed on all the IMRT plans. However, reliable independent dose calculation methods for dosimetry QA are also being developed [12, 13]. Most treatment optimization systems use simple dose calculation algorithms to compute the beamlet dose distributions used by the inverse planning process, which may introduce significant uncertainty in the optimized dose distribution, owing to the presence of heterogeneities, especially near tissue–air, tissue–lung and tissue–bone interfaces. For example, the commonly used finite sized pencil beam algorithm can modify the beamlet dose distribution based on equivalent path length, but it does not handle the dose perturbation due to electron transport at beam edges and near interfaces. Simplified algorithms–models are also used to account for the effect of photon scatter in the treatment head and leakage through the collimators. Some treatment planning systems implement more accurate dose algorithms, such as superposition convolution and Monte Carlo simulations for the final dose calculation after the MLC leaf sequences have been determined, in order to correct for the photon leakage effect. The FCCC has developed a Monte Carlo dose verification tool for IMRT QA, which may partially replace the phantom monitor unit check and the relative dose measurement with film.

### 3.5. Position verification and target localization

Position verification is critical for IMRT, both for the initial plan validation and for subsequent IMRT treatments. The goal is to verify that the treatment isocentre matches the planned isocentre. Positioning techniques based on bony structures provide adequate positioning accuracy for head and neck and spinal areas. Specially designed imaging systems based on ultrasound, CT and optical and radiographic detectors may be used for soft tissue target localization. The BAT ultrasound system (Fig. 5) has been shown to be an effective and efficient target relocation device for a prostate treatment set-up. The positioning accuracy is about 3 mm for the more than 3000 patients investigated. An extra 3–5 min is added to the treatment time and an IMRT prostate treatment is scheduled for 20 min. The FCCC has acquired a Siemens CT on rails system (a CT machine in the treatment room) for targets anywhere in the body (Fig. 6), which uses either bony structures or surgically inserted fiducial markers. A 2 mm accuracy is expected using this unit for body surgery and for hypofractionated IMRT treatments. A body localizer with vacuum fixation (Fig. 1) will reduce the movement of internal organs for high precision beam delivery for stereotactic body surgery or stereotactic IMRT. A CyberKnife system (Accuray) is being investigated for extracranial sites, including the prostate, lung, liver and pancreas, which uses a combined optical and radiographic system to correlate the movements of markers on the surface of the patient and the internal organs. Based on the real time organ motion, information dynamic target tracking can be performed. A 5 mm ( $2\sigma$ ) accuracy may be achieved using such real time image guidance for breast, thoracic and abdominal treatments.

### 3.6. Treatment delivery

There are several ways to deliver intensity modulated beams for IMRT, including dynamic MLC beam delivery, segmented beam delivery using static MLCs, intensity modulated arc therapy and compensator based IMRT. The Siemens SMLC (static MLC) is used at the FCCC to deliver intensity modulated fields. The FCCC treatment time for the prostate is 20 min for IMRT, compared with 15 min for 3-D CRT. The treatment time for the head and neck is variable, from 20 min to 40 min, depending on the complexity and number of field segments. A Radionics mMLC with a 4 mm leaf width is used for stereotactic body surgery and IMRT. The CyberKnife system uses a 6 MV X band linac mounted on a robotic arm, and is being investigated for hypofractionated treatments of the prostate, liver, pancreas and lung.





*FIG. 5. The BAT ultrasound system for soft tissue target localization.*



*FIG. 6. The Siemens CT on rails system for IMRT target localization.*



#### 4. SUMMARY

IMRT is an advanced form of 3-D CRT. The clinical implementation of IMRT needs much more work than that needed to implement 3-D CRT. This is only the first step in bringing this modality into the clinic. More effort is needed to keep it running smoothly and to keep pace with upgrades and future enhancements in IMRT technology. IMRT is an integrated process and is rapidly evolving. The QA programme for IMRT treatment planning and beam delivery will change with time to include the various new issues that will arise.

#### ACKNOWLEDGEMENTS

This work is in part supported by National Cancer Institute grant No. CA 78331. The authors would like to thank the other members of the therapy and physics team, especially J. Yang, O. Chibani and W. Xiong, for their contributions to the clinical implementation of IMRT and routine QA at the FCCC.

#### REFERENCES

- [1] BRAHME, A., Optimal setting of multileaf collimators in stationary beam radiation therapy, *Strahlenther. Onkol.* **164** (1988) 343–350.
- [2] CONVERY, D.J., WEBB, S., “Calculation of the distribution of head-scattered radiation in dynamically-collimated MLC fields”, *Use of Computers in Radiation Therapy* (Proc. Int. Conf. Salt Lake City, UT, 1997), Medical Physics Publishing, Madison, WI (1997) 350–353.
- [3] BOYER, A.L., GEIS, P.B., GRANT, W., KENDALL, R., CAROL, M., Modulated-beam conformal therapy for head and neck tumors, *Int. J. Radiat. Oncol. Biol. Phys.* **39** (1997) 227–236.
- [4] WANG, X., et al., Dosimetric verification of intensity modulated fields, *Med. Phys.* **23** (1996) 317–328.
- [5] WEBB, S., *The Physics of Conformal Radiotherapy: Advances in Technology*, Institute of Physics Publishing, Bristol, UK (1997).
- [6] CHUI, C.S., LOSASSO, T., SPIROU, S., Dose calculations for photon beams with intensity modulation generated by dynamic jaw or multileaf collimators, *Med. Phys.* **21** (1994) 1237–1243.
- [7] HOUNSELL, A.R., Monitor chamber backscatter for intensity modulated radiation therapy using multileaf collimators, *Phys. Med. Biol.* **43** (1998) 445–454.
- [8] LOW, D.A., et al., Quantitative dosimetric verification of an IMRT planning and delivery system, *Radiother. Oncol.* **49** (1998) 305–316.

- [9] MUTIC, S., LOW, D.A., KLEIN, E.E., DEMPSEY, J.F., PURDY, J.A., Room shielding for intensity modulated radiation therapy treatment facilities, *Int. J. Radiat. Oncol. Biol. Phys.* **50** (2001) 239–246.
- [10] BOYER, A.L., et al., Theoretical considerations of monitor unit calculations for intensity modulated beam treatment planning, *Med. Phys.* **26** (1999) 187–195.
- [11] CHEN, Y., XING, L., LUXTON, G., LI, J.G., BOYER, A.L., “A multi-purpose quality assurance tool for MLC-based IMRT”, *Use of Computers in Radiation Therapy (Proc. Int. Conf. Heidelberg, 2000)*, Springer-Verlag, Heidelberg (2000).
- [12] MA, C.-M., et al., Monte Carlo verification of IMRT dose distributions from a commercial treatment planning optimization system, *Phys. Med. Biol.* **45** (2000) 2483–2495.
- [13] PAWLICKI, T., MA, C.-M., Monte Carlo dose modelling for MLC-based IMRT, *Med. Dosim.* **26** (2001) 157–168.

# **QUASIMODO: AN ESTRO PROJECT FOR PERFORMING THE QUALITY ASSURANCE OF TREATMENT PLANNING SYSTEMS AND INTENSITY MODULATED RADIATION THERAPY**

B.J. MIJNHEER\*, C. DE WAGTER\*\*, S. GILLIS\*\*,  
A. OLSZEWSKA\*,\*\*\*

\* Radiotherapy Department, Netherlands Cancer Institute,  
Antoni van Leeuwenhoek Hospital,  
Amsterdam, Netherlands  
E-mail: bmijnh@nki.nl

\*\* Radiotherapy Division, Ghent University Hospital,  
Ghent, Belgium

\*\*\* Medical Physics Department, Centre of Oncology,  
Warsaw, Poland

## **Abstract**

In the framework of a European Society for Therapeutic Radiology and Oncology project on the quality assurance of treatment planning systems and intensity modulated radiation therapy (IMRT), radiotherapy institutions from nine European countries combined their efforts in designing and testing a new methodology for applying these tools in a safe and consistent way in the clinic. In the first part of the project a limited number of tests have been designed that should be carried out before a treatment planning system is used clinically. In the second part of the project the participating institutions will carry out tests for the verification of IMRT techniques for prostate cancer and head and neck tumours. The preliminary experience in applying these tests shows the necessity of having uniform guidelines for both purposes.

## **1. INTRODUCTION**

A computerized treatment planning system (TPS) is an essential tool in designing the radiotherapeutic treatment of a cancer patient. Although there are a number of reports on the quality assurance (QA) of the treatment planning process [1–5], only limited information is available on how to perform QA tests for a TPS in a systematic and efficient way. Particularly with respect to the three dimensional (3-D) aspects of planning systems, there are currently

no practical recommendations to guide a user in performing specific tests before implementing a 3-D TPS in clinical use. Two organizations, the IAEA [6] and the Nederlandse Commissie voor Stralingsdosimetrie (NCS) [7], are in the process of designing these types of test, but it might be expected that their recommendations require too many resources to allow for application in all radiotherapy institutions. For that reason it was decided that the European Society of Therapeutic Radiology and Oncology (ESTRO) would start two activities in the field of the QA of a TPS. First there is a need for a minimum number of tests to be performed in those institutions that have only limited resources. These tests should not be too cumbersome to perform and should cover the most essential parts of a TPS required for accurately planning the established conformal radiotherapy techniques to be used.

A rapidly increasing number of institutions have started the clinical introduction of intensity modulated radiotherapy (IMRT), a new form of conformal radiotherapy. By varying the beam intensity over a treatment field it is possible to deliver the radiation dose to conform more closely with irregularly shaped target volumes. In this way it is possible to deliver a higher dose to the tumour, while at the same time reducing the dose to the volume of surrounding healthy tissues. A high geometric and dosimetric accuracy is required for these advanced techniques. The acceptance testing of the IMRT TPS, as well as the verification of the delivery of these IMRT dose distributions, is therefore a prerequisite for the safe application of IMRT (see, for example, Ref. [8]). Various types of QA test are in use in individual institutions, but no internationally accepted guidelines are yet available. It is the second aim of this ESTRO project to design tests and to provide guidelines for the verification of IMRT techniques.

## 2. METHODS

The QUASIMODO (quality assurance of intensity modulated beams in radiation oncology) ESTRO project can be divided into two interrelated parts.

### 2.1. Part 1: Drafting a list of essential tests for a TPS

These recommendations are intended for all institutions applying conformal radiotherapy, including centres that have limited resources, use old releases of commercial software or apply non-standard TPSs. Recommendations should consider both the geometric and dosimetric aspects of a TPS, as formulated by other committees drafting guidelines for the QA of a TPS. For example, working groups of the IAEA [6] and the NCS [7] are preparing a report on accep-

tance testing, commissioning and the QA of computerized radiation treatment planning. Since the aim of the ESTRO project is more restricted than that of the IAEA or the NCS, only some parts of these reports, related to practical tests, have been used as a starting point for the ESTRO activities. This part of the project will mainly be performed in Amsterdam.

## **2.2. Part 2: The verification of static and dynamic IMRT fields**

An interesting and extremely timely activity is the verification of newly designed IMRT techniques for which general guidelines are not yet available. It is not sufficient for this activity to test the accuracy of the TPS alone. The various parts of the chain of an IMRT procedure, such as the design of the IMRT beam profile, the sequencing of the position of the leaves and the actual delivery of the dose by the treatment machine, are interrelated. This activity therefore concerns the development of procedures for the verification of specific IMRT applications using data measured on various treatment machines. In principle there are two ways of delivering IMRT profiles: the use of static or segmental multileaf collimator (MLC) fields, often called the step and shoot method, and the dynamic use of MLC leaves, of which the sliding window technique is the most commonly employed method.

IMRT techniques of varying degrees of complexity for the treatment of prostate cancer and head and neck tumours will be designed and tested in this part of the project. It was decided to verify the end product (i.e. the complete treatment delivery, not the dose distributions delivered by the individual fields separately). A phantom was made in Ghent specifically for this project (the CarPet phantom) to verify IMRT treatments of prostate cancer (Fig. 1). This phantom, as well as a set of photographic films, will be sent to each of the participating centres. Inside the phantom are some inserts for positioning an ionization chamber for absolute dose measurements, for the purposes of normalizing the film data.

All institutions will be asked to design an IMRT technique using their specific software and hardware, applying the same set of dose-volume criteria. For the prostate case these are: the planning target volume (PTV) should receive a mean dose of 200 cGy, which should be given as uniformly as possible (i.e. less than 10% of the PTV should receive a dose of less than 190 cGy, and less than 5% more than 210 cGy). The dose in the organ at risk (OAR) should not exceed 140 cGy, and not more than 10% of the volume of the remaining tissues should receive a dose higher than 160 cGy, while the maximum dose should be less than 200 cGy. It can be expected that some centres will deliver these fields with the static IMRT method, while others will apply the dynamic IMRT technique. The maximum delivery time for both techniques should be

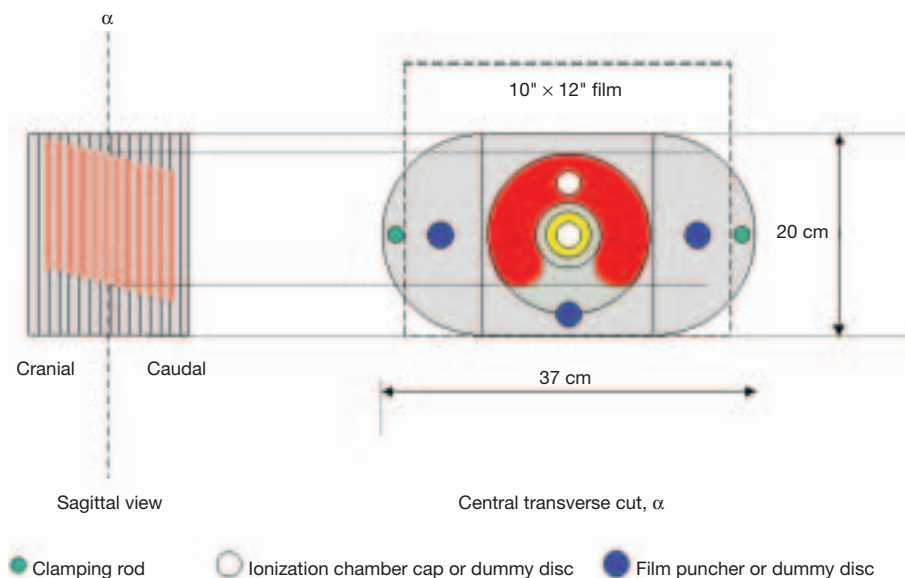


FIG. 1. Transversal and sagittal view of the CarPet phantom used for the verification of IMRT treatments of prostate cancer. Indicated are the PTV (in yellow) and an OAR (in red), which have to be considered in the optimization process. Films can be put between any of the 1 cm thick polystyrene slabs.

less than 20 min. This part of the project, including the film processing and data analysis, will mainly be performed in Ghent. The experience obtained with the prostate case will be used to design a second phantom to be used for the verification of the IMRT of head and neck tumours.

### 3. RESULTS

#### 3.1. Review of the current status of IMRT

The project started on 1 August 2001, and is funded for a period of two years. In order to have an overview of the current status of IMRT in the institutions participating in the QUASIMODO project, a questionnaire was distributed, and was returned by 13 participating centres. Information was provided concerning the delivery technique, the computer optimization software, the type of objective functions, the leaf sequencer software, the software for the calculation of the dose distribution and monitor units, the phantoms and dosimetry systems applied for verification and clinical experience. A general

conclusion drawn from this survey was that all major accelerator and TPS manufacturers are represented in the QUASIMODO project. As a consequence, it will be possible to compare most IMRT optimization–delivery combinations that are currently possible to apply clinically.

From the answers to the questionnaire it also became evident that until now most institutions have used IMRT to treat patients with prostate and head and neck cancer. Phantoms will therefore be designed to verify the techniques as applied in the participating institutions for these treatment sites.

### 3.2. Drafting a list of essential tests for a TPS

In order to estimate the usefulness and workload involved in applying QA tests for a TPS, the examples given in Ref. [7] were applied to a commercial TPS (Pinnacle, Philips ADAC Laboratories) recently installed in the Netherlands Cancer Institute for research purposes. Table I shows some of the tests that have been performed to verify the correctness of the anatomical description of the patient in the TPS. These tests, taken from chapter 2 of Ref. [7], are presented to ensure that the data for building an anatomical description are correctly linked to the specific patient, that the input of data, for example images, constituting the anatomical description is correct and that the anatomical description itself is correct.

TABLE I. EXAMPLES OF TESTS PERFORMED TO VERIFY THE CORRECTNESS OF THE ANATOMICAL DESCRIPTION OF THE PATIENT IN A TPS

(taken from Ref. [7])

Basic patient entry	Image conversion, input and use	Anatomical structures
Two patients with the same last name	A patient data set with a duplicated slice	A new structure with a name that already exists
Two patients with the same identification number	Various slice thicknesses	Correct geometry in automatic contouring
The same patient twice	Computed tomography number representation	Addition of a margin in axial slices
The same patient with two different targets	Patient orientation	3-D surface computation, volume check
Deletion of the patient	Geometry of reconstructed images	Structure expansion

The preliminary results have already demonstrated some of the limitations of this particular TPS, for example with respect to the input of patient data. Another observation was that the time involved in performing these tests is substantial. For instance, testing the anatomical description and beam description took several person-months, while currently a lot of effort is put into performing the dosimetric tests. Obviously a selection of the most important tests is necessary.

### **3.3. Verification of static and dynamic IMRT fields**

The performance of the CarPet phantom has been tested in three centres. After adapting the phantom and modifying the procedure slightly, the phantoms will now be distributed to all participating centres. The IMRT plans and the irradiated films, as well as the results of the ionization chamber measurements, will be sent to Ghent for analysis. Software has been developed to compare in a number of slices the calculated and measured dose distributions. The ionization chamber measurements will allow for a renormalization of the film measured dose distributions. A combination of a spatial criterion (e.g. 3 mm) and a dosimetric criterion (e.g. 3%) is implemented in accordance with the gamma concept, as introduced by Low et al. [9]. The resulting maps can be laid over the computed dose distributions, possibly indicating regions where the criteria were not met.

## **4. CONCLUSIONS**

A preliminary conclusion from the work done so far is that a clearer separation has to be made between tests to be performed by the vendor of a specific TPS, by user groups (test sites) of that system and by an individual user. It is therefore necessary to strive for a close co-operation with the vendors of TPSs at a later stage of the project, to get their input and comments on these proposals. Performing the proposed tests by users of various TPSs seems very useful before distributing the recommendations on a larger scale, which will most likely be done in the form of an ESTRO booklet.

An interesting observation from the survey on the current status of IMRT in Europe was that almost every institution applied its own phantom–dosimetry systems for the verification of treatment delivery. An evaluation of these methods, as well as of the methodology applied in this project, followed by drafting of general guidelines by ESTRO for the QA of IMRT planning and delivery, therefore seems the logical next step.



## ACKNOWLEDGEMENTS

The authors appreciate the enthusiastic co-operation in this project of the following: R. Arrans, Spain, J. Bohsung, Germany, W. Bulski, Poland, C. Fiorino, Italy, G. Hartmann, Germany, G. Heeren, Belgium, J.-M. d'Hooghe, Belgium, D. Huyskens, Belgium, T. Knöös, Sweden, J.-C. Rosenwald, France, D. Thwaites, United Kingdom, H. Welleweerd, Netherlands, and P. Williams, United Kingdom.

QUASIMODO is funded by the European Commission, Directorate General Health and Consumer Protection, Europe Against Cancer Programme, and is part of the ESQUIRE Project, grant agreement 2001CVG2-005.

## REFERENCES

- [1] VAN DYK, J., BARNETT, R.B., CYGLER, J., SHRAGGE, P.C., Commissioning and quality assurance of treatment planning computers, *Int. J. Radiat. Oncol. Biol. Phys.* **26** (1992) 261–273.
- [2] SHAW, J.E., A Guide to Commissioning and Quality Control of Treatment Planning Systems, Rep. 68, Institution of Physics and Engineering in Medicine and Biology, York, UK (1994).
- [3] SWISS SOCIETY FOR RADIOBIOLOGY AND MEDICAL PHYSICS, Quality Control of Treatment Planning Systems for Teletherapy, Rep. 7, Swiss Society for Radiobiology and Medical Physics (1997).
- [4] FRAASS, B., et al., American Association of Physicists in Medicine Radiation Therapy Committee Task Group 53: Quality assurance for clinical radiotherapy treatment planning, *Med. Phys.* **25** (1998) 1773–1829.
- [5] MAYLES, W.P.M., et al., Physics Aspects of Quality Control in Radiotherapy, Rep. 81, Institute of Physics and Engineering in Medicine, York, UK (1999) 60–95.
- [6] INTERNATIONAL ATOMIC ENERGY AGENCY, Commissioning and Quality Assurance of Computerized Treatment Planning (in preparation).
- [7] NEDERLANDSE COMMISSIE VOOR STRALINGSDOSIMETRIE, Quality Assurance of 3-D Treatment Planning Systems, draft report, NCS, Delft (2000).
- [8] INTENSITY MODULATED RADIATION THERAPY COLLABORATIVE WORKING GROUP, Intensity-modulated radiotherapy: Current status and issues of interest, *Int. J. Radiat. Oncol. Biol. Phys.* **51** (2001) 880–914.
- [9] LOW, D.A., HARMS, W.B., MUTIC, S., PURDY, J.A., A technique for the quantitative evaluation of dose distributions, *Med. Phys.* **25** (1998) 656–661.

**BLANK**

# FACTORS AFFECTING THE EXTRACTION OF ABSORBED DOSE INFORMATION IN 3-D POLYMER GEL DOSIMETERS BY X RAY COMPUTED TOMOGRAPHY

J.V. TRAPP, G. MICHAEL, Y. DE DEENE, C. BALDOCK  
Centre for Medical, Health, and Environmental Physics,  
Queensland University of Technology,  
Brisbane, Australia  
E-mail: c.baldock@qut.edu.au

## Abstract

Two sources of uncertainty in the X ray computed tomography imaging of polymer gel dosimeters are investigated in the paper. The first cause is a change in post-irradiation density, which is proportional to the computed tomography signal and is associated with a volume change. The second cause of uncertainty is reconstruction noise. A simple technique that increases the residual signal to noise ratio by almost two orders of magnitude is examined.

## 1. INTRODUCTION

There is a requirement to measure accurately three dimensional radiation dose distributions in radiotherapy, which has led to a growing body of research in the use of polymer gel dosimeters [1]. It has been shown that a post-irradiation change in the linear attenuation coefficient,  $\mu$ , of a polymer gel dosimeter can be measured by the use of X ray computed tomography (CT) [2, 3]. This paper examines two aspects of spatial uncertainty in the CT of polymer gel dosimeters. The first is spatial uncertainty within the dosimeter and the second is uncertainty within the image of the gel.

It has been postulated that the change in  $\mu$  may be primarily due to a change in physical density,  $\rho$ , of the polymer gel dosimeter [4]. To investigate spatial uncertainty in the dosimeter itself the relationship between  $\mu$  and  $\rho$  was examined and the implications of a density change in relation to spatial resolution were considered.

CT scanner settings and the reconstruction matrix size can affect both the noise and the spatial resolution in an image. The field of view (FOV) and its effect on both spatial resolution and noise in a CT image of a polymer gel dosimeter was examined.

2. METHODS AND MATERIALS

2.1. Polymer gel dosimeter spatial resolution

The linear attenuation coefficient,  $\mu$ , and physical density,  $\rho$ , were measured in polymer gel dosimeters irradiated to various doses. The polymer gel dosimeter was comprised of 5% gelatin (Sigma Aldrich), 3% acrylamide (Sigma Aldrich), 3% N,N'-methylene-bis-acrylamide (Sigma Aldrich) and 89% water. The gels were manufactured in a glovebox using a method previously described [3, 5] and poured into either polystyrene spectrophotometry cuvettes (Sigma Aldrich), for attenuation measurements, or volumetric flasks with capillary stoppers, for density measurements. Three batches of polyacrylamide gel (PAG) dosimeter were produced, as shown in Table I.

The linear attenuation coefficient was measured using a collimated beam of 59.54 keV photons from an  $^{241}\text{Am}$  source. This energy was selected as it is close to the typical effective energy (not peak energy) of a clinical CT scanner;  $\mu$  was also measured for deionized distilled water, for the calculation of the CT number. The detector was a high purity germanium detector (EG&G Ortec). Background counts were subtracted from the recorded counts and the remainder was normalized in accordance with a count taken at each set of measurements. A diagram of the apparatus is shown in Fig. 1.

The linear attenuation coefficient was calculated as the gradient of a weighted least squares fit (Fig. 2), with the path length of the radiation through the polymer gel dosimeter,  $t$ , being the abscissa and the ordinate  $y$  being:

$$y = \ln \left( \frac{C_1(A - B)}{C_2(A_0 - B)} \right) \tag{1}$$

TABLE I. BATCHES OF POLYMER GEL DOSIMETER MANUFACTURED

Sample	Parameter measured	Day of measurement (post-irradiation)
PAG <sub>1</sub>	$\mu$ and $\rho$	13–21 ( $\rho$ and $\mu$ measured on same day for each data point)
PAG <sub>2</sub>	$\mu$	19–25
PAG <sub>3</sub>	$\rho$	3

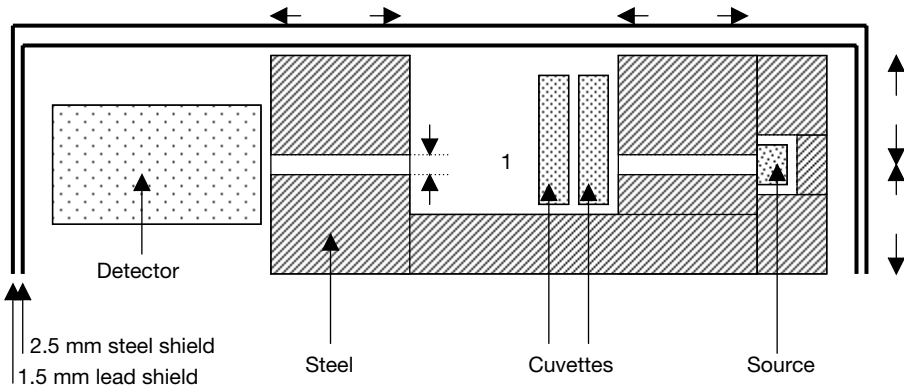


FIG. 1. Geometry of the collimating apparatus.

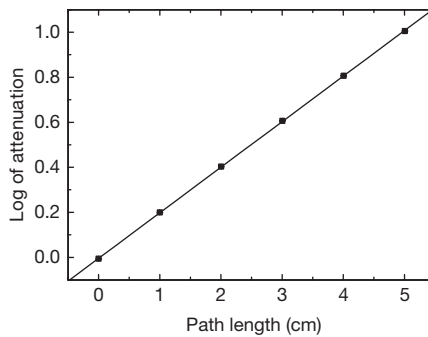


FIG. 2. Log of the attenuation of photons through various thicknesses of PAG.

where  $A$  is the counts with water or polymer gel dosimeter in the apparatus,  $A_0$  is the counts with empty cuvettes in the apparatus,  $B$  is the background counts, and  $C_1$  and  $C_2$  are the values of the normalization counts.  $A_0$  was measured for each number of cuvettes used; for example, for  $t$  of 2 cm,  $A_0$  was measured with two empty cuvettes to allow for attenuation by the cuvettes themselves. The uncertainty in  $y$  was calculated by a first order Taylor expansion of Eq. (1) [6].

Density was measured three days post-irradiation using glass density flasks with capillary stoppers. The mass of the flasks was determined empty, containing gel only, containing gel and the remainder filled with water, and filled with water only. Measurements were made at room temperature (24°C). The density of the gel was calculated as:

$$\rho_{\text{gel}} = m_{\text{gel}} \left( \frac{\rho_{\text{water}}}{m_{\text{tot}} - m_{\text{wat}}} \right) \quad (2)$$

where  $\rho_{\text{gel}}$  is the density of the polymer gel dosimeter,  $\rho_{\text{water}}$  is the density of water,  $m_{\text{tot}}$  is the mass of water that the flask can hold,  $m_{\text{wat}}$  is the mass of water required to fill the flask when containing gel and  $m_{\text{gel}}$  is the mass of gel in the flask. Uncertainty was calculated using a first order Taylor expansion of Eq. (2) [6].

## 2.2. Image spatial resolution

Two simulations were performed to examine the effects on noise of different pixel sizes in the final image. Projection data through a homogenous circle were simulated using Matlab software (Mathworks, Inc.).

In the first simulation projection data of 1024 ray sums per projection with 720 projections were produced, and various levels of Gaussian noise were added. The noisy projection data were grouped into pairs of ray sums and pairs of projections, which were averaged, producing data with 512 ray sums per projection and 360 projections. The process was repeated with groups of four ray sums and four projections to produce data with 256 ray sums per projection and 180 projections. All sets were produced from the original data set, ensuring that the same random numbers used in the noise generation were applied to all data sets representing the same simulated photon fluxes. The images were then reconstructed.

In the second simulation the first reconstructed image from the first simulation was used (the image reconstructed from the 1024 ray sum per projection data). In this simulation pixels in the reconstructed image were grouped into  $2 \times 2$  pairs and  $4 \times 4$  pairs and averaged within each group to produce larger pixels.

Both simulations produced images of the same size; however, the first simulation represents grouping of data prior to reconstruction (FOV settings varied on the scanner), and the second simulation represents grouping of data after reconstruction (post-acquisition).

## 3. RESULTS

### 3.1. Polymer gel dosimeter spatial resolution

Figures 3(a) and (b) show  $\mu$  for PAG<sub>1</sub> and PAG<sub>2</sub> as a function of dose. The inserts show the calculated CT numbers. A biexponential curve is fitted to the

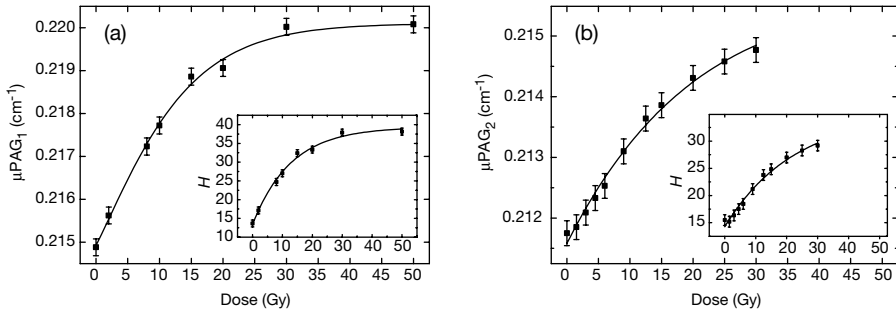


FIG. 3. Linear attenuation coefficient dependence on dose for (a)  $\text{PAG}_1$  and (b)  $\text{PAG}_2$ . The inserts show calculated  $H$ .

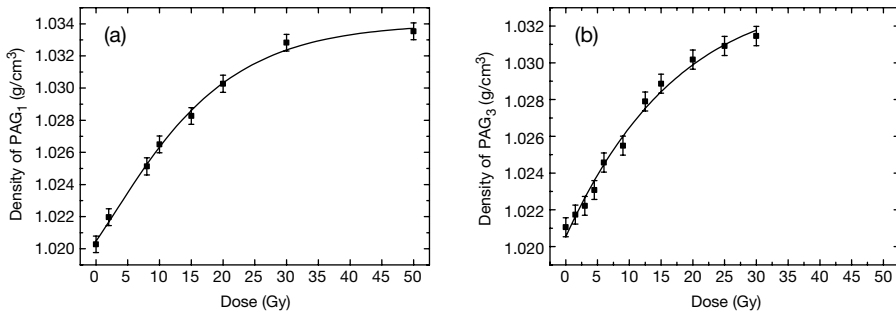


FIG. 4. Density dependence on dose for (a)  $\text{PAG}_1$  and (b)  $\text{PAG}_3$ .

data. The behaviour has been discussed previously in the context of magnetic resonance imaging measurements [7]. At high doses the asymptotic behaviour is due to monomer consumption, while the non-linear behaviour at low doses can be attributed to the presence of inhibitors, such as oxygen, which compete with the polymerization reaction [7].

Figures 4(a) and (b) show the measured  $\rho$  for  $\text{PAG}_1$  and  $\text{PAG}_3$  with biexponential curves fitted to the data. These figures show that the density of the polymer gel dosimeters appears to increase in a fashion that can be approximated as linear with dose to approximately 20 Gy, with further increases in density before reaching an upper plateau of density after approximately 30 Gy.

Figure 5(a) is a plot of  $\mu$  against  $\rho$  for  $\text{PAG}_1$  and Fig. 5(b) is a plot of  $\mu$  for  $\text{PAG}_2$  against  $\rho$  of  $\text{PAG}_3$ . A weighted least squares linear fit is shown. The least squares fit in Fig. 5(a) has a  $P$  value of  $<0.0001$  and an  $r^2$  value of 0.99605 and Fig. 5(b) has a  $P$  value of  $<0.0001$  and an  $r^2$  value of 0.99953. This indicates that

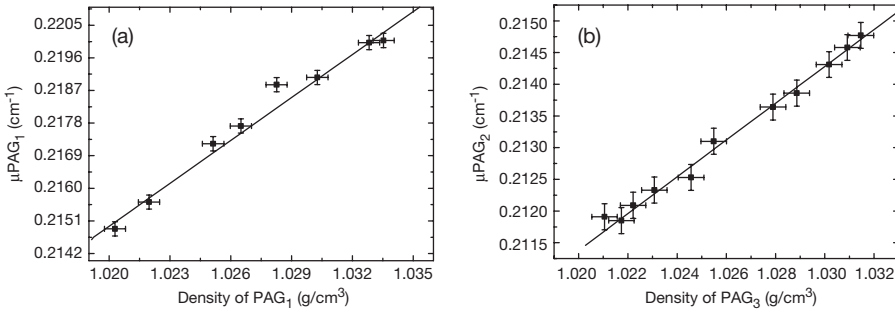


FIG. 5. Comparison of  $\mu$  and  $\rho$  for (a)  $\text{PAG}_1$  and (b) between  $\text{PAG}_2$  and  $\text{PAG}_3$ .

the function relating absorbed dose to density is proportional to that of the linear attenuation coefficient. Figure 5(b) shows that the linearity remains when the data for  $\mu$  and  $\rho$  are that of different batches and measured at different times.

The change in  $\mu$  is proportional to an increase in  $\rho$  of the polymer gel dosimeter. The increase in  $\rho$  of the polymer gel dosimeter during irradiation may introduce uncertainties in the absorbed dose as the radiation attenuation properties change. There is no mass lost from the gel during irradiation, therefore the increase in density must be related to a reduction in the volume of the irradiated gel. Initial measurements indicate that the change in volume is within acceptable levels for meeting the spatial resolution requirements of International Commission on Radiation Units and Measurements Report 42 [8].

### 3.2. Image resolution

The results of the effect of reconstruction matrix size on noise can be seen in Figs 6(a) and (b). The figures represent noise as the signal to noise ratio (SNR) prior to and after reconstruction. The portion of the figures with a pre-reconstruction SNR below approximately  $10^6$  represents stochastic noise typical in a CT image. The portion with a greater pre-reconstruction SNR represents CT images with very little stochastic noise, such as when several images are averaged together (effectively increasing the mAs) [2, 3]. The stochastic noise regions of Figs 6(a) and (b) behave as expected (i.e. as noise in the projections decreases so does noise in the final image). The figures show that there is a limit to the attainable SNR, due to an underlying noise component, which has been known since the 1970s [9] (the cause of this noise will be examined in future work).



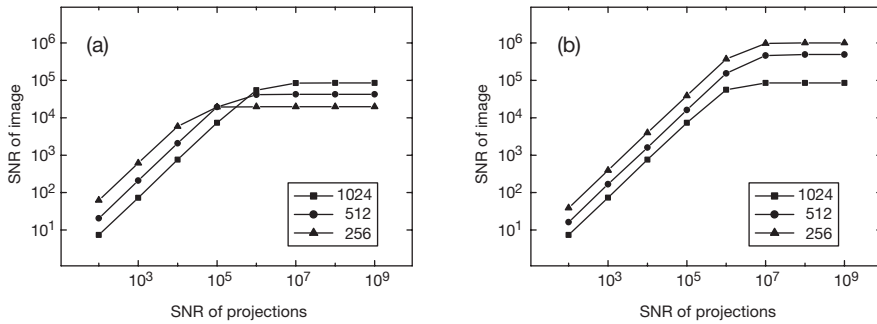


FIG. 6. (a) Pixels grouped prior to reconstruction; (b) pixels grouped after reconstruction.

A comparison of Figs 6(a) and (b) shows that in the stochastic noise region there is little difference between averaging before and after reconstruction; however, there are significant differences in the region of low noise representing high mAs or image averaging. Grouping of data after reconstruction gives a greater SNR in all cases, representing a lower noise level in the final image. A comparison of the 256 data between the figures shows that there is an improvement of almost two orders of magnitude. These data show that, when a large number of images are averaged together in the CT of gel dosimeters, better results will be achieved if images are acquired using the smallest pixel size settings available on the scanner, with the final image then reduced to the spatial resolution required for the particular application by grouping pixels into blocks. For example, if a 1 mm spatial resolution is required in the final gel dosimeter image and the scanner is capable of a 0.5 mm resolution, then the images should be acquired at a 0.5 mm resolution and then grouped to 1 mm to reduce noise.

#### 4. CONCLUSION

It has been shown that the change in  $\mu$  that gives rise to the CT signal is proportional to an increase in  $\rho$ . The increase in  $\rho$  will introduce uncertainties in the absorbed dose distribution within a polymer gel dosimeter, regardless of the imaging modality. To reduce noise when imaging a polymer gel dosimeter with CT, the image should be acquired at the smallest pixel size setting available on the scanner. The pixels should then be grouped, in order to meet the spatial uncertainty requirements of the particular application.

## REFERENCES

- [1] MARYANSKI, M.J., GORE, J.C., KENNAN, R.P., SCHULZ, R.J., NMR relaxation enhancement in gels polymerized and cross-linked by ionizing radiation: A new approach to 3D dosimetry by MRI, *Magn. Reson. Imag.* **11** (1993) 253–258.
- [2] HILTS, M., DUZENLI, C., ROBAR, J., AUDET, C., Polymer gel dosimetry using X-ray computed tomography: A feasibility study, *Phys. Med. Biol.* **45** (2000) 2559–2571.
- [3] TRAPP, J.V., BÄCK, S.Å.J., LEPAGE, M., MICHAEL, G., BALDOCK, C., An experimental study of the dose response of polymer gel dosimeters imaged with x-ray computed tomography, *Phys. Med. Biol.* **46** (2001) 2939–2951.
- [4] TRAPP, J.V., MICHAEL, G., DE DEENE, Y., BALDOCK, C., Attenuation of diagnostic energy photons by polymer gel dosimeters, *Phys. Med. Biol.* (in press).
- [5] BALDOCK, C., et al., Experimental procedure for the manufacture and calibration of polyacrylamide gel (PAG) for magnetic resonance imaging (MRI) radiation dosimetry, *Phys. Med. Biol.* **43** (1998) 695–702.
- [6] INTERNATIONAL ORGANIZATION FOR STANDARDIZATION, Guide to the Expression of Uncertainty in Measurement, 2nd edn, ISO, Geneva (1995).
- [7] DE DEENE, Y., HANSELAER, P., DE WAGTER, C., ACHTEN, E., DE NEVE, W., An investigation of the chemical stability of a monomer/polymer gel dosimeter, *Phys. Med. Biol.* **45** (2000) 859–878.
- [8] INTERNATIONAL COMMISSION ON RADIATION UNITS AND MEASUREMENTS, Use of Computers in External Beam Radiotherapy Procedures with High Energy Photons and Electrons, Rep. 42, ICRU, Bethesda, MD (1987).
- [9] COHEN, G., DI BIANCA, F.A., The use of contrast-detail-dose evaluation of image quality in a computed tomographic scanner, *J. Comput. Assist. Tomogr.* **3** (1979) 189–195.

## ACOUSTIC EVALUATION OF POLYMER GEL DOSIMETERS

M.L. MATHER, Y. DE DEENE, C. BALDOCK

Centre for Medical, Health and Environmental Physics,  
Queensland University of Technology  
E-mail: c.baldock@qut.edu.au

A.K. WHITTAKER

Centre for Magnetic Resonance, University of Queensland

Brisbane, Australia

### Abstract

The effect of polymer gel dosimeter composition, temperature and ultrasonic signal frequency on ultrasonic dose response was investigated. Ultrasonic attenuation and speed were measured in PAG and MAGIC polymer gel dosimeters to assess the effect of dosimeter composition on dose response. Ultrasonic attenuation and speed were also determined in PAGs for a range of temperatures (10–25°C) and the ultrasonic attenuation coefficient was measured for three different ultrasonic frequencies (25.7, 46.3 and 66.2 MHz). Variations in dosimeter composition, temperature and ultrasonic frequency were found to alter the dynamic range and dose sensitivity of ultrasonic dose response curves, as well as the absolute values of speed and attenuation.

### 1. INTRODUCTION

Advances in radiotherapy treatment techniques such as intensity modulated radiotherapy are placing increasing demands on radiation dosimetry for the verification of dose distributions in three dimensions. In response, polymer gel dosimeters capable of recording dose distributions in three dimensions are currently being developed. A new technique for the evaluation of absorbed dose distributions in these dosimeters using ultrasound was recently introduced [1]. Ultrasound attenuation and speed were shown to vary with absorbed dose over a large dynamic range (up to 50 Gy). This work demonstrated the potential of ultrasound for the evaluation of polymer gel dosimeters. The full potential of ultrasound evaluation techniques, however, is yet to be realized, as this method of investigation has not been optimized.

Ultrasound evaluations of polymer gel dosimeters may be optimized through a variation of dosimeter composition and temperature. Magnetic resonance imaging (MRI) evaluations of these dosimeters have shown dosimeter dose response to vary with dosimeter composition and evaluation temperature [2, 3]. As the ultrasonic properties of materials can be significantly affected by a material's structure and temperature it is predicted that the ultrasonic dose response of polymer gel dosimeters will also be affected by variations in dosimeter formulation and temperature [4]. The ultrasonic dose response of polymer gel dosimeters may also be affected by the ultrasonic signal frequency, as both ultrasonic attenuation and speed can be frequency dependent [5].

The work described in this paper investigates the effect of changes in polymer gel dosimeter composition, temperature and the frequency of the ultrasonic signal on the ultrasonic dose response. Specifically, the dose response of polyacrylamide gel (PAG) dosimeters and a normoxic gel dosimeter (MAGIC gel) were compared to assess the effect of dosimeter composition on the ultrasonic response. PAG samples were also investigated as a function of dose for a range of dosimeter temperatures and ultrasonic frequencies.

## 2. EXPERIMENT

### 2.1. Polymer gel preparation

A batch of PAG with a formulation of 3% acrylamide, 3% N,N'-methylene-bis-acrylamide, 5% gelatin and 89% water by mass was prepared in a nitrogen filled glovebox, the details of which may be found elsewhere [6]. Once prepared the gel was poured into polystyrene spectrophotometer cuvettes and sealed in nitrogen filled glass tubes to prevent oxygen contamination. A batch of MAGIC gel consisting of 9% methacrylic acid by weight was manufactured on the bench top, details of which can be found elsewhere [7, 8]. MAGIC gel was also poured into polystyrene spectrophotometer cuvettes; however, the MAGIC gel samples were not sealed in glass tubes, as MAGIC gel responds to ionizing radiation in the presence of oxygen. Once set, the PAG and MAGIC gel samples were irradiated with up to 50 Gy using a Gammacell 200  $^{60}\text{Co}$  irradiation facility, which had previously been calibrated [9].

### 2.2. Single frequency ultrasound experiments

Ultrasonic measurements were performed in a water tank, the temperature of which could be controlled to within 0.1°C (Fig. 1). Samples were placed in the tank one at a time in a reproducible position. An ultrasonic transducer

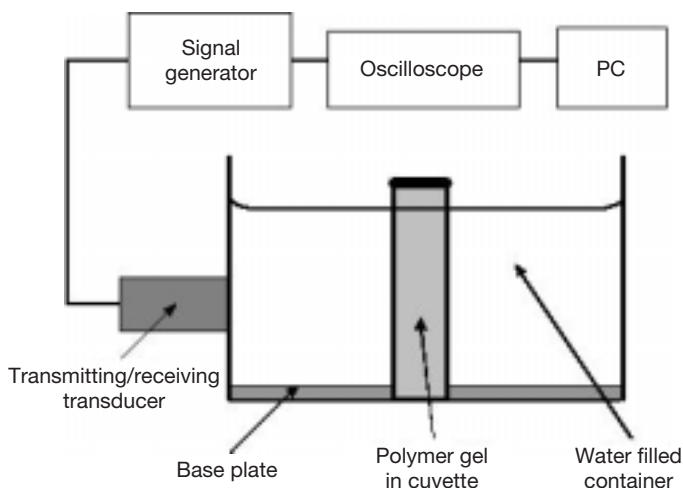


FIG. 1. Experimental set-up for single frequency ultrasound experiments.

(Panametrics A310S, Panametrics, Inc.) was coupled with ultrasound transmission gel (Aquasonic 100, Parker Labs, Inc.) to one end of the tank. A single cycle sinusoid was transmitted by the transducer at its resonant frequency ( $\sim 4$  MHz). The resulting reflected signals from the cuvette and polymer gel dosimeter interfaces were received by the transducer and recorded on a digitizing oscilloscope (Tektronics TDS 220). Digitized signals were transferred to a computer and analysed to determine the ultrasonic attenuation and speed. Attenuation and speed measurements were made at 10, 15, 20 and 25°C.

### 2.3. Ultrasound interferometer experiments

The dependence of ultrasonic attenuation on ultrasonic signal frequency was investigated using a pulsed ultrasonic interferometer operating at frequencies of 25.7, 46.3 and 66.2 MHz [1]. The interferometer consisted of a sample cell, tuneable transmitting and receiving ultrasonic transducers and a delay rod to adjust the path length between the two transducers. Ultrasonic attenuation was measured as a function of dosimeter path length, allowing the ultrasonic attenuation coefficient,  $\alpha$ , to be determined. Measurements were performed at room temperature (20°C).

### 3. RESULTS AND DISCUSSION

The variation of ultrasonic attenuation with absorbed dose is shown in Fig. 2 for PAG and MAGIC gel. Ultrasonic attenuation is seen to increase with absorbed dose over the full dose range for both formulations. In PAG the ultrasonic attenuation increases in a quasi-linear fashion up to approximately 15 Gy, with an ultrasonic attenuation dose sensitivity of  $(3.9 \pm 0.3)$  dB/m/Gy, while the quasi-linear region for MAGIC gel extends up to approximately 50 Gy, with an ultrasonic attenuation dose sensitivity of  $(4.7 \pm 0.3)$  dB/m/Gy. The overall attenuation found in MAGIC gel was greater than in PAG. The change in attenuation with dose in MAGIC gel was also greater than in PAG, as indicated by the dose sensitivity. The change in polymer gel dosimeter composition resulted in changes in the overall value of ultrasonic attenuation, dose sensitivity and the dynamic range of the attenuation dose response curve.

The variation in the ultrasonic speed of the propagation of bulk longitudinal waves in polymer gel dosimeters with absorbed dose is shown in Fig. 3. The ultrasonic speed is found to vary with absorbed dose for both formulations; however, there is a significant difference in the way it varies for the two dosimeter formulations investigated. Ultrasonic speed decreases with absorbed dose in PAG, while speed increases with absorbed dose in MAGIC gel. The decrease in ultrasonic speed in PAG continues up to approximately 30 Gy, with an ultrasonic speed dose sensitivity of  $(-0.44 \pm 0.02)$  m/s/Gy, while the increase in ultrasonic speed in MAGIC gel continues over the full dose range investigated, with

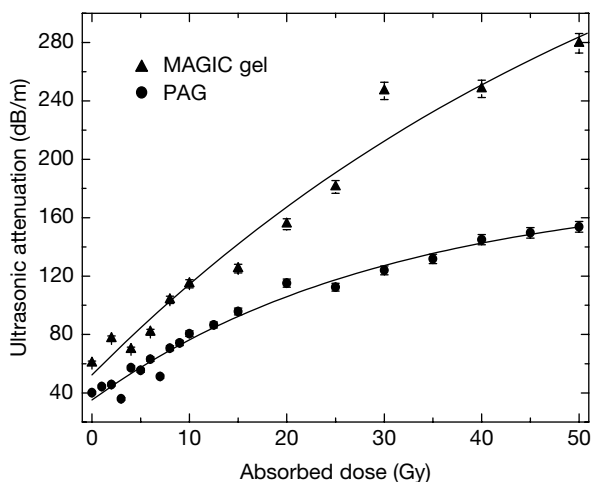


FIG. 2. Ultrasonic attenuation as a function of absorbed dose for PAG and MAGIC gel.

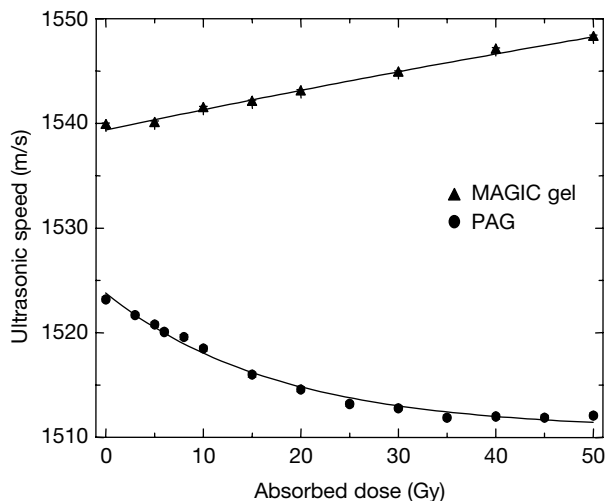


FIG. 3. Ultrasonic speed as a function of absorbed dose for PAG and MAGIC gel.

a dose sensitivity of  $(0.178 \pm 0.006)$  m/s/Gy. These results show that the ultrasonic dose sensitivity and dynamic range are significantly affected by the dosimeter composition. The different sensitivities of ultrasonic speed to radiation for PAG and MAGIC gel indicate fundamental differences in the two dosimeter formulations. Such differences have not been detected previously in MRI investigations.

The variation of ultrasonic attenuation with absorbed dose for different dosimeter temperatures is shown in Fig. 4. Ultrasonic attenuation increases with absorbed dose for all the dosimeter temperatures investigated. Attenuation is highest for the lowest dosimeter temperature investigated. Dose sensitivity is found to be affected by dosimeter temperature, with dose sensitivity increasing with a decrease in temperature for the samples investigated. For example, the ultrasonic attenuation dose sensitivity at 10°C,  $(2.5 \pm 0.3)$  dB/m/Gy, is higher than that at 25°C,  $(1.0 \pm 0.3)$  dB/m/Gy. From a practical point of view, the dosimeter temperature is relatively easy to control, and might be a convenient way to vary the dose sensitivity.

The dependence of ultrasonic speed on absorbed dose for a range of dosimeter temperatures is shown in Fig. 5. Ultrasonic speed is temperature dependent, with ultrasonic speed being highest at 25°C. The observed increase in ultrasonic speed with increase in temperature follows the variation of ultrasonic speed with temperature in water. The similarity in the response of the dosimeters to water is not unexpected, owing to the high water content of the dosimeters (~90%). Ultrasonic speed dose sensitivity is not as sensitive to temperature changes as ultrasonic attenuation dose sensitivity.

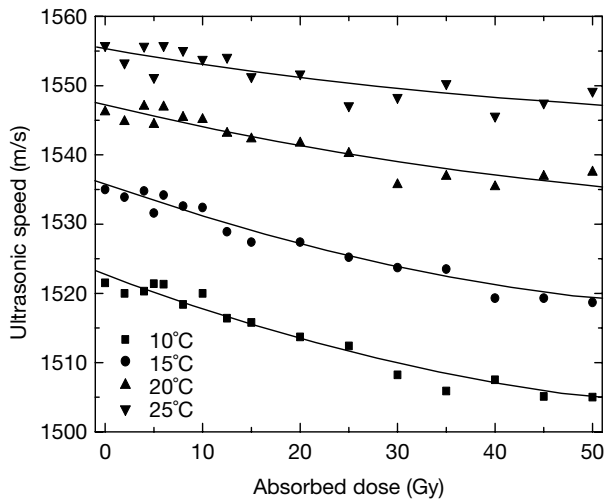


FIG. 4. Ultrasonic attenuation as a function of absorbed dose from 10°C to 25°C.

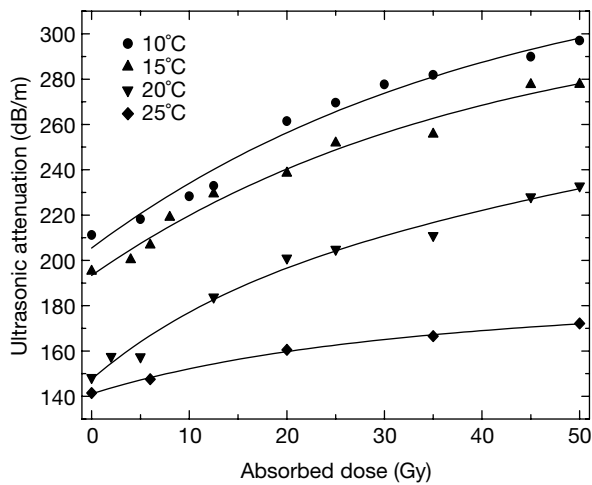


FIG. 5. Ultrasonic speed as a function of absorbed dose from 10°C to 25°C.

Figure 6 shows the variation of the ultrasonic attenuation coefficient with absorbed dose for three different ultrasonic frequencies. The attenuation coefficient is highest at 66.2 MHz and lowest at 25.7 MHz. Dose sensitivity is also found to be frequency dependent, with an increase in frequency from 25.7 MHz to 66.2 MHz resulting in the ultrasonic attenuation coefficient dose sensitivity almost doubling. The ability to vary dose sensitivity is attractive from a dosime-



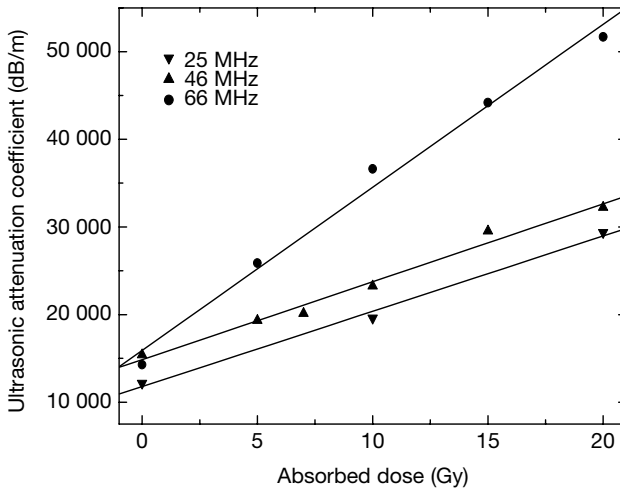


FIG. 6. Ultrasonic attenuation as a function of absorbed dose at 25.7, 46.3 and 66.2 MHz.

try point of view; however, an increase in frequency is accompanied with an increase in attenuation, so a compromise between the dose sensitivity and the signal to noise ratio must be found.

#### 4. CONCLUSION

This work has demonstrated that the ultrasonic dose response of polymer gel dosimeters can be altered by dosimeter composition, temperature and the frequency of the ultrasonic signal. Specifically, this work has shown that the dynamic range and dose sensitivity of ultrasonic dose response curves can be changed. Also, the absolute values of speed and attenuation can be altered. An understanding of how ultrasonic dose response curves can be altered will assist the further advancement of ultrasound evaluation techniques of polymer gel dosimeters. Future work involves the development of an instrument capable of imaging dose distributions with ultrasound.

#### ACKNOWLEDGEMENTS

The authors would like to thank A.F. Collings and N. Bajenov for their assistance with ultrasonic interferometry measurements.

## REFERENCES

- [1] MATHER, M.L., WHITTAKER, A.K., BALDOCK, C., Ultrasound evaluation of polymer gel dosimeters, *Phys. Med. Biol.* **47** (2002) 1449–1458.
- [2] LEPAGE, M., WHITTAKER, A.K., RINTOUL, L., BÄCK, S.Å.J., BALDOCK, C., The relationship between radiation-induced chemical processes and transverse relaxation times in polymer gel dosimeters, *Phys. Med. Biol.* **46** (2001) 1061–1074.
- [3] DE DEENE, Y., DE WAGTER, C., Artefacts in multi-echo  $T_2$  imaging for high-precision gel dosimetry: III. Effects of temperature drift during scanning, *Phys. Med. Biol.* **46** (2001) 2697–2711.
- [4] MAFFEZZOLI, A., QUARTA, E., LUPRANO, V.A.M., MONTAGNA, G., NICOLAIS, L., Cure monitoring of epoxy matrices for composites by ultrasonic wave propagation, *J. Appl. Polym. Sci.* **73** (1999) 1969–1977.
- [5] KINSLER, L.E., *Fundamentals of Acoustics*, Wiley, New York (1982).
- [6] BALDOCK, C., et al., Experimental procedure for the manufacture and calibration of polyacrylamide gel (PAG) for magnetic resonance imaging (MRI) radiation dosimetry, *Phys. Med. Biol.* **43** (1998) 695–702.
- [7] FONG, P., KEIL, D.C., DOES, M.D., GORE, J.C., Polymer gels for magnetic resonance imaging of radiation dose distributions at normal room atmosphere, *Phys. Med. Biol.* **46** (2001) 3105–3113.
- [8] DE DEENE, Y., et al., A basic study of some normoxic polymer gel dosimeters, *Phys. Med. Biol.* **47** (2002) 3441–3463.
- [8] BALDOCK, C., FITCHEW, R., MURRY, P.M., KRON, T., Calibration of Gammacell irradiator for irradiation of polymer dosimetry gels, *Med. Phys.* **26** (1999) 1130 (abstract).
- [9] COLLINGS, A.F., BAJENOV, N., The velocity of sound in human blood, *Australas. Phys. Eng. Sci. Med.* **7** (1984) 127–130.

# **PHOTON ENERGY DEPENDENCE OF THE ELECTRON PARAMAGNETIC RESONANCE ALANINE DOSIMETRY SYSTEM: AN EXPERIMENTAL INVESTIGATION**

E.S. BERGSTRAND\*, K.R. SHORTT\*\*,\*\*\*, C.K. ROSS\*\*, E.O. HOLE\*

\* Department of Physics, University of Oslo,  
Oslo, Norway  
E-mail: e.s.bergstrand@fys.uio.no

\*\* Ionizing Radiation Standards, National Research Council,  
Ottawa, Canada

## **Abstract**

Electron paramagnetic resonance (EPR) dosimetry with the amino acid alanine as the dosimeter material is widely used for transfer dosimetry, mostly for  $^{60}\text{Co}$  gamma irradiation. The alanine dosimeters are nearly water equivalent, and, with the efforts of recent years to improve accuracy for low doses, the EPR alanine dosimetry system represents a promising candidate for clinical application. Cobalt-60 gamma irradiation is often used for calibrating the alanine dosimetry system to make it traceable for that energy. As the photon energies used in radiation therapy are often different from those of  $^{60}\text{Co}$ , it is important to verify if the dose to water response of alanine dosimeters varies with photon energy. In the work described in the paper the dose to water response of alanine dosimeters (containing polyethylene as a binder) was investigated experimentally using three photon X ray beams of 10, 20 and 30 MV, with  $^{60}\text{Co}$  gamma rays (1.25 MeV) as a reference. The doses delivered ranged from 8 Gy to 54 Gy and were determined for all the beams using calorimetry. All irradiations were performed at the National Research Council in Ottawa, Canada, whereas all EPR measurements and the analysis were performed at the EPR laboratory at the University of Oslo, Norway. Comparing the dose to water responses averaged for the three high energy photon qualities to that of  $^{60}\text{Co}$  gamma rays gave a dose response reduction of 0.8%. Thus it is concluded that the EPR alanine dosimetry system may have a small energy dependence in the relative dose to water response averaged over the X ray beams investigated, as compared with  $^{60}\text{Co}$  gamma rays.

---

\*\*\* Present address: Division of Human Health, International Atomic Energy Agency, Vienna.

## 1. INTRODUCTION

Over some decades electron paramagnetic resonance (EPR) dosimetry, using alanine as the dosimeter material, has gained popularity as a dosimetry system for measuring high doses of ionizing radiation, and the dosimeter system has been used as a transfer system for  $^{60}\text{Co}$  gamma rays by the IAEA, among others [1]. There are several advantages of the EPR alanine dosimetry system: the radiation induced radicals are quite stable [2]; the dose to water response versus dose is constant up to about 5 kGy [3]; and the radiation sensitivity is rather high. Furthermore, the dosimeters are physically robust and fairly small in size. These facts make the EPR alanine system suitable for mailed dosimetry.

The EPR powder spectrum from amorphous alanine pellets or other types of disordered alanine samples is used for dose monitoring, commonly using the peak to peak amplitude of the central spectral line as the dose probe. It has recently been shown that at least three different radicals are formed and stabilized in alanine following irradiation with X rays at room temperature [4]. The three radicals contribute, in different degree, to the central EPR line [5].

Efforts have been made to enhance the accuracy as well as the reporting of statistical uncertainties in EPR alanine dosimetry [6, 7]. Depending on the composition and physical properties of the dosimeter material, the reading of the dosimeter material per dose absorbed in water may vary with changes in the quality of the radiation beam. Since the composition of alanine is nearly water equivalent, EPR alanine dosimetry offers promise as a suitable system to provide quality assurance measurements of the doses associated with radiotherapy. Cobalt-60 gamma ray beams (1.25 MeV) are usually used for the calibration of EPR alanine dosimetry. For those cases when transferring this dosimetry system to other radiation qualities, it is important to investigate any radiation energy dependence for the alanine reading per dose to water relative to that for photons of  $^{60}\text{Co}$ ; otherwise, neglecting the possible energy dependence of a dosimetry system may introduce systematic errors in the measured dose.

Others have previously investigated the behaviour of alanine with respect to different radiation qualities [8–11]. Olsen et al. [10] found a small energy dependence for 4–16 MV X rays compared with  $^{60}\text{Co}$ , which could be corrected for by very simple theoretical approximations, while Sharpe and Septhon [11] reported no significant energy dependence for the range of 4 MV to 20 MV X rays. Ciesielski and Wielopolski [9] found that radiation quality affected the qualitative EPR spectrum of alanine. It is not clear if the known dependence on the linear energy transfer of the alanine EPR spectrum shape affects the peak to peak dependence on the dose.

This paper investigates the behaviour of alanine peak to peak intensity with respect to radiation quality, and has been limited to photons in the energy range from  $^{60}\text{Co}$  to 30 MV X rays (tissue phantom ratio,  $\text{TPR}_{20,10}$ , in the range of 0.68 to 0.79). The dose to water response for each of the 10, 20 and 30 MV X ray beams compared with  $^{60}\text{Co}$  gamma irradiation has been used to quantify any possible energy dependence.

## 2. METHODS

Alanine dosimeters (Bruker Bronze batch 603995/2) were obtained from Bruker GmbH and were cylindrically shaped, with a height of 4.5 mm and a diameter of 4.7 mm and a weight of  $87 \text{ mg} \pm 2\%$ . The dosimeters contained 80% L- $\alpha$ -alanine and 20% polyethylene binder material.

### 2.1. Irradiation

The alanine dosimeters were irradiated at the National Research Council (NRC) in Ottawa, Canada, using a high energy photon linac at 10, 20 and 30 MV and the NRC  $^{60}\text{Co}$  source situated in an Eldorado 6 (AECL) therapy head. The dosimeters were given an absorbed dose to water in the range of approximately 10 Gy to 50 Gy for each beam quality. For each dose point and for all beam qualities, three dosimeters were irradiated simultaneously. The phantom temperature was monitored during each irradiation session. The largest temperature variation in one session was  $0.6^\circ\text{C}$ , and the variation between radiation qualities was  $3.3^\circ\text{C}$ .

To provide reference data sets independent of time, each linac irradiated set (10, 20 and 30 MV) was accompanied by a separate set, which was irradiated by  $^{60}\text{Co}$  gamma rays almost simultaneously, and the EPR signal was assumed to decay at the same rate for both members of each pair.

During irradiation, the dosimeters were placed, three in a stack, in a polymethylmethacrylate (PMMA) holder with a total wall thickness of approximately 1 mm and with outer dimensions like a Farmer like ionization chamber. The holder ensured identical dosimeter positions in the radiation field for each irradiation set-up. The holder fitted snugly into another water-proofing PMMA sleeve (wall thickness of 1 mm) that also was used for the ionization chambers, placed at a water depth of 10 cm (5 cm for  $^{60}\text{Co}$ ) in a full scatter water phantom.

The radiation beam was calibrated in terms of absorbed dose to water using a sealed water calorimeter. To verify the dose on each day of irradiations, a graphite walled NE 2571 ionization chamber that was originally calibrated using the calorimeter was placed into the same outer PMMA sleeve used for

the alanine dosimeters. The relative standard uncertainties in the applied doses to water are given as 0.5% for the linac irradiations and 0.4% for the  $^{60}\text{Co}$  irradiations, as measured with the ionization chamber and calorimeter [12].

## 2.2. EPR measurements

All alanine dosimeters were evaluated at the EPR laboratory at the University of Oslo, Norway, using a Bruker ESP 300E spectrometer equipped with a standard X band bridge, including a frequency counter. A Bruker rectangular  $\text{TE}_{104}$  double resonator was used with a  $\text{Mn}^{2+}/\text{MgO}$  reference sample (JEOL Co.) permanently mounted in the second cavity. A sample support system consisting of Teflon pedestals and thin quartz tubes was used to ensure identical positions for all the samples measured. The  $\text{Mn}^{2+}$  spectrum was recorded after each sample spectrum to correct the alanine signal for short and long term variations in the spectrometer sensitivity. Furthermore, the corresponding linac and  $^{60}\text{Co}$  irradiated dosimeters were evaluated, in random order, during the same EPR measurement session to ensure a fairly constant spectrometer configuration for the corresponding dosimeters. All alanine EPR spectra were a resultant spectrum of nine added scans, recorded with a sweep width of 1.5 mT, a microwave power of 1.00 mW and a modulation amplitude of 0.79 mT. The mass of each dosimeter was determined using a Mettler Toledo AG245 balance with a precision of 0.1 mg.

Typical conditions affecting the radical concentration, and thus the EPR signal intensity, are irradiation temperature and radical decay over time, the rate of which is influenced by the storage conditions. In the work described in this paper, in addition to the mentioned spectrometer sensitivity correction, a small irradiation temperature correction was applied [13], while the radical decay correction could be neglected, since the two corresponding dosimeter sets were irradiated and evaluated simultaneously and stored together. Thus all alanine readings reported are corrected peak to peak values of the central EPR line divided by the dosimeter mass, with a zero dose reading subtracted. The zero dose reading was evaluated as the abscissa intersection resulting from applying a weighted least squares regression [14] to the plot of alanine readings (without subtraction of the zero dose reading) versus dose to water for each of the six dosimeter sets. These plots are referred to as reading versus dose curves. One pair of reading versus dose curves is shown in Fig. 1.

## 2.3. Evaluation of the energy dependence

The dose to water response, also referred to as the dose response, is defined as the alanine reading per dose to water. The relative dose response is

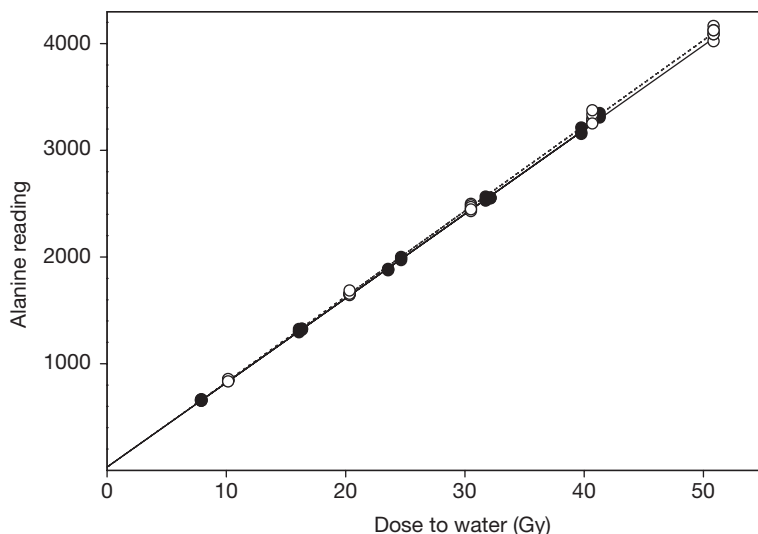


FIG. 1. The alanine reading as a function of dose to water for alanine dosimeters exposed to 10 MV X rays (black circles) and  $^{60}\text{Co}$  (white circles). The solid and dashed lines represent the weighted least squares regression for 10 MV X rays and  $^{60}\text{Co}$  gamma rays, respectively. The size of the symbols exceeds the standard uncertainties in both the x and y directions.

defined as the dose response for a certain beam quality relative to a reference quality ( $^{60}\text{Co}$ ). The energy dependence is hence the variation with beam quality in the relative dose response [15]. In this paper the relative dose response is calculated as the average of the dose responses for all the dosimeters irradiated with a certain linac quality, normalized to the average of the dose responses for all the associated dosimeters that were irradiated using  $^{60}\text{Co}$  gamma rays. Since the individual dose responses in Fig. 2 display an approximately constant variance relative to dose, a weighted average is not necessary.

For the estimation of the combined uncertainty of the experimental relative dose response, taking into account the varying absolute uncertainties over the dose range in both dose and the alanine reading, the following approach is used. The ratio of slopes, as calculated using weighted least squares regression to each reading versus dose curve, between each linac beam quality and the associated  $^{60}\text{Co}$  gamma irradiated set, can also be used to calculate the experimental relative dose response (indeed, each method produces results that are equal within three decimal places). The pair of reading versus dose curves for the 10 MV linac beam and the associated  $^{60}\text{Co}$  gamma irradiation is shown in Fig. 1. Thus the standard uncertainty of the ratio of slopes, as calculated in accordance with the recommended practice of the International Organization

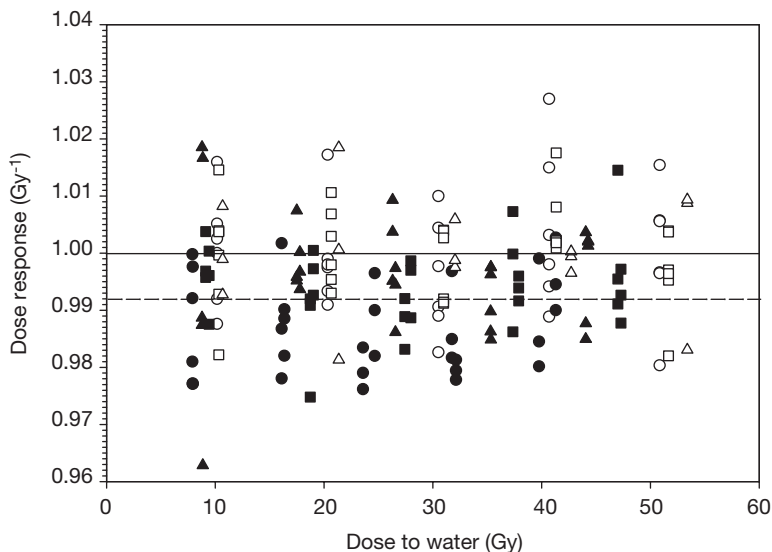


FIG. 2. The individual normalized dose responses as a function of dose for all the alanine dosimeters. Black circles, squares and triangles denote dosimeters exposed to 10, 20 and 30 MV X rays, respectively. White circles, squares and triangles denote dosimeters of the corresponding  $^{60}\text{Co}$  gamma irradiated reference set. Each corresponding X ray and gamma irradiated dose point is normalized with the same value (which was the average dose response of each  $^{60}\text{Co}$  set). The dashed line indicates the normalized dose response, which is averaged over the three linac beam qualities.

for Standardization [16], represents the standard uncertain of the relative dose to water response. This calculation involves the slope uncertainties, which were obtained using the expressions reported by Moreno and Bruzzone [17].

### 3. RESULTS AND ANALYSIS

Figure 2 shows the normalized individual dose to water responses versus dose to water for all six dosimeter sets. As expected for doses below 5 kGy [3], the dose responses show no systematic dependence versus dose over the dose range investigated (10–50 Gy). The experimental relative dose response values for the different linac beam qualities, calculated as the average relative dose response for each linac beam quality, are given in Table I, together with their respective standard uncertainties. As observed in Table I, all three experimental values for the relative dose response were close to unity, with a maximum deviation of 1.3% for the 10 MV linac/ $^{60}\text{Co}$  set. This can also be seen in Fig. 1,



TABLE I. EXPERIMENTAL RELATIVE DOSE TO WATER RESPONSE OF THE ALANINE DOSIMETERS IRRADIATED WITH 10, 20 AND 30 MV LINAC X RAYS

Linac potential (MV)	Experimental dose to water response $\pm$ standard uncertainty
10	$0.987 \pm 5.0 \times 10^{-3}$
20	$0.994 \pm 5.1 \times 10^{-3}$
30	$0.996 \pm 6.4 \times 10^{-3}$

**Note:** Calculated as the average normalized (with respect to the associated  $^{60}\text{Co}$  irradiation) dose response for each linac beam quality. Also shown are the standard uncertainties of the relative dose response values.

as the pair of slopes, although having the maximum deviation of the three linac qualities, still coincides rather well.

Owing to the high precision in the applied doses, a reasonably large number of dosimeters in each radiation quality data set and quite accurate EPR measurements, the combined standard uncertainties of the experimental relative dose responses were very small, ranging from 0.5% to 0.6%. The results agree rather well with the findings of Sharpe et al. [11], who reported that the alanine dose to water response was within 1% for several photon energies ranging from 4 MV to 20 MV. If the mass energy absorption coefficients as used by Olsen et al. [10] are applied to the measured dose to water responses obtained from the work reported in this paper, the resulting calculated dose to alanine responses agree rather well with those of Olsen et al. However, this paper reports an average small reduction in the dose response for high energy photons, and thus deviates from the previous work.

#### 4. DISCUSSION

Only the central part of the EPR spectrum (1.5 mT wide) was recorded in the work discussed in this paper, whereas the total EPR spectrum of irradiated alanine is close to 10 mT wide. Thus, apart from the central peak to peak, the data yielded no information regarding spectrum differences. Even if there should be an energy dependence in the relative yield of the different alanine radicals formed at room temperature [4], the amplitude of the central EPR line could nevertheless remain independent of this.

The experimental relative dose to water responses obtained for alanine dosimeters were  $0.987 \pm 0.005$ ,  $0.994 \pm 0.005$  and  $0.996 \pm 0.006$  relative to unity for  $^{60}\text{Co}$  gamma rays for 10, 20 and 30 MV X rays, respectively. Within the precision limits it is not possible to deduce any significant variation in the dose response between the different linac beam qualities. Thus the average dose response for the high energy linac beam qualities investigated was calculated, and gives  $0.992 \pm 0.005$  (0.8% below unity). The results apply for the present irradiation set-up, which consisted of alanine dosimeters (alanine and 20% polyethylene binder material) surrounded by 2 mm thick PMMA walls at the reference depth in a water phantom. For estimating the dose response for alanine dosimeters with no sleeve, the results may need to be corrected. Thus the presented results lead the authors to recommend that, when using a similar set-up when applying EPR alanine dosimetry for similar photon beam qualities ( $\text{TPR}_{20,10}$  in the range of 0.68 to 0.79), a beam quality correction factor of 1.008 should be applied to the dose to water response when calibrated using  $^{60}\text{Co}$  gamma rays.

### ACKNOWLEDGEMENTS

The authors wish to acknowledge the Research Council of Norway for funding the PhD project (project No. 68136/410) of E.S. Bergstrand, H. Bjerke at the Norwegian Radiation Protection Authorities for contributing with initial ideas and discussions, I. Glad, of the Department of Mathematics, University of Oslo, for clarifying discussions about statistics, and E. Malinen for stimulating discussions.

### REFERENCES

- [1] MEHTA, K., GIRZIKOWSKY, R., IAEA high-dose intercomparison in  $^{60}\text{Co}$  field, *Appl. Radiat. Isot.* **52** (2002) 1179–1184.
- [2] SLEPTCHONOK, O.F., NAGY, V., DESROSIERS, M.F., Advancements in accuracy of the alanine dosimetry system. Part 1. The effects of environmental humidity, *Radiat. Phys. Chem.* **57** (2000) 115–133.
- [3] NAGY, V., Accuracy considerations in EPR dosimetry, *Appl. Radiat. Isot.* **52** (2000) 1039–1050.
- [4] SAGSTUEN, E., HOLE, E.O., HAUGEDAL, S.R., NELSON, W.H., Alanine radicals: Structure determination by EPR and ENDOR of single crystals X-irradiated at 295 K, *J. Phys. Chem. A* **101** (1997) 9763–9772.
- [5] HEYDARI, M.Z., MALINEN, E., HOLE, E.O., SAGSTUEN, E., Alanine radicals. 2: The composite polycrystalline alanine EPR spectrum studied by

- ENDOR, thermal annealing, and spectrum simulations, *J. Phys. Chem. A* **106** (2002) 8971–8977.
- [6] HAYES, R.B., et al., Assessment of an alanine EPR dosimetry technique with enhanced precision and accuracy, *Nucl. Instrum. Methods Phys. Res. A* **440** (2000) 453–461.
- [7] NAGY, V., SHOLOM, S.V., CHUMAK, V.V., DESROSIERS, M.F., Uncertainties in alanine dosimetry in the therapeutic dose range, *Appl. Radiat. Isot.* **56** (2002) 917–929.
- [8] HANSEN, J.W., OLSEN, K.J., Theoretical and experimental radiation effectiveness of the free radical dosimeter alanine to irradiation with heavy charged particles, *Radiat. Res.* **104** (1985) 15–27.
- [9] CIESIELSKI, B., WIELOPOLSKI, L., The effects of dose and radiation quality on the shape and power saturation of the EPR signal in alanine, *Radiat. Res.* **140** (1994) 105–111.
- [10] OLSEN, K.J., HANSEN, W., WILLE, M., Response of the alanine radiation dosimeter to high-energy photon and electron beams, *Phys. Med. Biol.* **35** (1990) 43–52.
- [11] SHARPE, P.H.G., SEPTHON, J.P., “Alanine dosimetry at NPL — The development of a mailed reference dosimetry service at radiotherapy dose levels”, *Techniques for High Dose Dosimetry in Industry, Agriculture and Medicine*, IAEA-TECDOC-1070, IAEA, Vienna (1999) 183–189.
- [12] SEUNTJENS, J.P., ROSS, K., SHORTT, K.R., ROGERS, D.W.O., Absorbed-dose beam quality conversion factors for cylindrical chambers in high energy photon beams, *Med. Phys.* **27** (2000) 2763–2779.
- [13] NAGY, V., PUHL, J.M., DESROSIERS, M.F., Advancements in accuracy of the alanine dosimetry system. Part 2. The influence of the irradiation temperature, *Radiat. Phys. Chem.* **57** (2000) 1–9.
- [14] LISÝ, J.M., CHOLVADOVÁ, A., KUTEJ, J., Multiple straight-line least-squares analysis with uncertainties in all variables, *Comput. Chem.* **14** (1990) 189–192.
- [15] ATTIX, F., *Introduction to Radiological Physics and Radiation Dosimetry*, Wiley, New York (1986).
- [16] INTERNATIONAL ORGANIZATION FOR STANDARDIZATION, *Guide to the Expression of Uncertainty in Measurement*, 2nd edn, ISO, Geneva (1995).
- [17] MORENO, C., BRUZZONE, H., Parameters variances of a least-squares determined straight-line with errors in both coordinates, *Meas. Sci. Technol.* **4** (1993) 635–636.

**BLANK**

## **EXPERIENCE WITH IN VIVO DIODE DOSIMETRY FOR VERIFYING RADIOTHERAPY DOSE DELIVERY: THE PRACTICAL IMPLEMENTATION OF COST EFFECTIVE APPROACHES**

D.I. THWAITES\*, C. BLYTH\*\*, L. CARRUTHERS\*, P.A. ELLIOTT\*,  
G. KIDANE\*, C.J. MILLWATER\*, A.S. MacLEOD\*, M. PAOLUCCI\*,  
C. STACEY\*

\* Western General Hospital, University of Edinburgh  
E-mail: dit@holyrood.ed.ac.uk

\*\* Queen Margaret University College

Edinburgh, United Kingdom

### **Abstract**

Ten years' experience of using diodes to verify radiotherapy delivered doses is summarized in the paper. The initial aim of the programme was to quantify the accuracy and precision achieved in the radiotherapy process, for a range of disease sites, treatment units and treatment techniques, and then to identify any causes of systematic uncertainties or clinically significant random uncertainties and to rectify or improve them. Later objectives were to assess the balance of costs and benefits of their use and to optimize the methodology applied for their routine implementation. A number of practical measures were developed to simplify the routine use of diodes in normal clinical practice.

### **1. INTRODUCTION**

A systematic programme of in vivo dosimetry using diodes to verify radiotherapy delivered doses began in Edinburgh in 1992. The aims were: to investigate the feasibility of the routine systematic use of diodes as part of a comprehensive quality assurance programme; to carry out clinical pilot studies to assess the accuracy of dose delivery on each machine and for each site and technique; to identify and rectify systematic deviations; and to assess departmental dosimetric precision and to compare with clinical requirements. A further aim was to carry out a cost-benefit evaluation based on the results from the pilot studies to consider how best to use diodes routinely. Questions to be addressed included: when should diode dose verification be used and on

which patients; what should be measured in a routine programme; which staff members should carry out which tasks; what are the appropriate tolerance and action levels; and which actions should be taken at these levels. The diodes purchased and used were all from Scanditronix, including old style EDE, EDP-10, EDP-20 and later EDD-2, EDD-5, new-style EDP-10 and EDP-20 devices.

A subsequent programme assessed simplifications for routine use, including: omitting correction factors or reducing the set used; the use of additional metal buildup caps on the standard diodes to match buildup thicknesses, to reduce the ranges of correction factors required; the use of combined mid-range generic correction factors for a specific machine, modality, treatment site-field and diode position; how data is communicated and recorded to and from the treatment unit; how the diodes are mounted and handled in the treatment room; the quality control required for the diodes themselves; and the assessment of falsely recorded discrepancies to minimize the resource implications.

The Edinburgh Cancer Centre (ECC) has been fortunate in having a supply of multidisciplinary postgraduate level students (physicists, radiation oncologists and one part-time research radiographer), who have carried out dissertation projects on the testing and development stages.

## 2. INITIAL COMMISSIONING, TESTING AND WORKUP OF THE DIODES

The initial commissioning, testing and workup of the diodes by the physics group followed methods that are now accepted as conventional [1, 2]. While this is time consuming, it is necessary to have a complete understanding of the diodes' behaviour from the outset to give confidence in the measurements. The initial testing included: the stability of the signal (leakage); the reproducibility of the response; the linearity; the water equivalent depth of the detector; and the relative perturbation behind the diodes in a range of beams. This was followed by entrance and exit dose calibrations [3] comparing diodes on the phantom surface to a calibrated ionization chamber at the depth of dose maximum (entrance) and at the same depth from the exit surface (exit), ensuring that the diode and the ionization chamber were not shielding each other. Entrance and exit dose correction factors were then obtained relative to the calibration conditions, using standard methods [1, 2, 4] for each diode individually and over the range of conditions to be used clinically. Phantom measurements were carried out, partly to verify the methodology in various situations and also to aid in future interpretation and the transfer of diode dose measurements to the estimation of doses at the isocentre. Also at this stage a regular quality control programme was initiated for the diodes [2, 4], including regular checks on the calibration and correction factors.

### 3. PILOT CLINICAL STUDIES

Comprehensive clinical pilot studies were carried out for different treatment machines, treatment sites and treatment techniques, choosing to assess simpler situations first to test the methodology in practical situations, then gradually working up to more complex treatments. Measurements were carried out on patients once a week through the course of their treatment. A full data analysis was carried out, which included all relevant correction factors, to assess doses as precisely as possible. Entrance and exit doses were measured on all patients in each group once a week until sufficient data were accumulated to provide a confident analysis [5, 6]. Normally the diode was positioned on the beam central axis (although not for breast measurements), but it was ensured that there was no shadowing of one diode by another. The measured doses were compared with the expected doses taken from the patient treatment plan or from planning data. As is standard in these measurements, and as linked to the calibration methodology, 'entrance dose' means the dose at the depth of dose maximum and 'exit dose' means the dose at a similar depth upstream from the exit surface, so it is the doses planned at these positions that must be compared. Typical entrance dose distributions showed mean differences (between measured and expected doses) close to zero. Standard deviations (SDs) of distributions were in the range of 1.2% to 4.1%, depending on the site and on the linac used. For exit doses typical equivalent values were: means 1% to 4% below expected and SDs in the range of 2% to 5%. For each patient, where sufficient measurements were made, target volume doses were estimated from the deviations of the entrance and exit fields, aided by the phantom studies. For all treatment sites, except the breast, these were estimated at the isocentre. For breast treatments the point taken was in the middle of the irradiated volume. Total deviations for a particular treatment fraction were estimated from the deviations for each field, weighted in proportion to the dose delivered by that field. A best estimate of overall dose delivery for the total treatment course was obtained by averaging these values over all measured fractions. Examples of mean deviations for total treatments (with the SD given in brackets) are:

- (a) Head and neck:  $-0.2\%$  to  $+1.0\%$  (1.5–3%).
- (b) Breast (old technique, isocentre on surface):  $-4.0\%$  (2.5%).
- (c) Breast (new technique, isocentre at depth):  $-2.0\%$  (2.7%).
- (d) Pelvic:  $-0.4\%$  (2.7%).
- (e) Conformally blocked prostate–bladder (initial):  $+1.5\%$  (2.6%).
- (f) Conformally blocked prostate–bladder:  $+0.1\%$  (2.6%)  
(corrected, see text).
- (g) Electron (lower energies,  $E \leq 10$  MeV):  $+0.9\%$  (2.5%).

The SDs for the overall estimates of the total treatment course delivery were normally lower than the distributions for individual measurements and individual field data. Approximately 97% of estimated target volume doses over all the pilot studies have been within  $\pm 5\%$  of the expected (prescribed) doses (100% have been within 7% of the expected (prescribed) doses).

Some reasons for discrepancies were found to be: false positives arising from problems with the measurements, for example due to the diode methods used, such as diode positioning problems including contact and cable pulling; the difficulty to position if the relevant patient surface is directly on the couch or under an immobilization device; the limiting resolution of the electrometer for small dose components (particularly exit wedge doses); and positioning uncertainties under steep wedges or on steeply angled surfaces.

However, the studies identified some real systematic dose delivery problems and significant individual patient outliers. This has led to practice improvements. Causes have included: treatment machine performance; patient data acquisition; dose calculation errors (e.g. with the older technique used for breast field irradiation); non-CT (computed tomography) planning (so not all inhomogeneities were accounted for); patient set-up variations; and incorrect treatment parameters. Some causes were due to changes in patient size and shape between planning and treatment, for example systematic, such as weight loss, or random, such as bowel gas. Some causes were identified as a combination of factors, for example for the conformally blocked treatments, for which part of the systematic difference of 1.5% observed initially was due to the need for an extra correction factor for the diode measurements when conformal blocks were used (i.e. due to diode use and methodology) and part was due to the monitor unit calculation for conformal blocks (i.e. due to a real change to the delivered dose to patients). Correcting both of these gave a mean deviation of 0.1%. The studies indicated that diode dosimetry can identify problems at the level of 1% between the measured and stated dose values with good methodology, implementation and quality control, but that the diode methodology itself could introduce some errors.

Tolerance levels for individual measurements for standard treatments were chosen on the basis of the pilot studies, at approximately 2 SD in the observed distributions of differences between measured and stated doses. The aim was to have the tolerances wide enough that investigations were not triggered unnecessarily, yet narrow enough that clinically significant discrepancies were not missed: 5% was selected for entrance dose measurements and 8% for exit dose measurements, although tighter tolerances (3% and 6%, respectively) have been discussed for conformal treatments, especially if a dose escalation is involved. These were to be used as initial triggers for investigation. Where necessary, entrance and exit dose measurements were combined, as detailed above, to check the dose at the isocentre.



#### 4. ROUTINE IMPLEMENTATION

For routine use for conventional treatments, multidisciplinary discussions in the ECC agreed a number of points. These included:

- (a) To use normal treatment unit radiographers to carry out routine measurements, guided by the research radiographer.
- (b) To evaluate the procedures to ensure that the time involved at the treatment units was minimized.
- (c) To measure only entrance doses, with a 5% tolerance, as this programme was being added to an already existing comprehensive quality assurance system, including independent monitor unit checks, quality assurance of record and verify data and independent radiographer checks on set-up and treatment parameters; the aim of routine diode use is to identify significant errors not picked up by other levels of the quality system.
- (d) To develop gradually to measuring all patients, but to reassess this regularly.
- (e) To measure each patient usually only once within the first few days of treatment, so that any problems identified can be investigated and rectified early in the treatment course; often measurements are carried out on a particular machine on only one day a week, and all new patients on that machine are monitored, implying that 10 to 15 patients are monitored on that day.
- (f) To set the action level the same as the tolerance level (5%).
- (g) To have a clear protocol for actions in the event of a significant discrepancy being observed. Immediate checks are carried out in these cases. At the earliest opportunity, and before the next treatment fraction, a physicist checks the plan, treatment instructions, calculations, and diode method and measurement. A second diode measurement is carried out, by a member of the physics department, at the next treatment. If this is within tolerance, the treatment is deemed acceptable and the deviation is assigned to problems with diode positioning on the patient in the previous treatment. If it is not within tolerance, a detailed investigation is initiated by the physics group, using phantoms to simulate the treatment, in order to identify the cause (i.e. the treatment or the diode measurement).
- (h) To retain full entrance and exit dose measurements for some special cases, for example: for newly commissioned treatment equipment or techniques, as an overall test of the system; for critical patient groups, or critical techniques; and for occasional full audit studies, to evaluate performance.

As an overall measure of routine global accuracy of treatment delivery in the department, an analysis of roughly the first 5000 individual entrance dose

measurements showed a mean ratio of measured dose to expected dose close to unity (1.001) and an SD close to 3%. This, of course, inherently includes the uncertainties associated with the diode methodology. This is very similar to the figures from the first fraction entrance dose measurements taken over all the detailed pilot studies. Based on the analysis from those studies discussed above (Section 3), this implies that the uncertainties for total treatments will also be similar (i.e. that approximately 97% of estimated target volume doses will be within  $\pm 5\%$  of the expected (prescribed) doses and almost all within 7%).

## 5. METHODS TO SIMPLIFY ROUTINE USE

A number of practical measures were assessed to simplify routine use and to reduce the time required, as each linac typically treats 40 or more patients per day. These practical measures have included:

- (a) The non-use of diode correction factors to provide a simpler methodology and less quality control for the diodes. This was found not to be acceptable, as it could lead to situations in which real deviations were missed. In any case, the same diodes are used for critical groups, so correction factors are needed.
- (b) The use of buildup caps. Tight fitting buildup caps of brass, copper and steel have been investigated [7]. The caps match the buildup thickness more closely to the beam in question and reduce the range of correction factors required such that many entrance factors can be ignored at levels acceptable for routine use. The changes going from no cap to with cap are less on the newer style diodes than on the older. However, the newer style caps typically have smaller correction factor variations. Some factor variations (e.g. angle) may be worsened and, of course, the shadowing effect is worsened. This has therefore to be evaluated against the frequency of use. For routine use, where typically only one or two measurements are carried out throughout a treatment course, this is not a significant problem. Gains from the use of caps were less obvious for higher energy beams than for lower energy beams. Current practice in the department is to use additional buildup caps of 0.6 mm of brass on EDP-10 diodes for 6 MV beams (Fig. 1); EDP-20 diodes are being used for 8 MV beams without the need for any caps, while caps are currently not being used on EDP-20 diodes in 15 MV beams. Although the EDP-20 is thinner than the full buildup for the 15 MV beam, thus increasing the contaminant electron effects, this decision was taken to reduce shielding



*FIG. 1. Examples of diodes and brass buildup caps.*

- effects (and to reduce the number of diodes in use in the department). The secondary electron effects are accounted for in the correction factors.
- (c) The use of generic factors has been adopted for the diodes with buildup caps. The range of correction factors has been investigated for a typical range of patients and parameters for a given site, technique and field. A representative mid-range value is taken as the generic factor for that situation. Full sets of factors are still used in any detailed audit studies, critical group studies, etc.
  - (d) Methods have been implemented to streamline data flow from the planning to the treatment unit and for the physical handling of the diodes in the treatment room. The radiographers are provided with a range of values within which the practical diode reading should fall in order to be within tolerance, giving an immediate yes/no decision. Diode mounts have been designed for quick and easy operation in the treatment room (Fig. 2). Typical times added to planning are very small. In the treatment room the diode operations tend to be carried out in parallel with other operations, so adding minimal time.
  - (e) Diode quality control can be simplified by carrying out quick checks frequently, in conjunction with daily linac checks, and using these as a warning system, so that a major re-evaluation of factors is only required when the checks at this level indicate possible changes.



*FIG. 2. The ceiling mount for the diodes. It can swing in an almost complete circle to any position around the linac. Diodes are hooked to the base of the swinging arm.*

The time for the initial commissioning workup of new diodes, for quality control and for investigations of observed discrepancies, can be significant. However, the recognition of false positives and their causes has improved with experience, to the extent that the time lost from these is now significantly reduced. Currently the ECC is re-assessing routine use in some sites for which no discrepancies have been observed over long use, for example the breast, and is considering putting more effort into some other sites for which deviations would be more critical, for example during conformal radiotherapy and dose escalation studies.

## 6. CONCLUSIONS

The use of diodes (or other *in vivo* dosimetry) to verify delivered radiotherapy treatment doses is cost effective and is recommended. It can quantify the accuracy and precision achieved in the radiotherapy process in the department as well as deviations for individual patients. With appropriate methodology and quality control it is effective down to the sub-1% level. Observed problems can be identified and rectified. Relatively simple measures can be

implemented to optimize diode use in routine clinical practice. Implementation can be gradual, to make the task initially more acceptable to or manageable by staff. Different levels of the implementation process may be in place at the same time on different linacs. The optimum solutions described in this paper are applicable to the specific situation in the ECC and may not be best for the circumstances in all institutions. However, similar solutions have been independently arrived at by other departments [2].

## REFERENCES

- [1] VAN DAM, J., MARINELLO, G., Methods for In Vivo Dosimetry in External Radiotherapy, ESTRO Booklet No. 1, European Society of Therapeutic Radiology and Oncology, Brussels (1994).
- [2] HUYSKENS, D., et al., Practical Guidelines for the Implementation of In Vivo Dosimetry with Diodes in External Beam Radiotherapy with Photon Beams (Entrance Dose), ESTRO Booklet No. 5, European Society of Therapeutic Radiology and Oncology, Brussels (2001).
- [3] KIDANE, G., Evaluation of Radiation Diodes for In Vivo Dosimetry during Radiotherapy, MSc dissertation, St. Andrews Univ. (1992).
- [4] MAYLES, P., HEISIG, S., MAYLES, H., "Treatment verification and in vivo dosimetry", Radiotherapy Physics in Practice (WILLIAMS, J.R., THWAITES, D.I., Eds), 2nd edn, Oxford University Press, Oxford (2000).
- [5] BLYTH, C., MacLEOD, A.S., THWAITES, D.I., A pilot study of in vivo dosimetry for quality assurance in radiotherapy, Radiography **3** (1997) 131–142.
- [6] MILLWATER, C.J., MacLEOD, A.S., THWAITES, D.I., In vivo semiconductor dosimetry as part of routine quality assurance in a radiotherapy department, Br. J. Radiol. **71** (1998) 661–668.
- [7] PAOLUCCI, M., THWAITES, D.I., The use of build-up caps on diodes for in vivo dosimetry, Radiother. Oncol. **51** (1999) S54.

**BLANK**

## CONCLUSIONS AND RECOMMENDATIONS

(Session 15)

**Chair**

**P.J. ALLISY-ROBERTS**

Bureau international des poids et mesures

**Co-Chair**

**K.R. SHORTT**

IAEA

**Rapporteur**

**A. DUTREIX**

European Society for Therapeutic Radiology and Oncology

**BLANK**



## CONCLUSIONS AND RECOMMENDATIONS

Recommendations following the papers and discussions were prepared by the Chairs, Co-chairs and Rapporteurs of each session and presented to the participants of the symposium in the final session for their approval.

Although many of these recommendations concern the scientific community, some are directed to governments and industry, as these affect practical application in developing countries. However, as was pointed out during Session 15, some of the developed countries would also benefit from following these latter recommendations. The IAEA would obviously be a good choice to take the lead in many of these actions.

### Session 1: Setting the Scene

After the description of the operation of the mutual recognition arrangement (MRA), it was clear that developing countries would benefit from being included in MRA comparisons and declaring their calibration and measurement capabilities (CMCs), as this would encourage them to clarify their methods and uncertainties. As it is a matter for individual countries to decide whether they should sign the MRA, the symposium simply recommended that:

1. Secondary standards dosimetry laboratories (SSDLs) holding national dosimetry standards for signatories of the MRA should be encouraged to participate in comparisons and to declare their CMCs through their regional metrology organization (RMO).

To support the SSDLs in this dosimetry work, it was recommended that:

2. Additional RMO comparisons should be developed and participation in these comparisons by Member States should be encouraged.

For more than 30 years the IAEA has developed dosimetry codes of practice pertinent to external beam radiotherapy and has arrived at a situation in which all forms of dosimetry measurements are linked together in one coherent protocol. Consequently, the symposium recommended that:

3. Organizations recommending the use of the IAEA dosimetry code of practice in Technical Reports Series No. 398 (TRS 398) should encourage users to follow its most recently released version.

4. The use of TRS 398 should be encouraged in all Member States.
5. The translation of TRS 398 should be encouraged.

It was recommended that, through the maintenance and support of the IAEA/World Health Organization (WHO) SSDL network:

6. The dissemination of dosimetry standards and expertise in the developing world should continue.
7. The consistency and quality of dosimetry standards should be maintained and developed through comparisons.

### **Session 2: Absorbed Dose Standards and Calorimetry**

Absorbed dose to water is the necessary quantity for dosimetry measurements for radiotherapy. Many papers were presented on the different methods of determining absorbed dose to water using primary methods. However, there are many issues related to this that need to be addressed by the primary standards dosimetry laboratories (PSDLs) in the national metrology institutes. The symposium recommended that:

8. Absorbed dose to water should be derived from as many independent methods as possible.
9. Direct comparisons of water and graphite calorimeters should be encouraged.
10. Uncertainties assigned to absorbed dose to water primary standards should be examined in detail, preferably by a working group of the international Consultative Committee for Ionizing Radiation (CCRI), in order to rationalize any apparent discrepancies.
11. Research should be supported for all forms and new applications of calorimetry, for example for brachytherapy.
12. Absorbed dose standards for electron beams should be developed further.
13. Development of absorbed dose to water standards for kilovoltage X rays should be encouraged.
14. More PSDLs should participate in the high energy X ray comparison piloted by the Bureau international des poids et mesures (BIPM).

### **Session 3: Air Kerma and Absorbed Dose to Water Standards for Photons**

Currently, most dosimetry measurements are made in terms of air kerma. However, as all these measurements are related to a common primary method

using cavity ionization chambers, it is particularly important that the physical constants used in the measurement equations, and the corrections necessary for cavity ionization chambers, be well understood. Consequently, the symposium recommended that:

15. PSDLs and the International Commission on Radiation Units and Measurements (ICRU), as appropriate, should address the unresolved issues pertaining to air kerma dosimetry standards, including the re-evaluation of:
  - $k_{\text{wall}}$  and  $k_{\text{an}}$  (including the BIPM standard);
  - $W_{\text{air}}$  values and uncertainties;
  - Stopping power ratios;
  - Type B uncertainties related to Monte Carlo methods, taking account of the underlying interaction coefficients.

#### **Session 4: Meeting the Needs**

During Session 4 the WHO clearly presented the dramatic increase that is likely in the number of cancer patients in developing countries within the foreseeable future. Since nuclear technology in the form of radiotherapy will remain central for the treatment of cancer in both developed and developing countries within the same time frame, the symposium felt that:

16. Organizations engaged in assisting countries to develop and implement cancer control strategies should be proactive in order to address their current and future needs for cancer treatment.

It is clear that cobalt teletherapy and brachytherapy source trains will be the mainstays of radiotherapy for most developing countries for the foreseeable future. To support these therapies, the symposium felt that:

17. Appropriate staffing — medical, technical, nursing and scientific — is crucial for treatments to be effective.
18. Treatment equipment must be accompanied by the appropriate techniques for diagnosis, tumour localization and staging, immobilization, shielding, treatment simulation and planning, clinical dosimetry (including displays), treatment verification and follow-up.
19. Appropriate dosimetry equipment must be made available for equipment commissioning and continuing quality control.

With regard to therapy and supporting diagnostic equipment, the symposium felt that a number of issues could be addressed. There were particular concerns raised during the final discussion session that low dose rate brachytherapy equipment was no longer being produced, whereas this was considered by some radiation oncologists to be better or less expensive than high dose rate brachytherapy. Consequently, the symposium recommended that:

20. The equipment industry should be encouraged to recommence the production of low dose rate brachytherapy equipment and also to strive to make high dose rate brachytherapy equipment more affordable.
21. The equipment industry should be made aware of the future needs of the Member States regarding the increasing demands for cancer services.

While collaboration between industry and government was seen as useful for developing countries, concern was expressed that voluntary organizations often donated equipment without taking account of the consequent needs. Understanding that this is the domain of the WHO and PAHO, the symposium felt that:

22. WHO advice that provides guidance to organizations donating technologies to the developing countries should be disseminated widely.
23. Supporting guidance covering all factors required to implement such radiation technologies for safe and effective diagnosis and therapy should be developed.

Where the necessary infrastructure and expertise for maintaining linacs are missing, cobalt therapy may be much safer and more reliable for patients than linacs. Hence the symposium felt that:

24. Manufacturers should be encouraged to continue the production of cobalt therapy units.

The current lack of properly trained radiotherapy personnel is as serious as the lack of equipment in many developing — and indeed in some developed — Member States. It was noted that optimizing the use of existing equipment through the proper use of personnel could sometimes be more cost effective than simply adding new equipment. In view of the current lack of and future need for trained personnel and in order to increase awareness of this need among organizations such as the IAEA, European Commission (EC), European Federation of Organisations for Medical Physics (EFOMP),

European Society for Therapeutic Radiology and Oncology (ESTRO), International Organization for Medical Physics (IOMP), International Society for Radiation Oncology (ISRO), PAHO and WHO the symposium recommended that:

25. Training programmes should be implemented on a large scale for professional staff working in radiotherapy, not just to follow the basic curricula but also to comply with a requirement for continuing professional development.
26. National or regional centres of excellence for training should be developed and supported in co-operation with international organizations.

### **Sessions 5, 6 and 8b: Dosimetry Protocols and Comparisons**

The symposium felt very strongly that radiotherapy dosimetry within a given country should be consistent. To achieve this, ideally the same dosimetry protocol should be used in all radiotherapy centres of that particular country. Keeping in mind that some countries have developed their own national dosimetry protocol (e.g. TG 51<sup>1</sup> in the United States of America), for those countries that prefer to use TRS 398 the symposium recommended that:

27. TRS 398 should be adopted initially at the national level in collaboration with the national scientific societies and the SSDLs.
28. Training and education on TRS 398 should be encouraged prior to its implementation.
29. The differences from existing protocols expected with the practical implementation of TRS 398 should be disseminated.
30. The necessary changes in quality assurance procedures should be assessed before the adoption of TRS 398.
31. Both TRS 398 and the code of practice previously adhered to should be used in parallel for a short time and differences between the codes of practice outside those expected should be explained.
32. A specific date should be chosen for the adoption of the new code of practice by all hospitals in the country.
33. Independent dosimetry checks in co-operation with peers should be encouraged.

---

<sup>1</sup> AMERICAN ASSOCIATION OF PHYSICISTS IN MEDICINE, AAPM's TG-51 protocol for clinical reference dosimetry of high-energy photon and electron beams, *Med. Phys.* **26** (1999) 1847–1870.

34. External audits should be performed, if available.
35. The practical aspects of the adoption of TRS 398 for kilovoltage X rays should be studied and a pilot study should be encouraged for the adoption of the kilovoltage code of practice in the clinic.

It is recognized that several PSDLs and many SSDLs do not have their own accelerators for calibrating secondary standards for clinics. It has been suggested that the SSDLs could use hospital equipment (out of normal operating hours) for this purpose. However, the setting up of a facility for calibration takes time and the uncertainties associated with setting up may be larger than the uncertainties associated with using a protocol's calculated values. Consequently, the symposium recommended that:

36. A feasibility study (including the assessment of uncertainties) should be carried out in order that SSDLs can disseminate experimentally determined  $N_{D,w}$  calibrations — traceable to PSDLs — to radiotherapy centres for both megavoltage photon and electron beams.

Further recommendations concerning the dissemination of dosimetry protocols were that:

37. PSDLs should be encouraged to measure  $k_Q$  factors, which should be compiled in a single document.
38. Clinical electron dosimetry (at the hospital level) should be based, in order of preference, on:
  - Ionization chamber calibrations in electron beams based on a standard traceable to a PSDL; or
  - Cross-calibration in an electron beam against a  $^{60}\text{Co}$  calibrated reference chamber; or, if no other option is possible
  - Direct  $^{60}\text{Co}$  calibrations.

### Sessions 7 and 8a: Dosimetry Issues for Diagnostic Radiology

A large number of quantities have been used for dosimetry measurements in diagnostic radiology, in particular for dosimetry in computed tomography. This has caused considerable confusion, so it was strongly recommended that:

39. The quantities used for these purposes should be harmonized.

40. New codes of practice for dosimetry in diagnostic radiology should use the quantities agreed.
41. The determination of diagnostic reference levels, a process in which image quality also needs to be assessed, should use the quantities agreed.

Some SSDLs have established or are in the process of establishing calibration services for dosimetry in diagnostic radiology. The number of laboratories that can provide these services is not sufficient to meet national needs. The symposium recommended that:

42. SSDLs should develop calibration services for dosimetry in diagnostic radiology in order to be able to cover their national needs.
43. A set of recommendations should be developed to provide an interim approach to traceability for countries with no access to an SSDL undertaking the calibration of diagnostic dosimeters.

The symposium noted that computed tomography could deliver significant doses to the patient, although these doses were not always simple to assess, and that interventional radiology had caused irreversible skin damage to some patients. The discussions provoked the recommendations that:

44. Appropriate methods for quality assurance and quality control in digital and interventional radiology should be developed urgently.
45. New dosimetry methods should be developed to meet the needs of current and future X ray diagnostic methods.

It is important that all measurements in X ray diagnostic radiology be performed with the required accuracy. The symposium recommended that:

46. Dosimetry audits to check the performance of calibration laboratories and of end users should be developed and implemented for these diagnostic radiology techniques.

It was further noted that new skills need to be acquired by those performing diagnostic radiology measurements. Consequently, the symposium recommended that:

47. Education and training programmes should be developed for physicists and technical staff working in clinical diagnostic radiology.

**Session 9: Nuclear Medicine Dosimetry**

During Session 9 a number of concerns were expressed about the state of radionuclide measurements and patient dosimetry in nuclear medicine. The use of unsealed sources for radiotherapy is increasing, but there does not seem to be a concerted effort to improve the quality of the therapies, although standardization is becoming increasingly important, especially in view of multinational trials. The symposium summarized the concerns by making the recommendations that:

48. Clinical radioactivity measurements should be traceable to national or international activity standards in each country in which nuclear medicine is practised.
49. PSDLs should be encouraged to focus on establishing reliable procedures for measuring low energy gamma emitters, beta emitters, low energy electron emitters and alpha emitters.
50. Quality assurance/quality control programmes should be established and implemented, particularly for quantitative dosimetry analyses in nuclear medicine; guidance for such programmes should be developed.

With reference to patient dosimetry, the symposium recommended that:

51. The use of current dosimetry models should continue with the collection of adequate data to obtain good dose estimates, using as many patient specific modifications as possible.
52. The dissemination of better dosimetric models, particularly those based on patient images in a voxel format, should be encouraged in order that internal dose calculations can be more accurate and detailed and able to provide better correlations between calculated dose and observed effect.
53. Comparison programmes for the quantification of radioactivity should be established, especially for in-phantom measurement and for the calculation of organ doses from multiple image sets.
54. The development of standardized and well documented software programs for traditional dose calculation methods, and for implementing newer, voxel based methods, should be encouraged.

Finally, in Session 9, the symposium recommended that:

55. A standardized code of practice for simple and for more complicated dosimetry calculations should be developed.



**Sessions 10 and 12a: Brachytherapy**

Although brachytherapy has been practised for decades, it is a many faceted area in which the dosimetry is neither always clear nor always practised well. The symposium considered that the time had come to take definite steps to improve the situation. Consequently, it was recommended that:

56. PSDLs should establish dosimetry standards for brachytherapy sources that SSDLs then disseminate using an internationally agreed method.
57. Dosimetry comparisons between PSDLs and SSDLs should be developed and implemented.
58. Dosimetry audits for clinical end users should be developed and implemented.
59. Research efforts should be focused on dosimetry standards based on absorbed dose to water for photon emitting brachytherapy sources.
60. Beta dosimetry for brachytherapy should be improved, in particular for  $^{106}\text{Ru}/^{106}\text{Rh}$  sources.
61. Quality assurance programmes for brachytherapy dosimetry should be developed and implemented.
62. Education and training programmes should be developed for SSDL staff and for clinical personnel.

**Sessions 11 and 12b: Radiotherapy Dosimetry Audits**

Quality assurance and quality audit of a number of areas in the radiotherapy process were covered in Sessions 11 and 12b, which resulted in a large number of recommendations. In particular, to set the scene, the symposium felt that:

63. Radiotherapy at levels 1 (basic) and 2 (advanced) should be strengthened through education and training, equipment provision and expert support, while at level 3 (developmental) it should be advanced through research programmes.

The symposium strongly expressed the view that quality assurance and quality audits are a very effective way to ensure the correct delivery of the radiation dose to the patient and to enable the therapeutic outcome to be assessed in a consistent manner. Consequently, it was recommended that:

64. Quality assurance programmes for radiotherapy equipment, dosimetry and processes should be promoted, implemented and strengthened in order to ensure accurate, reproducible dose delivery to each radiotherapy patient.

65. Quality assurance programmes should cover the medical aspects of radiotherapy as well as the physics and technical aspects.
66. Audits should be encouraged for all levels of radiotherapy.

The many facets of the auditing of dosimetry were considered, and the symposium recommended that:

67. Dosimetry audit should be included within the scope of clinical audit, as assured dosimetry is required to enable assured clinical practice.
68. An external audit should be available to all radiotherapy centres for all clinically used external beam treatment units, as recommended internationally (e.g. in the International Basic Safety Standards for Protection against Ionizing Radiation and for the Safety of Radiation Sources<sup>2</sup> and the EC Medical Exposure Directive 97/43/Euratom<sup>3</sup>).
69. The level of external audit should be appropriate to the level of the radiotherapy department and of the national expertise (see also Recommendation 73).
70. As a minimum external audit for radiotherapy beam dosimetry, each beam dose output should be measured independently of the institution's procedures, for example using a mailed thermoluminescent dosimeter from an external laboratory, at least once every two years.

It was agreed that nationally adopted quality assurance programmes provide consistency for radiotherapy practice, and consequently the symposium recommended that:

71. The development of national quality assurance programmes should be encouraged and supported, especially in developing countries.

---

<sup>2</sup> FOOD AND AGRICULTURE ORGANIZATION OF THE UNITED NATIONS, INTERNATIONAL ATOMIC ENERGY AGENCY, INTERNATIONAL LABOUR ORGANISATION, OECD NUCLEAR ENERGY AGENCY, PAN AMERICAN HEALTH ORGANIZATION, WORLD HEALTH ORGANIZATION, International Basic Safety Standards for Protection against Ionizing Radiation and for the Safety of Radiation Sources, Safety Series No. 115, IAEA, Vienna (1996).

<sup>3</sup> EUROPEAN UNION, Council Directive 97/43/Euratom of 30 June 1997, Health Protection of Individuals against the Dangers of Ionizing Radiation in Relation to Medical Exposure (Repealing Directive 84/466/Euratom, O.J. No. L 265/1, 5.10.1984), Official Journal of the European Communities No. L 180/22–27, Luxembourg (1997).

72. National programmes should include guidelines on quality assurance procedures for radiotherapy centres and also for audit networks or audit systems at the national level.
73. National audit systems for radiotherapy dosimetry should be operated by qualified groups involving co-operation between SSDLs and clinical medical physicists.

The symposium understood that complex radiotherapy techniques require a significantly increased effort for their safe and effective implementation and use. Consequently, it was recommended that:

74. The development of quality assurance recommendations and programmes should be promoted for complex treatment situations (e.g. total body irradiation, stereotactic radiosurgery and intensity modulated radiotherapy).

A range of audit tools has been developed by several audit programmes, including that successfully run by the IAEA, for dosimetry audit. Postal dose audits based on thermoluminescence dosimetry are widely used and well established. However, it was noted that other systems (e.g. alanine) are being considered at the research level. The symposium recommended that:

75. Support should be given, through research programmes, to the development and evaluation of audit methodologies suitable for the various radiotherapy levels.

Appreciating the particular importance of audit when used to assure the dosimetry of patients from multiple countries participating in co-operative clinical trials, the symposium recommended that:

76. Activities in quality audit should be co-ordinated internationally and different audit systems should be compared.

### **Session 13: Proton and Hadron Dosimetry**

The symposium noted that the number of treatment facilities using proton beams and heavier ion beams (mostly  $^{12}\text{C}$ ) was growing, with 24 currently operational and another 20 planned worldwide over the next five years. There is still a divergence of opinion internationally and even nationally about the dosimetry methods to use for these therapy beams. However, the results presented indicate that the adoption of TRS 398 would provide a coherent approach. Consequently,

the symposium felt that the dosimetry of these beams should be in keeping with conventional radiotherapy beam dosimetry and recommended that:

77. Proton and heavier ion beam dosimetry should be based on absorbed dose to water standards.
78. Comparisons based on absorbed dose to water calibrations should be organized between centres.

For ion dosimetry, the symposium felt that considerable research was still needed to improve knowledge on basic physics data for dosimetry, and consequently recommended that:

79. Research projects on ion dosimetry techniques should be supported.

#### **Session 14: Developments in Clinical Radiotherapy Dosimetry**

At the clinical level two areas of concern were discussed, dose measurements and dose calculations. The practicalities of dosimetry systems were evidently a problem and the symposium recommended that:

80. Industry should be encouraged to develop affordable systems for practical use in quality assurance and dosimetry (e.g. tissue equivalent materials, easy to use phantoms and equipment that is robust and reliable).
81. Gel dosimetry methodology should be developed to evaluate its potential for routine use in radiotherapy centres.
82. In vivo dosimetry should be promoted, including its use in developing countries.
83. Alternative methods of clinical dosimetry should be tested and compared with traditional techniques.

With regard to dose calculations, the symposium recommended that:

84. Advanced computing methods for dose calculation should be encouraged where appropriate expertise is available.
85. Guidelines should be developed on which quality assurance tests of treatment planning systems should be performed by manufacturers, user groups and individual users.

Recognizing that errors in treatment monitor units and treatment time calculations have caused accidents, the symposium also recommended that:

86. All radiotherapy institutions should implement an independent monitor unit or time calculation protocol for each patient.

### **Session 15: Conclusions and Recommendations**

Some additional discussion points were raised during the round-up session. In particular, concern was expressed on the lack of understanding of the role of the medical physicist, specifically regarding dosimetry for the patient. The symposium recommended that:

87. During the training of administrators, the different roles of professionals working in radiotherapy should be clearly identified.
88. National, regional and international professional societies such as the IOMP should be encouraged to work together to register the profession of medical physicist with the International Labour Organization.
89. Medical physicists should involve themselves in the education and training of clinical practitioners.

Views were also exchanged on the lack of medical physics staff currently available and on the need for more staff in the future. Evidence of the lack of staff currently employed, even in developed countries, can be seen in the report commissioned by a United Kingdom government department on the need for nuclear skills (<http://www.dti.gov.uk/energy/nuclear/skills/nsg.shtml>). The symposium recommended that:

90. National, regional and international professional societies should work towards promoting the profession of medical physics to university undergraduates.

In conclusion, the symposium was greatly appreciated by all participants and each felt personally involved with the recommendations. The view was expressed that the time interval since the last symposium had been too long. Recognizing the importance of recent changes in the field of medical radiation dosimetry and notwithstanding the heavy organizational burden on any organization willing to host future such meetings, it was recommended that:

91. A further dosimetry symposium should be held in six years' time (2008).

**BLANK**

## **CHAIRS OF SESSIONS**

Session 1	K.R. SHORTT	IAEA
Session 2	A.R. DuSAUTOY	United Kingdom
Session 3	I. CSETE	Hungary
Session 4	S. GROTH	IAEA
Session 5	V.G. SMYTH	New Zealand
Session 6	S.M. VATNITSKY	IAEA
Session 7	F. PERNIČKA	IAEA
Session 8a	H.-M. KRAMER	Germany
Session 8b	A. MEGHZIFENE	IAEA
Session 9	B.E. ZIMMERMAN	United States of America
Session 10	H. TÖLLI	IAEA
Session 11	H. SVENSSON	European Society for Therapeutic Radiology and Oncology
Session 12a	I.-L.C. LAMM	European Federation of Organisations for Medical Physics
Session 12b	D.I. THWAITES	European Society for Therapeutic Radiology and Oncology and International Society for Radiation Oncology
Session 13	P. ANDREO	Sweden
Session 14	B. MIJNHEER	European Society for Therapeutic Radiology and Oncology
Session 15	P.J. ALLISY-ROBERTS	Bureau international des poids et mesures

## **CO-CHAIRS OF SESSIONS**

Session 1	A. MEGHZIFENE	IAEA
Session 2	J. SEUNTJENS	Canada
Session 3	L. BÜERMANN	Germany
Session 4	K.R. SHORTT	IAEA
Session 5	D.I. THWAITES	European Society for Therapeutic Radiology and Oncology and International Society for Radiation Oncology

Session 6	M. SAIFUL HUQ	United States of America
Session 7	J. ZOETELIEF	Netherlands
Session 8a	F. PERNIČKA	IAEA
Session 8b	P. ANDREO	Sweden
Session 9	M.G. STABIN	United States of America
Session 10	C.G. SOARES	United States of America
Session 11	J. IZEWSKA	IAEA
Session 12a	H. TÖLLI	IAEA
Session 12b	J. IZEWSKA	IAEA
Session 13	S.M. VATNITSKY	IAEA
Session 14	C. BALDOCK	Australia
	C.-M. MA	United States of America
Session 15	K.R. SHORTT	IAEA

## RAPPORTEURS OF SESSIONS

Session 1	G. IBBOTT	United States of America
Session 2	M.R. McEWEN	United Kingdom
Session 3	M.R. McEWEN	United Kingdom
Session 4	B. VIKRAM	IAEA
Session 5	K.E. ROSSER	United Kingdom
Session 6	K.E. ROSSER	United Kingdom
Session 7	H.-M. KRAMER	Germany
Session 8a	C. BORRÁS	Pan American Health Organization
Session 8b	K.E. ROSSER	United Kingdom
Session 9	H. ZAIDI	Switzerland
Session 10	I.-L.C. LAMM	European Federation of Organisations for Medical Physics
Session 11	R. HUNTLEY	Australia
Session 12a	I.-L.C. LAMM	European Federation of Organisations for Medical Physics
Session 12b	R. HUNTLEY	Australia
Session 13	A. KACPEREK	United Kingdom
Session 14	A. KACPEREK	United Kingdom
Session 15	A. DUTREIX	European Society for Therapeutic Radiology and Oncology



## PROGRAMME COMMITTEE

<i>Chair</i>	K.R. SHORTT	IAEA
<i>Members</i>	P. ANDREO	Sweden
	C. BORRÁS	Pan American Health Organization
	J. IZEWSKA	IAEA
	H.-M. KRAMER	Germany
	I.-L.C. LAMM	European Federation of Organisations for Medical Physics
	A. MEGHZIFENE	IAEA
	A. NIROOMAND-RAD	International Organization for Medical Physics
	P. ORTIZ LOPEZ	IAEA
	H. ØSTENSEN	World Health Organization
	F. PERNIČKA	IAEA
	K. SCHNUER	European Commission
	C.G. SOARES	American Association of Physicists in Medicine
	D.I. THWAITES	European Society for Therapeutic Radiology and Oncology and International Society for Radiation Oncology
	H. TÖLLI	IAEA
	S.M. VATNITSKY	IAEA
	A. WAMBERSIE	International Commission on Radiation Units and Measurements

## SECRETARIAT OF THE SYMPOSIUM

K.R. SHORTT	Scientific Secretary
R. PERRICOS	Conference Services
S. COHEN-UNGER	Records Officer
J. DENTON-MacLENNAN	Proceedings Editor

**BLANK**

## LIST OF PARTICIPANTS

- Aalbers, A.H.L.                      Nederlands Meetinstituut,  
P.O. Box 654,  
NL-2600 AR Delft,  
Netherlands  
Fax: +31152612971  
E-mail: aaalbers@nmi.nl
- Abushammala, R.A.H.              Radiotherapy Department,  
Mafrag Hospital,  
P.O. Box 2951,  
Abu Dhabi,  
United Arab Emirates  
Fax: +97125821549  
E-mail: rshamala@hotmail.com
- Affonseca, M.S.                      Laboratório de Ciências Radiológicas,  
Universidade do Estado do Rio de Janeiro,  
Rua São Francisco Xavier 524,  
Maracanã, CEP 2055-013 Rio de Janeiro RJ,  
Brazil  
Fax: +552122867146  
E-mail: florita@uperi.br or  
         mariella7@vol.com.br
- Aguirre, J.F.                          Department of Radiation Physics,  
University of Texas  
         M.D. Anderson Cancer Center,  
1515 Holcombe Blvd,  
P.O. Box 547,  
Houston, TX 77071,  
United States of America  
Fax: +17137941364  
E-mail: faguirre@mdanderson.org
- Al Nowais, S.A.A.                      Radiotherapy Department,  
Mafrag Hospital,  
P.O. Box 2951,  
Abu Dhabi,  
United Arab Emirates  
Fax: +9712582154  
E-mail: s\_alnowais@yahoo.com

- Al-Kinani, A.-T.                      Radiation Protection Department,  
Iraq Atomic Energy Commission,  
P.O. Box 765,  
Tuwaitha-Baghdad,  
Iraq  
Fax: +96417181929  
E-mail: a.alkinani@warkaa.net
- Allisy-Roberts, P.J.                      Bureau international des poids et mesures,  
Pavillon de Breteuil,  
F-92312 Sèvres Cedex,  
France  
Fax: +33145342021  
E-mail: allisy-roberts@bipm.org
- Alonso-Samper, J.L.                      Centro Nacional de Seguridad Nuclear (CNSN),  
Calle 4 No. 455 e/19 y 21,  
Vedado,  
C.P. 11300 Habana,  
Cuba  
Fax: +537551930  
E-mail: papa.samper@infomed.sld.cu
- Alvarez-Romero, J.T.                      Instituto Nacional de  
Investigaciones Nucleares,  
P.O. Box 181027,  
Colonia Escandón,  
Miguel Hidalgo,  
C.P. 11801 Mexico, D.F.,  
Mexico  
Fax: +525553297302  
E-mail: jtar@nuclear.inin.mx
- Andreo, P.                                  Medical Radiation Physics,  
University of Stockholm–Karolinska Institute,  
P.O. Box 260,  
SE-171 76 Stockholm,  
Sweden  
Fax: +468343525  
E-mail: pedro.andreo@ks.se

- Angliss, R.F. National Physical Laboratory,  
Queens Road,  
Teddington,  
Middlesex TW11 OLW,  
United Kingdom  
Fax: +442089436139  
E-mail: robert.angliss@npl.co.uk
- Anton, M. Physikalisch-Technische Bundesanstalt,  
Bundesallee 100,  
D-38116 Braunschweig,  
Germany  
Fax: +495315926405  
E-mail: mathias.anton@ptb.de
- Antropova, T.Y. Kazakh Research Institute of Oncology  
and Radiology,  
Abai Avenue 91,  
480072 Almaty,  
Kazakhstan  
Fax: +73272955234  
E-mail: tantropova@mail.ru
- Appukuttan, S. Radiological Physics and Advisory Division,  
Bhabha Atomic Research Centre,  
Trombay, Mumbai 400 085,  
India  
Fax: +91225519209  
E-mail: shanta13c@hotmail.com
- Arib, M. Centre de recherche nucléaire d'Alger,  
2 Bd. Frantz Fanon,  
B.P. 399 Alger Gare,  
Alger 16000,  
Algeria  
Fax: +2132434280  
E-mail: amehenna@hotmail.com
- Aznar, M.C. Radiation Physics Department,  
Risø National Laboratory,  
Building 201,  
DK-4000 Roskilde,  
Denmark  
Fax: +4546774959  
E-mail: marianne.aznar@risoe.dk

- Baldock, C. Centre for Medical, Health and  
Environmental Physics,  
Queensland University of Technology,  
G.P.O. Box 2434,  
Brisbane,  
Queensland 4001,  
Australia  
Fax: +61738641521  
E-mail: c.baldock@qut.edu.au
- Baranczyk, R. Centre of Oncology,  
Krakow Division,  
ul. Garncarska 11,  
PL-31-115 Kraków,  
Poland  
Fax: +48124226680  
E-mail: 25baranc@cyfronet.krakow.pl
- Beal, A.D.R. Department of Medical Physics,  
Tawam Hospital,  
P.O. Box 15258,  
Al Ain,  
Abu Dhabi,  
United Arab Emirates  
Fax: +97137511401  
E-mail: tonybeal@emirates.net.ae
- Beauvais-March, H. Institut de radioprotection et de sûreté nucléaire,  
Site du Vésinet,  
B.P. 35,  
F-78116 Le Vésinet Cedex,  
France  
Fax: +33139760896  
E-mail: helene.beauvais@opri.fr
- Becerril, A. Instituto Nacional de Investigaciones Nucleares,  
km 36.5 Carretera México,  
Toluca, Salazar Edo,  
52045 Municipio de Ocoyoacac,  
Mexico  
Fax: +525553297302  
E-mail: abv@nuclear.inin.mx

- Ben Omrane, L. Centre national de radioprotection,  
Hospital d'enfants,  
Bab Souika,  
1006 Tunis,  
Tunisia  
Fax: +21671571697  
E-mail: benomrane.latifa@planet.tn
- Ben-Shlomo, A. Radiation Safety Division,  
Soreq Nuclear Research Center,  
81800 Yavne,  
Israel  
Fax: +97289434196  
E-mail: abenshlomo@hotmail.com
- Bera, P. Agency's Laboratories at Seibersdorf,  
Department of Nuclear Sciences and Applications,  
International Atomic Energy Agency,  
A-2444 Seibersdorf,  
Austria  
Fax: +431260028222  
E-mail: P.Bera@iaea.org
- Bergstrand, E.S. Department of Physics,  
University of Oslo,  
P.O. Box 1048 Blindern,  
N-0316 Oslo,  
Norway  
Fax: +4722855671  
E-mail: e.s.bergstrand@fys.uio.no
- Bergström, B.D. ONCOlog Medical QA AB,  
Ultunaallén 2 A,  
SE-756 51 Uppsala,  
Sweden  
Fax: +4618300685  
E-mail: berndt.bergstrom@oncolog.net
- Besbes, M. Institut Salah Azaiz,  
Boulevard 9 Avril,  
Bab Saadoun,  
1006 Tunis,  
Tunisia  
Fax: +21671571380  
E-mail: mounir.besbes@rns.tn

- Bjerke, H. Norwegian Radiation Protection Authority,  
Grini Naeringspark 13,  
P.O. Box 55,  
N-1332 Østerås,  
Norway  
E-mail: hans.bjerke@nrpa.no
- Blaha, J. Faculty of Nuclear Sciences and  
Physical Engineering,  
Czech Technical University,  
Brehova 7,  
CZ-115-19 Prague 1,  
Czech Republic  
Fax: +420222320861  
E-mail: jan.blaha@fjfi.cvut.cz
- Bocharova, I.A. Moscow Oncology Research Institute,  
2nd Botkinsky,  
RU-125284 Moscow,  
Russian Federation  
Fax: +70959456882  
E-mail: i\_bocharova@mail.ru
- Bochud, F. Institut universitaire de radiophysique appliquée,  
Grand-Pré 1,  
CH-1007 Lausanne,  
Switzerland  
Fax: +41216233435  
E-mail: francois.bochud@inst.hospvd.ch
- Böhm, J.R. Physikalisch-Technische Bundesanstalt,  
Bundesallee 100,  
D-38116 Braunschweig,  
Germany  
Fax: +495315926015  
E-mail: juergen.boehm@ptb.de
- Bokulic, T. Department of Oncology and Nuclear Medicine,  
University Hospital "Sestre Milosrdnice",  
Vinogradska Street 29,  
HR-10000 Zagreb,  
Croatia  
Fax: +38513768303  
E-mail: tbokulic@public.srce.hr



- Borrás, C. Pan American Health Organization,  
Regional Office for the  
World Health Organization,  
525 23rd Street, NW,  
Washington, DC 20037-2895,  
United States of America  
Fax: +12029743610  
E-mail: borrasca@paho.org
- Bridier, A. Physics Department,  
Institut Gustave-Roussy,  
39, rue Camille Desmoulins,  
F-94805 Villejuif Cedex,  
France  
Fax: +33142115299  
E-mail: bridier@igr.fr
- Brunetto, M.G. Centro Médico Dean Funes,  
Dean Funes 2869,  
5000 Córdoba,  
Argentina  
Fax: +543514892624  
E-mail: brunetto@mail.famaf.unc.edu.ar
- Brunzendorf, J. Physikalisch-Technische Bundesanstalt,  
Bundesallee 100,  
D-38116 Braunschweig,  
Germany  
Fax: +495315926405  
E-mail: jens.brunzendorf@ptb.de
- Bubula, E.T. Computerized Medical Systems GmbH,  
Sundgauallee 25,  
D-79114 Freiburg,  
Germany  
Fax: +497618818811  
E-mail: friederike.schreiber@cms-euro.com
- Bucciolini, M. Dipartimento di Fisiopatologia Clinica,  
Università di Firenze,  
Viale Morgagni 85,  
I-50134 Florence,  
Italy  
Fax: +39554379930  
E-mail: marta@dfc.unifi.it

- Budzinski, P. MDS Nordion Gmbh,  
Heinrich von Stephan-Strasse 8,  
D-79100 Freiburg,  
Germany  
Fax: +497614551310  
E-mail: p.budzinski@mds.nordion.com
- Büermann, L. Physikalisch-Technische Bundesanstalt,  
Bundesallee 100,  
D-38116 Braunschweig,  
Germany  
Fax: +495315926405  
E-mail: ludwig.bueermann@ptb.de
- Bulski, W. Maria Sklodowska-Curie Memorial Cancer Center  
and Institute of Oncology,  
Roentgena Street 5,  
PL-02-781 Warsaw,  
Poland  
Fax: +48226449182  
E-mail: w.bulski@rth.coi.waw.pl
- Burkart, W. Department of Nuclear Sciences and Applications,  
International Atomic Energy Agency,  
Wagramer Strasse 5, P.O. Box 100,  
A-1400 Vienna,  
Austria  
Fax: +43126007  
E-mail: w.burkart@iaea.org
- Burns, D.T. Bureau international des poids et mesures,  
Pavillon de Breteuil,  
F-92312 Sèvres Cedex,  
France  
Fax: +33145342021  
E-mail: dburns@bipm.org
- Byrski, E. Centre of Oncology,  
ul. Garnearska 11,  
PL-31-115 Kraków,  
Poland  
Fax: +48124226680  
E-mail: z5byrski@cyf.edu.pl

- Caldas, L.V.E. Instituto de Pesquisas Energéticas e Nucleares,  
IPEN/CNEN,  
Av. Prof. Lineau Prestes,  
2242 Cidade Universitária,  
05508-900 São Paulo SP,  
Brazil  
Fax: +551138169117  
E-mail: lcaldas@net.ipen.br
- Casar, B. Institute of Oncology,  
Zaloska 2,  
SI-1000 Ljubljana,  
Slovenia  
Fax: +38614319108  
E-mail: bcasar@onko-i.si
- Castelo Branco Viegas, C. National Cancer Institute,  
Rua do Rezende 128,  
Sala 322,  
20230-092 Rio de Janeiro RJ,  
Brazil  
Fax: +552139707829;+552125512205  
E-mail: viegaspqrt@yahoo.com.br
- Chavaudra, J. Physics Department,  
Institut Gustave-Roussy,  
Service de Médecine Nucléaire,  
39, rue Camille Desmoulins,  
F-94805 Villejuif Cedex,  
France  
Fax: +33142115299  
E-mail: chavaudr@igr-fr
- Chen, Y. M. Department of Nuclear Medicine,  
Great Wall Hospital,  
Fuxing Road 28,  
Beijing 100853,  
China  
Fax: +861066937424823  
E-mail: chen.ym@263.net

- Chervyakov, A.M. Central Research Institute of Roentgenology  
and Radiology,  
Pesochny 2,  
Leningradskaya 70/4,  
RU-198005 St. Petersburg,  
Russian Federation  
Fax: +78125966705  
E-mail: cherviakov.a@cards.lanck.net
- Choi, Jin-ho Radiation Oncology Department,  
Gachon Medical School,  
Gil Medical Center,  
1198 Guwall-Dong,  
Namdong-Gu,  
Inchon 405-220,  
Republic of Korea  
Fax: +82025046152  
E-mail: jinhoc@ghil.com
- Coray, A. Department of Radiation Medicine,  
Paul Scherrer Institute,  
CH-5232 Villigen PSI,  
Switzerland  
Fax: +41563103515  
E-mail: doelf.coray@psi.ch
- Csete, I. National Office of Measures,  
Nemetvolgyi ut. 37-39,  
H-1124 Budapest,  
Hungary  
Fax: +3614585937  
E-mail: icsete@omh.hu
- Czap, L. Division of Human Health,  
Department of Nuclear Sciences and Applications,  
International Atomic Energy Agency,  
Wagramer Strasse 5, P.O. Box 100,  
A-1400 Vienna,  
Austria  
Fax: +431260028222  
E-mail: l.czap@iaea.org

- Dadasbilge, A. Institute of Oncology,  
Istanbul University,  
Gapat,  
TR-34390 Istanbul,  
Turkey  
Fax: +902125343078  
E-mail: alparbay@netone.com.tr
- Daures, J. Bureau national de métrologie–Laboratoire  
national Henri Becquerel,  
Commissariat à l'énergie atomique Saclay,  
DIMRI–LNHB,  
F-91191 Gif-sur-Yvette Cedex,  
France  
Fax: +33169084773  
E-mail: josiane.daures@cea.fr
- de Affonseca, M.S. Laboratório de Ciências,  
Radiológicas LCR-DBB-IBRAG,  
UERJ,  
Rua Sao Francisco Xavier, 524,  
PAV. HLC Sala 136 Térreo,  
20550-013 Rio de Janeiro RJ,  
Brazil  
Fax: +552122867146  
E-mail: florita@uperi.br
- de Angelis, C. Laboratorio di Fisica,  
Istituto Superiore di Sanita,  
Viale Regina Elena 299,  
I-00161 Rome,  
Italy  
Fax: +390649387075  
E-mail: cinzia.deangelis@iss.it
- de Regge, P. Agency's Laboratories at Seibersdorf,  
Department of Nuclear Sciences and Applications,  
International Atomic Energy Agency,  
A-2444 Seibersdorf,  
Austria  
Fax: +431260028222  
E-mail: P.de-Regge@iaea.org

- del Gallo Rocha, F. Instituto de Pesquisas Energeticas e Nucleares,  
IPEN/CNEN,  
Av. Prof. Lineau Prestes,  
2242 Cidade Universitária,  
05508-900 São Paulo SP,  
Brazil  
Fax: +551138169209  
E-mail: fgrocha@net.ipen.br
- Delaunay, F. Commissariat à l'énergie atomique Saclay,  
DIMRI/LNHB/LMDO,  
Bâtiment 534,  
F-91191 Gif-sur-Yvette Cedex,  
France  
Fax: +33169084773  
E-mail: franck.delaunay@cea.fr
- Derikum, K. Physikalisch-Technische Bundesanstalt,  
Bundesallee 100,  
D-38116 Braunschweig,  
Germany  
Fax: +495315926405  
E-mail: klaus.derikum@ptb.de
- Dobrovodsky, J. Slovak Institute of Metrology,  
Karloveská 63,  
SK-84255 Bratislava,  
Slovakia  
Fax: +421260294670  
E-mail: dobrovodsky@smu.gov.sk
- Douysset, G. Commissariat à l'énergie atomique Saclay,  
DIMRI/LNHB/LMDO,  
Bâtiment 534,  
F-91191 Gif-sur-Yvette Cedex,  
France  
Fax: +33169084773  
E-mail: douysset@ortolan.cea.fr

- Dryák, P. Inspectorate for Ionizing Radiation,  
Czech Metrological Institute,  
Radiova 1,  
CZ-102-00 Prague 10,  
Czech Republic  
Fax: +420266020466  
E-mail: pdryak@cmi.cz
- DuSautoy, A. National Physical Laboratory,  
Queens Road,  
Teddington,  
Middlesex TW11 OLW,  
United Kingdom  
E-mail: alan.dusautoy@npl.co.uk
- Duane, S. National Physical Laboratory,  
Queens Road,  
Teddington,  
Middlesex TW11 OLW,  
United Kingdom  
Fax: +442089436070  
E-mail: simon.duane@npl.co.uk
- Dutreix, A. European Society for Therapeutic Radiology  
and Oncology,  
EQUAL Measuring Laboratory,  
Service de physique,  
Institut Gustave-Roussy,  
39, rue Camille Desmoulins,  
F-94805 Villejuif Cedex,  
France  
Fax: +33142115299  
E-mail: equal@igr.fr
- Dvorak, P. Department of Dosimetry and Application of  
Ionizing Radiation,  
Czech Technical University,  
Brehova 7,  
CZ-115-19 Prague 1,  
Czech Republic  
Fax: +420224434710  
E-mail: dvorak@fjfi.cvut.cz

- Edelmaier, R. Bundesamt für Eich- und Vermessungswesen,  
Arltgasse 35,  
A-1160 Vienna,  
Austria  
Fax: +4314920875  
E-mail: r.edelmaier@metrologie.at
- Falcão, R.C. National Nuclear Energy Commission,  
Rua General Severiano 90,  
Sala 2116,  
22294-900 Rio de Janeiro RJ,  
Brazil  
Fax: +552125462494  
E-mail: ross@cnen.gov.br
- Ferraro, A. Ministerio de Salud Pública,  
Avda. 18 de Julio 1892, Of. 304,  
Montevideo,  
Uruguay  
Fax: +59824086524  
E-mail: dicoca@msp.gub.uy
- Ferreira, I.H. European Society for Therapeutic Radiology  
and Oncology,  
EQUAL Measuring Laboratory,  
Service de physique,  
Institut Gustave-Roussy,  
39, rue Camille Desmoulins,  
F-94805 Villejuif Cedex,  
France  
Fax: +33142115299  
E-mail: ferreira@igr.fr
- Fiume, A. Servizio di Fisica Sanitaria,  
Spedali Civili 1,  
I-25100 Brescia,  
Italy  
Fax: +390303995075  
E-mail: fisicasan.bs@numerica.it



- Fukumura, A. National Institute of Radiological Sciences,  
4-9-1, Anagawa, Inage-ku,  
Chiba-shi 263-8555,  
Japan  
Fax: +81432063246  
E-mail: fukumura@nirs.go.jp
- Gábris, F. Bundesamt für Eich- und Vermessungswesen,  
Arltgasse 35,  
A-1160 Vienna,  
Austria  
Fax: +4314920875  
E-mail: f.gabris@metrologie.at
- Gaudiano, J. Centro de Medicina Nuclear,  
Hospital de Clínicas,  
Av. Italia s/n,  
Montevideo,  
Uruguay  
Fax: +59827081774  
E-mail: gaudiano@hc.edu.uy
- Georg, D. Division of Medical Radiation Physics,  
Department of Radiotherapy and Radiobiology,  
Allgemeines Krankenhaus Wien,  
Währinger Gürtel 18–20,  
A-1090 Vienna,  
Austria  
Fax: +431404002696  
E-mail: dietmar.georg@str.akh.magwien.gv.at
- Gershkevitsh, E. Department of Radiotherapy,  
North Estonia Regional Hospital,  
Cancer Centre,  
Hiiu Str. 44,  
EE-11619 Tallinn,  
Estonia  
Fax: +3726504303  
E-mail: eduardger@yahoo.co.uk

- Giczi, F. Győr–Moson–Sopron County Health and Medical Office,  
National Public Health and Medical Officer Service,  
P.O. Box 66,  
H-9002 Győr,  
Hungary  
Fax: +3696418068  
E-mail: fgiczi.gyor@antsz.gov.hu
- Girzikowsky, R. Division of Human Health,  
Department of Nuclear Sciences and Applications,  
International Atomic Energy Agency,  
c/o Agency's Laboratories at Seibersdorf,  
A-2444 Seibersdorf,  
Austria  
Fax: +431260028222  
E-mail: R.Girzikowsky@iaea.org
- Gomola, I. IBA Advanced Radiotherapy,  
Bahnhofstrasse 5,  
D-90592 Schwarzenbruck,  
Germany  
Fax: +49912860710
- González, J.A. Instituto Oncológico Nacional,  
Antiguo Hospital Gorgas,  
Edif. 254, Ancón,  
Apartado Postal 83-0669,  
Zona 3,  
Panamá,  
Panama  
Fax: +5072616646 or +5072271106  
E-mail: jagonzalezr@angelfire.com
- Gorlachev, G.E. Moscow Engineering Physics Institute (MEPHI),  
MSIEM,  
Malaya Pionerskaya str. 12,  
OF. 279,  
RU-113054 Moscow,  
Russian Federation  
Fax: +70953247135  
E-mail: ggorl@dol.ru

- Govinda Rajan, K.N. Medical Physics and Safety Section,  
Radiological Physics and Advisory Division,  
Bhabha Atomic Research Centre,  
Trombay, Mumbai 400 085,  
India  
E-mail: grajanmpss@usnl.com or  
grajanmpss@yahoo.co.in
- Grindborg, J.-E. Swedish Radiation Protection Authority,  
SE-171 16 Stockholm,  
Sweden  
Fax: +4687297108  
E-mail: jan-erik.grindborg@ssi.se
- Groll, J. MDS Nordion GmbH,  
Heinrich von Stephan-Strasse 8,  
D-79100 Freiburg,  
Germany  
Fax: +497614551310  
E-mail: jgroll@mds.nordion.com
- Groth, S. Division of Human Health,  
Department of Nuclear Sciences and Applications,  
International Atomic Energy Agency,  
Wagramer Strasse 5, P.O. Box 100,  
A-1400 Vienna,  
Austria  
Fax: +43126007  
E-mail: s.groth@iaea.org
- Gürdalli, S. Department of Radiation Oncology,  
Hacettepe University,  
TR-06100 Sıhne, Ankara,  
Turkey  
Fax: +903123092912  
E-mail: sgurdal@hacettepe.edu.tr
- Gutt, F. Laboratorio Secundario de  
Calibración Dosimétrica,  
Instituto Venezolano de  
Investigaciones Científicas,  
Carretera Panamericana km 11,  
Apartado 21827, Caracas 1020A,  
Venezuela  
Fax: +582125041577  
E-mail: fgutt@ivic.ve

- Gwiazdowska, B.A. Maria Sklodowska-Curie Memorial Cancer Center  
and Institute of Oncology,  
Roentgena Street 5,  
PL-02-781 Warsaw,  
Poland  
Fax: +48226449182
- Hafner, H.P. Kantonsspital Luzern,  
Radio-Onkologie,  
CH-6000 Luzern 16,  
Switzerland  
Fax: +412055804  
E-mail: hp.hafner@ksl.ch
- Hartmann, G.H. Department of Medical Physics,  
German Cancer Research Center (DKFZ),  
Im Neuenheimer Feld 280,  
D-69120 Heidelberg,  
Germany  
Fax: +496221422572  
E-mail: g.hartmann@dkfz.de
- Hassan, Z. Radiotherapy Department,  
National Cancer Institute,  
Cairo University,  
Fom El-Khalig,  
Kasr El-Ari,  
Cairo,  
Egypt  
Fax: +2023644720  
E-mail: zeinab\_el\_taher@hotmail.com
- Hein, G.H. PTW-Freiburg,  
Lörracher Strasse 7,  
D-79115 Freiburg,  
Germany  
Fax: +497614905570  
E-mail: guenter-hein@ptw.de
- Hilgers, G. Physikalisch-Technische Bundesanstalt,  
Bundesallee 100,  
D-38116 Braunschweig,  
Germany  
Fax: +49531592696464  
E-mail: gerhard.hilgers@ptb.de

- Hobeila, F. Department of Medical Physics,  
McGill University Medical Center,  
Montreal General Hospital,  
L5-107, 1650 avenue Cedar,  
Montreal, Quebec, QU H2G 1A4,  
Canada  
Fax: +15149348229  
E-mail: fadi@medphys.mcgill.ca
- Holaday, W. Division of Planning and Co-Ordination,  
Department of Technical Co-Operation,  
International Atomic Energy Agency,  
Wagramer Strasse 5, P.O. Box 100,  
A-1400 Vienna,  
Austria  
Fax: +43126007  
E-mail: w.holaday@iaea.org
- Hourdakis, C.J. Hellenic Ionizing Radiation Calibration Laboratory,  
Greek Atomic Energy Commission,  
GR-15310 Aghia Paraskevi Attiki,  
Greece  
Fax: +302106506748  
E-mail: khour@eeae.gr
- Hranitzky, C. ARC Seibersdorf Research GmbH,  
Division of Health Physics/Radiation Protection,  
A-2444 Seibersdorf,  
Austria  
Fax: +431505502502  
E-mail: christian.hranitzky@arcs.at
- Hult, E.A. Norwegian Radiation Protection Authority,  
Grini Naeringspark 13,  
P.O. Box 55,  
N-1332 Østerås,  
Norway  
Fax: +4767147407  
E-mail: elin.agathe.hult@nrpa.no

- Huntley, R.B. Australian Radiation Protection and  
Nuclear Safety Agency,  
619 Lower Plenty Road,  
Yallambie,  
Victoria 3085,  
Australia  
Fax: +61394332305  
E-mail: robert.huntley@health.gov.au
- Ibbott, G.S. Department of Radiation Physics,  
University of Texas M.D. Anderson Cancer Center,  
1515 Holcombe Blvd,  
P.O. Box 547,  
Houston, TX 77071,  
United States of America  
Fax: +17137941364  
E-mail: gibbott@mdanderson.org
- Ibrahim, M.S. Nuclear Safety and Radiation Control  
National Center,  
Atomic Energy Authority,  
3 Ahmed El-Zomor Street,  
Nasr City,  
Cairo,  
Egypt  
Fax: +2022876031  
E-mail: mohamedsafaa3@yahoo.com
- Izewska, J. Division of Human Health,  
Department of Nuclear Sciences and Applications,  
International Atomic Energy Agency,  
Wagramer Strasse 5, P.O. Box 100,  
A-1400 Vienna,  
Austria  
Fax: +43126007  
E-mail: j.izewska@iaea.org
- Jäkel, O. Department of Medical Physics,  
German Cancer Research Center (DKFZ),  
Im Neuenheimer Feld 280,  
D-69120 Heidelberg,  
Germany  
Fax: +496221422572  
E-mail: o.jaekel@dkfz.de

- Janeczek, J. Department of Medical Physics,  
Tawam Hospital,  
P.O. Box 15258,  
Al Ain,  
Abu Dhabi,  
United Arab Emirates  
Fax: +97137075803  
E-mail: jacek@tawam-hosp.gov.ae
- Järvinen, H.E.J. Radiation and Nuclear Safety Authority (STUK),  
P.O. Box 14,  
FIN-00881 Helsinki,  
Finland  
Fax: +358975988248  
E-mail: hannu.jarvinen@stuk.fi
- Jobs, J.-T. PTW-Freiburg,  
Lörracher Strasse 7,  
D-79115 Freiburg,  
Germany  
Fax: +497614905570  
E-mail: jens-thomas.jobs@ptw.de
- Johansson, K.E.L. Radiation Physics Department,  
Umeå University Hospital,  
SE-90185 Umeå,  
Sweden  
Fax: +469078515188  
E-mail: lennart.johansson@vll.se
- Kacperek, A. Douglas Cyclotron,  
Clatterbridge Centre for Oncology,  
Bebington, Wirral CH63 4JY,  
United Kingdom  
Fax: +441513342845  
E-mail: andrzej@ccotrust.co.uk
- Kadni, T.B. Malaysian Institute for  
Nuclear Technology Research,  
Bangi,  
43000 Kajang, Selangor,  
Malaysia  
Fax: +60389250575  
E-mail: taiman@mint.gov.my

- Kappas, C. European Society for Therapeutic Radiology  
and Oncology,  
EQUAL Measuring Laboratory,  
Service de physique,  
Institut Gustave-Roussy,  
39, rue Camille Desmoulins,  
F-94805 Villejuif Cedex,  
France  
Fax: +3314215299  
E-mail: kappas@med.upatras.gr
- Kapsch, R.-P. Physikalisch-Technische Bundesanstalt,  
Bundesallee 100,  
D-38116 Braunschweig,  
Germany  
Fax: +495315926405  
E-mail: ralf-peter.kapsch@ptb.de
- Karppinen, K.J. Radiation and Nuclear Safety Authority (STUK),  
P.O. Box 14,  
FIN-00881 Helsinki,  
Finland  
Fax: +358975988248  
E-mail: juhani.karppinen@stuk.fi
- Kern, W. Computerized Medical Systems GmbH,  
Sundgaullee 25,  
D-79114 Freiburg,  
Germany  
Fax: +497618818811  
E-mail: friederike.schreiber@cms-euro.com
- Kessler, C. Bureau international des poids et mesures,  
Pavillon de Breteuil,  
F-92312 Sèvres Cedex,  
France  
Fax: +33145342021  
E-mail: ckessler@bipm.org
- Kim, Gwe-Ya Korean Food and Drug Administration,  
5 Nokbun-Dong Eunpyung-Gu,  
Seoul 122-704,  
Republic of Korea  
Fax: +8223513726  
E-mail: yaya@kfda.go.kr



- Klimesch, H.                      Computerized Medical Systems GmbH,  
Sundgauallee 25,  
D-79114 Freiburg,  
Germany  
Fax: +497618818811  
E-mail: friederike.schreiber@cms-euro.com
- Koch, J.                              Multidata Systems Deutschland GmbH,  
Rizzastrasse 44,  
D-56068 Koblenz,  
Germany  
Fax: +492619154599  
E-mail: jkoch@multidata-systems.de
- Kosunen, A.A.                      Radiation and Nuclear Safety Authority (STUK),  
P.O. Box 14,  
FIN-00881 Helsinki,  
Finland  
Fax: +358975988450  
E-mail: antti.kosunen@stuk.fi
- Králik, G.                              St. Elizabeth Cancer Institute,  
Heydukova 10,  
SK-81250 Bratislava,  
Slovakia  
Fax: +421252923711  
E-mail: gkralik@ousa.sk
- Kramer, H.M.                        Physikalisch-Technische Bundesanstalt,  
Bundesallee 100,  
D-38116 Braunschweig,  
Germany  
Fax: +495315926405  
E-mail: hans-michael.kramer@ptb.de
- Krauss, A.                              Physikalisch-Technische Bundesanstalt,  
Bundesallee 100,  
D-38116 Braunschweig,  
Germany  
Fax: +495315926405  
E-mail: achim.krauss@ptb.de

- Krus, K. Gammex-RMI,  
Adesheimer Weg 17,  
D-53902 Bad Münstereifel,  
Germany  
Fax: +4922571692  
E-mail: kkrus.gammex-rmi@t-online.de
- Krutoff, B.M. Radiation Therapy Service,  
VA Greater Los Angeles Healthcare System,  
11301 Willshire Blvd,  
Los Angeles, CA 90073,  
United States of America  
Fax: +3102684925  
E-mail: bradford.krutoff@med.va.gov
- Kurniawan, B. Department of Physics,  
Faculty of Mathematics and Natural Sciences,  
University of Indonesia,  
Depok 16424,  
Indonesia  
Fax: +62217863441  
E-mail: bkuru@fisika.ui.ac.id
- Kurosawa, T. National Metrology Institute of Japan (AIST),  
1-1-1 Umezono,  
Tsukuba,  
Ibaraki 305-8568,  
Japan  
Fax: +81298615673  
E-mail: tadahiro-kurosawa@aist.go.jp
- Kuzmanovic, Z. Institute of Oncology,  
Novi Sad,  
Institutski put 4,  
YU-21204 Sremska Kamenica,  
Serbia and Montenegro  
Fax: +38121613741  
E-mail: zoran-k@EUnet.yu
- Lamm, I.-L.C. Radiation Physics,  
Lund University Hospital,  
SE-221 85 Lund,  
Sweden  
Fax: +4646 136156  
E-mail: inger-lena.lamm@skane.se

- |             |   |
|-------------|---|
| Lavoie, C.  | Consumer and Clinical Radiation Protection<br>Bureau,<br>Health Canada,<br>Radiation Protection Building,<br>775 Brookfield Road PL6301A,<br>Ottawa, Ontario, K1A 1C1,<br>Canada<br>Fax: +16139411734<br>E-mail: christian_lavoie@hc-sc.gc.ca |
| Leitner, A. | Bundesamt für Eich- und Vermessungswesen,<br>Arltgassee 35,<br>A-1160 Vienna,<br>Austria<br>Fax: +43149110334<br>E-mail: a.leitner@metrologie.at  |
| Lencart, J. | Instituto Português de Oncologia do Porto,<br>Rua António Bernardino de Almeida,<br>P-4200-072 Porto,<br>Portugal<br>Fax: +351225026489<br>E-mail: jlencart@portugalmail.pt   |
| Lesiak, J.  | Centre of Oncology,<br>ul. Garnarska 11,<br>PL-31-115 Kraków,<br>Poland<br>Fax: +48124226680<br>E-mail: z5lesiak@cyf-kr.edu.pl  |
| Levin, C.V. | Division of Human Health,<br>Department of Nuclear Sciences and Applications,<br>International Atomic Energy Agency,<br>Wagramer Strasse 5, P.O. Box 100,<br>A-1400 Vienna,<br>Austria<br>Fax: +43126007<br>E-mail: c.v.levin@iaea.org        |

- Linero, D. Medical Physics Department,  
Institut Català d'Oncologia,  
L'Hospitalet de Lionbregat,  
Avda. Gran Via s/n, km 2,7,  
E-08907 Barcelona,  
Spain  
Fax: +34932607731  
E-mail: dlinero@ico.scs.es
- Lingatong, N. Bureau of Health Devices and Technology,  
Department of Health,  
Bldg 24, San Lazaro Compound,  
Rizal Avenue,  
Santa Cruz 1003,  
Manila,  
Philippines  
Fax: +6327116016  
E-mail: n\_lingatong@hotmail.com
- Lopes, M.C. Instituto Português de Oncologia de Coimbra  
do IPOFG,  
Avenida Bissaya Barreto,  
P-3000-075 Coimbra,  
Portugal  
Fax: +351239 484317  
E-mail: mclopes@croc.min-saude.pt
- Ma, C.-M.C. Department of Radiation Oncology,  
Fox Chase Cancer Center,  
7701 Burholme Avenue,  
Philadelphia, PA 19111,  
United States of America  
Fax: +12157284789  
E-mail: c\_ma@fccc.edu
- Machula, G. National Office of Measures,  
Nemetvolgyi ut. 37-39,  
H-1124 Budapest,  
Hungary  
Fax: +3614585937  
E-mail: g.machula@omh.hu

- Marechal, M.H.H. Instituto de Radioproteção e Dosimetria,  
IRD/CNEN,  
Av. Salvador Allende,  
C.P. 37750,  
22780-160 Rio de Janeiro RJ,  
Brazil  
Fax: +552124422325  
E-mail: mhelena@ird.gov.br
- Matache, G. Institute of Oncology “Prof. Al. Trestioreanu”,  
Sos. Fundeni No. 252, Sector 2,  
RO-72435 Bucharest,  
Romania  
Fax: +4012406160  
E-mail: matache@mail.iob.ro
- Mazzocchi, S. Azienda Ospedaliera Careggi,  
U.O. Fisica Sanitaria,  
Viale Pieraccini 17,  
I-50139 Florence,  
Italy  
Fax: +39554279321  
E-mail: mazzocchis@ao-careggi.toscana.it
- McEwen, M.R. Ionizing Radiation Standards,  
National Research Council,  
Montreal Rd,  
Ottawa, Ontario, K1A OR6,  
Canada  
E-mail: malcolm.mcewen@nrc.ca
- Meade, A.D. School of Physics,  
Dublin Institute of Technology,  
Kevin’s Street,  
Dublin 8,  
Ireland  
Fax: +35314103478  
E-mail: aidan.meade@dit.ie

- Medin, J.A.T. Department of Radiation Physics,  
Lund University,  
Malmö University Hospital,  
SE-205 02 Malmö,  
Sweden  
Fax: +4640963185  
E-mail: joakim.medin@rfa.mas.lu.se
- Meghzifene, A. Division of Human Health,  
Department of Nuclear Sciences and Applications,  
International Atomic Energy Agency,  
Wagramer Strasse 5, P.O. Box 100,  
A-1400 Vienna,  
Austria  
Fax: +43126007  
E-mail: a.meghzifene@iaea.org
- Meghzifene, K. Institut für Biomedizinische Technik und Physik,  
Universität Wien,  
AKH-4L,  
Währinger Gürtel 18–20,  
A-1090 Vienna,  
Austria  
Fax: +431404003988  
E-mail: k.meghzifene@bmtbakh-wien.ac.at
- Meriaty, H. Safety Division,  
Australian Nuclear Science and Technology  
Organisation,  
New Illawarra Road,  
Lucas Heights,  
New South Wales 2234,  
Australia  
Fax: +61297173899  
E-mail: ham@ansto.gov.au
- Mijnheer, B.J. Radiotherapy Department,  
Netherlands Cancer Institute,  
Plesmanlaan 121,  
NL-1066 CX Amsterdam,  
Netherlands  
Fax: +3120 6691101  
E-mail: bmijnh@nki.nl

- Milano, F. Department of Clinical Physiopathology,  
University of Florence,  
Viale Morgagni 85,  
I-50134 Florence,  
Italy  
Fax: +390554379930  
E-mail: f.milano@dfe.unifi.it
- Miljanic, S. Ruder Boskovic Institute,  
P.O. Box 180,  
Bijenicka 54,  
HR-10002 Zagreb,  
Croatia  
Fax: +38514680098  
E-mail: saveta@rudjer.irb.hr.
- Millar, R.M. William Buckland Radiotherapy Centre,  
The Alfred Hospital,  
Commercial Road,  
Prahran,  
Victoria 3181,  
Australia  
Fax: +61392762669  
E-mail: malcolm.millar@wbrc.org.au
- Miller, C.R.E. Medical Physics Radiotherapy Department,  
Kingston Public Hospital,  
North Street,  
Kingston,  
Jamaica  
Fax: +18769671636  
E-mail: cmiller@cwjamaica.com
- Moaierifar, K. IBA Scanditronix AB,  
Stalgatan 14,  
SE-754 50 Uppsala,  
Sweden  
Fax: +4618127552  
E-mail: kiarash@scsxmedical.se

- Moiseenko, A. Department of Radiotherapy,  
Oncological Scientific Center,  
76 Fanarjyan Street,  
Kanaker,  
375052 Yerevan,  
Armenia  
E-mail: alla@moon.yerphi.am
- Munck af Rosenschöld, P.M. Department of Radiation Physics,  
Lund University Hospital,  
Klinik 7,  
SE-221 85 Lund,  
Sweden  
Fax: +4646136156  
E-mail: per.munck@skane.se
- Nani, K.E. National Centre for Radiotherapy and  
Nuclear Medicine,  
P.O. Box KB 369,  
Korle-Bu,  
Ghana  
Fax: +23321400807  
E-mail: kwakunani@yahoo.com
- Nasukha Center of R&D for Radiation Safety and  
Nuclear Biomedicine,  
National Atomic Energy Agency,  
P.O. Box 7043 JKSKL,  
Jakarta 12070,  
Indonesia  
Fax: +62217657950  
E-mail: aljabar2@hotmail.com
- Newhauser, W.D. Department of Radiation Physics,  
University of Texas M.D. Anderson Cancer Center,  
1515 Holcombe Blvd,  
P.O. Box 94,  
Houston, TX 77030,  
United States of America  
E-mail: wnewhaus@mdanderson.org



- Nicolai, J.P. Centre de Fontenay aux Roses,  
Commissariat à l'énergie atomique,  
DRT/SEII Bât. 38.2,  
Route du Panorama, B.P. No. 6,  
F-92265 Fontenay-aux-Roses Cedex,  
France  
E-mail: jean-philippe.nicolai@cea.fr
- Nikodemová, D. Institute of Preventive and Clinical Medicine,  
Limbová Str. 14,  
SK-83301 Bratislava,  
Slovakia  
Fax: +421259369338  
E-mail: nikodem@upkm.sk
- Nilsson, N.B. Department of Medical Radiation Physics,  
Stockholm University,  
P.O. Box 260,  
SE-171 76 Stockholm,  
Sweden  
Fax: +468343525  
E-mail: bo.nilsson@radfys.ki.se
- Niroomand-Rad, A. International Organization for Medical Physics,  
Department of Radiation Medicine,  
L.L. Bles Building,  
Georgetown University Hospital,  
3800 Reservoir Road,  
Washington, DC 20007,  
United States of America  
Fax: +1202 7843323  
E-mail: nirooma@gunet.georgetown.edu
- Nishiwaki, Y. Institut für Medizinische Physik,  
Universität Wien,  
Währingerstrasse 13,  
A-1090 Vienna,  
Austria  
Fax: +4318764259

- Novák, L. National Radiation Protection Institute,  
Srobarova 48,  
CZ-100-00 Prague 10,  
Czech Republic  
Fax: +420267311410  
E-mail: lnovak@suro.cz
- Novakovic, M. EKOTEH Dosimetry Radiation Protection Co.,  
V. Ruzdjaka 21,  
HR-10000 Zagreb,  
Croatia  
Fax: +38516043866  
E-mail: mlnovako@inet.hr
- Novotný, J. Department of Stereotactic and Radiation  
Neurosurgery,  
Na Homolce Hospital,  
Roentgenova 2,  
CZ-150-30 Prague 5,  
Czech Republic  
Fax: +420257210688  
E-mail: josef.novotny@homolka.cz
- Nowotny, R. Institut für Biomedizinische Technik und Physik,  
Universität Wien,  
AKH-4L,  
Währinger Gürtel 18–20,  
A-1090 Vienna,  
Austria  
Fax: +431404003988  
E-mail: robert.nowotny@univie.ac.at
- Oberdorfer, M. Nuklearmedizinische Fakultät,  
R.D. Isar,  
Technische Universität München,  
Ismaninger Strasse 22,  
D-81675 Munich,  
Germany  
Fax: +498941404938  
E-mail: M.Oberdorfer@lrz.tum.de

- Olsen, K.J. Department of Radiation Therapy,  
Physics 54C3,  
University Hospital Herlev,  
DK-2730 Herlev,  
Denmark  
Fax: +4544883065  
E-mail: kjol@herlevhosp.kbhamt.dk
- Olšovcová, V. Inspectorate for Ionizing Radiation,  
Czech Metrological Institute,  
Radiova 1,  
CZ-102-00 Prague 10,  
Czech Republic  
Fax: +420266020466  
E-mail: volsovcova@cmi.cz
- Onori, S. Laboratorio di Fisica,  
Istituto Superiore di Sanità,  
Viale Regina Elena 299,  
I-00161 Rome,  
Italy  
Fax: +3906493877075  
E-mail: sandro.onori@iss.it
- Ortiz Lopez, P. Division of Radiation and Waste Safety,  
Department of Nuclear Safety and Security,  
International Atomic Energy Agency,  
Wagramer Strasse 5, P.O. Box 100,  
A-1400 Vienna,  
Austria  
Fax: +43126007  
E-mail: p.ortiz-lopez@iaea.org
- Osorio, A. Laboratorio Secundario de  
Calibración Dosimetrica,  
Dirección General de Energía,  
Universidad de San Carlos,  
24 Calle 21-12 Zona 12,  
01012 Guatemala,  
Guatemala  
Fax: +5024762007  
E-mail: arot23@yahoo.com

- Parkkinen, R.T.                      Radiation and Nuclear Safety Authority (STUK),  
P.O. Box 14,  
FIN-00881 Helsinki,  
Finland  
Fax: +358975988248  
E-mail: ritva.parkkinen@stuk.fi
- Patel, V.                                Department of Radiation Oncology,  
Royal Prince Alfred Hospital,  
Missenden Road,  
Camperdown,  
New South Wales 2050,  
Australia  
Fax: +61295158070  
E-mail: vpatel@E-mail.cs.nsw.gov.au
- Paviotti de Corcuera, R.            Division of Physical and Chemical Sciences,  
Department of Nuclear Sciences and Applications,  
International Atomic Energy Agency,  
Wagramer Strasse 5, P.O. Box 100,  
A-1400 Vienna,  
Austria  
Fax: +43126007  
E-mail: r.paviotti-corcuera@iaea.org
- Peixoto, J.G.P.                        Instituto de Radioproteção e Dosimetria,  
IRD/CNEN,  
Av. Salvador Allende,  
C.P. 37750,  
22780-160 Rio de Janeiro RJ,  
Brazil  
Fax: +552134118163  
E-mail: guilherm@ird.gov.br
- Pellet, S.                                “Frederic Joliot Curie”,  
National Research Institute for Radiobiology and  
Radiohygiene,  
Anna u. 5,  
H-1221 Budapest,  
Hungary  
Fax: +3612291931  
E-mail: pellet@hp.osski.hu

- Pernička, F. Division of Human Health,  
Department of Nuclear Sciences and Applications,  
International Atomic Energy Agency,  
Wagramer Strasse 5, P.O. Box 100,  
A-1400 Vienna,  
Austria  
Fax: +43126007  
E-mail: f.pernicka@iaea.org
- Picard, Y. Consumer and Clinical Radiation Protection  
Bureau,  
Health Canada,  
Radiation Protection Building,  
775 Brookfield Road PL6301A,  
Ottawa, Ontario, K1A 1C1,  
Canada  
Fax: +16139411734  
E-mail: yani\_picard@hc-sc.gc.ca
- Pieksma, M. Nederlands Meetinstituut,  
P.O. Box 654,  
NL-2600 AR Delft,  
Netherlands  
Fax: +31302539095  
E-mail: mpieksma@nmi.nl
- Plompen, R. IBA Advanced Radiotherapy,  
Bahnhofstrasse 5,  
D-90592 Schwarzendruck,  
Germany  
Fax: +49912860710  
E-mail: rob.plompen@wellhofer.com
- Ponte, F. Instituto Português de Oncologia do Porto,  
Rua António Bernardino de Almeida,  
P-4200-072 Porto,  
Portugal  
Fax: +351225026489  
E-mail: fponte@portugalmail.pt

- Potiens, M.P.A. Instituto de Pesquisas Energéticas e Nucleares,  
IPEN/CNEN,  
Av. Prof. Lineau Prestes,  
2242 Cidade Universitária,  
05508-900 São Paulo SP,  
Brazil  
Fax: +551138169209  
E-mail: mppalbu@net.ipen.br
- Pszona, S. Andrzej Soltan Institute for Nuclear Studies,  
PL-05-400 Otwock-Swierk,  
Poland  
Fax: +48227793481  
E-mail: pszona@ipj.gov.pl
- Pychlau, H.C.H. PTW-Freiburg,  
Lörracher Strasse 7,  
D-79115 Freiburg,  
Germany  
Fax: +497614905570  
E-mail: pychlau@ptw.de
- Rascon Caballero, A. Ministerio de Ciencia y Tecnología,  
Avda. Complutense 22,  
E-28040 Madrid,  
Spain  
Fax: +34913066442  
E-mail: angel.rascon@ciemat.es
- Rehani, M.M. Division of Radiation and Waste Safety,  
Department of Nuclear Safety and Security,  
International Atomic Energy Agency,  
Wagramer Strasse 5, P.O. Box 100,  
A-1400 Vienna,  
Austria  
Fax: +43126007  
E-mail: m.rehani@iaea.org

- Ridziková, A. Faculty of Nuclear Sciences and  
Physical Engineering,  
Czech Technical University,  
Brehova 7,  
CZ-115-19 Prague 1,  
Czech Republic  
Fax: +420222320861  
E-mail: anri@orangE-mail.sk
- Rodrigues, L.L.C. Instituto de Pesquisas Energéticas e Nucleares,  
IPEN/CNEN,  
Av. Prof. Lineau Prestes,  
2242 Cidade Universitária,  
05508-900 São Paulo SP,  
Brazil  
Fax: +551138169209  
E-mail: lcrodri@net.ipen.br
- Rodrigues, L.N. Instituto de Pesquisas Energéticas e Nucleares,  
IPEN/CNEN,  
Av. Prof. Lineau Prestes,  
2242 Cidade Universitária,  
05508-900 São Paulo SP,  
Brazil  
Fax: +551138169117  
E-mail: lnatal@net.ipen.br
- Rosser, K.E. National Physical Laboratory,  
Queens Road,  
Teddington,  
Middlesex TW11 0LW,  
United Kingdom  
E-mail: karen.rosser@npl.co.uk
- Rudder, D. National Radiotherapy Centre,  
Ministry of Health,  
112 Western Main Road,  
St. James,  
Trinidad and Tobago  
Fax: +8686283232  
E-mail: damianr@wow.net

- Saiful Huq, M. Department of Radiation Oncology,  
Thomas Jefferson University,  
111 South 11th Street,  
Philadelphia, PA 19107-5097,  
United States of America  
Fax: +12159555331  
E-mail: saiful.huq@mail.tju.edu
- Salikin, M.S. Malaysian Institute for  
Nuclear Technology Research,  
Bangi,  
43000 Kajang, Selangor,  
Malaysia  
Fax: +60389250575  
E-mail: saion@mint.gov.my
- Saravi, M.C. Comisión Nacional de Energía Atómica,  
Avenida del Libertador 8250,  
1429 Buenos Aires,  
Argentina  
Fax: +541143798228  
E-mail: saravi@cae.cnea.gov.ar
- Schachner, J. Institut für Krankenhausphysik,  
Krankenhaus Lainz,  
Wolkersbergenstrasse 1,  
A-1130 Vienna,  
Austria  
E-mail: joschach@eunet.at
- Schaeken, B. Algemeen Ziekenhuis Middelheim,  
AFD Radiotherapie,  
Lindendreef 1,  
B-2020 Antwerpen,  
Belgium  
Fax: +3232810719  
E-mail: bob.schaeken@ocmw.antwerpen.be



- Schmidt, W.F.O.                      Institut für Radioonkologie,  
Donauspital,  
Langobardenstrasse 122,  
A-1220 Vienna,  
Austria  
Fax: +431288022728  
E-mail: werner.schmidt@smz.magwien.gv.at
- Schnuer, K.                            Radiation Protection Unit,  
Directorate General for Environment,  
European Commission,  
Bât. Wagner C/320,  
Plateau de Kirchberg,  
L-2920 Luxembourg,  
Luxembourg  
Fax: +352430134646/3628  
E-mail: klaus.schnuer@cec.eu.int
- Schreiner, T.                          Fotec GmbH,  
Viktor Kaplan-Straße 2,  
A-2700 Wiener Neustadt,  
Austria  
E-mail: schreiner@fotec.at
- Seemann, R.                          Fotec GmbH,  
Viktor Kaplan-Straße 2,  
A-2700 Wiener Neustadt,  
Austria  
E-mail: seemann@fotec.at
- Selbach, H.-J.                        Physikalisch-Technische Bundesanstalt,  
Bundesallee 100,  
D-38116 Braunschweig,  
Germany  
Fax: +495315926405  
E-mail: hans-joachim.selbach@ptb.de

- Seuntjens, J. McGill University,  
Medical Physics Unit,  
Montreal General Hospital,  
1650 avenue Cedar,  
Montreal, Quebec, H3G 1A4,  
Canada  
Fax: +15149348229  
E-mail: jseuntjens@medphys.mcgill.ca
- Shortt, K.R. Division of Human Health,  
Department of Nuclear Sciences and Applications,  
International Atomic Energy Agency,  
Wagramer Strasse 5, P.O. Box 100,  
A-1400 Vienna,  
Austria  
Fax: +43126007  
E-mail: k.shortt@iaea.org
- Silberbach, A. Computerized Medical Systems GmbH,  
Sundgauallee 25,  
D-79114 Freiburg,  
Germany  
Fax: +497618818811  
E-mail: silber@cms-euro.com
- Smyth, V. National Radiation Laboratory,  
108 Victoria Street, P.O. Box 25-099,  
Christchurch,  
New Zealand  
Fax: +6433661156  
E-mail: vere\_smyth@nrl.moh.govt.nz
- Soares, C.G. National Institute of Standards and Technology,  
100 Bureau Drive,  
Stop 8460,  
Gaithersburg, MD 20899-8460,  
United States of America  
Fax: +13018697682  
E-mail: csoares@nist.gov
- Spanswick, K.A. Radcal Europe,  
20 Milton Drive,  
Ravenshead,  
Nottingham NG15 9BE,  
United Kingdom  
E-mail: kspanswick@radcal.com

- Stabin, M.G. Department of Radiology,  
Radiological Sciences,  
Vanderbilt University,  
1161 21st Ave S,  
Nashville, TN 37232,  
United States of America  
E-mail: stabin@bellsouth.net
- Stadtman, H. ARC Seibersdorf Research GmbH,  
Division of Health Physics/Radiation Protection,  
A-2444 Seibersdorf,  
Austria  
Fax: +431505502502  
E-mail: hannes.stadtman@arcs.ac.at
- Staykova, V.I. Laboratory of Clinical Dosimetry and  
Metrology of Ionizing Radiation,  
Univ. Hospital "Queen Giovanna",  
8, Bialo More Street,  
BG-1504 Sofia,  
Bulgaria  
Fax: +3592467176  
E-mail: vstaykova@hotmail.com
- Stewart, K.J. Department of Medical Physics,  
McGill University Health Center,  
Montreal General Hospital,  
L5-107, 1650 avenue Cedar,  
Montreal, Quebec, H3G 1A4,  
Canada  
Fax: +15149348229  
E-mail: kristins@medphys.mcgill.ca
- Stisova, V. Faculty of Nuclear Sciences and  
Physical Engineering,  
Czech Technical University,  
Brehova 7,  
CZ-115-19 Prague 1,  
Czech Republic  
Fax: +420222320861  
E-mail: viktorie.stisova@centrum.cz

- Stserbakov, V. Department of Radiotherapy,  
North Estonia Regional Hospital,  
Cancer Centre,  
Hiiu Str. 44,  
EE-11619 Tallinn,  
Estonia  
Fax: +3726504303  
E-mail: shch@onkoloogia.ee
- Stucki, G. Swiss Federal Office of Metrology and  
Accreditation,  
Federal Department of Justice and Police,  
Lindenweg 50,  
CH-3003 Bern-Wabern,  
Switzerland  
Fax: +41313233210  
E-mail: gerhard.stucki@metas.ch
- Suliman, I.I. Delft University of Technology,  
Interfaculty Reactor Institute,  
Mekelweg 15,  
NL-2629 JB Delft,  
Netherlands  
Fax: +31152789011  
E-mail: i.i.suliman@iri.tudelft.nl
- Suriyapee, S. Department of Radiology,  
Chulalongkorn University,  
King Chulalongkorn Memorial Hospital,  
Rama IV Road,  
Bangkok 10330,  
Thailand  
Fax: +6622564334/162  
E-mail: ssivalee@chula.ac.th
- Svensson, H. European Society for Therapeutic Radiology and  
Oncology,  
Avenue Mounier Laan 83,  
B-1200 Brussels,  
Belgium  
Fax: +468343525  
E-mail: hans.svensson@radfys.umu.se

- Takeyeddin, M. Atomic Energy Commission of Syria,  
P.O. Box 6091,  
Damascus,  
Syrian Arab Republic  
Fax: +963116112289  
E-mail: atomic@net.sy
- Tannanonta, C. Department of Radiology,  
Faculty of Medicine,  
Mahidol University,  
Ramathibodi Hospital,  
Rama VI Road,  
Bangkok 10400,  
Thailand  
Fax: +6622011191  
E-mail: ractn@mahidol.ac.th
- Tarutin, I.G. Research Institute of Oncology and  
Medical Radiology,  
P.O. Box Lesnoy-2,  
223052 Minsk,  
Belarus  
Fax: +375172024704  
E-mail: tarutin@omr.med.by or itarutin@tut.by
- Thomas, R.A.S. National Physical Laboratory,  
Queens Road,  
Teddington,  
Middlesex TW11 0LW,  
United Kingdom  
Fax: +442089436070  
E-mail: russell.thomas@npl.co.uk
- Thomson-Miller, M. Thomson Nielsen Electronics Ltd,  
25B Northside Road,  
Ottawa, Quebec, K2H 8S1,  
Canada  
Fax: +16135965243  
E-mail: mmiller@thomson-elec.com

- Thwaites, D.I. Department of Oncology Physics,  
Edinburgh Cancer Centre,  
University of Edinburgh,  
Western General Hospital,  
Edinburgh EH4 2XU,  
United Kingdom  
Fax: +441315371092  
E-mail: dit@holyrood.ed.ac.uk
- Tiefenboeck, W. Bundesamt für Eich- und Vermessungswesen,  
Arltgasse 35,  
A-1160 Vienna,  
Austria  
Fax: +4314920875  
E-mail: w.tiefenboeck@metrologie.at
- Tölle, H. Division of Human Health,  
Department of Nuclear Sciences and Applications,  
International Atomic Energy Agency,  
Wagramer Strasse 5, P.O. Box 100,  
A-1400 Vienna,  
Austria  
Fax: +43126007  
E-mail: h.toelli@iaea.org
- Tolwinski, J. Maria Skłodowska-Curie Memorial Cancer Center  
and Institute of Oncology,  
Roentgena Street 5,  
PL-02-781 Warsaw,  
Poland  
Fax: +48226449182
- Tonhäuser, P. MDS Nordion GmbH,  
Heinrich von Stephan-Strasse 8,  
D-79100 Freiburg,  
Germany  
Fax: +497614551310  
E-mail: ptonhauser@mds.nordion.com
- Tosi, G. European Institute of Oncology,  
Department of Medical Physics,  
Via Ripamonti 435,  
I-20141 Milan,  
Italy  
Fax: +39257489208  
E-mail: giampiero.tosi@ieo.it

- Tovar Muñoz, V.M. Instituto Nacional de Investigaciones Nucleares,  
P.O. Box 181027,  
Colonia Escandón,  
Miguel Hidalgo,  
11801 Mexico, D.F.,  
Mexico  
Fax: +525553297302  
E-mail: vmtm@nuclear.inin.mx
- Twydle, J.P. Agfa NDT Ltd,  
Unit 30,  
Robert Cort Industrial Estate,  
Britten Road,  
Reading RG2 OAU,  
United Kingdom  
Fax: +441189314711  
E-mail: john.twydle.jt@agfa.co.uk
- Valen, H.J. Haukeland University Hospital,  
Haukeland Sykenus,  
Radiofysisk Avd.,  
N-5021 Bergen,  
Norway  
Fax: +4755976089  
E-mail: harald.valen@haukeland.no
- van der Marel, J. Nederlands Meetinstituut,  
P.O. Box 80000,  
NL-3508 TA Utrecht,  
Netherlands  
Fax: +31302539095  
E-mail: hvdmarel@nmi.nl
- van der Merwe, D.G. Area 249: Radiation Services,  
Johannesburg Hospital,  
7 York Road,  
Parktown 2193,  
South Africa  
Fax: +27116429185  
E-mail: vandermerwedg@mediarie.wits.ac.za
- van Dijk, E. Nederlands Meetinstituut,  
P.O. Box 80000,  
NL-3508 TA Utrecht,  
Netherlands  
Fax: +31302539095  
E-mail: evandijk@nmi.nl





- Vynckier, S.                      Université Catholique de Louvain,  
Avenue Hippocrate 10,  
B-1200 Brussels,  
Belgium  
Fax: +3227644749  
E-mail: vynckier@rbnt.ucl.ac.be
- Wagner, M.                      Abteilung für Medizinische Physik,  
Landeskrankenhaus Feldkirch,  
Carinagasse 47,  
A-6800 Feldkirch,  
Austria  
Fax: +55223037523
- Waligórski, M.                      Centre of Oncology,  
ul. Garnearska 11,  
PL-31-115 Kraków,  
Poland  
Fax: +48124226680  
E-mail: z5waligo@cyf-kr.edu.pl
- Wambersie, A.                      Unité de radiobiologie et de radioprotection,  
Université Catholique de Louvain,  
Avenue Hippocrate 54,  
B-1200 Brussels,  
Belgium  
Fax: +3227649425  
E-mail: wambersie@rbnt.ucl.ac.be
- Weninger, F.                      Fotec GmbH,  
Viktor Kaplan-Straße 2,  
A-2700 Wiener Neustadt,  
Austria  
E-mail: weninger@fotec.at
- Westermarck, M.                      Department of Hospital Physics,  
Karolinska Hospital,  
P.O. Box 260,  
SE-171 76 Stockholm,  
Sweden  
Fax: +4687366280  
E-mail: mathias.westermarck@ks.se

- Whelan, S. International Agency for Research on Cancer,  
World Health Organization,  
150, Cours Albert-Thomas,  
F- 69372 Lyons Cedex 08,  
France  
Fax: +33472738575  
E-mail: whelan@iarc.fr
- Wickman, C.G. Radiation Physics,  
Department of Physics,  
Umeå University,  
SE-90185 Umeå,  
Sweden  
Fax: +46907851588  
E-mail: goran.wickman@vll.se
- Witzani, J. Bundesamt für Eich- und Vermessungswesen,  
Arltgasse 35,  
A-1160 Vienna,  
Austria  
Fax: +4314920875  
E-mail: j.witzani@metrologie.at
- Woods, M.J. National Physical Laboratory,  
Queens Road,  
Teddington,  
Middlesex TW11 OLW,  
United Kingdom  
Fax: +442086140480  
E-mail: michael.woods@npl.co.uk
- Zaidi, H. Division of Nuclear Medicine,  
Geneva University Hospital,  
CH-1211 Geneva,  
Switzerland  
Fax: +41223727169  
E-mail: habib.zaidi@hcuge.ch
- Zatelli, G. Azienda Ospedaliera Careggi,  
U.O. Fisica Sanitaria,  
Viale Pieraccini 17,  
I-50139 Florence,  
Italy  
Fax: +39554279321  
E-mail: zatellig@ao-careggi.toscana.it

Zdesar, U.

Institute of Occupational Safety,  
Slovenian Nuclear Safety Authority,  
Bohoriceva 22A,  
SI-1000 Ljubljana,  
Slovenia  
Fax: +38661312562  
E-mail: urban.zdesar@zvd.si

Zimmerman, B.E.

National Institute of Standards and Technology,  
100 Bureau Drive,  
Stop 8462,  
Gaithersburg, MD 20899,  
United States of America  
Fax: +13019267416  
E-mail: bez@nist.gov

Zoetelief, J.

Delft University of Technology,  
Interfaculty Reactor Institute,  
Mekelweg 15,  
NL-2629 JB Delft,  
Netherlands  
Fax: +31152789011  
E-mail: j.zoetelief@iri.tudelft.nl

**BLANK**

## AUTHOR INDEX

- Aalbers, A.H.L.: I 93  
 Aguirre, J.F.: II 191  
 Akagi, T.: II 321  
 Allahverdi, M.: II 183  
 Allisy-Roberts, P.J.: I 11  
 Alm Carlsson, G.: I 387  
 Andersen, C.E.: II 353  
 Andreo, P.: I 21, 297, 375; II 279  
 Aukett, R.J.: I 271  
 Aznar, M.C.: II 353  
 Bäck, S.Å.J.: II 353  
 Bahar-Gogani, J.: II 121  
 Baker, M.: II 45  
 Baldock, C.: II 339, 389, 397  
 Balter, P.: II 209  
 Barone Tonghi, L.: II 311  
 Beach, M.: II 361  
 Beaudré, A.: I 313  
 Ben Omrane, L.: I 367  
 Bergstrand, E.S.: II 405  
 Bjerke, H.: I 279  
 Blyth, C.: II 415  
 Bochud, F.O.: I 429  
 Boehringer, T.: II 295  
 Böhm, J.: II 111  
 Borrás, C.: I 231  
 Bøtter-Jensen, L.: II 353  
 Bridier, A.: I 313; II 157  
 Buchillier, T.: I 429  
 Büermann, L.: I 125  
 Bulski, W.: II 231  
 Burkart, W.: I 3  
 Burns, D.T.: I 11, 141  
 Carruthers, L.: II 415  
 Chahed, N.: I 367  
 Chauvenet, B.: I 83  
 Chen, L.: II 369  
 Christensen, P.: I 439  
 Coray, A.: II 295  
 Csete, I.: I 125  
 Cuttone, G.: II 311  
 Czap, L.: I 375  
 Dance, D.R.: I 387  
 Daneš, J.: I 449  
 Daures, J.: I 83  
 de Almeida, C.E.: II 221  
 de Deene, Y.: II 389, 397  
 de Prez, L.A.: I 93  
 de Wagter, C.: II 381  
 Derikum, K.: I 287, 353  
 DeWerd, L.A.: I 387  
 Ding, M.: II 369  
 Dowling, A.: I 421  
 Drexler, G.: I 387  
 Dryák, P.: II 67  
 Duane, S.: I 67, 115, 335, 467;  
     II 201  
 DuSautoy, A.R.: I 37  
 Dutreix, A.: II 157  
 Egger, E.: II 311  
 Elliott, P.A.: II 415  
 Ferreira, I.H.: I 313; II 157, 221  
 Followill, D.: II 209  
 Fourkal, E.: II 369  
 Fukuda, S.: II 321  
 Fukumura, A.: II 321  
 Gaudiano, J.: II 59  
 Giczi, F.: I 449  
 Gillis, S.: II 381  
 Goitein, G.: II 295  
 Govinda Rajan, K.N.: I 467  
 Greener, A.G.: I 271  
 Hanson, W.F.: II 191, 209  
 Harrison, R.M.: I 271  
 Hartmann, G.H.: I 323; II 303  
 Hasegawa, T.: II 321

- Heeg, P.: II 303  
 Hilgers, G.: II 121  
 Hobeila, F.: I 177  
 Hole, E.O.: II 405  
 Ibbott, G.: II 139, 191, 209, 361  
 Izewska, J.: II 139, 249  
 Jäkel, O.: II 303  
 Jansen, J.T.M.: I 411  
 Järvinen, H.: I 263, 361, 387, 405  
 Jiménez, P.: I 231  
 Jokelainen, I.: I 263  
 Julius, H.W.: I 439  
 Kacperek, A.: II 311  
 Kanai, T.: II 321  
 Kanematsu, N.: II 321  
 Kapsch, R.-P.: I 287  
 Karger, C.P.: II 303  
 Karppinen, J.: I 405  
 Kaulich, T.W.: II 111  
 Kidane, G.: II 415  
 Kocik, B.: II 231  
 Kosunen, A.: I 263, 361  
 Koyama, Y.: I 151  
 Kramer, H.-M.: I 159, 387  
 Krauss, A.: I 75  
 Kroutilíková, D.: II 269  
 Kurosawa, T.: I 151  
 Kusano, Y.: II 321  
 Laban, J.A.: II 177  
 Layangkul, T.: II 239  
 Levin, C.V.: I 221  
 Li, J.S.: II 369  
 Lin, S.: II 295  
 Lomax, A.: II 295  
 Luraschi, F.: II 311  
 Ma, C.-M.: II 369  
 Maccia, C.: I 449  
 MacLeod, A.S.: II 415  
 Malone, J.F.: I 421  
 Marre, D.: I 313  
 Maruhashi, A.: II 321  
 Maryanski, M.: II 361  
 Marzoli, L.: II 311  
 Masuda, Y.: II 321  
 Mather, M.L.: II 397  
 Mattsson, S.: II 353  
 McEwen, M.R.: I 67, 115, 335, 467; II 201  
 McNeeley, S.: II 369  
 Meade, A.D.: I 421  
 Medin, J.: II 353  
 Meghzifene, A.: I 375  
 Mello da Silva, C.N.: I 257  
 Michael, G.: II 389  
 Mijnheer, B.J.: II 381  
 Millwater, C.J.: II 415  
 Milu, C.: I 449  
 Moyers, M.F.: II 327  
 Mtimet, S.: I 367  
 Muench, W.: I 103  
 Nahum, A.E.: I 271, 367  
 Nelson, A.: II 209  
 Ng, K.-H.: I 387  
 Nikodemová, D.: I 449  
 Nisbet, A.: II 183  
 Nishio, T.: II 321  
 Nohtomi, A.: II 321  
 Novák, L.: II 269  
 Novotný, J.: I 475; II 269  
 Ochoa, R.: II 221  
 Olšovcová, V.: II 67  
 Olszewska, A.: II 381  
 Oresegun, M.: I 449  
 Orkongiat, C.: II 239  
 Ostrowsky, A.: I 83  
 Padovani, R.: I 449  
 Paolino, A.: II 59  
 Paolucci, M.: II 415  
 Parkkinen, R.: I 263, 361  
 Pedroni, E.: II 295  
 Perníčka, F.: I 387, 449  
 Picard, Y.: I 457

- Pieksma, M.: I 93  
 Powley, S.K.: II 183  
 Price, R.: II 369  
 Pszona, S.: II 231  
 Pychlau, C.: II 167  
 Qin, L.: II 369  
 Quast, U.: II 111  
 Quintel, H.: I 103  
 Raffaele, L.: II 311  
 Rodrigues, L.N.: I 257  
 Ross, C.K.: II 405  
 Rosser, K.E.: I 271; II 201  
 Rovelli, A.: II 311  
 Rudder, D.: I 231  
 Sabini, M.G.: II 311  
 Saiful Huq, M.: I 297, 313  
 Savio, E.: II 59  
 Selbach, H.-J.: II 101  
 Seuntjens, J.P.: I 37, 177, 343  
 Shigwan, J.B.: I 467  
 Shimbo, M.: II 321  
 Shortt, K.R.: I 375; II 405  
 Sipilä, P.: I 263, 361  
 Smyth, V.G.: II 177  
 Soares, C.G.: II 79, 101  
 Soukup, M.: I 475  
 Stabin, M.G.: II 3  
 Stacey, C.: II 415  
 Staniszewska, M.A.: I 449  
 Stewart, K.J.: I 343  
 Stoker, I.: I 67  
 Stovall, M.: II 191  
 Stucki, G.: I 103  
 Suliman, I.I.: I 411  
 Svensson, H.: II 139, 157  
 Tabarelli de Fatis, P.: II 311  
 Tailor, R.C.: II 191  
 Takata, N.: I 151  
 Tannanonta, C.: II 239  
 Tapiovaara, M.: I 405  
 Tatsuzaki, H.: I 221  
 Thomas, R.A.S.: I 335; II 201  
 Thwaites, D.I.: I 243; II 183, 239, 415  
 Tölle, H.: II 79  
 Trapp, J.V.: II 389  
 Valley, J.-F.: I 429  
 van der Marel, J.: II 93  
 van Dijk, E.: I 93; II 93, 129  
 van Dyk, J.: I 205  
 Vandana, S.: I 467  
 Vano, E.: I 449  
 Vatnitsky, A.S.: II 327  
 Vatnitsky, S.M.: II 279, 327  
 Verhaegen, F.: I 367  
 Vijayam, M.: I 467  
 Walsh, C.L.: I 421  
 Wambersie, A.: I 7  
 Wang, L.: II 369  
 Whelan, S.L.: I 189  
 Whittaker, A.K.: II 397  
 Wickman, G.: II 121  
 Wincel, K.: II 231  
 Woods, M.J.: II 45  
 Yanou, T.: II 321  
 Yusa, K.: II 321  
 Zaidi, H.: II 29  
 Zareba, B.: II 231  
 Zimmerman, B.E.: II 17  
 Zoetelief, J.: I 387, 411, 439